NNT: 2017SACLS470

UNIVERSITÉ PARIS SUD
Comprendre le monde, construire l'avenir®

Understanding Cell Dynamics in Cancer from Control and Mathematical Biology Standpoints: Particular Insights into the Modeling and Analysis Aspects in Hematopoietic Systems and Leukemia

Thèse de doctorat de l'Université Paris-Saclay
préparée à l'Université Paris-Sud

École doctorale n°580 Sciences et technologies de l'information et de la communication (STIC)
Spécialité de doctorat: Automatique

Thèse présentée et soutenue à Paris, le 27 novembre 2017, par

Walid Djema

Composition du Jury :

Françoise Lamnabhi-Lagarrigue Directrice de recherche CNRS, L2S, CentraleSupélec,	Présidente
Pierdomenico Pepe Associate Professor, *L'Aquila University, Italy*	Rapporteur
Mostafa Adimy Directeur de recherche INRIA, Rhône-Alpes	Rapporteur
Alexander Medvedev Professeur, *Upsala University, Sweden*	Examinateur
Catherine Bonnet Directrice de recherche Inria, L2S (CNRS) CentraleSupélec	Directrice de thèse
Frédéric Mazenc Chargé de recherche Inria, L2S (CNRS), CentraleSupélec	Co-Directeur de thèse
Jean Clairambault Directeur de recherche Inria, Université de Sorbonne	Co-Directeur de thèse

université PARIS-SACLAY
ÉCOLE DOCTORALE
Sciences et technologies de l'information et de la communication (STIC)

Titre : Modélisation et analyse de stabilité des dynamiques de populations cellulaires cancéreuses: applications au cas de l'hématopoïèse et de la leucémie aiguë myéloblastique

Mots clés : Modélisation, Stabilité, Systèmes à retards, Théorie de Lyapunov, Cancer, Cycle cellulaire

Résumé : Cette thèse porte sur la modélisation et l'analyse de stabilité de certains mécanismes biologiques complexes en rapport avec le cancer. Un intérêt particulier est porté au cas de l'hématopoïèse et de la leucémie aiguë myéloblastique (LAM). Les modèles utilisés et/ou introduits dans cette thèse se décrivent par des équations aux dérivées partielles structurées en âge, qui se réduisent à des systèmes à retards de plusieurs types (retards ponctuels ou distribués, à support fini ou infini). Ces modèles à retards sont parfois couplés à des équations aux différences, et possiblement avec des paramètres variant dans le temps. Un des principaux challenges dans ce travail consiste à développer des méthodes temporelles, qui se basent sur la construction de fonctionnelles de Lyapunov-Krasovskii strictes, pour les systèmes non-linéaires à retards étudiés.
Les principales notions abordées dans ces travaux incluent : l'analyse de stabilité/stabilisation et de robustesse, l'emploi de techniques de modélisation des populations cellulaires saines et malades, l'étude de différentes classes de systèmes dynamiques, (possiblement à temps variant ou à commutation), et également l'introduction de quelques outils issus de l'intelligence artificielle (planification et recherche de solution) dans un contexte de modèles biologiques.
Ainsi, les méthodes de modélisation et d'analyse employées dans ce travail ont permis d'une part d'étendre les résultats de stabilité de cette classe de systèmes biologiques, et d'autre part de mieux comprendre certains mécanismes biologiques liés au cancer et sa thérapie. Plus précisément, certains concepts récemment établis en biologie et en médecine sont mis en évidence dans ce travail pour la première fois dans cette classe de systèmes, telles que : la dédifférenciation des cellules (plasticité), ou encore la dormance des cellules cancéreuses dans des modèles tenant compte de la cohabitation entre cellules saines et mutées. Les résultats obtenus sont interprétés dans le cas de l'hématopoïèse et de la LAM, mais ce travail s'applique également à d'autres types de tissus où le cycle cellulaire se produit de façon similaire.

Title : Understanding Cell Dynamics in Cancer from Control and Mathematical Biology Standpoints: Particular Insights into the Modeling and Analysis Aspects in Hematopoietic Systems and Leukemia

Keywords: Modeling, Stability, Time-delay systems, Lyapunov theory, Cancer, Cell cycle

Abstract : The thesis deals with the modeling and analysis issues of (cancer) cell population dynamics, with particular insights on the process of blood cell formation and acute myeloid leukemia (AML). Models are described through some age-structured partial differential equations, which are suitably reduced to nonlinear time-delay systems of different types (with pointwise or finite and infinite distributed delays, possibly involving time-varying parameters, and coupled to difference equations). Thus, this work provides analysis tools for stability and control, mainly of the class of retarded functional differential equations, coupled with continuous time difference equations. The main contribution relies on the stability analysis of the different (biologically) meaningful steady states of the resulting systems. Thus, whether for healthy or unhealthy (e.g. leukemic) cases, the studied models are investigated through time-domain analysis tools.
More precisely, stability properties of the steady states of interest are provided by means of sophisticated strict Lyapunov-like functionals, suitable for the studied models. At any step, insights and medical interpretations of the theoretical results, in light of cancer evolution, are provided. In addition, recent biological and medical evidences on cancer are introduced in the class of systems studied here. This is the case of cell plasticity phenomena and cancer dormancy in models taking into account cohabitation between ordinary and mutated stem cells. Thus, through suitable theoretical studies, it becomes possible to provide a better understanding of the complex mechanisms behind the triggering of some pathological disorders, such as AML. The ultimate aim behind these (stability) studies is to finally suggest some suitable optimized strategies in order to improve cancer treatment through selective combined drug infusions.

Université Paris-Saclay
Espace Technologique / Immeuble Discovery
Route de l'Orme aux Merisiers RD 128 / 91190 Saint-Aubin, France

À mon père, à qui je souhaite un prompt rétablissement.

Rien n'aurait pu se faire sans l'aide, le soutien et les encouragements de ceux qui m'aiment. Du fond de mon cœur, je vous dis Merci !

Mes remerciements vont particulièrement à mes encadrants, avec qui j'ai partagé tant de moments enrichissants, ainsi qu'aux membres du jury qui m'ont honoré par leur présence. Je n'oublie pas toutes les belles rencontres, les collègues et les amis que j'ai pu me faire durant cette période.

Résumé en français des travaux de thèse de Walid Djema.

Titre : « Modélisation et analyse de stabilité des dynamiques de populations cellulaires cancéreuses: applications au cas de l'hématopoïèse et de la leucémie aiguë myéloblastique »

Titre originel en anglais: «*Understanding Cell Dynamics in Cancer from Control and Mathematical Biology Standpoints: Particular Insights into the Modeling and Analysis Aspects in Hematopoietic Systems and Leukemia* »

Les mathématiques appliquées en biologie et en médecine connaissent actuellement un essor sans précédent, à la fois dans la description, la compréhension et la maîtrise du monde du vivant. En effet, la modélisation des systèmes biologiques complexes vise à contrôler ces processus, à valider des observations ou des données médicales, ainsi qu'à prédire le comportement de ces systèmes dans diverses situations (il s'agit par exemple d'anticiper l'effet de certaines thérapies en se basant sur des modèles mathématiques et sur des simulations).

L'analyse mathématique du cas du cancer, parmi une multitude de désordres qui touchent les organismes et tissus vivants, est d'une importance capitale pour deux raisons principales : d'une part la gravité et l'agressivité de cette maladie qui s'étend à tous les organismes et les tissus, de toutes les tranches d'âge, etc., et d'autre part, la complexité des mécanismes déclencheurs, des évolutions et des stades de maladie, ainsi que des traitements appliqués (chirurgie, médicaments ciblés, chimiothérapie, radiothérapie, etc.). D'autant plus que plusieurs éléments intervenant dans le cancer, comme les mutations génétiques et/ou épi-génétiques ou la résistance aux traitements, rendent ce phénomène biologique encore plus difficile à élucider. Par conséquent, les biologistes et les médecins font appel à la modélisation et l'analyse mathématique à chaque fois que l'intuition et les observations ne suffisent plus à comprendre les interactions entre les mécanismes majeurs qui déclenchent le cancer puis favorisent son évolution. Certaines de ces notions clés, relatives au cancer, seront abordées dans le cadre de ces travaux de thèse. Ainsi, par exemple, un modèle tenant compte de la coexistence entre des cellules souches saines et des cellules mutées est introduit et analysé[1]. Ce dernier décrit la dynamique de ces populations cellulaires saines et cancéreuses avec, comme objectif thérapeutique principal, le maintien en dormance des cellules cancéreuses. Ce modèle introduit et aborde également un aspect du rôle – parfois ambigu – du système immunitaire dans le déclenchement du cancer et le maintien en dormance des cellules tumorales.

[1] **Djema, W.**, Bonnet, C., Mazenc, F., Clairambault, J., Fridman, E., Hirsch, P. and Delhommeau, F., "***Control in Dormancy or Eradication of Cancer Stem Cells: Mathematical Modeling and Stability Issues***". *Journal of theoretical biology (JTB)*. 2018.

Plus généralement, les problématiques abordées dans ces travaux de thèse concernent la modélisation et l'analyse du cycle cellulaire, incluant une phase de quiescence. Nous nous focalisons particulièrement sur le cas de l'hématopoïèse – qui est le processus de fabrication et de régénération continue de toutes les cellules sanguines – et de la leucémie aiguë myéloblastique. En effet, l'hématopoïèse est considérée en biologie et en médecine comme un paradigme pour l'analyse du cycle cellulaire, et particulièrement quand il s'agit du processus de différenciation cellulaire. À noter également que les *Cancer Stem Cells (CSCs)* ont été identifiées pour la première fois dans le cas de la leucémie aiguë myéloblastique. Les paramètres biologiques qui interviennent de façon récurrente dans ce type de modèles représentent les fonctionnalités biologiques telles que la différenciation cellulaire, l'apoptose (ou la mort programmée des cellules), l'auto-renouvellement cellulaire et la prolifération cellulaire (voir l'***Introduction*** de la thèse, le chapitre ***A Glimpe into Biology***, ainsi que les travaux pionniers de Mackey et d'Adimy dans ce domaine). Nous nous focalisons sur les propriétés de stabilité des systèmes – ou des modèles – résultants puisque leurs trajectoires représentent l'évolution de différentes densités cellulaires, et leurs comportements reflètent les situations saines ou malades d'intérêt médical. Par conséquent, nous continuons dans le cadre de ces travaux de thèse l'effort d'amélioration des modèles mathématiques de dynamique de populations cellulaires déjà existants, ainsi que leur analyse de stabilité[2]. Nous introduisons également de nouveaux modèles qui tiennent compte d'observations biologiques récentes, qui n'ont pas été abordées précédemment dans la classe de systèmes qui nous intéressent, telles que la dédifférenciation et la transdifférenciation cellulaires (*cell plasticity*[3]), le blocage d'une minorité de cellules durant la mitose (*cell-cycle arrest*), la dormance des cellules cancéreuses, ou encore le rôle que pourrait avoir le système immunitaire dans le maintien du phénomène de dormance du cancer (*immunoediting*).

Les modèles mathématiques que nous étudions sont des modèles déterministes (par opposition aux modèles stochastiques), qui se décrivent par des équations aux dérivées partielles (EDPs) structurées en âge (l'âge étant la durée ou le temps que passent les cellules soit dans le compartiment de prolifération soit dans celui de quiescence ; voir les modèles de Mackey et d'Adimy pour plus de détails). Ces modèles se réduisent par la suite à des systèmes à retards de différents types, en appliquant la méthode dite des caractéristiques. Ainsi, nous allons étudier tout au long de cette thèse des systèmes non-linéaires à retards distribués à supports finis et infinis, des retards ponctuels et des systèmes non-linéaires à retards couplés à des équations aux différences (*differential-difference systems*). Certains de ces modèles peuvent avoir des paramètres variant dans le temps. C'est le cas par exemple lorsque des paramètres de taux d'apoptose et de différenciation varient sous l'effet de la maladie (le blocage de la différenciation est une caractéristique de la leucémie aiguë myéloide) ou des thérapies possiblement appliquées. Des perturbations additives non-nulles peuvent aussi être considérées dans nos modèles, afin de représenter certains phénomènes biologiques non-modélisés explicitement ou bien le manque d'exactitude dans les modèles résultants. Nous abordons également au dernier chapitre de la thèse la question de

---

[2] **Djema, W.**, Mazenc, F. and Bonnet, C., **"Stability analysis and robustness results for a nonlinear system with distributed delays describing hematopoiesis".** *Systems & Control Letters*, 2017.

[3] **Djema, W.**, Bonnet, C., Mazenc, F., Clairambault, J., **"Introducing Cell-Plasticity Mechanisms into a Class of Cell Population Dynamical Systems".** *American Control Conference (ACC), IEEE*, 2018.

l'effet de certaines injections de médicaments ciblés ou de sécrétions de facteurs de croissance, qui agissent sur les différents paramètres biologiques de nos modèles, dans un système où les paramètres peuvent commuter entre plusieurs valeurs discrètes.

Dans notre étude de stabilité, nous allons nous consacrer à l'application d'approches d'analyse de stabilité dans le domaine temporel, et plus précisément aux techniques issues de la théorie de Lyapunov pour les systèmes non-linéaires et à temps variant. Nous rappelons dans ce résumé que l'aspect héréditaire des systèmes à retards, qui les rend de dimension infinie, complique leur analyse de stabilité et de stabilisation. Cependant, l'extension de la théorie classique de Lyapunov, à savoir précisément les théorèmes de Lyapunov-Krasovskii et de Lyapunov-Razumikhin, ont permis l'analyse d'une plus grande classe de systèmes dynamiques à retards. Par contre, la difficulté majeure qui est classiquement rencontrée lors de l'analyse des systèmes non-linéaires, avec ou sans retards, se trouve dans le fait qu'aucune méthode systématique n'existe pour la construction de fonctionnelles de Lyapunov-Krasovkii appropriées pour les systèmes à analyser. Par conséquent, une contribution fondamentale apportée par ces travaux de thèse, réside dans les différents types de fonctionnelles de Lyapunov-Krasovskii que nous proposons pour l'étude de nos modèles biologiques présentant des retards de différentes natures. Nous utilisons parfois des approches d'analyse basées sur la nature du système à étudier, qui est un système positif (*positive and compartmental systems*), pour la construction de fonctionnelles de Lyapunov-Krasovskii appropriées. Nous rappelons également que même lorsqu'un équilibre est connu pour être asymptotiquement stable, il est toujours important de chercher à construire une fonction/fonctionnelle de Lyapunov pour le système en question, vu les multiples avantages qui en découlent (stabilité exponentielle, estimation du taux de convergence des solutions, analyse de robustesse de type *Input-to-State Stability (ISS)*, etc., voir Section 3.3 de la thèse). Les résultats de stabilité, et de robustesse par rapport aux perturbations, qui ont été ainsi obtenus sont largement commentés, d'un point de vue biologique et médical, et différentes illustrations numériques sont présentées tout au long de la thèse.

L'objectif principal de ce travail de thèse est donc de consolider nos connaissances en matière de modélisation et d'analyse de stabilité des dynamiques de populations cellulaires cancéreuses. Pour ce faire, nous avons tenu compte des observations les plus récentes concernant les origines des *cancer stem cells*, ou plus exactement de la « souchitude » (*stemness*) qui caractérise les cellules cancéreuses, incluant l'option de dormance dans le cancer, ainsi que le rôle du système immunitaire dans ce mécanisme de dormance, et l'option de dédifférenciation cellulaire. Nous avons également évoqué les thérapies actuelles et émergentes dans le cas de la leucémie aiguë myéloïde. Ainsi, nous avons d'une part mis en évidence plusieurs phénomènes biologiques, liés au cancer, dans la classe de systèmes que nous étudions, et d'autre part, nous avons utilisé plus d'outils mathématiques pour l'analyse de stabilité des systèmes résultants. Par ailleurs, nous avons proposé une solution algorithmique originale – dans le dernier chapitre de la thèse – pour ce qui pourrait s'apparenter à une technique de stabilisation de densités cellulaires par perfusion médicamenteuse. Cette dernière approche s'inspire des techniques de planification stratégique (*pathfinding algorithms*), largement utilisées dans le domaine de l'intelligence artificielle.

Understanding Cell Dynamics in Cancer from Control and Mathematical Biology Standpoints

Particular Insights into the Modeling and Analysis Aspects in Hematopoietic Systems and Leukemia

Walid Djema

Jury members: Mostafa Adimy **(referee)**
Catherine Bonnet **(supervisor)**
Jean Clairambault **(supervisor)**
Raphaël Itzykson **(examiner)**
Françoise Lamnabhi-Lagarrigue **(examiner)**
Frédéric Mazenc **(supervisor)**
Alexandre Medvedev **(examiner)**
Pierdomenico Pepe **(referee)**

French Institute for Research in Computer Science and Automation (Inria)
CentraleSupélec, Laboratory of Signal and Systems (L2S)
University Paris-Sud, University Paris-Saclay

This dissertation is submitted for the degree of
Ph.D. in Control Engineering and Mathematical Biology

November 2017

Table of contents

Chapter 1

Introduction

Applied mathematics have an impressive success in describing the natural word. Modeling complex systems is essential for many practical reasons, including system understanding, control and validation, prediction and behavior anticipation. For biologic phenomena, mathematics have been used for describing/modeling dynamical processes during centuries. Related fields as epidemiology and ecology have also attracted a great mathematical interest which continues to grow (see [211, 210]). Early biological models were basically investigating the way populations grow or decline over time [19]. In more recent years, the greatest objectives of mathematical modeling and simulation techniques consist in providing ways of better understanding the underlying mechanisms of grave diseases. For instance, Dale & Mackey traced recently in [71] their mathematical modeling and analysis work, during four decades, to understand and treat the periodic hematological disease known as *cyclical neutropenia (CN)*.

Some other successful biomathematical applications are discussed in [182]. We can mention for instance the study of the dynamics of molecular regulatory networks that monitor eukaryotic cells during their cell cycle [287], the mathematical analysis of neuro-oncology and cell proliferation in neuro-tumors [143], and also the mathematical analysis of plaque formation in atherosclerosis, as well as their regression under different therapeutic strategies [109].

Mathematics is biology's next microscope, only better; biology is mathematics' next physics, only better (J.E. Cohen, 2004, [65]).

«Although mathematics has long been intertwined with the biological sciences, an explosive synergy between biology and mathematics seems poised to enrich and extend both fields greatly in the coming decades. Biology will increasingly stimulate the creation of qualitatively new realms of mathematics. Why? In biology, ensemble properties emerge at each level of organization from the interactions of heterogeneous biological units at that level and at lower and higher levels of organization (larger and smaller physical scales, faster and slower temporal scales). New mathematics will be required to cope with these ensemble properties and with the heterogeneity of the biological units that compose ensembles at each level. Mathematics will benefit increasingly from its involvement with biology, just as mathematics has already benefited and will continue to benefit from its historic involvement with physical problems. In classical times, physics, as first an applied then a basic science, stimulated enormous advances in mathematics. In the coming century, biology will stimulate the creation of entirely new realms of mathematics. In this sense, biology is mathematics's next physics, only better. Biology will stimulate fundamentally new mathematics because living nature is qualitatively more heterogeneous than non-living nature» (J.E. Cohen, 2004, [65]).

In the modern era, cancer is one of the most devastating causes of morbidity and mortality all over the world [29]. Through modeling, analysis and simulation tools, mathematical biology is involved in cancer understanding, and particularly in the study of cell population growth. In fact, the main objective of multi-disciplinary cancer research is the development of efficient anti-tumor therapeutic strategies, and for that, the input provided by mathematical studies are required. For instance, cancer-triggering mechanisms, along with all the complications that follow this disease (such as drug resistance, mutation accrual, etc.), are highly complex phenomena that cannot be easily understood, and for which mathematical tools are becoming increasingly necessary. This is already the case in hematology (e.g. [189, 240, 59, 182]), and in various other biological fields (e.g. [249, 154, 287, 234, 211, 210]).

Hematopoiesis - the process of blood cell formation - provides a model for studying and understanding all the mammalian stem cells and their niches [209], as well as all the mechanisms involved in the cell cycle and particularly in cell differentiation. The hematopoietic paradigm is in fact already used in biology and medicine, as well as in mathematical modeling and analysis of living organisms. In [240], L. Pujo-Menjouet reviewed the mathematical modeling of blood cell dynamics, along with some related pathological disorders, during the past five decades. It is within this framework that we situate our work, as a continuity of modeling and stability analysis of blood cell dynamics. As for the majority of works discussed in [240], the models that we study can be extended to cover other tissues and mechanisms, even if they follow a long line of work that has much more focused on the hematopoietic system. However, at this point, it is worth mentioning that pioneering works that introduced early blood cell dynamical models have been formulated for any type of cells [268], or they were borrowed from models describing other tissues (see, e.g., [49] for a dorsal epidermis cell model that inspired all the cell cycle models containing a resting phase). Concretely, medical research is looking for new combined targeted therapies able to overcome the challenge of cancer cells overproliferation, to restore apoptosis mechanisms and normal differentiation of immature cells, and also to avoid the high toxicity effects that characterize heavy non-selective (chemo)therapy. In that quest, the ultimate goal behind mathematical studies is to provide some inputs that should help biologists to suggest and test new treatments, and to contribute within multi-disciplinary groups in the opening of new perspectives against cancer. Our research project is imbued within a similar spirit and fits the expectations of a better understanding of the behavior of healthy and unhealthy blood cell dynamics. It involve intensive collaboration with hematologists from *Hôpital Saint-Antoine* in Paris, and aims to analyze the cell fate evolution in treated or untreated leukemia, allowing for the suggestion of new anti-leukemic combined chemotherapy. In a fairly general way, we discuss in this dissertation some issues that are related to the modeling of the cell cycle, with a particular insight into hematopoietic systems. Stability features of mathematical models are highlighted, since systems' trajectories reflect the most prominent healthy or unhealthy behaviors of the biologic processes under study. We indeed perform stability analysis of systems describing healthy and unhealthy situations, particularly in the case of acute myeloblastic leukemia (AML). We pursue the objectives of earlier works in order to understand the interactions between the various parameters and functions involved in the studied mechanisms. We extend sometimes the stability analysis and the application of some already existing models, whereas news models and variants are other times introduced, to cover novel biological evidences such as: mutations accumulation, cohabitation between ordinary and mutated cells in niches ([137]), control in dormancy and eradication of cancer stem cells, cancer dormancy ([93, 102]) and cellular

plasticity ([301, 52]). The content of the thesis is developed in the last section of the introduction, but before that, we briefly give a glimpse into Mackey-type models of cell dynamics and Lyapunov concept for stability analysis.

Population dynamical models

Some of the classical issues that drive mathematical population models are listed in [19] as follows: «*Why do populations sometimes grow and sometimes decline? Must populations grow to such a point that they are unsustainably large and then die out? If not, must a population reach some equilibrium? If an equilibrium exists, what factors are responsible for it? Is such an equilibrium so delicate that any disruption might end it? What determines whether a given population follows one of these courses or another?*» [19]. Some early models have been proposed to address such questions, as the Malthusian model (introduced in 1798, see [188]), Verhulst logistic model (introduced in 1845, see e.g. [284]), and their variants. Since then, more sophisticated populations models have emerged, starting from the pioneer works of Sharpe and Lotka (in 1911, see [262]) and McKendrick (in 1925, [205]) which introduced partial differential equations (PDE) based modeling framework. Thus, a new area of age-structured cell populations (and, similarly, of size or any phenotype-structured populations) has been extensively developed ([22]).

Age-structured population models

Definition 1. *«A structured population model is a model of population dynamics where the state variable, the variable which at each time t characterizes a given population, is a distribution of the individuals over a set of values, each individual being associated, at each time t, to one and only one value. As examples, let us quote age-structured models where each individual is characterized by its age. All the individuals who, at a given time t, have the same age determine what is known as an age-cohort. Other characters of an individual can be the size, the weight, or the quantity of a certain product» (Arino, 1995 [21]).*

The first age-structured model (applied in demography in 1911, by Sharpe and Lotka [262])

We consider that $p(t,a)$ is the population density at time t and of age a. The evolution of p is governed by the following PDE:

$$\frac{\partial p(t,a)}{\partial t} + \frac{\partial p(t,a)}{\partial a} = -d(a)p(t,a), \tag{1.1}$$

where $d(a)$ is the death rate at age a, per unit of individual. The age a is the structure variable in the model (1.1). The number of newborn at time $t \geq 0$ is given by the **renewal equation**:

$$p(t,0) = \int_0^{+\infty} b(a)p(t,a)da, \tag{1.2}$$

where $b(a)$ is the birth rate. For each $t \geq 0$, the function $p(t,\cdot)$ is a density function. The quantity $\int_{\underline{a}}^{\overline{a}} p(t,a)da$ gives the total number of alive individuals within the population at time $t \geq 0$, whose age lies in $(\underline{a},\overline{a})$. Overall, it has to be noted that rigorous mathematical analysis of the fundamental linear age-structured systems has been based on Volterra theory and it was developed many years later (e.g., Bellman & Cooke, 1961, [32]).

Mackey's model for hematopoietic stem cells (HSCs) in 1978, [180]

Burns & Tannock proposed in 1970 an ODE model with delay to describe the cell cycle involving a quiescent phase G_0 [49]. Few years later, an age-structed model describing the population cell dynamics in hematopoiesis was introduced by Mackey [180]. In this system, $r(t,a)$ represents the density of quiescent cells at time $t \geq 0$ and age $a \geq 0$, and $\lim_{a\to+\infty} r(t,a) = 0$ for all $t \geq 0$, while $p(t,a)$ represents the density of proliferating cells (i.e. active in the cell cycle) at time $t \geq 0$ and age $a \in [0,\tau]$, where $\tau > 0$ is a finite age limit (i.e. assumed to be the average duration of the cell cycle, in days). Evolution of $r(t,a)$ and $p(t,a)$ are described by the following PDE-model:

$$\begin{cases} \frac{\partial}{\partial t} r(t,a) + \frac{\partial}{\partial a} r(t,a) = -\big(\delta + \beta(R(t))\big)\, p(t,a), \quad t > 0,\ a > 0, \\ \frac{\partial}{\partial t} p(t,a) + \frac{\partial}{\partial a} p(t,a) = -\gamma p(t,a), \quad t > 0,\ 0 < a < \tau, \end{cases} \tag{1.3}$$

where δ is the degradation rate of resting cells (in day^{-1}) and γ is the programmed cell death rate (apoptosis rate in day^{-1}). The function β is the re-introduction function from resting to proliferating phases, which has been considered in the form of a Hill function [180]:

$$\beta(\ell) = \frac{\beta_0 \theta^\alpha}{\theta^\alpha + \ell^\alpha}, \text{ where, } \beta_0 > 0,\ \theta > 0, \text{ and, } \alpha > 1. \tag{1.4}$$

The total density of resting cells is defined by: $R(t) = \int_0^\infty r(t,a)da$, and, similarly, the total density of proliferating cells is defined by: $P(t) = \int_0^\tau p(t,a)da$. The boundary conditions associated to (1.3) give the new births for $t > 0$:

$$\begin{cases} r(t,0) = 2p(t,\tau), \\ p(t,0) = \int_0^{+\infty} \beta(R(t)) r(t,a) da = \beta(R(t)) R(t). \end{cases} \tag{1.5}$$

The system is completed by adequate initial conditions (at time $t = 0$) which are L^1-functions denoted by $n(0,a) = n_0(a)$ and $p(0,a) = p_0(a)$. Using the classical method of characteristics (see in particular [31] and [101]), Mackey's model [180] is rewritten for sufficiently large $t > 0$ as:

$$\begin{cases} \dot{R}(t) = -\big(\delta + \beta(R(t))\big) R(t) + 2e^{-\delta\gamma} \beta(R(t-\tau)) R(t-\tau), \\ \dot{P}(t) = -\gamma P(t) + \beta(R(t)) R(t) - e^{-\delta\gamma} \beta(R(t-\tau)) R(t-\tau). \end{cases} \tag{1.6}$$

Since then, and for many decades, several versions of Mackey's model have emerged. The reader is referred again to the recent paper by L. Pujo-Menjouet (2016, [240]) for a review on hematological modeling. Here we mention some variants of Mackey's model that are also considered in this thesis:

❍ The models of J. Bélair, M. Mackey, and J. Mahaffy, in 1995 [31] and in 1998 [185], F. Billy *et al.* in 2012 [39], and M. Adimy and F. Crauste in 2009 [7], where growth-factor dependent biological parameters have been considered.

❍ The model of M. Adimy, F. Crauste and A. El Abdllaoui in 2008 [8], where several discrete maturity stages have been introduced (see also A. Marciniak-Czochra, *et al.* in 2009 [189] for an ODE model with several maturity stages).

❍ The model of M. Adimy, A. Chekroun and T. Touaoula in 2015 [4], where a recent fast-self renewing mechanism has been considered.

Modeling cell population dynamics through time-delay systems

Mackey's model in (1.6) leads us to consider hematopoiesis models through time-delay systems. In fact, in order to go even further than the case of hematopoiesis, we emphasize that delay systems is a major class of dynamical systems in biology and in many other fields (e.g. chemistry, economics, mechanics, sensors and field network [251]). However, the particularity of delays in biological systems is that they often result from maturation and proliferation processes which take a large time that cannot be neglected. Delays may be source of stability or, more often, of instability [218]. Thus, since delays lead to changes of stability properties in dynamical systems, it becomes essential to develop adequate tools for the analysis of time-delay biological systems. The theory of time-delay systems is now a vast area, and has continued to grow strongly during the last two decades (see e.g. [251, 120, 106, 219, 30, 222, 266, 16, 192], to name only a few). Many time-delay models have been developed in the literature to study hematopoietic systems and all their related pathological disorders (see the review in [101]). For instance, we mention the following contributions:

❍ S. Bernard *et al.* in 2003 [37] studied a model with constant point delays in cyclical neutropenia.

❍ C. Haurie *et al.* in 2000 [133] studied a model with distributed delay for the peripheral regulation of neutrophil production mediated by granulocyte colony-stimulating factor.

❍ J. Mahaffy *et al.* in 1998 [185] studied a model with state-dependent delay for erythropoiesis -the process of red blood cell formation- involving growth factor dynamics.

❍ M. Adimy *et al.* in 2015 [4] studied a differential-difference (i.e. a differential system coupled to an algebraic equation) model for overproliferating blood disorders.

We point out that many ODE-based models have been developed in the literature to describe hematopoiesis (see for instance [275] and [189]). In other cases, ODE-based representations have been used instead of some classical delay systems, even if delays appear by nature (to model the duration of the cell cycle or maturation) in hematopoietic systems as the adequate modeling approach (see Section 3.2 of [101]). Clearly, this modeling simplification aims to reduce the difficulty of analysis that generally characterizes infinite-dimensional systems. However, for technical details, reducing the model into ODEs is not always possible for hematopoietic models (see [101]); this is for instance the case of the white blood cell formation model studied in [135]. Thus, ODE-based models of hematopoiesis are beyond the scope of our work, where only some age-structured PDEs and time-delay systems are discussed.

Various types of nonlinear time-delay systems modeling cell population dynamics appear throughout this thesis. When cell proliferation is described as a phase in which cells divide with a certain degree of freedom, nonlinear systems with distributed delays are used (e.g. [8]). The length of the distributed delays may be finite (if cells are obliged to die or divide before an age limit), or infinite (if few cells are arrested during their cell cycle - at some checkpoints - and do not die by apoptosis). Models involve discrete delay when the cell division (mitosis) is assumed to occur at a fixed average age for all the proliferating cells. So, with the aim of giving an estimation of the basin of attraction of the steady states of these models, and having in mind the analysis of similar models with time-varying parameters, we have chosen a state-space framework for our study.

Some aspect of the mathematical analysis of cell dynamics in hematopoiesis have not been fully addressed in earlier works. We can mention for instance the analysis of time-varying models, the

investigation of global stability properties of the nonlinear systems, or the estimate of the size of the basin of attraction of steady states. These are in fact common issues in many biological models where some functionalities depend on time (e.g. circadian rhythms) or when they are temporarily affected by therapy (e.g. drug infusion). Also some systems are known to evolve far from their equilibria (e.g. chemostat's models) and a local stability analysis may be insufficient. In the case of hematopoiesis, the biological parameters can be time-varying if affected by the disease (e.g. blockade of differentiation process and apoptosis in leukemia), or by therapies that change the model parameters. In addition, in normal or abnormal hematopoiesis, blood count may temporary deviate or oscillate far from its steady states.

Time-delay systems

Time-delay systems are generally represented in the framework of *functional differential equations (FDEs)*, see for instance [165], [106] and [120].
We denote $\mathscr{C}\left([-\tau,0],\mathbb{R}^n\right)$ the set of continuous functions mapping the interval $[-\tau,0]$ to $\mathbb{R}^n$.
For any $A>0$ and any continuous function of time $u\in\mathscr{C}\left([t_0-\tau,t_0+A],\mathbb{R}^n\right)$, and $t_0\le t\le t_0+A$, we denote by $u_t\in\mathscr{C}$ the segment of the function u defined as:

$$u_t(\theta)=u(t+\theta),\ -\tau\le\theta\le 0. \tag{1.7}$$

Thanks to the notation (1.7), a general form[a] of FDEs is given by:

$$\dot{x}(t)=f(t,x_t), \tag{1.8}$$

where $x(t)\in\mathbb{R}$, $\dot{x}(t)$ is the right-hand derivative of $x(t)$, and $f:\mathbb{R}\times\mathscr{C}\to\mathbb{R}^n$.

❍ The system (1.8) indicates that the derivative of the state variable x at time t depends on t and $x(m)$ for $t-\tau\le m\le t$. Therefore, in order to determine the future evolution of the state, it is necessary to specify the initial state variable in a time interval of length τ, i.e. from $t_0-\tau$ to t_0,

$$x_{t_0}=\phi,\ \text{where } \phi\in\mathscr{C}\left([-\tau,0],\mathbb{R}^n\right)\ \text{is given.} \tag{1.9}$$

The notation (1.9) means that $x(t_0+\theta)=x_{t_0}(\theta)=\phi(\theta),-\tau\le\theta\le 0$.

❍ For a function $\phi\in\mathscr{C}\left([a,b],\mathbb{R}^n\right)$, we define the continuous norm $\|.\|_c$ by

$$\|\phi\|_c=\max_{a\le\theta\le b}\|\phi(\theta)\|. \tag{1.10}$$

❍ The general form of functional differential equations includes the class of **differential-difference systems**, and the class of **systems with distributed delays**, i.e. integro-differential equations (see [165], Chapter 1).

[a] but which does not include the case of neutral functional differential equations.

Control systems and biological models

Remarkably, the powerful techniques of *Control* (for instance, theory of stability and stabilization [158, 292, 187]) have demonstrated innumerable applications in mathematical biology ([211, 210]). This is particularly the case in cancer-related issues, in growth tumors and oncology, but also in neuronal connectivity and cardiovascular systems, as well as in epidemiology and infectious diseases. The complex problems encountered in these fields are nowadays requiring increasingly sophisticated mathematical methods for suitable analysis.

In our case, cell population dynamics are modeled through structured PDEs or time-delay systems, possibly coupled to difference equations. Due to their hereditary feature, time-delay systems are more complicated to handle than finite dynamical systems [164]. However, since the middle of the last century, the extension of the classical theory of Lyapunov to systems with delay, through Lyapunov-Krasovskii and Lyapunov-Razumikhin theorems, have allowed stability analysis of this major class of systems.

Lyapunov stability analysis of time-delay systems

Lyapunov theory offers efficient tools for stability analysis of nonlinear systems. The extension of this theory to the case of time-delay systems has allowed the analysis of a larger class of systems. The advantages of knowing Lyapunov functions or functionals (LKFs) are fundamental in *Control* theory, since they make it possible to estimate rates of convergence of solutions and to establish robustness results of Input-to-State-Stability type [198]. Moreover, LKFs can also be used to determine estimates of the basin of attraction ([126, 119, 114]) of locally asymptotically stable steady states. Unfortunately, the construction of Lyapunov-Krasovskii functionals is sometimes a difficult task since there are no systematic method for dealing with nonlinear systems. This is a difficulty that we face when analyzing models of cell population dynamics. In addition, some technical difficulties may arise when investigating differential-difference models where solutions are not uniformly continuous (since *invariance principles* and *Barbalat's lemma* are not applicable to establish asymptotic stability of solutions). Finally, it is worth mentioning that the resulting biological models of interest belong to the family of *positive* and *compartmental systems* [124]. Therefore, it becomes possible to take advantage of some suitable non-quadratic LKFs (approximated at the origin by linear functionals), that can be used only when systems trajectories are positive [124] (the use of a positive approach in the analysis of dynamical systems appeared first in [55]). These constructions will be often used throughout this thesis.

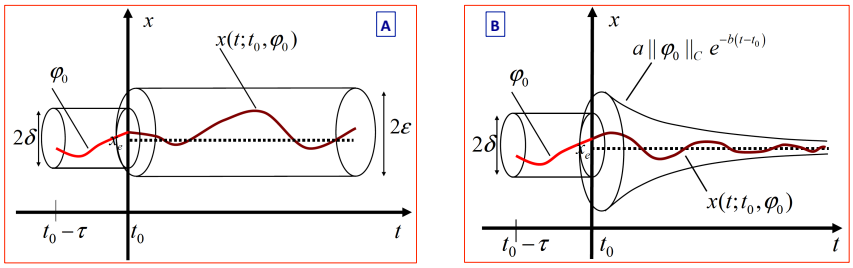

Fig. 1.1 **A**. The equilibrium point denoted x_e is Lyapunov stable, i.e. for *sufficiently small* initial conditions (small perturbations), the trajectories remain *close* to the steady state x_e. **B**. The steady state x_e is locally exponentially stable. These illustrative figures are taken from [304].

Lyapunov-Krasovskii Theorem for stability of time-delay systems

Definition 2. *(Kolmanovskii and Myshkis, 1992 [164]; Hale and Verduyn-Lunel, 1993 [127]). For the system* (1.8)*, the trivial solution $x(t) = 0$ is **stable** if for any $t_0 \in \mathscr{R}$ and any $\varepsilon > 0$, there exists a $\delta = \delta(t_0, \varepsilon) > 0$ such that $\|x_{t_0}\|_c < \delta$ implies $\|x(t)\| < \varepsilon$.*
*It is said to be **asymptotically stable** if it is **stable** and for any $t_0 \in \mathscr{R}$ and any $\varepsilon > 0$, there exists a $\delta_a = \delta_a(t_0, \varepsilon) > 0$ such that $\|x_{t_0}\|_c < \delta_a$ implies $\lim_{t\to\infty} x(t) = 0$.*
*Moreover, it is said to be **exponentially stable** if there exist positive constants a, b and δ such that*

$$\|x_{t_0}\|_c < \delta \Rightarrow \|x(t, t_0, x_{t_0})\| < a\|x_{t_0}\|_c e^{-b(t-t_0)}.$$

*If a, b and δ do not depend on t_0, then the origin is **uniformly exponentially stable**.*

It is generally difficult to establish stability using these definitions. The extension of the Lyapunov theory to systems of infinite dimension offers an alternative way to prove stability. Two approaches have been introduced: Lyapunov-Krasvoskii theorem and Lyapunov-Razumikhin theorem. Lyapynov-Krasovskii functionals (LKFs) are the most recurrent tool in the current work:

Lyapunov-Krasovskii approach (K. Gu, V. Kharitonov and J. Chen, 2003 [120])

«As in the study of systems without delay, an effective method for determining the stability of a time-delay system is the Lyapunov method. For a system without delay, this requires the construction of a Lyapunov function $V(t, x(t))$, which in some sense is a potential measure quantifying the deviation of the state $x(t)$ from the trivial solution 0*. Since for a delay-free system $x(t)$ is needed to specify the system's future evolution beyond t, and since in a time-delay system, the corresponding Lyapunov function be a functional $V(t, x_t)$ depending on x_t, which also should measure the deviation of x_t from the trivial solution* 0*. Such a functional is known as a Lyapunov-Krasovskii functional»*
K. Gu, V. Kharitonov and J. Chen, 2003 [120].

Lyapunov-Krasovskii theorem

Suppose $f : \mathbb{R} \times \mathscr{C}\left([-\tau, 0], \mathbb{R}^n\right) \to \mathbb{R}^n$, and that $u, v, w : \mathbb{R}_+ \to \mathbb{R}_+$ are continuous nondecreasing functions, where additionally $u(s)$ and $v(s)$ are positive for $s > 0$, and $u(0) = v(0) = 0$. If there exists a continuous differentiable functional $V : \mathbb{R} \times \mathscr{C}\left([-\tau, 0], \mathbb{R}^n\right) \to \mathbb{R}$, which is positive definite

$$u(\|\phi(0)\|) \leq V(t, \phi) \leq v(\|\phi\|_c) \tag{1.11}$$

and such that its derivative along (1.8) is non-positive

$$\dot{V}(t, \phi) \leq -w(\|\phi(0)\|), \tag{1.12}$$

then the origin of (1.8) is uniformly stable. If in addition $w(s) > 0$ for $s > 0$, then it is uniformly asymptotically stable. If, in addition, $\lim_{s\to\infty} u(s) = \infty$, then it is globally uniformly asymptotically stable. Finally, if for all $t \geq 0$, $\dot{V}(t, \phi) \leq -\alpha V(t, \phi)$, where $\alpha > 0$, then the origin of the system (1.8) is exponentially stable.

Organization of the thesis

The manuscript is organized as follows:

■ In **Chapter 2**, we give an overview on a number of interesting biological principles. Some of them have recently emerge (e.g. cancer stem cells, dormancy and cell plasticity), and they are currently undergoing intensive biological research. Our aim is to ease the reading of the manuscript, since these notions will be re-evoked throughout the upcoming three parts of the thesis.

❍ **Part I. The class of nonlinear systems with distributed delays.**

■ In **Chapter 3**, we perform a stability analysis of a particular class of nonlinear systems with finite distributed delays, that extends some existing models from the literature ([8], [24]). A key feature of our analysis is that the conceived technique relies on the construction of suitable strict Lyapunov functionals for nonlinear time-delay systems.

■ In **Chapter 4**, we consider a model of proliferation and quiescence in living organisms, where we extend the work of Chapter 3 in two directions:

(a) Firstly, we discuss how to reconcile some earlier modeling ways of the cell cycle in one common framework. Then, accordingly, we consider a model that contains a compartment where cells may be quiescent for an unlimited time, along with a proliferating phase (modeling the cell cycle) in which most of the cells may divide, or die, while few of them may be arrested during their cycle for unlimited time. The resulting system is a nonlinear system with infinite distributed delays, and a Lyapunov technique is developed for the analysis of its origin.

(b) In the second part of the chapter, we consider for the first time some cell plasticity features in the class of systems that we study. As a first step, we are going to discuss some simple cases of cell-plasticity in unhealthy tissues, and we highlight the role that dedifferentiation may play in the survival of cancer cells (this hypothesis is in line with some recent medical observations). The main analysis is performed on a simpler model involving two maturity stages and a dedifferentiation function from progeny to SCs.

❍ **Part II. The class of differential-difference systems**

■ **Chapter 5** is an introductory work which opens up the analysis of a class of hematopoietic systems, described by some differential-difference (or, more generally, *descriptor*) systems, following the work in [4]. More precisely, the study is conducted on a model of stem cell population dynamics introduced in [4], and which admits two equilibrium points: zero, and - under some conditions on the biological parameters - a strictly positive steady state. We revisit the stability properties of the 0-equilibrium by extending the Lyapunov construction of [4], in order to establish global exponential stability of the trajectories. For the strictly positive steady state, the available analysis in [4] is local and is based on the frequency analysis of the characteristic equation associated to the linear approximation of the model. Here we discuss the nonlinear analysis of the positive steady state, in the time-domain framework, going through Lyapunov-like functionals of two types:

First, we test an adaptation of a method recently developed for the analysis of quasi-linear time-varying systems via *Comparative* and *Positive Systems* ([196]). Based on the techniques of [196], [124], [206], we get the advantage of deriving decay conditions for non-positive trajectories of our model, through a linear degenerate Lyapunov functional.

The second approach is more classical, since it is based on a quadratic functional. Sufficient conditions for the regional exponential stability, an estimate of the decay-rate of the solutions, and a subset of the basin of attraction of the positive steady state, are then provided.

■ In **Chapter 6**, an age-structured model describing the coexistence between tumor (or, cancer stem cells) and ordinary stem cells is developed and explored. Firstly, the model is transformed into a nonlinear time-delay system that describes the dynamics of healthy cells, coupled to a nonlinear differential-difference system governing the dynamics of unhealthy cells. These model generalizes some early coupled systems of hematopoiesis ([23], [26]).

The main features of the resulting model are highlighted and an advanced stability analysis of several coexisting steady states is performed, through a Lyapunov-like approach for descriptor-type systems.

We pursue an analysis that provides a theoretical treatment framework following different medical orientations, among which:

i) the case where therapy aims to eradicate cancer cells while preserving healthy cells,

ii) a less demanding, more realistic, scenario that consists in maintaining healthy and unhealthy cells in a controlled stable steady-state (cancer dormancy).

Biological interpretations and therapeutic strategies are discussed according to our findings throughout this chapter. Notice that a more recent version of this chapter **(mainly focused on the role of the immune system in cancer dormancy)** is provided in the (updated) journal version of this work (see [77]).

❍ **Part III. Nonlinear systems involving growth factors and drugs**

■ In **Chapter 7**, we discuss some issues related to the role of growth-factors and drugs in hematopoietic systems. This is a step-forward in refining the modeling aspects presented in the previous chapters. First, we propose a description of cell proliferation and quiescence, where almost all the involved parameters and functions are affected by multiple growth-factor concentrations. We interpret the resulting system as a possibly switching one. Event-triggered mechanisms in our system may result from drug infusions or from practical situations where the body requires to adapt efficiently its blood cell count (e.g. for combating an infection). The key point consists in the formulation of what can be interpreted as *stabilization* issue -in our context- through artificial intelligence planning tools. In that framework, an optimal solution is discovered via planning and scheduling algorithms. For unhealthy hematopoiesis, we address the treatment issue through multiple drug infusions. In that case, we determine the *best* therapeutic strategy that restore an ordinary hematopoietic system. We claim that a large spectrum of applications of our method can be envisaged. For instance, healthy hematopoiesis can be considered as an *intelligent agent*, able to set objectives -that correspond to body requirements- and to achieve them in an optimal way. Biological interpretations and numerical simulations are provided throughout the chapter.

Finally, a general conclusion, along with some perspectives, are outlined at the end of the thesis.

Chapter 2

A Glimpse into Biology

2.1 The cell-division cycle in living organisms

Cells are the fundamental units of life and the *building blocks* of all the living organisms. Eukaryotic cells (these are cells with nucleus) that engage in the division process (i.e. *cell-division cycle*, [131]) usually undergo a series of transformations and a mechanism of nuclear division (*mitosis*), that ends with a division of each engaged cell (*cytokinesis*, [208]). Figure 2.1 illustrates the cell-division process of a single mother cell that divides into two daughter cells. Many processes are in fact involved in the cell-division mechanism, as well as in the several sequential maturation and differentiation stages of cells. These biological and physiological phenomena frequently occur in the human body, and particularly in quickly dividing tissues such as skin and bone marrow. Basically, the repetition of cell-division cycle processes leads to the growth of tissues in all the multicellular organisms.

Definition 3. *«Actively dividing eukaryote cells pass through a series of stages known collectively as the **cell cycle**, formed by two gap phases (G_1 and G_2), a synthesis phase S, in which the genetic material is duplicated, and a mitosis phase M, in which mitosis partitions the genetic material and the cell divides (cytokinesis)»*[1]*. The main events that occur during the phases G_1, S, G_2, and M, of the cell cycle (Figure 2.1-**(A)**) are discussed in a chronological order in the next section.*

2.1.1 An overview of the main steps defining the eukaryote cell cycle

We provide some basic definitions of the cell cycle phases, that are sufficient for the thesis context. The interested reader may refer - for instance - to [208] for more information.

❍ ***G_1* phase:** The cell cycle starts from the interphase G_1, which is also known as the growth phase. It covers the period from the last cell mitosis until the beginning of the DNA replication. Many enzymes, essential to S phase, are formed during G_1. The G_1 phase is also characterized by a highly variable duration, even for cells belonging to the same species.

❍ ***S* phase:** After G_1, each mother-dividing cell starts a process of DNA replication, which marks the beginning of the synthetic phase S. Each chromosome has two sister chromatids at the end of the S phase, i.e. the amount of DNA inside the mother-dividing cell is doubled.

[1] From *The Cell Cycle, Mitosis and Meiosis*, The official website of the Leicester University. `https://le.ac.uk/`

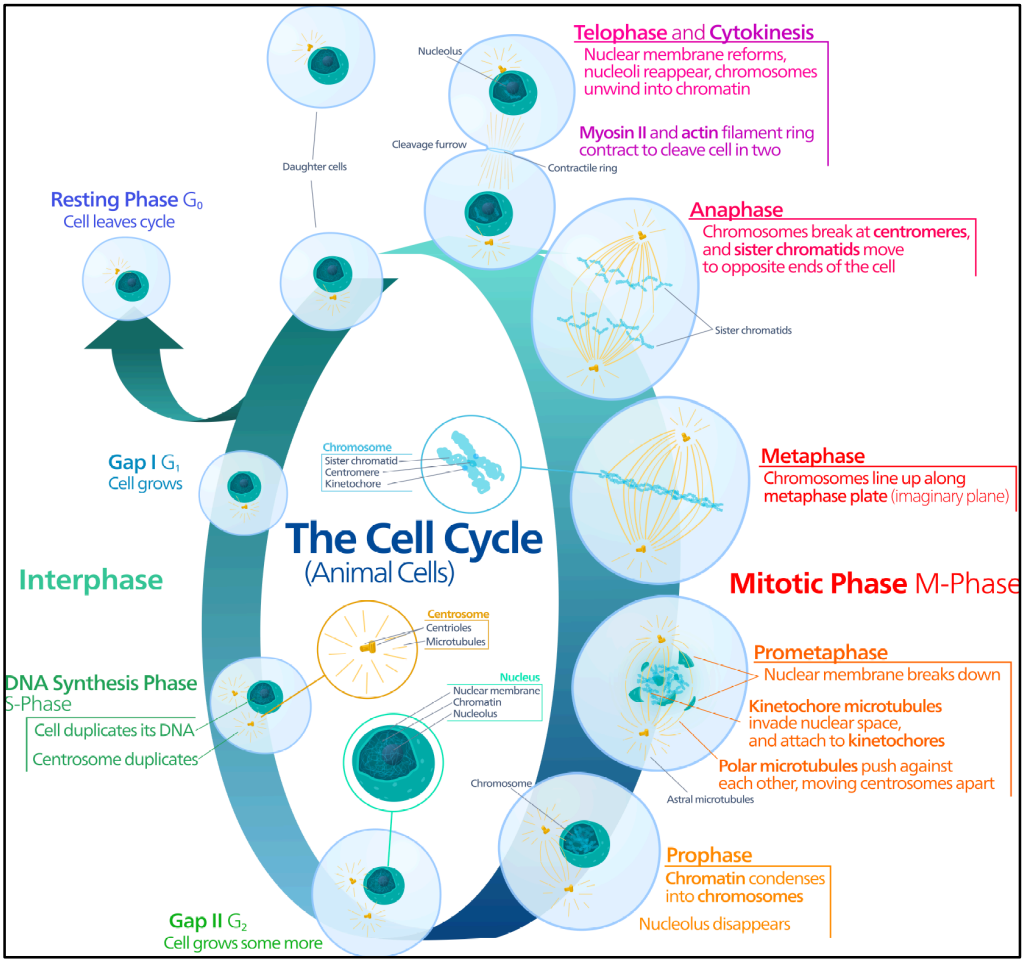

Fig. 2.1 The main steps and events in the (animal) cell cycle process, and a resting phase G_0.

❍ ***G_2* phase:** Eukaryotic cells enter a gap phase G_2, right after the S phase, where a series of events occurs to prepare the mitosis phase M. For instance, the production of many microtubules (required for the mitosis process) is performed during the G_2 phase. The overall process bringing together G_1, S, and G_2, i.e. the period of the cell cycle that precedes mitosis, is known as the *interphase*.

❍ ***M* phase:** Mitosis is the process by which the mother cell separates the chromosomes in its nucleus into two identical (in the general case, even if asymmetric cell division also exists) sets in two separated nuclei. The M phase is actually composed of several subphases, the last one is cytokinesis, which divides the nuclei, cytoplasm, organelles and cell membrane into two completely separated daughter cells.

Remark 1. *Even in fast-renewing tissues such as gut, bone marrow, and skin, cells are not always proliferating, but on the contrary, most of them are in a non-proliferating state, called resting or quiescent phase, G_0 [208]. The quiescent phase G_0 is indicated in Figure 2.1-(**A**) (and also in Figure 2.2), where cells stopped dividing and left the cell-division cycle.*

2.1.2 Checkpoints, principle of control of the cell cycle

Some well-defined checkpoints are used by the body to control the mother cells during their cycle. These checkpoints regroup a set of regulatory proteins that monitor and control the overall progression of cells through the different cell-cycle stages. More precisely, if some requirements are not fulfilled at specific moments, a proteins network takes over the issue by preventing the cell progression through the cycle. Consequently, abnormal cells (e.g. with damaged DNA) cannot move forward in the division process, i.e. cell arrest, where they are obliged to undergo DNA repair, or they are doomed to die by apoptosis.

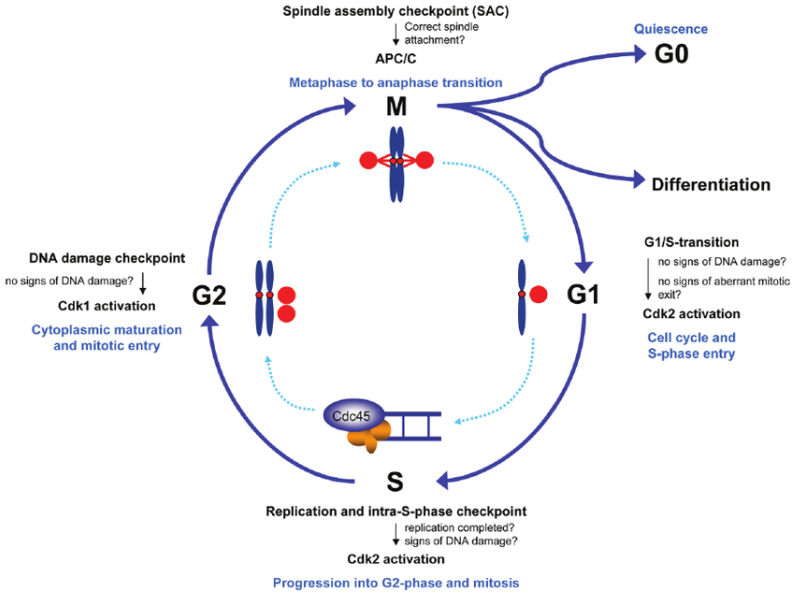

Fig. 2.2 Cells go through the cycle in an unidirectional manner, where they cannot enter the next phase in the cell cycle until all the transition exigences of the previous one are satisfied. Thus, the cycle progression is restricted to the cells fulfilling specific requirements, necessary for the formation of healthy tissues. The figure is from [260].

There are three main checkpoints (G_1/S, G_2/M, and the metaphase checkpoints) that ensure that damaged DNA is not passed on to daughter cells (see Figure 2.2). We can briefly mention that:

❍ ***G_1/S* checkpoint** is a transition and a kind of rate-limiting checkpoint in the cell-division cycle. In this stage (Figure 2.2), the mother-dividing cell checks whether it has enough materials to successfully replicate its DNA. All unhealthy and/or malnourished cells are arrested at this checkpoint.

❍ ***G_2/M* checkpoint** represents a transition step where the cell ensures that it has enough cytoplasm and phospholipids to form two daughter cells. It is also the stage where the cell checks if it is the right time to replicate. Inhibition of protein synthesis during the gap G_2 will prevent the cell from undergoing mitosis M.

❍ **Metaphase checkpoint** is the one that occurs during the **metaphase**. Here, the cell wants to ensure that the spindle has formed and that all of the chromosomes are aligned at the spindle equator before anaphase begins.

Remark 2. ***i)*** *The p53 gene (also known as tumor protein p53, or, cellular tumor antigen p53) plays an important role in triggering the control mechanisms at both G_1/S and G_2/M checkpoints. In fact, a damaged p53 (due to abnormal mutations) causes some severe health consequences [139]. In addition to p53,*

checkpoint regulators are being heavily researched for their roles in cancer growth and overproliferation. ***ii)*** *Cancer are usually caused by mutations that allow the cells to speed through the various checkpoints, and even skip them altogether (i.e. cells perform a $S \rightarrow M \rightarrow S$ cycle, consecutively, such that the gap phases are skipped). Because these cells are no longer arrested in the previously mentioned checkpoints, any DNA mutation that occurs is disregarded and transmitted to the formed daughter cells. This partly explains why cancer cells tend to exponentially accrue mutations.*

Finally, it is worth mentioning that the regulatory process that controls committed cells before and during mitosis, by triggering a series of physiological events during the cell-division cycle, is not perfectly understood. Indeed, we point out that, for instance, our understanding of the underlying mechanisms of translational regulation in the somatic cell cycle is still limited [229], while our knowledge of the energy regulation (generation and consumption) during the cycle progression is still in a primitive stage [255].

2.2 Stem Cells (SCs)

A fascinating category of cells is known as stem cells (SCs). These are undifferentiated cells characterized by their extensive ability to self-renew and their multipotency, which is the ability to differentiate into more mature and specialized cells [285]. Figure 2.3 gives a cartoon representation of the common possible fates of eukaryotic (stem) cells.

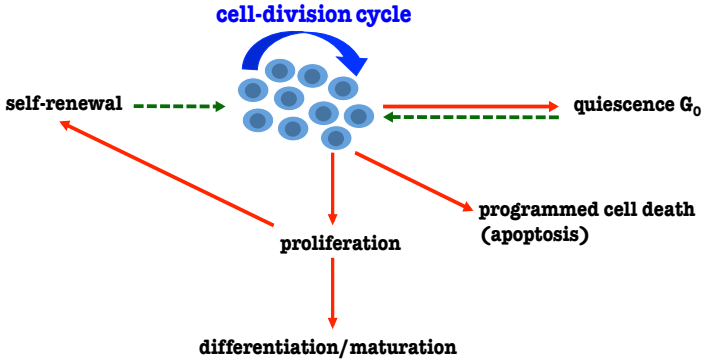

Fig. 2.3 Schematic illustration of the different (stem) cell fates: proliferation, death, self-renewal, differentiation, quiescence. Quiescent (or resting) cells may recover their division activity. The recent cell plasticity concepts (dedifferentiation and trandifferentiation, Box 2 and Section 2.4.2) are not represented here.

The general and common concepts defined below are, in a similar way, also valid for non-stem cells.

Definition 4. Cell proliferation.
Proliferation of cells is the mechanism that results in an increase of the number of cells. It is defined by the balance between cell divisions and cell loss through cell death or differentiation. One of the characteristics of cancer is that cancerous cells generally overproliferate[2].

Definition 5. Cell self-renewal.
Self-renewal of cells is the process by which SCs divide to produce more stem cells, thus perpetuating

[2] See the definition given in *Nature*, available at: `https://www.nature.com/subjects/cell-proliferation`

the SC pool throughout life. In other words, self-renewal is cell-division with maintenance of the undifferentiated state that characterizes SCs ([264]). In the process of maturation, cells gradually lose their ability to self-renew, as they become more and more mature.

Definition 6. Cell differentiation.
Differentiation of cells represents the process by which cells change from one state to a more specialized type, which has specific functions. Differentiation ***commonly*** *occurs in an irreversible way*[3]*, many times during the development of a multicellular eukaryotic organism.*

Definition 7. Apoptosis
Apoptosis is a highly regulated process of programmed cell death that occurs in multicellular organisms. Biochemical events lead to morphological cell changes resulting in cell death. If launched, apoptosis cannot be stopped and causes irreversible nuclear and chromosomal DNA fragmentation.

2.3 Cancer Stem Cells (CSCs)

Basic features of normal SCs have been shortly discussed in the previous section. Now, we point out that sometimes a pathological population of cells, that does not initially necessarily belong to the SC family ([93]), acquires self-renewing and proliferating capabilities similar to those of normal SCs ([93, 230]). These stem-like cells are very often out of control [247] and they are capable of initiating, developing and regenerating cancers [93], hence their designation as cancer stem cells (CSCs) [150].

2.3.1 What is cancer?

Cancer is one of the most devastating causes of morbidity and mortality all over the world [29]. A brief definition of cancer, given by the *National Cancer Institute (NCI)* [4], is as follows:

Definition 8. *«**Cancer** is a term for diseases in which abnormal cells divide without control and can invade nearby tissues. Cancer cells can also spread to other parts of the body through the blood and lymph systems. There are several main types of cancer. Carcinoma is a cancer that begins in the skin or in tissues that line or cover internal organs. Sarcoma is a cancer that begins in bone, cartilage, fat, muscle, blood vessels, or other connective or supportive tissue. Leukemia is a cancer that starts in blood-forming tissue, such as the bone marrow, and causes large numbers of abnormal blood cells to be produced and enter the blood. Lymphoma and multiple myeloma are cancers that begin in the cells of the immune system. Central nervous system cancers are cancers that begin in the tissues of the brain and spinal cord. Also called malignancy.» National Cancer Institute (NCI, 2017). See also: [297].*

In fact healthy tissues are maintaining homeostasis (i.e. maintain a constant internal environment in response to environmental challenges) through a heavy regulation mechanism. Unfortunately, several types of disturbances and disorders may occur, causing many severe dysregulation including cancers. In other words, cancer emerges after some disorders that lead an irreversible neoplastic transformation (i.e. conversion of a tissue with a normal growth pattern into a malignant tumor) [29]. Neoplastic cells are

[3] But see Section 2.4, for *cell plasticity* features (dedifferentiation and transdifferentiation of cells).
[4] NCI is the federal government's principal agency for cancer research and training, USA. `https://www.cancer.gov`

aggressive, continuously self-renewing, proliferating and in addition, they have the ability to escape to apoptosis, mitotic checkpoints, and the hole immune regulation system [29].

In particular, a hostile subpopulation of cells within a tumor mass is known to be highly resistant to anti-tumor drugs currently used in therapeutics [29]. These cells are known as *Cancer Stem Cells (CSCs)* [247], as discussed in the next section.

2.3.2 On the Cancer Stem Cell (CSC) hypothesis

CSCs were identified in 1994 and, since then, their research field is generating an increasing interest. Indeed, their biological properties together with their formation mechanisms become clearly a major focus of current medical research. The reason behind such an interest is that CSCs are able of initiating and fueling tumor growth, and moreover, they show a strong resistance to conventional cancer therapies [231].

Box 1. ***The CSCs hypothesis***

Definition 9. *CSCs form a limited subpopulation of cancer cells that have indefinite potential for self-renewal, and most of the time, an overproliferating activity resulting in tumorigenesis.*

*The **CSCs hypothesis** postulates that only a subpopulation of the total population of cancer cells, that form a tumor, is capable of initiating, sustaining and regenerating tumors, while non-stem cancer cells are considered to be without any tumor initiation potential (see [93, 94]).*
*In fact, in such a framework, cancer cells include CSCs, and striking parallels exist between normal SCs and CSCs. One interpretation of cancer[a] is that: **CSCs may originate from the transformation of normal SCs**. In addition, it appears clear that similar signalling pathways are regulating self-renewal mechanisms in SCs and cancer cells (see [247]).*

Remark 3. *The CSCs hypothesis is actually still controversial, even if this concept has gained ground in the recent years and is now better accepted. For some authors, the reference as a "CSCs paradigm" may appear to be more appropriate than "hypothesis" (see for instance [93]). In fact, medical observations have approved the existence of multiple subpopulations of cancer cells in a tumor, with different tumor-initiating powers ([93, 94]), including a subpopulation of cells showing a "stem-like" status [116, 117]. However, it appears that "stemness" is not a permanent state, but rather a transient cell state that is associated to epigenetic changes [54, 116, 117].*

[a] We will see later a second interpretation of cancer, based on cell plasticity features (Section 2.4.2), in which it is argued that CSCs emerge from the dedifferentiation of more mature cancer cells.

In addition, as reported in [231], the discovery that activation in carcinoma[5] cells of the *epithelial-to-mesenchymal transition* (*EMT*)[6] program can give rise to cells with stem-like properties has provided one possible mechanism explaining how CSCs arise, with possible therapeutic manipulations (see [231]).

[5] Carcinoma is a type of cancer that starts in cells that make up the skin or the tissue lining organs, such as the liver or kidneys. It is developed from epithelial cells and started in the tissues that lines the inner or outer surfaces of the body. As it is usually the case of all cancers, carcinomas are abnormal cells that overproliferate without control.

[6] Roughly speaking, EMT is the mechanism by which epithelial cells lose their cell polarity and cell-cell adhesion, and gain migratory and invasive properties to become mesenchymal stem cells (these are multipotent stromal cells that can differentiate into a variety of cell types).

Next, we mention that CSCs have the feature of dividing asymmetrically, since mother CSCs give birth to daughters that remain as CSCs (self-renewal) and they give also birth to differentiated cells that generate the non-stem cancer cells [93]. In the sequel, we will see that these (non-stem) cancer cells may also (re)generate CSCs [29] through a sophisticated process known as dedifferentiation ([52], which is a *cell-plasticity* feature [280]) as developed in the next section.

2.4 Can cells undergo dedifferentiation?

In view of the broad range of options available for cells in general (including self-renewal, differentiation, lineage specification, programmed cell death, and quiescence, see Figure 2.3), and SCs in particular, it becomes clear that determining the fate of a given cell is a key challenge [95]. This task is further complicated by the discovery of unexpected biological mechanisms that are known as cell plasticity abilities. More precisely, it has been believed for a long time that once a cell differentiates into a particular cell type that has a distinctive function in the human body (e.g. when an hematopoietic SC differentiates into a type of, for instance, mature white blood cells), it permanently loses the potential for diverse functions and stably maintains its identity [301]. The discovery of dedifferentiation contradicted this biological postulate, and thus opening the way to a much richer and complex cellular behavior.

Box 2. ***Crucial definitions: cell-plasticity (dedifferentiation & transdifferentation)***

Definition 10. *«**Dedifferentiation** is an important biological phenomenon whereby cells regress from a specialized function to a simpler state reminiscent of stem cells» [52].*

Definition 11. *«**Transdifferentiation** is defined as the conversion of one cell type to another. It belongs to a wider class of cell type transformations called metaplasias which also includes cases in which SCs of one tissue type switch to a completely different SC» [263].*

It has been believed that once a cell differentiates into a particular cell type that has a distinctive function in the human body, it permanently maintains its identity [301]. The discovery of dedifferentiation contradicted this biological postulate and allowed a much richer and complex cellular behavior. Even more surprisingly, transdifferentiation stated that adult SCs may first reside in one tissue and then contribute to another tissue [280]. In fact, in normal tissues, when the process of cell generation and continuous replenishment is perturbed (e.g. tissue injury, hemorrhage), the homeostatic mechanisms are invoked to allow adequate regeneration of damaged tissue [280].

As previously mentioned, the mechanisms regulating the cell-division cycle are not yet perfectly assimilated. Nevertheless, it is agreed by everyone that understanding how the fate of cell (including SCs) is guided will, firstly, elucidate the causes of cancer and, secondly, allow the use of cells/SCs in *regenerative medicine*[7] (see for instance [95], and the references therein).

[7] «Regenerative medicine aims to replace the lost or damaged cells in the human body through a new source of healthy transplanted cells or by endogenous repair» [83].

2.4.1 Evidences about cell plasticity: the case of induced pluripotent stem cells (iPSCs)

The two main human SC types[8] are **embryonic stem cells** and **adult stem cells** (e.g. epidermal stem cells to renew skin, epithelial stem cells in the gut, hematopoietic stem cells in bone marrow for fabrication of blood, bronchoalveolar stem cells in the lungs). By artificially reprogramming adult cells a new category of cells that expresses embryonic stem cells characteristics is obtained (sometimes called **induced pluripotent stem cells** (iPSCs)[9]. Not surprisingly, the clinical potential of stem cells is eliciting huge scientific and commercial interest [95].

Box 3. ***Yamanaka factors (Oct3/4, Sox2, Klf4, c-Myc)***

A research team in Kyoto University, in Japan, have successfully identified in 2006 the mechanism that would allow genetic reprogramming of differentiated adult cells to become SCs. The resulting stem-like cells are known as induced pluripotent stem cells (iPSCs), and they are similar to embryonic stem cells. Since then, researchers have rapidly improved the initial techniques of generating iPSCs, creating a powerful new way to "dedifferentiate" cells whose developmental fates had been previously assumed to be determined.

***Yamanaka**[a] **Factors (Oct3/4, Sox2, Klf4, c-Myc)** are highly expressed in embryonic SCs, where they regulate the developmental signaling network inducing pluripotency. The over-expression of these factors is used to transform human somatic cells into pluripotent embryonic-like cells [175].*

[a] Shinya Yamanaka has been awarded the *Nobel Prize in Physiology or Medicine*, in 2012, for «the discovery that mature cells can be reprogrammed to become pluripotent».

Finally, since some ethical issues arise regarding the use of embryonic SCs in research, cell plasticity appears as an acceptable way to produce SCs without sacrificing embryos [52]. Consequently, therapy research is focusing on adult cells due, as previously mentioned, to their potential in regenerative medicine and tumor biology, but also because dedifferentiation (or, reprogramming) may offer an abundant source of SCs without any risk of immune rejection from the intended recipient (see [95, 230, 52, 41]).

2.4.2 Cell plasticity in normal tissues

In normal tissues, it has been believed that once a cell differentiates into a particular cell type that has a distinctive function in the human body (e.g. when an hematopoietic SC differentiate into a type of mature white blood cells), it permanently loses the potential for diverse functions and stably maintains its identity [301]. However, nowadays, it becomes clear that the traditional lineages and functions are, physiologically, no longer sufficient to describe the fate of a cell [280]. Indeed, the discovery of dedifferentiation in normal tissues has contradicted the classical biological visions, and thus, opens the way to a much richer cellular behavior and fates, even when no malignancy is involved. In addition, transdifferentiation and transdetermination [280], these even more surprising phenomena where adult SCs may first reside in one tissue and then contribute to another, are also present is healthy cases.

[8] See the website of the *International Society for Stem Cells Research (ISSCR)*: `www.closerlookatstemcells.org`
See also the *Nature Reports*: `www.nature.com/stemcells/2007/0706/070614/full/stemcells.2007.14.html`

[9] See the website of *GE healthcare*: `www.gelifesciences.com`

Finally, we notice that cell plasticity in healthy tissues is evoked when the process of cell generation and continuous replenishment is perturbed (e.g. after tissue injury, or hemorrhage) [280]. Indeed, in such situations, the homeostatic mechanisms are invoked to allow adequate and fast regeneration of damaged tissues (see Figure 2.4).

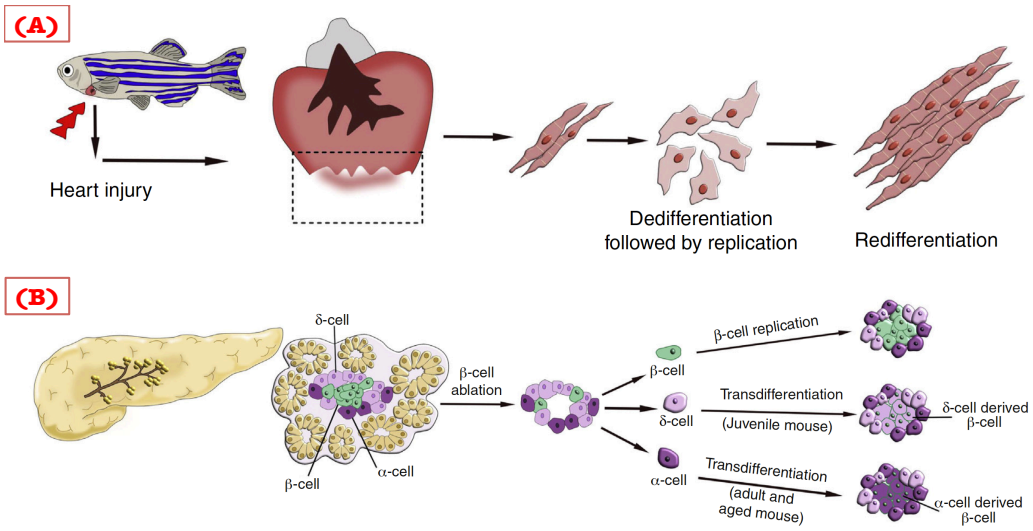

Fig. 2.4 **(A)** A differentiation example: After a ventricular amputation of zebrafish, a dedifferentiation (followed by a replication -proliferation-, then, a redifferentiation) is observed in cardiomycocytes ([280]). **(B)** A transdifferentiation example in which hypatocytes become biliary duct epithelial cells. This process occurs after a toxin-induced biliary injury. These images are from [280] (**(A)** is from Fig. 2 and **(B)** is from Fig. 3 of [280]).

2.4.3 Dedifferentiation meets cancer

Cell-plasticity has provided new hypothesis about the origin of cancer, as well as new therapeutic insights for its treatment (see the review articles on this topic: [83, 110, 171, 149], and the references therein).

At this juncture, the issue is whether cancer emerge from SC disorder or a reacquisition of SC characteristics? (see [230], for a similar issue in the typical case of leukemia). The latter question is equivalent to the one already tackled in Section 2.3, about the origin of CSCs. We have already put forward one interpretation that assumes that CSCs may originate from a transformation (i.e. mutation) in a part of normal SCs (see Box 1). Several relevant works support this theory that appears consistent. However, another interpretation strongly relate cancer to dedifferentiation (see [83, 110, 171, 149], and the example in Figure 2.5). In fact, both ways of generating cancerous cells may exist in the same type of cancer, as illustrated in the following example in Box 4.

Definition 12. Epigenetics *is the analysis of any potentially heritable change in gene expression, which actually affects how cells read the genes, while it does not involve changes in the corresponding DNA sequence. In other words, it is about a modification in phenotype without changing genotype. See [116, 117].*

Box 4. ***The example of leukemic (i.e. blood cancerous) cells***

We quote from Tung & Knoepfler work [286] that:

« The CSC hypothesis postulates that immortality is a pathological offshoot of the normally exquisitely controlled proliferation machinery in normal SCs from which mis-regulated cell expansion occurs due to oncogenic mutations [150, 72]. This CSC model further proposes that there is a subpopulation of cancer cells within tumors that possesses some sSC-related properties such as self-renewal and that give rise to tumors [42]. However, ***whether CSCs originate from normal SCs or from differentiated cells, which reacquire SC attributes through a dedifferentiation process, is a long-standing question [217].*** *The answer to this key open question may vary depending on tumor type and stage as well. Take the hematopoietic system for example;* ***leukemia SCs have been shown to arise from both self-renewing SCs and also from transient repopulating progenitors, providing evidence that stem cells and late-stage precursors can both undergo oncogenic transformation and result in similar tumor phenotypes*** *[68] » [286].*

In the majority of cancers, the genetic/epigenetic heterogeneity is reflected by genome instability (i.e. genetic or epigenetic alterations [214]). We define the phenotypic heterogeneity as the diversity in functional features and behaviors in different lineage markers that cancer cells can adopt during their cancer progression (growth). Based on cell surface markers ([174, 246, 279]), we can identify distinct (heterogeneous) populations of cancer cells within the same tumors, i.e. cancer cells within the tumor may exist at different states of differentiation and maturation, including the subpopulation of CSCs [93, 94].

In [110], the authors reported that although CSCs exhibit the SC characteristics (self-renewal, proliferation and differentiation), they do not necessarily originate from the transformation of normal tissue SCs. Several recent works are suggesting that not all cancers strictly conform to the unidirectional hierarchical CSC model, and highlight the theory of **tumor cell plasticity**, where non-CSCs dedifferentiate and acquire CSC-like properties under certain conditions as demonstrated by the concrete examples given in [110]. Finally, we refer to [142], and the references therein, for a quantitative experience highlighting the role of dedifferentiation in cancerous cell surviving during radiotherapy.

Box 5. ***Summary of the main medical research focuses in cell plasticity***

All the research efforts in recent years are mainly focusing on the following aspects of cell plasticity:

- *Adult cells manipulation and artificial reprogramming into iPSCs.*
- *CSCs origin and the role of cell plasticity in the appearance and maintenance of tumors.*
- *Drug-resistance, chemotherapy and radiotherapy resistance, induced by cell-plasticity.*

2.5 Cancer dormancy

Very often, CSCs and cancer cells are characterized by unhealthy behaviors such as excessive proliferation and abnormal loss of their differentiation faculties (this is what we observe in leukemia, for instance). On the other hand, it cannot be disregarded that in some cases (as in breast cancer and leukemia [88], [18]) CSCs do not overproliferate (cancer without disease [102], or, *in situ* tumor). However, even during their

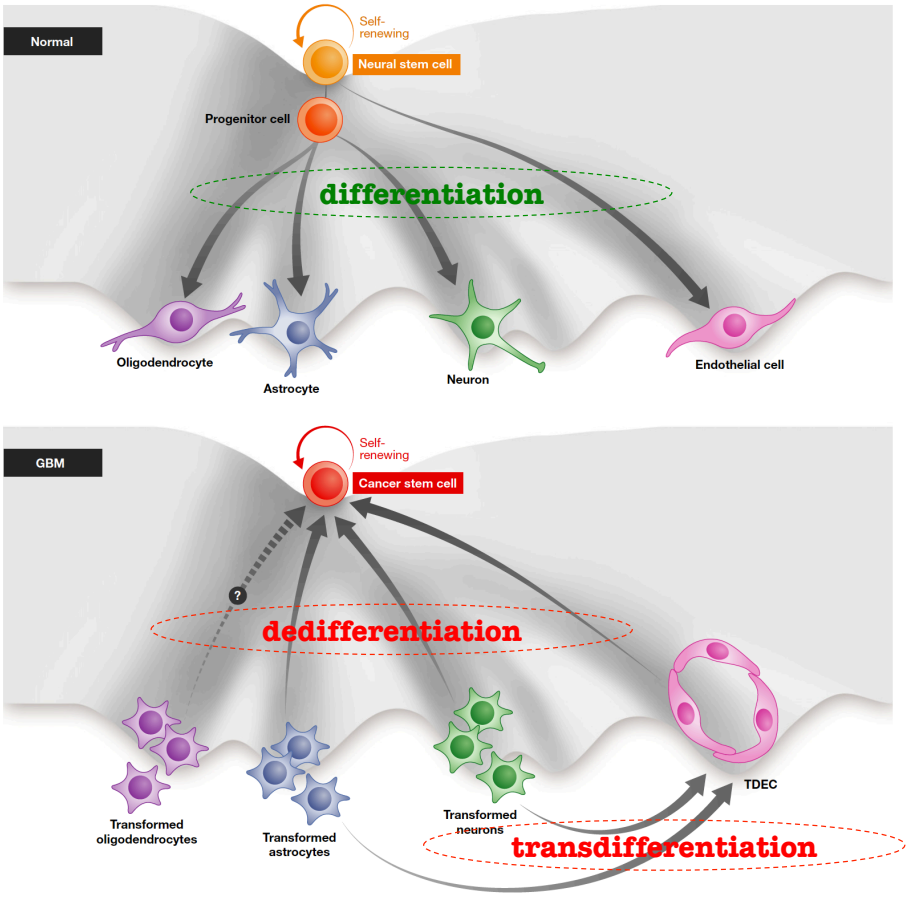

Fig. 2.5 Dedifferentiation and cancer. A model for the generation of malignant gliomas. Normal mechanism of neuronal differentiation: Neural stem cell can self-renew, go through an intermediate progenitor cell, and differentiate into oligodendrocytes, astrocytes, neurons, and endothelial cells. In the formation of glioblastoma, the transformed neurons, astrocytes, and possibly oligodendrocytes can dedifferentiate/reprogram to become cancer stem cells (CSCs), which can then continue to self-proliferate and differentiate to more transformed neurons and astrocytes. The transformed neurons and astrocytes can also transdifferentiate into endothelial cells (TDECs), which can again dedifferentiate to CSCs. [110].

non-overproliferating states, CSCs remain in general distinguishable through specific markers on their surface[10] [247].

2.5.1 Evidences and underlying assumptions about cancer dormancy

Strong evidence about the existence of this stalled growth, commonly referred to as *tumor dormancy*, has been established many years ago when microscopic tumors were frequently encountered during autopsy examinations ([220], [102]). The most likely explanations (see [15, 261, 102]) of CSCs dormancy state are:

i) blood and nutrient supply issues that prevent tumor growth, or delay its clinical manifestation [213],

ii) vigilance of the immune system which, in some rare cases, suffices to stop tumor development (see [98, 261, 213, 299, 291]). In fact, there has been a lengthy debate on the role of the immune system in

[10] For instance, stems cells in acute myeloid leukemia have some *interleukin-3–receptor α chain* surface markers, which are not found in normal hematopoietic stems cells (see [150, 99]).

the defense against cancer: a process called *cancer immunosurveillance* [291]. The ambiguity about the immunosurveillance concept stems from the fact that often the immune system favors the development of the tumor instead of trying to eliminate it. The concept that attempts to integrate the diverse effects of the immune system on tumor progression is known as *cancer immunoediting* (see the review articles [261] and [291]). However, even if it appears as an unsystematic process, the immune response remains one of the most likely justifications for cancer dormancy.

Illustrative interpretations of CSC eradication, dormancy, and escape of dormancy, in terms of cancer immunoediting, are provided in Figure 2.6 (see also Figure 3 of [261] and in Figure 1 of [291]).

Not surprisingly, an interest arises for cancer therapies that are oriented on the immune system, bearing the name of *immunotherapy*[11]. In a similar spirit, monoclonal antibodies, e.g. gemtuzumab ozogamicin, have been approved in the treatment protocols of some cancers (as in acute myeloid leukemia [115]), even if more trials are still needed to identify their exact benefits [253, 115]. Other cancer therapies, sometimes assimilated to immunotherapy, are using some *immune checkpoint inhibitors* (see for instance, [228], [169] and [44]). In the last part of our work, we will be shortly adopting some of these immuno-oriented concepts, associated with classical chemotherapy, as it is frequently adopted in practice.

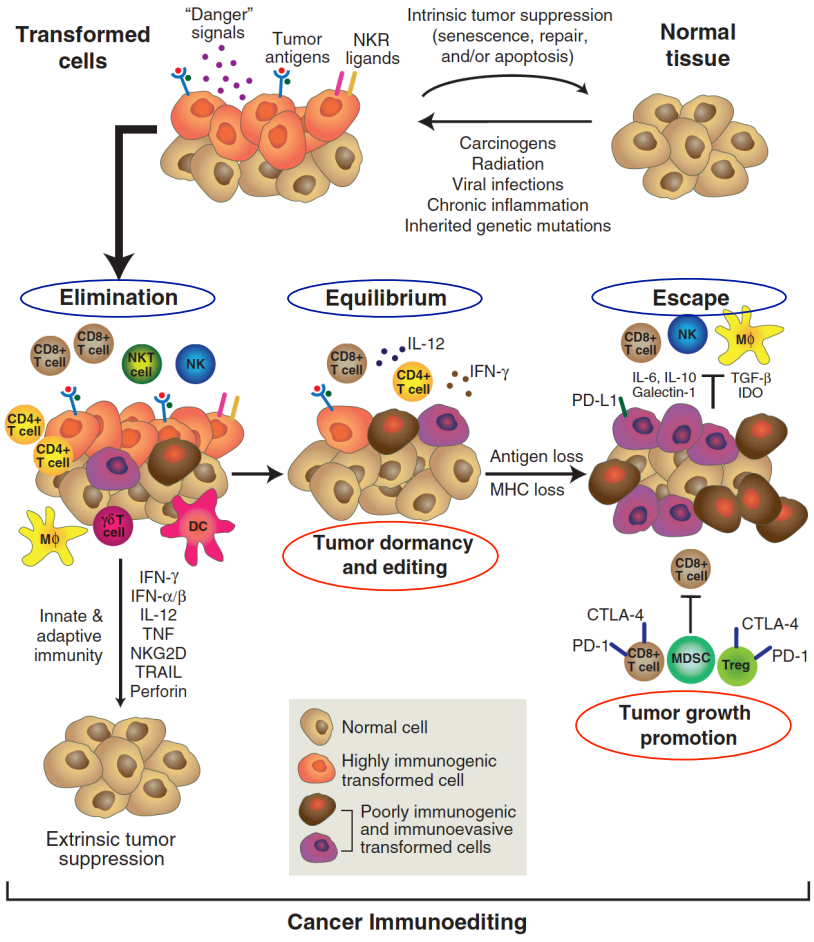

Fig. 2.6 Illustrative figure (**taken from [261]**) of escape from dormancy and immunoediting concepts.

[11] Immunotherapy aims to help the immune system destroy cancer cells. It is given after -or at the same time as- another cancer treatment such as chemotherapy. (`http://www.cancer.net/`)

2.5.2 Is cancer dormancy a promising therapeutic option?

In a general perspective, apart from the interpretation of tumor dormancy as an observed natural phenomenon in human cancers, the idea to transform cancer into a chronic disease is in the voices of many people in the medical world nowadays [111], [14]. Indeed, the interesting issue here is about: *how can we bring CSCs from an overproliferating activity to a dormant state?* More precisely, since cancer treatments most often consist of delivering the maximum tolerable doses of drugs in order to kill diagnosed tumors, and knowing that a non-completely eradicated tumor frequently grows again, even more aggressively than the initial one [93], the option of maintaining the tumor in dormancy is more appealing than trying to eradicate it [147]. Further discussions on the opportunities offered by cancer dormancy in therapeutics can be found for instance in [14], [289], [111], and the references therein.

The development of a relevant mathematical framework appears as a necessary tool to apprehend tumor dormancy as a biological mechanism [154], with the ultimate goal to apply it in therapeutic settings. However, the task of mastering CSCs, i.e. bringing them into a dormant state, seems to be difficult to conduct. Indeed, one of the first dormancy-oriented therapeutic approaches has not been very fruitful. It was based on the use of *angiogenesis inhibitors* (substances that inhibit the growth of new blood vessels [102]) as drugs that choke off the blood supply of the tumor, in order to maintain it in dormancy. However, unexpected effects occurred in practice, in some situations, where targeting the blood vessels that feed tumors actually accelerated the spread of cancer [134], [248].

In the clinic of cancers today, eradication of CSCs remains the predominant treatment approach (although there is still a long way to improve the existing eradication treatment strategies [277]). In light of the previously mentioned observations, one can say that dormancy has actually generated more issues than answers, in the process of understanding cancer. Among the open issues, we emphasize the following ones: *when a treatment protocol is elaborated for CSCs eradication with a given rate of success, how can we actually administer it (or a part of it) in order to achieve dormancy?* In addition, since eradication techniques may generate some surviving tumors which become even more aggressive than the initial ones, a key question is to determine *whether it is effective to consider the same targets and drugs, as for CSCs eradication, in order to achieve dormancy?* These are some open questions in this topic.

2.6 A presentation of the process of blood cell production

Among a wide range of physiological mechanisms occurring in the human body, our research axis particularly highlight one fundamental and major process, leading to the formation and continuous replenishment of all the blood cells, known as hematopoiesis [138]. Clearly, *hematopoietic stem cells (HSCs)* are the most clinically studied type of SC. Due to their vital importance, extensive work (particularly in biology and medicine) is carried out on HSCs, since they sustain haematopoiesis [69].

More precisely, in a healthy bone marrow resides a rare population of HSCs. The critical role of HSCs is to create and replenish all the types of blood cells, including red blood cells, white blood cells and platelets, as illustrated in Figure 2.8. These distinctive categories of differentiated blood cells arise from HSCs by a process of commitment to (and execution of) complex programs of cell differentiation [138]. Thus, lineage committed progenitor cells subsequently proliferate and differentiate to produce

the circulating mature blood cells, under the control of what is collectively known as *colony-stimulating factors* (CSFs) (i.e. a group of hormonal-like growth factors) [61, 265]. In fact, the blood cells (both the myeloid and lymphoid lineages in Figure 2.8) differentiate inside the bone marrow (Figure 2.7), they leave and enter bloodstream when they become mature.

The complexity of the hematopietic system is enormous, since as many as $1-5\times10^9$ erythrocytes and $1-5\times10^9$ white blood cells are produced per day during the lifetime of an individual. Additional complexities include the need to maintain a pool of undifferentiated SCs, from which mature cells arise by a differentiation process.

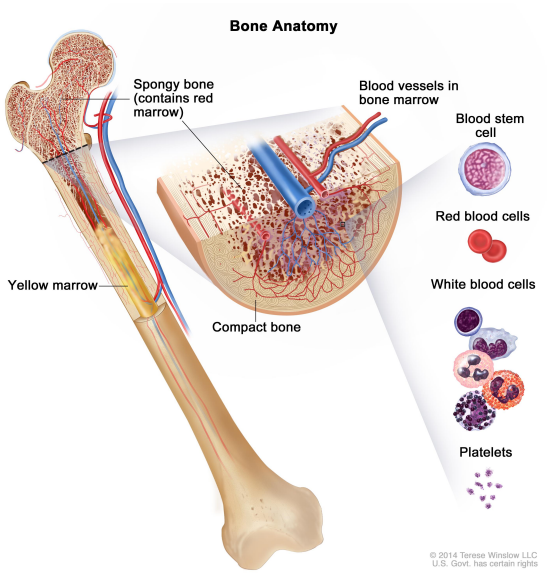

Fig. 2.7 The hematopoietic cells are formed inside the bone marrow. When blood cells become mature, they leave the bone marrow and go into circulation, in order to fulfill their specif tasks. This figure is from the *National Cancer Institute* (available at: `https://www.cancer.gov/types/leukemia/patient/adult-aml-treatment-pdq`).

On the importance of HSCs

In 2017, G. Crane and his co-authors wrote in [69] about hematopoiesis:

« *Hematopoiesis is required for the ongoing production of blood cells and immune cells — including erythrocytes, platelets and white blood cells — throughout life. To generate these cells, HSCs give rise to an array of restricted progenitors, which proliferate extensively and then differentiate into mature cells. Without hematopoiesis, we would not be able to maintain blood cell counts and would die within weeks as a result of anaemia (due to erythrocyte depletion), bleeding (due to platelet depletion) and infection (due to the depletion of myeloid and lymphoid immune effector cells). Although restricted progenitors are responsible for most steady-state hematopoiesis, HSCs must be maintained throughout life to replenish these progenitors, and to regenerate hematopoietic cells after stresses such as severe infection or blood loss* » [69].

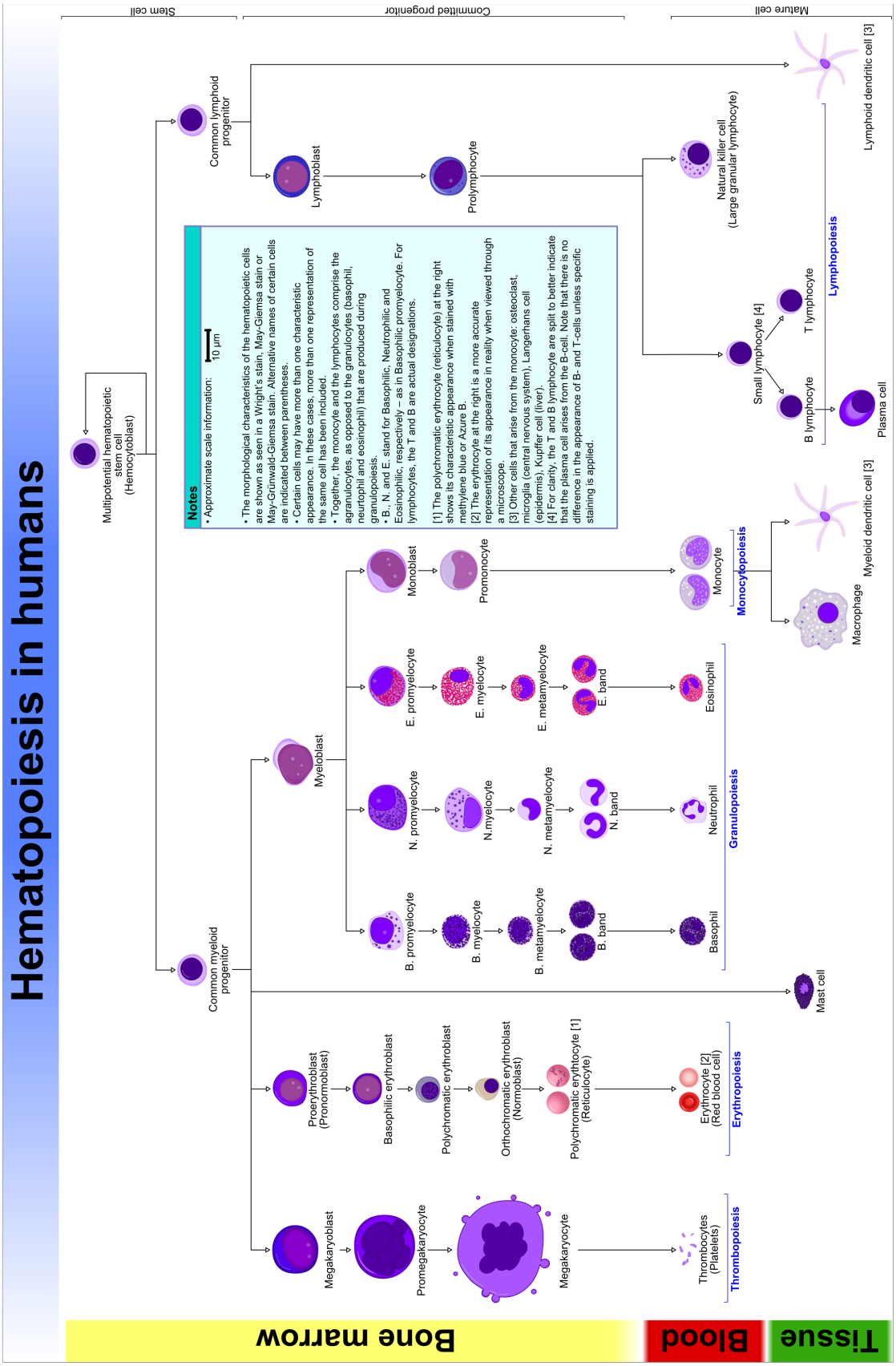

Fig. 2.8 Blood cells production (hematopoiesis). Hematopoietic SCs are at the root of this process: they give birth to common myeloid progenitors (that differentiate and give birth to all the cell in the myeloid lineage), and/or to common lymphoid progenitors (that differentiate and give birth to all lymphoid cells). This figure is an Open Access material from Wikipedia (under CC BY-SA 3.0 license) - Available from: `https://en.wikipedia.org/wiki/Lymphocyte`.

2.7 Hematopoietic niches

The local specialized tissue microenvironment that promotes the maintenance and ongoing production of SCs is known as *niche* [69, 209]. Inside the bone marrow, the hematopoietic niche regulates the function of adult HSCs, via the production of factors that directly act on SCs (some other factors, from more distant tissues, also affect the SCs in their niche [69]).

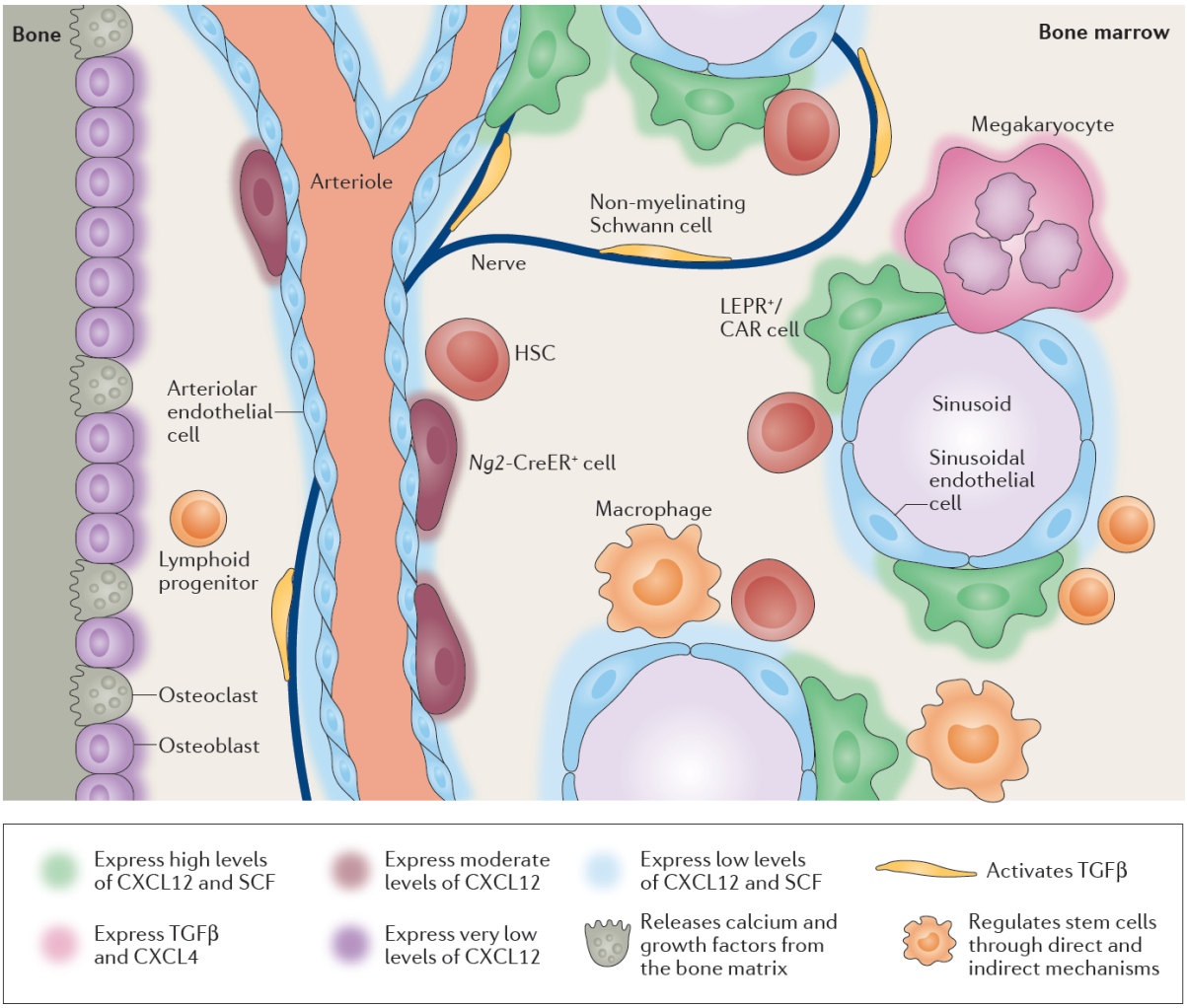

Fig. 2.9 **This figure is taken from [69]**. It illustrates niches location of adult HSCs and their regulation processes. Inside an adult bone marrow, HSCs position themselves in close contact to sinusoid (see [209, 69]), since these locations usually express high levels of *stem cells factors (SCF)* as explained in [69]. SCF and CXCL12 are indeed necessary for the maintenance of HSCs [69]. Approximately 10% of HSCs localize near to small-diameter arterioles [69]. Many growth factors, nerve fibers and cells, through very complex mechanisms, are also required for HSC maintenance (see also [308], and the references therein). Osteoblasts appear to promote a subset of early lymphoid progenitors. Some other lymphoid progenitors reside inside sinusoidal niches, where they depend on CXCL12 synthesized by LEPR+ (leptin receptor +) cells [69]. Surprisingly, it appears that, in turn, HSCs regulate the maintenance of the niches through the secretion of angiopoietin-1 (see [308]).

For further reading on the HSCs niches, we refer to [159, 76], and also to [129] for a recent review of the neural regulation of hematopoietic niches through sympathetic nervous system (SNS).

2.8 Regulation of hematopoietic cell growth

The process of hematopoietic cell differentiation is heavily regulated through cytokines (see [200]), in order to maintain an adequate mature-cell density in the bloodstream.

Cytokines: these are small proteins that play a major role in cell signaling. Their release has an effect on the cell around them, by affecting their behavior and determining their fates. Here we list some important facts about cytokines: **i)** They are involved in autocrine signalling, paracrine signalling and endocrine signalling as immunomodulating agents. **ii)** They include chemokines, interferons, interleukins, lymphokines, and tumour necrosis factors but generally not hormones or growth factors[a]. **iii)** They are produced by a broad range of cells, including immune cells like macrophages, B lymphocytes, T lymphocytes and mast cells, as well as endothelial cells, fibroblasts, and various stromal cells.

[a] **Difference between cytokines and growth-factors:** Hormones (growth-factors) are also important cell signaling molecules. In fact, the distinction between cytokines and hormones is still part of ongoing research. Most commonly, cytokines include chemokines, interferons, interleukins, lymphokines, and tumor necrosis factors but generally not growth factors (despite some overlap in the terminology). Notice that one type of cytokine may be produced by more than one type of cells, while hormones tend to be made by specific kinds of cells.

2.8.1 Regulation of red blood cells: Erythropoeietin (EPO)

We define ***erythropoiesis*** as the process of production of red blood cells (RBCs or *erythrocytes*). In the simplest scenario, a decrease of oxygen O_2 is detected by the kidneys, which stimulates the secretion (by some interstitial fibroblasts in the kidneys) of a cytokine (or a growth factor) called *erythropoietin* (EPO). More generally, EPO is a glycoprotein that plays the most relevant control in erythropoiesis: it promotes both the proliferation and differentiation of red blood cell precursors (see Figure 2.8), which favors the erythropoiesis process and results in red blood cells production.

2.8.2 Regulation of white blood cells: Granulocyte colony-stimulating factor (G-CSF)

The Granulocyte-colony stimulating factor (G-CSF, [75]), is a *glycoprotein* that stimulates the bone marrow to produce *granulocytes* (see Figure 2.8) that go into the bloodstream [281].

G-CSF is considered both as a cytokine and as a hormone. As mentioned in [200], several tissues may release G-CSF in the body, and it may in addition have different roles (stimulates the survival, differentiation, and proliferation of neutrophils, Figure 2.8).

2.8.3 Regulation of platelets production: Thrombopoietin (THPO)

Megakaryocyte growth and development factor (MGDF), or, more commonly, Thrombopoietin (THPO), is a protein (more precisely, a glycoprotein hormone) produced by liver and kidney, and which regulates the platelets formation. In fact, THPO stimulates the production and differentiation of *megakaryocytes* (see Figure 2.8), the bone marrow cells that lead to platelets [155].

2.9 Some pathological blood disorders

A huge number of diseases and disorders may occur in the hematologic systems. Here we are listing some examples of these diseases.

- **Anemia** is one of the most frequent blood disorders which is mainly characterized by a decrease in the number of red blood cells and hemoglobin in the bloodstream. Numerous kinds of anemia exist, and several classifications are introduced to categorize them (for instance, nutritional *vs* non-nutritional anemias). We can mention for instance:
  - **Pernicious anemia** is a type of megaloblastic anemias, characterized by an inability to absorb B_{12}-vitamins (due to a loss of gastric parietal cells).
  - **Iron deficiency anemia** is a disorder where hemoglobin cannot be produced. Indeed, as its name indicates, iron is very low during this kind of anemia, while hemoglobin contains iron.
  - **Megaloblastic hereditary anemia** is an unhealthy situation, which is characterized by an inhibition of DNA synthesis during erythropoiesis.
  - **Alphastic anemia** is a blood disorder in which the bone marrow cannot produce sufficient blood cells to replenish the circulating mature blood cells.
- **Infectious diseases (bacterium-related and protozoan-related)**
  - **Cholera infection**, which is a bacterium-related.
  - **Plasmodium infection (Malaria)**, which is protozoan-related.
- **Immunodeficiency**
- **Blood cancers**, which belong to the family of cancers (see Section 2.3.1), but they are limited to those originating, evolving, or affecting the bone marrow, blood cells, or lymph glands[12].
  - **Myeloma**
    - **Malignant plasma cell tumor NOS**
  - **Malignant immunoproliferative diseases**
    - **T-gamma lymphoproliferative disease**
  - **Lymphoma**
    - ***B*-cell lymphoma**
    - **Burkitt lymphoma**
  - **Leukemia:** unlike solid tumors, leukemia is a liquid cancer that starts in the bone marrow, which is the place of production of all blood cells. Leukemic cells are most of the time immature white blood cells, that abnormally and excessively proliferate in the bone marrow until they overrun the healthy blood cells (see Figure 2.10). Moreover, since leukemia is not a solid tumor, cells may travel through the bloodstream and contaminate other organs in the body.

    First, we distinguish between **acute** leukemia and **chronic** leukemia. Roughly speaking, the **acute** one growths very quickly, at the point of becoming deadly in weeks or months, if not treated. On the other hand, chronic leukemia types are generally slow and long-term developing cancers. There two

[12] Lymph gland is a part of both the lymphatic and adaptive immune systems. Lymph nodes are major sites of *B* and *T* lymphocytes (see Figure 2.8), and other white blood cells.

main types of acute leukemia: the first one appears in the myeloid lineage while the second one appears in the lymphoid lineage (see blood lineages in Figure 2.8).

- ➢ **Acute myeloid leukemia (AML)**
- ➢ **Acute lymphoblastic leukemia (ALL)**

On the other hand, we can distinguish between three types of chronic leukemia:

- ➢ **Chronic myeloid leukemia (CML)**
- ➢ **Chronic lymphocytic leukemia (CLL)**
- ➢ **Hairy cell leukemia (HCL)**

In practice, the most commonly encountered types of leukemia, in adults, are CLL and AML.

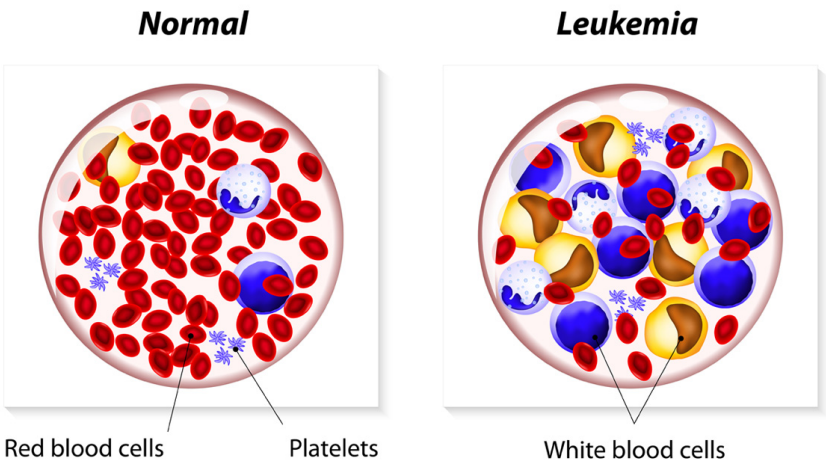

Fig. 2.10 Normal blood includes a large variety of cells of different shapes, reflecting the normal developmental stages and the different types of cells (mature red blood cells, mature white blood cells, platelets, see Figure 2.8). This diversity is vital for the healthy functioning of blood throughout the body. On the other hand, leukemia is characterized by a poor cell diversity resulting from the overproliferation of cancer (immature) blood cells, with a similar appearance. In AML, blast cells (immature white blood cells, Figure 2.8), which are enable to perform their functions in blood, invade the bone marrow and possibly the bloodstream. In fact, their overproliferating and self-renewing activities prevent the formation of other (normal) blood cells.
`Figure source: http://www.cancerexpertnow.com/resource/cancer-resources/leukemia-diagnosis/`

2.10 A particular emphasis on Acute Myeloid Leukemia (AML)

In [85], H. Döhner and co-authors defined AML as follows:

Definition 13. Acute Myeloid Leukemia (AML) [85].
«AML is a form of cancer that is characterized by infiltration of the bone marrow, blood, and other tissues by proliferative, clonal, abnormally differentiated, and occasionally poorly differentiated cells of hematopoietic system» [85].

Box 6. ***Some facts and figures about AML***

❍ *AML is clinically identified if leukemic myeloid blasts (Figure 2.11) exceed* 20% *in the bloodstream: this is in fact the conventional diagnosis criterion of AML, or, if at least* 50% *of blood cells belonging to different myeloid lineages are dysplastic*[a] *[84].*

❍ *The success rate of therapies in AML for patients younger than 60 years is approximately* 40%*, while it never exceeds* 15% *for patients over 60 years [85, 84].*

❍ *At the time of this writing, striking statistics and previsions about acute myeloid leukemia (AML) are provided by the American Cancer Society for the current year (2017), in the United States of America. Some of these data are summarized in Table 2.1.*

[a]Dysplastic cells are unhealthy cells with severe abnormal development.

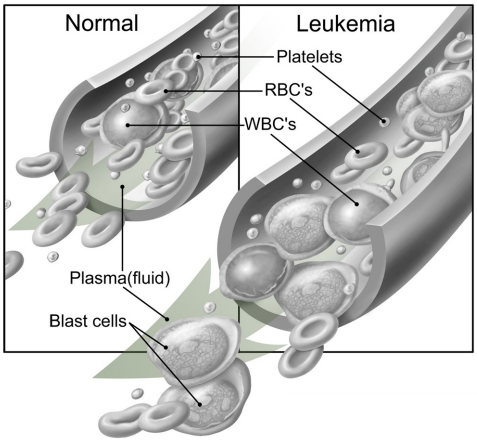

Fig. 2.11 A two-panel drawing of normal blood cells and blood cells with leukemia. Platelets, red blood cells, white blood cells, plasma (fluid), and blast cells are labeled. Blasts are not typically found in bloodstream when hematopoiesis is normal. Usually, AML diagnosis criterion consists in the identification of -at least- 20% of blasts in the bloodstream. This figure is under a free licence from the *National Cancer Institute (NCI)*, by *A. Hoofring*.

Estimates of new cases in leukemia (all kinds)	$\approx$ 62130 new cases in 2017
Estimates of deaths from leukemia (all kinds)	$\approx$ 24500 deaths in 2017
Estimates of new cases in Acute Myeloid Leukemia	$\approx$ 21380 new AML cases in 2017
Estimates of of deaths from in Acute Myeloid Leukemia	$\approx$ 10590 deaths in 2017

Table 2.1 Estimates (USA, 2017) provided by the **Cancer Statistic Center** affiliated to the **American Cancer Society**.

According to the type of cell which is affected, AML has been divided into eight types, by the **French-American-British (FAB) classification**. A pioneer FAB classification proposal was introduced in [34]. Since then, many revisions have been performed [125]. A different classification exists, it is known as **WHO - World Health Organization - classification** (last update in 2008, [221]). Roughly speaking, the FAB Classification relies on morphological criteria of the cells, while WHO Classification separates malignant cells according to chromosome translocations. An overview of the FAB classification is given in Table 2.2, while an extensive discussion on the WHO classification can be found in [85, 84].

M0	undifferentiated AML	immature while blood cells
M1	myeloblastic leukemia with minimal maturation	immature while blood cells
M2	myeloblastic leukemia with maturation	immature while blood cells
M3	promyelocytic leukemia	immature while blood cells
M4	myelomonocytic leukemia	immature while blood cells
M4 eos	myelomonocytic leukemia with eosinophilia	immature while blood cells
M5	monocytic leukemia	immature while blood cells
M6	erythroid leukemia	immature red blood cells
M7	megakaryoblastic leukemia	immature cells that produce platelets

Table 2.2 The French-American-British (FAB) classification divides AML mainly into eight subtypes[13].

2.10.1 FLT3 (fms-like tyrosine kinase) mutations in AML

FLT3 (fms-like tyrosine kinase), is a member of the type III receptor tyrosine kinase (RTK) family. It is mainly expressed in multipotential HSCs and progenitors [243]. Severe FLT3 mutations are found in blast cells in nearly 30% of newly diagnosed AML in adults [305, 160, 277]. Cells with FLT3 mutations have an important overproliferating advantage, typically through RAS-RAF, JAK-STAT and PI3K-AKT signaling pathways (see Figure 2.12) [85, 258].

There are in fact two types of FLT3 mutations in AML:

- ❍ **FLT3-ITD subtype** (internal tandem duplication mutation, see [166], [282], [298]).
- ❍ **FLT3-TKD subtype** (point mutation in the tyrosine kinase domain, see [199]).

The first subtype (i.e., FLT3-ITD), represents approximately 70% of AML with FLT3 mutations, and it has a severely poor prognosis [305, 277]. In fact, several molecules kinase inhibitor have been evaluated against FLT3 mutations in the typical case of AML. For instance, we can mention: AC220 [305], lestaurtinib [161], and, more recently, midostaurin [277]. A glimpse into some AML therapies is discussed in the next section (see Box 8).

Finally, we mention that many other mutations may occur -sometimes simultaneously- in the hematopoietic cell population. These mutations have more or less devastating consequences (see [137]). For instance, we can mention the DNMT3A mutations, TET2 mutations, IDH1 and IDH2 mutations, etc. The appearance of the latter types of mutations in AML lead to deregulation of the DNA methylation (see the review paper about genomic and epigenomic landscapes in AML [214], see also Table 1 in [85] that gives only the most frequent gene mutations in adult AML).

2.10.2 Current and emerging therapies for AML

Even after decades of intensive medical research, the treatment of AML has not encountered too much success [85]. Indeed, it is surprising to notice that AML drug protocols have remained substantially unchanged over the last four decades [85, 258].

In the general case, two main chemotherapy phases are considered during the treatment:

[13] See the *StayWell* official webpage:
`http://poc.select.kramesstaywell.com/Content/cancer-source-v1/understanding-acute-myeloid-leukemia-am`,
And the *American Cancer Society* official webpage:
`https://www.cancer.org/cancer/acute-myeloid-leukemia/detection-diagnosis-staging/how-classified.html`

❍ **Induction therapy:** this is an intensive chemotherapy phase that generally uses some continuous-infusions of cytarabine with anthracycline (possibly with anti-CD33 monoclonal antibody such as gemtuzumab orogamicin [253]). See [85], and also [295].

❍ **Postremission therapy:** if a complete remission is obtained within the intensive induction phase, a suitable consolidation program is prescribed. This essential phase includes chemotherapy and hematopoietic cell transplantation.

Box 7. On classical and emerging therapies for AML (2017, [258])

The classical chemotherapy-based treatment of AML is known as (7+3), meaning that the patient undergoes an intensive induction consisting of cytarabine (during 7) and/plus anthracycline (during 3 days). This treatment is generally followed by consolidation chemotherapy andhematopoietic cell transplant (HCT), in order to ensure a complete remission.
In [112], one attempt - among many others - to improve the classical regiment (7+3) is discussed:
« Efforts to improve the outcome of patients with AML have included the replacement of daunorubicin with idarubicin or mitoxantrone; the intensification of cytarabine or daunorubicin during induction; and the addition of maintenance therapy. With the exception of maintenance therapy, which was associated with an inferior survival, most regimen modifications have had modest effects and most randomized trials have shown no significant difference in outcome between treatment arms» [112]. Nevertheless, the overall results of ongoing treatments suggest that an improvement of the global prognosis of patients is possible, ***but a better understanding of leukemogenesis mechanisms is necessary in order to develop new selective combined targeted therapeutic strategies****. In fact, various promising agents are evaluated in clinical trials: a summary is given in Table 1 of the recent work [258].*

Let us now briefly mention some new promising therapies in the case of AML.

- ❍ **New cytotoxic agents**
  - ➡ **Vosaroxin**
- ❍ **FLT3 inhibitors**
  - ➡ **Sorafenib** (first generation, [252])
  - ➡ **Midostaurin** (first generation, [277])
  - ➡ **Quizartinib** (second generation)
- ❍ **PLK inhibitor**
  - ➡ **Dasatinib**
  - ➡ **Midostaurin** (which is also an FLT3 inhibitor)
- ❍ **Antibody-based therapies**
  - ➡ **antibodies targeting CD33 (e.g. gemtuzumab orogamicin)**
  - ➡ **antibodies targeting antigens such as CD123**
- ❍ **Epigenetic-modifiers therapies**
  - ➡ **inhibition of the mutant metabolic enzymes IDH1 and IDH2 (e.g. by infusing AG-120 and AG-221)**
- ❍ **Immune checkpoint blockade**

  Ipilimumab

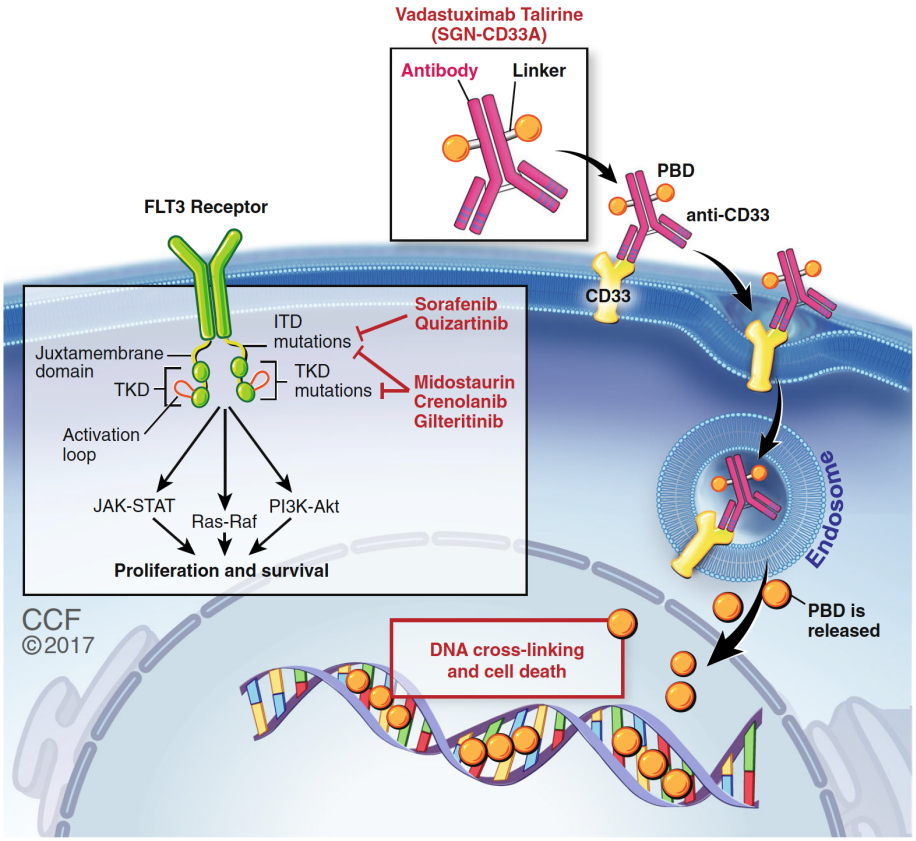

Fig. 2.12 FLT3 mutations in the signaling genes are of two subtypes (ITD and TKD) [166, 199, 258]. Mutated cells in these cases have an overproliferating advantage through RAS-RAF, JAK-STAT and PI3K-AKT ([163]) signaling pathways, along with a survival ability [85, 258]. **This figure is taken from [258]**.

Box 8. FLT3 inhibitors and therapies for AML (2017, [277])

Patients with acute myeloid leukemia (AML) and a FLT3 mutation have poor outcomes [277]. Since FLT3 mutations are frequently encountered in AML, several tyrosine kinase inhibitors are developed as possible effective drugs.

The third clinical trial of midostaurin has been conducted recently in [277]. The conclusion is outlined as follows ([277]):

«The addition of midostaurin to chemotherapy resulted in a 22% lower risk of death than that among patients who received chemotherapy plus placebo. Although the trial was not powered for subgroup analyses, overall survival was longer in the midostaurin group than in the placebo group among patients with a FLT3 mutation of the TKD subtype and among those with a FLT3 mutation of the ITD subtype with either a high ratio or a low ratio of mutant to wild-type alleles. »[277].

Finally, we mention that therapies targeting FLT3 mutations are highly toxic (due to their nonselectivity), and in addition, a FLT3-resistance mutations can be developed.

2.11 How do these biological concepts appear in this thesis?

The sections developed in this chapter give a limited overview on a number of interesting biological principles: some of them have recently emerge (e.g. CSCs, dormancy, and cell plasticity), and they are currently undergoing intensive biological research. The interested reader is referred to the references therein the sections for further detail on the topic. Our aim is to ease the reading of the manuscript, since the notions introduced here will be re-evoked throughout the upcoming three parts of the thesis.

Box 9. Hematopoiesis as a general modeling framework

Hematopoiesis provides a model for studying and understanding all the mammalian stem cells and their niches [209], but also all mechanisms of cell cycle, differentiation and maturation processes. One of the objectives behind the study of cell population growth is the development of new anti-tumor therapeutic strategies. Indeed, cancer-triggering mechanisms (including the case of AML), as well as all the complications that follow (such as drug resistance, mutation accrual, etc), are highly complex, and the contribution provided by mathematical tools in representing and understanding them is becoming increasingly necessary (in hematology [182, 240], and in various other biological fields [211, 210]). This is actually the concept of our project, in which we expect that a better understanding of the behavior of healthy and unhealthy blood cell dynamics, allows us to predict the cell fate evolution in treated or untreated leukemia, and then participates to the suggestion/elaboration of new anti-AML therapeutic drugs.

Concretely, medical research is looking for new combined targeted therapies able to counter overproliferation of cancer cells, to restore normal apoptosis and differentiation, and to avoid the high toxicity effects that characterize heavy non-selective chemotherapy. The ultimate goal behind mathematical modeling and analysis is to provide some inputs that should help biologists to suggest and test new treatment, and to contribute within multi-disciplinary groups in the opening of new perspectives against cancer.

Now, in this section, we want to guide the reader by briefly pointing out some key elements that link the upcoming chapters to the biological concepts discussed in the current one. In other words, the issue here is to specify how, where, and from what angle, we are going to approach the biological phenomena introduced in this chapter, in our mathematical work. For that purpose, we state the following details:

❍ The models we study in this thesis describe the dynamics of cell populations. All these models consider that cells may be in quiescence G_0, or they undergo a cell-division cycle (a proliferating phase). Our systems may be applied to different biological processes and tissues where a cell cycle is involved. However, we dedicate particular considerations to the case of hematopoiesis, and especially acute myeloblastic leukemia (AML). We recall that the hematopoietic system together with its regulatory mechanism, serve as a paradigm for the other biological systems with self-renewal SC populations sustaining the production of both short -and long-lived mature cells ([265]). However, a distinction between the hematopoietic system and other similar biological processes appears in our work, when it comes to discuss some treatment strategies and anti-cancer drugs. Indeed, in that context, we will only refer to the molecules already used -or currently undergoing trial phases- in the case of leukemia.

❍ We consider healthy situations (e.g. normal hematopoiesis), and other times we study some unhealthy cases (such as AML). In general, we separate between the studies of the healthy and unhealthy cell dynamics, while in some other situations we consider coexistence between heterogeneous cells (e.g. healthy and mutated cells), meaning that:

❑ Sometimes, the same mathematical model of cell population dynamics can be interpreted once in a healthy situation, and another one in an unhealthy situation, under some circumstances:

➢ if all the biological parameters (representing biological functions such as differentiation, cell death, proliferation, etc) involved in a model are healthy, then the model describes a healthy situation.

➢ if the model contains at least one abnormal parameter (such as an over-proliferation parameter, or a blockade in differentiation process, as frequently encountered in cancer), then the resulting system is said to be unhealthy.

The advantage of this separation is to highlight the medical insights in each situation, since the analysis objectives may differ depending on whether the situation is healthy or unhealthy.

❑ At other times, we will analyze some coupled models where heterogeneous healthy and mutated populations of cells may coexist in the same environment. The latter modeling approach takes into account the cohabitation between different categories of cells, such as the shared environment (i.e. niches) between healthy SCs population and CSCs population. In this case, we will particularly highlight the role of SCs (not necessarly hematopoietic ones), instead of studying the whole maturation process.

Box 10. A model of cohabitation between SCs and CSCs to study cancer dormancy (see [77] for an updated version)

At this juncture, we can mention that in the perspective of taking into account the coexistence between ordinary SCs and mutated SCs (CSCs, Section 2.3), and in light of AML clinical manifestation and treatments (discussed in Sections 2.10.1-2.10.2), we explore in Chapter 5 a coupled model between SC and CSC dynamics. In that configuration, a healthy SC compartment together with an abnormal (or unhealthy, mutated) cell compartment are involved. The latter subpopulation is affected by a first mutation that occurs in some genes encoding enzymes in epigenetics (e.g. TET2, DNMT3A [74, 238]). This event results in an increase of the self-renewing activity of the affected cells. A more serious pathological situation arises when a second mutation, affecting this time the pathways regulating the differentiation process such as NPM1 or transcription factors, appears on some cells. The superposition of these two events yields a blockade in differentiation. Finally, a subsequent mutation impairing proliferation control (e.g. FLT3, Section 2.10.1) appears in a subpopulation of cells that have already accumulated one or more of the previously mentioned mutations. The latter event activates an uncontrolled overproliferation of cells (i.e. they become CSCs), and thereby causes AML (see [137] for more information on the series of mutations - causing AML - described above).

The main motivation behind the work presented in Chapter 5 is to provide a framework for studying the issue of cancer dormancy, along with its therapeutic opportunities (see Sections 2.5). The analysis is focused on the maintenance of unhealthy cells at a controlled stable steady state, while ensuring that healthy cells survive.

❍ Differentiation and maturation processes (as in Figure 2.8) are important modeling aspects in the majority of models (those discussed in Chapters 3, 4 and 7), different from the model with one maturity level discussed in Box 10. This is in fact a modeling approach which goes through multi-maturity stages, where SCs are at the root of the process (i.e. the first maturity state), and cells gradually mature from one discrete stage into another. The notions dedifferentiation and transdifferentiation (cell plasticity, Section 2.4), as well as those related to the cell arrest at the cell-cycle checkpoints, appear in the the first part of the thesis, in models involving different maturity stages within a given cell hierarchy.

❍ Finally, we emphasize that the issue of AML treatment -current and emerging chemotherapy (Section 2.10.2)- is recurrent throughout the thesis, and particularly in Part II. The notions of blood regulation (Section 2.8), through growth factors or drugs (that are considered to act as growth factors) is widely discussed in Chapter 7 (Part III of the thesis).

Part I

The class of nonlinear systems with distributed delays

Chapter 3

Stability analysis of a nonlinear hematopoietic system with finite distributed delays

Synopsis. **We perform a stability analysis of a particular class of nonlinear systems with finite distributed delays, that extend some existing models from the literature ([8], [24]). A key feature of our analysis is that the conceived technique relies on the construction of suitable strict Lyapunov functionals for nonlinear time-delay systems. Even when a system is known to be asymptotically stable, it is always more advantageous to construct a *strict* Lyapunov functional for it. It is precisely from this point of view that we adopt a Lyapunov approach, which allows us to complement some analysis aspects and to address some new issues which are of importance -in practice- for hematopoietic systems.**

3.1 Overview of the chapter

We develop in the time-domain a Lyapunov technique of stability analysis for a nonlinear system with distributed delays describing cell dynamics in hematopoiesis. Based on previous studies by Mackey (see in particular [180]), the first revisited model was proposed and studied by Adimy *et al.* in [8], then it was widely analyzed by Özbay *et al.* in ([226], [225]) via an Input-Output approach. We also revisit the model proposed by Avila *et al.* in [24], via a construction of a novel Lyapunov-Krasovskii functional (LKF). Notice that the system introduced in [24] generalizes the one presented in [8] by considering some extra-dynamics describing the advantage of proliferation of unhealthy cells. For analysis purposes, two interesting biological situations lead us to investigate the stability properties of two meaningful steady states of the revisited models: the 0-equilibrium for unhealthy hematopoiesis and the positive equilibrium for the healthy case. Biologically, convergence to the 0-equilibrium means the extinction of all the generations of blood cells while the positive equilibrium reflects the normal process in which all the generations of blood cells will survive.

The Lyapunov constructions that we propose for these two steady states are slightly different in the sense that we take advantage of the positivity of the system under study in order to construct linear

functionals to analyze the 0-equilibrium, while we use some quadratic functionals to investigate the stability properties of the positive steady state. In addition, we complement some previous results given in [180], [8], [9], [226], [225] and [24], by establishing, for both equilibria, the exponential stability of solutions and by providing an estimate of their rate of convergence. In particular, we prove the global exponential stability of the trivial steady state under a less conservative condition than the one proposed in [9] for global asymptotic stability. Moreover, we investigate the case of time-varying differentiation and self-renewing rates: the latter case is expected to be useful when describing the blockade of differentiation in an unhealthy hematopoietic system and to model the drug effect (i.e. re-differentiation ability) when infusing treatments. Next, for the positive steady state, we complement already published results ([8], [225]) by providing an explicit approximation of its basin of attraction: this is a specific region defined as a sub-level of the suitable LKF that we are going to introduce, and which imposes a restriction on the initial conditions of the nonlinear system in order to ensure the exponential convergence of the trajectories to the positive steady state.

In addition, we perform a robustness analysis when the model is subject to some nonvanishing perturbations. Recall that many uncertainties may arise when one is mathematically modeling such a complex living process. For instance, the re-introduction function from resting to proliferating stages, modelled as a Hill-type function (as proposed by Mackey in [180] and then used in all subsequent works) is a striking source of uncertainties in the model, since it relies on approximate assumptions. Furthermore, it is important to be aware that several assumptions were made in order to establish the mathematical models that we revisit here. For instance, phenomena like dedifferentiation and transdifferentiation -known as *cell plasticity* features- are neglected in Mackey-type models. Plasticity mechanisms are briefly discussed in this chapter where they are introduced as uncertainties, and therefore followed by a robustness analysis. We will need to await Chapter 4 to deepen the study of hematopoietic systems which take into account some simple cases of plasticity abilities, by adapting a mathematical framework for dedifferentiation features in healthy and unhealthy tissues[1].

In light of the description mentioned above, we organize this chapter as follows: in Section 3.2 we expose the basics of the model of interest along with its important features. We subsequently establish an insight in Section 3.3 into the pursued objectives and novel expectations from the analysis that we perform. In particular, we highlight the importance of performing robustness analysis, considering time-varying parameters, estimating rate of convergence of solutions together with region attraction of the positive steady state. Then, in Section 3.5, we propose our stability analysis approach in the case of unhealthy hematopoiesis. It is mainly about the stability analysis of the trivial steady state of the models in [8] and [24] and their extensions. Next, in Section 3.6, the stability analysis of the strictly positive steady state is discussed in the context of healthy hematopoiesis. Numerical examples along with biological interpretations are provided throughout the different sections of the chapter. Finally, in Section 3.7 we bring some concluding remarks.

[1] In the Chapter 4, we enhance the role of differentiation and transdifferentiation by considering a hematopoietic models where cell plasticity is no more a marginal phenomenon, and cannot be considered as a perturbation, but it is fully modeled.

3.2 Models with finite distributed delays describing immature cell dynamics

In [8] and [24], hematopoietic cell dynamics are described through nonlinear transport equations which can be reduced with the characteristic method to some nonlinear systems with finite distributed delays. As in many other previous contributions (for instance, [8], [226], [9] and [225]), our interest in the current work is to find theoretical stability conditions depending on the different biological parameters involved in the hematological process. Going even further, we want to extend our approach to study nonlinear systems instead of their linear approximations, to prove exponential stability instead of asymptotic one, and to investigate robustness and the effect of some uncertain parameters. But now, some quick comments about the models of interest and their related literature are needed.

Let us now describe precisely the mathematical formulation of the models of interest (i.e. the systems in [8], and [24]). In fact, from a mathematical point of view, the model in [8] appears as a particular case of the one in [24]. More explicitly, they are equivalent when the fast self-renewing process introduced in [24] is zero. However, from a biological standpoint, the model in [24] is an extension which only applies for unhealthy hematopoiesis (since high proliferation is a symptom of disease. See Chapter 2). Therefore, in order to achieve the best presentation of this Chapter, we start from the model in [8], that we will first extend according to our expectations (by considering time-varying parameters and uncertainties), and analyze in both unhealthy (Section 3.5) and healthy (Section 3.6) cases. The analysis of the model in [24] (that we also extend by considering time-varying parameters) is performed in the Section 3.5, that deals with the unhealthy case.

Consequently, we begin now with the model in [8]. First, we recall from Chapter 2 that HSCs are immature undifferentiated and unspecialized cells, which are at the root of hematopoiesis, and which are responsible of blood cells production and their continuous replenishment. More precisely, HSCs are able to produce cells with the same maturity-level and also to differentiate into more mature and specialized cells with advanced features. During their proliferation, and more precisely during their *M-phase* (see Chapter 2), mitosis occurs for the cells which do not die by apoptosis, and each one of them divides into two daughter cells. At the maturation stage i, x_i denotes the total density of resting cells. We let δ_i denote the death rate of the resting cell population, while the apoptosis rate (i.e. the death rate of proliferating cells), is represented by γ_i, for all $i \in \{1,\dots,n\}$. At each division, a proportion $K_i \in (0,1)$ of dividing cells goes to the next more mature resting stage while the other part ($L_i = 1 - K_i$) stays at the same level i. Finally, $\beta_i(\cdot)$ is the re-introduction function from resting sub-population into the proliferating one, of the i-th immature generation of cells [180].

In this model, it is considered that proliferating cells can divide between the moment they enter to the proliferating phase and a maximum age $\tau_i > 0$. Moreover, immature cells enter into maturity after passing through n successive (immature) stages. It can be shown (see [8]) that for each compartment $i \in I_n = \{1,\dots,n\}$, the dynamics of immature cells are governed by the system:

$$\begin{aligned}\dot{x}_i(t) = &-\delta_i x_i(t) - w_i(x_i(t)) + 2L_i \int_0^{\tau_i} g_i(a) w_i(x_i(t-a))da \\ &+ 2K_{i-1} \int_0^{\tau_{i-1}} g_{i-1}(a) w_{i-1}(x_{i-1}(t-a))da,\end{aligned} \tag{3.1}$$

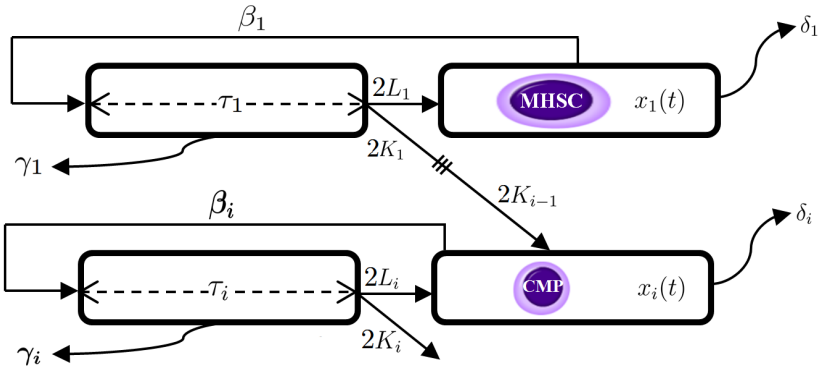

Fig. 3.1 Schematic representation of the primary phases in the production of immature myeloid progenitor cells, as introduced in the discrete-maturity model of [8]. In this age-structured model, for all $i \in \{1,\dots,n\}$, immature cells are in a resting phase (right hand side compartment, called G_0-phase) or in a proliferating phase (left hand side). This is a well-established representation since the work of Burns and Tannock in 1970 [49]. See the text for the details on the notations.

when $i > 1$ and

$$\dot{x}_1(t) \quad = \quad -\delta_1 x_1(t) - w_1(x_1(t)) + 2L_1 \int_0^{\tau_1} g_1(a) w_1(x_1(t-a)) da, \tag{3.2}$$

where, for all $i \in \{1,\dots,n\}$, the functions w_i are defined by $w_i(x_i) = \beta_i(x_i)x_i$, and,

$$g_i(a) = e^{-\gamma_i a} f_i(a), \tag{3.3}$$

where the function f_is describe cell divisions (mitosis), which are probability density functions. Since the mitosis occurs before the age limit τ_i, it follows that

$$f_i(a) \geq 0, \quad \text{for all}, a \in [0,\tau_i], \quad \text{and}, \quad \int_0^{\tau_i} f_i(a) da = 1. \tag{3.4}$$

Figure 3.2 shows that after n immature compartments, the cells only proliferate and differentiate (at rates k_j, $j \in \{1,\dots,m\}$). Thus, here it is considered that mature cells need to pass through m maturity compartments before becoming completely differentiated and then being ready to perform their functions in the bloodstream. Similarly to the immature proliferating cells (Figure 3.1), mature cells divide before reaching a maximum age θ_j and they can be lost by apoptosis with a rate σ_j.

It is sufficient to study the dynamics of the total densities of quiescent cells (x_i) given by (3.1)-(3.2), since the population of proliferating cells together with the dynamics of mature cells (Figure 3.2), have no impact on the dynamics of the resting immature cells x_i, for all $i \in I_n$ (see [8] and [225]). More precisely, the asymptotic behavior of proliferating immature cells and mature cells can be deduced from the study of the resting cells. Therefore, we focus on the stability properties of the system represented by equations (3.1)-(3.2).

Obvious biological facts induce that the parameters δ_i, L_i, K_i, τ_i and γ_i are positive for all $i \in \{1,\dots,n\}$ (recall that $K_i \in (0,1)$ and, $L_i = 1 - K_i$). Moreover, we assume that, for each $i \in \{1,\dots,n\}$, the function

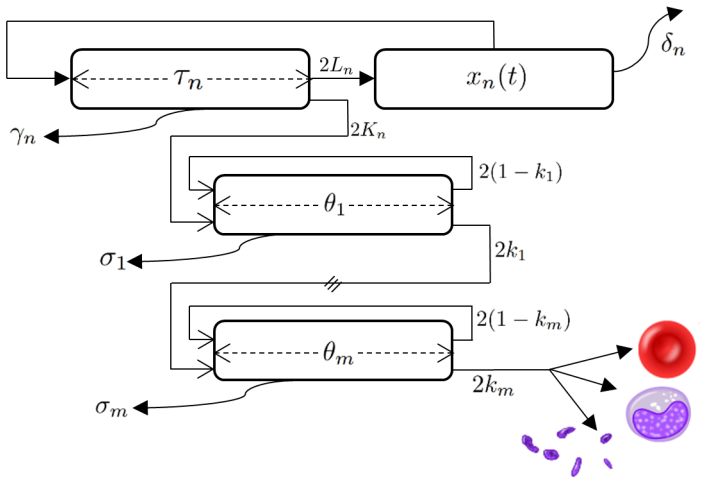

Fig. 3.2 The m mature compartments ([8]) in the myeloid lineage are precursors of the red blood cells, white blood cells and platelets. At the end of the maturation process, mature cells leave the bone marrow and go into the bloodstream [8].

$\beta_i(\cdot)$ is differentiable and decreasing, satisfying,

$$\lim_{a\to+\infty} \beta_i(a) = 0 \tag{3.5}$$

Furthermore, the following parameters are introduced to ease the notation,

$$C_i = \int_0^{\tau_i} g_i(d\ell)d\ell, \tag{3.6}$$

$$\alpha_i = 2L_iC_i - 1. \tag{3.7}$$

Remark 4. *For the sake of simplicity, we assume throughout the current chapter that the parameters α_i satisfy the conditions $\alpha_i > 0$, for all $i \in \{1,\dots,n\}$. In fact, biologically, the constants α_i quantify the difference between surviving self-renewing daughter cells and pre-existing mother cells [8]. The later assumption is necessary for the existence of a positive equilibrium (see the corresponding assumption in [225], argued by the growth-principle). However, the conditions $\alpha_i > 0$ are not necessary when studying the 0-equilibrium of the model* (3.1)-*(3.2), as illustrated in the next chapter, on even a more general model including infinite distributed delays.*

Let us now say some words about the model in [24], in which fast self-renewing dynamics have been introduced. This represents a generalization of the model of [8], since the latter model can be deduced from the former one. In practical terms, extra-dynamics are added to the model (3.1)-(3.2), in a way that makes possible to distinguish between cells entering a *normal* resting phase G_0 and a second one, denoted $\tilde{G}_0$ (see Figure (3.3)). Thus, cells entering $\tilde{G}_0$ are allowed to re-start a proliferating-cycle, via $\tilde{\beta}$, faster than the classical way from G, through β [24].

Remark 5. *In our analysis of the model presented in [24] (Section 5.1), we only focus on its 0-equilibrium, since it is the most biologically meaningful steady state for unhealthy hematopoiesis. Our interest in dormancy (see Chapter 2) is relevant only in coupled models, where healthy and unhealthy cells coexist.*

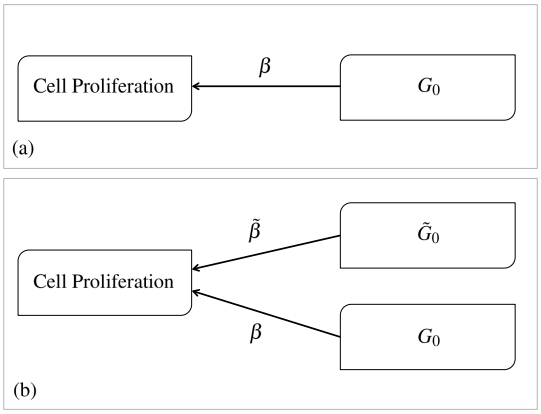

Fig. 3.3 The re-introduction function β, from the resting phase G_0 to the proliferating one is the unique available way in (a) that allows quiescent cells to start a cell-cycle (division). However, in (b), a sub-population of cells can follow a faster path through $\tilde{G}_0$ and $\tilde{\beta}$. By introducing the $\tilde{\beta}$ path, a distinction between healthy and unhealthy cells can be represented.

Having said that, we begin now by the stability properties of the model (3.1)-(3.2). First, we state some fundamental features of the studied model.

Positivity of the solutions

Proposition 1. *The solutions of system (3.1)-(3.2) associated with positive initial conditions are positive.*

Proof. First, let us prove that if $x_1(m) > 0$ for all $m \in [-\tau_1, 0]$ then $x_1(t) > 0$ for all $t \geq -\tau_1$. We prove this result by contradiction. Assume that there exists $t_1 > 0$ such that for all $t \in [0, t_1[$, $x_1(t) > 0$ and $x_1(t_1) = 0$ then from (3.2) we obtain

$$\dot{x}_1(t_1) = 2L_1 \int_0^{\tau_1} g_1(a) w_1(x_1(t_1 - a)) da > 0. \tag{3.8}$$

Since x_1 is of class C^1, there is Θ continuous such that $x_1(t) = \dot{x}_1(t_1)(t - t_1) + \Theta(t)(t - t_1)^2$. It follows there is $t_2 \in]0, t_1[$ such that $x_1(t_2) < 0$. This yields a contradiction. We deduce that for all $t \geq 0$, $x_1(t) > 0$.

Arguing similarly, we can prove that, if for all integer $i \in \{1, \ldots, n\}$, and all $m \in [-\tau_i, 0]$, $x_i(m) > 0$, then $x_i(t) > 0$, for all $t \in [-\tau_i, +\infty)$. We conclude that the positive orthant is forward invariant. Thus, throughout this paper, we consider only positive solutions of (3.1)-(3.2). □

We will say that an equilibrium point of a system is globally asymptotically stable when all its *positive* solutions converge to it. In the following part we give the main condition of existence of a positive steady state of system (3.1)-(3.2). The reader is referred to [8] for more details on the existence of equilibrium points, especially for the so-called *axial steady states* (equilibrium points belonging to the boundaries of the positive orthant, apart from the origin), that we do not emphasize here, since they are biologically irrelevant (moreover, their analysis is readily deduced from the one of the origin and the positive steady state). Therefore, our main objectives in Sections 3.5 and 3.6 concern the analysis of the origin and the strictly positive steady state using a new approach.

Existence of Steady states

One notices that the *trivial steady state* $X^0 = (0,\dots,0)$ always exists. Biologically, convergence to this point means the extinction of all generations of immature cells. In contrast, the *positive steady state*, we shall denote by $X^e = (x_1^e,\dots,x_n^e)$, where $x_i > 0$ for all $i \in I_n$, does not always exist. The following result gives a necessary and sufficient condition of existence of X^e.

Proposition 2. *The system (3.1)-(3.2) admits a positive equilibrium point $X^e = (x_1^e,\dots,x_n^e)$, where $x_i > 0$ for all $i \in I_n$, if and only if the condition*

$$\beta_1(0) > \frac{\delta_1}{\alpha_1}, \tag{3.9}$$

is satisfied.

Proof. Let us assume that the system (3.1)-(3.2) admits a positive equilibrium point X^e. Then one can check readily that, necessarily,

$$\left[\alpha_1\beta_1(x_1^e) - \delta_1\right] x_1^e = 0. \tag{3.10}$$

Since β_1 is a continuous positive and decreasing function such that (3.5) is satisfied, we deduce that (3.10) admits a solution $x_1^e > 0$ if and only if the condition (3.9) is satisfied. We conclude that if (3.1)-(3.2) admits a positive equilibrium point, then necessarily the condition (3.9) is satisfied. Now, assume that the condition (3.9) is satisfied. Then necessarily, there exists $x_1^e > 0$ such that (3.10) is satisfied. Next, let us proceed by induction. Assume there is $j \in \{1,\dots,n-1\}$ such that there are positive constants $x_i^e > 0$ such that

$$\delta_i x_i^e - \alpha_i\beta_i(x_i^e)x_i^e = 2K_{i-1}C_{i-1}\beta_{i-1}(x_{i-1}^e)x_{i-1}^e \tag{3.11}$$

when $i \in \{2,\dots,j\}$ and $\delta_1 x_1^e - \alpha_1\beta_1(x_1^e)x_1^e = 0$. Now, observe that (3.5) implies that the function $\varpi(m) = \delta_{j+1}m - \alpha_{j+1}\beta_{j+1}(m)m$ satisfies $\varpi(0) = 0$ and $\lim_{m\to+\infty}\varpi(m) = +\infty$. It follows that there exists $x_{j+1}^e > 0$ such that

$$\delta_{j+1}x_{j+1}^e - \alpha_{j+1}\beta_{j+1}(x_{j+1}^e)x_{j+1}^e = 2K_jC_j\beta_j(x_j^e)x_j^e. \tag{3.12}$$

We conclude that for all $i \in \{2,\dots,n\}$, there are positive constants $x_i^e > 0$ such that

$$\delta_i x_i^e - \alpha_i\beta_i(x_i^e)x_i^e = 2K_{i-1}C_{i-1}\beta_{i-1}(x_{i-1}^e)x_{i-1}^e. \tag{3.13}$$

We deduce easily that the system (3.1)-(3.2) admits a positive equilibrium point X^e. □

3.3 Pursued objectives in hematopoietic models

In order to highlight the issues to be addressed, we need to situate ourselves and clearly position the work in context. For that, we will give a very short summary of the main aspects in the analysis of time-delay hematopoietic systems. Here, we want to point out the trends and the objectives fixed/reached by research

in this field. Several mathematical models are developed in the literature, all of them share in common the aim of modeling a healthy behavior of hematopoietic cells. Then, from this normal/healthy model, an abnormal case is derived, modeled, and analyzed. The goal is to enhance the understanding of the unhealthy situation by studying the conditions that disturb the healthy model and cause pathology (e.g. by considering an epigenetic mutation that induces a sudden change in the healthy model parameters).

3.3.1 Strengths and weaknesses of the formerly used approaches

In a series of works by Mackey and his co-authors -during more than four decades- a paramount interest was given to hematological disorders where an oscillatory (periodic) behavior is observed [132] (starting from earliest works [181], [180], until the most recent ones [170]). We can for instance mention the importance attached to *neutrophenia* in [37] and [66]. In these two papers -and the references therein- the authors deal with a pathological disorder in which oscillations are observed in the count of red blood cells, white blood cells and platelets (by the way, these oscillations often occur under the same oscillatory period). We can also mention the contribution [66], in which *periodic chronic myeloid leukemia* is studied. In the latter case, objectives behind the analysis are the same as those of [37]-[66], and their conclusions emphasize how periodic behavior may occur in all blood compartments count.

We focus now on one of the most recent works, namely [170]. In this study, the interesting case of *cyclical thrombocytopenia* (CT) is revisited. It is worth mentioning that during CT disease, large period oscillations in platelets compartment are observed, whereas red and white cell counts remain unchanged. Therefore, the model introduced in [170] includes only platelets dynamics, while the one presented in [66] is concerned with different lineages (see Figure 3.4). In summary, most of the time, Mackey's team focuses on blood lineages that are likely to exhibit abnormal oscillations. Thus, from a mathematical point of view, the analysis is often oriented towards the existence of a *Hopf bifurcation* from which oscillatory solutions emerge.

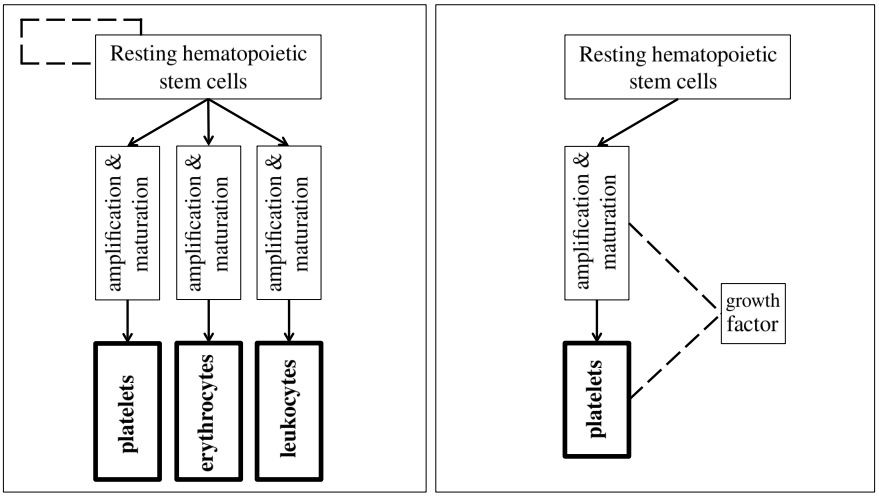

Fig. 3.4 An approximate reproduction of the cartoon representations of the models in [66] (on the left) and [170] (on the right). One notices that the recent model in [170] focuses only on platelets dynamics, since it is the unique compartment in which cyclical thrombocytopenia causes large fluctuations (oscillations). On the other hand, the model in [66] contains all the lineages, since period chronic myeloid leukemia may cause oscillations in all cell types [132].

Turning now to the works of Adimy *et al.* ([8], [2], [9], [4]), Avila *et al.* ([24], [23]), Özbay *et al.* ([225], [224] [226]). There is no doubt on the fact that all these models find their origin in the Mackey's type model (particularly in the pioneer work [180]). However, the perspectives are slightly different and a new interest is rising for the case of *acute myeloid leukemia*. Recall that in the latter blood disorder, an overproliferation of abnormal -immature- white blood cells is observed. Coherently, the search for a Hopf Bifurcation (i.e. oscillatory solutions) should no longer be the main issue (but, as an exception, it is further noted in [4] that the existence of Hopf Bifurcations is investigated, even if the model seems to be designed for a non-periodic disease). Nevertheless, for above quoted contributions by Özbay, Avila, and their respective collaborators, it is clearly noted that serious interest is being paid to the regional asymptotic stability of constant steady states. Therefore, the idea of the existence of a Hopf bifurcation is now abandoned when studying the typical case of acute myeloid leukemia. Clearly, throughout our work, we are fully committed to this vision and we continue to develop and complement the work started in [225].

To summarize, in light of the above discussion, we conclude that notable advances have been made in the field of hematopoietic systems modeling and analysis, which is an active area. The major achievements are completed within the topic of periodic diseases, while some complementary material need to be developed to model and analyze non-periodic diseases, mainly characterized by overproliferation of unhealthy cells.

A second point (particularly highlighted in [225]) that we have already raised in the introduction, regards the analysis of nonlinear systems instead of their linear approximations. This remark is valid for almost all the previously mentioned works, when it comes to study the positive steady states of the systems. In fact, here we are facing a common requirement for many types of models where it is well-known that analyzed systems may evolve far from their steady states. Thus, it is a general problem which extends beyond the hematopoietic systems (for instance, we can mention *chemostat* models [197]). In fact, as things now stand, the analysis of hematopoietic systems is mainly done without considering the nonlinear aspects of the models (e.g. [170]) or the effect of disturbances and uncertain parameters.

3.3.2 Alternative approaches to meet novel expectations

Now, we are able to situate ourselves in the current study of hematological disorders. First, local asymptotic stability (in particular when studying the positive steady states of (3.1)-(3.2)), is the only result that can be achieved using frequency approaches. On the other hand, we want to extend the study and provide regional exponential stability of this steady state. Indeed, from a biological standpoint, in order to understand a physiological phenomenon and to possibly improve its therapy strategy (let say for instance that we want to adapt a dosage of medication), it appears clear that a result giving a local asymptotic stability is less useful than a one giving local exponential stability, with an estimate of the rate of convergence of the solutions (see Section 3.5.2) and a subset of the basin of attraction of the steady state, as well as establishing results when parameters are uncertain or time-varying (both under the effect of the disease and the drugs).

Few years after [8], the system (3.1)-(3.2) was widely analyzed in [225] using an Input-Output approach. In particular, results regarding the stability properties of the positive equilibrium were improved

(see Section 2.3 of [225]), then they prepared the next steps in the study of acute myeloid leukemia. More precisely, in the concluding remarks of [225], we can read that: «*Of course, periodic medications will make the system parameters vary in time; analysis of such a time varying nonlinear system with distributed delays requires a separate study*», and, a few lines further on: «*Although leukemia is the best understood cancer, as far as dynamical modeling is concerned, there are still practical difficulties in determining the parameters of the mathematical model considered here*», then, they continue to say: «*Other lines of future work include consideration of different types of (possibly higher order) cell division rates* f_i ».

In the light of -but not exclusively- all the the remarks mentioned above, we revisit in this chapter the models studied in ([8], [9], [225], [24]) describing hematopoiesis. We have chosen to approach these matters by a Lyapunov approach, since this theory offers strong and effective tools in order to deal with the above mentioned issues. However, we need first to find a suitable Lyapunov functional, which is not always an easy task.

3.3.3 What can Lyapunov theory bring more?

Since the middle of the last century, the extension of the classical theory of Lyapunov to systems with delay ([251]) allowed stability analysis of a large class of dynamical systems constantly encountered in biology, physiology, population dynamics and many other real-life problems (see [211] for more information). The advantages of knowing Lyapunov functions or functionals are fundamental: for instance, they make it possible to establish robustness results of Input-to-State-Stability type (see for instance [187]), to estimate rates of convergence of solutions, and they can also be used to determine estimates of the basin of attraction for locally asymptotically stable equilibrium points. However, in many cases, the construction of Lyapunov Krasovskii-functionals is a difficult task. This is indeed the case for the model of hematopoiesis that we are studying here (and, more generally, throughout all our work).

It is worth mentioning that the stability results of the origin of the models in [8] and [4], are already provided using Lyapunov techniques. Later, we perform a comparison between our results and earlier ones. However, we can already point out that our constructions slightly relax some earlier stability conditions and ensure global exponential stability with an estimate on the decay rate of the solutions. Finally, the LKF approach for the positive equilibrium point is a novel approach that will allow us to complement the already published work (using frequency and Input-Output frameworks), and thus offering the opportunity to consolidate our general knowledge on the analysis aspects of the studied models.

3.4 Extending the description of the mathematical model

In view of what has been brought up in the previous section, we enhance the flexibility of the model (3.1)-(3.2) by considering its new version:

$$\begin{aligned}\dot{x}_i(t) =& -\delta_i x_i(t) - w_i(x_i(t)) + 2L_i(t)\int_0^{\tau_i} g_i(a)w_i(x_i(t-a))da \\ &+ 2K_{i-1}(t)\int_0^{\tau_{i-1}} g_{i-1}(a)w_{i-1}(x_{i-1}(t-a))da + \varepsilon_i(t),\end{aligned} \tag{3.14}$$

where $\varepsilon_i(t) \in [0, \overline{\varepsilon_i}]$, $\overline{\varepsilon} > 0$, and $L_i(\cdot)$ are functions of class $\mathscr{C}^1$, and similarly to (3.1)-(3.2), $K_i(t) = 1 - L_i(t)$, for all $t \geq 0$, with the convention $K_0(t) \equiv 0$. In explicit terms, here we are considering a system in which differentiation and self-renewing rates are time-varying (or, uncertain), and, in addition, subject to nonvanishing perturbations ε_i. In fact, it can be proven that nonvanishing perturbations arise from cell plasticity, if considered as unknown input for the resting population, and thereby lead to system (3.14) with $\varepsilon_i(t) \in [0, \overline{\varepsilon}_i]$, as illustrated in the sequel.

3.4.1 Origin of nonvanishing perturbations

First, as already mentioned in [225] the parameters of the studied model, at the time being, are not well-estimated even if some nominal healthy values are given in the literature (see for instance, [180], [4]). Moreover, we notice that many uncertainties may arise when one is mathematically modeling such a complex living process. A striking illustration in the models of [180], [8], [24] -among others- comes from the reintroduction function β (and $\tilde{\beta}$, which has a similar form): the Hill function that we consider was proposed by Mackey in [180] (and used in all subsequent works) under several assumptions (four main assumptions which are given in [180], page 951, the paragraph between Eq (3.1) and Eq (3.2)). In fact, it is not difficult to observe that uncertainties on that function fall within the scope of *nonvanishing perturbations* (see Chapter 1). In addition, several assumptions were made in order to determine the studied mathematical models (even if some of them are not explicitly mentioned). For instance, differentiation is considered in this model, while *dedifferentiation* and *transdifferentiation* (see Chapter 2, *cell plasticity*) are not modeled. Let us assume now that some differentiated cells that belong to a given hierarchy $i \in I_n = \{1, \ldots, n\}$ may join a less mature cell compartment by dedifferentiation (in fact, even cells which do not belong to the studied hierarchy may join any compartment by transdifferentiation). Therefore, if we consider that for any $i \in I_n$, $d \equiv \varepsilon_i$ is the input coming from a different (non-modeled) hierarchy (e.g. the lymphoid one) by dedifferentiation or transdifferentiation, then ε_i corresponds to a bounded disturbance, under the assumption that cells plasticity is a limited phenomenon, of acceptable scale, which is biologically reasonable. Therefore, we can show that it is possible to describe the dynamics of the total population of resting cells by model (3.14). More precisely, in this case, the hematopoietic system is described by the age-structured (McKendrick-type) PDE system:

$$\begin{cases} \frac{\partial p_i(t,a)}{\partial t} + \frac{\partial p_i(t,a)}{\partial a} + \gamma_i p_i(t,a) + h_i(a) p_i(t,a) = 0, \\ \frac{\partial r_i(t,a)}{\partial t} + \frac{\partial r_i(t,a)}{\partial a} + \delta_i r_i(t,a) + \beta_i \left(\int_0^\infty r_i(t,a) da \right) r_i(t,a) = 0, \end{cases} \tag{3.15}$$

where $p_i(t,a)$ is the density of proliferating cells at the immature stage i, of age a and at time t, and, similarly, $r_i(t,a)$ represents the density of resting cells at the immature stage i. The renewal conditions (new births) -which give the birth rate at the initial age $a = 0$ (see Chapeter 1)- are introduced through the following boundary conditions:

$$\begin{cases} p_i(t,0) = \beta_i \left(\int_0^\infty r_i(t,a) da \right) \int_0^{\tau_i} r_i(t,a) da, \\ r_i(t,0) = 2K_{i-1}(t) \int_0^{\tau_{i-1}} h_{i-1}(a) p_{i-1}(t,a) da + 2L_i(t) \int_0^{\tau_i} h_i(a) p_i(t,a) da + \varepsilon_i(t), \end{cases}$$

where the second equation of $r_i(t,0)$ expresses the fact that new births at time $t \geq 0$ are composed by: i) the new density of cells coming from the same generation $i \in I_n$ by the self renewing process (i.e. the term containing L_i), ii) the density of cells coming from the previous generation $i-1$ by differentiation (i.e. the term containing K_{i-1}), and, iii) the density of new births coming from some non-modelled hierarchies (e.g. Pre-B cells from the lymphoid lineage that become stem cells [259]), by dedifferentiation or transdifferentiation (the flux that we are denoting ε_i).

Hence, using the method of characteristics, we prove that for $t \geq 0$ sufficiently large we get

$$p_i(t,a) = p_i(t-a,0)e^{-\gamma_i a}e^{-\int_0^a h_i(m)dm}.$$

Therefore, by integrating the second equation of the PDE system, with respect to the age variable a between 0 and ∞, and using the boundary conditions, we can easily prove that the total density of resting cells $x_i(t) = \int_0^{+\infty} r_i(t,a)da$, satisfies (3.14), with $\varepsilon_i(t) \in [0, \overline{\varepsilon}_i]$.

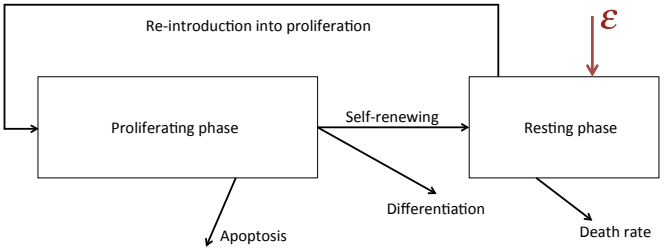

Fig. 3.5 A first step to model cell plasticity is to consider it as an unknown disturbance. The input ε represents the flux of cells generated by dedifferentiation/transdifferentiation, and it leads to the model (3.14) with nonvanishing perturbations.

In summary, two main reasons are retained for the origin of disturbances: i) the lack of accuracy when modeling the laws governing complex living organisms, and, ii) difficulties in modelling more complex phenomena.

3.4.2 Summary of the model equations, without fast-renewing dynamics

Using an alternative approach, our aim here is to deepen the analysis as well as to solve some open issues of the models in [8] and [24] which are of importance in practice. For that, we are considering the model described by:

$$\begin{aligned} \dot{x}_i(t) = &-\delta_i x_i(t) - w_i(x_i(t)) + 2L_i(t)\int_0^{\tau_i} g_i(a)w_i(x_i(t-a))da \\ &+ 2K_{i-1}(t)\int_0^{\tau_{i-1}} g_{i-1}(a)w_{i-1}(x_{i-1}(t-a))da + \varepsilon_i(t), \end{aligned} \tag{3.16}$$

with the convention $K_0(\cdot) = 0$, and where for all $i \in I_n = \{1,\ldots,n\}$, $n \geq 1$, x_i denotes the total density of resting cells of generation i. A resting cell is a cell that is not active in the process of dividing. The constant δ_i denotes the death rate for the resting cell population. The re-introduction function from resting into proliferating sub-population of the i-th generation is denoted $\beta_i(\cdot)$, and depends on the the total density of resting cells x_i. It is assumed to be a differentiable and decreasing function such that $\lim_{a\to+\infty} \beta_i(a) = 0$.

Proliferating cells can divide between the moment they enter the proliferating phase and a maximal age $\tau_i > 0$, while the apoptosis rate, γ_i, is the death rate of proliferating cells. Moreover, biological facts induce that the parameters δ_i, L_i, K_i, τ_i and γ_i are positive for all $i \in I_n$. Next, we have $w_i(x_i) = \beta_i(x_i)x_i$, $g_i(a) = e^{-\gamma_i a} f_i(a)$, where the f_is are $\mathscr{C}^1$ functions representing the cell division probability densities, such that $f_i(a) \geq 0$ for all $a \in [0, \tau_i]$, and $\int_0^{\tau_i} f_i(a)da = 1$, since the mitosis occurs before the limit age τ_i. At each division, and at any time $t \geq 0$, a proportion $K_i(t) \in [K_{i\min}, K_{i\max}] \subset (0,1)$ of dividing cells goes to the next resting stage while the other part ($L_i(t) = 1 - K_i(t)$, for all $t \geq 0$) stays at the same level i. Finally, we are going to perform a robustness analysis of (3.16) under nonvanishing perturbation terms $\varepsilon_i(t) \in [0, \overline{\varepsilon}_i]$, where $\overline{\varepsilon}_i > 0$, for all $i \in I_n$ and $t \geq 0$. Below are some fundamental remarks that complete the description of the model and its equations.

Remark 6. *We are assuming basic concepts in order to distinguish between healthy and unhealthy situations in the models that we are studying in this chapter (more refined descriptions will be achieved for models involving cohabitation between healthy and unhealthy cells in Part II). Thus, intuitively, we consider that the model* (3.16) *describes a cancer state when some of its biological parameters are abnormal (i.e. being different from healthy parameters, or becoming time-varying to model the effect of appropriate infused drugs) and it reflects a healthy situation when all its parameters are normal. Then, using a Lyapunov technique, our aim is to improve some existing results in two different contexts: i) we provide theoretical conditions to eradicate cancer cells in an unhealthy situation (Section 3.5), and, ii) we ensure the survival of healthy cells in normal hematopoiesis (Section 3.6).*

Remark 7. *From biological considerations, and given what we know about cell-plasticity, it is suggested that the flux of cells (the input ε_i in Figure (3.5)) generated by dedifferentiation, is a permanent excitation, such that $\varepsilon_i(t) \to \overline{\varepsilon}_i$ when $x_i \to 0$. This is due to the fact that dedifferentiation increases in order to compensate cell loss in perturbed tissues (e.g. after injury). In other words, cells plasticity is often interpreted as a mechanism which is invoked to allow regeneration of damaged tissue [280]. However, we do not require this information when performing the stability analysis.*

Remark 8. *Considering a time-varying apoptosis is also useful for therapeutic issues, since this parameters can be targeted by drugs. However, this issue is not addressed in the current chapter and will be covered in the next one. The reason behind this choice is that the apoptosis rate parameter appears in the PDE-equations modelling cell dynamics (that lead to the time-delay system studied here), while differentiation and self-renewing functions appear in the boundary conditions. Therefore, it is straightforward to consider differentiation and self-renewal processes as time-varying parameters in the time-delay system, while the transition between the transport equations to the time-delay system (using the method of characteristics, see Chapter 1) needs to be carefully rechecked (as illustrated in Chapter 4).*

Remark 9. *Since the nonvanishing perturbations $\varepsilon_i(t)$, for all $t \geq 0$ and $i \in I_n$, satisfy $\varepsilon_i(t) \geq 0$, we can prove by arguing as in Proposition 1, that the positive orthant is forward invariant.*

3.5 Stability analysis of the trivial steady state in the unhealthy hematopoiesis

In this section, we emphasize the case of unhealthy hematopoiesis. We start with the model (3.1)-(3.2) (i.e. (3.16), with time-independent parameters and without disturbances).

3.5.1 Global asymptotic stability of the 0-equilibrium

First, we construct a global nonlinear LKF for the system (3.1)-(3.2), from which, in conjunction with Barbalat's lemma, the global asymptotic stability of the origin is proved. In fact, in this first step, we are already improving the existing results -provided in [8] and [9]- by proving global asymptotic stability of the origin under a less conservative condition than the one provided in [9].

Theorem 1. *The system (3.1)-(3.2) admits the origin X^0 as a globally asymptotically stable equilibrium point if for all $i \in \{1,\dots,n\}$,*

$$s_i := \delta_i - (2C_iL_i - 1)\,\beta_i(0) > 0 \tag{3.17}$$

Remark 10. *i) We can readily check that if* (3.17) *is satisfied, then the origin is the unique equilibrium of the nominal system* (3.1)-(3.2)*.*
ii) Using a frequency domain approach, it was proved in [8] that (3.17) *guarantee local asymptotic stability of the origin. In [9], more restrictive conditions than* (3.17) *(due to the fact that $L_i < 1$, for all $i \in I_n$) were given to ensure global asymptotic stability of the origin.*
iv) Notice that the Lyapunov functional that we will introduce in this section is unusual since it is approximated at the origin by a linear function (see [124] for linear functional for positive systems).

Proof. Let us introduce for all $i \in \{1,\dots,n\}$ the functionals

$$\rho_i(x_{it}) = \int_{t-\tau_i}^{t}\int_{m}^{t} g_i(m-a+\tau_i)w_i(x_i(a))\,da\,dm. \tag{3.18}$$

Simple calculations give:

$$\dot{\rho}_i(t) = C_i w_i(x_i(t)) - \int_{t-\tau_i}^{t} g_i(t-a)w_i(x_i(a))\,da, \tag{3.19}$$

where C_i is the constant defined in (3.6). Now, we focus on the first compartment ($i = 1$). Let us introduce a functional:

$$\zeta_1(x_{1t}) = x_1(t) + 2L_1\rho_1(x_{1t}). \tag{3.20}$$

Then its derivative along the trajectories of (3.2) satisfies

$$\begin{aligned}\dot{\zeta}_1(t) &= 2L_1\int_0^{\tau_1} g_1(a)w_1(x_1(t-a))\,da - \delta_1 x_1(t) - w_1(x_1(t)) \\ &\quad +2L_1C_1w_1(x_1(t)) - 2L_1\int_{t-\tau_1}^{t} g_1(t-a)w_1(x_1(a))\,da \\ &= [-\delta_1 + \alpha_1\beta_1(x_1(t))]x_1(t).\end{aligned} \tag{3.21}$$

Next, we consider the case where the inequalities (3.17) are satisfied and we show that X^0 is globally asymptotically stable. We consider a positive solution of (3.1)-(3.2).

Since β_1 is decreasing and $x_1(t) > 0$ for all $t \geq 0$, the inequality

$$\dot{\zeta}_1(t) \leq -s_1x_1(t) \tag{3.22}$$

with $s_1 = \delta_1 - \alpha_1\beta_1(0)$ is satisfied for all $t \geq 0$.

Now, consider the functional:

$$\zeta_2(x_{1t},x_{2t}) \quad = \quad x_2(t)+2L_2\rho_2(x_{2t})+2K_1\rho_1(x_{1t})+\tfrac{3K_1C_1\beta_1(0)}{s_1}\zeta_1(x_{1t}). \tag{3.23}$$

Simple calculations give

$$\begin{array}{rcl}\dot{\zeta}_2(t) & = & 2K_1\int_0^{\tau_1} g_1(a)w_1(x_1(t-a))da+2L_2\int_0^{\tau_2} g_2(a)w_2(x_2(t-a))da \\ & - & \delta_2x_2(t)-w_2(x_2(t))+2L_2C_2w_2(x_2(t))-2L_2\int_{t-\tau_2}^{t} g_2(t-a)w_2(x_2(a))da \\ & + & 2K_1C_1w_1(x_1(t))-2K_1\int_{t-\tau_1}^{t} g_1(t-a)w_1(x_1(a))da+\tfrac{3K_1C_1\beta_1(0)}{s_1}\dot{\zeta}_1(t).\end{array} \tag{3.24}$$

Using (3.22), we obtain

$$\dot{\zeta}_2(t) \quad \leq \quad \left[-\delta_2+\alpha_2\beta_2(x_2(t))\right]x_2(t)+K_1C_1\left[2\beta_1(x_1(t))-3\beta_1(0)\right]x_1(t). \tag{3.25}$$

Since the functions β_1 and β_2 are decreasing, the inequality

$$\dot{\zeta}_2(t)\leq\left[\underbrace{-\delta_2+\alpha_2\beta_2(0)}_{-s_2}\right]x_2(t)-K_1C_1\beta_1(0)x_1(t) \tag{3.26}$$

holds. Next, by induction, with $X=(x_1,\ldots,x_n)$, we easily determine constants $\nu_i>0$, $\tilde{\nu}_i>0$ and $\lambda_n>0$ such that the derivative along the trajectories of (3.1)-(3.2) of the functional

$$\zeta_n(X_t)=\sum_{i=1}^{n}[\nu_ix_i(t)+\tilde{\nu}_i\rho_i(x_{it})] \tag{3.27}$$

satisfies

$$\dot{\zeta}_n(t)\leq-\lambda_n\sum_{i=1}^{n}x_i(t). \tag{3.28}$$

By integrating this inequality, we get, for all $t\geq 0$,

$$\zeta_n(X_t)-\zeta_n(X_0)\leq-\lambda_n\int_0^t\sum_{i=1}^{n}x_i(a)da. \tag{3.29}$$

Since $\zeta_n(X_t)>0$ for all $t\geq 0$, it follows that

$$\sum_{i=1}^{n}\int_0^t x_i(a)da\leq\frac{\zeta_n(X_0)}{\lambda_n}. \tag{3.30}$$

Moreover the inequality $\zeta_n(X_t)\geq\sum_{i=1}^{n}\nu_ix_i(t)$ and (3.29) imply that $X(t)$ is bounded. We deduce easily that $X(t)$ is uniformly continuous. Then from (3.30) and Barbalat's lemma (see Chapter 1), we deduce that, for all $i\in\{1,\ldots,n\}$,

$$\lim_{t\to\infty}x_i(t)=0. \tag{3.31}$$

□

3.5.2 Global exponential stability of the 0-equilibrium

In the previous section, we proved asymptotic stability of X^0 of the system (3.1)-(3.2). Now, we establish its global exponential stability and we estimate the rate of convergence of the solutions under the same stability conditions. Thus, we slightly modify the analytic expression of the Lyapunov functional by adding exponential functions in the double integral terms.

Theorem 2. *The nominal system (3.1) admits the origin, X^0, as a globally exponentially stable equilibrium point if for all $i \in I_n$, the inequalities*

$$s_i := \delta_i - (2C_iL_i - 1)\,\beta_i(0) > 0, \tag{3.32}$$

are satisfied. If

$$s_1 := \delta_1 - (2C_1L_1 - 1)\beta_1(0) < 0, \tag{3.33}$$

then no positive solution converges to X^0.

Remark 11. *Using a frequency domain approach, it was proven in [8] that if* (3.33) *is satisfied then the system is unstable. So here, in the second part of Theorem 2, we are proving a similar result (i.e. that the origin is not attractive, see Chapter 1) using a different approach that relies on a construction of LKF*[2].

Proof. First, let us pick a family of positive constants $\rho_i^\dagger$, to be selected later, and define for all $i \in I_n$, the functionals

$$v_i(x_{it}) = \int_{t-\tau_i}^{t}\int_{m}^{t} e^{-\rho_i^\dagger(t-m-\tau_i)} g_i(m+\tau_i-a) w_i(x_i(a))\,da\,dm. \tag{3.34}$$

For all $i \in I_n$, the derivative of the functional (3.34) along the trajectories of the nominal system (3.1) satisfies

$$\begin{aligned}\dot{v}_i(t) &= -\rho_i^\dagger v_i(x_{it}) - \int_{t-\tau_i}^{t} g_i(t-a) w_i(x_i(a))\,da + w_i(x_i(t)) \int_0^{\tau_i} e^{\rho_i^\dagger a} g_i(a)\,da \\ &\leq -\rho_i^\dagger v_i(x_{it}) - \int_{t-\tau_i}^{t} g_i(t-a) w_i(x_i(a))\,da + w_i(x_i(t)) e^{\rho_i^\dagger \tau_i} C_i,\end{aligned}$$

where the last inequality is a consequence of (3.6). Let us introduce the following functional for the first compartment of hematopoietic stem cells:

$$\mathscr{V}_1(x_{1t}) = x_1(t) + 2L_1 v_1(x_{1t}). \tag{3.35}$$

Its derivative along the trajectories of the nominal system (3.1) satisfies

$$\dot{\mathscr{V}}_1(t) \leq -\delta_1 x_1(t) - 2L_1\rho_1^\dagger v_1(x_{1t}) - \left[1 - 2L_1 e^{\rho_1^\dagger \tau_1} C_1\right] w_1(x_1(t)). \tag{3.36}$$

[2] Although Lyapunov theory is usually used to provide *sufficient* stability conditions, sometimes the Lyapunov functional candidate can be used to prove *instability* results. Instability Lyapunov techniques are much less prevalent than stability ones, but when they apply, it becomes sometimes possible to provide necessary and sufficient stability conditions. For instance, in Theorem 2, we notice that for the sub-system $i = 1$ the condition (3.32) is a necessary and sufficient condition for the global exponential stability of the origin of system (3.2).

Since $\alpha_1 > 0$, we conclude that for all $\rho_1^\dagger > 0$, the inequality $2L_1 e^{\rho_1^\dagger \tau_1} C_1 - 1 > 0$ is satisfied. Therefore, using $w_1(x_1(t)) \leq \beta_1(0) x_1(t)$, it follows from (3.36) that:

$$\dot{\mathscr{V}}_1(t) \leq -\left[\delta_1 - \left(2L_1 e^{\rho_1^\dagger \tau_1} C_1 - 1\right) \beta_1(0)\right] x_1(t) - 2L_1 \rho_1^\dagger v_1(x_{1t}). \tag{3.37}$$

Now, if (3.32) is satisfied, we choose $\rho_1^\dagger = \frac{1}{2\tau_1} \ln\left(\frac{\delta_1 + \beta_1(0) + 2L_1 C_1 \beta_1(0)}{4L_1 C_1 \beta_1(0)}\right)$, which satisfies $\rho_1^\dagger > 0$ since $s_1 > 0$. Then we obtain $\delta_1 - \left(2L_1 e^{\rho_1^\dagger \tau_1} C_1 - 1\right) \beta_1(0) \geq \frac{s_1}{2} > 0$.

It follows that the inequality (3.37) gives $\dot{\mathscr{V}}_1(t) \leq -\frac{s_1}{2} x_1(t) - 2L_1 \rho_1^\dagger v_1(x_{1t})$, and from the definition of $\mathscr{V}_1$, we get

$$\dot{\mathscr{V}}_1(t) \leq -\tilde{s}_1 \mathscr{V}_1(x_{1t}) - \frac{s_1}{4} x_1(t), \tag{3.38}$$

with $\tilde{s}_1 = \min\left\{\frac{s_1}{4}, \rho_1^\dagger\right\}$. Consequently, the origin of the subsystem $i = 1$ is globally exponentially stable.

Next, in order to extend the result to the overall system, we introduce the following functional which takes into account the cells dynamics of the first and the second generations of immature cells:

$$\mathscr{V}_2(x_{2t}, x_{1t}) = x_2(t) + 2L_2 v_2(x_{2t}) + 2K_1 v_1(x_{1t}) + \frac{8K_1 \beta_1(0) e^{\rho_1^\dagger \tau_1} C_1}{s_1} \mathscr{V}_1(x_{1t}). \tag{3.39}$$

Using (3.38), we prove that the derivative of $\mathscr{V}_2$ along the trajectories of the nominal system (3.1) satisfies

$$\begin{aligned} \dot{\mathscr{V}}_2(t) \leq & -\delta_2 x_2(t) - \left(1 - 2L_2 e^{\rho_2^\dagger \tau_2} C_2\right) w_2(x_2(t)) - 2L_2 \rho_2^\dagger v_2(x_{2t}) \\ & - 2K_1 \rho_1^\dagger v_1(x_{1t}) - \frac{8K_1 \beta_1(0) e^{\rho_1^\dagger \tau_1} C_1 \tilde{s}_1}{s_1} \mathscr{V}_1(x_{1t}) \\ & - 2K_1 e^{\rho_1^\dagger \tau_1} C_1 \left[\beta_1(0) - \beta_1(x_1(t))\right] x_1(t). \end{aligned} \tag{3.40}$$

Using the assumption $\alpha_2 > 0$, together with the fact that the function β_2 is strictly decreasing, it follows that,

$$\begin{aligned} \dot{\mathscr{V}}_2(t) \leq & -\left[\delta_2 - \left(2L_2 e^{\rho_2^\dagger \tau_2} C_2 - 1\right) \beta_2(0)\right] x_2(t) - 2L_2 \rho_2^\dagger v_2(x_{2t}) \\ & - 2K_1 \rho_1^\dagger v_1(x_{1t}) - \frac{8K_1 \beta_1(0) e^{\rho_1^\dagger \tau_1} C_1 \tilde{s}_1}{s_1} \mathscr{V}_1(x_{1t}). \end{aligned} \tag{3.41}$$

When the conditions (3.32) are satisfied, we select $\rho_2^\dagger > 0$ (similarly to $\rho_1^\dagger$), such that the inequality $\delta_2 - \left(2L_2 e^{\rho_2^\dagger \tau_2} C_2 - 1\right) \beta_2(0) \geq \frac{s_2}{2}$, is satisfied. It follows from (3.41) that there exists a strictly positive constant $\tilde{s}_2$, such that

$$\dot{\mathscr{V}}_2(t) \leq -\tilde{s}_2 \mathscr{V}_2(x_{1t}, x_{2t}) - \frac{s_2}{4} x_2(t), \tag{3.42}$$

is satisfied. Next, by induction, we easily check that there exist a positive constant $\tilde{s}_n$ and a family of strictly positive weighting constants $\nu_i^\dagger$ and $\tilde{\nu}_i^\dagger$, such that the derivative of the functional $\mathscr{V}(x_t) = \sum_{i=1}^n \left[\nu_i^\dagger x_i(t) + \tilde{\nu}_i^\dagger v_i(x_{it})\right]$, which is taking into account all the n generations of immature blood cells,

along the trajectories of the nominal system (3.1), satisfies

$$\dot{\mathscr{V}}(t) \leq -\tilde{s}_n \mathscr{V}(x_t). \tag{3.43}$$

From the inequality (3.43) and the properties of the functional $\mathscr{V}$, we conclude that, if the conditions (3.32) are satisfied, the origin of the nominal model (3.1)-(3.2) is globally exponentially stable.

In order to complete the proof, we consider the case where the inequality (3.33) is satisfied and we show that no positive solution converges to X^0. We prove this result by contradiction, i.e. we assume that a positive solution $x(t)$ converges to X^0. Now, we select $\rho_1^\dagger = 0$ and we observe that the derivative of the functional $\mathscr{V}_1$, introduced in (3.35), is given by

$$\dot{\mathscr{V}}_1(t) = \left[-\delta_1 + \alpha_1 \beta_1(x_1(t))\right] x_1(t). \tag{3.44}$$

When (3.33) is verified, using the facts that the function β_1 is decreasing and $x_1(t)$ converges to zero, we deduce that there exists $t_r > 0$ such that, for all $t \geq t_r$,

$$-\delta_1 + \alpha_1 \beta_1(x_1(t)) \geq \frac{-\delta_1 + \alpha_1 \beta_1(0)}{2}.$$

It follows from (3.44) that, for all $t \geq t_r$,

$$\dot{\mathscr{V}}_1(t) \geq \frac{-\delta_1 + \alpha_1 \beta_1(0)}{2} x_1(t). \tag{3.45}$$

From (3.33), and the positivity of the solutions, it follows that for all $t \geq t_r$, $\dot{\mathscr{V}}_1(t) > 0$. Consequently, we deduce that, for all $t \geq t_r$,

$$\mathscr{V}_1(x_{1t}) \geq \mathscr{V}_1(x_{1t_r}) > 0. \tag{3.46}$$

It follows that $\mathscr{V}_1(x_{1t})$ does not converge to zero. On the other hand, $\mathscr{V}_1(x_{1t})$ converges to zero because $x_1(t)$ converges to $X^0 = (0, \ldots, 0)$. This yields a contradiction. □

Example 1. *A possible selection of the cell division probability densities, which was considered in [226] and [225], is given by* $f_i(a) = \frac{m_i}{e^{m_i \tau_i} - 1} e^{m_i a}$, *with* $m_i > 0$, *for all* $i \in I_n$. *Let us consider the following biological functions and parameters:*

	$\beta_i(x_i)$	$f_i(a)$	δ_i	L_i	τ_i	γ_i
$i=1$	$\frac{1.22}{1+x_1^2}$	$\frac{5e^{5a}}{e^{5\tau_1}-1}$	0.9	0.85	1.2	0.22
$i=2$	$\frac{1.33}{1+4x_2^4}$	$\frac{7e^{7a}}{e^{7\tau_2}-1}$	0.96	0.8	1.3	0.33

The form given to β_i *[180] normalizes the values taken by the total density* x_i.

Simple calculations give: $(2L_1C_1 - 1)\beta_1(0) = 0.4448$, $(2L_2C_2 - 1)\beta_2(0) = 0.4392$. *Therefore, according to Proposition 2, the positive equilibrium of system* (3.1)-(3.2) *does not exist. Moreover, according to Theorem 2, the origin* $X^0 = (0,0)$ *of system* (3.1)-(3.2) *is globally exponentially stable, as shown in Figure 7.4.5.*

Remark 12. *In fact, the point made above -in Example 1- about the normalized value of* x_i *is available throughout all the manuscript. Indeed, the function* β_i *given [180] can be normalized as stated in [4],*

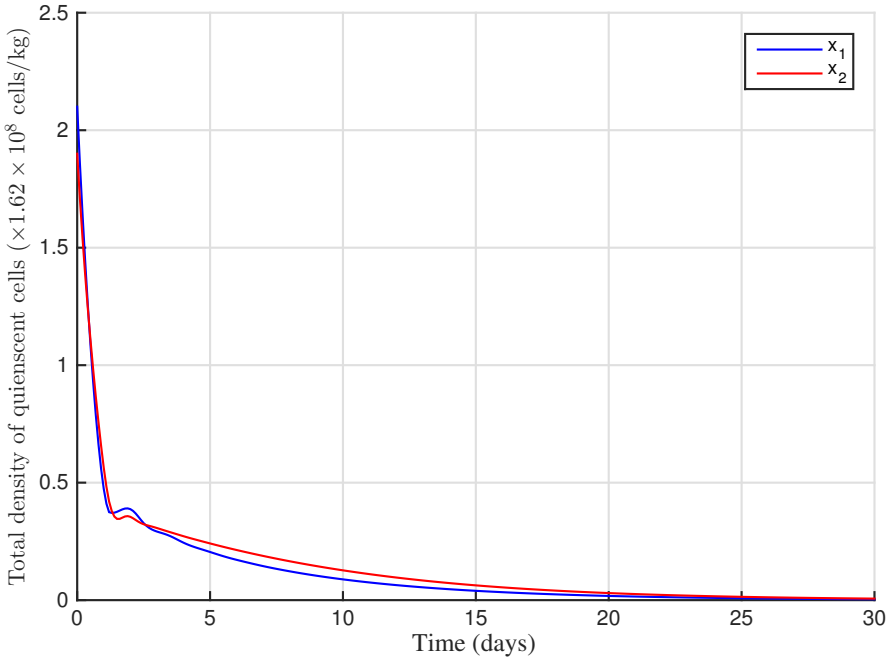

Fig. 3.6 Trajectories of Example 1 showing the exponential convergence to X^0

such that in the considered scale, a value $x_i = 1$ *expresses approximately* 1 *unity of* 1.62×10^8 *cells/kg ([4]).*

3.5.3 Global exponential stability under time-varying parameters

Convergence to X^0 means the eradication of all the immature blood cells. This case may be suitable when the model is assumed to describe the dynamics of unhealthy cells. We recall that one of the characteristics of leukemia is the blockade in the differentiation process (see Figure 3.7), which can become a target for the drugs used in treatments. Thus, it is interesting to consider the case where differentiation and self-renewal rates are uncertain or time-varying (see Remark 8 regarding the case of time-varying apoptosis).

Global exponential stability under time-varying differentiation and self-renewing rates

In this part, we extend the result of Theorem 2 to the nominal model that describes the immature cell dynamics under time-varying differentiation rates, $K_i(t)$ for all $t \geq 0$, and $i \in I_n$, and which is given by

$$\begin{aligned} \dot{x}_i(t) = {} & 2K_{i-1}(t) \int_0^{\tau_{i-1}} g_{i-1}(a) w_{i-1}(x_{i-1}(t-a)) da \\ & + 2L_i(t) \int_0^{\tau_i} g_i(a) w_i(x_i(t-a)) da - \delta_i x_i(t) - w_i(x_i(t)), \end{aligned} \tag{3.47}$$

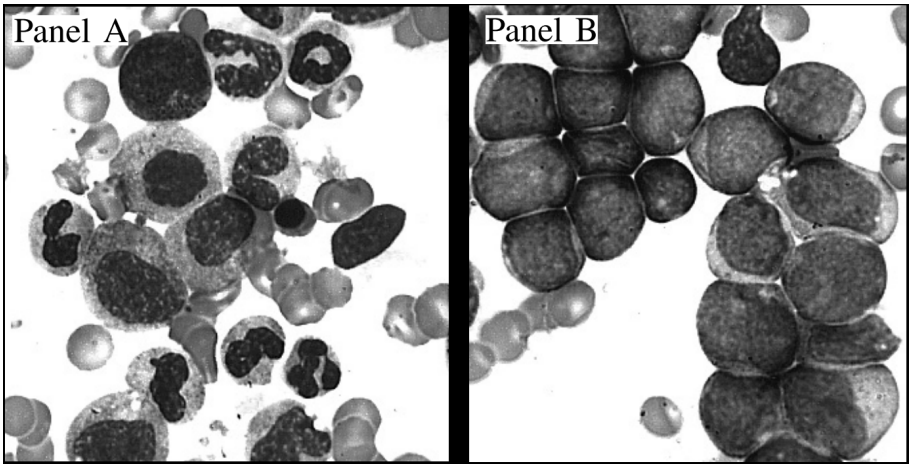

Fig. 3.7 **Panel A** shows normal bone marrow cells that express a large variety of shapes, reflecting the diversity in developmental stages in healthy hematopoiesis. In contrast, **Panel B** shows blast cells, with similar appearance, in the case of AML. Blasts in healthy hematopoiesis represent less than 5% of the total density of cells in the bone marrow. A sudden blockade in the differentiation process of blasts in **Panel A** leads to AML illustrated in **Panel B**. It was thought that drugs encouraging the re-differentiation of blasts are not effective to cure AML. However, very recently, this therapeutic strategy have been relaunched after good clinical results [278], where inhibition of DHODH restored the differentiation of unhealthy cells. The microscopic images are from the free educational materials proposed by the *Leukemia & Lymphoma Society*.

where $K_i(t)+L_i(t)=1$ and $L_i(t)\in[L_{i\min},L_{i\max}]\subset(0,1)$. We recall that, by convention, $K_0(t)=0$, for all $t\geq 0$, and we assume that $K_i(\cdot)$, $L_i(\cdot)$ are of class C^0, for all $i\in I_n$. Based on Theorem 2, we prove the following result:

Corollary 1. *The conditions*

$$\bar{s}_i=\delta_i-(2L_{i\max}C_i-1)\,\beta_i(0)>0,\ \ \forall i\in I_n, \tag{3.48}$$

ensure that the origin of the system (3.47) *is globally exponentially stable.*

Proof. We give some indications for the proof, which is slightly different from the one of Theorem 2. Here we consider $L_{1\max}$ instead of L_1 in the definition of the functional $\mathscr{V}_1(x_{1t})$ introduced in (3.35). Similarly, we consider $L_{2\max}$, $K_{1\max}=1-L_{1\min}$ and $\bar{s}_1$, instead of L_2, K_1, and s_1, respectively, in the definition of the functional $\mathscr{V}_2(x_{2t},x_{1t})$, introduced in (3.39). Then, we can prove that the derivative of the former functional along the trajectories of the system (3.47) satisfies an inequality in the form of (3.38), and similarly the derivative of the latter functional satisfies an inequality similar to (3.42). Therefore, arguing by induction we can prove that the origin of the system (3.47) is globally exponentially stable. □

Example 2. *Let us consider* $n=2$ *and for all* $t\geq 0$, $L_1(t)=\frac{1}{2}\big(1+0.96\cos(25t)\big)$ *and* $L_2(t)=\frac{1}{2}\big(1+0.96\sin(15t)\big)$. *Sine function sounds reasonable to model the variation in differentiation rates since drugs are -usually- infused quasi-periodically. Nevertheless, many other time-varying functions may be used instead of sine ones. Let us assume that:*

	$\beta_i(x_i)$	$f_i(a)$	δ_i	τ_i	γ_i
$i=1$	$\frac{2.87}{1+x_1^2}$	$\frac{e^a}{e^{\tau_1}-1}$	0.973	0.8	0.9
$i=2$	$\frac{2.7}{1+x_2^4}$	$\frac{e^a}{e^{\tau_2}-1}$	0.965	0.7	0.97

Elementary calculations give: $\bar{s}_1 = 0.0592$*, and,* $\bar{s}_2 = 0.0099$*, which means that the stability conditions* (3.48) *are satisfied for* $i \in \{1,2\}$.

Therefore, according to Corollary 1, the origin $X^0 = (0,0)$*, which is the unique equilibrium point of* (3.47)*, is globally exponentially stable.*

Figure 3.8 illustrates the trajectories x_1 *and* x_2 *for the parameters and biological functions of Example 2.*

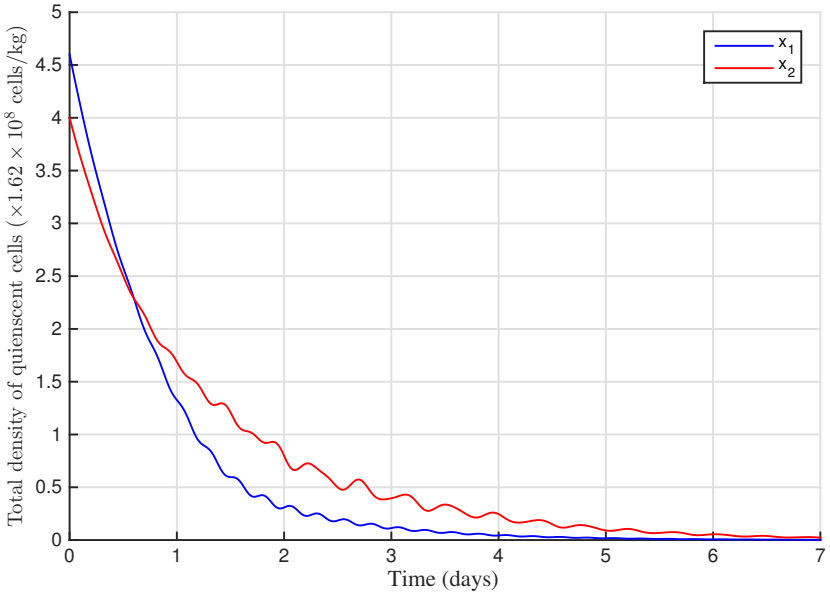

Fig. 3.8 Trajectories of the system (3.47) for the time-varying functions K_i and L_i and the parameters given in Example 2.

Further comments in the case of time-varying differentiation and self-renewing processes

A) At this juncture, we briefly comment the results in the AML case, in which a blockade of differentiation, i.e. K_i decreases in early maturity stages, is usually observed. Not surprisingly, the conditions (3.48) suggest that therapeutic strategies to eradicate cells must be oriented towards increasing the death rates γ_i (recall that increasing the apoptosis rate γ_i decreases C_i), and δ_i, and also towards decreasing L_{imax} (i.e. increasing differentiation).

Although very partial results for particular cases of AML (with myelodysplastic syndrome, MDS), and on cell cultures only, have been obtained using tyrosine kinase inhibitors (TKIs, in particular dasatinb [167]) in stimulating differentiation, the only clinically efficient case of redifferentiation therapy known until recently was by using all-trans retinoic acid (ATRA) and arsenic tri-oxide in acute promyelocytic leukemia (APL). However, this therapeutic track has lately been relaunched by establishing that inhibition of

Dihydroorotate Dehydrogenase (DHODH) is efficient in releasing cells from differentiation arrest [278] (see also [179]). Finally, increasing apopotosis may be achieved classically by using cytosine arabinoside (see Chapter 2).

B) We recall that Theorem 2 and Corollary 1 complement the previous published results, by establishing global exponential stability instead of asymptotic stability and by extending the result to cover the case of time-varying differentiating and self-renewing rates.

Hence the question that arises is whether we know how do L_i and K_i parameters vary under the effect of the disease and the drugs that may be infused. The answer is not that apparent due to the complexity of the real phenomena that occur during healthy or unhealthy processes (e.g. accumulation of mutations, signal pathways break, growth-factors, body response, drug efficiency and toxicity). In addition, even in the healthy case, the mechanisms controlling hematopoiesis are not perfectly known, at the time being.

Thus, based on the model that we study, we propose to separate some concepts and provide conceptional interpretations of some typical observed phenomena.

First, we consider that if the disease appears suddenly (due to a mutation that occurs for unknown reasons) we can expect a brutal change in model parameters from healthy to unhealthy states. For instance, a mutation in the pathways regulating differentiation such as NPM1 [146] or transcription factors that induces blockade of cell differentiation. In this case, the functions $K_i(\cdot)$ and $L_i(\cdot)$ can be interpreted as *switching* parameters.

A different interpretation can be given to the effect of growth-factors and drugs on the model parameters, however it leads also to a similar representation. More precisely, growth-factor effect on model parameters can be approximated by switching functions. Indeed, it turns out that the secretion of growth factors is very fast in comparison to cell response (see Marciniak *et al.* [189]) and thereby the levels of growth-factor concentrations converge very quickly to their steady states. This is the time to bring up that the latter assertion (i.e. the difference between time-scales of cell population dynamics and small molecule dynamics) is at the origin of the studied models with constant parameters. Thus, in all the models of hematopoiesis, all the biological parameters (e.g. differentiation, apoptosis rates, etc) actually depend on the concentration of growth factors (see [31], [3], [82] and the references therein). However, it is assumed these concentrations do not vary or that they reach very quickly their equilibrium state. Hence the models with constant parameters (e.g. (3.1)-(3.2)).

Now it seems clear that through a description of cell dynamics with possibly switching parameters (see for instance the situation illustrated in Figure 3.9), we will be able to combine constant and dynamical parameters. More importantly, we can represent the (external) events that change the nature of the system during a long period of time, such that a mutation that suddenly occurs or an instantaneous drug effect.

On the other hand, notice that Corollary 1 does not require $K_i(\cdot)$ and $L_i(\cdot)$ to be of class $\mathscr{C}^0$ (as initially introduced in (3.47)) and the result can be extended to piecewise continuous functions $K_i(\cdot)$ and $L_i(\cdot)$. Therefore, we conclude that Corollary 1 applies for the switching version of system (3.47)[3], which is a nice point.

Of course, a parameter behavior as illustrated in Figure 3.9 remains an idealistic situation, that results from an approximation of the actual behavior. Therefore, we suggest that small variations may continuously occur throughout the process of hematopoiesis. By small variations we mean that the

[3]But we need to ensure that the corresponding switching system has a unique solution.

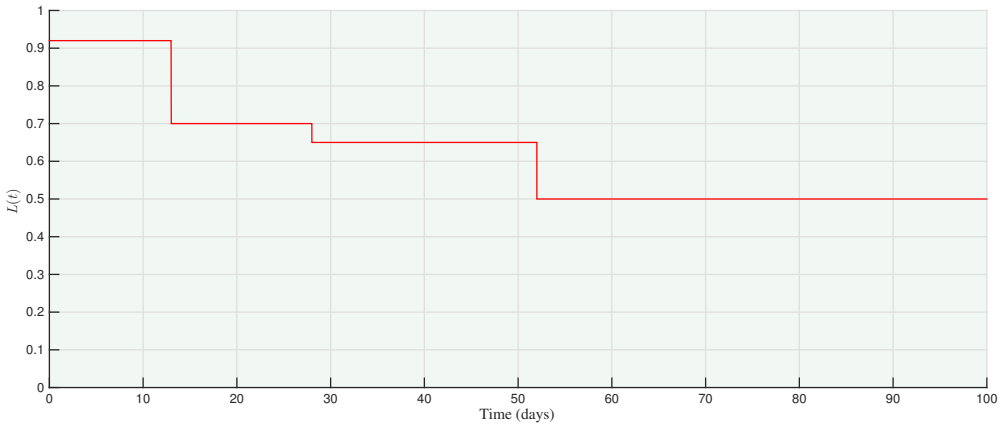

Fig. 3.9 An example of evolutionary self-renewing parameter. Switching may result as a reaction to drug infusion (therapy), mutations and anomalies (disease), or other external factors (body requirement, injury).

fluctuations remain limited and less significant than major changes like those induced by mutations or an effective drug). We propose to illustrate the above discussion on a pedagogical illustration as follows.

Example 3. *We consider an example with one stage ($n = 1$). Since there is no confusion between parameters in the discussion that follows, we omit the subscript* 1.

The parameters of the model are: $\delta = 0.25$, $\tau = 0.8$, $\gamma = 0.25$, $f(a) = \frac{e^a}{e^\tau - 1}$, *and* $\beta(x) = \frac{2.87}{1+x^2}$. *We consider two experiences (denoted respectively* ***Sit. 1*** *and* ***Sit. 2****) with two different functions* $L(t)$, *for all* $t \in [0, 250]$.

Each L-function is a result of three superimposed signals: a piecewise continuous signal, a cosine signal, and a white noise.

The former signal (i.e. the piecewise continuous one) is a step-function that switches at several isolated time instants (similar to the one illustrated in Figure 3.9). More precisely, we consider that in ***Sit. 1****, the step-function switches from the value* 0.92 *to the value* 0.7 *at* $t = 13$. *Then, it switches again to* 0.65 *at* $t = 28$. *Then it switches from the previous value to* 0.58 *at* $t = 52$. *Finally, at* $t = 175$, *it switches again to its initial value* 0.92. *In* ***Sit. 2****, we replace* 0.58 *by* 0.5 *at the transition occurring at* $t = 52$.

Thus, we construct a theoretical example of therapy in which the differentiation ability (recall that $K(t) = 1 - L(t)$, *for all* $t \in [0, 250]$*) is gradually recovered (i.e. the so-called re-differentiation therapeutic track). Thus, at* $t = 0$, *we notice that* $K(0) = 0.08$, *which is relatively low (assimilated to an unhealthy situation where differentiation is blocked). The time instants* $t = 13$, $t = 28$ *and* $t = 52$ *are considered as three successive (gradual) drug infusions that progressively increase the differentiation rate. Finally, the time instant* $t = 175$ *is assumed to be the time instant at which the drug is eliminated from the body (thereby its effect disappears).*

It seems reasonable to consider that in the absence of drugs that act on self-renewing (i.e. for all $t \geq 175$*), the blockade of differentiation re-appears as for* $t = 0$. *In fact, the goal of therapy is to ensure that malignant cells will be eradicated during the therapy-time (i.e. from* $t = 13$ *to* $t = 175$*). If cancerous cells are not eliminated during this period of time, we expect a regeneration of the disease. The meaning of cell eradication in the studied model will be discussed later.*

Now, we observe the Figure 3.10 that illustrates the evolution of the total density of unhealthy quiescent cells in ***Sit. 1*** *and* ***Sit. 2****. We notice from it that for* $t \in [52, 175]$*, the total density of cells* x *is asymptotically converging to zero, and that in both situations* ***Sit. 1*** *and* ***Sit. 2****. Moreover, for that time-interval, we can check that the global exponential stability conditions* (3.48) *are satisfied. Next, from* $t = 175$ *and thereafter, the trajectory* x *increases progressively until recovering the initial unhealthy situation. This is an expected result since, mathematically, asymptotic convergence cannot reproduce the total eradication of cells (a notion that requires convergence to zero in finite-time). However, we can intuitively define a threshold from which* x *is considered to be zero.*

For instance, we are observing that cells take much more time to reach their initial value in ***Sit. 2****, in comparison with* ***Sit. 1****. This is due to the fact that in* ***Sit 2*** *(in which the mean value of* $K(t)$ *for* $t \in [52, 175]$ *is bigger), the state* x *is closer to zero than in* ***Sit. 1****. In more accurate terms, we have* $x(t = 175) = 0.0035$ *in* ***Sit. 1****, while* $x(t = 175) = 5.910^{-13}$ *in* ***Sit. 2****. Here we want to highlight an important fact about the mathematical models that we are studying. In fact, the McKendrick-type models that we study here describe the dynamics of large numbers -or population- of cells [234]. Therefore, when the state variable* x *is too small, our models do not describe the cell dynamics and some stochastic phenomena lead to total cell eradication [234]. Nevertheless, we can see in our models that when* x *is sufficiently close to zero (for instance, in* ***Sit. 2****, where* $x(t = 175) = 5.910^{-13}$*), and knowing that the normalized scaling between the value of the state variable and the total density of cells is given by:* $x_{normalized} = 1 \Rightarrow x_{real} = 1.62 \times 10^8$ *(see [4]), then we deduce that the value of* $x(t)$*, at* $t = 1.75$ *is equivalent to an effective cell count which is less than* 1*. Therefore, we can roughly consider that in this case, cell eradication is actually achieved.*

The consequence is that by considering a threshold for the density of cells after which x *is zero, the unhealthy cell regeneration observed in Figure 3.10-* ***Sit. 2*** *is no longer possible. On the other hand, the scenario* ***Sit. 1*** *is different, since we cannot consider that* $x(t = 175) = 0.0035$ *(*$\approx 5.67 \times 10^5$ *cells/kg) is negligible. In this respect, the role of the estimates of the* ***rate of convergence of the solutions*** *appears clearly. More precisely, using the estimate of the decay rate given in Theorem 2, and given a threshold* $x_\ell > 0$*, the initial density of cells* $x(t = 0)$*, and the effect of drug infusions, we can readily determine the duration of treatment* T*, which is necessary to ensure that for all* $t > T$*,* $x(t) \leq x_\ell$*.*

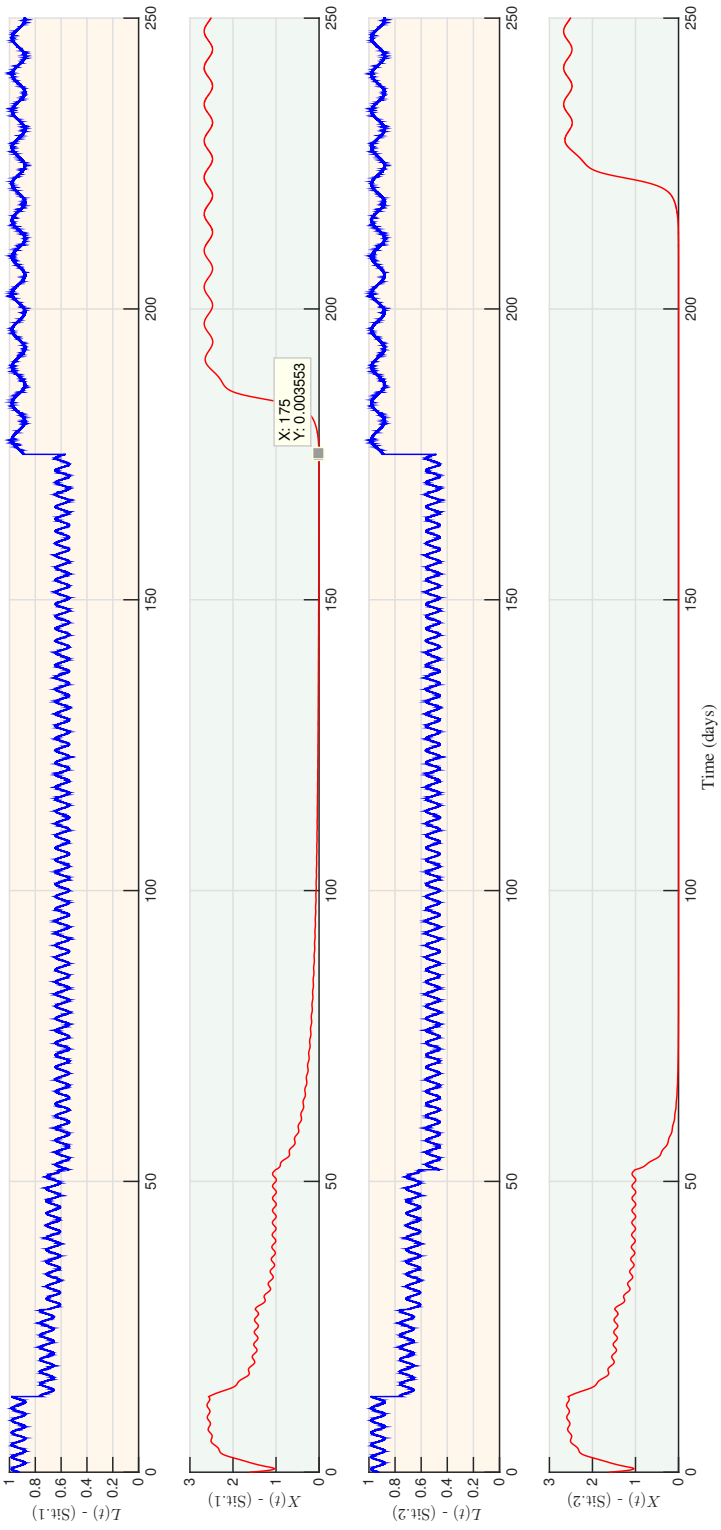

Fig. 3.10 In blue the signals $L_1(t)$ in two different situations (Sit. 1 and Sit. 2). The difference between L_1 is Sit. 1 and Sit. 2 is that for $t \in [52, 175]$, L_1 in Sit.1 has a mean value 0.5, while in Sit. 2 it is mean value is 0.4. Otherwise, L_1 is the same in both situations. In red, the total density of resting unhealthy cells in both situations.

3.5.4 Robustness analysis of the trivial steady state

In this section, we use the strict functionals $\mathscr{V}_i$, introduced in Theorem 2, to perform a robustness analysis in the case of nonvanishing perturbations $\varepsilon_i(t) \in (0, \overline{\varepsilon}_i]$, for all $i \in I_n$, $t \geq 0$. Let us observe that the derivative of the functional $\mathscr{V}_1$, defined in (3.35), along the trajectories of the perturbed system (3.1), satisfies,

$$\dot{\mathscr{V}}_1(t) \leq -\tilde{s}_1 \mathscr{V}_1(x_{1t}) - \frac{s_1}{4} x_1(t) + \overline{\varepsilon}_1. \tag{3.49}$$

We consider any constant $\theta \in (0,1)$ and we define the family of sets:

$$\mathscr{T}_{i\overline{\varepsilon}_i} = \left\{ \varphi \in \mathscr{C}\left([-\tau_i, 0], \mathbb{R}\right), \ \ \mathscr{V}_i(\varphi) \leq \frac{\overline{\varepsilon}_i}{\theta \tilde{s}_i} \right\}. \tag{3.50}$$

Notice for later use that the sets $\mathscr{T}_{i\overline{\varepsilon}_i}$ are the smallest possible for θ close to 1. Clearly, if $x_{1t} \notin \mathscr{T}_{1\overline{\varepsilon}_1}$, then (3.49) gives $\dot{\mathscr{V}}_1(t) \leq -(1-\theta)\tilde{s}\mathscr{V}_1(x_{1t}) - \frac{s_1}{4} x_1(t)$. Therefore, the state x_{1t} converges exponentially to the set $\mathscr{T}_{1\overline{\varepsilon}_1}$. However, a refined result can be provided, in the sense that we can determine smaller positive invariant sets than the family $\mathscr{T}_{i\overline{\varepsilon}_i}$. For that, let us introduce the functional,

$$\mathscr{A}_1(x_{1t}) = \mathscr{V}_1(x_{1t}) - \psi_1 x_1(t). \tag{3.51}$$

It is worth mentioning that the functional $\mathscr{A}_1$ is positive on the positive orthant for $\psi_1 = \frac{s_1}{8\left(\delta_1 + \beta_1(0)\right)} < 1$, where s_1 is the constant defined in (3.32). Using the expression of ψ_1, we can check that the derivative of $\mathscr{A}_1$, along the trajectories of the perturbed system (3.1), satisfies:

$$\dot{\mathscr{A}_1}(t) \leq -\tilde{s}_1 \mathscr{V}_1(x_{1t}) - \frac{s_1}{8} x_1(t) - 2\psi_1 L_1 \int_{t-\tau_1}^{t} g_1(t-a) w_1(x_1(a)) da + (1-\psi_1)\overline{\varepsilon}_1.$$

Now, if we define the family of sets

$$\tilde{\mathscr{T}}_{i\overline{\varepsilon}_i} = \left\{ \varphi \in \mathscr{C}\left([-\tau_i, 0], \mathbb{R}\right), \mathscr{V}_i(\varphi) + \frac{2\psi_i L_i}{\tilde{s}_i \theta} \int_{-\tau_i}^{0} g_i(a) w_i(\varphi) da \leq \frac{(1-\psi_i)\overline{\varepsilon}_i}{\theta \tilde{s}_i} \right\},$$

where $0 < \psi_i < 1$, for all $i \in I_n$. Observe that $\tilde{\mathscr{T}}_{i\overline{\varepsilon}_i} \subset \mathscr{T}_{i\overline{\varepsilon}_i}$, for all $\psi_i > 0$, and $\tilde{\mathscr{T}}_{i\overline{\varepsilon}_i} = \mathscr{T}_{i\overline{\varepsilon}_i}$, for $\psi_i = 0$. Now, notice that for all $x_{1t} \notin \tilde{\mathscr{T}}_{1\overline{\varepsilon}_1}$, the derivative of the functional $\mathscr{A}_1$ satisfies

$$\dot{\mathscr{A}_1}(t) \leq -\tilde{s}_1(1-\theta)\mathscr{V}_1(x_{1t}) - \frac{s_1}{8} x_1(t) \leq -\tilde{s}_{1\theta} \mathscr{A}_1(x_{1t}) - \frac{s_1 + \psi_1 \theta}{8} x_1(t), \tag{3.52}$$

where $\tilde{s}_{1\theta} = \min\left\{\tilde{s}_1(1-\theta), \theta/8\right\} > 0$, for all $\theta \in (0,1)$. Therefore, from the definition of the functional $\mathscr{A}_1$, we conclude that the state x_{1t} converges exponentially to $\tilde{\mathscr{T}}_{1\overline{\varepsilon}_1}$, and the decay rate of the trajectory $x_1(t)$ is smaller than, or equal to, $\tilde{s}_{1\theta}$. On the other hand, we readily check, by contradiction, that the sets $\tilde{\mathscr{T}}_{i\overline{\varepsilon}_i}$ are positively invariant (i.e. a trajectory in $\tilde{\mathscr{T}}_{i\overline{\varepsilon}_i}$ remains in $\tilde{\mathscr{T}}_{i\overline{\varepsilon}_i}$ for all the future time). Arguing as in the proof of Theorem 2, we generalize this result to the overall system. In other words, we have proved the following result:

Theorem 3. *If the conditions $s_i > 0$ are satisfied, for all $i \in I_n$, then the states x_{it} of the perturbed system* (3.16)*, where $\varepsilon_i(t) \in (0, \overline{\varepsilon}_i]$, for all $t \geq 0$, converge exponentially to the sets $\tilde{\mathscr{T}}_{i\overline{\varepsilon}_i}$, where $0 < \psi_i < 1$, for all $i \in I_n$.*

Remark 13. *i) Since dedifferentiation is the mechanism whereby cells regress to undifferentiated cells, it seems reasonable to focus more on the first compartment of cells. ii) The proof of Theorem 3 can be easily extended to the case of time-varying differentiation and self-renewing rates.*

Example 4. *Here we intend to make use of Example 3 in order to illustrate some basics about the effect of cell plasticity (considered here as an uncertain input in our system). In the next chapter we will return to this issue. Let us consider the parameters of Example 3 and the self-renewing process as illustrated in* ***Sit. 1****. Moreover, we consider stochastic uncertainties as the sequence illustrated in Figure 3.11 for $t \in [0,1]$. Integrating the dynamical systems with and without uncertainties leads to the trajectories illustrated in Figure 3.11.*

3.5.4.1 Further comments in the case of uncertainties induced by cell-plasticity

It is trendy to interpret many cancer types as a phenomenon induced by an abnormal dedifferentiation (see for instance [64] for leukemia, and also [110], [73], [301], for other types of cancer).

Intuitively, we have underscored in Example 3 how exponential stability can be -in practice- roughly interpreted as a *finite* time convergence (the duration that we called $T > 0$), when the state is *sufficiently* small ($x(t) < x_\ell$, for all $t \geq T$). In such a situation we can assume that, in practice, cancer regeneration is theoretically excluded.

On the other hand, the case described in Figure 3.11 is different. Indeed, in Example 4 we assume that cell-plasticity generates an uncertain nonvanishing bounded input that leads to a practical stability result (i.e. Theorem 3). The trajectories illustrated in Figure 3.11 show that in the presence of nonnegligible cell-plasticity activity, the cell count will not go under the threshold x_ℓ during the treatment period (e.g. the treatment period in Example 4 starts at $t = 13$ and ends at $t = 175$). Thus, due to cell-plasticity, it is expected that therapy will not succeed in completely eradicating malignant cells during the treatment period. It is worth mentioning that both experimental and theoretical recent results seem to confirm some closed statements. For instance, in the mathematical study presented in [249] (that relies on the experimental results in [142], from lung cancer) the hypothesis that when cancer cells are attacked by radiotherapy, they dedifferentiate into cancer stem cells (i.e. dedifferentiation to regress to $i = 1$) because stem cells are less sensitive to radiotherapy. Interestingly, they suggest that therapy works better inhibiting *survivin* (see, [144]) expression, that decreases dedifferentiation of cancer cells.

Fig. 3.11 Uncertainties with $\overline{\varepsilon} = 0.2$. Trajectories of Example 4 with and without uncertainties.

3.5.5 Model equations in the case involving fast self-renewing dynamics

We pursue what we said previously on the model with fast self-renewing dynamics (the model introduced in [24]). In this case, a sub-population of cells has an advantage of proliferation, if compared to *ordinary* cells. A schematic representation of the cell dynamics is given in Figure 5.94. For all $i \in I_n = \{1,\dots,n\}$ (recall that $n \geq 1$ is the number stages of maturity), we denote by x_i the total density of *ordinary* resting cells and by $\tilde{x}_i$ the total density of fast self-renewing cells.

3.5.6 LKF constructions for a model with fast self-renewing dynamics

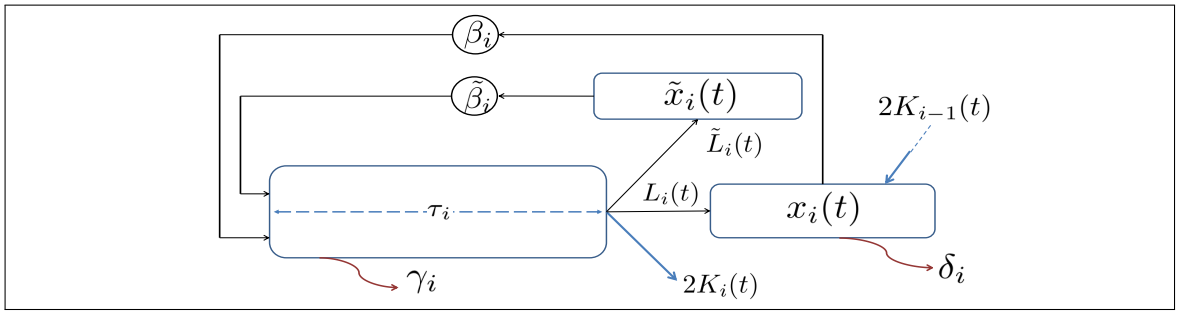

Fig. 3.12 Schematic representation of the age-structured model describing unhealthy hematopoeisis. The dynamics $\tilde{x}_i$ represent the extra-dynamics introduced to quantify the total density of fast-renewing cells.

Similarly to the model introduced in the previous sections, the constant δ_i represents the death rate of quiescent cells. We recall that the function $g_i(a)$ is defined by $g_i(a) = e^{-\gamma_i a} f_i(a)$ where f_i is a density function describing the mitosis and is such that $\int_0^{\tau_i} f_i(a)da = 1$, and γ_i is the death rate of the proliferating cells (apoptosis). Proliferating cells can divide between the moment they enter the proliferating phase and a maximal age $\tau_i > 0$. The reintroduction functions $\beta_i(x_i)$ and $\tilde{\beta}_i(\tilde{x}_i)$ from the resting to the proliferating phases are considered to be nonlinear, continuous, decreasing functions, and $\lim_{a\to+\infty} \tilde{\beta}_i(a) = \lim_{a\to+\infty} \beta_i(a) = 0$.

The total population densities x_i and $\tilde{x}_i$ are described by the following time-delay system, for all $i \in I_n = \{1,\dots,n\}$,

$$\left\{\begin{array}{ll} \dot{x}_i(t) = & -(\delta_i + \beta_i(x_i(t)))x_i(t) + L_i(t)\Im_i(w_i,\tilde{w}_i) + 2K_{i-1}(t)\Im_{i-1}(w_{i-1},\tilde{w}_{i-1}) \\ \dot{\tilde{x}}_i(t) = & -\tilde{w}_i(\tilde{x}_i(t)) + \tilde{L}_i(t)\Im_i(w_i,\tilde{w}_i), \quad t \geq 0, \end{array}\right. \tag{3.53}$$

where (with an abuse of notation) the distributed delay terms are defined by,

$$\Im_i(w_i,\tilde{w}_i) = \int_0^{\tau_i} g_i(a)[w_i(x_i(t-a)) + \tilde{w}_i(\tilde{x}_i(t-a))]da, \tag{3.54}$$

where a is the age of cells. As similarly done for the case of the model without fast self-renewing dynamics, we assume first that the functions $L_i(\cdot)$ and $\tilde{L}_i(\cdot)$ are of class C^0, for all $i \in I_n$. Moreover, these functions satisfy

$$L_i(t) := 2\sigma_i(t)(1-K_i(t)),\ \tilde{L}_i(t) := 2(1-\sigma_i(t))(1-K_i(t)),\ \text{and, } K_0 = 0, \tag{3.55}$$

for all $t \geq 0$, where we recall that the rates $K_i(t)$ represent the proportion of cells that differentiate, while the functions $1-\sigma_i(t)$ characterize the probability of fast self-renewal at the time instant t. We recall that:

$$C_i = \int_0^{\tau_i} g_i(a)da, \quad \text{for all} \quad i \in I_n.$$

Originally, the model described by (3.53) was introduced in [24] with constant parameters K_i, L_i, $\tilde{L}_i$ and σ_i, for all $i \in I_n$. As repeatedly mentioned throughout the chapter, AML is characterized by a blockade in the differentiation process which becomes also a target for some drugs already used in its treatment. Thus, we consider here the time-varying system (3.53).

Since each proliferating cell, which does not die by apoptosis and completes its mitosis, gives birth to two daughter cells, we deduce that $K_i(t) \in [0,1]$ for all $t \geq 0$. In fact, we assume that $K(t) \in [K_{i\min}, K_{i\max}] \subset (0,1)$, for all $t \geq 0$, meaning that even for an unhealthy hematopoiesis, the differentiating process will not completely vanish. More precisely, in the AML case, due to the blockade in the differentiation process, we expect that $\lim_{t\to\infty} K(t) = K_{i\min} \neq 0$.

Similarly, we consider the case where for all $t \geq 0$, $\sigma_i(t) \in [\sigma_{i\min}, \sigma_{i\max}] \subseteq [0,1]$. From medical practice we know that, in the AML case, a blockade in the differentiation process $\left(\text{i.e. } \lim_{t\to\infty} K_i(t) = K_{i\min}\right)$ and a high rate of fast self-renewing $\left(\text{i.e. } \lim_{t\to\infty} \sigma_i(t) = \sigma_{i\min}\right)$ are simultaneously observed. This fact yields to $\lim_{t\to\infty} \tilde{L}_i(t) = \tilde{L}_{i\max}$, in the AML case, with $\tilde{L}_{i\max} = 2(1-\sigma_{i\min})(1-K_{i\min})$.

The situation in which $\sigma_i = 0$ describes the worst unhealthy case in which all the proliferating cells that complete their mitosis will be engaged in the fast self-renewing process. On the other hand, we observe that the case where $\sigma_i = 1$, and all the parameters involved in the model are constant, is in fact well suited to healthy hematopoiesis. Indeed, note that the case $\sigma_i = 1$ is equivalent to consider $\tilde{x} = 0$, and if the parameters in (3.53) are constants, then the system (3.53) is equivalent the model (3.1).

Moreover, we define for all $i \in I_n$,

$$\hat{L}_i(t) := L_i(t) + \tilde{L}_i(t) = 2\left(1 - K_i(t)\right), \ \ t \geq 0.$$

Notice that $\hat{L}(t) \in [\hat{L}_{i\min}, \hat{L}_{i\max}] \subset (0,2)$, for all $t > 0$, where $\hat{L}_{i\max} = 2(1-K_{i\min})$.

It is easy to prove that system (3.53) is positive. Throughout this section, we employ the positivity of the system to construct a suitable Lyapunov-Krasovskii functional in order to investigate the stability properties of the overall system. We start with the following proposition:

Proposition 3. *If the condition*

$$C_i \tilde{L}_{i\max} < 1, \tag{3.56}$$

for all $i \in I_n$, is not satisfied, then there exists a system in the family of systems (3.53) *whose origin is not globally asymptotically stable.*

Proof. We prove Proposition 3 by contradiction. Let us assume that (3.56) is not satisfied for a given $j \in I_n$ and that all the positive solutions of the system (3.53), with for all $i \in I_n$, $\tilde{L}_i(t) = \tilde{L}_{i\max}$, for all $t \geq 0$, converges to the origin.

Observe that

$$\dot{\tilde{x}}_i(t) \geq -\tilde{w}_i(\tilde{x}_i(t)) + \tilde{L}_{i\max} \int_{t-\tau_i}^{t} g_i(t-a)\tilde{w}_i(\tilde{x}_i(a))da. \tag{3.57}$$

Let us introduce the functionals

$$h_i(\tilde{x}_{it}) = \int_{t-\tau_i}^{t} \int_{m}^{t} g_i(m-a+\tau_i)\tilde{w}_i(\tilde{x}_i(a))dadm. \tag{3.58}$$

Simple calculations give

$$\dot{h}_i(t) = C_i\tilde{w}_i(\tilde{x}_i(t)) - \int_{t-\tau_i}^{t} g_i(t-a)\tilde{w}_i(\tilde{x}_i(a))da. \tag{3.59}$$

From (3.57) and (3.59), it follows that the derivatives of the functionals $H_i(\tilde{x}_{it}) = \tilde{x}_i(t) + \tilde{L}_{i\max}h_i(\tilde{x}_{it})$, along the trajectories of (3.53), satisfy

$$\dot{H}_i(t) \geq (C_i\tilde{L}_{i\max} - 1)\tilde{w}_i(\tilde{x}_i(t)). \tag{3.60}$$

Since there exists $j \in I_n$ such that $C_j\tilde{L}_{j\max} > 1$, we get $\dot{H}_j(t) \geq 0$. It follows that,

$$H_j(\tilde{x}_{jt}) \geq H_j(0) > 0.$$

Therefore, $H_j(\tilde{x}_{jt})$ does not converge to zero. But we consider a solution that converges to the origin, which implies that $H_j(\tilde{x}_{jt})$ converges to zero. This yields a contradiction. □

Remark 14. *If $\sigma_{i\min} = 0$, we obtain $\hat{L}_{i\max} = \tilde{L}_{i\max}$. Therefore, from Proposition 3, we observe that if the condition $C_i\hat{L}_{i\max} < 1$ is not satisfied for all $i \in I_n$, then there exists a system* (3.53) *whose origin is not globally asymptotically stable. Consequently, we can not establish global exponential stability of the origin of system* (3.53) *if the condition*

$$C_i\hat{L}_{i\max} > 1$$

holds true for some $i \in I_n$.

Now, let us state and prove the following result:

Theorem 4. *For all $i \in I_n$, if the conditions*

$$C_i\hat{L}_{i\max} < 1, \tag{3.61}$$

are satisfied, then all the positive trajectories of (3.53) *converge exponentially to the origin.*

Proof. Let us consider a family of strictly positive constants λ_i, for all $i \in I_n$. First, we observe that when the conditions (3.61) are satisfied, then for all $\lambda_i \in \left(1, \frac{1+C_i\hat{L}_{i\max}}{2C_i\hat{L}_{i\max}}\right)$, the following inequalities are verified

$$1 - \lambda_i C_i\hat{L}_{i\max} > \frac{1 - C_i\hat{L}_{i\max}}{2} > 0. \tag{3.62}$$

Next, let us introduce, for all $i \in I_n$, the functionals defined along the trajectories of system (3.53), by

$$v_i^{\ddagger}(x_{it}, \tilde{x}_{it}) = \int_{t-\tau_i}^{t} \int_{m}^{t} e^{-\rho_i^{\ddagger}(t-m-\tau_i)} g_i(m-a+\tau_i)\left[w_i(x_i(a)) + \tilde{w}_i(\tilde{x}_i(a))\right] dadm, \tag{3.63}$$

where $\rho_i^{\ddagger}$ are strictly positive constants to be selected later. The derivatives of the functionals (3.63), along the trajectories of (3.53), satisfy (with an abuse of notation for $\Im_i$),

$$\dot{v}_i^{\ddagger}(t) \leq -\rho_i^{\ddagger} v_i^{\ddagger}(x_{it}, \tilde{x}_{it}) - \Im_i(w_i, \tilde{w}_i) + \left[w_i(x_i(t)) + \tilde{w}_i(\tilde{x}_i(t))\right] e^{\rho_i^{\ddagger}\tau_i} C_i. \tag{3.64}$$

Let us introduce the following functional for the first compartment of unhealthy cells

$$\mathscr{V}_1^{\ddagger}(x_{1t}, \tilde{x}_{1t}) = x_1(t) + \tilde{x}_1(t) + \lambda_1 \hat{L}_{1\max} v_1^{\ddagger}(x_{1t}, \tilde{x}_{1t}), \tag{3.65}$$

where λ_1 satisfies (3.62). Using (3.64), it follows that

$$\begin{aligned} \dot{\mathscr{V}}_1^{\ddagger}(t) \leq & -\left[\delta_1 + \left(1 - \lambda_1 e^{\rho_1^{\ddagger}\tau_1} \hat{L}_{1\max} C_1\right) \beta_1(x_1(t))\right] x_1(t) - \lambda_1 \rho_1^{\ddagger} \hat{L}_{1\max} v_1^{\ddagger}(x_{1t}, \tilde{x}_{1t}) \\ & - \left(1 - \lambda_1 e^{\rho_1^{\ddagger}\tau_1} \hat{L}_{1\max} C_1\right) \tilde{w}_1(\tilde{x}_1(t)) + \left(\hat{L}_1(t) - \lambda_1 \hat{L}_{1\max}\right) \Im_1(w_1, \tilde{w}_1), \end{aligned} \tag{3.66}$$

since λ_1 satisfies (3.62). It follows that by selecting any

$$\rho_1^{\ddagger} \in \left(0, \frac{1}{\tau_1} \ln\left(\frac{1 + \lambda_1 C_1 \hat{L}_{1\max}}{2\lambda_1 C_1 \hat{L}_{1\max}}\right)\right), \tag{3.67}$$

we obtain

$$1 - \lambda_1 e^{\rho_1^{\ddagger}\tau_1} \hat{L}_{1\max} C_1 > \frac{1 - \lambda_1 \hat{L}_{1\max} C_1}{2} > 0.$$

Moreover, since $\hat{L}_1(t) \leq \hat{L}_{1\max}$, we deduce that (3.66) gives

$$\begin{aligned} \dot{\mathscr{V}}_1^{\ddagger}(t) \leq & -\left[\delta_1 + \theta_1^{\ddagger} \beta_1(0)\right] x_1(t) - \theta_1^{\ddagger} \tilde{w}(\tilde{x}_1(t)) \\ & - \lambda_1 \hat{L}_{1\max} \rho_1^{\ddagger} v_1^{\ddagger}(x_{1t}, \tilde{x}_{1t}) - \overline{\lambda}_1 \Im_1(w_1, \tilde{w}_1), \end{aligned} \tag{3.68}$$

where,

$$\theta_1^{\ddagger} = 1 - \lambda_1 e^{\rho_1^{\ddagger}\tau_1} \hat{L}_{1\max} C_1 > 0, \text{ and, } \overline{\lambda}_1 = (\lambda_1 - 1)\hat{L}_{1\max} > 0.$$

Since the right hand side of (3.68) is always nonpositive, we deduce by integrating (3.68) that for all $t \geq 0$,

$$\mathscr{V}_1^{\ddagger}(x_{1t}, \tilde{x}_{1t}) \leq \mathscr{V}_1^{\ddagger}\left(\varphi_{x_1}, \varphi_{\tilde{x}_1}\right). \tag{3.69}$$

This means in particular that $\tilde{x}(t)$ is bounded by a constant $\tilde{x}_{1b} > 0$. Since the function $\tilde{\beta}_1$ is decreasing, it follows that, for all $t \geq 0$, the inequality (3.68) gives, with an abuse of notation,

$$\begin{aligned} \dot{\mathscr{V}}_1^{\ddagger}(t) \leq & -\left[\delta_1 + \theta_1^{\ddagger} \beta_1(0)\right] x_1(t) - \theta_1^{\ddagger} \tilde{\beta}_1(\tilde{x}_{1b}) \tilde{x}_1(t) \\ & - \lambda_1 \hat{L}_{1\max} \rho_1^{\ddagger} v_1^{\ddagger}(x_{1t}, \tilde{x}_{1t}) - \overline{\lambda}_1 \Im_1(w_1, \tilde{w}_1). \end{aligned} \tag{3.70}$$

We conclude that for all $t \geq 0$,

$$\dot{\mathscr{V}}_1^{\ddagger}(t) \leq -\tilde{s}_1 \mathscr{V}_1^{\ddagger}(x_{1t}, \tilde{x}_{1t}) - \overline{\lambda}_1 \Im_1(w_1, \tilde{w}_1), \tag{3.71}$$

where,

$$\tilde{s}_1 = \min\left\{\delta_1 + \theta_1^\ddagger \beta_1(0), \theta_1^\ddagger \tilde{\beta}_1(\tilde{x}_{1b}), \lambda_1 \rho_1^\ddagger \hat{L}_{1\max}\right\}.$$

By virtue of the functional $\mathscr{V}_1^\ddagger$, we conclude that the origin of the subsystem $i = 1$ is globally exponentially stable, with a decay rate smaller than, or equal to, $\tilde{s}_1$.

Next, in the rest of the proof, we consider the case where the conditions (3.61) are satisfied for any number of compartments ($i \in I_n$). Let us introduce the following functional that takes into account the first and the second generations of cells:

$$\mathscr{V}_2^\ddagger(X_{2t}) = x_2(t) + \tilde{x}_2(t) + \lambda_2 \hat{L}_{2\max} v_2^\ddagger(x_{2t}, \tilde{x}_{2t}) + \frac{2K_{1\max}}{\overline{\lambda}_1} \mathscr{V}_1^\ddagger(x_{1t}, \tilde{x}_{1t}), \tag{3.72}$$

with $X_2 = (x_1, \tilde{x}_1, x_2, \tilde{x}_2)$. Similarly to the case $i = 1$, we select $\rho_2^\ddagger$ such that the derivative of the functional (3.72) along the trajectories of (3.53) satisfies

$$\begin{aligned}\dot{\mathscr{V}}_2^\ddagger(t) \leq &-\left[\delta_2 + \theta_2^\ddagger \beta_2(0)\right] x_2(t) - \theta_2^\ddagger \tilde{w}_2(\tilde{x}_2(t)) - \lambda_2 \hat{L}_{2\max} \rho_2^\ddagger v_2^\ddagger(x_{2t}, \tilde{x}_{2t}) \\ &+ 2K_1(t)\Im_1(w_1, \tilde{w}_1) - \overline{\lambda}_2 \Im_2(w_2, \tilde{w}_2) + \frac{2K_{1\max}}{\overline{\lambda}_1} \dot{\mathscr{V}}_1^\ddagger(t).\end{aligned} \tag{3.73}$$

Combining (3.73) and (3.71), we deduce that for all $t \geq 0$,

$$\begin{aligned}\dot{\mathscr{V}}_2^\ddagger(t) \leq &-\left[\delta_2 + \theta_2^\ddagger \beta_2(0)\right] x_2(t) - \theta_2^\ddagger \tilde{\beta}_2(\tilde{x}_{2b}) \tilde{x}_2(t) - \lambda_2 \hat{L}_{2\max} \rho_2^\ddagger v_2^\ddagger(x_{2t}, \tilde{x}_{2t}) \\ &- \overline{\lambda}_2 \Im_2(w_2, \tilde{w}_2) - \frac{2\tilde{s}_1 K_{1\max}}{\overline{\lambda}_1} \mathscr{V}_1^\ddagger(x_{1t}, \tilde{x}_{1t}) - 2\left(K_{1\max} - K_1(t)\right)\Im_1(w_1, \tilde{w}_1).\end{aligned} \tag{3.74}$$

Since $K_1(t) \leq K_{1\max}$, we straightforwardly deduce that there exists $\tilde{s}_2 > 0$ such that, for all $t \geq 0$,

$$\dot{\mathscr{V}}_2^\ddagger(t) \leq -\tilde{s}_2 \mathscr{V}_2^\ddagger(X_{2t}) - \lambda_2 \Im_2(w_2, \tilde{w}_2). \tag{3.75}$$

Next, by induction, one can readily determine families of constants $\mathfrak{a}_i^\ddagger > 0$, $\mathfrak{b}_i^\ddagger > 0$ and a constant $\tilde{s}_n > 0$, such that the derivative of the functional

$$\mathscr{V}_n^\ddagger(X_{nt}) = \sum_{i=1}^{n} \left[x_i(t) + \mathfrak{a}_i^\ddagger \tilde{x}_i(t) + \mathfrak{b}_i^\ddagger v_i^\ddagger(x_{it}, \tilde{x}_{it})\right], \tag{3.76}$$

with $X_n = (x_1, \tilde{x}_1, \ldots, x_n, \tilde{x}_n)$, along the trajectories of (3.53), satisfies

$$\dot{\mathscr{V}}_n^\ddagger(t) \leq -\tilde{s}_n \mathscr{V}_n^\ddagger(X_{nt}), \text{ with } \tilde{s}_n > 0. \tag{3.77}$$

From (3.77) and the properties of the functional $\mathscr{V}_n^\ddagger$, we conclude that the origin of the system (3.53) is globally exponentially stable with a decay rate smaller than, or equal to, $\tilde{s}_n$. □

Technical Note 1. *The reader may have noticed the technical differences between the proofs of Theorem 2 and Theorem 4. For instance, the detour through the boundedness of $\tilde{x}_1$ that allowed us to obtain $\tilde{x}$ in the right-hand side of $\dot{\mathscr{V}}_1^\ddagger$* (3.68)-(3.70)*, and thereby recover $\mathscr{V}_1^\ddagger$ in the right-hand side of* (3.70)*, which*

establishes exponential stability of the solutions, was not necessary in Theorem 2. We also notice that the generalization of the result to the overall system ($i \in I_n, n \geq 2$) is different (by comparing (3.71) *with* (3.38)*). Indeed, in* (3.38) *we required an extra-negative term in $x_1(t)$ in order to handle the effect of the coupling that appears in $\mathcal{V}_2$. On the other hand, in* (3.71)*, we manage to ensure a negative integral term $\left(-\overline{\lambda}_1 \Im_1(w_1, \tilde{w}_1)\right)$, in order to compensate the coupling terms appearing in $\mathcal{V}_2^{\ddagger}$. In both cases, we extended the results to any number of generations of cells without conservatism, which is a nice point.*

Remark 15. *In the case where $\sigma_{i\max} = 1$, all the cells that complete their mitosis without dying by apoptosis may join -entirely- the fast-self renewing process, through $\tilde{G}_0$. This is an extreme unhealthy case, in which all cells are abnormally fast-proliferating. Since this case is allowed in our study (the one presented in [80]), it appears clear that the only way to ensure that the exponential convergence of the solutions to zero is to force the proliferating cells to have a negative balance between mother cells entering from G_0 and $\tilde{G}_0$ (normalized to 1), and daughter cells that rise from mitosis and survive to apoptosis ($C_i\hat{L}_{i\max}$), which is expressed by the condition $C_i\hat{L}_{i\max} < 1$. On the other hand, if limited extent is imposed to the abnormal behavior (i.e. reflected in the model by assuming $\sigma_{i\max} < 1$), we expect that less restrictive (from a biological standpoint) conditions can be determined, as illustrated in the sequel.*

In one among the works done collaboratively with Professor Emilia Fridman [107], further results on the stability of model with fast self-renewing dynamics are provided. In particular, global asymptotic stability and regional exponential stability are discussed in the case of system (3.53) has constant parameters. Notice also that the analysis of the PDE version of the system (3.53) is addressed. Here we retain only one corollary from [107] which goes along with Theorem 4 of the current chapter (see Remark 15). So the following result deals with the case in which K_i and L_i in (3.53) are constant and $\sigma_i(t) \in [\sigma_{i\min}, \sigma_{i\max}]$, where $\sigma_{i\max} < 1$, for all $i \in I_n$ and $t \geq 0$.

$$\sigma_{i\min} \leq \sigma_i(t) \leq \sigma_{i\max}, \text{ for all, } i \in I_n. \tag{3.78}$$

Corollary 2. *Assume that there exist $\kappa_1^1 > 0, \ldots, \kappa_n^1 > 0$ such that the following $4n$ linear inequalities are satisfied:*

$$\begin{array}{l} [(L_i + \kappa_i^1 \tilde{L}_i) \int_0^{\tau_i} e^{-\gamma_i a} f_i(a) da - 1] \beta_i(0)_{\sigma_i = \sigma_{i\min}} < \delta_i, \\ [(L_i + \kappa_i^1 \tilde{L}_i) \int_0^{\tau_i} e^{-\gamma_i a} f_i(a) da - 1] \beta_i(0)_{|\sigma_i = \sigma_{i\max}} < \delta_i, \\ (L_i + \kappa_i^1 \tilde{L}_i) \int_0^{\tau_i} e^{-\gamma_i a} f_i(a) da_{|\sigma_i = \sigma_{i\min}} < \kappa_i^1, \\ (L_i + \kappa_i^1 \tilde{L}_i) \int_0^{\tau_i} e^{-\gamma_i a} f_i(a) da_{|\sigma_i = \sigma_{i\max}} < \kappa_i^1, \text{ for all, } i \in I_n. \end{array} \tag{3.79}$$

Then, the zero solution of the system (3.53)-(3.55)*, where σ_i satisfies (3.78), is globally asymptotically stable.*

Example 5. *Let us consider the following parameters and functions:*
for i=1: $\delta_1 = 3.3$, $K_1 = 0.1$, $m_1 = 1$, $\tau_1 = 0.8$, $\gamma_1 = 0.2$, $\beta_1(x_1) = \frac{0.8}{1+x_1^3}$ and $\tilde{\beta}_1(\tilde{x}_1) = \frac{10}{1+2\tilde{x}_1^2}$.
for i=2: $\delta_2 = 4$, $K_2 = 0.08$, $m_2 = 1$, $\tau_2 = 0.8$, $\gamma_2 = 0.3$, $\beta_2(x_2) = \frac{1}{1+x_2^3}$ and $\tilde{\beta}_2(\tilde{x}_1) = \frac{10}{1+\tilde{x}_2^2}$.
We assume that σ_i is uncertain for $i \in \{1,2\}$. For instance, we consider that

$$0.5 = \sigma_{i\min} \leq \sigma_i(t) \leq \sigma_{i\max} = 0.9, \text{ for } i = 1,2 \tag{3.80}$$

and,

$$\sigma_i(t) = \frac{\sigma_{i\max} + \sigma_{i\min}}{2} + \frac{\sigma_{i\max} - \sigma_{i\min}}{2}\cos(t). \tag{3.81}$$

The conditions (3.79) *are satisfied for* $\kappa_1^1 = \kappa_2^1 = 5$*:*

- $\left[(L_1 + \kappa_1^1\tilde{L}_1)\int_0^{\tau_1} e^{-\gamma_1 a} f_1(a)da - 1\right] \beta_1(0)|_{\sigma_1=\sigma_{1\min}} = 3.1501 < 3.3 = \delta_1$
  $\left[(L_1 + \kappa_1^1\tilde{L}_1)\int_0^{\tau_1} e^{-\gamma_1 a} f_1(a)da - 1\right] \beta_1(0)|_{\sigma_1=\sigma_{1\max}} = 1.0434 < 3.3 = \delta_1$
  $(L_1 + \kappa_1^1\tilde{L}_1)\int_0^{\tau_1} e^{-\gamma_1 a} f_1(a)da|_{\sigma_1=\sigma_{1\min}} = 4.9376 < 5 = \kappa_1^1$
  $(L_1 + \kappa_1^1\tilde{L}_1)\int_0^{\tau_1} e^{-\gamma_1 a} f_1(a)da|_{\sigma_1=\sigma_{1\max}} = 2.3042 < 5 = \kappa_1^1$
- $\left[(L_2 + \kappa_2^1\tilde{L}_2)\int_0^{\tau_2} e^{-\gamma_2 a} f_2(a)da - 1\right] \beta_2(0)|_{\sigma_2=\sigma_{2\min}} = 3.8302 < 4 = \delta_2$
  $\left[(L_2 + \kappa_2^1\tilde{L}_2)\int_0^{\tau_2} e^{-\gamma_2 a} f_2(a)da - 1\right] \beta_2(0)|_{\sigma_2=\sigma_{2\max}} = 1.2541 < 4 = \delta_2$
  $(L_2 + \kappa_2^1\tilde{L}_2)\int_0^{\tau_2} e^{-\gamma_2 a} f_2(a)da|_{\sigma_2=\sigma_{2\min}} = 4.8302 < 5 = \kappa_2^1$
  $(L_2 + \kappa_2^1\tilde{L}_2)\int_0^{\tau_2} e^{-\gamma_2 a} f_2(a)da|_{\sigma_2=\sigma_{2\max}} = 2.2541 < 5 = \kappa_2^1$

According to Corollary 2, the origin of the studied model in Example 5 is globally asymptotically stable.

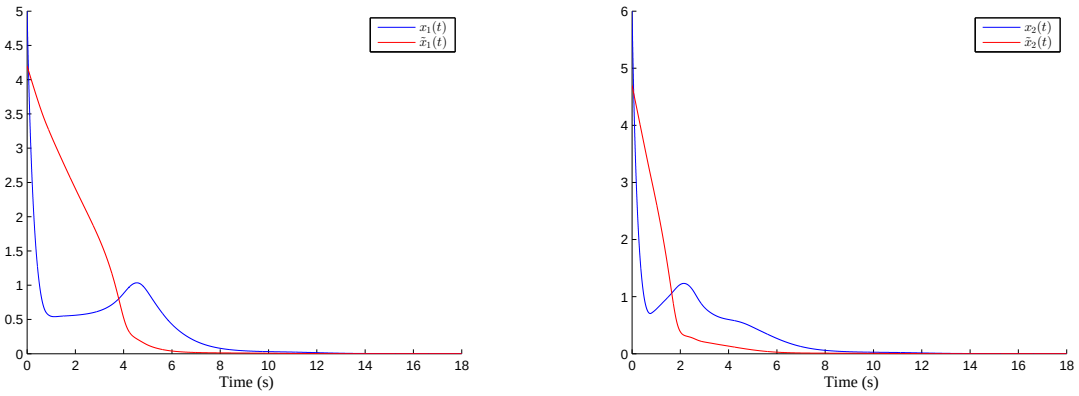

Fig. 3.13 Qualitative behavior of the trajectories x_i and $\tilde{x}_i$ for the model in Example 5.

3.6 Stability analysis of the positive steady state in the healthy hematopoiesis

A strictly positive equilibrium X^e reflects the surviving of all the generations of blood cells, which is the aim of a *healthy* hematopoiesis. When the condition (3.9) is satisfied, a unique X^e exists. In this section, we are interested in finding an estimate of the basin of attraction of X^e.

Let us also recall that the components of X^e can be computed from the equation,

$$\beta_1(x_1^e) = \frac{\delta_1}{\alpha_1}, \tag{3.82}$$

and for $i \in \{2,\ldots,n\}$, from the equations (3.13), which always admit a unique solution.

Let us start by looking to the reintroduction functions β_i, from the resting to the proliferating stages. We previously mentioned that, owing to some biological considerations, the following Hill functions were

proposed by Mackey in [180],

$$\beta_i(x_i) = \frac{\beta_i(0)}{1 + b_i x_i^{\mathfrak{n}_i}}, \tag{3.83}$$

with $\beta_i(0) > 0$, $b_i > 0$ and $\mathfrak{n}_i \geq 2$. This typical choice was assumed in subsequent works ([8] and [226]). Actually, many other decreasing functions β_i, with a finite maximum $\beta_i(0)$ and adjustable slope and inflection point can be chosen to match the biological assumptions [180].

Throughout this section, we consider the functions β_i in the form (3.83) and we indicate later for which other forms our results remain valid.

Since we are interested in the positive equilibrium X^e, we perform the classical changes of coordinates, $\hat{x}_i = x_i - x_i^e$, for $i \in I_n$. It follows from (3.1)-(3.2) that

$$\begin{aligned}
\dot{\hat{x}}_i(t) = &- \delta_i \left[\hat{x}_i(t) + x_i^e\right] - w_i\left(\hat{x}_i(t) + x_i^e\right) \\
&+ 2L_i \int_{t-\tau_i}^{t} g_i(t-a) w_i\left(\hat{x}_i(a) + x_i^e\right) da \\
&+ 2K_{i-1} \int_{t-\tau_{i-1}}^{t} g_{i-1}(t-a) w_{i-1}\left(\hat{x}_{i-1}(a) + x_{i-1}^e\right) da.
\end{aligned} \tag{3.84}$$

However, a new representation of (3.84) that eases the analysis of its origin can be obtained. Indeed, observe that, with an abuse of notation, $w_i(\hat{x}_i + x_i^e) = w_i(x_i^e) + \mu_i \hat{x}_i + R_i(\hat{x}_i)$, where,

$$\mu_i = \beta_i(x_i^e) + \beta_i'(x_i^e) x_i^e, \quad \text{and,} \quad R_i(\hat{x}_i) = \int_{x_i^e}^{x_i^e + \hat{x}_i} [\hat{x}_i + x_i^e - l] w_i^{(2)}(l) dl. \tag{3.85}$$

Moreover, we denote $\beta_{i*} = \delta_i + \mu_i$. It follows that (3.84) is equivalent to

$$\begin{aligned}
\dot{\hat{x}}_i(t) = &- \beta_{i*} \hat{x}_i(t) + 2L_i \mu_i \int_{t-\tau_i}^{t} g_i(t-a) \hat{x}_i(a) da \\
&- R_i(\hat{x}_i(t)) + 2L_i \int_{t-\tau_i}^{t} g_i(t-a) R_i(\hat{x}_i(a)) da \\
&+ 2K_{i-1} \mu_{i-1} \int_{t-\tau_{i-1}}^{t} g_{i-1}(t-a) \hat{x}_{i-1}(a) da \\
&+ 2K_{i-1} \int_{t-\tau_{i-1}}^{t} g_{i-1}(t-a) R_{i-1}(\hat{x}_{i-1}(a)) da.
\end{aligned} \tag{3.86}$$

Remark 16. *Compared with Section 3.5, the stability analysis of the origin of* (3.86) *is more complicated due to the shifting. Indeed, linear functionals can no longer be used since the system* (3.86) *is not positive. A common approach to investigate the stability properties of such a class of systems is by using quadratic functions or functionals, as illustrated in the sequel.*

3.6.1 Introductory result based on Razumikhin's Theorem

To get a first intuition, let us consider the subsystem (3.86) for $i = 1$. A linear approximation at its origin is obtained by neglecting the terms where R_1 is present. The following linear system is obtained:

$$\dot{z}_1(t) = - \beta_{1*} z_1(t) + 2L_1 \mu_1 \int_{t-\tau_1}^{t} g_1(t-a) z_1(a) da. \tag{3.87}$$

Let us consider the positive definite quadratic function

$$Q(a) = \frac{1}{2}a^2. \tag{3.88}$$

We apply the Razumikhin's Theorem (see Chapter 1): Pick a constant $q > 1$ and consider $t \geq 0$ such that $qQ(z_1(t)) \geq Q(z_1(a)),\ \ \forall a \in (t-\tau_1, t)$. Then the derivative of Q along the trajectories of the (3.87) satisfies:

$$\begin{aligned} \dot{Q}(t) &\leq -2\beta_{1*}Q(z_1(t)) + 4\sqrt{Q(z_1(t))}L_1|\mu_1| \int_{t-\tau_1}^{t} g_1(t-a)\sqrt{Q(z_1(a))}da \\ &\leq -2\left[\beta_{1*} - 2\sqrt{q}L_1|\mu_1|C_1\right] Q(z_1(t)). \end{aligned} \tag{3.89}$$

We conclude from Razumikhin's theorem that the condition $\beta_{1*} - 2L_1|\mu_1|C_1 > 0$ is sufficient for the asymptotic stability of the origin of the system (3.87). This leads us to introduce, for all $i \in I_n$, the constants

$$\varsigma_i = \beta_{i*} - 2L_i|\mu_i|C_i = \delta_i + \mu_i - 2L_i|\mu_i|C_i, \tag{3.90}$$

that will be of use later in the stability analysis of the nonlinear system, in the analytic expression of the quadratic Lyapunov-Krasovskii functionals and in the size of the region of attraction that we will provide.

3.6.2 Introductory result based on Lyapunov-Krasovskii Theorem

Here we prove a similar result to the one provided in the previous section: we extend it to any number of stages n. Recall that the positive equilibrium point of the system (3.1)-(3.2) has never been studied by Lyapunov techniques. For our application, the Lyapunov-Krasovskii approach is more advantageous than the Razumikhin's one, since the LKF can be used to provide an estimate of the basin of attraction of the positive steady state.

In this section, we consider the case where a positive equilibrium point exists and determine a quadratic Lyapunov-Krasovskii functional whose derivative along the trajectories of the system is smaller, in a neighborhood of the equilibrium point, than a negative definite function of the state variable.

$$\begin{cases} \dot{z}_1(t) = -\beta_{1*}z_1(t) + M_1\mu_1 \displaystyle\int_{t-\tau_1}^{t} g_1(t-l)z_1(l)dl, \\ \dot{z}_i(t) = -\beta_{i*}z_i(t) + M_i\mu_i \displaystyle\int_{t-\tau_i}^{t} g_i(t-l)z_i(l)dl \\ \qquad\qquad +2K_{i-1}\mu_{i-1} \displaystyle\int_{t-\tau_{i-1}}^{t} g_{i-1}(t-l)z_{i-1}(l)dl, \ \text{ when } \ i \in \{2,\dots,n\}, \end{cases} \tag{3.91}$$

with $M_i = 2L_i$ for all $i \in \{1,\dots,n\}$,

$$\beta_{i*} = \delta_i + \mu_i, \tag{3.92}$$

$$\mu_i = \left[\frac{\partial w_i(x_i)}{\partial x_i}\right]_{x_i = x_i^e} = \beta_i(x_i^e) + \beta_i'(x_i^e)x_i^e, \tag{3.93}$$

for all $i \in \{1,\dots,n\}$. Let us recall the definition of the constants ς_i, which are given for all $i \in \{1,\dots,n\}$ by

$$\varsigma_i = \beta_{i*} - M_i|\mu_i| \int_0^{\tau_i} g_i(a)da, \tag{3.94}$$

and observe for later use that

$$\varsigma_i = \delta_i + \mu_i - 2L_i|\mu_i|C_i. \tag{3.95}$$

Let us also define the constants

$$\xi_1 = 0\ ,\ \xi_i = \frac{8K_{i-1}^2|\mu_{i-1}|^2C_{i-1}}{\varsigma_i},\ \forall i \in \{2,\dots,n\}, \tag{3.96}$$

$$\eta_1 = 0\ ,\ \eta_i = \frac{2}{3\varsigma_i}\xi_i C_{i-1},\ \forall i \in \{2,\dots,n\}, \tag{3.97}$$

and,

$$q_n = 1\ ,\quad q_i = 2^{n-i}\prod_{k=i+1}^{n}\eta_k\ ,\quad \forall i \in \{1,...,n-1\}. \tag{3.98}$$

We recall that

$$Q(a) = \frac{1}{2}a^2, \tag{3.99}$$

for all $i \in \{1,\dots,n\}$,

$$\Omega_i(z_{it}) = \int_{t-\tau_i}^{t}\int_{l}^{t} g_i(l-a+\tau_i)Q(z_i(a))dadl, \tag{3.100}$$

$$R_1(z_{1t}) = \frac{1}{\varsigma_1}\left[\frac{1}{2}Q(z_1(t)) + L_1|\mu_1|\Omega_1(z_{1t})\right], \tag{3.101}$$

$$S_i(z_{it}) = \frac{1}{2}Q(z_i(t)) + L_i|\mu_i|\Omega_i(z_{it}) \tag{3.102}$$

and, for all $i \in \{2,\dots,n\}$,

$$R_i(z_{it}, z_{i-1t}) = \frac{4}{3\varsigma_i}\left[S_i(z_{it}) + \frac{\xi_i}{2}\Omega_{i-1}(z_{i-1t})\right]. \tag{3.103}$$

We are ready to state and prove the main result of the section.

Theorem 5. *The conditions*

$$\varsigma_i > 0, \tag{3.104}$$

for all $i \in \{1,\dots,n\}$, ensure that the origin of (3.86) is locally asymptotically stable. Moreover, the functional U

$$U(Z_t) = \sum_{i=1}^{n} q_i R_i(z_{it}, z_{i-1t}) \tag{3.105}$$

with $Z = (z_1,\dots,z_n)$ and where the constant q_i are the constants defined in (3.98) is such that its derivative along the solutions of system (3.91) *satisfies*

$$\dot{U}(t) \le -Q(z_n(t)) - \sum_{j=1}^{n-1} 2^{n-j-1}\prod_{k=j+1}^{n}\eta_k Q(z_j(t)). \tag{3.106}$$

Remark 17. *One can check easily that the functional U satisfies the conditions of Lyapunov-Krasovskii's theorem.*

Proof. **i) Lyapunov-Krasovskii result for $i = 1$:**

The derivative along the trajectories of (3.91) of $Q(z_1)$, where Q is the function defined in (3.99), satisfies the inequality

$$\dot{Q}(t) \quad \leq \quad -\beta_{1*}z_1(t)^2 + 2L_1|\mu_1| \int_{t-\tau_1}^{t} g_1(t-a)|z_1(t)z_1(a)|da. \tag{3.107}$$

Using the inequality $|z_1(t)z_1(a)| \leq \frac{1}{2}|z_1(t)|^2 + \frac{1}{2}|z_1(a)|^2$, we obtain

$$\dot{Q}(t) \leq -2\beta_{1*}Q(z_1(t)) + 2L_1|\mu_1| \int_{t-\tau_1}^{t} g_1(t-a)Q(z_1(t))da + 2L_1|\mu_1| \int_{t-\tau_1}^{t} g_1(t-a)Q(z_1(a))da.$$

As an immediate consequence,

$$\frac{1}{2}\dot{Q}(t) \leq \left[-\beta_{1*} + L_1|\mu_1| \int_0^{\tau_1} g_1(a)da\right] Q(z_1(t)) + L_1|\mu_1| \int_{t-\tau_1}^{t} g_1(t-a)Q(z_1(a))da. \tag{3.108}$$

Now, we consider the functional S_1 defined in (3.102). Using

$$\dot{\Omega}_1(t) = \int_{t-\tau_1}^{t} g_1(l-t+\tau_1)dlQ(z_1(t)) - \int_{t-\tau_1}^{t} g_1(t-a)Q(z_1(a))da, \tag{3.109}$$

we deduce that its derivative along the trajectories of (3.91) satisfies

$$\dot{S}_1(t) \leq -\varsigma_1 Q(z_1(t)), \tag{3.110}$$

with ς_1 defined in (3.94). Thus, we recover the result given by Razumikhin Theorem in the previous section. Next, we extend the proof for any $i \in I_n$.

ii) Lyapunov-Krasovskii functional for the overall system:

Now, we consider the overall maturity-structured model of cell differentiation (3.91). Let us rewrite this system with simplifying notations:

$$\begin{cases} \dot{z}_1(t) = -\beta_{1*}z_1(t) + M_1\mu_1\Im_1(z_{1t}) \\ \dot{z}_i(t) = -\beta_{i*}z_i(t) + M_i\mu_i\Im_i^{\dagger}(z_{it}) + 2K_{i-1}\mu_{i-1}\Im_{i-1}^{\dagger}(z_{i-1t}) \text{ , when } \quad i > 1, \end{cases} \tag{3.111}$$

with,

$$\Im_i^{\dagger}(z_{it}) = \int_{t-\tau_i}^{t} g_i(t-a)z_i(a)da \tag{3.112}$$

for all $i \in \{1, \ldots, n\}$. Then we deduce from the previous part of the proof of Theorem 5 that

$$\begin{aligned} \dot{S}_i(t) &\leq \left[-\beta_{i*} + M_i|\mu_i| \int_0^{\tau_i} g_i(a)da\right] Q(z_i(t)) + \frac{1}{2}z_i(t)2K_{i-1}\mu_{i-1}\Im_{i-1}^{\dagger}(z_{i-1t}) \\ &= \left[-\beta_{i*} + M_i|\mu_i| \int_0^{\tau_i} g_i(a)da\right] Q(z_i(t)) + K_{i-1}z_i(t)\mu_{i-1}\Im_{i-1}^{\dagger}(z_{i-1t}). \end{aligned} \tag{3.113}$$

It follows that

$$\dot{S}_i(t) \leq -\varsigma_i Q(z_i(t)) + \nu_{i-1} \int_{t-\tau_{i-1}}^{t} g_{i-1}(t-l) z_i(t) z_{i-1}(l) dl, \tag{3.114}$$

with ς_i defined in (3.94) and $\nu_{i-1} = K_{i-1}|\mu_{i-1}|$.

Notice that for any constant $c > 0$, $|z_i(t)z_{i-1}(a)| \leq \frac{1}{2c}|z_i(t)|^2 + \frac{c}{2}|z_{i-1}(a)|^2$. It follows that

$$\begin{aligned}\dot{S}_i(t) \leq & -\varsigma_i Q(z_i(t)) + \frac{1}{2c}\nu_{i-1}\int_{t-\tau_{i-1}}^{t} g_{i-1}(t-a)|z_i(t)|^2 da + \frac{c}{2}\nu_{i-1}\int_{t-\tau_{i-1}}^{t} g_{i-1}(t-a)|z_{i-1}(a)|^2 da \\ = & -\varsigma_i Q(z_i(t)) + \frac{1}{c}\nu_{i-1}C_{i-1}Q(z_i(t)) + c\nu_{i-1}\int_{t-\tau_{i-1}}^{t} g_{i-1}(t-a)Q(z_{i-1}(a))da.\end{aligned}$$

Choosing $c = \frac{4\nu_{i-1}C_{i-1}}{\varsigma_i}$, we obtain

$$\dot{S}_i(t) \leq -\tfrac{3}{4}\varsigma_i Q(z_i(t)) + \tfrac{\xi_i}{2}\int_{t-\tau_{i-1}}^{t} g_{i-1}(t-a)Q(z_{i-1}(a))da. \tag{3.115}$$

Now, consider the functional R_1 defined in (3.101) and, for $i \in \{2,\dots,n\}$ the functionals R_i defined in (3.103). Then it follows from (3.102) and (3.110) that

$$\dot{R}_1(t) \leq -Q(z_1(t)) \tag{3.116}$$

and, for $i \in \{2,\dots,n\}$, (3.115) implies that

$$\begin{aligned}\dot{R}_i(t) \leq & -Q(z_i(t)) + \frac{2}{3\varsigma_i}\xi_i\int_{t-\tau_{i-1}}^{t} g_{i-1}(t-a)Q(z_{i-1}(a))da \\ & + \frac{2}{3\varsigma_i}\xi_i\int_{t-\tau_{i-1}}^{t} g_{i-1}(l+\tau_{i-1}-t)Q(z_{i-1}(t))dl \\ & - \frac{2}{3\varsigma_i}\xi_i\int_{t-\tau_{i-1}}^{t} g_{i-1}(t-a)Q(z_{i-1}(a))da \\ = & -Q(z_i(t)) + \frac{2}{3\varsigma_i}\xi_i\int_{0}^{\tau_{i-1}} g_{i-1}(l)dl Q(z_{i-1}(t)) \\ = & -Q(z_i(t)) + \eta_i Q(z_{i-1}(t)).\end{aligned} \tag{3.117}$$

Let us consider the functional U defined in (3.105). Then we straightforwardly deduce from (3.116) and (3.117) that

$$\begin{aligned}\dot{U}(t) \leq & \sum_{i=2}^{n} q_i[-Q(z_i(t)) + \eta_i Q(z_{i-1}(t))] - q_1 Q(z_1(t)) \\ \leq & -\sum_{i=2}^{n} q_i Q(z_i(t)) + \sum_{j=2}^{n-1} q_{j+1}\eta_{j+1}Q(z_j(t)) + q_2\eta_2 Q(z_1(t)) - q_1 Q(z_1(t)).\end{aligned} \tag{3.118}$$

By grouping the terms, we obtain

$$\dot{U}(t) \leq -q_n Q(z_n(t)) + \sum_{j=1}^{n-1}\left(q_{j+1}\eta_{j+1} - q_j\right)Q(z_j(t)). \tag{3.119}$$

Using (3.98), we obtain

$$q_{j+1}\eta_{j+1} - q_j = 2^{n-j-1}\prod_{k=j+1}^{n}\eta_k - 2^{n-j}\prod_{k=j+1}^{n}\eta_k.$$

We deduce that (3.106) is satisfied. The functional U defined in (3.105) satisfies the conditions of Lyapunov-Krasovskii's Theorem. It follows that X^e is a locally asymptotically stable equilibrium point of the system (3.91). □

3.6.3 Exponential stability of the positive equilibrium via a novel LKF

In the previous section, we discussed the local asymptotic stability of the positive steady state of the system (3.86). In this section, we will extend this result by designing a novel Lyapunov-Krasovskii functional implying local exponential stability under the same previous sufficient conditions and making possible to estimate the rate of convergence. For technical reasons that will appear along our constructions, the analytic expression of the novel functional is slightly different from the one proposed in the previous section. This functional will allow us to achieve our next objective, which is to determine an approximation of the basin of attraction of the positive equilibrium of the nonlinear system (3.86).

Let us state and prove the following result:

Theorem 6. *The conditions*

$$\varsigma_i > 0, \tag{3.120}$$

for all $i \in I_n$, ensure that the origin of (3.86) *is locally exponentially stable.*

Proof. We recall that the linear approximation of the system (3.86) at its origin (which is obtained by neglecting in (3.86) all the terms where R_i is present for all $i \in I_n$), can be written as follows

$$\begin{aligned}\dot{z}_i(t) = &-\beta_{i*}z_i(t) + 2L_i\mu_i\int_{t-\tau_i}^{t} g_i(t-a)z_i(a)da \\ &+ 2K_{i-1}\mu_{i-1}\int_{t-\tau_{i-1}}^{t} g_{i-1}(t-a)z_{i-1}(a)da.\end{aligned} \tag{3.121}$$

Contrary to Section 3.5, the nonpositivity of the system under study motivates the introduction of the positive definite function in (3.99). Let us consider also the following two functionals:

$$\Omega_i(\varphi_{it}) = \int_{t-\tau_i}^{t}\int_{l}^{t} g_i(l-a+\tau_i)Q(\varphi_i(a))dadl, \tag{3.122}$$

$$\Lambda_i(\varphi_{it}) = \int_{t-\tau_i}^{t} e^{l-t}\int_{l}^{t} g_i(l-a+\tau_i)Q(\varphi_i(a))dadl. \tag{3.123}$$

In fact, other types of functionals may be used instead of (3.122) and (3.123). However, for the sake of clarity, we use a weighted combination of them in order to compensate the distributed delayed terms and estimate the exponential decay rates. Moreover, we define for all $i \in I_n$, the following functionals:

Let us define for all $i \in I_n$ the following functionals

$$S_i(z_{it}) = \frac{1}{2}Q(z_i(t)) + L_i|\mu_i|\Omega_i(z_{it}), \tag{3.124}$$

$$N_1(z_{1t}) = S_1(z_{1t}) + \frac{\varsigma_1}{2C_1}\Lambda_1(z_{1t}), \tag{3.125}$$

and for all $i \in \{2,\dots,n\}$,

$$N_i(z_{it}, z_{i-1t}) = S_i(z_{it}) + \frac{\varsigma_i}{2C_i}\Lambda_i(z_{it}) + \psi_i\Lambda_{i-1}(z_{i-1t}), \tag{3.126}$$

where ψ_i is an appropriate strictly positive constant to be determined later for all $i \in \{2,\dots,n\}$.

First of all, observe for later use that the derivatives of the functionals Ω_i and Λ_i, for all $i \in I_n$, along the trajectories of (3.121) satisfy,

$$\dot{\Omega}_i(t) = C_iQ(z_i(t)) - \int_{t-\tau_i}^{t} g_i(t-a)Q(z_i(a))da, \tag{3.127}$$

$$\begin{aligned}\dot{\Lambda}_i(t) &= -\Lambda_i(z_{it}) - e^{-\tau_i}\int_{t-\tau_i}^{t} g_i(t-a)Q(z_i(a))da + \int_0^{\tau_i} e^{l-\tau_i}g_i(l)dlQ(z_i(t)) \\ &\leq -\Lambda_i(z_{it}) - e^{-\tau_i}\int_{t-\tau_i}^{t} g_i(t-a)Q(z_i(a))da + C_iQ(z_i(t)),\end{aligned} \tag{3.128}$$

where the last inequality is a consequence of the definition of the constants C_i given by (3.5.6).

For the sake of clarity, we will decompose now the proof of Theorem 6 into two parts: we start the construction of a Lyapunov functional for the first compartment and next we generalize this construction to any number of compartments.

i) Lyapunov-Krasovskii functional for the first compartment:

Using the inequality $|z_1(t)z_1(a)| \leq \frac{1}{2}|z_1(t)|^2 + \frac{1}{2}|z_1(a)|^2$, one can readily check that the derivative along the trajectories of (3.91) of $Q(z_1)$, where Q is the function defined in (3.99), satisfies the inequality

$$\frac{1}{2}\dot{Q}(t) \leq [-\beta_{1*} + L_1|\mu_1|C_1]\,Q(z_1(t)) + L_1|\mu_1|\int_{t-\tau_1}^{t} g_1(t-a)Q(z_1(a))da. \tag{3.129}$$

The derivative of the functional N_1, defined in (3.125), along the trajectories of (3.91) satisfies

$$\dot{N}_1(t) \leq -\frac{\varsigma_1}{2}Q(z_1(t)) - \frac{\varsigma_1}{2C_1}\Lambda_1(z_{1t}). \tag{3.130}$$

On the other hand, observe that

$$\begin{aligned}N_1(z_{1t}) \leq &\frac{1}{2}Q(z_1(t)) + \frac{\varsigma_1}{2C_1}\int_{t-\tau_1}^{t} e^{l-t}\int_l^t g_1(l-a+\tau_1)Q(z_1(a))dadl \\ &+ L_1|\mu_1|\int_{t-\tau_1}^{t}\int_l^t e^{(l-(t-\tau_1))}g_1(l-a+\tau_1)Q(z_1(a))dadl.\end{aligned}$$

Then

$$N_1(z_{1t}) \leq \frac{1}{2}Q(z_1(t)) + \left(\frac{\varsigma_1 + 2L_1C_1|\mu_1|e^{\tau_1}}{2C_1}\right)\Lambda_1(z_{1t}). \tag{3.131}$$

From (3.130) and (3.131) we deduce that

$$\dot{N}_1(t) \leq -\tilde{\varsigma}_1 N_1(z_{1t}) - \frac{\varsigma_1}{4}Q(z_1(t)), \tag{3.132}$$

for all $\xi_1 \in \left(0, \min\left\{\frac{\varsigma_1}{2}, \frac{\varsigma_1}{\varsigma_1+2L_1C_1|\mu_1|e^{\tau_1}}\right\}\right)$.

ii) Lyapunov-Krasovskii functional for the overall system:

Now observe that for $i>1$, the derivatives of the functions $Q(z_i(t))$ along the trajectories of (3.91) satisfy

$$\begin{aligned}\dot{Q}(t) \leq & -\beta_{i*}z_i^2(t)+2L_i|\mu_i|\int_{t-\tau_i}^{t} g_i(t-a)|z_i(t)z_i(a)|da \\ & +2K_{i-1}|\mu_{i-1}|\int_{t-\tau_{i-1}}^{t} g_{i-1}(t-a)|z_i(t)z_{i-1}(a)|da.\end{aligned}$$

Using the inequalities: $|z_i(t)z_i(a)| \leq Q(z_i(t))+Q(z_i(a)$, for all $i \in I_n$, and $|z_i(t)z_{i-1}(a)| \leq \xi_i Q(z_i(t))+\frac{1}{\xi_i}Q(z_{i-1}(a))$, with $\xi_i>0$, for all $i>1$, it follows that

$$\begin{aligned}\dot{Q}(t) \leq & 2\left[-\beta_{i*}+L_i|\mu_i|C_i\right]Q(z_i(t))+2L_i|\mu_i|\int_{t-\tau_i}^{t} g_i(t-a)Q(z_i(a))da \\ & +2\xi_i K_{i-1}|\mu_{i-1}|C_{i-1}Q(z_i(t))+\frac{2K_{i-1}|\mu_{i-1}|}{\xi_i}\int_{t-\tau_{i-1}}^{t} g_{i-1}(t-a)Q(z_{i-1}(a))da.\end{aligned}$$

We keep in mind the inequality (3.132), and we observe that, for $i>1$, the derivatives of the functionals N_i, defined in (3.126), along the trajectories of (3.91) satisfy

$$\begin{aligned}\dot{N}_i(t) \leq & \left[-\beta_{i*}+2L_i|\mu_i|C_i\right]Q(z_i(t))+\xi_i K_{i-1}|\mu_{i-1}|C_{i-1}Q(z_i(t)) \\ & +\frac{K_{i-1}|\mu_{i-1}|}{\xi_i}\int_{t-\tau_{i-1}}^{t} g_{i-1}(t-a)Q(z_{i-1}(a))da \\ & -\frac{\varsigma_i}{2C_i}\Lambda_i(z_{it})+\frac{\varsigma_i}{2}Q(z_i(t))+\psi_i\dot{\Lambda}_i(t).\end{aligned} \tag{3.133}$$

Choosing

$$\psi_i = \frac{K_{i-1}|\mu_{i-1}|e^{\tau_{i-1}}}{\xi_i}+m_i e^{\tau_{i-1}}, \tag{3.134}$$

with $m_i>0$, the inequality (3.133) gives

$$\begin{aligned}\dot{N}_i(t) \leq & -\frac{\varsigma_i}{2}Q(z_i(t))-\frac{\varsigma_i}{2C_i}\Lambda_i(z_{it})-\psi_i\Lambda_{i-1}(z_{i-1t})+\psi_i C_{i-1}Q(z_{i-1}(t)) \\ & +\xi_i K_{i-1}|\mu_{i-1}|C_{i-1}Q(z_i(t))-m_i\int_{t-\tau_{i-1}}^{t} g_{i-1}(t-a)Q(z_{i-1}(a))da.\end{aligned} \tag{3.135}$$

Remark 18. *In the remainder of the current proof, one can choose $m_i=0$ for all $i \in \{2,\ldots,n\}$. In fact, the role of this parameter when it is strictly positive will appear in the proof of the next theorem -in the next section- where we analyze the nonlinear system and we determine a subset of the basin of attraction of its positive steady state.*

Now, observe that if we select $\xi_i = \frac{\varsigma_i}{4K_{i-1}|\mu_{i-1}|C_{i-1}}$, for all $i \in \{2,...,n\}$, then

$$\dot{N}_i(t) \leq -\frac{\varsigma_i}{4}Q(z_i(t))-\frac{\varsigma_i}{2C_i}\Lambda_i(z_{it})-\psi_i\Lambda_{i-1}(z_{i-1t})+\psi_i C_{i-1}Q(z_{i-1}(t)). \tag{3.136}$$

One can readily check that there exists a strictly positive real number $\tilde{\varsigma}_i$ such that

$$\dot{N}_i(t) \leq -\tilde{\varsigma}_i N_i(z_{it}, z_{i-1t}) - \frac{\varsigma_i}{8} Q(z_i(t)) + \frac{\theta_i^{\ominus} \varsigma_{i-1}}{8} Q(z_{i-1}(t)), \tag{3.137}$$

with $\theta_i^{\ominus} = \frac{8\psi_i C_{i-1}}{\varsigma_{i-1}}$. In order to establish that the conditions (3.120), for all $i \in I_n$, are sufficient to ensure that the origin of the cascaded system (3.91) is exponentially stable, we introduce the functional:

$$W(Z_t) = p_1 N_1(z_{1t}) + \sum_{i=2}^{n} p_i N_i(z_{it}, z_{i-1t}), \tag{3.138}$$

with

$$p_i = 2^{n-i} \prod_{k=i+1}^{n} \theta_k^{\ominus}, \quad p_n = 1. \tag{3.139}$$

From (3.132) and (3.137), we conclude that

$$\begin{aligned} \dot{W}(t) \leq & -\sum_{i=1}^{n} p_i \tilde{\varsigma}_i N_i(z_{it}, z_{i-1t}) - \frac{p_1 \varsigma_1}{4} Q(z_1(t)) \\ & - \sum_{i=2}^{n} \frac{p_i \varsigma_i}{8} Q(z_i(t)) + \sum_{i=2}^{n} \frac{p_i \theta_i^{\ominus} \varsigma_{i-1}}{8} Q(z_{i-1}(t)). \end{aligned} \tag{3.140}$$

On the other hand

$$p_i \theta_i^{\ominus} = 2^{n-i} \prod_{k=i+1}^{n} \theta_k^{\ominus} \theta_i^{\ominus} = \frac{1}{2} p_{i-1}. \tag{3.141}$$

By combining (3.140) and (3.141), we deduce that

$$\begin{aligned} \dot{W}(t) \leq & -\sum_{i=1}^{n} p_i \tilde{\varsigma}_i N_i(z_{it}, z_{i-1t}) - \frac{\varsigma_n}{8} Q(z_n(t)) - \frac{1}{2} \sum_{i=1}^{n-1} \frac{p_i \varsigma_i}{8} Q(z_i(t)) - \frac{p_1 \varsigma_1}{8} Q(z_1(t)) \\ \leq & -\xi W(Z_t), \end{aligned} \tag{3.142}$$

with $\xi > 0$. From the features of the functional W and the inequality (3.142) we conclude that the origin of the system (3.91) is exponentially stable. The next step in this work consists in determining an approximation of the basin of attraction of the strictly positive equilibrium of the nonlinear system (3.86).

□

3.6.4 Estimate of the region of attraction of the positive steady state

Here we will use the functionals N_i defined in the previous section (i.e. the functionals that allowed us to prove local exponential stability of the positive steady state), to provide an estimate of the basin of attraction of the positive steady state.

For that, let us first state and prove the following assertion:

Claim 1. *There exist constants $\hat{s}_i > 0$, for all $i \in I_n$, which depend on the biological parameters of the model and on the strictly positive equilibrium X^e, such that, for all $\hat{x}_i > -x_i^e$, $x_i^e > 0$, the inequality*

$$|R_i(\hat{x}_i)| \leq \hat{s}_i Q(\hat{x}_i), \tag{3.143}$$

is satisfied.

Proof. For notational convenience, we drop the subscript "i" and we use x_e instead of x_i^e to denote the positive equilibrium. Using the expression of β given in (3.83), we observe that for all $x_e > 0$ and $\mathfrak{z} > -x_e$,

$$R(\mathfrak{z}) = \beta(0)J(\mathfrak{z}) - \mu\mathfrak{z} \tag{3.144}$$

where $J(\mathfrak{z}) = \frac{\mathfrak{z}+x^e}{1+b(\mathfrak{z}+x_e)^{\mathfrak{n}}} - \frac{x_e}{1+bx_e^{\mathfrak{n}}}$. First, let us study the function

$$\rho(\mathfrak{z}) = \frac{1}{1+b(\mathfrak{z}+x_e)^{\mathfrak{n}}} - \frac{1}{1+bx_e^{\mathfrak{n}}} = \frac{b\left[{x_e}^{\mathfrak{n}} - (\mathfrak{z}+x_e)^{\mathfrak{n}}\right]}{p(\mathfrak{z})}, \tag{3.145}$$

where, $p(\mathfrak{z}) = \left[1+b(\mathfrak{z}+x_e)^{\mathfrak{n}}\right](1+bx_e^{\mathfrak{n}})$. Observe that,

$$(\mathfrak{z}+x_e)^{\mathfrak{n}} - x_e^{\mathfrak{n}} = \mathfrak{n}x_e^{\mathfrak{n}-1}\mathfrak{z} + \mathfrak{n}\int_0^{\mathfrak{z}}\int_{x_e}^{x_e+l}(\mathfrak{n}-1)m^{n-2}dmdl.$$

Consequently,

$$\rho(\mathfrak{z}) = -\frac{\mathfrak{n}bx_e^{\mathfrak{n}-1}}{p(\mathfrak{z})}\mathfrak{z} + \mathfrak{C}(\mathfrak{z}), \tag{3.146}$$

where $\mathfrak{C}(\mathfrak{z}) = -\frac{\mathfrak{n}b(\mathfrak{n}-1)}{p(\mathfrak{z})}\int_0^{\mathfrak{z}}\int_0^l (m+x_e)^{\mathfrak{n}-2}dmdl$. Denote $h = 1+bx_e^{\mathfrak{n}}$, and observe that

$$\frac{1}{p(\mathfrak{z})} = \frac{1}{h}\left(\rho(\mathfrak{z}) + \frac{1}{h}\right). \tag{3.147}$$

From (3.147) and (5.48), it follows that $\rho(\mathfrak{z}) = -\mathfrak{n}bx_e^{\mathfrak{n}-1}\left(\frac{\rho(\mathfrak{z})}{h} + \frac{1}{h^2}\right)\mathfrak{z} + \mathfrak{C}(\mathfrak{z})$. Consequently, we get the intermediate result:

$$\rho(\mathfrak{z}) = -\frac{\mathfrak{n}bx_e^{\mathfrak{n}-1}}{h^2}\mathfrak{z} + \mathfrak{C}(\mathfrak{z}) - \frac{\mathfrak{n}bx_e^{\mathfrak{n}-1}}{h}\rho(\mathfrak{z})\mathfrak{z}. \tag{3.148}$$

On the other hand, observe that,

$$J(\mathfrak{z}) = \left(\rho(\mathfrak{z}) + \frac{1}{h}\right)\mathfrak{z} + x_e\rho(\mathfrak{z}) = \mathfrak{c}_1\mathfrak{z} + \mathfrak{c}_2\mathfrak{C}(\mathfrak{z}) + \mathfrak{c}_3\rho(\mathfrak{z})\mathfrak{z}, \tag{3.149}$$

where the last equality is a direct consequence of (5.49), with $\mathfrak{c}_1 = \frac{1}{h} - \frac{\mathfrak{n}bx_e^{\mathfrak{n}}}{h^2}$, $\mathfrak{c}_2 = x_e$ and $\mathfrak{c}_3 = \left(1 - \frac{\mathfrak{n}bx_e^{\mathfrak{n}}}{h}\right)$. Now, we readily check that

$$\left|\mathfrak{C}(\mathfrak{z})\right| \leq \frac{\mathfrak{n}b(\mathfrak{n}-1)}{p(\mathfrak{z})}\left(|\mathfrak{z}|+x_e\right)^{\mathfrak{n}-2}\frac{\mathfrak{z}^2}{2}. \tag{3.150}$$

Now, from (5.48), we deduce that $\left|\rho(\mathfrak{z})\right| \leq \frac{\mathfrak{n}bx_e^{\mathfrak{n}-1}}{p(\mathfrak{z})}|\mathfrak{z}| + |\mathfrak{C}(\mathfrak{z})|$. Moreover, using (5.51), we get

$$\left|\mathfrak{z}\rho(\mathfrak{z})\right| \leq \frac{\mathfrak{n}bx_e^{\mathfrak{n}-1}}{p(\mathfrak{z})}\mathfrak{z}^2 + \frac{\mathfrak{n}b(\mathfrak{n}-1)}{2p(\mathfrak{z})}\left(|\mathfrak{z}|+x_e\right)^{\mathfrak{n}-2}|\mathfrak{z}|^3. \tag{3.151}$$

From (5.50), we deduce that,

$$|J(\mathfrak{z}) - \mathfrak{c}_1\mathfrak{z}| \leq \frac{\mathfrak{n}b(\mathfrak{n}-1)|\mathfrak{c}_3|}{2p(\mathfrak{z})}\left(|\mathfrak{z}|+x_e\right)^{\mathfrak{n}-2}|\mathfrak{z}|^3 + \left[\frac{\mathfrak{n}b(\mathfrak{n}-1)|\mathfrak{c}_2|\left(|\mathfrak{z}|+x_e\right)^{\mathfrak{n}-2}}{2p(\mathfrak{z})} + \frac{\mathfrak{n}bx_e^{\mathfrak{n}-1}|\mathfrak{c}_3|}{p(\mathfrak{z})}\right]\mathfrak{z}^2.$$

Now, observe that $\frac{1}{p(\mathfrak{z})} = \frac{1}{\left[1+b(\mathfrak{z}+x_e)^{\mathfrak{n}}\right]h}$. Therefore, for $\mathfrak{z} \geq 0$, we get $\frac{1}{p(\mathfrak{z})} = \frac{1}{\left[1+b(|\mathfrak{z}|+x_e)^{\mathfrak{n}}\right]h}$, and when $\mathfrak{z} \leq 0 \quad \Big(\text{i.e. } \mathfrak{z} \in (-x_e, 0]\Big)$, we get $\frac{1}{p(\mathfrak{z})} \leq \frac{1}{h} \leq \frac{1+b(2x_e)^{\mathfrak{n}}}{\left[1+b(|\mathfrak{z}|+x_e)^{\mathfrak{n}}\right]h}$. Consequently, for all $\mathfrak{z} > -x_e$, we have $\frac{1}{p(\mathfrak{z})} \leq \frac{1+b(2x_e)^{\mathfrak{n}}}{\left[1+b(|\mathfrak{z}|+x_e)^{\mathfrak{n}}\right]h}$. We deduce that

$$\begin{aligned}\left|J(\mathfrak{z}) - \mathfrak{c}_1\mathfrak{z}\right| \leq \Bigg[&\left(\frac{\mathfrak{n}b(\mathfrak{n}-1)|\mathfrak{c}_3|(1+b(2x_e)^{\mathfrak{n}})}{2h}\right)\frac{\left(|\mathfrak{z}|+x_e\right)^{\mathfrak{n}-2}|\mathfrak{z}|}{1+b(|\mathfrak{z}|+x_e)^{\mathfrak{n}}} \\ &+ \frac{\mathfrak{n}b(\mathfrak{n}-1)|\mathfrak{c}_2|\left(|\mathfrak{z}|+x_e\right)^{\mathfrak{n}-2}\left(1+b(2x_e)^{\mathfrak{n}}\right)}{2\left[1+b(|\mathfrak{z}|+x_e)^{\mathfrak{n}}\right]h} + \frac{\mathfrak{n}bx_e^{\mathfrak{n}-1}|\mathfrak{c}_3|\left(1+b(2x_e)^{\mathfrak{n}}\right)}{\left[1+b(|\mathfrak{z}|+x_e)^{\mathfrak{n}}\right]h}\Bigg]\mathfrak{z}^2.\end{aligned}$$

By distinguishing between the two cases $|\mathfrak{z}|+x_e \geq 1$ and $|\mathfrak{z}|+x_e \leq 1$, one can prove that the following inequalities are satisfied for all $\mathfrak{z} > -x_e$,

$$\frac{\left(|\mathfrak{z}|+x_e\right)^{\mathfrak{n}-2}|\mathfrak{z}|}{1+b(|\mathfrak{z}|+x_e)^{\mathfrak{n}}} \leq \frac{\left(|\mathfrak{z}|+x_e\right)^{\mathfrak{n}-1}}{1+b(|\mathfrak{z}|+x_e)^{\mathfrak{n}}} \leq \max\left\{b, b^{-1}\right\}.$$

It follows that

$$|J(\mathfrak{z}) - \mathfrak{c}_1\mathfrak{z}| \leq \mathfrak{c}_4\mathfrak{z}^2, \tag{3.152}$$

with the positive constant

$$\mathfrak{c}_4 = \frac{\mathfrak{n}b(\mathfrak{n}-1)(1+b(2x_e)^{\mathfrak{n}})\left(x_e+|\mathfrak{c}_3|\right)\max\left\{b, b^{-1}\right\}}{2h} + \frac{\mathfrak{n}bx_e^{\mathfrak{n}-1}\left(1+b(2x_e)^{\mathfrak{n}}\right)|\mathfrak{c}_3|}{h^2}.$$

On the other hand, we easily check that $\mu = \beta(0)\mathfrak{c}_1$, with μ defined in (3.85). It follows that, by combining (5.47) and (5.53), we obtain $|R(\mathfrak{z})| \leq \beta(0)\mathfrak{c}_4\mathfrak{z}^2$. Since $Q(\mathfrak{z}) = \frac{1}{2}\mathfrak{z}^2$, we conclude that $|R(\mathfrak{z})| \leq \hat{s}Q(\mathfrak{z})$,where one possible value of $\hat{s}$ is $\hat{s} = 2\mathfrak{c}_4\beta(0)$. □

Remark 19. *It is worth mentioning that the stability analysis which will be performed for the origin of the nonlinear system* (3.86) *is available for many other reintroduction functions β_i, as long as they satisfy the sector condition* (3.143).

Furthermore, in order to ease the notation, we denote

$$I_i(\hat{x}_{it}) = \int_{t-\tau_i}^{t} g_i(t-a)Q(\hat{x}_i(a))da. \tag{3.153}$$

Finally, we define the constants $\tilde{k}_i = \frac{\varsigma_i}{8\hat{s}_i}$, $\hat{k}_i = \frac{\varsigma_i}{4C_iL_i\hat{s}_ie^{\tau_i}}$ and $\overline{N}_i = \min\left\{\tilde{k}_i^2, \hat{k}_i^2\right\}$. Notice that for all $i \in I_n$, $\tilde{k}_i$ and $\hat{k}_i$ are only dependent on the constant biological parameters of the model.

Now we are ready to state and prove the following result:

Theorem 7. *Let the system* (3.86) *be such that*

$$\varsigma_i > 0, \tag{3.154}$$

for all $i \in I_n$. Then all the solutions of (3.86) *with initial conditions $\hat{\varphi}_i \in \mathscr{C}([-\tau_i, 0], \mathbb{R})$ satisfying*

$$N_i(\hat{\varphi}_i, \hat{\varphi}_{i-1}) < \overline{N}_i, \tag{3.155}$$

converge exponentially to the origin.

Remark 20. *Generally, Lyapunov theory provides sufficient conditions for stability. However, due to earlier published works we can comment conditions* (3.154)*. In previous works (using frequency domain approaches), it was claimed in [8] that the origin is locally asymptotically stable if $\delta_i + (2L_iC_i + 1)\,\mu_i > 0$ is satisfied. However, in [225], it was shown that the previous assertion holds true only when $-\delta_i < \mu_i < 0$. We notice that our stability conditions* (3.154) *are equivalent to those of [225] on that interval. Next, when $\mu_i > 0$, our exponential stability conditions* (3.154) *(which are provided without specifying a particular form of f_i), correspond to the conditions for local stability provided in [225] (and which have been slightly improved using Nyquist criterion for a typical selection of the functions f_i in [225]). It remains the case $\mu_i < -\delta_i$ which is not covered by the Lyapunov approach proposed here, and which was addressed in [225]. The region of attraction defined in* (3.155) *is rather difficult to interpret. In fact, based on some numerical simulations and the conjecture made in [225], we suggest that the region defined in* (3.155) *is conservative.*

Proof. **i) Lyapunov-Krasovskii functional for the first compartment:**

We start with the first generation of hematopoietic stem cells. Here we are using the results already proved in the previous section. Then, we deduce that the derivative of the function $Q(\hat{x}_1(t))$, introduced in (3.99), along the trajectories of (3.86) satisfies

$$\begin{aligned}\dot{Q}(t) \leq & 2\left[-\beta_{1*} + L_1|\mu_1|C_1\right]Q(\hat{x}_1(t)) + \hat{s}_1|\hat{x}_1(t)|Q(\hat{x}_1(t)) \\ & + 2L_1\left(|\mu_1| + \hat{s}_1|\hat{x}_1(t)|\right)I_1(\hat{x}_{1t}).\end{aligned} \tag{3.156}$$

It follows that the derivative of the functional N_1, introduced in (3.125), satisfies

$$\begin{aligned}\dot{N}_1(t) \leq & -\left[\frac{\varsigma_1}{8}Q(\hat{x}_1(t)) + \frac{\varsigma_1}{2C_1}\Lambda_1(\hat{x}_{1t})\right] + \left[\frac{\hat{s}_1}{2}|\hat{x}_1(t)| - \frac{\varsigma_1}{4}\right]Q(\hat{x}_1(t)) \\ & - \frac{\varsigma_1}{8}Q(\hat{x}_1(t)) + \left[L_1\hat{s}_1|\hat{x}_1(t)| - \frac{\varsigma_1 e^{-\tau_1}}{2C_1}\right]I_1(\hat{x}_{1t}).\end{aligned} \tag{3.157}$$

On the other hand, from the definition of N_1 we observe that

$$N_1(\hat{x}_{1t}) \leq \frac{1}{2}Q(\hat{x}_1(t)) + \left(\frac{\varsigma_1 + 2L_1C_1|\mu_1|e^{\tau_1}}{2C_1}\right)\Lambda_1(\hat{x}_{1t}). \tag{3.158}$$

From (3.157) and (3.158), we deduce that for all $\tilde{\varsigma}_1 \in \left(0, \min\left\{\frac{\varsigma_1}{4}, \frac{\varsigma_1}{\varsigma_1+2L_1C_1|\mu_1|e^{\tau_1}}\right\}\right)$, the derivative of the functional N_1 satisfies

$$\dot{N}_1(t) \leq -\tilde{\varsigma}_1 N_1(\hat{x}_{1t}) + \left[\frac{\hat{s}_1}{2}|\hat{x}_1(t)| - \frac{\varsigma_1}{4}\right] Q_1(\hat{x}_1(t)) + \left[L_1\hat{s}_1|\hat{x}_1(t)| - \frac{\varsigma_1 e^{-\tau_1}}{2C_1}\right] I_1(\hat{x}_{1t}) - \frac{\varsigma_1}{8} Q(\hat{x}_1(t)).$$

From the definition of N_1, which is given in (3.125), we notice that $|\hat{x}_1(t)| \leq 2\sqrt{N_1(\hat{x}_{1t})}$. A direct consequence is that

$$\begin{aligned}\dot{N}_1(t) \leq & -\tilde{\varsigma}_1 N_1(\hat{x}_{1t}) + \left[\hat{s}_1\sqrt{N_1(\hat{x}_{1t})} - \frac{\varsigma_1}{4}\right] Q_1(\hat{x}_1(t)) \\ & + \left[2L_1\hat{s}_1\sqrt{N_1(\hat{x}_{1t})} - \frac{\varsigma_1 e^{-\tau_1}}{2C_1}\right] I_1(\hat{x}_{1t}) - \frac{\varsigma_1}{8} Q(\hat{x}_1(t)).\end{aligned}$$

Now, we conclude that if the condition (3.155) is satisfied, then

$$\dot{N}_1(t) \leq -\tilde{\varsigma}_1 N_1(\hat{x}_{1t}) - \frac{\varsigma_1}{8} Q(\hat{x}_1(t)). \tag{3.159}$$

This allows us to conclude that the origin of the subsystem (3.86), for $i = 1$, is exponentially stable, with a decay rate smaller than $\tilde{\varsigma}_1$.

ii) LKF for the overall system: Here we take into account all generations of immature blood cells. Using the inequality $|\hat{x}_i(t)\hat{x}_{i-1}(a)| \leq \xi_i Q(\hat{x}_i(t)) + \frac{1}{\xi_i} Q(\hat{x}_{i-1}(a))$, with $\xi_i > 0$ for $i > 1$, and the inequality $|\hat{x}_i(t)\hat{x}_i(a)| \leq Q(\hat{x}_i(t)) + Q(\hat{x}_i(a))$, for $i \in I_n$, we can show that if we select $\psi_i = \frac{K_{i-1}|\mu_{i-1}|e^{\tau_{i-1}}}{\xi_i} + \frac{\varsigma_i e^{-\tau_i} K_{i-1}\hat{s}_{i-1}}{2L_i\hat{s}_i C_i} e^{\tau_{i-1}}$, then the derivatives of the functions $Q(\hat{x}_i(t))$, for all $i > 1$, along the trajectories of (3.86) satisfy

$$\begin{aligned}\dot{Q}(t) \leq & 2\left[-\beta_{i*} + L_i|\mu_i|C_i\right] Q(\hat{x}_i(t)) + \hat{s}_i|\hat{x}_i(t)|Q(\hat{x}_i(t)) \\ & + 2L_i\left(|\mu_i| + \hat{s}_i|\hat{x}_i(t)|\right) I_i(\hat{x}_{it}) + 2K_{i-1}|\mu_{i-1}|C_{i-1}\xi_i Q(\hat{x}_i(t)) \\ & + 2K_{i-1}\left(\hat{s}_{i-1}|\hat{x}_i(t)| + \frac{|\mu_{i-1}|}{\xi_i}\right) I_{i-1}(\hat{x}_{i-1t}).\end{aligned} \tag{3.160}$$

Moreover, we choose $\xi_i = \frac{\varsigma_i}{4K_{i-1}|\mu_{i-1}|C_{i-1}}$. It follows that

$$\begin{aligned}\dot{N}_i(t) \leq & -\tilde{\varsigma}_i N_i(\hat{x}_i, \hat{x}_{i-1}) + \psi_i C_{i-1} Q(\hat{x}_{i-1}(t)) - \left[\frac{\varsigma_i}{8} - \frac{1}{2}\hat{s}_i|\hat{x}_i(t)|\right] Q(\hat{x}_i(t)) \\ & - \frac{\varsigma_i}{16} Q(\hat{x}_i(t)) + L_i\hat{s}_i\left[|\hat{x}_i(t)| - \frac{\varsigma_i e^{-\tau_i}}{2L_i\hat{s}_i C_i}\right] I_i(\hat{x}_{it}) \\ & + K_{i-1}\hat{s}_{i-1}\left[|\hat{x}_i(t)| - \frac{\varsigma_i e^{-\tau_i}}{2L_i\hat{s}_i C_i}\right] I_{i-1}(\hat{x}_{i-1t}),\end{aligned} \tag{3.161}$$

with $\tilde{\varsigma}_i > 0$. Finally, we conclude that if the conditions (3.155) are satisfied, then

$$\dot{N}_i(t) \leq -\tilde{\varsigma}_i N_i(\hat{x}_{it}, \hat{x}_{i-1t}) - \frac{\varsigma_i}{16} Q(\hat{x}_i(t)) + \psi_i C_{i-1} Q(\hat{x}_{i-1}(t)). \tag{3.162}$$

As we had done in the previous Section, we can prove that the derivative of the functional

$$W(\hat{X}_t) = \sum_{i=1}^{n} p_i N_i(\hat{x}_{it}, \hat{x}_{i-1t}), \text{ with } p_i = 2^{n-i} \prod_{k=i+1}^{n} \frac{8\psi_k C_{k-1}}{\varsigma_{k-1}}, \ p_n = 1,$$

where $\hat{X} = (\hat{x}_1, \ldots, \hat{x}_n)$, satisfies,

$$\dot{W}(t) \leq -\sum_{i=1}^{n} p_i \tilde{\varsigma}_i N_i(\hat{x}_{it}, \hat{x}_{i-1t}) - \frac{\varsigma_1}{8} Q(\hat{x}_1(t)) - \frac{\varsigma_n}{16} Q(\hat{x}_n(t)) - \frac{1}{2} \sum_{i=1}^{n-1} \frac{p_i \varsigma_i}{8} Q(\hat{x}_i(t)).$$

Finally, we obtain for all $t \geq 0$,

$$\dot{W}(t) \leq -\varsigma W(\hat{X}_t), \tag{3.163}$$

with $\varsigma = \min\{\tilde{\varsigma}_1, \ldots, \tilde{\varsigma}_n\} > 0$.

To summarize, by virtue of the properties of the functionals N_i, for all $i \in I_n$, and since the original system (3.1) is a positive system, we conclude that the set

$$\mathscr{A} = \left\{ \varphi_i \in \mathscr{C}([-\tau_i, 0], \mathbb{R}_+) : N_i(\varphi_i - x_i^e, \varphi_{i-1} - x_{i-1}^e) < \overline{N}_i \right\}, \tag{3.164}$$

is a subset of the basin of attraction of the positive steady state of system (3.1). □

Example 6. *In this numerical example, we consider the system with the following biological functions and parameters for $n = 3$:*

	$\beta_i(x_i)$	$f_i(a)$	δ_i	τ_i	γ_i	K_i
$i=1$	$\frac{0.5}{1+x_1^2}$	$\frac{10e^{10a}}{e^{10\tau_1}-1}$	0.1356	1.109402	0.3	0.05
$i=2$	$\frac{1}{1+x_2^4}$	$\frac{10e^{10a}}{e^{10\tau_2}-1}$	0.1669	1.2	0.4	0.07
$i=3$	$\frac{3}{1+x_3^2}$	$\frac{2e^{2a}}{e^{2\tau_2}-1}$	0.3559	1.36	0.45	0.085

From the selected parameters, it follows that: $C_1 = 0.7390$, $C_2 = 0.6445$, $C_3 = 0.6580$, and,

	x_i^e	α_i	ς_i	$\hat{s}_i$	$\overline{N}_i$
$i=1$	0.70036	0.40422	0.08924	0.65070	2.5935×10^{-4}
$i=2$	0.78225	0.19888	0.02329	3.00487	9.3935×10^{-7}
$i=3$	1.0050	0.20422	0.33938	2.98491	2.02×10^{-4}

We select the initial conditions: $\varphi_1 = 0.6850$, $\varphi_2 = 0.782$ and $\varphi_3 = 0.979$.
Therefore, $\mathscr{N}_1(\varphi_1 - x_1^e) = 7.16 \times 10^{-5} < \overline{N}_1$,
$\mathscr{N}_2(\varphi_2 - x_2^e, \varphi_1 - x_1^e) = 6.65 \times 10^{-7} < \overline{N}_2$,
$\mathscr{N}_3(\varphi_3 - x_3^e, \varphi_2 - x_2^e) = 1.94 \times 10^{-4} < \overline{N}_3$.
According to Theorem 3, the positive steady state $X^e = \left(x_1^e, x_2^e, x_3^e\right)$ is exponentially stable (Figure 3.14).

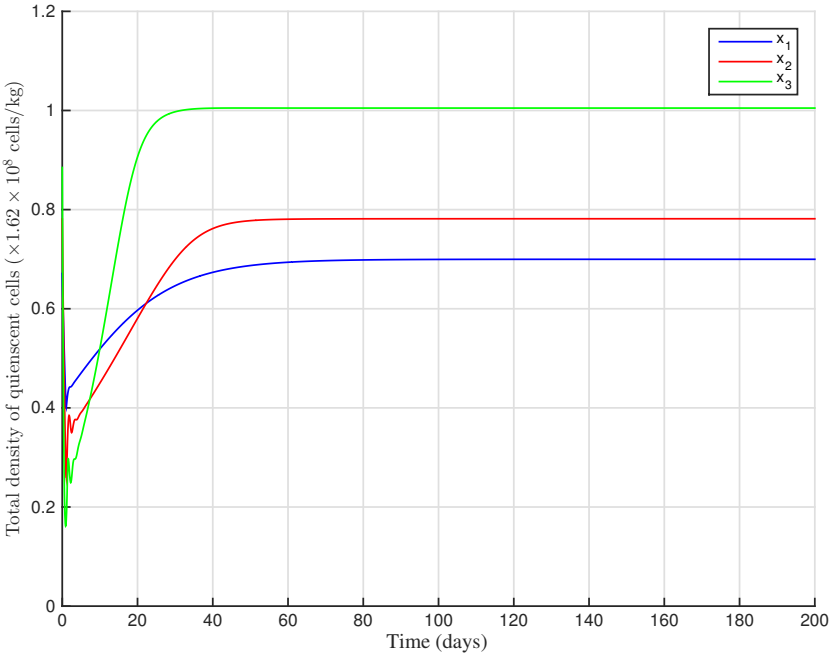

Fig. 3.14 Trajectories of Example 6.

3.6.5 Robustness analysis of the positive equilibrium

In this section, we consider the perturbed system (3.1), that we write in the form (3.86), which is determined by performing the change of coordinate $\hat{x}_i(t) = x_i(t) - x_i^e$. Based on the functionals constructed in Theorem 3, we prove the following result:

Corollary 3. *Let the system* (3.86) *be perturbed by a nonvanishing additive disturbances* $\varepsilon(t) \in (0, \varepsilon_i]$, $\overline{\varepsilon}_i > 0$, *for all* $t > 0$ *and* $i \in I_n$. *If the conditions*

$$\varsigma_i > 0 \tag{3.165}$$

are satisfied for all $i \in I_n$, *then all the solutions of* (3.86) *with initial conditions* $\varphi_i \in \mathscr{C}([-\tau_i, 0], \mathbb{R}^+)$ *satisfying*

$$\left(\frac{2\overline{\varepsilon}_i}{\theta\tilde{\varsigma}_i}\right)^2 \leq N_i(\varphi_i - x_i^e, \hat{\varphi}_{i-1} - x_{i-1}^e) < \overline{N}_i, \tag{3.166}$$

with $\theta \in (0,1)$, *converge exponentially to the domain,*

$$\mathscr{G}_{\overline{\varepsilon}_i} = \left\{ \varphi_i \in \mathscr{C}([-\tau_i, 0], \mathbb{R}),\ \ N_i(\varphi_i - x_i^e, \varphi_{i-1} - x_{i-1}^e) \leq \left(\frac{2\overline{\varepsilon}_i}{\theta\tilde{\varsigma}_i}\right)^2 \right\}. \tag{3.167}$$

Proof. Let us prove the previous result for $i = 1$. Arguing as we did in the proof of Theorem 3, one can generalize to the overall system. First, observe that the derivative of $Q(\hat{x}_1(t))$ along the trajectories of the

perturbed system satisfies:

$$\begin{aligned}\dot{Q}(t) \leq & 2\left[-\beta_{1*}+L_1|\mu_1|C_1\right]Q(\hat{x}_1(t))+\hat{s}_1|\hat{x}_1(t)|Q(\hat{x}_1(t)) \\ & +2L_1\left(|\mu_1|+\hat{s}_1|\hat{x}_1(t)|\right)I_1(\hat{x}_{1t})+|\hat{x}_1(t)|\overline{\varepsilon}_i.\end{aligned} \tag{3.168}$$

Consequently, the derivative of the functional N_1, introduced in (3.125), along the trajectories of the perturbed system, verifies

$$\begin{aligned}\dot{N}_1(t) \leq & -\left[\frac{\varsigma_1}{8}Q(\hat{x}_1(t))+\frac{\varsigma_1}{2C_1}\Lambda_1(\hat{x}_{1t})\right]+\left[\frac{\hat{s}_1}{2}|\hat{x}_1(t)|-\frac{\varsigma_1}{4}\right]Q(\hat{x}_1(t)) \\ & -\frac{\varsigma_1}{8}Q(\hat{x}_1(t))+\left[L_1\hat{s}_1|\hat{x}_1(t)|-\frac{\varsigma_1 e^{-\tau_1}}{2C_1}\right]I_1(\hat{x}_{1t})+|\hat{x}_1(t)|\overline{\varepsilon}_i.\end{aligned} \tag{3.169}$$

Using (3.158), and the fact that $|\hat{x}_1(t)| \leq 2\sqrt{N_1(\hat{x}_{1t})}$, we obtain

$$\begin{aligned}\dot{N}_1(t) \leq & -\tilde{\varsigma}_1 N_1(\hat{x}_{1t})+\left[\hat{s}_1\sqrt{N_1(\hat{x}_{1t})}-\frac{\varsigma_1}{4}\right]Q_1(\hat{x}_1(t)) \\ & +\left[2L_1\hat{s}_1\sqrt{N_1(\hat{x}_{1t})}-\frac{\varsigma_1 e^{-\tau_1}}{2C_1}\right]I_1(\hat{x}_{1t})-\frac{\varsigma_1}{8}Q(\hat{x}_1(t))+2\overline{\varepsilon}_i\sqrt{N_1(\hat{x}_{1t})},\end{aligned}$$

where $\tilde{\varsigma}_1 \in \left(0, \min\left\{\frac{\varsigma_1}{4}, \frac{\varsigma_1}{\varsigma_1+2L_1C_1|\mu_1|e^{\tau_1}}\right\}\right)$. Therefore, when $N_1(\varphi_1-x_1^e)<\overline{N}_1$ is satisfied, we deduce that

$$\dot{N}_1(t) \leq -\tilde{\varsigma}_1 N_1(\hat{x}_{1t})-\frac{\varsigma_1}{8}Q(\hat{x}_1(t))+2\overline{\varepsilon}_i\sqrt{N_1(\hat{x}_{1t})}. \tag{3.170}$$

Now, let us consider any $\theta \in (0,1)$ and observe that for all initial conditions φ_1 satisfying $N_1(\varphi_1-x_1^e)<\overline{N}_1$ with $\varphi_1 \notin \mathscr{G}_{\overline{\varepsilon}_i}$, the inequality (3.170) gives

$$\dot{N}_1(t) \leq -(1-\theta)\tilde{\varsigma}_1 N_1(\hat{x}_{1t}). \tag{3.171}$$

We conclude that the states x_{1t} satisfying (3.166) converge exponentially to the invariant set $\mathscr{G}_{\overline{\varepsilon}_1}$, defined in (3.167), with a decay rate smaller or equal to $\frac{(1-\theta)\tilde{\varsigma}_1}{2}$. □

3.7 Concluding remarks and discussion

With the aim of constantly refining and improving the modeling and the analysis of hematopoietic mechanisms, we proposed explicit constructions of suitable strict Lyapunov-Krasovksii functionals for some nonlinear hematopoietic systems with finite distributed delays ([8], [24]). Within a broader framework regarding unhealthy hematopoiesis, we had begun the chapter with a review of earlier trends and objectives behind mathematical analysis in this field. Later, we showed how our (Lyapunov) approach allowed us to solve some practical and technical issues, which complement already published results on the topic. For instance, in comparison with the previous work in [225], we complement and improved some analysis aspects by providing exponential stability with an estimate on the decay rate of the solutions

and a basin of attraction formulation, without any extra assumption on the mitosis functions. Then, for the first time in the analysis of the studied models, a robustness analysis is performed when they are subject to some nonvanishing perturbations. We have also illustrated how dedifferentiation flux (cell-plasticity abilities), together with model uncertainties -that may for instance rise from reintroduction functions from resting to proliferating stages- can generate nonvanishing perturbations in the studied time-delay models.

In addition, we covered some practical situations such as time-varying differentiating rates (to model the action on the blockade in differentiation and redifferentiation), that we discussed in several examples, using switching parameters (i.e. piecewise continuous functions) or periodic behaviors. Throughout the chapter, we discussed some recent biological facts (e.g. redifferentiation therapy trends and cell-plasticity interpretations). Then, in the last part of the chapter, emphasis was given to the positive steady state that is well-suited to describe healthy hematopoiesis. For the first time we proposed a study which is based on Lyapunov theory for the strictly positive steady state. Then, in that framework, we provided an explicit formulation of a subset of its region of attraction, which is the first one to be established, even if -practically- the basin associated to the Lyapunov-Krasovskii functionals seems to be conservative if compared with simulation results.

The work that we will present in the next chapter will particularly enhance the role of dedifferentiation and transdifferentiation by considering a simple hematopoietic model where cell plasticity is no more a marginal phenomenon, and cannot be considered as a perturbation, but has to be fully modeled.

Chapter 4

A model with infinite distributed delays involving cell arrest and plasticity

Synopsis. **A model of proliferation and quiescence in living organisms is studied. Here we extend the work presented in the previous chapter in two directions.** ***(I)*** **Firstly, we discuss how to reconcile some earlier modeling ways of the cell cycle in one common framework. Then, accordingly, we consider a model that contains a compartment where cells may be quiescent for an unlimited time, along with a proliferating phase (modeling the cell cycle) in which most of the cells may divide, or die, while few of them may be arrested during their cycle for unlimited time. The resulting system extends the model of [8] - studied in the previous chapter - by considering the possibly case of infinite distributed delays. A Lyapunov technique is then developed for the analysis of the origin of the system.** ***(II)*** **In the second part of the chapter, we consider for the first time some cell plasticity features in the class of systems that we study. As a first step, we are going to discuss some simple cases of cell-plasticity in unhealthy tissues, and we highlight the role that dedifferentiation may play in the survival of cancer cells (this hypothesis is in line with some medical observations). The main analysis is performed on a simpler model involving two maturity stages and a dedifferentiation function from progeny to SCs.**

4.1 Overview of the chapter

Generally, the length of the cycle is approximately 24 hours for fast-dividing mammalian cells. However, this duration varies from one type of tissue to another, and even from one cell to another. In addition, if a problem occurs in some cells within the total cell population, they may be arrested in one of the cell-cycle checkpoints (See Chapter 1). Several biological works have particularly focused on the length of the G_1 phase, as well as its possible applications (see [168] and [256]). For instance, the manipulation of the G_1 length in neural SCs is discussed in [256], including also its impacts on the differentiation of neural precursors. For other type of cells, we refer to Figure 1 in [168] that gives the lengths of the cell cycle (particularly G_1) of some important categories of cells, including blood lineages, gut lineage and neural lineage. Note that, in the classification given in [168], the cycle length of the *common myeloid progenitors* (CMP) - in the hematopoietic system - appears as unknown or undetermined (see also [40, 209] for the

mechanisms involved in hematopoietic SCs niches regulation). We also mention that cancer dormancy ([93, 15]) is sometimes justified by cellular dormancy, i.e. G_0 and G_1-arrest (see [15]). In addition, some drugs have cell arresting power and are used to stop the uncontrolled growth that characterizes proliferating cancer cells [244].

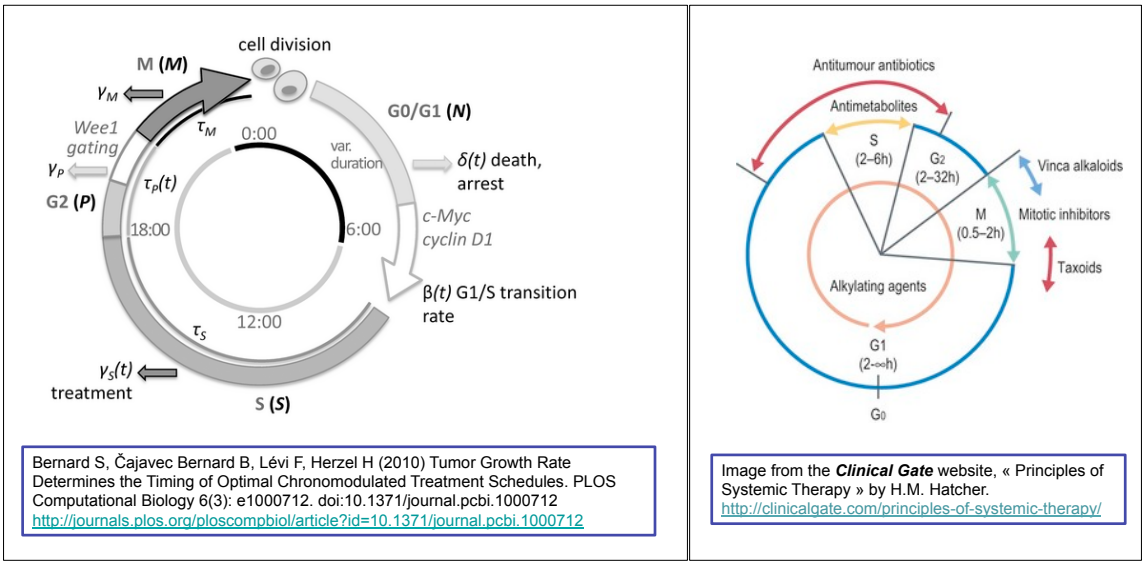

Bernard S, Čajavec Bernard B, Lévi F, Herzel H (2010) Tumor Growth Rate Determines the Timing of Optimal Chronomodulated Treatment Schedules. PLOS Computational Biology 6(3): e1000712. doi:10.1371/journal.pcbi.1000712
http://journals.plos.org/ploscompbiol/article?id=10.1371/journal.pcbi.1000712

Image from the ***Clinical Gate*** website, « Principles of Systemic Therapy » by H.M. Hatcher.
http://clinicalgate.com/principles-of-systemic-therapy/

Fig. 4.1 The Figure on the right is extracted from the online reference indicated at the bottom of the Figure. It shows the cell-cycle phases with their lengths and give some examples of drugs that act at a specific moment of the cycle (e.g. taxanes, which are mitotic inhibitors), or alkylating agents, which are independent-drugs that act at any cell-cycle sub-phase. The Figure on the left is from [38], and it belongs to the Open-i service of the National Library of Medicine that enables search and retrieval of abstracts and images from the open source literature. The figure on the left is taken from [38]. It shows the successive steps of the normal cell-cycle, starting from G_1 (of variable duration) until mitosis where two daughter cells are illustrated. The figure on the right is extracted from the online reference indicated at its bottom. It shows the phases of the cell-cycle according to their lenghts, as well as some classical drugs that impact the duration of the cycle at specific sub-phases (e.g. mitotic inhibitors such as taxanes) and alkylating agents (e.g. ifosfamide), which can target the cells at any moment during their cell-cycle.

In summary, we say that cell-cycle arrest may occur for many reasons, among which: **i)** if a DNA damage is detected by cells at some checkpoints, **ii)** due to insufficient nutriments, **iii)** resulting from drug infusions. More details are given in Box 11 for the interested reader.

We pointed out that an heterogeneous distribution of the cell-cycle length over the total density of cells within the same population exists, and it may complicate the modeling aspect of the cell-cycle. Indeed, basically, the questions that arise here are the following ones:

If some models take into account the cell arrest (i.e. the fact that some cells can be blocked during their cycle), while other models consider that all the cells must divide or die before a finite age, can we expect equivalent results in both frameworks? Does the minority of arrested cells cause a change in the asymptotic behavior of the model and on the stability properties of its steady states?

To answer these questions, we begin by briefly reviewing some existing models of the cell cycle. Then, we revisit the model in [8], studied in the previous chapter, and we extend it to the case where few cells can take infinite time to divide or die.

Box 11. Some extra-facts about the length of the cell cycle

① **Some uncertainty on the duration of the healthy cell-cycle:** This is particularly true for the growth-phase G_1, and the gap G_2, as illustrated in Figure 4.1.

② **A probable link between the cell-cycle arrest and cancer dormancy:** Cancer dormancy is still poorly understood, and is currently undergoing intensive research ([261]). In [15], the author reviewed some of the main clinical explanations justifying cancer dormancy. His key points include **cellular dormancy**, i.e. G_0 and G_1-arrest (but also angiogenic dormancy and immunosurveillance, or cancer immunoediting [15]).

③ **Drugs increase the duration of the cell-cycle and cause G_1-arrest:** Most of the anti-tumor drugs are targeting dividing cells in their cell-cycle (Figure 4.1). Drugs increase the duration of the cell-cycle and cause G_1-arrest, in order to halt cell overproliferation and achieve cancer dormancy. In fact, the idea to transform cancer into a chronic disease is in the voices of many people in the medical world nowadays ([111], [14]). *erlotinib*.

④ **The impact of changes in cell cycle duration on the biological properties of living tissues:** We have also noticed that some works focus on the impact of the variable length of the growth-phase G_1 ant its possible applications (see [168] and [256]). For instance, the manipulation of the G_1 length in neural stem cells is discussed in [256], including its impact on the differentiation features of neural precursors.

From a mathematical point of view, the resulting system (Section 4.3) that we study in the first part of this chapter has infinite distributed delays. A stability analysis of the 0-equilibrium is performed in Section 4.4, via the introduction of a novel Lyapunov-Krasovskii functional (LKF). The extension of the stability analysis of the positive steady state to the nonlinear model involving infinite distributed delays is performed in Section 4.6.

In the second part of the chapter, we highlight some cell plasticity features. We recall that cells have the ability to guide their development paths and determine their individual and collective fates (Chapter 2). Dedifferentiation allows cells to regress from an advanced differentiated state to a less differentiated one, including the case where cells lose their specific functions and become stem cells (Figure 4.2).

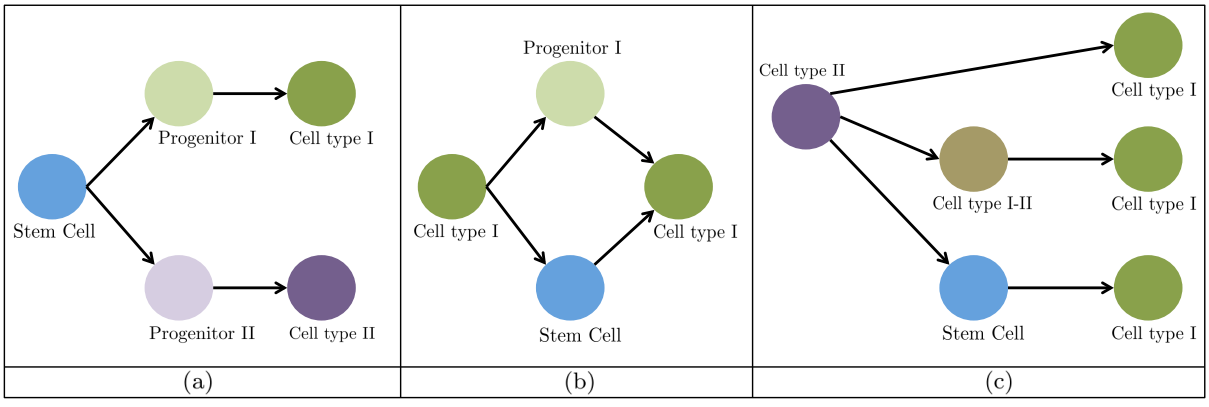

Fig. 4.2 **(a)** Cells development **(b) Dedifferentiation**: a lineage reversion in which differentiated cells acquire the properties of more immature cells within the same lineage hierarchy. **(c) Transdifferentiation**: the conversion of one differentiated cell type into another, or, the conversion of one progenitor/SC population into another SC type. Contrary to the case **(b)**, we notice in **(c)** that a cell of type I can be transformed to a cell of type II, without pasing through a SC state. **This illustrative figure of cell-plasticity features is adapted from [280]**.

Our aim is to introduce the process of cell dedifferentiation in living organisms in the models we study. Firstly, in Section 4.7, we briefly discuss the case in which more mature cells dedifferentiate into SCs, and join the resting SC phase. A more interesting situation is observed when, in Section 4.8, the dedifferentiated subpopulation of cells that join the SC compartment is directly active in proliferation. In the latter case, we are going to introduce a general modeling framework involving cell plasticity functions is given in Section 4.8.1. functions (Section 4.8.1), and then analyze a simpler case in which an unhealthy differentiated subpopulation of cells regresses to a CSC state. This is in fact the expected behavior of cancer cells when dedifferentiation is associated with cancer [286] (e.g. epigenetic mutations that increase the self-renewing activity of CSCs [173, 286]).

In Section 4.8.2, we study a specific (unhealthy) dedifferentiation process in which a (mutated) subpopulation of cancer cells belonging to the j-th generation in the cell hierarchy, where $j \in \{2, \dots, n\}$, dedifferentiates through a typical function to a SC stage. A stability analysis is carried out in Section 4.8.3, in the typical case involving two maturity stages and a dedifferentiation function from progeny to SCs.

4.2 An insight on some cell cycle modeling trends

Now, we compare between some early cell-cycle models and we situate the one we focus on in this chapter according to them. Firstly, it is worth mentioning that the objective behind the introduction of some models is to investigate the behavior of cells that undergo proliferation at their specific checkpoints (i.e. the transition from a given sub-phase to the next one). Accordingly, some mathematical models make a separation between some four sub-phases of the cell cycle (e.g. [25, 26, 39]), however, the latter perspective is beyond the scope of our work. Indeed, here we give a particular focus to the transition between the resting phase G_0 (which is not explicitly modeled in [39]) and the proliferating compartment (i.e. the cell-cycle, which is the sum of the four sub-phases G_1, S, G_2 and M), together with their respective lengths. This is described in Figure 4.3, where we point out some differences between two main modeling approaches: on the one hand, we observe the configurations **(A)** and **(B)** where a G_0 phase is considered, and on the other hand, we have the configuration **(C)** where G_0 is assimilated to G_1. These two trends may be reconciled by adopting the representation **(D)** (see the arguments given in Figure 4.3). We recall from the previous chapter that cell population models containing quiescent and proliferating phases date back to some pioneers works such as Burns & Tannok [49] and Mackey [180], which have been more recently improved by Adimy *et al.* [8].

In our context, the configuration **(D)** improves the one illustrated in **(C)** by clearly separating the G_0 compartment from the cell-cycle. From a biological point of view, the fact that G_0 and G_1 are separated is no longer a matter for debate [208]. In addition, contrary to **(A)** and **(B)**, the representation **(D)** extends the representation of the cell-cycle by considering it of unlimited length. Thus, the role of the growth phase G_1 and the gap phase G_2 (which are of variable duration in healthy and unhealthy cases, and which may halt some dividing cells in the cell cycle) is highlighted. The configuration in **(D)**-Figure 4.3 is the one that we consider in the first part of this chapter. Extending the LKF constructions we provided in the previous chapter to study the origin of the version involving infinite distributed delays is not a trivial task.

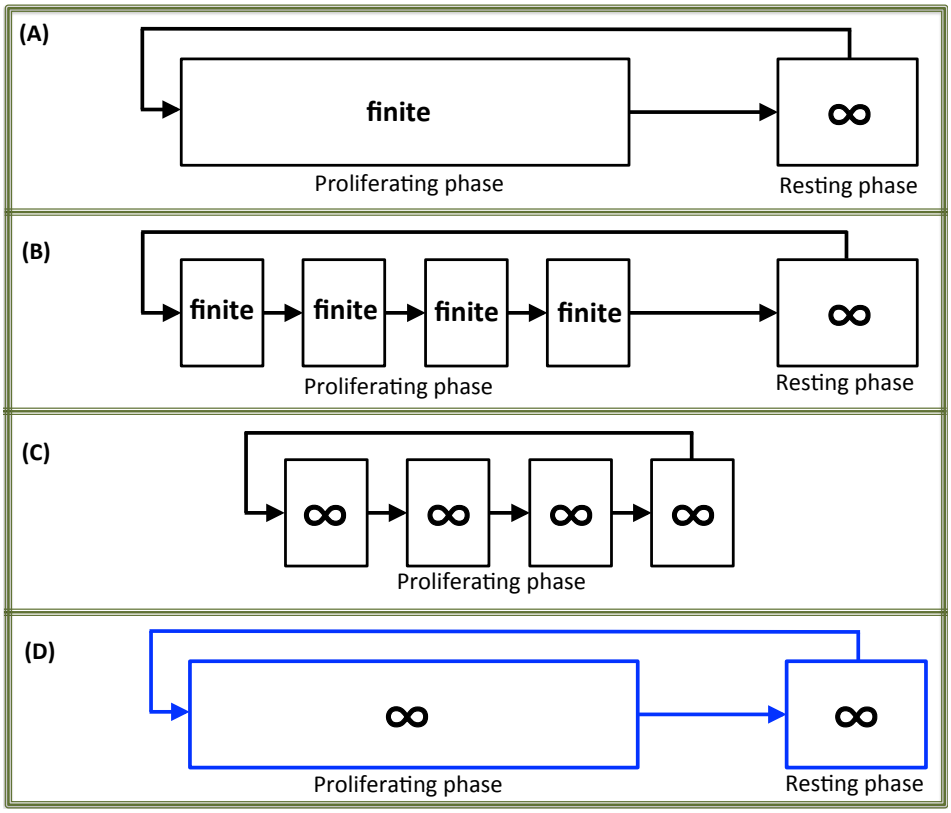

Fig. 4.3 Cartoon approximate representation of some cell cycle models from the literature. Configuration **(A)** is the one in which cells may be quiescent during their entire life, or they can enter to a proliferating stage of finite length (as in [8, 9, 225, 81]). In **(B)**, the cell cycle is splited into four sub-phases G_1, S, G_2 and M, each one has a finite duration (as in [25]), i.e. in **(B)** the length of the proliferating phase is finite since all the sub-phases were assumed to be finite. Next, the situation in **(C)** (as in [39]) is completeley different, since in this approach the cell cycle is described as an infinite support without an explicit resting phase G_0 (that can be associated with G_1). Thus, in **(C)**, the lengths of the sub-phases G_1, S, G_2 and M are infinite, and a focus is placed on how the transition from one sub-phase to the next one occurs. Finally, we notice that **(D)** (which is the model we introduce in this work) represents a genaral case in which -at least- G_1 or G_2 may be of infinite length in the cell cycle (which is compacted in a single infinite phase), along with a separated infinite G_0 compartment. In summary, one notices that the configuration **(D)** separates quiescence from proliferation (as in **(A)-(B)**), while proliferation is of infinite length (as in **(C)**). Some slightly different models are considered for instance in [47, 46], where a molecular structured population (involving age-and-cyclin structured-PDEs) have been studied, considering that the length of the cell cycle $G_1 - S - G_2 - M$ is infinite.

4.3 A nonlinear cell population model involving infinite distributed delays and time-varying parameters

We introduce in this section the model of interest, illustrated in Figure 4.12, in which we have n distinguishable maturity levels ($i \in I_n = \{1,\dots,n\}$, where $i = 1$ is the compartment of SCs). For the sake of clarity, as a first step, we will neglect the cell-plasticity features (dedifferentiation and transdifferentiation), that appear in Figure 4.4, and we perform a stability analysis of the model that takes into account cell arrest.

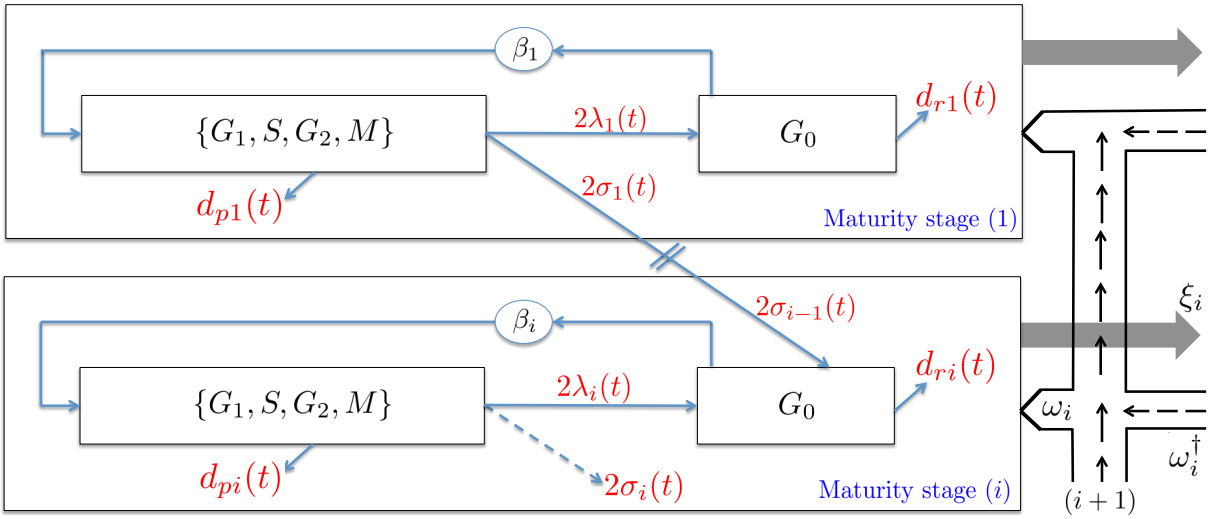

Fig. 4.4 A cartoon representation of the discrete maturity model of interest, that extends those of Mackey, Adimy *et al*. Cells of the i-th maturity-generation, where $i \in I_n = \{1, \dots, n\}$, $n > 1$, are in a resting phase G_0, or in proliferation (cell-division cycle) $\{G_1, S, G_2, M\}$ of infinite support (i.e. few cells may be arrested in the cell cycle for unlimited time). In the general case, we can consider that all the involved biological parameters (rate of differentiation $\sigma_i \in (0,1)$, rate of self-renew $\lambda_i = 1 - \sigma_i$, apoptosis rate d_{pi}, death rate of resting cells d_{ri}) are time-varying. On the right, the flux due to the cell-plasticity functions (ξ_i and ω_i for all $i \in I_n$) is represented.

The dynamics of resting cells $r_i(t,a)$, and proliferating cells $p_i(t,a)$, of the i-th generation ($i \in I_n$), of age $a > 0$, at time $t \geq 0$, are governed by

$$\begin{cases} \frac{\partial p_i}{\partial t} + \frac{\partial p_i}{\partial a} = -\left[d_{pi}(t) + h_i(a)\right] p_i(t,a), \\ \frac{\partial r_i}{\partial t} + \frac{\partial r_i}{\partial a} = -\left[d_{ri}(t) + \beta_i\left(x_i(t)\right)\right] r_i(t,a), \end{cases} \tag{4.1}$$

where we recall that for all $i \in I_n$, $x_i(t) = \int_0^{+\infty} r_i(t,a)da$, and, for all $i \in I_n$ and $t \geq 0$, $d_{ri}(t)$ is the death rate of the resting cells, while $d_{pi}(t)$ is the death rate of proliferating cells. We recall also that the reintroduction function β_i is decreasing and $\lim_{\ell \to \infty} \beta_i(\ell) = 0$.

The renewal conditions, which give the birth rate at the initial age $a = 0$, are introduced through the following boundary conditions:

$$\begin{cases} p_i(t,0) = \beta_i\left(\int_0^{+\infty} r_i(t,a)da\right) \int_0^{+\infty} r_i(t,a)da, \\ r_i(t,0) = 2\sigma_{i-1}(t) \int_0^{+\infty} h_{i-1}(t,a) p_{i-1}(t,a)da + 2\left(1 - \sigma_i(t)\right) \int_0^{+\infty} h_i(t,a) p_i(t,a)da, \end{cases} \tag{4.2}$$

where $\sigma_i(t)$ represents the time-varying rate of differentiation and, consequently, $\lambda_i(t) = 1 - \sigma_i(t)$ is the rate of self-renewal of the i-th cell generation. Then, we complete the system (4.83)-(4.86) with $\mathscr{L}^1$-functions as initial conditions (i.e. initial age distributions when $t = 0$):

$$\begin{cases} p_i(0,a) = p_i^0(a), \quad \text{for all} \quad a \in [0, +\infty), \\ r_i(0,a) = r_i^0(a), \quad \text{for all} \quad a \in [0, +\infty). \end{cases} \tag{4.3}$$

Finally, we assume from biological considerations that, for any fixed time $t \geq 0$,

$$\lim_{a\to+\infty} p_i(t,a) = \lim_{a\to+\infty} r_i(t,a) = 0. \tag{4.4}$$

Remark 21. *Apart from the aforementioned extension to the case of unlimited cell-cycle length, we also notice that all the parameters (differentiation, self-renewing and apoptosis rates), involved in* (4.83)-(4.86)*, are time-varying (which was not the case of similar earlier models).*

4.3.1 On the modeling of the mitosis function

Remark 22. *The densities of proliferating cells $p_i(t,a)$ -first equation in* (4.83)- *were defined in [8] over $0 < a < \tau_i$, where τ_i is finite. Therefore, the division rate h_i in [8], which must fulfill the condition*[1] *$\int_0^{\tau_i} h_i(a)da = +\infty$, has been considered as a continuous non-decreasing function satisfying*

$$\lim_{a\to\tau_i} h_i(a) = +\infty.$$

Now, in our work, we consider that the (continuous) cumulative distribution function h_i is defined over an infinite support $[0,+\infty)$, is nondecreasing, and it satisfies

$$\lim_{a\to+\infty} h_i(a) = 1. \tag{4.5}$$

Indeed, we consider that when the age a increases, the cells which do not die by apoptosis, have an increasing probability to divide, and this probability goes to 1 when a goes to infinity. The latter description captures the fact that a majority of cells may divide (if they do not die by apoptosis), while few of them may be arrested within the cycle. The qualitative form of h_i in this case is given in Figure 4.5.

4.3.2 A time-delay system with infinite distributed delays and time-varying apoptosis rates

Similarly to the model studied in the previous chapter (involving finite distributed delays), we want to study the time-delay version of the cell population dynamical model. We recall that the finite value $\tau_i > 0$ - in the previous chapter - represents the maximum age at which all the dividing cells (that do not die by apoptosis), at the i-th maturity stage, must divide. Thus, here we assume that the PDE model (4.83)-(4.86)-(4.85) is written in the following nonlinear system with **infinite** distributed delays (i.e. where $\tau_i = \infty$):

$$\begin{aligned}\dot{x}_i(t) = &- d_{ri}(t)x_i(t) - \beta_i(x_i(t))x_i(t) + 2\lambda_i(t)\int_0^{+\infty} g_i(t,a)\beta_i(x_i(t-a))x_i(t-a)da \\ &+ 2\sigma_{i-1}(t)\int_0^{+\infty} g_{i-1}(t,a)\beta_{i-1}(x_{i-1}(t-a))x_{i-1}(t-a)da,\end{aligned} \tag{4.6}$$

[1] This assumption describes the fact that all the proliferating cells which do not die by apoptosis during the cell cycle, are obliged to divide before they reach the maximal age τ_i.

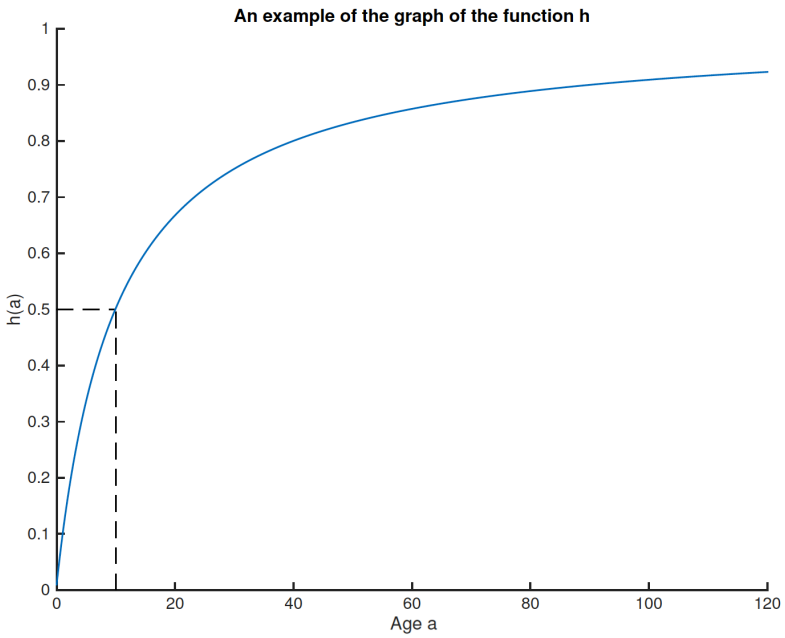

Fig. 4.5 Representative - qualitative - graph of the cumulative distribution function h_i in (4.83). This form describes the fact that cells have a low probability to divide at early stages of the cycle, then the probability tends to 1 when the age of the proliferating cells increases.

where $f_i(a) = h_i(a)e^{-\int_0^a h_i(m)dm}$, for all $a \in [0,+\infty)$, and

$$g_i(t,a) = f_i(a)e^{-\int_0^a d_{pi}(m+t-a)dm}, \text{ for all } a \in [0,+\infty), \text{ and } t \geq 0, \tag{4.7}$$

and, $\lambda_i(t) \in [\underline{\lambda}_i, \overline{\lambda}_i] \subset (0,1)$, $\sigma_i(t) \in [\underline{\sigma}_i, \overline{\sigma}_i] \subset (0,1)$, and $\lambda_i(t) = 1 - \sigma_i(t)$. Moreover, we consider that for all $t \geq 0$, the death rates satisfy: $d_{ri}(t) \in [\underline{d}_{ri}, \overline{d}_{ri}] \subset (0,\infty)$, and $d_{pi}(t) \in [\underline{d}_{pi}, \overline{d}_{pi}] \subset (0,\infty)$. A direct consequence is that

$$e^{-a\overline{d}_{pi}} \leq e^{-\int_0^a d_{pi}(m+t-a)dm} \leq e^{-a\underline{d}_{pi}}. \tag{4.8}$$

Then, for all $t \geq 0$, and for all $a \in [0,+\infty)$,

$$f_i(a)e^{-a\overline{d}_{pi}} \leq g_i(t,a) \leq f_i(a)e^{-a\underline{d}_{pi}}. \tag{4.9}$$

Let us denote for later use

$$\overline{C}_i = \int_0^{+\infty} f_i(\ell)e^{-\underline{d}_{pi}\ell}d\ell, \tag{4.10}$$

and observe for that $\overline{C}_i < 1$, for all $i \in I_n$.

The system (4.6) is positive, i.e. for positive initial conditions the trajectories are positive for all $t \geq 0$. Throughout the work, we consider only positive solutions of (4.6). As a qualitative example, we consider a function $f_i(a) = h_i(a)e^{-\int_0^a h_i(m)dm}$, where h_i is the cumulative distribution function in Figure 4.5, for all $a \in [0,+\infty)$. For constant apoptosis rate (d_p is 0.01 days^{-1}), then g_i is defined by[2] $g_i(a) = e^{-d_{pi}a}f_i(a)$.

[2] and let us recall for later use that if the apoptosis rate is constant, then: $\int_0^\infty g(m)dm < \int_0^\infty f(m)dm = 1$

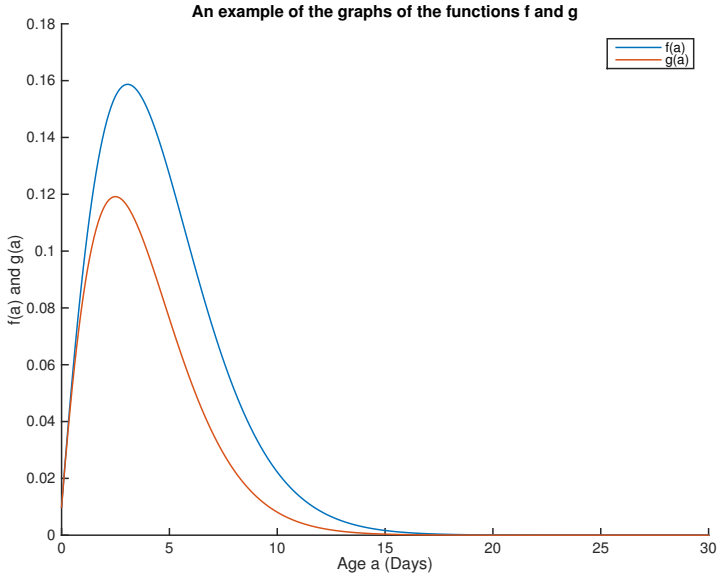

Fig. 4.6 Illustrative - qualitative - graphs of the probability density function $f_i(a)$, and the function $g_i(a)$ (for constant apoptosis rate d_{pi}), for all $a \in [0, +\infty)$.

4.4 Stability analysis of the 0-equilibrium

In this section, we analyze the stability properties of the origin of the model (4.6), since the aim of anti-cancer therapy is the eradication of unhealthy cells. More precisely, we prove in this section the following result (that generalizes those given by Adimy *et al.* and those in Chapter 3, to the case of **infinite** distributed delays):

Theorem 8. *For all $i \in I_n = \{1, \ldots, n\}$, the following statements hold true:*

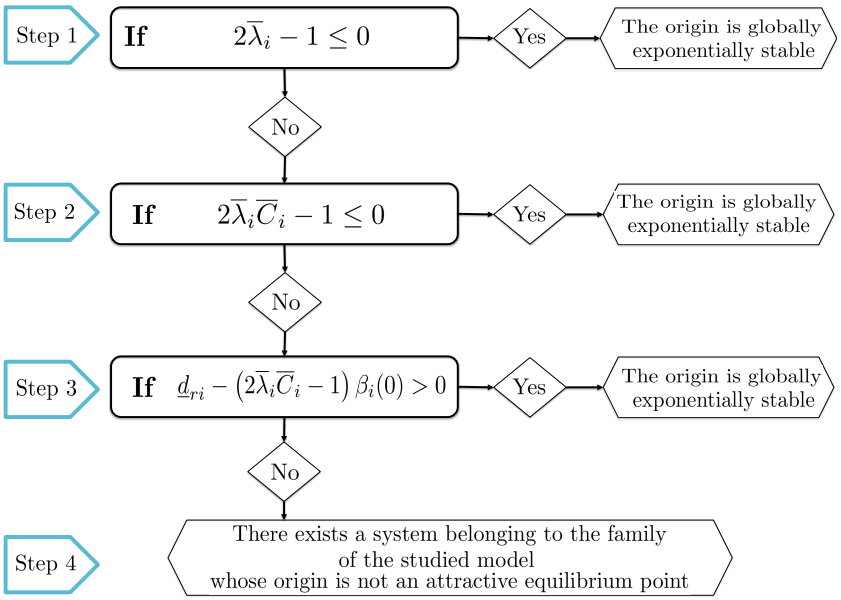

Remark 23. *The condition in **Step 3** is a direct generalization of the well-known necessary and sufficient stability condition for the 0-equilibrium of the class of systems with finite distributed delays and constant*

parameters (introduced in [8]). More precisely, the latter stability condition has been provided in [8] for local asymptotic stability of the origin, and in the previous chapter for global exponential stability of the origin of the model with finite distributed delays and constant apoptosis rates. However, proving this statement requires a novel Lyapunov-Krasovskii functional, different from the one already used in the previous chapter.

Proof. Let us start by introducing for all $i \in I_n$, the family of functionals:

$$N_i(x_{it}) = \int_0^{+\infty} f_i(\ell) \int_{t-\ell}^{t} e^{-\underline{d}_{pi}(t-s)} \beta_i(x_i(s)) x_i(s) ds d\ell. \tag{4.11}$$

The time derivative of N_i is given for all $t \geq 0$ by:

$$\dot{N}_i(t) = -\underline{d}_{pi} N_i(x_{it}) + \int_0^{+\infty} f_i(\ell) \beta_i(x_i(t)) x_i(t) d\ell - \int_0^{+\infty} f_i(\ell) e^{-\underline{d}_{pi}\ell} \beta_i(x_i(t-\ell)) x_i(t-\ell) d\ell. \tag{4.12}$$

Since $\int_0^{\infty} f_i(\ell) d\ell = 1$, it follows that:

$$\begin{aligned} \dot{N}_i(t) &= -\underline{d}_{pi} N_i(x_{it}) + \beta_i(x_i(t)) x_i(t) - \int_0^{+\infty} f_i(\ell) e^{-\underline{d}_{pi}\ell} \beta_i(x_i(t-\ell)) x_i(t-\ell) d\ell \\ &\leq -\underline{d}_{pi} N_i(x_{it}) + \beta_i(x_i(t)) x_i(t) - \int_0^{+\infty} g_i(t,\ell) \beta_i(x_i(t-\ell)) x_i(t-\ell) d\ell, \end{aligned} \tag{4.13}$$

where the last inequality is a consequence of (4.9). Next, let us observe that the derivatives of the functionals,

$$M_i(x_{it}) = \int_0^{+\infty} f_i(\ell) e^{-\underline{d}_{pi}\ell} \int_{t-\ell}^{t} \beta_i(x_i(s)) x_i(s) ds d\ell, \tag{4.14}$$

along the trajectories of (4.6), satisfy for all $i \in I_n$,

$$\dot{M}_i(t) = \beta_i(x_i(t)) x_i(t) \int_0^{+\infty} f_i(\ell) e^{-\underline{d}_{pi}\ell} d\ell - \int_0^{+\infty} f_i(\ell) e^{-\underline{d}_{pi}\ell} \beta_i(x_i(t-\ell)) x_i(t-\ell) d\ell. \tag{4.15}$$

It follows that,

$$\begin{aligned} \dot{M}_i(t) &= \overline{C}_i \beta_i(x_i(t)) x_i(t) - \int_0^{+\infty} f_i(\ell) e^{-\underline{d}_{pi}\ell} \beta_i(x_i(t-\ell)) x_i(t-\ell) d\ell \\ &\leq \overline{C}_i \beta_i(x_i(t)) x_i(t) - \int_0^{+\infty} g_i(t,\ell) \beta_i(x_i(t-\ell)) x_i(t-\ell) d\ell. \end{aligned} \tag{4.16}$$

For later use, we notice that:

$$\begin{aligned} N_i(x_{it}) &= \int_0^{+\infty} f_i(\ell) \int_{t-\ell}^{t} e^{-\underline{d}_{pi}(t-s)} \beta_i(x_i(s)) x_i(s) ds d\ell \\ &\geq \int_0^{+\infty} \int_{t-\ell}^{t} f_i(\ell) e^{-\underline{d}_{pi}\ell} \beta_i(x_i(s)) x_i(s) ds d\ell \\ &= M_i(x_{it}). \end{aligned} \tag{4.17}$$

For the sake of brevity, **Step 1** and **Step 2** will be established only for the subsystem $i = 1$. The results can be extended for all $i \geq 1$ using similar arguments as those we will provide in the proof of **Step 3**.

Step 1: Let us introduce the following functional for the first compartment:

$$U_1(x_{1t}) = x_1(t) + 2\overline{\lambda}_1 N_1(x_{1t}). \tag{4.18}$$

Its derivative along the trajectories of (4.6) satisfies:

$$\begin{aligned}\dot{U}_1(t) \leq & -\left[d_{r1}(t) + \beta_1(x_1(t))\right] x_1(t) + 2\lambda_1(t) \int_0^{+\infty} g_1(t,\ell)\beta_1(x_1(t-\ell))x_1(t-\ell)d\ell \\ & - 2\overline{\lambda}_1 \underline{d}_{p1} N_1(x_{1t}) + 2\overline{\lambda}_1 \beta_1(x_1(t))x_1(t) - 2\overline{\lambda}_1 \int_0^{+\infty} g_1(t,\ell)\beta_1(x_1(t-\ell))x_1(t-\ell)d\ell.\end{aligned} \tag{4.19}$$

Since for all $i \in I_n$ and for all $t \leq 0$, $\lambda_1(t) \leq \overline{\lambda}_1$, we obtain

$$\dot{U}_1(t) \leq -\left[d_{r1}(t) - \left(2\overline{\lambda}_1 - 1\right)\beta_1(x_1(t))\right] x_1(t) - 2\overline{\lambda}_1 \underline{d}_{p1} N_1(x_{1t}). \tag{4.20}$$

From (4.20) we deduce that if the condition $2\overline{\lambda}_1 - 1 \leq 0$ is satisfied, then the origin of the subsystem ($i = 1$) is globally exponentially stable.

Next, we focus on the case $2\overline{\lambda}_1 - 1 > 0$. From (4.6) and (4.16), we observe that the derivative of the functional

$$V_1(x_{1t}) = x_1(t) + 2\overline{\lambda}_1 M_1(x_{1t}), \tag{4.21}$$

satisfies

$$\dot{V}_1(t) \leq -\left[d_{r1}(t) - \left(2\overline{\lambda}_1 \overline{C}_1 - 1\right)\beta_1(x_1(t))\right] x_1(t). \tag{4.22}$$

Now, let us distinguish between two cases:

i) If $2\overline{\lambda}_1 \overline{C}_1 - 1 < 0$. In this case we conclude from (4.22) that the origin of the subsystem ($i = 1$) is globally asymptotically stable, and we prove in the sequel that it is also globally exponentially stable (i.e. the statement in **Step 2**).

Step 2: By combining (4.20) and (4.22), we check that the functional

$$W_1(x_{1t}) = U_1(x_{1t}) + 2\overline{\lambda}_1 \frac{1-\overline{C}_1}{1-2\overline{\lambda}_1\overline{C}_1} V_1(x_{1t}), \tag{4.23}$$

satisfies,

$$\dot{W}_1(t) \leq -d_{r1}(t)\left[1 + 2\overline{\lambda}_1 \frac{1-\overline{C}_1}{1-2\overline{\lambda}_1\overline{C}_1}\right] x_1(t) - 2\overline{\lambda}_1 \underline{d}_{p1} N_1(x_{1t}) + \left(1 - 2\overline{\lambda}_1\overline{C}_1\right)\beta_1(x_1(t))x_1(t).$$

Using the fact that $2\overline{\lambda}_1\overline{C}_1 - 1 < 0$, it follows that

$$\dot{W}_1(t) \leq -\alpha_1 d_{r1}(t)x_1(t) - 2\overline{\lambda}_1 \underline{d}_{p1} N_1(x_{1t}), \tag{4.24}$$

where $\alpha_1 = \frac{1-2\overline{\lambda}_1\overline{C}_1 + 2\overline{\lambda}_1\left(1-\overline{C}_1\right)}{1-2\overline{\lambda}_1\overline{C}_1}$. Since $2\overline{\lambda}_1\overline{C}_1 - 1 < 0$ and $1 - \overline{C}_1 > 0$, we deduce that $\alpha_1 > 0$.

Finally, using (4.17) we conclude that (4.24) gives

$$\begin{aligned}\dot{W}_1(t) \leq & -\alpha_1 d_{r1}(t)x_1(t) - \overline{\lambda}_1 \underline{d}_{p1} N_1(x_{1t}) - \overline{\lambda}_1 \underline{d}_{p1} N_1(x_{1t}) \\ \leq & -\alpha_1 \underline{d}_{r1} x_1(t) - \overline{\lambda}_1 \underline{d}_{p1} N_1(x_{1t}) - \overline{\lambda}_1 \underline{d}_{p1} M_1(x_{1t}) \\ \leq & -\delta_1 W_1(x_{1t}),\end{aligned} \tag{4.25}$$

where $\delta_1 > 0$. Consequently, the origin of the subsystem $i = 1$ is globally exponentially stable with a decay rate smaller or equal to δ_1.

ii) If $2\overline{\lambda}_1\overline{C}_1 - 1 \geq 0$. Now, we recall that the functions β_i are decreasing. It follows that the functionals U_1 and V_1 satisfy, respectively,

$$\dot{U}_1(t) \leq -\left[d_{r1}(t) - \left(2\overline{\lambda}_1 - 1\right)\beta_1(0)\right] x_1(t) - 2\overline{\lambda}_1 \underline{d}_{p1} N_1(x_{1t}), \tag{4.26}$$

and

$$\dot{V}_1(t) \leq -\left[d_{r1}(t) - \left(2\overline{\lambda}_1\overline{C}_1 - 1\right)\beta_1(0)\right] x_1(t). \tag{4.27}$$

Since for all $t \geq 0$, $\underline{d}_{r1} \leq d_{r1}(t)$, we end up with

$$\dot{U}_1(t) \leq -\left[\underline{d}_{r1} - \left(2\overline{\lambda}_1 - 1\right)\beta_1(0)\right] x_1(t) - 2\overline{\lambda}_1 \underline{d}_{p1} N_1(x_{1t}), \tag{4.28}$$

and

$$\dot{V}_1(t) \leq -\left[\underline{d}_{r1} - \left(2\overline{\lambda}_1\overline{C}_1 - 1\right)\beta_1(0)\right] x_1(t). \tag{4.29}$$

Step 3: Firstly, let us assume that

$$\underline{d}_{r1} - \left(2\overline{\lambda}_1\overline{C}_1 - 1\right)\beta_1(0) > 0.$$

A direct consequence is that the functional

$$R_1(x_{1t}) = U_1(x_{1t}) + \frac{2\overline{\lambda}_1\beta_1(0)\left(1-\overline{C}_1\right)}{\underline{d}_{r1} - \left(2\overline{\lambda}_1\overline{C}_1 - 1\right)\beta_1(0)} V_1(x_{1t}), \tag{4.30}$$

is positive on the positive orthant. Moreover, there exists $\tilde{\delta}_1 > 0$, such that the derivative of R_1 along the trajectories of (4.6) satisfies

$$\begin{aligned}\dot{R}_1(t) \leq & -\left[\underline{d}_{r1} - \left(2\overline{\lambda}_1\overline{C}_1 - 1\right)\beta_1(0)\right] x_1(t) - 2\overline{\lambda}_1 \underline{d}_{p1} N_1(x_{1t}), \\ \leq & -\tilde{\delta}_1 R_1(x_{1t}),\end{aligned} \tag{4.31}$$

where the last inequality is a consequence of (4.17). By virtue of the functional R_1, we conclude that the origin of the subsystem ($i = 1$) is globally exponentially stable.

Now we extend the result to the overall system. Let us assume that the conditions

$$\underline{d}_{ri} - \left(2\overline{\lambda}_i \overline{C}_i - 1\right) \beta_i(0) > 0, \tag{4.32}$$

are verified for all $i \in I_n$, and let us prove that the origin of the system (4.6) is globally exponentially stable.

Firstly, we define a family of constants $\mathfrak{K}_i$ such that:

$$\mathfrak{K}_i \in \left(1, \frac{\underline{d}_{ri} + \left(2\overline{\lambda}_i \overline{C}_i + 1\right) \beta_i(0)}{4\overline{\lambda}_i \overline{C}_i \beta_i(0)} \right), \text{ for all } i \in I_n. \tag{4.33}$$

One can check that when the inequalities (4.32) are satisfied then $\mathfrak{K}_i$ exist for all $i \in I_n$. Moreover, for all $\mathfrak{K}_i$ verifying (4.33), the following inequalities are satisfied,

$$\underline{d}_{ri} - \left(2\mathfrak{K}_i \overline{\lambda}_i \overline{C}_i - 1\right) \beta_i(0) > \frac{\underline{d}_{ri} - \left(2\overline{\lambda}_i \overline{C}_i - 1\right) \beta_i(0)}{2} > 0, \tag{4.34}$$

for all $i \in I_n$. Secondly, we slightly modify the functional V_1, introduced in (4.21), in order to get some additional negative terms in its derivative. For that matter, we set,

$$\tilde{V}_1(x_{1t}) = x_1(t) + 2\mathfrak{K}_1 \overline{\lambda}_1 M_1(x_{1t}), \tag{4.35}$$

where $\mathfrak{K}_1$ satisfies (4.33). Its derivative along the trajectories of (4.6) verifies

$$\dot{\tilde{V}}_1(t) \leq -\left[d_{r1}(t) - \left(2\mathfrak{K}_1 \overline{\lambda}_1 \overline{C}_1 - 1\right) \beta_i(0) \right] x_1(t) - 2\left(\mathfrak{K}_1 \overline{\lambda}_1 - \lambda_1(t)\right) \int_0^{+\infty} g_1(t,\ell) \beta_1(x_1(t-\ell)) x_1(t-\ell) d\ell.$$

Since $\mathfrak{K}_1 > 1$, and for all $t \geq 0$, $\lambda_1(t) \leq \overline{\lambda}_1$, we get:

$$\dot{\tilde{V}}_1(t) \leq -\left[d_{r1}(t) - \left(2\mathfrak{K}_1 \overline{\lambda}_1 \overline{C}_1 - 1\right) \beta_i(0) \right] x_1(t) - \overline{\mathfrak{K}}_1 \int_0^{+\infty} g_1(t,\ell) \beta_1(x_1(t-\ell)) x_1(t-\ell) d\ell,$$

where $\overline{\mathfrak{K}}_1 = 2\overline{\lambda}_1 (\mathfrak{K}_1 - 1) > 0$. Moreover, using (4.34) we conclude that

$$\dot{\tilde{V}}_1(t) \leq -\frac{1}{2}\left[d_{r1}(t) - \left(2\overline{\lambda}_1 \overline{C}_1 - 1\right) \beta_i(0) \right] x_1(t) - \overline{\mathfrak{K}}_1 \int_0^{+\infty} g_1(t,\ell) \beta_1(x_1(t-\ell)) x_1(t-\ell) d\ell. \tag{4.36}$$

If we compare the derivatives $\dot{V}_1$ and $\dot{\tilde{V}}_1$, that satisfy, respectively, (4.29) and (4.36), we notice that a negative integral extra-term appears in (4.36). The latter term will be used in order to compensate an input from the first generation of cells (i.e. $i = 1$) when we study the subsystem formed by $i = 1, 2$.

More precisely, let us introduce the following functional that takes into account the dynamics of the first and the second generations of immature cells ($i \in \{1, 2\}$):

$$R_2(x_{2t}, x_{1t}) = x_2(t) + 2\overline{\lambda}_2 N_2(x_{2t}) + \tilde{a}\tilde{V}_2(x_{2t}) + \tilde{\tilde{a}}\tilde{V}_1(x_{1t}) + \hat{a} N_1(x_{1t}), \tag{4.37}$$

where, similarly to $\tilde{V}_1$, we consider $\tilde{V}_2$ given by:

$$\tilde{V}_2(x_{2t}) = x_2(t) + 2\Re_2\overline{\lambda}_2 M_2(x_{2t}), \tag{4.38}$$

and the weighting constants $\tilde{a} > 0$, $\tilde{\tilde{a}} > 0$, and $\hat{a} > 0$ are given by:

$$\tilde{a} = \frac{4\overline{\lambda}_2\beta_2(0)\left(1-\overline{C}_2\right)}{\underline{d}_{r2} - \left(2\overline{\lambda}_2\overline{C}_2 - 1\right)\beta_2(0)}, \ \tilde{\tilde{a}} = \frac{2\overline{\sigma}_1(1+\tilde{a})}{\overline{\Re}_1}, \text{ and, } \hat{a} = \frac{\tilde{\tilde{a}}\left[\underline{d}_{r1} - \left(2\overline{\lambda}_1\overline{C}_1 - 1\right)\beta_1(0)\right]}{4\beta(0)}.$$

Observe that the conditions (4.32) ensure that $\tilde{a}$ is strictly positive, which in turn guarantees that the functional R_2 is positive on the positive orthant.

Now observe that the derivative of R_2 along the trajectories of (4.6) satisfies

$$\begin{aligned}
\dot{R}_2(t) \leq & -\left[d_{r2}(t) + \beta_2(x_2(t))\right]x_2(t) + 2\lambda_2(t)\int_0^{+\infty} g_2(t,\ell)\beta_2(x_2(t-\ell))x_2(t-\ell)d\ell \\
& + 2\sigma_1(t)\int_0^{+\infty} g_1(t,\ell)\beta_1(x_1(t-\ell))x_1(t-\ell)d\ell - 2\overline{\lambda}_2\underline{d}_{p2}N_2(x_{2t}) + 2\overline{\lambda}_2\beta_2(x_2(t))x_2(t) \\
& - 2\overline{\lambda}_2\int_0^{+\infty} g_2(t,\ell)\beta_2(x_2(t-\ell))x_2(t-\ell)d\ell - \frac{\tilde{a}}{2}\left[d_{r2}(t) - \left(2\overline{\lambda}_2\overline{C}_2 - 1\right)\beta_2(0)\right]x_2(t) \\
& \hat{a}\beta(0)x_1(t) - \hat{a}\underline{d}_{p1}N_1(x_{1t}) - \tilde{a}\overline{\Re}_2\int_0^{+\infty} g_2(t,\ell)\beta_2(x_2(t-\ell))x_2(t-\ell)d\ell \\
& + 2\tilde{a}\sigma_1(t)\int_0^{+\infty} g_1(t,\ell)\beta_1(x_1(t-\ell))x_1(t-\ell)d\ell - \frac{\tilde{\tilde{a}}}{2}\left[d_{r1}(t) - \left(2\overline{\lambda}_1\overline{C}_1 - 1\right)\beta_1(0)\right]x_1(t) \\
& - \tilde{\tilde{a}}\overline{\Re}_1\int_0^{+\infty} g_1(t,\ell)\beta_1(x_1(t-\ell))x_1(t-\ell)d\ell.
\end{aligned} \tag{4.39}$$

By grouping the terms and since for all $t \geq 0$, $\lambda_2(t) \leq \overline{\lambda}_2$, we deduce that

$$\begin{aligned}
\dot{R}_2(t) \leq & -\left[d_{r2}(t) - \left(2\overline{\lambda}_2 - 1\right)\beta_2(x_2(t))\right]x_2(t) \\
& - \frac{\tilde{a}}{2}\left[d_{r2}(t) - \left(2\overline{\lambda}_2\overline{C}_2 - 1\right)\beta_2(0)\right]x_2(t) - 2\overline{\lambda}_2\underline{d}_{p2}N_2(x_{2t}) \\
& + 2\sigma_1(t)\left[1+\tilde{a}\right]\int_0^{+\infty} g_1(t,\ell)\beta_1(x_1(t-\ell))x_1(t-\ell)d\ell \\
& - \tilde{a}\overline{\Re}_2\int_0^{+\infty} g_2(t,\ell)\beta_2(x_2(t-\ell))x_2(t-\ell)d\ell \\
& - \frac{\tilde{\tilde{a}}}{2}\left[d_{r1}(t) - \left(2\overline{\lambda}_1\overline{C}_1 - 1\right)\beta_1(0)\right]x_1(t) + \hat{a}\beta(0)x_1(t) \\
& - \tilde{\tilde{a}}\overline{\Re}_1\int_0^{+\infty} g_1(t,\ell)\beta_1(x_1(t-\ell))x_1(t-\ell)d\ell - \hat{a}\underline{d}_{p1}N_1(x_{1t}).
\end{aligned} \tag{4.40}$$

By substituting $\tilde{\tilde{a}}$ and $\hat{a}$, we get for all $t \geq 0$,

$$\begin{aligned}\dot{R}_2(t) \leq & -\left[d_{r2}(t) - \left(2\overline{\lambda}_2\overline{C}_2 - 1\right)\beta_2(0)\right] x_2(t) - 2\overline{\lambda}_2\underline{d}_{p2}N_2(x_{2t}) \\ & - \tilde{a}\overline{\Re}_2 \int_0^{+\infty} g_2(t,\ell)\beta_2(x_2(t-\ell))x_2(t-\ell)d\ell \\ & - \frac{\tilde{\tilde{a}}}{4}\left[d_{r1}(t) - \left(2\overline{\lambda}_1\overline{C}_1 - 1\right)\beta_1(0)\right] x_1(t) - \hat{a}\underline{d}_{p1}N_1(x_{1t}).\end{aligned} \tag{4.41}$$

We conclude that there exists a strictly positive constant $\tilde{\tilde{\delta}}_2 > 0$, such that

$$\dot{R}_2(t) \leq -\tilde{\tilde{\delta}}_2 R_2(x_{2t}, x_{1t}) - \tilde{a}\overline{\Re}_2 \int_0^{+\infty} g_2(t,\ell)\beta_2(x_2(t-\ell))x_2(t-\ell)d\ell. \tag{4.42}$$

Consequently, by virtue of the functional R_2, we conclude that the origin $(0,0)$ of the subsystem $i = \{1,2\}$, is globally exponentially stable.

Therefore, by induction, we conclude that there exists a family of strictly positive constants ρ_i, $\tilde{\rho}_i$, for all $i \in I_n = \{1,\ldots,n\}$, such that the derivative of

$$R_n(x_{nt},\ldots,x_{1t}) = x_n(t) + \sum_{i=1}^{n}\left(\rho_i N_i(x_{it}) + \tilde{\rho}_i\tilde{V}_i(x_{it})\right), \tag{4.43}$$

where, $\tilde{V}_i(x_{it}) = x_i(t) + 2\Re_i\overline{\lambda}_i M_i(x_{it})$ for all $i \in I_n$, satisfies

$$\dot{R}_n(t) \leq -\tilde{\tilde{\delta}}_n R_n(x_{nt},\ldots,x_{1t}), \text{ where } \tilde{\tilde{\delta}}_n > 0. \tag{4.44}$$

By virtue of the functional R_n, we conclude that the origin $(0,\ldots,0)$ of the overall system $i \in I_n$ is globally exponentially stable.

Step 4: The last part of the proof consists in proving that there exists a system belonging to the family of systems (4.6) whose origin is not attractive. For that purpose, it is sufficient to consider a particular case of system (4.6) where all the biological parameters are constant. More precisely, we consider that the death rate $d_{pi}(t) = d_{pi}$, for all $t \geq 0$, where d_{pi} is any constant parameter belonging to $[\underline{d}_{pi}, \overline{d}_{pi}]$, and similarly for the other parameters involved in the model (4.6) (i.e. d_{pi}, λ_i and $\sigma_i = 1 - \lambda_i$).

We use similar arguments as those for the finite distributed delays in the previous chapter. So, we consider the functional,

$$v_1(x_{1t}) = x_1(t) + 2\lambda_1 \int_0^{+\infty}\int_{t-\ell}^{t} f_1(\ell)e^{-d_{p1}\ell}\beta_1(x_1(m))x_1(m)dmd\ell. \tag{4.45}$$

The derivative of v_1 satisfies for all $t \geq 0$,

$$\begin{aligned}\dot{v}_1(t) = & -\left[d_{r1} + \beta_1(x_1(t))\right] x_1(t) + 2\lambda_1 \int_0^{+\infty} g_1(\ell)\beta_1(x_1(t-\ell))x_1(t-\ell)d\ell \\ & + 2\lambda_1 C_1\beta_1(x_1(t))x_1(t) - 2\lambda_1 \int_0^{+\infty} g_1(\ell)\beta_1(x_1(t-\ell))x_1(t-\ell)d\ell \\ = & -\left[d_{r1} - (2\lambda_1 C_1 - 1)\beta_1(x_1(t))\right] x_1(t).\end{aligned} \tag{4.46}$$

Now we proceed by contradiction: we consider that $x_1(t)$ converges to the origin and that $d_{r1} - (2\lambda_1 C_1 - 1)\beta_1(0) \geq 0$. Since β_1 is decreasing and $\beta_1(0)$ is its maximum, we deduce that there exists a time instant t_1, such that for all $t \geq t_1$, we obtain

$$\dot{v}_1(t) \geq -\left[\frac{d_{r1} - (2\lambda_1 C_1 - 1)\beta_1(0)}{2}\right] x_1(t). \tag{4.47}$$

Since $x_1(t) > 0$, we deduce that $v_1(x_{1t}) > v_1(t_{1t})$ for all $t > t_1$. It follows that the functional v_1 does not converge to zero. On the other hand, v_1 converges to the zero if x_1 converge to zero. This yields to a contradiction. □

Remark 24. *In Theorem 8, it is clear that if **Step 1** is satisfied, then **Step 2** is also satisfied (since $\overline{C}_i < 1$, for all $\underline{d}_{pi} > 0$). Similarly, we see that if **Step 2** holds true then **Step 3** is also verified, since $\underline{d}_{ri} > 0$. In fact, by assuming that $2\overline{\lambda}_i\overline{C}_i - 1 > 0$ (which is otherwise the generalization of the assumption $2L_iC_i - 1 > 0$ in [225], see also [8]), we rewrite Theorem 8 in a compact form similar to the one in Theorem 3 of [81] for the model with finite distributed delays. It is also worthy of note that biologically **Step 1** is an extreme condition that ensures exponential eradication of unhealthy cells even if apoptosis is stalled to zero (i.e. $d_{pi} = 0$ and $\overline{C}_i = 1$). The condition in **Step 2** is less strong than the first one, while **Step 3** is the most reasonable. Indeed, **Step 3** provides a necessary and sufficient condition for all-cell extinction, less strong than the two previous ones.*

4.5 Some comments on the reintroduction function from quiescence into proliferation

In Section 4.3.1, we have revisited the description of the mitosis function. Now, we want to highlight some features of the re-introduction function β_i. The motivation is as follows: in numerical experiments, we observed that for different forms of β_i, such that β_i is continuously decreasing and $\lim_{m\to+\infty}\beta_i(m) = \mathfrak{b} > 0$, the corresponding system may have unbounded solutions. In fact, having some unbounded solutions can be interpreted as the invasion of the bone marrow and the bloodstream by blasts (leukemic cells) and it represents an interesting model to investigate.

Similarly, in [47, 46], a *"getting in the cycle"* or *"recruitment"* function (which has the same role as the reintroduction function β_i in our case), of the form: $G_i(m) = \frac{\alpha_1 \nu^n + \alpha_2 m^n}{\nu^{\mathfrak{n}} + m^{\mathfrak{n}}}$, where, $0 < \alpha_2 < \alpha_1$, was considered for unhealthy tissues. The authors have shown that in this case, unbounded solutions may exist in their model [47, 46].

Here we are wondering about the biological meaning of $\lim_{m\to+\infty}\beta_i(m) = \mathfrak{b} > 0$ and its possible interpretation. Let us firstly revisit the assumptions considered by Mackey in [180], the first time he introduced the re-introduction function $\beta_i(x_i) = \frac{\beta(0)\nu^{\mathfrak{n}}}{\nu^{\mathfrak{n}} + x_i^{\mathfrak{n}}}$, where $\nu > 0$ and $\mathfrak{n} \geq 2$.

Origin of the reintroduction function from resting to proliferation

We list here the assumptions made by Mackey in [180] (see also [241]) on the reintroduction function β_i.

First, it is assumed that each cell contains a receptor for a mitotic regulatory molecule, considered as an inhibitor (i.e. mitosis occurs in a regular fashion if the cell receptor is in an uncombined form). The reaction between the receptor and regulatory inhibitors proceeds as follows:

❶ **H1**, of [180]: $\vartheta_{\mathfrak{ac}} + \mathfrak{n} \times \mathfrak{c} \rightleftharpoons \vartheta_{\mathfrak{inc}}$, where $\vartheta_{\mathfrak{ac}}$ is the active form of the receptor while $\vartheta_{\mathfrak{inc}}$ is its inactive form; and $\mathfrak{c}$ is the regulatory molecule.

❷ **H2**, of [180]: The equilibrium constant ν for the reaction is so that $[\vartheta_{\mathfrak{ac}}] \times [\mathfrak{c}]^{\mathfrak{n}} = \nu[\vartheta_{\mathfrak{inc}}]$.

❸ **H3**, of [180]: There are a fixed number of receptors $[T_{\mathfrak{c}}]$ per cell, thus: $[T_{\mathfrak{c}}] = [\vartheta_{\mathfrak{ac}}] + [\vartheta_{\mathfrak{inc}}]$.

❹ **H4**, of [180]: The number of regulatory molecules is directly proportional to the number of resting phase stem cells; $[\mathfrak{c}] = \tilde{\mathfrak{a}} x_i$, where $\tilde{\mathfrak{a}}$ is a strictly positive constant.

The hypothesis **H4** is the one that interests us most. Indeed, basically it means that the body is assumed to be able to produce a quantity of regulatory molecules which is proportional to the total density of resting cells x_i. In other words, the model assumes that when the number of cells is about to grow excessively (to infinity), the body is capable of delivering an infinity of inhibitor ligands (which are capable of preventing cell division). So, it is not surprising that trajectories remain bounded in this case.

Modifying the re-introduction function from quiescence into proliferation

Let us now modify the hypothesis **H4** introduced in [180]. In fact, we are going to consider the case where the concentration $[c]$ is saturated (i.e. the quantity of regulatory molecules that the body may produce is limited). One possible form is the following:

$$[\mathfrak{c}] = \frac{\mathfrak{a}_0 x_i}{\mathfrak{a}_0 - 1 + x_i} = \psi_{\mathfrak{a}_0}(x_i), \text{ where, } \mathfrak{a}_0 > 1. \tag{4.48}$$

Consequently, by denoting $\beta_i(0)$ the maximal reintroduction rate, we end-up with the following form of the re-introduction function:

$$\beta_i(x_i) = \frac{\beta_i(0)\tilde{\nu}}{\tilde{\nu} + \psi_{\mathfrak{a}_0}(x_i)^{\mathfrak{n}}}, \ \beta_i(0) > 0, \ \tilde{\nu} > 0, \text{ and, } \mathfrak{n} \geq 2. \tag{4.49}$$

In this case we notice that $\lim_{x_i \to \infty} \beta_i(x_i) = \mathfrak{b} > 0$. In numerical experiments, we observe that for the new form of β_i, unbounded solutions may exist for some initial conditions. A rigorous proof of that result is currently under investigation. For example, we consider that $\mathfrak{a}_0 = 15 \times 10^{12}$, $\beta_i(0) = 1.84$ days^{-1}, $\tilde{\nu} = 1.62 \times 10^8$ cells/kg, and $\mathfrak{n} = 2$. The saturated production of mitotic inhibitors with respect to the cell density x_i is illustrated in Figure 4.7, the function β_i is illustrated in Figure 4.8, and an example in which unbounded solutions may occur is given in Figure 4.9.

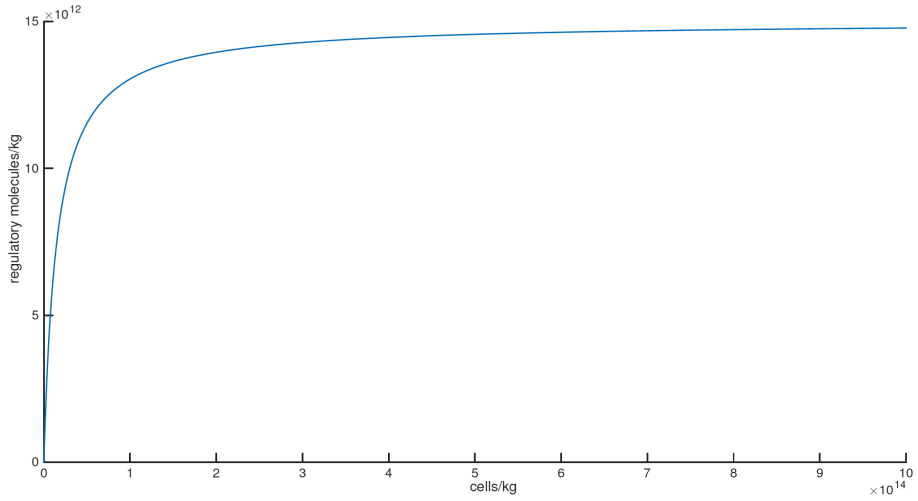

Fig. 4.7 The density of the regulatory molecules is limited, while the cell population continue to grow. Illustration of the function $\psi_{\mathfrak{a}_0}$, when $\mathfrak{a}_0 = 15 \times 10^{12}$.

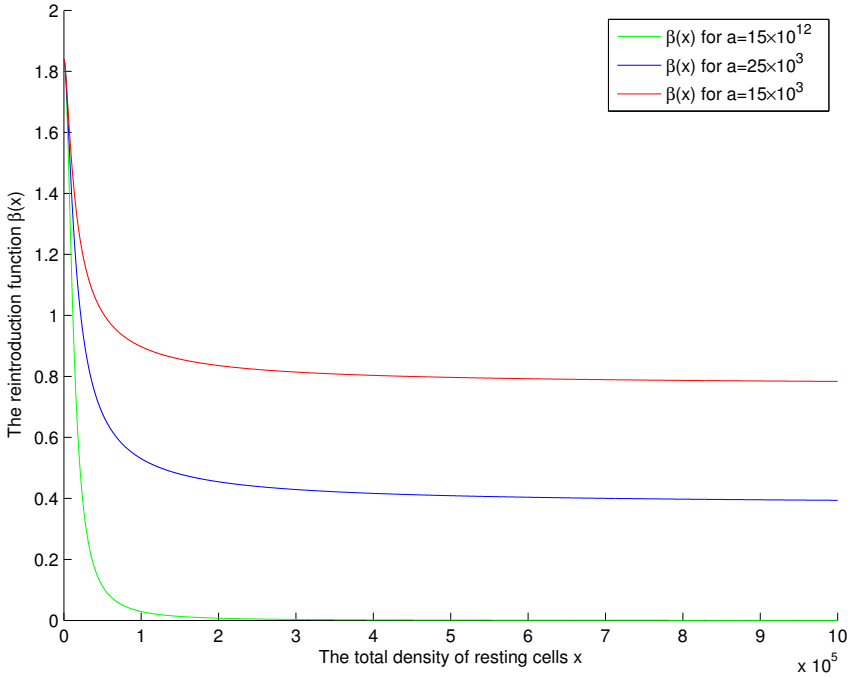

Fig. 4.8 Some illustrations of the form of the re-introduction function β. We have here $\lim_{m\to+\infty}\beta_i(m) = \mathfrak{b} > 0$, where the value of $\mathfrak{b}$ increases with respect to $\mathfrak{a}_0$.

4.6 Healthy tissues: Stability analysis of the positive steady state

As in the previous chapter: we associate the strictly positive steady state to a healthy hematopoiesis, describing the normal process in which cell generations survive and are stable. When all the biological parameters are constant, the model (4.6) admits a strictly positive steady state $E = \left(x_1^e, \ldots, x_n^e\right)$, where

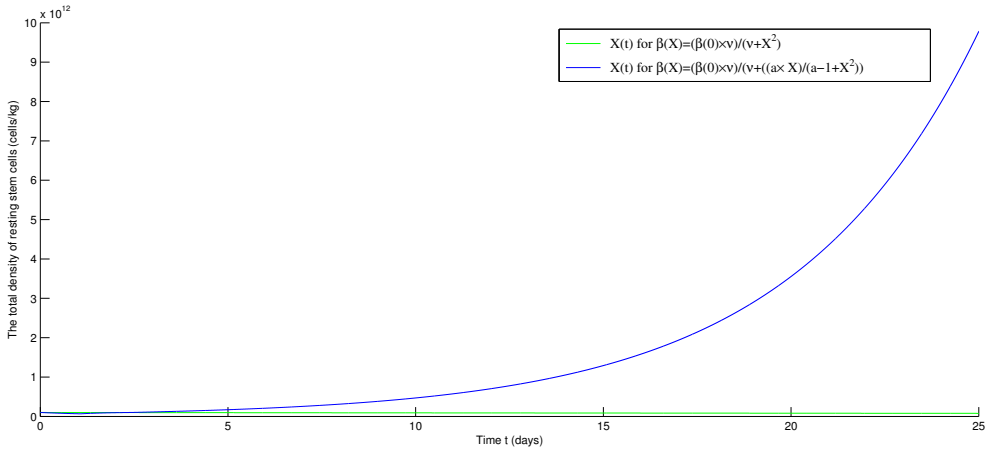

Fig. 4.9 The invasion of the bone marrow by cancer stem cells can be modeled by an appropriate selection of the reintroduction function from resting-into-proliferating phases.

$x_i^e > 0$ for all $i \in I_n$. In fact, the condition of existence of E is exactly similar to the one for finite delays in the previous chapter, while its stability analysis is slightly different. We illustrate briefly the LKF construction in this case.

The version of system (4.6) with constant parameters is given by:

$$\begin{aligned}\dot{x}_i(t) = &- d_{ri}x_i(t) - \beta_i(x_i(t))x_i(t) + 2\lambda_i \int_0^{+\infty} g_i(a)\beta_i(x_i(t-a))x_i(t-a)da \\ &+ 2\sigma_{i-1} \int_0^{+\infty} g_{i-1}(a)\beta_{i-1}(x_{i-1}(t-a))x_{i-1}(t-a)da,\end{aligned} \tag{4.50}$$

where,

$$g_i(a) = f_i(a)e^{-d_{pi}a}, \text{ for all } a \in [0,+\infty], \int_0^{+\infty} f_i(a)da = 1, \text{ and } \lambda_i + \sigma_i = 1. \tag{4.51}$$

We can see that the positive steady state $E = \left(x_1^e, \ldots, x_n^e\right)$ where $x_i^e > 0$ for all $i \in I_n$, exists if and only if

$$d_{r1} < [2\lambda_1 C_1 - 1]\,\beta_1(0), \text{ where, } C_1 = \int_0^{+\infty} g_1(a)da, \text{ for all } a \in [0,+\infty). \tag{4.52}$$

We assume in this section that the condition (4.52) is satisfied and we perform the change of coordinates $\tilde{x}_i = x_i - x_i^e$, for all $i \in I_n$, and using the Taylor formula, with an abuse of notation, $\left(\tilde{x}_i + x_i^e\right)\beta_i(\tilde{x}_i + x_i^e) = x_i^e\beta_i(x_i^e) + \mu_i\tilde{x}_i + r_i(\tilde{x}_i)$, where $\mu_i = \beta_i(x_i^e) + \beta_i'(x_i^e)x_i^e$, and, $r_i(\tilde{x}_i) = \int_{x_i^e}^{x_i^e+\tilde{x}_i} \left(\tilde{x}_i + x_i^e - \ell\right)\left[\beta_i(\ell)\ell\right]^{(2)} d\ell$, we end up with the system:

$$\begin{aligned}\dot{\tilde{x}}_i(t) = &- d_i^*\tilde{x}_i(t) + 2\mu_i\lambda_i \int_0^{+\infty} g_i(a)\tilde{x}_i(t-a)da + 2\mu_{i-1}\sigma_{i-1} \int_0^{+\infty} g_{i-1}(a)\tilde{x}_{i-1}(t-a)da \\ &- r_i(\tilde{x}_i(t)) + 2\lambda_i \int_0^{+\infty} g_i(a)r_i(\tilde{x}_i(t-a))da + 2\sigma_{i-1} \int_0^{+\infty} g_{i-1}(a)r_{i-1}(\tilde{x}_{i-1}(t-a))da,\end{aligned} \tag{4.53}$$

where $d_i^* = d_{ri} + \mu_i$. If the trajectories of (4.53) converge exponentially to the origin, then the trajectories of (4.50) converge exponentially to the positive steady state E.

Theorem 9. *The conditions*

$$\psi_i^\dagger = d_i^* - 2\lambda_i|\mu_i|C_i > 0, \text{ where, } C_i = \int_0^{+\infty} g_i(a)da, \text{ for all } a \in [0,+\infty) \tag{4.54}$$

for all $i \in I_n$, ensure that the positive steady state E of the system (4.50) *is regionally exponentially state and a subset of its basin of attraction is provided.*

Proof. We give the proof only for $i = 1$. Using exactly the same arguments as in the previous chapter, we can extend the result to all $i \in I_n$. First, we observe that the derivative of the quadratic function,

$$\mathfrak{Q}(m) = \frac{1}{2}m^2. \tag{4.55}$$

along the trajectories of system (4.53), satisfies for all $t \geq 0$

$$\begin{aligned}
\dot{\mathfrak{Q}}(t) =& -2d_1^*\mathfrak{Q}(\tilde{x}_1(t)) + 2\mu_1\lambda_1\tilde{x}_1(t)\int_0^{+\infty} g_1(a)\tilde{x}_1(t-a)da \\
&- \tilde{x}_1(t)r_1(\tilde{x}_1(t)) + 2\lambda_1\tilde{x}_1(t)\int_0^{+\infty} g_1(a)r_1(\tilde{x}_1(t-a))da \\
\leq& -2\left[d_1^* - |\mu_1|\lambda_1 C_1\right]\mathfrak{Q}(\tilde{x}_1(t)) + 2|\mu_1|\lambda_1\int_0^{+\infty} g_1(a)\mathfrak{Q}(\tilde{x}_1(t-a))da \\
&- \tilde{x}_1(t)r_1(\tilde{x}_1(t)) + 2\lambda_1\tilde{x}_1(t)\int_0^{+\infty} g_1(a)r_1(\tilde{x}_1(t-a))da,
\end{aligned} \tag{4.56}$$

We recall from the previous chapter that the nonlinearities r_i satisfy the sector conditions:

$$|r_i(\tilde{x}_i)| \leq \bar{r}_i\mathfrak{Q}(\tilde{x}_i), \tag{4.57}$$

where $\bar{r}_i > 0$, for all $i \in I_n$, and for all $\tilde{x}_i \in (-x_i^e, +\infty)$. Therefore, using (4.57), it follows that

$$\begin{aligned}
\dot{\mathfrak{Q}}(t) \leq& -2\left[d_1^* - |\mu_1|\lambda_1 C_1\right]\mathfrak{Q}(\tilde{x}_1(t)) + 2|\mu_1|\lambda_1\int_0^{+\infty} g_1(a)\mathfrak{Q}(\tilde{x}_1(t-a))da \\
&+ |\tilde{x}_1(t)|\bar{r}_1\mathfrak{Q}(\tilde{x}_1(t)) + 2\lambda_1|\tilde{x}_1(t)|\bar{r}_1\int_0^{+\infty} g_1(a)\mathfrak{Q}(\tilde{x}_1(t-a))da
\end{aligned} \tag{4.58}$$

Now, let us introduce the functional:

$$\mathscr{N}_i(\tilde{x}_{it}) = \int_0^{+\infty} f_i(\ell)\int_{t-\ell}^{t} e^{-d_{pi}(t-m)}\mathfrak{Q}(\tilde{x}_i(m))dmd\ell. \tag{4.59}$$

Its derivative satisfies, for all $i \in I_n$,

$$\begin{aligned}
\mathscr{N}_i(t) =& -d_{pi}\mathscr{N}_i(\tilde{x}_{it}) + \mathfrak{Q}(\tilde{x}_i(t)) - \int_0^{+\infty} f_i(\ell)e^{-d_{pi}\ell}\mathfrak{Q}(\tilde{x}_i(t-\ell))d\ell \\
=& -d_{pi}\mathscr{N}_i(\tilde{x}_{it}) + \mathfrak{Q}(\tilde{x}_i(t)) - \int_0^{+\infty} g_i(\ell)\mathfrak{Q}(\tilde{x}_i(t-\ell))d\ell
\end{aligned} \tag{4.60}$$

Let us introduce the following functional:

$$\mathscr{M}_i(\tilde{x}_{it}) = \int_0^{+\infty}\int_{t-\ell}^{t} g_i(\ell)\mathfrak{Q}(\tilde{x}_i(m))dmd\ell. \tag{4.61}$$

Its derivative is given by

$$\dot{\mathscr{M}}_i(t) = C_i\mathfrak{Q}(\tilde{x}_{it}) - \int_0^{+\infty} g_i(\ell)\mathfrak{Q}(\tilde{x}_i(t-\ell))d\ell. \tag{4.62}$$

It follows that the derivative of the functional

$$\mathscr{V}_1(\tilde{x}_{1t}) = \mathfrak{Q}(\tilde{x}_1(t)) + 2|\mu_1|\lambda_1\mathscr{M}_1(\tilde{x}_{1t}) + \psi_1^\dagger\mathscr{N}_1(\tilde{x}_{1t}), \tag{4.63}$$

where $\psi_i^\dagger > 0$ is defined in (4.54), along the trajectories of (4.53), satisfies

$$\begin{aligned}
\dot{\mathscr{V}}_1(t) \leq & -2\left[d_1^* - |\mu_1|\lambda_1 C_1\right]\mathfrak{Q}(\tilde{x}_1(t)) + 2|\mu_1|\lambda_1\int_0^{+\infty} g_1(a)\mathfrak{Q}(\tilde{x}_1(t-a))da \\
& + |\tilde{x}_1(t)|\bar{r}_1\mathfrak{Q}(\tilde{x}_1(t)) + 2\lambda_1|\tilde{x}_1(t)|\bar{r}_1\int_0^{+\infty} g_1(a)\mathfrak{Q}(\tilde{x}_1(t-a))da \\
& + 2|\mu_1|\lambda_1 C_1\mathfrak{Q}(\tilde{x}_{1t}) - 2|\mu_1|\lambda_1\int_0^{+\infty} g_1(\ell)\mathfrak{Q}(\tilde{x}_1(t-\ell))d\ell \\
& - d_{p1}\psi_1^\dagger\mathscr{N}_1(\tilde{x}_{1t}) + \psi_1^\dagger\mathfrak{Q}(\tilde{x}_{1t}) - \psi_1^\dagger\int_0^{+\infty} g_1(\ell)\mathfrak{Q}(\tilde{x}_1(t-\ell))d\ell \\
\leq & -\psi_1^\dagger\mathfrak{Q}(\tilde{x}_1(t)) + |\tilde{x}_1(t)|\bar{r}_1\mathfrak{Q}(\tilde{x}_1(t)) - d_{p1}\psi_1^\dagger\mathscr{N}_1(\tilde{x}_{1t}) \\
& + \left(2\lambda_1\bar{r}_1|\tilde{x}_1(t)| - \psi_1^\dagger\right)\int_0^{+\infty} g_1(a)\mathfrak{Q}(\tilde{x}_1(t-a))da.
\end{aligned}$$

Since $|\tilde{x}_1(t)| \leq \sqrt{2\mathscr{V}_1(\tilde{x}_{1t})}$, it follows that

$$\begin{aligned}
\dot{\mathscr{V}}_1(t) \leq & -\frac{\psi_1^\dagger}{2}\mathfrak{Q}(\tilde{x}_1(t)) + \left(\bar{r}_1\sqrt{2\mathscr{V}_1(\tilde{x}_{1t})} - \frac{\psi_1^\dagger}{2}\right)\mathfrak{Q}(\tilde{x}_1(t)) - d_{p1}\psi_1^\dagger\mathscr{N}_1(\tilde{x}_{1t}) \\
& + \left(2\lambda_1\bar{r}_1\sqrt{2\mathscr{V}_1(\tilde{x}_{1t})} - \psi_1^\dagger\right)\int_0^{\infty} g_1(a)\mathfrak{Q}(\tilde{x}_1(t-a))da
\end{aligned} \tag{4.64}$$

Since $\lambda_i < 1$ for all $i \in I_n$, we conclude that for all initial condition $\varphi_1 \in \mathscr{C}\left([-\infty, 0], \mathbb{R}^+\right)$ satisfying

$$\mathscr{V}_1(\tilde{\varphi}_1) < \left(\frac{\psi_1^\dagger}{2\sqrt{2}\bar{r}_1}\right)^2, \tag{4.65}$$

the derivative of the functional $\mathscr{V}$ satisfies for all $t \geq 0$,

$$\dot{\mathscr{V}}_1(t) \leq -\frac{\psi_1^\dagger}{2}\mathfrak{Q}(\tilde{x}_1(t)) - d_{p1}\psi_1^\dagger\mathscr{N}_1(\tilde{x}_{1t}) \tag{4.66}$$

On the other hand, we notice from the definitions of $\mathscr{N}$ and $\mathscr{M}$ that:

$$\begin{aligned}
\mathscr{N}_i(\tilde{x}_{it}) = & \int_0^{+\infty} f_i(\ell)\int_{t-\ell}^{t} e^{-d_{pi}(t-m)}\mathfrak{Q}(\tilde{x}_i(m))dmd\ell \\
\geq & \int_0^{+\infty}\int_{t-\ell}^{t} f_i(\ell)e^{-d_{pi}\ell}\mathfrak{Q}(\tilde{x}_i(m))dmd\ell \\
= & \mathscr{M}_i(\tilde{x}_{it}).
\end{aligned} \tag{4.67}$$

A direct consequence is that

$$\begin{aligned}\dot{\mathscr{V}}_1(t) &\leq -\frac{\psi_1^\dagger}{2}\mathfrak{Q}(\tilde{x}_1(t)) - d_{p1}\psi_1^\dagger \mathscr{N}_1(\tilde{x}_{1t}) \\ &\leq -\frac{\psi_1^\dagger}{2}\mathfrak{Q}(\tilde{x}_1(t)) - \frac{d_{p1}\psi_1^\dagger}{2}\mathscr{M}_1(\tilde{x}_{1t}) - \frac{d_{p1}\psi_1^\dagger}{2}\mathscr{N}_1(\tilde{x}_{1t}) \\ &\leq -\tilde{\psi_1}^\dagger \mathscr{V}_1(\tilde{x}_{1t}), \text{ where, } \tilde{\psi_1}^\dagger > 0.\end{aligned} \tag{4.68}$$

We conclude that for all initial conditions satisfying (4.65), the trajectories of (4.53) (for $i = 1$) converge exponentially to the origin (which is E of model (4.50)) with a decay rate smaller or equal to $\frac{\tilde{\psi}^\dagger}{2}$. □

In the previous sections, we revisited the description of the cell cycle and we generalized the stability results of Chapter 3 to the case of nonlinear systems with infinite distributed delays and time-varying parameters, through the construction of novel Lyapunov-Krasovskii functionals. From a biological point of view, we have seen that the stability conditions in Theorem 4.12 and 8 are substantially similar to those given in the previous chapter.

In the sequel, we introduce for the first time some cell-plasticity functions in the model of interest.

4.7 First observations on transdifferentiation and dedifferentiation

We briefly illustrate two situations: transdifferentiation as a disturbance (as in Chapter 3) and a dedifferentiation process in which more mature cells regress to a SC resting (quiescent) compartment.

4.7.1 Transdifferentiation as an input for HSCs-compartment

We recall that in Chapter 3, cell-plasticity has been considered as a perturbation (nonvanishing disturbances). In fact, using the LKF that we introduced in Section 4.4, we can perform a robustness analysis when the system is subject to external perturbations.

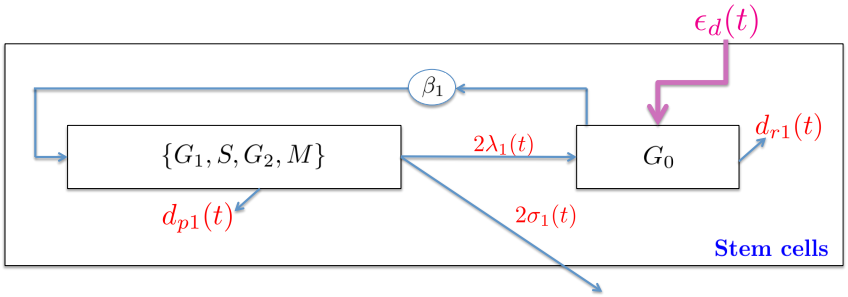

Fig. 4.10 $\varepsilon_d(\cdot)$ is introduced to model the effect of the transdifferentiation from other cell types, that join the compartment of HCSs.

In this case, the studied model is given by The studied model is given by:

$$\begin{cases} \frac{\partial p_1(t,a)}{\partial t} + \frac{\partial p_1(t,a)}{\partial a} + d_{p1}(t)p_1(t,a) + h_1(a)p_1(t,a) = 0, \\ \frac{\partial r_1(t,a)}{\partial t} + \frac{\partial r_1(t,a)}{\partial a} + d_{r1}(t)r_1(t,a) + \beta_1\left(\int_0^{+\infty} r_1(t,a)da\right) r_1(t,a) = 0. \end{cases} \tag{4.69}$$

The renewal conditions which give the birth rate at the initial age $a = 0$ are introduced through the following boundary conditions:

$$\begin{cases} p_1(t,0) = \beta_1\left(\int_0^{+\infty} r_1(t,a)da\right)\int_0^{\infty} r_1(t,a)da, \\ r_1(t,0) = 2\lambda_1(t)\int_0^{+\infty} h_1(a)p_1(t,a)da + \varepsilon_d(t). \end{cases} \tag{4.70}$$

where, $\varepsilon_d(t) \in (0,\overline{\varepsilon}]$, for all $t \geq 0$. Using the method of characteristics, we prove that for all $t \geq 0$ and $a \geq 0$,

$$\dot{x}_1(t) = -d_{r1}(t)x_1(t) - \beta_1(x_1(t))x_1(t) + 2\lambda_1(t)\int_0^{+\infty} g_1(t,a)\beta_1(x_1(t-a))x_1(t,a)da + \varepsilon_d(t). \tag{4.71}$$

Remark 25. ***i)*** *We observe that in this case, investigating the stability properties of the origin of system* (4.71) *is equivalent to performing a robustness analysis when the nominal system describing stem cells dynamics is subject to external disturbances. We establish a common result about practical stability (see Chapter 9, Khalil).* ***ii)*** *It is well known that a strict Lyapunov functional that allows us to establish exponential stability result guarantees robustness.* ***iii)*** *We can take advantage from the positive infinite distributed terms in* (4.71) *in order to refine the stability set obtained using* R_1.

We introduce the functional

$$\mathscr{R}(x_{1t}) = R_1(x_{1t}) - \theta x_1(t), \tag{4.72}$$

where,

$$\theta = \frac{1}{2}\min\left\{ \frac{\underline{d}_{r1} - \left(4\overline{\lambda}_1\overline{C}_1 - \left(1 + 2\overline{\lambda}_1\right)\right)\beta_1(0)}{\underline{d}_{r1} - \left(2\overline{\lambda}_1\overline{C}_1 - 1\right)\beta_1(0)}, \frac{\underline{d}_{r1} - \left(2\overline{\lambda}_1\overline{C}_1 - 1\right)\beta_1(0)}{\overline{d}_{r1} + \beta(0)} \right\} = \frac{\underline{d}_{r1} - \left(2\overline{\lambda}_1\overline{C}_1 - 1\right)\beta_1(0)}{2\left(\overline{d}_{r1} + \beta(0)\right)},$$

and the functional R_1 is the one defined in (4.30). One of the selection criteria of the weighted constant θ is to ensure that the functional $\mathscr{R}$ is positive on the positive orthant. Finally, we consider $\tilde{\theta} > 0$ and we define the set

$$\mathscr{S}_{\varepsilon_d} = \left\{ \varphi \in \mathscr{C}\left((-\infty,0],\mathbb{R}^+\right), R_1(\varphi) + 2\theta\underline{\lambda}_1\int_{-\infty}^{0} f_1(-a)e^{\underline{d}_{p1}a}\beta_1(\varphi)\varphi < \tilde{\theta} \right\}. \tag{4.73}$$

Based on the LKF used in Section 4.4, we are ready to prove the following result:

Corollary 4. *If the condition*

$$\underline{d}_{r1} - \left(2\overline{\lambda}_1\overline{C}_1 - 1\right)\beta_1(0) > 0, \tag{4.74}$$

is satisfied, then the state x_{1t} of system (4.71)*, where for all $t \geq 0$, $\varepsilon_d(t) \in (0, \overline{\varepsilon}_d]$, converges exponentially to the set $\mathscr{S}_{\varepsilon_d}$.*

Proof. We are going to use the functionals N_1 and M_1 introduced respectively in (4.11) and (4.14); as well as their derivatives satisfying respectively (4.13) and (4.16). Therefore, the derivative of the functional U_1, introduced in (4.18), along the trajectories of the perturbed system (4.71) satisfies

$$\dot{U}_1(t) \leq -\left[\underline{d}_{r1} - \left(2\overline{\lambda}_1 - 1\right)\beta_1(0)\right] x_1(t) - 2\overline{\lambda}_1 \underline{d}_{p1} N_1(x_{1t}) + \varepsilon_d(t), \tag{4.75}$$

and, similarly, the derivative along the trajectories of the perturbed system (4.71) of the functional V_1 introduced in (4.21) satisfies

$$\dot{V}_1(t) \leq -\left[\underline{d}_{r1} - \left(2\overline{\lambda}_1\overline{C}_1 - 1\right)\beta_1(0)\right] x_1(t) + \varepsilon_d(t). \tag{4.76}$$

Thus, the derivative of the functional R_1, introduced in (4.30), satisfies

$$\dot{R}_1(t) \leq -\left[\underline{d}_{r1} - \left(2\overline{\lambda}_1\overline{C}_1 - 1\right)\beta_1(0)\right] x_1(t) - 2\overline{\lambda}_1 \underline{d}_{p1} N_1(x_{1t}) + \frac{\underline{d}_{r1} - \left(4\overline{\lambda}_1\overline{C}_1 - \left(1 + 2\overline{\lambda}_1\right)\right)\beta_1(0)}{\underline{d}_{r1} - \left(2\overline{\lambda}_1\overline{C}_1 - 1\right)\beta_1(0)}\overline{\varepsilon}_d. \tag{4.77}$$

A direct consequence is that the derivative of the functional $\mathscr{R}$, defined in (4.72), along the trajectories of (4.71) satisfies

$$\begin{aligned}\dot{\mathscr{R}}(t) \leq & -\left[\underline{d}_{r1} - \left(2\overline{\lambda}_1\overline{C}_1 - 1\right)\beta_1(0)\right] x_1(t) + \theta\left(\overline{d}_{r1} + \beta(0)\right) x_1(t) \\ & - 2\overline{\lambda}_1 \underline{d}_{p1} N_1(x_{1t}) - 2\theta\lambda_1(t)\int_0^{+\infty} g_1(t,a)\beta_1(x_1(t-a))x_1(t-a)da \\ & + \frac{\underline{d}_{r1} - \left(4\overline{\lambda}_1\overline{C}_1 - \left(1 + 2\overline{\lambda}_1\right)\right)\beta_1(0)}{\underline{d}_{r1} - \left(2\overline{\lambda}_1\overline{C}_1 - 1\right)\beta_1(0)}\overline{\varepsilon}_d.\end{aligned}$$

Using the expression $\theta = \frac{\underline{d}_{r1} - \left(2\overline{\lambda}_1\overline{C}_1 - 1\right)\beta_1(0)}{2\left(\overline{d}_{r1} + \beta(0)\right)}$, it follows that

$$\begin{aligned}\dot{\mathscr{R}}(t) \leq & -\frac{1}{2}\left[\underline{d}_{r1} - \left(2\overline{\lambda}_1\overline{C}_1 - 1\right)\beta_1(0)\right] x_1(t) - 2\overline{\lambda}_1 \underline{d}_{p1} N_1(x_{1t}) \\ & - 2\theta\lambda_1(t)\int_0^{+\infty} g_1(t,a)\beta_1(x_1(t-a))x_1(t-a)da \\ & + \frac{\underline{d}_{r1} - \left(4\overline{\lambda}_1\overline{C}_1 - \left(1 + 2\overline{\lambda}_1\right)\right)\beta_1(0)}{\underline{d}_{r1} - \left(2\overline{\lambda}_1\overline{C}_1 - 1\right)\beta_1(0)}\overline{\varepsilon}_d.\end{aligned} \tag{4.78}$$

Using the definition of $\mathscr{R}$, R_1, and the inequality (4.17), we easily determine a strictly positive constant $\hat{\delta} > 0$, such that

$$\begin{aligned}\dot{\mathscr{R}}(t) \leq & -2\hat{\delta}\mathscr{R}(x_{1t}) - 2\theta\lambda_1(t)\int_0^{+\infty} g_1(t,a)\beta_1(x_1(t-a))x_1(t-a)da \\ & + \frac{\underline{d}_{r1} - \left(4\overline{\lambda}_1\overline{C}_1 - \left(1+2\overline{\lambda}_1\right)\right)\beta_1(0)}{\underline{d}_{r1} - \left(2\overline{\lambda}_1\overline{C}_1 - 1\right)\beta_1(0)}\overline{\varepsilon}_d.\end{aligned} \tag{4.79}$$

We conclude that for all $x_{1t} \notin S_{\varepsilon_d}$, we have $\dot{\mathscr{R}}(t) \leq -\hat{\delta}\mathscr{R}(x_{1t})$. Therefore, for all $t \geq 0$, $\varepsilon_d(t) \in (0, \overline{\varepsilon}_d]$, $\varphi \in \mathscr{C}\left((-\infty, 0], \mathbb{R}^+\right)$, and $x_{1t} \notin S_{\varepsilon_d}$, we have $x_1(t) \leq \mathscr{R}(\varphi)e^{-\hat{\delta}t}$, meaning that the trajectory $x_1(t)$ converges to the origin as long as $x_{1t} \notin S_{\varepsilon_d}$, and that the state x_{1t} converges exponentially to the set $\mathscr{S}_{\varepsilon_d}$. □

4.7.2 Dedifferentiation towards the stem cell resting compartment

Now, let us say few words about the case in which any generation $j \in \{2, \ldots, n\}$ may dedifferentiate to join the **resting** stem cell compartment. The model in this case is illustrated in Figure 4.11, and it is governed by:

$$\begin{cases} \frac{\partial p_i(t,a)}{\partial t} + \frac{\partial p_i(t,a)}{\partial a} + d_{pi}(t)p_i(t,a) + h_i(a)p_i(t,a) = 0, \\ \frac{\partial r_i(t,a)}{\partial t} + \frac{\partial r_i(t,a)}{\partial a} + d_{ri}(t)r_i(t,a) + \beta_i\left(x_i(t)\right)r_i(t,a) = 0, \\ \text{for all } i \geq 1 \text{ where } i \neq j, \text{ and,} \\ \frac{\partial p_j(t,a)}{\partial t} + \frac{\partial p_j(t,a)}{\partial a} + d_{pj}(t)p_j(t,a) + h_j(a)p_j(t,a) = 0, \\ \frac{\partial r_j(t,a)}{\partial t} + \frac{\partial r_j(t,a)}{\partial a} + \left[d_{rj}(t) + \varepsilon_d(t)\right]r_j(t,a) + \beta_j\left(x_j(t)\right)r_j(t,a) = 0. \end{cases} \tag{4.80}$$

The renewal conditions which give the birth rate at the initial age $a = 0$ are introduced through the following boundary conditions:

$$\begin{cases} r_1(t,0) = 2\left(1-\sigma_1(t)\right)\int_0^{+\infty} h_1(a)p_1(t,a)da + \int_0^{+\infty}\varepsilon_d(t)r_j(t,a)da, \\ r_i(t,0) = 2\left(1-\sigma_i(t)\right)\int_0^{+\infty} h_i(a)p_i(t,a)da \\ \qquad\qquad +2\sigma_{i-1}(t)\int_0^{+\infty} h_{i-1}(a)p_{i-1}(t,a)da, \text{ for all } i > 1, \text{ and,} \\ p_i(t,0) = \beta_i\left(x_i(t)\right)x_i(t), \text{ for all } i \in \{1, \ldots, n\}. \end{cases} \tag{4.81}$$

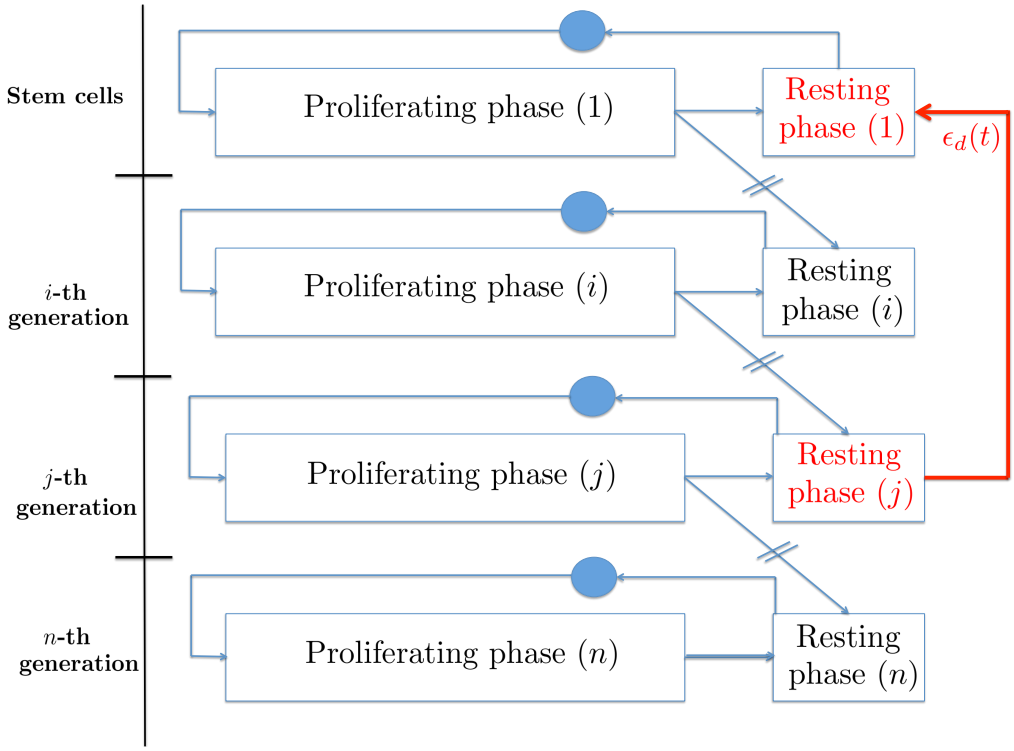

Fig. 4.11 The cell generation j can be chosen to be any generation between the 2nd and the n-th generation. A subpopulation of the j-th generation is assumed to undergo dedifferentiation mechanisms and thus join the first compartment of (hematopoietic) stem cells.

Through classical arguments, we show the model in Figure 4.11 is described for all $t \geq 0$ by the system:

$$\begin{cases} \dot{x}_1(t) = 2\lambda_1(t)\int_0^{+\infty} g_1(t,a)\beta_1(x_1(t-a))x_1(t-a)da + \epsilon_d(t)x_j(t) \\ \qquad -d_{r1}(t)x_1(t) - \beta_1(x_1(t))x_1(t) \\ \dot{x}_j(t) = 2\lambda_j(t)\int_0^{+\infty} g_j(t,a)\beta_j(x_j(t-a))x_j(t-a)da \\ \qquad +2\sigma_{j-1}(t)\int_0^{+\infty} g_{j-1}(t,a)\beta_{j-1}(x_{j-1}(t-a))x_{j-1}(t-a)da \\ \qquad -\left[d_{rj}(t)+\epsilon_d(t)\right]x_j(t) - \beta_j(x_j(t))x_j(t), \\ \text{and, for all } i \notin \{1,j\}, \\ \dot{x}_i(t) = 2\lambda_i(t)\int_0^{+\infty} g_i(t,a)\beta_i(x_i(t-a))x_i(t-a)da \\ \qquad +2\sigma_{i-1}(t)\int_0^{+\infty} g_{i-1}(t,a)\beta_{i-1}(x_{i-1}(t-a))x_{i-1}(t-a)da \\ \qquad -d_{ri}(t)x_i(t) - \beta_i(x_i(t))x_i(t). \end{cases} \tag{4.82}$$

Using LKF constructions as in Section 4.4, we can prove that if the stability conditions in **Step 3** of Theorem 8 are satisfied for all $i \in \{1,\dots,n\}$, then the origin of the system (4.82) -involving dedifferentiation as in Figure 4.11- is globally exponentially stable. In other words, the dedifferentiation process as represented in Figure 4.11 has no major effect if all the cell generations are already dying. On the other hand, some medical experiments (e.g. [142], [249]) mention that cancer cells avoid their extinction during therapy by undergoing dedifferentiation processes.
In order to determine a model that reproduce effectively the expected dynamics in dedifferentiation of unhealthy tissues, we introduce in the next section another configuration of the cell plasticity function, in which the dedifferentiated cells are directly active in the **proliferating** phase. In other words, we modify the representation given in Figure 4.11, by introducing a dedifferentiation function from the unhealthy more mature cell generations towards the stem cell compartment, where CSCs are directly active in the cell cycle. Then, we study the resulting system and we show that in this configuration, it is possible to have the conditions in **Step 3** of Theorem 8 that are satisfied, while cells do not vanish thanks to the dedifferentiation mechanism.

4.8 Dedifferentiation of a subpopulation of cells into cancer stem cells

We discuss in this section a refined model (illustrated in Figure 4.12-4.13) that highlights, qualitatively, the impact of dedifferentiation on the behavior of cancer cells. More precisely, we consider that cancer cells may dedifferentiate into CSCs (i.e. they join the SC compartement, are they are directly active in proliferation).

4.8.1 Introduction of a general model involving unhealthy cell-plasticity mechanisms

We recall the general form of the model in Figure 4.12, in which we have n distinguishable maturity levels ($i \in I_n = \{1,\dots,n\}$, where $i = 1$ is the compartment of SCs). Now, we focus on the role of the cell-plasticity functions ω_i and ξ_i, for all $i \in I_n$ (the flux functions on the right of Figure 4.12).

The dynamics of resting cells, $r_i(t,a)$, and proliferating cells, $p_i(t,a)$, of the i-th generation ($i \in I_n$), of age $a > 0$, at time $t \geq 0$, are governed by the age-structured (McKendrick) PDEs :

$$\begin{cases} \frac{\partial p_i}{\partial t} + \frac{\partial p_i}{\partial a} = -\left[d_{pi}(t) + h_i(a)\right] p_i(t,a), \\ \frac{\partial r_i}{\partial t} + \frac{\partial r_i}{\partial a} = -\left[d_{ri}(t) + \beta_i\left(x_i(t)\right)\right] r_i(t,a) - \xi_i(t), \end{cases} \tag{4.83}$$

where, for all $i \in I_n$, $x_i(t) = \int_0^{+\infty} r_i(t,a)da$, and, for all $i \in I_n$ and $t \geq 0$, $d_{ri}(t)$ is the death rate of the resting cells, while $d_{pi}(t)$ is the death rate of proliferating cells. The reintroduction function β_i is decreasing and $\lim_{\ell\to\infty} \beta_i(\ell) = 0$. Moreover, we consider with an abuse of notation (see the explanation below) that for all $t \geq 0$,

$$\xi_i(t) = \xi_i\left(\underbrace{x_1(t),\dots,x_{i-1}(t)}_{\text{out. dediff}}, x_i(t), \overbrace{\xi_i^{\dagger}(t)}^{\text{out. transdiff}}\right). \tag{4.84}$$

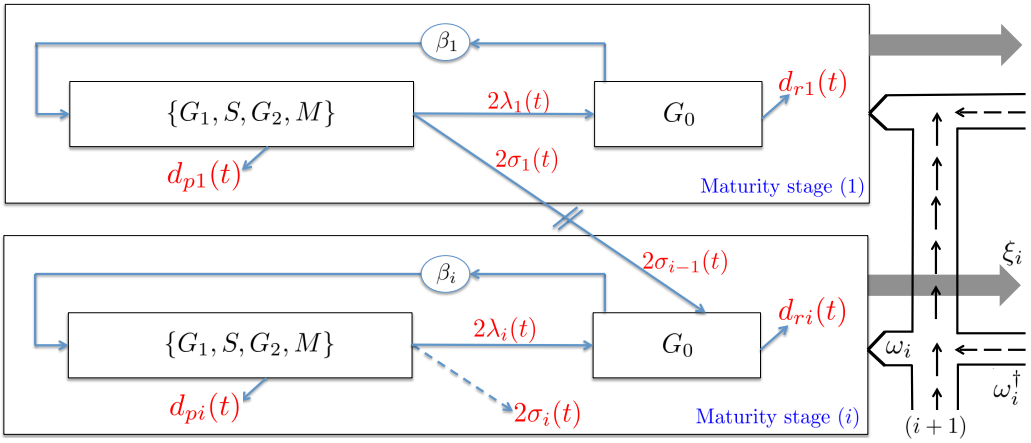

Fig. 4.12 A cartoon representation of the discrete maturity model of interest, involving multiple dedifferentiation and transdifferentiation functions. Cells of the i-th maturity-generation, where $i \in I_n = \{1,\dots,n\}$, $n > 1$, are in a resting phase G_0, or in proliferation (cell-division cycle) $\{G_1, S, G_2, M\}$. In the general case, we can consider that all the involved biological parameters (rate of differentiation $\sigma_i \in (0,1)$, rate of self-renew $\lambda_i = 1 - \sigma_i$, apoptosis rate d_{pi}, death rate of resting cells d_{ri}) are time-varying. On the right, the flux due to the cell-plasticity functions, ξ_i and ω_i for all $i \in I_n$, is represented. In fact, both ξ_i and ω_i have a part related to dedifferentiation and a part related to transdifferentiation. The former one depends on the (modeled) state variables, which represent the total densities of the resting cells x_i, while the parts quantifying trandifferentiation (denoted $\xi_i^\dagger$ and $\omega_i^\dagger$, in equations (5.95), (5.105)) depend on time, since they are biologically related to distant (external) cell tissues and lineages (i.e. which are not explicitely modeled). This model extends the one in [8].

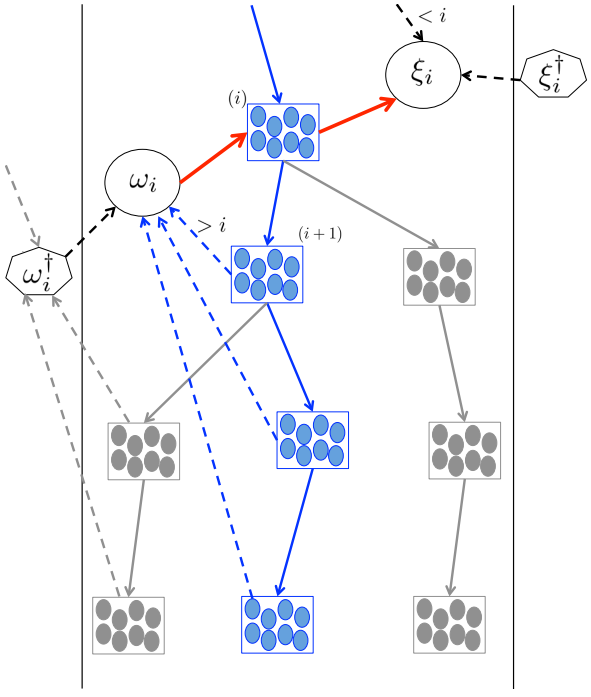

Fig. 4.13 The blue lineage hierarchy is the one we are focusing on. Grey lineages are those which cannot be explicitly modeled in our mathematical framework. For the i-th cell generation, the function w_i quantifies the input by dedifferentiation from the next more mature generations of the studied blue lineage, together with the input by transdifferentiation ($\omega_i^\dagger$), which comes from non-modeled distant cell types. In a similar spirit, ξ_i quantifies the loss in cell account of the i-th generation, in response to some requirements from less mature generation of the blue hierarchy (i.e. dedifferentiation), or by other types of cells (i.e. the loss due to transdifferentiation, $\xi_i^\dagger$).

About the functions ξ_i

As illustrated in Figure 4.13, the function ξ_i quantifies the **output (cell loss)** either by dedifferentiation or by transdifferentiation. As formulated in (5.95), the function ξ_i depends on x_i and may be affected by some of, or all, the generations of cells which are less mature than the i-th generation, i.e. the cell densities $x_1,\dots,x_{i-1}$. This is -by definition- justified by the fact that dedifferentiation of the i-th generation addresses a need (either healthy or cancerous) that arises in a less mature generation within the same hierarchy (i.e. at least one of the densities $x_1,\dots,x_{i-1}$).
In addition, the loss by transdifferentiation, $\xi_i^\dagger$, aims to address a need from more distant tissues, i.e. $\xi_i^\dagger$ does not depend on the modeled cell populations x_i, but only on time (as a representation of any external event that occurs beyond the studied hierarchy).

The system (4.83) is associated with some initial conditions (i.e. initial age distributions when $t=0$) which are $\mathscr{L}^1$-functions defined by:

$$\begin{cases} p_i(0,a) = p_i^0(a), \ \text{ and,} \\ r_i(0,a) = r_i^0(a), \ \text{ for all } \ a \in [0,+\infty). \end{cases} \tag{4.85}$$

Moreover, we assume from biological considerations that for all $t \geq 0$, $\lim_{a\to\infty} p_i(t,a) = \lim_{a\to\infty} r_i(t,a) = 0$. Finally, the renewal conditions, which give the birth rate at the initial age $a=0$, are introduced through the following boundary conditions:

$$\begin{cases} p_i(t,0) = \beta_i \left(\int_0^{+\infty} r_i(t,a)da \right) \int_0^{+\infty} r_i(t,a)da + \omega_i(t) \\ \qquad\quad = \beta_i(x_i(t))x_i(t) + \omega_i(t), \\ r_i(t,0) = 2\sigma_{i-1}(t) \int_0^{+\infty} h_{i-1}(a)p_{i-1}(t,a)da \\ \qquad\quad +2\left(1-\sigma_i(t)\right) \int_0^{+\infty} h_i(a)p_i(t,a)da, \end{cases} \tag{4.86}$$

where $\sigma_i(t)$ represents the time-varying rate of differentiation and, consequently, $\lambda_i(t) = 1-\sigma_i(t)$ is the rate of self-renewal of the i-th cell generation. In addition, we consider with an abuse of notation that for all $t \geq 0$,

$$\omega_i(t) = \omega_i \left(x_i(t), \underbrace{x_{i+1}(t),\dots,x_n(t)}_{\text{in. dediff}}, \overbrace{\omega_i^\dagger(t)}^{\text{in. transdiff}} \right). \tag{4.87}$$

About the functions ω_i

The function ω_i appears in the boundary conditions (4.86), since it represents the new cell birth resulting from the dedifferentiation of more mature cell generations, together with the transdifferentiation of other cell lineages. The functions ω_i are implicitly related to the functions ξ_i in (5.95), since cells that join the i-th generation by dediffentiation (the input ω_i) are, for instance, the sum of the dedifferentiated cells from more mature generations (the outputs ξ_{i+1}, ξ_{i+2}, ...). Therefore, for all $i \in I_n$, the function ω_i depends on x_i and may depend on (all or some of) the more mature generations in the same hierarchy, $x_{i+1}, \ldots, x_n$. Moreover, the time-varying term $\omega_i^\dagger$ in (5.105) quantifies the incoming by trandifferentiation from distant cell lineages or types, outside the hierarchy of interest.

In summary, we say that generally in McKendrick type models, the removal terms (e.g. death rates) appear in the PDE system (model (4.83), in our case), while new births appear in the boundary conditions (given by (4.86), in our case). The PDE system (4.83)-(4.86)-(4.85) provides a general framework to describe the cell dynamics within a given hierarchy formed by n discrete-maturity stages. However, we still need to specify the nature and the operating mode of the dedifferentiation and the transdifferentiation functions (ξ_i and ω_i, for all $i \in I_n$), in order to determine the behavior of the overall system. For that purpose, we need to focus on a typical explicit dedifferentiation mechanism. More precisely, we start in this study with an unhealthy case in which a portion of the j-th cell generation ($j \in I_n$, $j > 1$) dedifferentiates and joins the SC compartment ($i = 1$), as presented in the sequel.

4.8.2 A specific (unhealthy) dedifferentiation process into CSCs

In order to allow mathematical analysis, we focus on the typical (explicit) case in which a proportion $\kappa \in [0,1]$ of the total density of resting cells of the j-th generation x_j becomes diseased, e.g. as a result of a series of abnormal mutations (see [300] for mutations inducing leukemia). Then, we consider that only the subpopulation of mutated cells can undergo dedifferentiation, and we denote by D the characteristic pattern that describes the dedifferentiation mechanism from the j-th generation into the SC-proliferating compartment.

Let $j \in [2,n]$ be the generation of cells that includes a malignant (mutated) subpopulation, capable of generating cancer stem cells (CSCs) by dedifferentiation. For the sake of brevity, we consider that the transdifferentiation mechanisms are negligible compared to dedifferentiation (i.e. we put $\xi_i^\dagger(t) = \omega_i^\dagger(t) = 0$, for all $i \in I_n$ and $t \geq 0$, otherwise, the study will be similar to the robustness analysis that we performed in Section 4.7.1).

We notice that -with an abuse of notation- the functions ξ_i and ω_i can be rewritten in this case as:

$$\begin{cases} \xi_i(x_1,\ldots,x_i) = 0, \text{ for all } i \in I_n,\ i \neq j, \\ \xi_j(x_1,\ldots,x_j) = \xi_j(x_j) = \kappa D(\kappa x_j) x_j, \\ \omega_1(x_1,\ldots,x_n) = \omega_1(x_j) = \kappa D(\kappa x_j) x_j, \\ \omega_i(x_i,\ldots,x_n) = 0, \text{ for all } i \in \{2,\ldots,n\}, \end{cases} \tag{4.88}$$

where we can select the function D as follows,

$$D(\ell) = \tanh\left(\ell^p\right), \text{ where, } p > 0, \text{ for all } \ell \geq 0. \tag{4.89}$$

One notices that the selected dedifferentiation functions (4.88) depend only on the mutated subpopulation of cells belonging to the j-th maturity generation x_j. The latter choice can be argued as an **unhealthy dedifferentiation process** triggered by abnormal mutations observed in a subpopulation κx_j of the j-th stage. Many other alternative choices may be considered if biological requirements are justified[3]

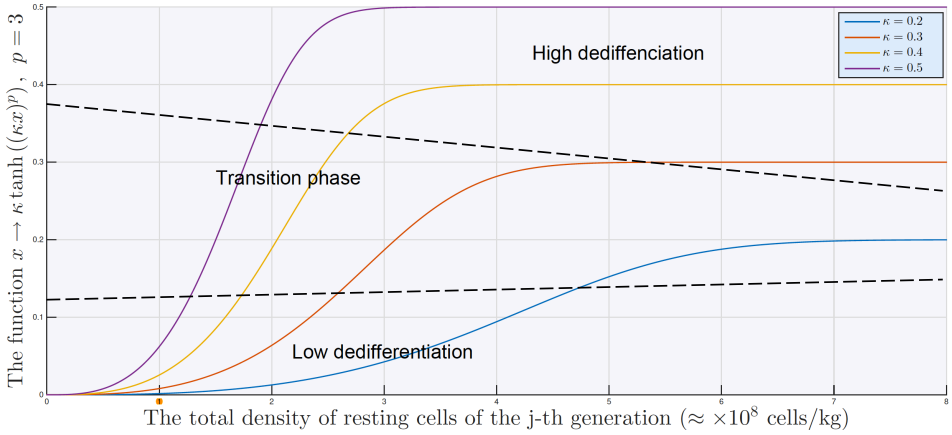

Fig. 4.14 The function $x_i \to \kappa D(\kappa x_i)$, for different values of κ, is suggested to represent qualitatively the effectiveness and the impact of dedifferentiation according to: **(1)** the size of the population where tumor mutations occur (quantified by the total cell density x_i), and **(2)** the proportion of mutated cells within the entire population (quantified by κ). See Remark 26-**(ii)**.

Remark 26. *Let us say few more words about the cell-plasticity functions ξ_i and ω_i that we defined in* (4.88). *Firstly, we recall that we are limiting ourselves to the case of constant κ, where $k \in [0,1]$. The features of the tangent hyperbolic function D defined in* (4.89) *lead to:*

i) *$\xi_j \equiv 0$ and $\omega_1 \equiv 0$, when $x_j = 0$ or $\kappa = 0$. The latter case means that dedifferentiation does not exist if no abnormal mutation occurs.*

ii) *when the j-th cell generation forms a relatively small population over all the n cell generations (i.e. a low density x_j), or when the portion of unhealthy cells is minimal within the genetic diversity landscape (i.e. a low mutated portion of cells, quantified by κ), then the gain of the dedifferentiation process is minimal. Indeed, the subpopulation of mutated cells is not expected to entirely dedifferentiate and join the SCs compartment. Actually, sometimes mutated cells do not dedifferentiate and they may also disappear over time if they do not overproliferate. In our model, the gain of the differentiation process is represented by the quantity $\kappa D(\kappa x_j)$, since $\xi_j(x_j) = \kappa D(\kappa x_j) x_j$. The gain is illustrated in Figure 4.14, where we notice that for low x_j and low κ, the amplitude of $\kappa D(\kappa x_j)$ is small. Then, it*

[3]Other choices different from (4.88) may be considered within the general framework introduced in Section 4.8.1. For instance, a **healthy dedifferentiation process** can be envisaged, in which the ξ_i and ω_i depend on the total density of resting SCs x_1. In this configuration, the density of SCs triggers the dedifferentiation of more mature differentiated cells, if needed (e.g. after hemorrhage or injury, when the body is in a hurry to regenerate itself). For the sake of brevity, this situation is beyond the scope of the current work.

increases in order to approach its maximum value, when the total size of the population x_j is too high, i.e. $\lim_{x_j\to\infty} \kappa D(\kappa x_j) = \kappa$.

Finally, we rewrite the model (4.83) describing the dynamics of resting and proliferating cells, in the form:

$$\begin{cases} \frac{\partial p_i}{\partial t} + \frac{\partial p_i}{\partial a} + \left[d_{pi}(t) + h_i(a)\right] p_i(t,a) = 0, \\ \frac{\partial r_i}{\partial t} + \frac{\partial r_i}{\partial a} + \left[d_{ri}(t) + \beta_i\left(x_i(t)\right)\right] r_i(t,a) = 0, \\ \text{for all } i \geq 1 \text{ where } i \neq j, \text{ and,} \\ \frac{\partial p_j}{\partial t} + \frac{\partial p_j}{\partial a} + \left[d_{pj}(t) + h_j(a)\right] p_j(t,a) = 0, \\ \frac{\partial r_j}{\partial t} + \frac{\partial r_j}{\partial a} + \left[d_{rj}(t) + \beta_j\left(x_j(t)\right)\right] r_j(t,a) + \kappa D\left(\kappa x_j(t)\right) x_j(t) = 0. \end{cases} \tag{4.90}$$

We emphasize the case of (4.86) described throughout the current section, in which the renewal conditions are introduced through the following boundary conditions:

$$\begin{cases} p_1(t,0) = \beta_1\left(x_1(t)\right) x_1(t) + \kappa D_j\left(\kappa x_j(t)\right) x_j(t), \\ p_i(t,0) = \beta_i\left(x_i(t)\right) x_i(t), \text{ for all } i \in \{2,\ldots,n\}, \\ r_1(t,0) = 2\left(1-\sigma_1(t)\right) \int_0^{+\infty} h_1(a) p_1(t,a) da, \\ \text{and for all } i > 1 : \\ r_i(t,0) = 2\left(1-\sigma_i(t)\right) \int_0^{+\infty} h_i(a) p_i(t,a) da + 2\sigma_{i-1}(t) \int_0^{+\infty} h_{i-1}(a) p_{i-1}(t,a) da. \end{cases} \tag{4.91}$$

Finally, we consider some suitable initial conditions as in (4.85). Now, using the method of characteristics, we reduce the model (4.90)-(4.91)-(4.85) into a nonlinear time-delay system (with infinite distributed delays and time-varying parameters). For the sake of clarity and due to space limitation, we illustrate here -without loss of generality- a case with two cell generations, in which a dedifferentiation mechanism is established from the 2nd generation into the SCs one, as illustrated in Figure 4.15.

For example, we consider that a progeny subpopulation κx_2, $\kappa \in [0,1]$, with abnormal mutations (e.g. DMNT3A increasing self-renewal), that may trigger dedifferentiation into CSCs [68], as it appears to be the case in leukemia [286, 173].

As a first approach, we consider a simplified version of the model of interest (with two maturity stages, finite distributed delays and constant parameters). For that:

Let $j \in [2,n]$ be the generation of cells that includes a malignant (mutated) subpopulation, capable of generating cancer stem cells (CSCs) by dedifferentiation. The method of characteristics ([31], [8]) gives, for sufficiently large time,

$$p_i(t,a) = p_i(t-a,0) e^{-\int_0^a d_{pi}(m+t-a)dm} e^{-\int_0^a h_i(m)dm}. \tag{4.92}$$

By integrating $r_i(t,a)$, for all $i \in I_n$, over the age-variable a between 0 and ∞, we obtain:

$$\begin{cases} \dot{x}_i(t) = -d_{ri}(t) x_i(t) - \beta_i(x_i(t)) x_i(t) + r_i(t,0), \quad \text{for all } i \geq 1, i \neq j, \text{ and,} \\ \dot{x}_j(t) = -d_{rj}(t) x_j(t) - \beta_j(x_j(t)) x_j(t) + r_j(t,0) - \kappa x_j(t) D\left(\kappa x_j(t)\right). \end{cases} \tag{4.93}$$

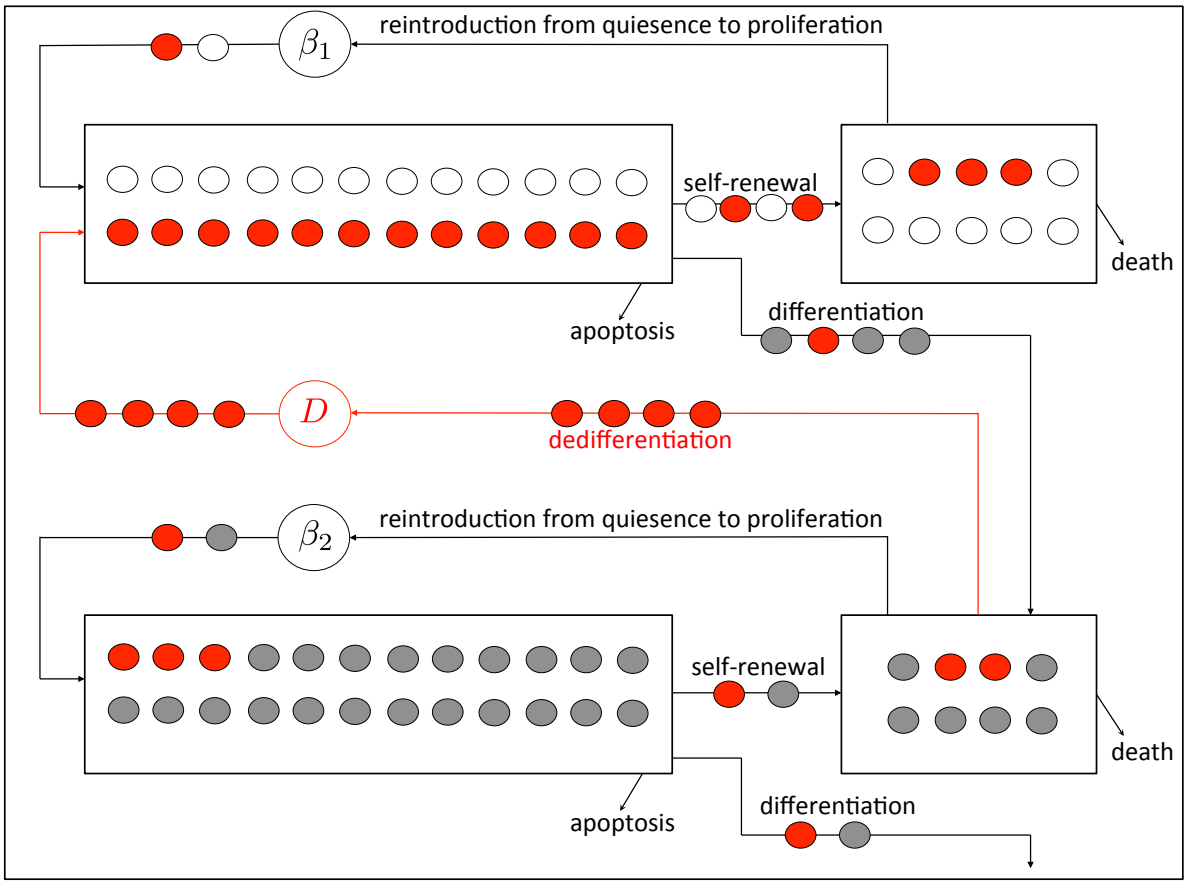

Fig. 4.15 Red cells are malignant (mutated) cells. White cells are ordinary stem cells (SCs), while the gray cell compartment is the one of (progeny) differentiated cells, that includes the subpopulation (in red) κx_2. A mechanism of dedifferentiation of malignant cells (in red, from $i = 2$ to $i = 1$) is established through the function D. In hematopoiesis, a translocation effect after some epigenetic mutations in the progeny compartment (here $i = 2$) may lead to a dedifferentiation of progeny ([68]) and the rise of cancer stem cells (CSCs), that trigger a quick progression of leukemia [286]. For instance, a DNMT3A mutation may provide abnormal cells with a self-renewal activity as important as the one of SCs [173, 286].

Using the boundary conditions (4.91), we substitute the expressions of $r_i(t,0)$, for all $i \in I_n$, we get

$$\begin{cases} \dot{x}_1(t) = -d_{r1}(t)x_1(t) - \beta_1(x_1(t))x_1(t) + 2\left(1-\sigma_1(t)\right)\int_0^{+\infty} h_1(a)p_1(t,a)da, \\ \dot{x}_i(t) = -d_{ri}(t)x_i(t) - \beta_i(x_i(t))x_i(t) + 2\left(1-\sigma_i(t)\right)\int_0^{+\infty} h_i(a)p_i(t,a)da \\ \qquad +2\sigma_{i-1}(t)\int_0^{+\infty} h_{i-1}(a)p_{i-1}(t,a)da, \ \text{ for all } \ i \geq 2, i \neq j, \ \text{ and,} \\ \dot{x}_j(t) = -d_{rj}(t)x_j(t) - \beta_j(x_j(t))x_j(t) - \kappa x_j(t) D\left(\kappa x_j(t)\right) \\ \qquad +2\left(1-\sigma_j(t)\right)\int_0^{+\infty} h_j(a)p_j(t,a)da \\ \qquad +2\sigma_{j-1}(t)\int_0^{+\infty} h_{j-1}(a)p_{j-1}(t,a)da. \end{cases} \tag{4.94}$$

Next, using (4.92) we deduce that

$$\begin{cases} \dot{x}_1(t) = -\left[d_{r1}(t)+\beta_1(x_1(t))\right]x_1(t)+2\left(1-\sigma_1(t)\right)\int_0^{+\infty}h_1(a)e^{-\int_0^a h_1(m)dm}p_1(t-a,0)e^{-\int_0^a d_{p1}(m+t-a)dm}da, \\ \dot{x}_i(t) = -\left[d_{ri}(t)+\beta_i(x_i(t))\right]x_i(t)+2\left(1-\sigma_i(t)\right)\int_0^{+\infty}h_i(a)e^{-\int_0^a h_i(m)dm}p_i(t-a,0)e^{-\int_0^a d_{pi}(m+t-a)dm}da \\ \qquad +2\sigma_{i-1}(t)\int_0^{+\infty}h_{i-1}(a)e^{-\int_0^a h_{i-1}(m)dm}p_{i-1}(t-a,0)e^{-\int_0^a d_{pi-1}(m+t-a)dm}da, \text{ for all } i\geq 2,\ i\neq j, \\ \dot{x}_j(t) = -d_{rj}(t)x_j(t)-\beta_j(x_j(t))x_j(t)-\kappa x_j(t)D\left(\kappa x_j(t)\right) \\ \qquad +2\left(1-\sigma_j(t)\right)\int_0^{+\infty}h_j(a)e^{-\int_0^a h_j(m)dm}p_j(t-a,0)e^{-\int_0^a d_{pj}(m+t-a)dm}da \\ \qquad +2\sigma_{j-1}(t)\int_0^{+\infty}h_{j-1}(a)e^{-\int_0^a h_{j-1}(m)dm}p_{j-1}(t-a,0)e^{-\int_0^a d_{pj-1}(m+t-a)dm}da. \end{cases} \tag{4.95}$$

Using again the boundary conditions (4.91), we deduce that:

$$\begin{cases} \dot{x}_1(t) = -\left[d_{r1}(t)+\beta_1(x_1(t))\right]x_1(t) \\ \qquad +2\left(1-\sigma_1(t)\right)\int_0^{+\infty}h_1(t,a)e^{-\int_0^a h_1(m)dm}\beta_1\left(x_1(t-a)\right)x_1(t-a)e^{-\int_0^a d_{p1}(m+t-a)dm}da \\ \qquad +2\left(1-\sigma_1(t)\right)\int_0^{+\infty}h_1(a)e^{-\int_0^a h_1(m)dm}\kappa x_j(t-a)D_j\left(\kappa x_j(t-a)\right)e^{-\int_0^a d_{p1}(m+t-a)dm}da, \\ \dot{x}_i(t) = -\left[d_{ri}(t)+\beta_i(x_i(t))\right]x_i(t) \\ \qquad +2\left(1-\sigma_i(t)\right)\int_0^{+\infty}h_i(a)e^{-\int_0^a h_i(m)dm}\beta_i\left(x_i(t-a)\right)x_i(t-a)e^{-\int_0^a d_{pi}(m+t-a)dm}da \\ \qquad +2\sigma_{i-1}(t)\int_0^{+\infty}h_{i-1}(a)e^{-\int_0^a h_{i-1}(m)dm}\beta_{i-1}\left(x_{i-1}(t-a)\right)x_{i-1}(t-a)e^{-\int_0^a d_{pi-1}(m+t-a)dm}da, \\ \qquad \text{for all } i\geq 2,\ i\neq j, \text{ and,} \\ \dot{x}_j(t) = -\left[d_{rj}(t)+\beta_j(x_j(t))\right]x_j(t)-\kappa D\left(\kappa x_j(t)\right)x_j(t) \\ \qquad +2\left(1-\sigma_j(t)\right)\int_0^{+\infty}h_j(a)e^{-\int_0^a h_j(m)dm}\beta_j\left(x_j(t-a)\right)x_j(t-a)e^{-\int_0^a d_{pj}(m+t-a)dm}da \\ \qquad +2\sigma_{j-1}(t)\int_0^{+\infty}h_{j-1}(a)e^{-\int_0^a h_{j-1}(m)dm}\beta_{j-1}\left(x_{j-1}(t-a)\right)x_{j-1}(t-a)e^{-\int_0^a d_{pj-1}(m+t-a)dm}da. \end{cases} \tag{4.96}$$

For the sake of clarity, we analyze the simpler version of the model (4.96), with finite distributed delays, constant parameters, and involving only two cell generations (as in Figure 4.15), given by:

$$\begin{cases} \dot{x}_1(t) = -\left[d_{r1}+\beta_1(x_1(t))\right]x_1(t)+2\left(1-\sigma_1\right)\int_0^{\tau_1}g_1(a)\beta_1\left(x_1(t-a)\right)x_1(t-a)da \\ \qquad +2\left(1-\sigma_1\right)\int_0^{\tau_1}g_1(a)\kappa x_2(t-a)D\left(\kappa x_2(t-a)\right)da, \\ \dot{x}_2(t) = -\left[d_{r2}+\beta_2\left(x_2(t)\right)+\kappa D\left(\kappa x_2(t)\right)\right]x_2(t)+2\left(1-\sigma_2\right)\int_0^{\tau_2}g_2(a)\beta_2\left(x_2(t-a)\right)x_2(t-a)da \\ \qquad +2\sigma_1\int_0^{\tau_1}g_1(a)\beta_1\left(x_1(t-a)\right)x_1(t-a)da+2\sigma_1\int_0^{\tau_1}g_1(a)\kappa x_2(t-a)D\left(\kappa x_2(t-a)\right)da. \end{cases} \tag{4.97}$$

4.8.3 Stability properties of the 0-equilibrium of a two maturity stages model involving dedifferentiation

Now, we want to determine stability conditions of the origin of the model (4.97). This is equivalent to the eradication of all the cells involved in this unhealthy process (Figure 4.15), through anti-cancer therapies. In fact, we can prove that the system (4.97) is positive [124]. Therefore, we take advantage from the positivity of the trajectories to develop a suitable Lyapunov approach and perform a stability analysis of the origin of the system (4.97).

Firstly, let us consider in this proof that: $s_i = d_{ri} - \alpha_i\beta_i(0)$ and $\alpha_i = 2\lambda_i C_i - 1$, for $i = 1,2$, and,

$$\mathfrak{a} = s_2 - \kappa\overline{D}\left[\frac{2\sigma_1\lambda_1 C_1^2\beta_1(0)}{s_1} + 2\sigma_1 C_1 - 1\right], \tag{4.98}$$

where, $\overline{D} = \sup_{\ell\geq 0} D(\ell)$. Notice that, $\overline{D} = 1$, when, $D(\ell) = \tanh(\ell^p)$, $p > 0$.

Now we are ready to state and prove the following result:

Theorem 10. *Let us assume that $s_i > 0$ for all $i \in I_n$. If, in addition, the conditions,*

$$\begin{cases} 1 - 2\sigma_1 C_1 - \frac{2\sigma_1\lambda_1 C_1^2\beta_1(0)}{s_1} < 0, \text{ and, } \mathfrak{a} > 0, \\ \text{or, } 1 - 2\sigma_1 C_1 - \frac{2\sigma_1\lambda_1 C_1^2\beta_1(0)}{s_1} \geq 0, \end{cases} \tag{4.99}$$

are satisfied, then the origin of the model (4.97) *is globally asymptotically stable.*

Proof. First, let us define the two operators:

$$v^{\dagger}(x_{1t}, x_{2t}) = \int_{t-\tau_1}^{t}\int_{m}^{t} e^{-\delta(t-m-\tau_1)} g_1(m-\ell+\tau_1)\left[\beta_1(x_1(\ell))x_1(\ell) + \kappa x_2(\ell)D(\kappa x_2(\ell))\right] d\ell dm, \tag{4.100}$$

and

$$u^{\dagger}(x_{2t}) = \int_{t-\tau_2}^{t}\int_{m}^{t} e^{-\tilde{\delta}(t-m-\tau_2)} g_2(m-\ell+\tau_2)\beta_2(x_2(\ell))x_2(\ell) d\ell dm, \tag{4.101}$$

where δ and $\tilde{\delta}$ are two nonnegative constants. It follows that for all $t \geq 0$,

$$\begin{aligned} \dot{v}^{\dagger}(t) \leq & -\delta v^{\dagger}(x_{1t}, x_{2t}) - \int_{t-\tau_1}^{t} g_1(t-\ell)\left[\beta_1(x_1(\ell))x_1(\ell) + \kappa x_2(\ell)D(\kappa x_2(\ell))\right] d\ell \\ & + \left[\beta_1(x_1(t))x_1(t) + \kappa x_2(t)D(\kappa x_2(t))\right] e^{\delta\tau_1} C_1, \end{aligned} \tag{4.102}$$

and

$$\dot{u}^{\dagger}(t) = -\tilde{\delta}u^{\dagger}(x_{2t}) - \int_{t-\tau_2}^{t} g_2(t-\ell)\beta_2(x_2(\ell))x_2(\ell) d\ell + C_2 e^{\tilde{\delta}\tau_2}\beta_2(x_2(t))x_2(t). \tag{4.103}$$

We introduce for the system (4.97) the following functional:

$$V^{\dagger}(x_{1t}, x_{2t}) = x_2(t) + 2\lambda_2 u(x_{2t}) + 2\sigma_1 v^{\dagger}(x_{1t}, x_{2t}) + \frac{2\sigma_1 C_1\beta_1(0)}{s_1}\left[\underbrace{x_1(t) + 2\lambda_1 v^{\dagger}(x_{1t}, x_{2t})}_{U^{\dagger}(x_{1t}, x_{2t})}\right], \tag{4.104}$$

Throughout the proof of Theorem 10, we consider that $s_i > 0$ for all $i \in I_n$.

We start by computing the derivative of $U^{\dagger}(x_{1t},x_{2t}) = x_1(t) + 2\lambda_1 v^{\dagger}(x_{1t},x_{2t})$, along the trajectories of (4.97), and we get, for all $t \geq 0$,

$$\begin{aligned}
\dot{U}^{\dagger}(t) =& -\left[d_{r1} + \beta_1(x_1(t))\right] x_1(t) + 2\lambda_1 \int_{t-\tau_1}^{t} g_1(t-\ell)\left[\beta_1(x_1(\ell))x_1(\ell) + \kappa x_2(\ell) D(\kappa x_2(\ell))\right] d\ell \\
& - 2\lambda_1 \int_{t-\tau_1}^{t} g_1(t-\ell)\left[\beta_1(x_1(\ell))x_1(\ell) + \kappa x_2(\ell) D(\kappa x_2(\ell))\right] d\ell \\
& + 2\lambda_1 C_1 \left[\beta_1(x_1(t))x_1(t) + \kappa x_2(t) D(\kappa x_2(t))\right] \\
=& -\left[d_{r1} - \alpha_1\beta_1(x_1(t))\right] x_1(t) + 2\kappa\lambda_1 C_1 D\left(\kappa x_2(t)\right) x_2(t),
\end{aligned} \tag{4.105}$$

where we choose $\delta = 0$ for the sake of clarity. Next, using the fact that $\beta_1(x_1) \leq \beta_1(0)$ for all $x_1 \geq 0$, we deduce that since $s_1 = \delta_1 - \alpha_1\beta_1(0) > 0$, then it follows that,

$$\dot{U}^{\dagger}(t) \leq -s_1 x_1(t) + 2\kappa\lambda_1 C_1 D\left(\kappa x_2(t)\right) x_2(t). \tag{4.106}$$

Next, we observe that the derivative of $V^{\dagger}$, introduced in (4.104), along the trajectories of (4.97), is

$$\begin{aligned}
\dot{V}^{\dagger}(t) =& -\left[d_{r2} + \beta_2(x_2(t)) + \kappa D\left(\kappa x_2(t)\right)\right] x_2(t) + 2\lambda_2 \int_{t-\tau_2}^{t} g_2(t-\ell)\beta_2(x_2(\ell))x_2(\ell)d\ell + 2\lambda_2 C_2 \beta_2(x_2(t))x_2(t) \\
& + 2\sigma_1 \int_{t-\tau_1}^{t} g_1(t-\ell)\left[\beta_1(x_1(\ell))x_1(\ell) + \kappa x_2(\ell) D(\kappa x_2(\ell))\right] d\ell - 2\lambda_2 \int_{t-\tau_2}^{t} g_2(t-\ell)\beta_2(x_2(\ell))x_2(\ell)d\ell \\
& + 2\sigma_1 \left[\beta_1(x_1(t))x_1(t) + \kappa x_2(t) D(\kappa x_2(t))\right] C_1 - 2\sigma_1 \int_{t-\tau_1}^{t} g_1(t-\ell)\left[\beta_1(x_1(\ell))x_1(\ell) + \kappa x_2(\ell) D(\kappa x_2(\ell))\right] d\ell \\
& + \frac{2\sigma_1 C_1 \beta_1(0)}{s_1} \left(\underbrace{-\left[d_{r1} - \alpha_1\beta_1(x_1(t))\right] x_1(t) + 2\kappa\lambda_1 C_1 D\left(\kappa x_2(t)\right) x_2(t)}_{\dot{U}^{\dagger}(t)} \right).
\end{aligned}$$

Using the intermediate result (4.106), we deduce that for $\tilde{\delta} = 0$, the derivative of $V^{\dagger}$ satisfies for all $t \geq 0$,

$$\begin{aligned}
\dot{V}^{\dagger}(t) \leq& -\left[d_{r2} - \left(2\lambda_2 C_2 - 1\right)\beta_2(x_2(t))\right] x_2(t) + 2\sigma_1 \left[\beta_1(x_1(t))x_1(t) + \kappa x_2(t) D(\kappa x_2(t))\right] C_1 \\
& - \kappa x_2(t) D\left(\kappa x_2(t)\right) + \frac{2\sigma_1 C_1 \beta_1(0)}{s_1} \left[-s_1 x_1(t) + 2\kappa\lambda_1 C_1 D\left(\kappa x_2(t)\right) x_2(t)\right] \\
\leq& -s_2 x_2(t) - \left[1 - 2\sigma_1 C_1 - \frac{2\sigma_1\lambda_1 C_1^2 \beta_1(0)}{s_1}\right] \kappa D\left(\kappa x_2(t)\right) x_2(t) \\
& - 2\sigma_1 C_1 \left[\beta_1(0) - \beta_1(x_1(t))\right] x_1(t).
\end{aligned} \tag{4.107}$$

Consequently, from the last inequality in (4.107) we deduce what follows:

❍ **The case:** $1 - 2\sigma_1 C_1 - \frac{2\sigma_1\lambda_1 C_1^2 \beta_1(0)}{s_1} < 0$. Now, we recall that,

$$\mathfrak{a} = s_2 - \kappa\overline{D}\left[\frac{2\sigma_1\lambda_1 C_1^2 \beta_1(0)}{s_1} + 2\sigma_1 C_1 - 1\right], \tag{4.108}$$

and we deduce that if the condition $\mathfrak{a} > 0$ is satisfied, then $\dot{V}^{\dagger}(t)$ satisfies for all $t \geq 0$,

$$\dot{V}^{\dagger}(t) \leq -\mathfrak{a} x_2(t) - 2\sigma_1 C_1 \left[\beta_1(0) - \beta_1(x_1(t))\right] x_1(t). \tag{4.109}$$

By integrating the inequality (4.109) we get,

$$V^{\dagger}(t) \leq V^{\dagger}(0) - \mathfrak{a}\int_0^t x_2(m)dm - 2\sigma_1 C_1 \int_0^t \left[\beta_1(0) - \beta_1(x_1(m))\right] x_1(m)dm,$$

for all $t \geq 0$. Therefore, from the definition of $V^{\dagger}$ in (4.104), we deduce that x_1 is bounded by a constant $\bar{x}_1 > 0$. Consequently, since β_1 is decreasing, we get for all $t \geq 0$,

$$\dot{V}^{\dagger}(t) \leq -\mathfrak{a}x_2(t) - \mathfrak{b}x_1(t), \text{ where, } \mathfrak{b} = 2\sigma_1 C_1 \left[\beta_1(0) - \beta_1(\bar{x}_1)\right] > 0. \tag{4.110}$$

Thus, we conclude that the origin of the model (4.97) is globally asymptotically stable.

❍ **The case:** $1 - 2\sigma_1 C_1 - \frac{2\sigma_1 \lambda_1 C_1^2 \beta_1(0)}{s_1} \geq 0$. It follows from (4.107) that for all $t \geq 0$ the derivative of V satisfies:

$$\dot{V}^{\dagger}(t) \leq -s_2 x_2(t) - 2\sigma_1 C_1 \left[\beta_1(0) - \beta_1(x_1(t))\right] x_1(t). \tag{4.111}$$

One notices the similarities between (4.109) and (4.111). Therefore, arguing similarly as in the previous case, we easily prove that the origin of model (4.97) is globally asymptotically stable. □

Remark 27. *We recall, from Section 4.4, that or a model without dedifferentiation ($\kappa = 0$), the conditions $s_i > 0$ (equivalent to **Step 3** in Theorem 8), for all $i \in I_n$ are necessary and sufficient for global exponential stability of the origin of the corresponding system, and that anti-cancer therapy aims to satisfy the decay conditions that ensure that the origin is stable, in order to eradicate malignant cells. However, we can show that the model* (4.97) *may admit a positive steady state even if $s_i > 0$, for all $i \in I_n$, which is not the case when $\kappa = 0$. Therefore, we notice that the conditions $s_i > 0$, for all $i \in I_n$ are no longer sufficient to ensure that the 0-equilibrium is stable when dedifferentiation exists. In light of Theorem 10, we deduce that zero is stable if we guarantee that an upper-bound on κ is satisfied, i.e. if dedifferentiation does not cross the threshold defined by the condition $\mathfrak{a} > 0$ in* (4.99)*. Medical practice supports this observation ([142], [249]), as discussed in the sequel.*

4.8.4 Concluding remarks and numerical experiments

We consider the situation observed in [142, 249], where medical practice shows that cancer cells may survive to therapy by undergoing dedifferentiation.

A glimpse into the medical experience

In [142], some experiences have been conducted on human non-small cell lung cancer. Their results suggested that non-stem cancer cells which were targeted through radiotherapy, have protected themselves by dedifferentiation processes (CSCs are particularly resistant to radiotherapy, see for example [28, 70]). In [249], an ODE-model was proposed to fit the data of [142]. In a second time, the experience was renewed by adding some *survivin inhibitors* (known as *YM155*), that undermined dedifferentiation of cancer cells. The therapy efficacy was substantially improved when *YM155* was used along with radiotherapy [249, 142].

We check the qualitative behavior of our system through some situations that are reflective of those encountered in [142, 249]. For that purpose, we consider for instance the cell division probability densities of the forms $f_i(a) = \frac{m_i}{e^{m_i\tau_i}-1}e^{m_i a}$, with $m_i > 0$, $i \in I_n$, along with the following functions and parameters:

	$\beta_i(x_i)$	$f_i(a)$	d_{ri}	λ_i	τ_i	d_{pi}
$i=1$	$\frac{1.11}{1+x_1^2}$	$\frac{10e^{10a}}{e^{10\tau_1}-1}$	0.112	0.7	1.19	0.27
$i=2$	$\frac{1.4}{1+x_2^4}$	$\frac{10e^{10a}}{e^{10\tau_2}-1}$	0.37	0.9	1.32	0.33

After simple calculations, we get: $s_1 = 0.0518$ and $s_2 = 0.2218$. Therefore, in the case where dedifferentiation does not exist (i.e. $\kappa = 0$), the origin of the studied model is globally exponentially stable [81, 8], as illustrated in Figure 4.16-(a). Next, let us assume that at $t = 20$ days, the dedifferentiation mechanism is triggered (by setting $\kappa = 0.8$ at $t = 20$ days). In that case, we still have $s_1 > 0$ and $s_2 > 0$, but, however, we note that the sufficient stability conditions (4.99), in Theorem 10, are not satisfied:

$$1 - 2\sigma_1 C_1 - \frac{2\sigma_1\lambda_1 C_1^2\beta_1(0)}{s_1} = -4.45, \tag{4.112}$$

and,

$$\mathfrak{a} = s_2 - \kappa\overline{D}\left[\frac{2\sigma_1\lambda_1 C_1^2\beta_1(0)}{s_1} + 2\sigma_1 C_1 - 1\right] = -3.33. \tag{4.113}$$

In simulation, we observe that for some initial conditions, the origin of the system (4.97) is not asymptotically stable, as illustrated in Figure 4.16-(b). More importantly, we can see/prove that the trajectories converge in this case to a strictly positive steady state, given by $x_1^* = 1.47$ and $x_2^* = 0.66$, that exists even if $s_i > 0$ (contrary to the case $\kappa = 0$, where zero is the unique steady state). In addition, we can determine the gain of the dedifferentiation function, which converges to $\kappa D(\kappa x_2^*) = 0.12$, when the trajectories of the system (4.97) approach the positive steady state. Thus, in this example, the unhealthy cells prevent themselves from total extinction thanks to their dedifferentiation ability (Figure 4.16 (a)-(b)).

Finally, we notice in Figure 4.16-(c) that for some sufficiently small initial conditions and $\kappa = 0.8$, the dedifferentiation process is not sufficient to avoid the total cell eradication.

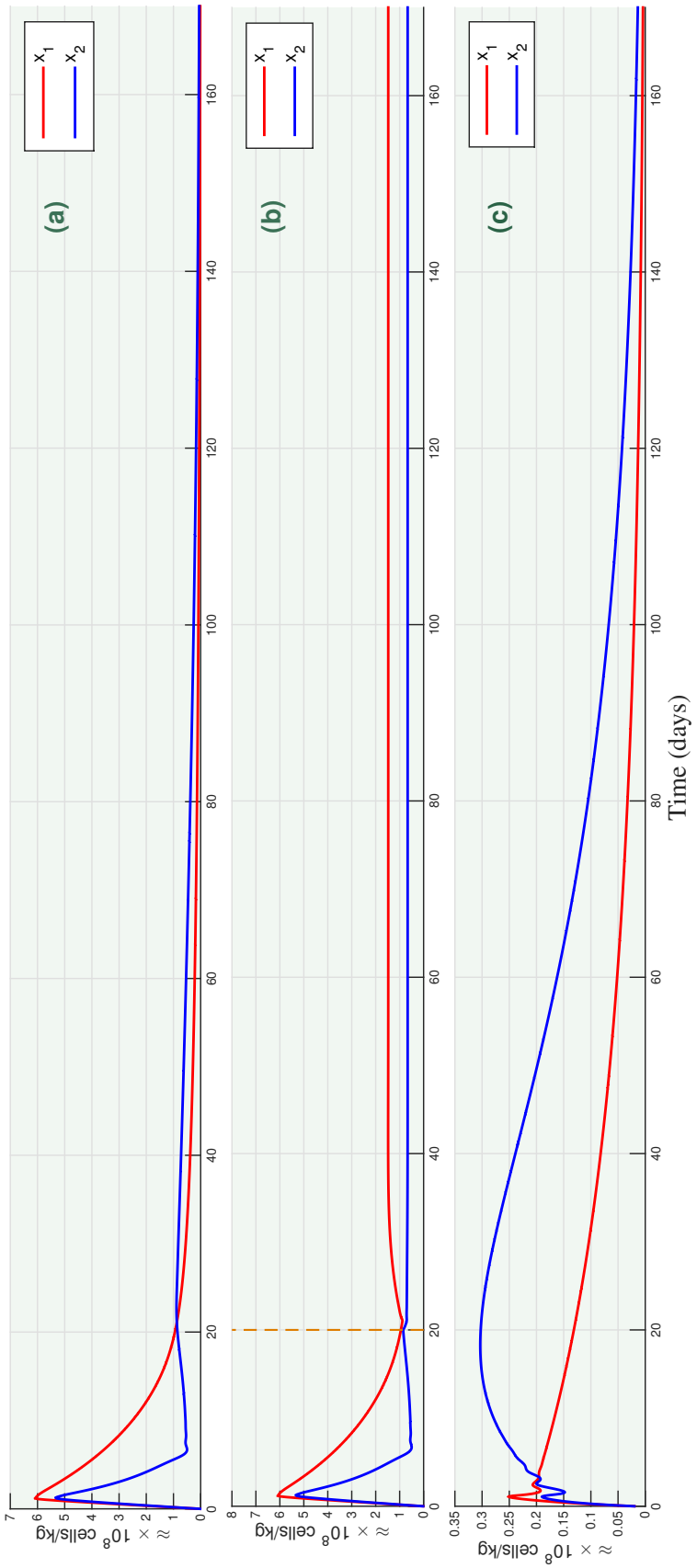

Fig. 4.16 In **(a)**, $\kappa = 0$, for all $t \geq 0$, and $s_i > 0$. The trajectories converge to zero. In **(b)** and **(c)** the dedifferentiation process is trigerred at $t = 20$. In **(b)**, the trajectories do not converge to zero (they converge to a small positive steady state), which means that dedifferentiation prevents cells from total extinction. This observation supports the hypothesis claiming that cancer cells protect themselves through dedifferentiation during anti-cancer therapy. We suggest that therapeutics should take into account cell plasticity features, by including drugs that target dedifferentiation mechanisms, in order to satisfy the conditions in Theorem 10 and therefore avoid the case **(b)**. Otherwise, malignant cells may regenerate themselves after therapy. In **(c)**, dedifferentiation is also triggered at $t = 20$, but this time, we consider that the initial mutated subpopulation κx_j is small. In this case, dedifferentiation is ineffective in ensuring unhealthy cell survival (mutated cells disapear over time without creating an agressive cancer).

4.9 Conclusion

Let us recall the key points discussed/analyzed throughout this chapter:

❶ A network of regulatory proteins monitor the progression of cells in the cycle at specific checkpoints, and some damaged cells may be arrested in G_1 or G_2 [92]. The cell cycle arrest may also be induced by chemotherapy, and some hypothesis are advanced to link the cell-cycle arrest with cancer dormancy.

❷ Different modeling trends have been used to represent the cell cycle. Some of them combine G_0 and the proliferating phase in a unique model with infinite duration, while other models include a separated G_0 phase along with a limited/finite proliferating cycle (with or without subdividing the proliferating phase).

❸ We reconcile some of the early modeling methodologies by taking into account a separated proliferating compartment of infinite support, in order to include a possible cell arrest, in G_1 or G_2, for a minority of cells during their cycle.

❹ The resulting model studied in the first part of the chapter is a nonlinear system with infinite distributed delays and time-varying parameters. We generalize the stability results of [8, 9], and particularly the LKF constructions provided in the previous chapter, to analyze the model of interest.

❺ In a second time, we emphasized cell-plasticity features. We introduced a general model for cell population dynamics involving several dedifferentiation and transdifferentiation (general) functions. Then, in order to allow analysis, we derived from the general description, a model (with explicit cell-plasticity functions) for the typical situation where a portion (or, a mutated subpopulation) of any generation of differentiated progenitor cells[4] regresses into an hematopoietic SC proliferating state.

❼ Since anti-cancer therapy aims to eradicate all the malignant cancer cells, we investigated the stability properties of the origin of the unhealthy model involving cancer cell dedifferentiation. In this case, we derived a study for a simpler model involving two maturity stages and a dedifferentiation function from progeny to SCs. We also checked the qualitative behavior of the model and we compared it to some medical observations that claim that cancer cells protect themselves through dedifferentiation during anti-cancer therapy.

Much remain to be done in the study of the concepts discussed throughout this chapter. Particularly the analysis and the interpretation (possibly related to dormancy?) of the positive steady state that occurs in the model involving dedifferentiation, when the stability conditions of the origin in the model without dedifferentiation, are satisfied (i.e. Section 4.8.4, Figure 4.16-**(b)**).

[4] Belonging for instance, to a specific blood lineage hierarchy as illustrated in Figure 4.13-blue hierarchy.

Part II

The class of coupled differential-difference systems

Chapter 5

Analysis of a differential-difference model through Lyapunov-like functionals design

Synopsis. **This is an introductory work which opens up the analysis of a class of hematopoietic systems, described by some differential-difference (or, more generally, *descriptor*) systems. In fact, our study is conducted on a model of stem cell population dynamics, recently introduced in the literature ([4]), that admits two equilibrium points: zero, and, under some conditions on the biological parameters, a strictly positive steady state. The latter one seems biologically more relevant ([4]).**

We revisit the stability properties of the 0-equilibrium by extending the Lyapunov construction of [4], in order to establish global exponential stability of the trajectories with an estimate on their rate of convergence.

For the strictly positive steady state, the available analysis in [4] is local, based on the frequency analysis of the characteristic equation associated to the linear approximation of the model. Here we discuss the nonlinear analysis of the positive steady state, in the time-domain framework, going through Lyapunov-like functionals of two types. Firstly, we test an adaptation of a method recently developed for the analysis of quasi-linear time-varying systems via *Comparative* and *Positive Systems* ([196]). Based on the techniques of [196], [124], [206], we get the advantage of deriving decay conditions for non-positive trajectories of the studied model, through a linear degenerate Lyapunov-like functional. The second approach that we use for the positive steady state is more classical, since it is based on the computation of the derivative of a quadratic functional along the non-positive trajectories of the shifted model whose origin is the strictly positive steady state of the initial system. Thus, sufficient conditions for regional exponential stability, an estimate of the decay-rate of the solutions, and a subset of the basin of attraction of the positive steady state, are then provided. We discuss the complementarity of both approaches and their limits throughout the chapter.

5.1 Overview of the chapter

A relevant model has been recently introduced in [8], improving the pioneering model proposed by Mackey in [180]. The work presented in this chapter is based on this new model, where fast self-renewing dynamics of hematopoietic stem cells is envisaged. In fact, this description takes into account a sub-population of cells that remains constantly active in the proliferating compartment.

In this chapter, we highlight the positive system approach as an effective way to establish stability results for nonlinear time-delay systems. The hematopoietic model that we are interested in can be put in the form of a differential-difference systems, that can admit two steady states: the 0-equilibrium which always exists, and a unique strictly positive steady state that may exist under some conditions on the biological parameters. The model of interest is briefly given in Section 5.2 (the interested reader is invited to refer to the original work [4] for more details). It has been proven through a Lyapunov functional that the origin is globally asymptotically stable if it is the unique equilibrium of the model. In Section 5.3, we are using a slightly different Lyapunov approach to extend the stability known results and thus establish global exponential stability of the origin, with an estimate of the decay rate of solutions. We recall that the positivity of the trajectories of the studied model is an asset that makes possible the analysis through linear Lyapunov functionals [124].

Clearly, linear functions are more convenient for the analysis of positive systems, particularly when time-delay is involved ([36], [216], [97], [124], [122], [50], [176], [215]), since it avoids painful computations which goes along with the use, for instance, of quadratic-type functions. Notice that, sometimes, the suitable quadratic functions are difficult to construct, while linear ones are readily available. This general observation motivates in fact the axis of fundamental search that aims to develop new ways to establish stability of non-positive systems, using the tools available for positive ones (see the recent works [196], [86], [190], [216], [51], [206], [136]). Similar techniques and applications are widely used for the construction of interval observers, as in [90], [89], [191], [245], [193], [118], and [207].

In light of the above mentioned remarks, the question arose as to whether it was possible to define a framework to study the stability properties of the strictly positive equilibrium point using a simple linear (i.e. non quadratic) Lyapunov functionals. We recall that initially the studied model is positive. However, the trajectories are no longer monotone when it comes to study the shifted version of the model (whose origin is the positive steady state of the initial one). Therefore, the first step that we perform in Section 5.4.1.1 is the determination of a linear *Comparative System* ([250]). The origin of the latter obtained system has the particularity of being globally exponentially stable if it is exponentially stable on only the positive orthant ([196]). Consequently, in Sections 5.4.1.2 and 5.4.1.3, global decay conditions are derived via the construction of a suitable linear functional. Exploitation of that study in the case of our hematopoietic system, together with the feasibility of the global results, are discussed through numerical applications in Section 5.4.1.4.

Finally, in Section 5.4.2, a more classical study, which is based on the direct analysis of the *non-positive* system through a quadratic Lyapunov-like construction, is established. Through this approach, sufficient conditions for the regional exponential stability are provided, and a subset of the basin of attraction is formulated in terms of a sub-level of the Lyapunov-like functional. Roughly speaking - and apart from the conservatism that characterizes Lyapunov methods - we can say that both studies that will

be presented for the strictly positive steady state appear to be complementary; in the sense that the former one provides sufficient conditions that are more likely to be satisfied for large state values (see Section 5.4.1.4), while the second approach gives local results, as summarized in Section 5.5.

5.2 Model presentation

The resulting model of interest is a nonlinear differential-difference system, whose piecewise-continuous trajectories can be bounded or unbounded [4]. Some tools making possible to construct Lyapunov functionals for some general nonlinear differential-difference equations are available (see, [233], [152], [121], and the references therein). Notice also that one may rewrite the model equations in the neutral time-delay framework, in order to take advantage from the existing literature devoted to this field (see [194, 104]). Even if an equilibrium is known to be asymptotically stable, we still need some explicit strict Lyapunov functionals for the multiple advantage that they offer (e.g. to establish some robustness results [218, 187]). Besides the difficulties related to the construction of suitable functionals for nonlinear time-delay systems, it is generally more difficult to prove stability when trajectories are not uniformly continuous [203], since Barbalat's lemma requires uniform continuity of solutions. In fact, almost all the issues related to stability and robustness can be addressed when a strict Lyapunov functional for the corresponding system is known.

In light of previous comments, we focus in this chapter on different Lyapunov-based analysis techniques, by developing a study dedicated to the delay differential-difference model of hematopoiesis of interest. In particular, for the strictly positive steady state, two ways to prove stability of the nonlinear system are investigated, thereby completing the linear frequency-domain analysis performed in [4]. The reader is invited to refer to Sections 1-3 in [4] for the complete presentation of the biological model in Figure 5.1. Here we give its differential-difference version of interest:

$$\left\{\begin{array}{rcl} \dot{x}(t) & = & -\big(\delta+\beta(x(t))\big)x(t)+2Le^{-\gamma\tau}u(t-\tau), \\ u(t) & = & \beta(x(t))x(t)+2Ke^{-\gamma\tau}u(t-\tau),\ \ t>0, \end{array}\right. \tag{5.1}$$

where we consider that the parameters δ, K, $L=1-K$, γ and τ are strictly positive real numbers and $K\in(0,1)$. x represents the total density of resting cells and u is the density of the new proliferating cells. As usual, the function β is continuous, decreasing and $\lim_{x\to\infty}\beta(x)=0$ ([180]). A unique piecewise continuous solution $(x(t),u(t))$ exists for all $t\geq 0$, when the system (6.8) is associated with the initial conditions $x(0)\in\mathbb{R}$ and $\varphi_u\in PC\big([-\tau,0],\mathbb{R}\big)$, (see [121]). Throughout this work, we assume that the solutions are piecewise continuous. Moreover, system (6.8) is positive, i.e. the solutions of system (6.8) associated with positive initial conditions $x(0)\in\mathbb{R}^+$ and $\varphi_u\in PC\big([-\tau,0],\mathbb{R}^+\big)$, are positive. Here, we consider only the positive solutions of (6.8).

We consider that β is the Hill function of Mackey's models, i.e.,

$$\beta(x)=\frac{\beta(0)}{1+bx^n} \tag{5.2}$$

where b, $\beta(0)$ are strictly positive real numbers, and, $n\geq 2$. To ease the notation, we define the following

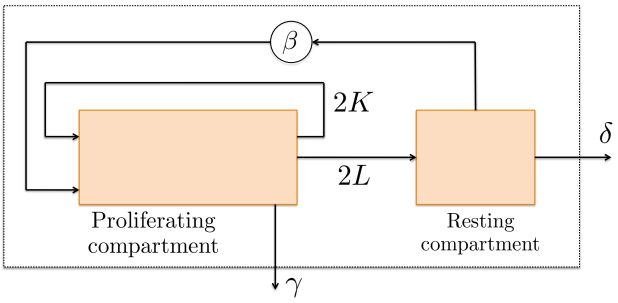

Fig. 5.1 Schematic representation of blood cells formation.

constants:

$$\overline{K} = \frac{1}{2}e^{\gamma\tau}, \tag{5.3}$$

$$\mu = \frac{\beta(0)}{\delta}, \tag{5.4}$$

$$\underline{K} = (\mu+1)\overline{K} - \mu. \tag{5.5}$$

Notice that $\overline{K}$ and μ are strictly positive. Finally, we prove for later use the following result:

Lemma 1. *The positive solution $\varpi(t)$, for all $t \geq 0$, of the perturbed scalar difference equation*

$$\varpi(t) = \xi^{\dagger}(t) + \upsilon\varpi(t-h),\ \ \xi^{\dagger}(t) \geq 0,\ \ \forall t \geq 0, \tag{5.6}$$

associated with a piecewise-continuous positive initial function $\varpi(t) = \varphi(t)$, for $t \in [-h, 0]$, $h > 0$, converges exponentially to zero if: ***(i)*** *the perturbation $\xi^{\dagger}(t)$ vanishes exponentially to zero, when $t \to \infty$, and,* ***(ii)*** *$\upsilon \in (0,1)$.*

Proof. From **(i)** it follows that there exist $\kappa_1 > 0$ and $\kappa_2 > 0$, such that, $\xi^{\dagger}(t) \leq \kappa_1 e^{-\kappa_2 t}$, for all $t \geq 0$. Let us denote $\rho(t) = \kappa_1 e^{-\kappa_2 t}$, for all $t \geq 0$. We notice that:

$$\rho(t) = e^{-\kappa_2 h}\kappa_1 e^{\kappa_2(t-h)} = \kappa_3\rho(t-h),\ \ \text{where}\ \ \kappa_3 \in (0,1)\,. \tag{5.7}$$

Therefore, from (5.6) we obtain:

$$\varpi(t) \leq \kappa_3\rho(t-h) + \upsilon\varpi(t-h),\ \ \text{where},\ \ \kappa_3 \in (0,1)\,,\ \ \text{and},\ \ \upsilon \in (0,1)\,. \tag{5.8}$$

Let us assume that $\upsilon > \kappa_3$, without loss of generality[1]. Now, we introduce the positive constant $\kappa_4 = \frac{\kappa_3}{\upsilon - \kappa_3}$, and we deduce that:

$$\begin{aligned} \varpi(t) + \kappa_4\rho(t) \leq & \upsilon\varpi(t-h) + \kappa_3(1+\kappa_4)\rho(t-h) \\ = & \upsilon\left[\varpi(t-h) + \kappa_4\rho(t-h)\right]. \end{aligned} \tag{5.9}$$

Since $\upsilon \in (0,1)$, we conclude that $\varpi(t)$ converges exponentially to zero. □

[1] Otherwise, if $\kappa_3 > \upsilon$, we observe that there always exists $\tilde{\upsilon} \in (\kappa_3, 1)$, such that $\varpi(t) \leq \kappa_3\rho(t-h) + \tilde{\upsilon}\varpi(t-h)$, typically we select $\tilde{\upsilon} = \frac{1-\kappa_3}{2}$. The remainder of the proof does not change, considering this time $\tilde{\upsilon}$ instead of υ.

Now we are ready to investigate the stability properties of the model (6.8), starting with its trivial steady state, and then its positive steady state.

5.3 Stability analysis of the 0-equilibrium

We revisit the 0-equilibrium $E^0 = (0,0)$ stability analysis provided in [4], by proving its global exponential stability. Non-attractivity of E^0 when its stability condition is not satisfied can also be deduced from the Lyapunov functional. The expression of the functional introduced here is slightly different from the one used in [4], and here we prove exponential stability, with an estimate of the rate of convergence of the solutions.

Theorem 11. *For all*

$$K \in \left(0, \overline{K}\right), \tag{5.10}$$

i) if the condition

$$s := \underline{K} - K > 0, \tag{5.11}$$

is satisfied, the origin of the system (6.8) *is globally exponentially stable.*
ii) if

$$s := \underline{K} - K < 0, \tag{5.12}$$

then no positive trajectory converges to the origin of system (6.8).

Remark 28. *In fact, when the condition* (5.11) *is satisfied, the origin is the unique equilibrium point of system* (6.8). *This explains why the stability results in Theorem 11 can be global.*

Proof. Firstly, we use the following functional:

$$\mathscr{M}\left(x(t), u_t\right) = x(t) + \left(\frac{\mu+1}{\mu} + \varepsilon\right) \int_{t-\tau}^{t} u(\ell) d\ell, \tag{5.13}$$

where,

$$\varepsilon = -\frac{s}{2(\overline{K} - K)\mu}. \tag{5.14}$$

Notice that, since $K \in (0, \overline{K})$, then $\varepsilon < 0$ when (5.11) is satisfied and $\varepsilon > 0$ when (5.12) holds.

We start by proving **ii).** Let us proceed by contradiction. We assume that the condition (5.12) is satisfied and a positive solution $(x(t), u(t))$ converges to the origin.

Since $\varepsilon > 0$, the functional $\mathscr{M}$ is positive on the positive orthant. Moreover, its derivative along the trajectories of (6.8) is

$$\begin{aligned} \dot{\mathscr{M}}(t) = &\left[-\delta + \left(\frac{\mu+1}{\mu} + \varepsilon - 1\right)\beta(x(t))\right] x(t) \\ &+ \left[-\frac{\mu+1}{\mu} - \varepsilon + \left(\frac{\mu+1}{\mu} + \varepsilon\right)\frac{K}{\overline{K}} + \frac{1-K}{\overline{K}}\right] u(t-\tau). \end{aligned} \tag{5.15}$$

On the other hand, from (5.4), we notice that

$$-\delta+\left(\frac{\mu+1}{\mu}+\varepsilon-1\right)\beta(0)=\varepsilon\beta(0)>0. \tag{5.16}$$

Since $x(t)$ converges to zero, and β is continuous and decreasing, we conclude that there exists a time instant $t_1>0$, such that for all $t\geq t_1$,

$$-\delta+\left(\frac{\mu+1}{\mu}+\varepsilon-1\right)\beta(x(t))\geq\frac{\varepsilon\beta(0)}{2}>0. \tag{5.17}$$

It follows from (5.15) and (5.17) that for all $t\geq t_1$,

$$\dot{\mathscr{M}}(t)\geq\frac{\varepsilon\beta(0)}{2}x(t)+\frac{1}{\mu\overline{K}}\Big[-(\mu+1)\overline{K}+\mu+K+\varepsilon\mu(K-\overline{K})\Big]u(t-\tau).$$

Since $s=(\mu+1)\overline{K}-\mu-K$, the previous inequality rewrites as

$$\begin{aligned}\dot{\mathscr{M}}(t)\geq&\frac{\varepsilon\beta(0)}{2}x(t)+\frac{1}{\mu\overline{K}}\left[-s+\varepsilon\mu(K-\overline{K})\right]u(t-\tau)\\=&\frac{\varepsilon\beta(0)}{2}x(t)-\frac{s}{2\mu\overline{K}}u(t-\tau),\end{aligned}$$

where the last equality is a consequence of (5.14). Since $s<0$ and $\varepsilon>0$, we conclude that for all $t\geq t_1$, $\dot{\mathscr{M}}(t)\geq 0$. It follows that

$$\mathscr{M}(x(t),u_t)\geq\mathscr{M}(x(t_1),u_{t_1})>0. \tag{5.18}$$

Therefore, $\mathscr{M}$ does not converge to zero when t goes to $+\infty$. On the other hand, $\mathscr{M}$ converges to zero since $\big(x(t),u(t)\big)$ converges to the origin. This yields a contradiction.

Next, let us prove **i).** We consider the case where the inequality (5.11) is satisfied. An immediate consequence is that $\varepsilon<0$. First, to ensure that the functional $\mathscr{M}$ is positive on the positive orthant, let us check that $\frac{\mu+1}{\mu}+\varepsilon>0$. From the definitions of ε and s, we get

$$\frac{\mu+1}{\mu}+\varepsilon=\frac{2\left[(\mu+1)\overline{K}-\mu K\right]-2K-s}{2(\overline{K}-K)\mu}. \tag{5.19}$$

Since $K\in(0,1)$, we deduce that

$$(\mu+1)\overline{K}-\mu K>(\mu+1)\overline{K}-\mu=\underline{K}.$$

It follows that

$$\frac{\mu+1}{\mu}+\varepsilon>\frac{2(\underline{K}-K)-s}{2(\overline{K}-K)\mu}=\frac{s}{2(\overline{K}-K)\mu}>0. \tag{5.20}$$

Consequently, the functional $\mathscr{M}$ is nonnegative. Moreover, its derivative along the trajectories of (6.8) satisfies

$$\begin{aligned}\dot{\mathscr{M}}(t) &= \left[-\delta + \left(\frac{\mu+1}{\mu} + \varepsilon - 1\right)\beta(x(t))\right]x(t) - \frac{s}{2\mu\overline{K}}u(t-\tau) \\ &\leq \left[-\delta + \left(\frac{\mu+1}{\mu} - 1\right)\beta(0)\right]x(t) + \varepsilon\beta(x(t))x(t) - \frac{s}{2\mu\overline{K}}u(t-\tau) \\ &= \varepsilon\beta(x(t))x(t) - \frac{s}{2\mu\overline{K}}u(t-\tau),\end{aligned} \tag{5.21}$$

where the last equality is a consequence of (5.4). By integrating (5.21), we get, for all $t \geq 0$,

$$\mathscr{M}(x(t), u_t) \leq \mathscr{M}(x(0), \varphi_u) + \varepsilon \int_0^t \beta(x(m))x(m)dm - \frac{s}{2\mu\overline{K}}\int_0^t u(m-\tau)dm. \tag{5.22}$$

Since $\varepsilon < 0$ and $s > 0$, it follows from (5.13) and (5.22) that for all $t \geq 0$, the trajectory $x(t)$ is upper bounded by a strictly positive constant x_b.

In order to complete the proof, let us introduce the following functional:

$$\mathscr{W}\left(x(t), u_t\right) = \mathscr{M}\left(x(t), u_t\right) - \psi\int_{t-\tau}^t u(\ell)d\ell + \tilde{\psi}\int_{t-\tau}^t\int_m^t e^{\ell-t}u(\ell)d\ell dm, \tag{5.23}$$

where ψ and $\tilde{\psi}$ are positive real numbers to be selected later. From (5.20), observe that if we choose

$$\psi = \min\left\{\frac{s}{4(\overline{K}-K)\mu}, \frac{s}{2\mu\overline{K}}\right\}, \tag{5.24}$$

then the functional $\mathscr{W}$ is nonnegative and its derivative along the trajectories of (6.8) is:

$$\dot{\mathscr{W}}(t) = \dot{\mathscr{M}}(t) - \psi\left[u(t) - u(t-\tau)\right] + \tilde{\psi}\left[-\int_{t-\tau}^t e^{\ell-t}u(\ell)d\ell + \tau u(t)\right] - \tilde{\psi}\int_{t-\tau}^t\int_m^t e^{\ell-t}u(\ell)d\ell dm.$$

By selecting $\tilde{\psi} = \frac{\psi}{\tau}$, we obtain

$$\begin{aligned}\dot{\mathscr{W}}(t) &= \dot{\mathscr{M}}(t) + \psi u(t-\tau) - \tilde{\psi}\int_{t-\tau}^t e^{\ell-t}u(\ell)d\ell - \tilde{\psi}\int_{t-\tau}^t\int_m^t e^{\ell-t}u(\ell)d\ell dm \\ &\leq \dot{\mathscr{M}}(t) + \psi u(t-\tau) - \tilde{\psi}e^{-\tau}\int_{t-\tau}^t u(\ell)d\ell - \tilde{\psi}\int_{t-\tau}^t\int_m^t e^{\ell-t}u(\ell)d\ell dm.\end{aligned} \tag{5.25}$$

Then from (5.21) and (5.25), we deduce that

$$\begin{aligned}\dot{\mathscr{W}}(t) &\leq \varepsilon\beta(x(t))x(t) - \left[\frac{s}{2\mu\overline{K}} - \psi\right]u(t-\tau) - \tilde{\psi}e^{-\tau}\int_{t-\tau}^t u(\ell)d\ell - \tilde{\psi}\int_{t-\tau}^t\int_m^t e^{l-t}u(\ell)d\ell dm \\ &\leq \varepsilon\beta(x(t))x(t) - \tilde{\psi}e^{-\tau}\int_{t-\tau}^t u(\ell)d\ell - \tilde{\psi}\int_{t-\tau}^t\int_m^t e^{\ell-t}u(\ell)d\ell dm,\end{aligned} \tag{5.26}$$

where the last inequality is a consequence of (5.24). Therefore, by combining the facts that $\varepsilon < 0$, β is a continuous decreasing function and $x(t)$ is upper bounded by $x_b > 0$, for all $t \geq 0$, we deduce that

$$\dot{\mathscr{W}}(t) \leq \varepsilon\beta(x_b)x(t) - \tilde{\psi}e^{-\tau}\int_{t-\tau}^{t} u(\ell)d\ell - \tilde{\psi}\int_{t-\tau}^{t}\int_{m}^{t} e^{l-t}u(\ell)d\ell dm. \tag{5.27}$$

Finally, we conclude that there exists a strictly positive $\tilde{s}$, such that

$$\dot{\mathscr{W}}(t) \leq -\tilde{s}\mathscr{W}\left(x(t), u_t\right). \tag{5.28}$$

We deduce that,

$$\mathscr{W}\left(x(t), u_t\right) \leq e^{-\tilde{s}t}\mathscr{W}\left(x(0), \varphi_u\right), \tag{5.29}$$

for all $t \geq 0$. Therefore,

$$x(t) \leq e^{-\tilde{s}t}\mathscr{W}\left(x(0), \varphi_u\right), \tag{5.30}$$

for all $t \geq 0$. It follows that x converges exponentially to zero. Consequently, using Lemma 1, we notice form the second equation in (6.8), that u converges exponentially to zero, since the condition (5.10) implies that $2Ke^{-\gamma\tau} < 1$. □

Remark 29. *Theorem 11 gives a necessary and sufficient condition for the exponential stability of the trivial steady state when $K \in \left(0, \overline{K}\right)$ (Eq.* (5.10)*). In the case where $\overline{K} \geq 1$, it follows that Theorem 11 can be used to address the stability of the system for all the possible K values, i.e. for all $K \in (0,1)$. However, we notice that if $\overline{K} < 1$, then the conditions* (5.11) *and* (5.12) *give stability/instability conditions only for $K \in (0, \overline{K})$. In order to complete the analysis (i.e. to establish the stability conditions for all the possible K values), we show that if $\overline{K} \leq 1$, then no positive trajectory converges to the origin for all $K \in (\overline{K}, 1)$, by similar arguments as in ii) in Theorem 11. For that, we can consider the functional $\mathscr{M}$, defined in* (5.15) *where now ε is in fact any strictly positive constant. Moreover, notice that $K > \overline{K}$ implies that $2Ke^{-\gamma\tau} > 1$. Therefore, using the second equation in* (6.8)*, one notices that in this case system* (6.8) *has unbounded solutions (see [4]).*

Example 7. *Let us define the following biological parameters:*

$\beta(x)$	γ	τ	δ	K
$\frac{\beta(0)}{1+x^3}$	0.4	1	1	0.2

Case 1: Let us select $\beta(0) = 2$. It follows that $\underline{K} = 0.2377$. and $s = 0.0377$. Then, according to Theorem 11, the origin $E^0 = (0,0)$ is the unique equilibrium point and it is globally exponentially stable.

Case 2: Now we assume that $\beta(0) = 4$. After simple calculations we find that $s = -0.4704$. We deduce, according to Theorem 11, that the origin $E^0 = (0,0)$ is not attractive.

In fact, this system has a stable strictly positive steady state $E = (x_e, u_e)$, where $x_e = 0.9516$ and $\tilde{u}_e = 2.7936$, that seems asymptotically stable. In fact, the system illustrated in Case. 2 (Figure 5.3) provides an opening example for the study of the positive steady state in the sequel.

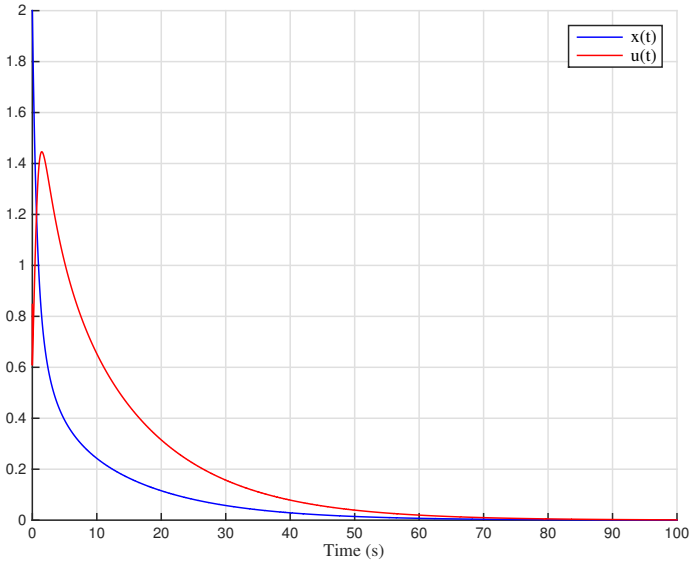

Fig. 5.2 The trajectories $x(t)$ and $u(t)$ for the parameters in Case 1.

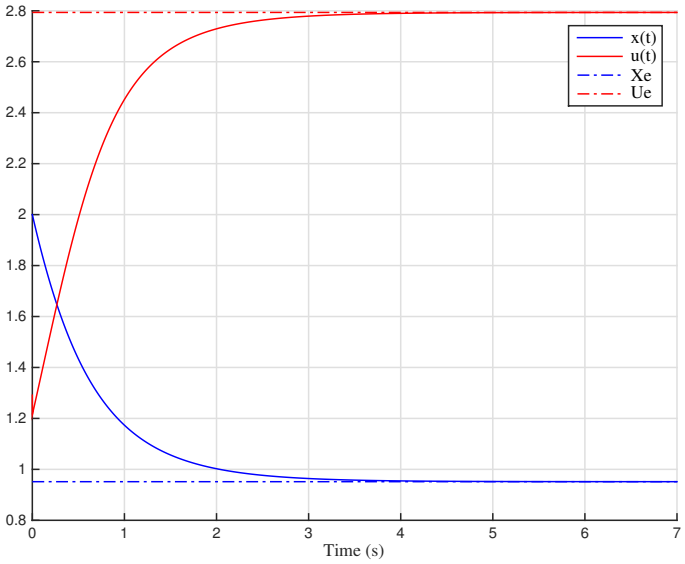

Fig. 5.3 The trajectories $x(t)$ and $u(t)$ for the parameters in Case 2.

5.4 Analysis of the positive steady state

Contrary to the trivial equilibrium $E^0 = (0,0)$ studied in the previous part, the strictly positive steady state $E = (x_e, u_e)$, where $x_e > 0$ and $u_e > 0$, does not always exist. In this section, first, we recall from [4] the conditions for its existence, then we investigate its stability properties by two Lyapunov-based approaches. The first one is inspired from [196] and uses the notions of *Comparative Systems* [250] and

linear Lyapunov-like functionals ([124], [122]). On the other hand, the second analysis is more classical, since it is performed through quadratic functionals directly defined along the model trajectories.

It is worth mentioning that in order to analyze the stability of the positive equilibrium, the authors in [4] developed a method which consists in writing the model (6.8) as a special case of a neutral differential system, then they investigated the local stability properties of the linear approximation of the neutral system by a frequency approach. The latter procedure assumes continuity of the solutions and provides a local result on the linear approximation. The results that we discuss here are complementary with those already provided, since we focus on the nonlinear behavior.

Existence of a strictly positive equilibrium point

If a positive equilibrium $E = (x_e, u_e)$ exists, then it satisfies:

$$\begin{cases} (\delta + \beta(x_e))x_e = 2Le^{-\gamma\tau}u_e, \\ \beta(x_e)x_e = (1 - 2Ke^{\gamma\tau})u_e. \end{cases} \tag{5.31}$$

From the second equation in (5.31), it follows that

$$u_e = \frac{\overline{K}}{\overline{K} - K}\beta(x_e)x_e. \tag{5.32}$$

From the previous equation, observe that the existence of E implies that necessarily $K < \overline{K}$. By substituting u_e in the first equation in (5.31), and since x_e is not zero, we get

$$\left(\frac{1 - \overline{K}}{\overline{K} - K}\right)\beta(x_e) = \delta.$$

Since $\delta > 0$ and $K < \overline{K}$, we deduce that

$$\overline{K} < 1. \tag{5.33}$$

Since β is continuous, decreasing and $\lim_{a\to\infty}\beta(a) = 0$, it follows from (5.32) that the existence and uniqueness of E are guaranteed by

$$\frac{1 - \overline{K}}{\overline{K} - K} > \frac{1}{\mu}.$$

Since $1 - \overline{K} > 0$, $\overline{K} - K > 0$ and $\underline{K} = (\mu + 1)\overline{K} - \mu$, the previous inequality is equivalent to

$$\underline{K} < K. \tag{5.34}$$

We conclude that the condition $K \in (\underline{K}, \overline{K})$ is necessary for the existence of E. This statement justifies what we have mentioned in Remark 1. We can easily check that if (5.33) holds, then $\underline{K} < \overline{K}$, and consequently E may exist. Next, since $\underline{K}$ may be positive or negative, and using the fact that $K > 0$, we conclude that we have proved the following:

Proposition 4. *A unique strictly positive steady state $E = (x_e, u_e)$ exists if and only if the conditions:*

$$0 < K < \overline{K} < \frac{\mu}{\mu + 1}, \tag{5.35}$$

or,

$$0 < \underline{K} < K < \overline{K} < 1, \tag{5.36}$$

are satisfied.

Remark 30. *In the previous statement, the uniqueness concerns the existence of the positive equilibrium E. We recall that the 0-equilibrium of system* (6.8) *always exists.*

A new representation of the system

In the sequel, we assume that the positive equilibrium E exists. First, the changes of coordinates, $\tilde{x} = x - x_e$ and $\tilde{u} = u - u_e$, give

$$\begin{cases} \dot{\tilde{x}}(t) = & -\big(\delta + \beta(\tilde{x}(t) + x_e)\big)(\tilde{x}(t) + x_e) + 2Le^{-\gamma\tau}(\tilde{u}(t-\tau) + u_e), \\ \tilde{u}(t) = & -u_e + \beta(\tilde{x}(t) + x_e)(\tilde{x}(t) + x_e) + 2Ke^{-\gamma\tau}(\tilde{u}(t-\tau) + u_e), \ \ t > 0, \end{cases} \tag{5.37}$$

or, equivalently,

$$\begin{cases} \dot{\tilde{x}}(t) = & -\delta\tilde{x}(t) - \beta(\tilde{x}(t) + x_e)(\tilde{x}(t) + x_e) + 2Le^{-\gamma\tau}\tilde{u}(t-\tau) - \delta x_e + 2Le^{-\gamma\tau}u_e, \\ \tilde{u}(t) = & \beta(\tilde{x}(t) + x_e)(\tilde{x}(t) + x_e) + 2Ke^{-\gamma\tau}\tilde{u}(t-\tau) + (2Ke^{-\gamma\tau} - 1)u_e, \ \ t > 0. \end{cases} \tag{5.38}$$

Analyzing the stability properties of the origin of (5.38) seems to be a difficult task. Therefore, we write the model (5.38) in an equivalent form that eases its analysis. Using the Taylor formula, we can write, with an abuse of notation,

$$\beta(\mathfrak{z} + x_e)(\mathfrak{z} + x_e) = \beta(x_e)x_e + \theta\mathfrak{z} + I(\mathfrak{z}), \tag{5.39}$$

where,

$$\theta = \beta(x_e) + \beta'(x_e)x_e, \tag{5.40}$$

and,

$$I(\mathfrak{z}) = \int_{x_e}^{x_e + \mathfrak{z}} (\mathfrak{z} + x_e - l)\,\tilde{\theta}(\ell)d\ell, \tag{5.41}$$

where, $\tilde{\theta}(\mathfrak{z}) = \big[\beta(\mathfrak{z})\mathfrak{z}\big]^{(2)}$. We deduce that for all $t > 0$, the system (5.38) is equivalent to

$$\begin{cases} \dot{\tilde{x}}(t) = & -\delta\tilde{x}(t) - \beta(x_e)x_e - \theta\tilde{x}(t) - I(\tilde{x}(t)) + 2Le^{-\gamma\tau}\tilde{u}(t-\tau) - \delta x_e + 2Le^{-\gamma\tau}u_e, \\ \tilde{u}(t) = & \beta(x_e)x_e + \theta\tilde{x}(t) + I(\tilde{x}(t)) + 2Ke^{-\gamma\tau}\tilde{u}(t-\tau) + (2Ke^{-\gamma\tau} - 1)u_e. \end{cases} \tag{5.42}$$

Using (5.31), we get for all $t > 0$,

$$\begin{cases} \dot{\tilde{x}}(t) & = & -(\delta + \theta)\tilde{x}(t) - I(\tilde{x}(t)) + 2Le^{-\gamma\tau}\tilde{u}(t-\tau), \\ \tilde{u}(t) & = & \theta\tilde{x}(t) + I(\tilde{x}(t)) + 2Ke^{-\gamma\tau}\tilde{u}(t-\tau). \end{cases} \tag{5.43}$$

Due to the shifting of the initial system coordinates, we notice that the trajectories $\tilde{x}$ and $\tilde{u}$ of system (5.43) are no longer positive. More precisely, we have, $\tilde{x} > -x_e$, and, $\tilde{u} > -u_e$, where $x_e > 0$ and $u_e > 0$, when Proposition 4 is satisfied.

In the analysis of the nonlinear system (5.43), we need to prove that the typical nonlinear term $I(\tilde{x})$ satisfies a kind of sector-condition, that is given by:

Claim 2. *For all $x_e > 0$ and $\tilde{x} > -x_e$, there exist two strictly positive constants z_1 and z_2, such that*

$$|I(\tilde{x})| \leq z_1 Q(\tilde{x}), \quad \textit{and,} \quad |I(\tilde{x})| \leq z_2 |\tilde{x}|. \tag{5.44}$$

A possible selection of z_1 and z_2 is:

$$z_1 = 2\mathfrak{c}_4 \beta(0), \tag{5.45}$$

$$z_2 = \beta(0) \max\left\{\mathfrak{c}_4, 2\max\{b, b^{-1}\} + |\mathfrak{c}_1|\right\}, \tag{5.46}$$

where, $Q(m) = \frac{1}{2}m^2$, and, $\mathfrak{c}_1 = \frac{1}{h} - \frac{nbx_e^n}{h^2}$, $\mathfrak{c}_2 = x_e$, $\mathfrak{c}_3 = \left(1 - \frac{nbx_e^n}{h}\right)$, $h = 1 + bx_e^n$, and,

$$\mathfrak{c}_4 = \frac{nb(n-1)(1+b(2x_e)^n)\left(|\mathfrak{c}_2| + |\mathfrak{c}_3|\right)\max\left\{b, b^{-1}\right\}}{2h} + \frac{nbx_e^{n-1}\left(1+b(2x_e)^n\right)|\mathfrak{c}_3|}{h^2}.$$

Proof. The first part of this proof (to determine z_1) is identical to the one presented in Chapter 3. Here we recall the main steps that allow us to determine the constant z_2. So, using the expression of β, which is given in (6.1), we observe that for all $x_e > 0$ and $\mathfrak{z} > -x_e$,

$$I(\mathfrak{z}) = \beta(0)G(\mathfrak{z}) - \theta\mathfrak{z} \tag{5.47}$$

where $G(\mathfrak{z}) = \frac{\mathfrak{z}+x_e}{1+b(\mathfrak{z}+x_e)^n} - \frac{x_e}{1+bx_e^n}$. First of all, let us study the function:

$$\rho(\mathfrak{z}) = \frac{1}{1+b(\mathfrak{z}+x_e)^n} - \frac{1}{1+bx_e^n} = \frac{b\left[x_e^n - (\mathfrak{z}+x_e)^n\right]}{p(\mathfrak{z})}, \text{ where, } p(\mathfrak{z}) = \left[1+b(\mathfrak{z}+x_e)^n\right](1+bx_e^n).$$

Thanks to the formula $(\mathfrak{z}+x_e)^n - x_e^n = nx_e^{n-1}\mathfrak{z} + n\int_0^{\mathfrak{z}}\int_{x_e}^{x_e+l}(n-1)m^{n-2}dmdl$, it follows that,

$$\rho(\mathfrak{z}) = -\frac{nbx_e^{n-1}}{p(\mathfrak{z})}\mathfrak{z} + \mathfrak{C}(\mathfrak{z}). \tag{5.48}$$

where $\mathfrak{C}(\mathfrak{z}) = -\frac{nb(n-1)}{p(\mathfrak{z})}\int_0^{\mathfrak{z}}\int_0^l (m+x_e)^{n-2}dmdl$. Let us denote $h = 1+bx_e^n$, and observe that $\frac{1}{p(\mathfrak{z})} = \frac{1}{h}\left(\rho(\mathfrak{z}) + \frac{1}{h}\right)$. Therefore, we obtain, $\rho(\mathfrak{z}) = -nbx_e^{n-1}\left(\frac{\rho(\mathfrak{z})}{h} + \frac{1}{h^2}\right)\mathfrak{z} + \mathfrak{C}(\mathfrak{z})$.

Consequently, we get the intermediate result:

$$\rho(\mathfrak{z}) = -\frac{nbx_e^{n-1}}{h^2}\mathfrak{z} + \mathfrak{C}(\mathfrak{z}) - \frac{nbx_e^{n-1}}{h}\rho(\mathfrak{z})\mathfrak{z}. \tag{5.49}$$

On the other hand, observe that

$$G(\mathfrak{z}) = \left(\rho(\mathfrak{z}) + \frac{1}{h}\right)\mathfrak{z} + x_e\rho(\mathfrak{z}) = \mathfrak{c}_1\mathfrak{z} + \mathfrak{c}_2\mathfrak{C}(\mathfrak{z}) + \mathfrak{c}_3\rho(\mathfrak{z})\mathfrak{z}, \tag{5.50}$$

where the last equality is a direct consequence of (5.49), and the constants $\mathfrak{c}_1$, $\mathfrak{c}_2$, and, $\mathfrak{c}_3$ are those provided in the statement of Claim 2. Now, we readily check that

$$\left|\mathfrak{C}(\mathfrak{z})\right| \leq \frac{nb(n-1)}{p(\mathfrak{z})}\left(|\mathfrak{z}| + x_e\right)^{n-2}\frac{\mathfrak{z}^2}{2}. \tag{5.51}$$

From (5.48) we deduce that $\left|\rho(\mathfrak{z})\right| \leq \frac{nbx_e^{n-1}}{p(\mathfrak{z})}|\mathfrak{z}| + |\mathfrak{C}(\mathfrak{z})|$. Using (5.51), it follows that

$$\left|\mathfrak{z}\rho(\mathfrak{z})\right| \leq \frac{nbx_e^{n-1}}{p(\mathfrak{z})}\mathfrak{z}^2 + \frac{nb(n-1)}{2p(\mathfrak{z})}\left(|\mathfrak{z}| + x_e\right)^{n-2}|\mathfrak{z}|^3. \tag{5.52}$$

From the second equality in (5.50), we deduce that,

$$|G(\mathfrak{z}) - \mathfrak{c}_1\mathfrak{z}| \leq \frac{nb(n-1)|\mathfrak{c}_3|}{2p(\mathfrak{z})}\left(|\mathfrak{z}| + x_e\right)^{n-2}|\mathfrak{z}|^3 + \left[\frac{nb(n-1)|\mathfrak{c}_2|\left(|\mathfrak{z}| + x_e\right)^{n-2}}{2p(\mathfrak{z})} + \frac{nbx_e^{n-1}|\mathfrak{c}_3|}{p(\mathfrak{z})}\right]\mathfrak{z}^2.$$

Through simple calculations (see in Chapter 3), we find that

$$|G(\mathfrak{z}) - \mathfrak{c}_1\mathfrak{z}| \leq \mathfrak{c}_4\mathfrak{z}^2, \tag{5.53}$$

where $\mathfrak{c}_4$ is the positive constant defined in the statement of the Claim 2. On the other hand, we easily check that $\theta = \beta(0)\mathfrak{c}_1$, where θ is the constant defined in (5.40). Therefore, by combining (5.47) and (5.53), we obtain

$$|I(\mathfrak{z})| \leq \beta(0)\mathfrak{c}_4\mathfrak{z}^2, \tag{5.54}$$

We conclude that $z_1 = 2\mathfrak{c}_4\beta(0)$, since by definition, $Q(\ell) = \frac{1}{2}\ell^2$.

Now, we wish to determine z_2. From (5.53), we have $\frac{|G(\mathfrak{z})-\mathfrak{c}_1\mathfrak{z}|}{|\mathfrak{z}|} \leq \mathfrak{c}_4|\mathfrak{z}|$. Then,

- if $|\mathfrak{z}| \leq 1$, we get $\frac{|G(\mathfrak{z})-\mathfrak{c}_1\mathfrak{z}|}{|\mathfrak{z}|} \leq \mathfrak{c}_4$, and,
- if $|\mathfrak{z}| > 1$, we get $\frac{|G(\mathfrak{z})-\mathfrak{c}_1\mathfrak{z}|}{|\mathfrak{z}|} \leq |\mathfrak{c}_1| + \frac{2\max\{b,b^{-1}\}}{|\mathfrak{z}|} \leq |\mathfrak{c}_1| + 2\max\{b,b^{-1}\}$.

We conclude that for all $\mathfrak{z} > -x_e$, we have $\frac{|G(\mathfrak{z})-\mathfrak{c}_1\mathfrak{z}|}{|\mathfrak{z}|} \leq \max\left\{\mathfrak{c}_4, 2\max\{b,b^{-1}\} + |\mathfrak{c}_1|\right\}$.

From (5.47), we conclude that

$$|I(\mathfrak{z})| \leq z_2|\mathfrak{z}|, \tag{5.55}$$

where, $z_2 = \beta(0)\max\left\{\mathfrak{c}_4, 2\max\{b,b^{-1}\} + |\mathfrak{c}_1|\right\}$. □

Now, we are ready to analyze the resulting model (5.43), for which we are going to highlight two different approaches. The method that we left for the end is more traditional, through quadratic Lyapunov-like constructions. While the technique that we address right after the present section is based on more recent concepts, including Comparative (Positive) Systems and linear Lyapunov functionals.

5.4.1 Stability analysis through a Comparative Positive System approach

The technique that we investigate here (recently presented in [196], see also the references therein) starts with the original step of representing the nonlinear system (5.43) as a linear time-varying system. Notice that both classes of systems, i.e., nonlinear and time-varying ones, are beyond the scope of classical frequency methods. However, Lyapunov techniques offer strong tools for performing their analyses.

5.4.1.1 Obtaining a Comparative System of higher dimension

We are looking for a Comparative System which enables us -from the analysis of its origin- to establish the exponential stability of the zero solution of the model given in (5.43). Therefore, using Claim 2, we notice that the function $J(\tilde{x}) = I(\tilde{x})/\tilde{x}$ is bounded on $(-x_e, +\infty)$. More precisely, we have

$$\left|J(\tilde{x})\right| < z_2, \text{ for all } \tilde{x} \in (-x_e, \infty), \text{ and, } x_e > 0. \tag{5.56}$$

Moreover, we take a specific well-defined non-zero trajectory $\tilde{x}_0(t)$, of the system (5.43), for all $t \geq 0$, and we set:

$$J(t) := I(\tilde{x}_0(t))/\tilde{x}_0(t), \text{ for all } t \geq -\tau. \tag{5.57}$$

The notation (5.57) implies that the model (5.43) is rewritten as a linear time-varying system of the form:

$$\left\{ \begin{array}{rcl} \dot{\tilde{x}}(t) & = & -\big(\delta + \theta + J(t)\big)\tilde{x}(t) + 2Le^{-\gamma\tau}\tilde{u}(t-\tau), \\ \tilde{u}(t) & = & \big(\theta + J(t)\big)\tilde{x}(t) + 2Ke^{-\gamma\tau}\tilde{u}(t-\tau), \quad t > 0. \end{array} \right. \tag{5.58}$$

Remark 31. *The notation* (5.57) *is a manner of concealing the nonlinear part of the dynamical system* (5.43)*. This will be beneficial in a first time, since it allows us to obtain a linear time-varying Comparative System, from which decay conditions can be derived. To be relevant, the decay conditions provided for the model* (5.58) *have to be independent from the choice of the fixed trajectory $x_0(t)$ in the model* (5.43)*, i.e., stability conditions have to be valid for all the system trajectories. The latter issue will be discussed in the sequel, when decay conditions will be provided. It seems clear that an analysis approach that omits the particular nature of the nonlinear terms (i.e. I defined in* (5.41)*) may lead to more conservatism in the stability conditions, than a dedicated approach which takes into account the model features. The latter observation applies also to the assertion in Claim 2, where the constants z_1 and z_2 are determined, globally, for all $\tilde{x} \geq -x_e$. However, we can notice that by exploiting the nature of the nonlinear term I, the constants z_1 and z_2 can be considerably improved over a large part of the domain of definition, where they are smaller than the global values. This will have a direct impact on the conservatism of the obtained decay conditions. Hence, in the second phase that follows the determination of the decay conditions for the time-varying system* (5.58)*, the above mentioned remarks will be taken into account in order to provide a more refined analysis dedicated to the system* (5.43)*.*

Now, along the trajectories of the system (5.43), we define the following operator for all $t \geq 0$,

$$\xi(t) = \tilde{x}(t) + \alpha \int_{t-\tau}^{t} \tilde{u}(\ell) d\ell, \tag{5.59}$$

where α is a positive constant to be chosen later. Next, observe that the derivative of $\xi(t)$, along the trajectories of the time-varying system (5.58), is given by

$$\dot{\xi}(t) = -\Big[\delta + (1-\alpha)\big(\theta + J(t)\big)\Big]\tilde{x}(t) + \big[\alpha(2Ke^{-\gamma\tau} - 1) + 2Le^{-\gamma\tau}\big]\tilde{u}(t-\tau). \tag{5.60}$$

Using the equality $\tilde{x}(t) = \xi(t) - \alpha \int_{t-\tau}^{t} u(\ell) d\ell$, we get

$$\begin{aligned} \dot{\xi}(t) = &-\Big[\delta + (1-\alpha)\big(\theta + J(t)\big)\Big]\xi(t) + \alpha\Big[\delta + (1-\alpha)\big(\theta + J(t)\big)\Big]\int_{t-\tau}^{t} \tilde{u}(\ell) d\ell \\ &+ \big[\alpha(2Ke^{-\gamma\tau} - 1) + 2Le^{-\gamma\tau}\big]\tilde{u}(t-\tau). \end{aligned} \tag{5.61}$$

Then, we fix the value of α to the constant that we denote in the sequel α_0, where, $\alpha_0 = \frac{2Le^{-\gamma\tau}}{1-2Ke^{-\gamma\tau}} > 0$. It follows that we can rewrite:

$$\dot{\xi}(t) = -A(t)\xi(t) + \alpha_0 A(t) \int_{t-\tau}^{t} \tilde{u}(\ell) d\ell, \tag{5.62}$$

where,

$$A(t) = \delta + (1-\alpha_0)\big(\theta + J(t)\big).$$

To ease the notation, we put $B(t) = \theta + J(t)$. Therefore, for all $t > 0$, we rewrite the system equations in the following compact form:

$$\left\{ \begin{array}{rcl} \dot{\xi}(t) & = & -A(t)\xi(t) + \alpha_0 A(t) \int_{t-\tau}^{t} \tilde{u}(\ell) d\ell, \\ \tilde{x}(t) & = & \xi(t) - \alpha_0 \int_{t-\tau}^{t} \tilde{u}(\ell) d\ell, \\ \tilde{u}(t) & = & B(t)\tilde{x}(t) + 2Ke^{-\gamma\tau}\tilde{u}(t-\tau). \end{array} \right. \tag{5.63}$$

In addition, we use the following decomposition: $A(t) = \overline{A}(t) - \underline{A}(t)$, $B(t) = \overline{B}(t) - \underline{B}(t)$, where, for all $t \geq 0$, $\overline{A}(t) \geq 0$, $\underline{A}(t) \geq 0$, $\overline{B}(t) \geq 0$ and $\underline{B}(t) \geq 0$. Consequently, the system (5.63) is equivalent to

$$\left\{ \begin{array}{rcl} \dot{\xi}(t) & = & -A(t)\xi(t) + \alpha_0 \overline{A}(t) \int_{t-\tau}^{t} \tilde{u}(l) dl - \alpha_0 \underline{A}(t) \int_{t-\tau}^{t} \tilde{u}(\ell) d\ell, \\ \tilde{x}(t) & = & \xi(t) - \alpha_0 \int_{t-\tau}^{t} \tilde{u}(\ell) d\ell, \\ \tilde{u}(t) & = & \overline{B}(t)\tilde{x}(t) - \underline{B}(t)\tilde{x}(t) + 2Ke^{-\gamma\tau}\tilde{u}(t-\tau), \;\; t > 0. \end{array} \right. \tag{5.64}$$

The latter form is equivalent to:

$$\left\{ \begin{array}{l} \dot{\xi}(t) = -A(t)\xi(t) + \alpha_0 \overline{A}(t) \int_{t-\tau}^{t} \tilde{u}(l) dl - \alpha_0 \underline{A}(t) \int_{t-\tau}^{t} \tilde{u}(\ell) d\ell, \\ \dot{\tilde{x}}(t) = -A(t)\xi(t) + \alpha_0 \overline{A}(t) \int_{t-\tau}^{t} \tilde{u}(l) dl - \alpha_0 \underline{A}(t) \int_{t-\tau}^{t} \tilde{u}(\ell) d\ell - \alpha_0 \tilde{u}(t) + \alpha_0 \tilde{u}(t-\tau), \\ \tilde{u}(t) = \overline{B}(t)\tilde{x}(t) - \underline{B}(t)\tilde{x}(t) + 2Ke^{-\gamma\tau}\tilde{u}(t-\tau), \;\; t > 0. \end{array} \right. \tag{5.65}$$

Technical Note 2. *At this juncture, let us point out the following assertions:*
(i) *If all the solutions of* (5.65) *with initial conditions satisfying the matching condition*

$$\varphi_{\tilde{x}}(0) = \varphi_{\xi}(0) + \alpha_0 \int_{-\tau}^{0} \varphi_{\tilde{u}}(\ell) d\ell, \ \textit{where,} \ \varphi_{\tilde{u}} \in \ PC\left([-\tau, 0], (-\tilde{u}_e, +\infty)\right), \tag{5.66}$$

converge exponentially to zero, then the solutions of (5.58) *converge exponentially to the origin, i.e. to the positive steady state E of the non-shifted system* (6.8).
(ii) *Notice that, in* ***(i)****, we require the condition* (5.66) *in order to match the trajectories of* (5.65) *to those of* (5.58)*, otherwise we cannot conclude*[a]*. On the other hand, the matching condition that ensures the continuity of the solutions in* (5.58) *(and therefore, in* (5.65)*), i.e. the condition:*

$$\varphi_{\tilde{u}}(0) = B(0)\varphi_{\tilde{x}}(0) + 2Ke^{-\gamma\tau}\varphi_{\tilde{u}}(-\tau), \tag{5.67}$$

is not required, i.e., the models (5.58) *and* (5.65) *have piecewise continuous solutions.*
(iii) *The solution* $\tilde{x}(t)$ *explicitly intervenes in the model* (5.65)*, through the terms A and B. Hence, it will be possible to conclude on the stability of the origin of* (5.65) *(and, therefore, of* (5.58)*) if and only if the* ***decay conditions****, and the expression of the* ***decay rate****, of the solutions will be determined independently* [b] *from the specific* $J(t)$.

[a] A counter-example: let us consider the zero initial condition $\varphi_{\tilde{x}}(0) = 0$, $\varphi_{\tilde{u}}(m) = 0$, for all $m \in [-\tau, 0]$, for the systems (5.58) and (5.65), while we set $\varphi_{\xi}(0) > 0$ in (5.65), i.e. the matching condition is not satisfied. We notice that if for all $t \geq 0$, $A(t) < 0$, then the solutions of the model (5.58) are identically zero for all $t \geq 0$, but this does not hold for the components $\left(\tilde{x}(t), \tilde{u}(t)\right)$ of the solution of (5.65).

[b] For that, the inequality (5.56) is crucial, since it gives an upper-bound on J regardless the specific trajectory $x_0(t)$ used to define $A(t)$ and $B(t)$ in (5.65).

Next, our objective is to investigate the stability properties of the resulting system (5.64), which is equivalent to (5.65). For that purpose, we use an approach that doubles the dimension of the system, as in [206] (see also, [196], [122]). More precisely, we consider the following system:

$$\left\{\begin{array}{rcl}
\dot{\xi}(t) & = & -A(t)\xi(t) + \alpha_0\overline{A}(t)\int_{t-\tau}^{t}\tilde{u}(\ell)d\ell + \alpha_0\underline{A}(t)\int_{t-\tau}^{t}\tilde{y}(\ell)d\ell, \\
\tilde{x}(t) & = & \xi(t) + \alpha_0\int_{t-\tau}^{t}\tilde{y}(\ell)d\ell, \\
\tilde{u}(t) & = & \overline{B}(t)\tilde{x}(t) + \underline{B}(t)\tilde{z}(t) + 2Ke^{-\gamma\tau}\tilde{u}(t-\tau), \\
\dot{\psi}(t) & = & -A(t)\psi(t) + \alpha_0\overline{A}(t)\int_{t-\tau}^{t}\tilde{y}(l)dl + \alpha_0\underline{A}(t)\int_{t-\tau}^{t}\tilde{u}(\ell)d\ell, \\
\tilde{z}(t) & = & \psi(t) + \alpha_0\int_{t-\tau}^{t}\tilde{u}(\ell)d\ell, \\
\tilde{y}(t) & = & \overline{B}(t)\tilde{z}(t) + \underline{B}(t)\tilde{x}(t) + 2Ke^{-\gamma\tau}\tilde{y}(t-\tau),
\end{array}\right. \tag{5.68}$$

for all $t > 0$, which is associated with the matching conditions,

$$\begin{array}{rcl}
\varphi_{\tilde{x}}(0) & = & \varphi_{\xi}(0) + \alpha_0\int_{-\tau}^{0}\varphi_{\tilde{y}}(\ell)d\ell, \\
\varphi_{\tilde{z}}(0) & = & \varphi_{\psi}(0) + \alpha_0\int_{-\tau}^{0}\varphi_{\tilde{u}}(\ell)d\ell.
\end{array} \tag{5.69}$$

5.4.1.2 Analyzing the Comparative System via a linear Lyapunov functional

For later use, let us check the following feature regarding the system (5.68).

Proposition 5. *For strictly positive initial conditions, i.e.,* $\varphi_\xi(0) \in \mathbb{R}^+$, $\varphi_{\tilde{x}}(0) \in \mathbb{R}^+$, $\varphi_\psi(0) \in \mathbb{R}^+$, $\varphi_{\tilde{z}}(0) \in \mathbb{R}^+$, $\varphi_{\tilde{u}} \in PC\left([-\tau,0],\mathbb{R}^+\right)$, *and,* $\varphi_{\tilde{y}} \in PC\left([-\tau,0],\mathbb{R}^+\right)$, *the trajectories of the system* (5.68) *remain strictly positive for all future time* $t \geq 0$.

Proof. We want to prove that the solutions of (5.68) associated with strictly positive initial conditions are strictly positive. Let us give a brief proof, by contradiction, for each component of the trajectories. First, we consider that all the initial conditions are positive. Then,

- We assume that $\xi(t) > 0$ for all $t \in [0,t_1[$, and that $\xi(t_1) = 0$, while all the other components of the trajectories are positive for all $t \leq t_1$. It follows from the first equation in (5.68) that

$$\dot{\xi}(t_1) = \alpha_0 \overline{A}(t_1) \int_{t_1-\tau}^{t_1} \tilde{u}(\ell)d\ell + \alpha_0 \underline{A}(t_1) \int_{t_1-\tau}^{t_1} \tilde{y}(\ell)d\ell > 0, \tag{5.70}$$

  which contradicts the fact that $\xi(t) > 0$ for all $t \in [0,t_1[$. Therefore, $\xi(t_1) > 0$.

- We assume that $\tilde{x}(t) > 0$ for all $t \in [0,t_1[$, and that $\tilde{x}(t_1) = 0$; all the other components of the trajectories are positive for all $t \leq t_1$. It follows from the second equation in (5.68) that

$$\alpha_0 \int_{t_1-\tau}^{t_1} \tilde{y}(\ell)d\ell = -\xi(t_1) < 0, \tag{5.71}$$

  which contradicts the positivity of $\tilde{y}(t)$ for all $t \leq t_1$. Therefore, $\tilde{x}(t_1) > 0$.

- We assume that $\tilde{u}(t) > 0$ for all $t \in [0,t_1[$, and that $\tilde{u}(t_1) = 0$; all the other components of the trajectories are positive for all $t \leq t_1$. It follows from the third equation in (5.68) that

$$\underline{B}(t_1)\tilde{z}(t_1) + 2Ke^{-\gamma\tau}\tilde{u}(t_1-\tau) = -\overline{B}(t_1)\tilde{x}(t_1) < 0, \tag{5.72}$$

  which contradicts the $\tilde{u}(t)$ for all $t < t_1$. Arguing similarly for ψ, $\tilde{z}$, and $\tilde{y}$, we prove that all the trajectories are positive when (5.68) is associated with positive initial conditions.

□

Remark 32. ***(i)*** *Similarly to Proposition 5, we can prove that the system* (5.68) *is negative, i.e., for negative initial conditions, the trajectories remain negative. More importantly, we highlight the fact that the proof of the positivity does not rely on the choice of the specific trajectory used to determine* $J(t)$ *in* (5.58).
(ii) *The second relevant feature to be pointed out for the higher dimensional system* (5.68) *is that if* $\left(\xi,\tilde{x},\tilde{u}\right)$ *is a solution of* (5.64)*, then automatically* $\left(\xi,\tilde{x},\tilde{u},-\xi,-\tilde{x},-\tilde{u}\right)$ *is a solution of* (5.68). *A direct consequence is that if all the solutions of* (5.68) *-that satisfy the matching conditions* (5.69)*- converge to the origin, then all the solutions of* (5.64) *converge to the origin too.*

Another key idea needs to be formulated before being able to apply the positive approach in the stability analysis of (5.68). Indeed, as discussed for the system studied in [196] (Section IV. Step 2), the linearity and the positivity of the Comparative System (5.68) ensure that its origin is globally exponentially stable if it is globally exponentially stable only on the positive orthant.

5.4.1.3 Sufficient decay conditions for global exponential stability

In this section, we consider only positive solutions of the Comparative System (5.68). This fact allows us to reduce the stability analysis to a system of lower dimension. Indeed, now we set $X_1 = \xi + \psi$, $X_2 = \tilde{x} + \tilde{z}$, and, $X_3 = \tilde{u} + \tilde{y}$. Then (5.68) gives

$$\left\{\begin{array}{lcl} \dot{X}_1(t) & = & A(t)X_1(t) + \alpha_0 A^s(t) \int_{t-\tau}^{t} X_3(l)dl, \\ X_2(t) & = & X_1(t) + \alpha_0 \int_{t-\tau}^{t} X_3(l)dl, \\ X_3(t) & = & B^s(t)X_2(t) + 2Ke^{-\gamma\tau}X_3(t-\tau), \end{array}\right. \tag{5.73}$$

where, $A^s = \overline{A} + \underline{A} \in [0, S)$. Therefore, we notice that (5.73) yields

$$\left\{\begin{array}{lcl} \dot{X}_1(t) & = & A(t)X_1(t) + \alpha_0 A^s(t) \int_{t-\tau}^{t} X_3(\ell)d\ell, \\ X_3(t) & = & B^s(t)X_1(t) + \alpha_0 B^s(t) \int_{t-\tau}^{t} X_3(\ell)d\ell + 2Ke^{-\gamma\tau}X_3(t-\tau), \end{array}\right. \tag{5.74}$$

Let us introduce the following linear functional:

$$W\left(X_1(t), X_{3t}\right) = X_1(t) + \sigma_1 \int_{t-\tau}^{t} X_3(m)dm + \sigma_2 \int_{t-\tau}^{t}\int_{m}^{t} e^{\sigma_3(\ell-t)}X_3(\ell)d\ell dm,$$

where σ_1, σ_2, and, σ_3, are strictly positive constants to be selected later.

The derivative of the functional W, along the trajectories of (5.74), is given for almost all $t \geq 0$, by:

$$\begin{aligned} \dot{W}(t) =& A(t)X_1(t) + \alpha_0 A^s(t) \int_{t-\tau}^{t} X_3(\ell)d\ell + \sigma_1\left[X_3(t) - X_3(t-\tau)\right] \\ &+ \sigma_2\left[\tau X_3(t) - \int_{t-\tau}^{t} e^{\sigma_3(\ell-t)}X_3(\ell)d\ell - \sigma_3\int_{t-\tau}^{t}\int_{m}^{t} e^{\sigma_3(\ell-t)}X_3(\ell)d\ell dm\right] \\ =& A(t)X_1(t) + \alpha_0 A^s(t) \int_{t-\tau}^{t} X_3(\ell)d\ell + (\sigma_1 + \tau\sigma_2)X_3(t) - \sigma_1 X_3(t-\tau) \\ &- \sigma_2 \int_{t-\tau}^{t} e^{\sigma_3(\ell-t)}X_3(\ell)d\ell - \sigma_2\sigma_3\int_{t-\tau}^{t}\int_{m}^{t} e^{\sigma_3(\ell-t)}X_3(\ell)d\ell dm. \end{aligned} \tag{5.75}$$

Thanks to the second equation in (5.74), we get for almost all $t \geq 0$,

$$\begin{aligned} \dot{W}(t) =& \Gamma(t)X_1(t) + \alpha_0 A^s(t) + \alpha_0\left[A^s(t) + (\sigma_1 + \tau\sigma_2)B^s(t)\right] \int_{t-\tau}^{t} X_3(\ell)d\ell \\ &- \sigma_2 \int_{t-\tau}^{t} e^{\sigma_3(\ell-t)}X_3(\ell)d\ell - \left[\sigma_1 - 2Ke^{-\gamma\tau}(\sigma_1 + \tau\sigma_2)\right]X_3(t-\tau) \\ &- \sigma_2\sigma_3 \int_{t-\tau}^{t}\int_{m}^{t} e^{\sigma_3(\ell-t)}X_3(\ell)d\ell dm, \end{aligned} \tag{5.76}$$

where,

$$\Gamma(t) = -A(t) + (\sigma_1 + \tau\sigma_2) B^s(t), \quad \text{for all } t \geq 0. \tag{5.77}$$

Using the fact that

$$\int_{t-\tau}^{t} e^{\rho(\ell-t)} X_3(\ell) d\ell \geq e^{-\rho\tau} \int_{t-\tau}^{t} X_3(\ell) d\ell, \tag{5.78}$$

for all $t \geq 0$, we deduce that for almost all $t \geq 0$,

$$\begin{aligned} \dot{W}(t) \leq & \Gamma(t) X_1(t) - \left[\sigma_2 e^{-\sigma_3\tau} - \alpha_0 \left(A^s(t) + (\sigma_1 + \tau\sigma_2) B^s(t)\right)\right] \int_{t-\tau}^{t} X_3(\ell) d\ell \\ & + \sigma_1 \left[2Ke^{-\gamma\tau}\left(1 + \frac{\sigma_2\tau}{\sigma_1}\right) - 1\right] X_3(t-\tau) - \sigma_2\sigma_3 \int_{t-\tau}^{t}\int_{m}^{t} e^{\sigma_3(\ell-t)} X_3(\ell) d\ell dm. \end{aligned} \tag{5.79}$$

Now, let us choose,

$$\sigma_2 = \frac{\sigma_1^2}{\tau}. \tag{5.80}$$

It follows that $2\left(1 + \frac{\sigma_2\tau}{\sigma_1}\right) Ke^{-\gamma\tau} - 1 = 2(1+\sigma_1) Ke^{-\gamma\tau} - 1$. Therefore, since $2Ke^{-\gamma\tau} < 1$, we deduce that for all $\sigma_1 \in \left(0, \frac{1-2Ke^{-\gamma\tau}}{4Ke^{-\gamma\tau}}\right)$, we get,

$$2(1+\sigma_1)Ke^{-\gamma\tau} - 1 < \frac{2Ke^{-\gamma\tau} - 1}{2} < 0. \tag{5.81}$$

Therefore, we observe that by choosing $\sigma_2 = \frac{\sigma_1^2}{\tau}$, and $\sigma_1 \in \left(0, \frac{1-2Ke^{-\gamma\tau}}{4Ke^{-\gamma\tau}}\right)$, then the derivative of W along the trajectories of (5.74), satisfies,

$$\begin{aligned} \dot{W}(t) \leq & \Gamma(t) X_1(t) - \left[\sigma_2 e^{-\sigma_3\tau} - \alpha_0 \left(A^s(t) + (\sigma_1 + \tau\sigma_2) B^s(t)\right)\right] \int_{t-\tau}^{t} X_3(\ell) d\ell \\ & - \sigma_2\sigma_3 \int_{t-\tau}^{t}\int_{m}^{t} e^{\sigma_3(\ell-t)} X_3(\ell) d\ell dm, \quad \text{for almost all } t \geq 0. \end{aligned} \tag{5.82}$$

A condition on the delay: We recall that $J(t) = J(\tilde{x}_0(t)) \leq z_2$, for all $t \geq -\tau$, $\tilde{x}_0 \in (-x_e, +\infty)$. Now, let $S > 0$ be such that $A^s(t) < S$, for all $t \geq 0$, and set,

$$h(\tau) = \frac{\alpha_0\tau}{\sigma_1^2}\left[S + \sigma_1(\sigma_1+1)(|\theta| + z_2)\right]. \tag{5.83}$$

It follows that if the delay τ satisfies the condition

$$h(\tau) < 1, \tag{5.84}$$

then, for a small enough $\sigma_3 > 0$, we readily check[2] that there exists $\sigma_4 > 0$ satisfying,

$$\sigma_2 e^{-\sigma_3\tau} - \alpha_0\left[A^s(t) + (\sigma_1 + \sigma_2\tau) B^s(t)\right] = \sigma_4 > 0. \tag{5.85}$$

[2]The condition (5.84) means that $1 - \alpha_0\sigma_2\left[S + \sigma_1(\sigma_1+1)(|\theta| + z_2)\right] > 0$. Therefore, for small enough σ_3, we have $e^{-\sigma_3\tau} - \alpha_0\sigma_2\left[S + \sigma_1(\sigma_1+1)(|\theta| + z_2)\right] > 0$.

Therefore, if the **first decay condition** (5.84) is satisfied, then we end up with,

$$\dot{W}(t) \leq \Gamma(t)X_1(t) - \sigma_4 \int_{t-\tau}^{t} X_3(\ell)d\ell - \sigma_2\sigma_3 \int_{t-\tau}^{t}\int_{m}^{t} e^{\sigma_3(\ell-t)}X_3(\ell)d\ell dm. \tag{5.86}$$

Now, let us focus on the function $\Gamma(t)$, for all $t \geq 0$, where,

$$\Gamma(t) = -\delta + \left(\frac{2e^{-\gamma\tau}-1}{1-2Ke^{-\gamma\tau}} + \sigma_1(\sigma_1+1)\right)\left(\theta + J(t)\right). \tag{5.87}$$

Our objective is to ensure that

$$\exists \Gamma^{\dagger} > 0, \ \text{ such that, } \ \Gamma(t) \leq -\Gamma^{\dagger}, \ \forall t \geq 0. \tag{5.88}$$

The latter condition is in fact satisfied if and only if the following **second decay condition**,

$$\delta > \left(\frac{2e^{-\gamma\tau}-1}{1-2Ke^{-\gamma\tau}} + \sigma_1(\sigma_1+1)\right)(|\theta| + z_2), \tag{5.89}$$

is satisfied.

Remark 33. *The decay conditions* (5.84) *and* (5.89) *are* ***sufficient conditions of global exponential stability*** *of the origin of* (5.74)*. Indeed, we observe that if* (5.84) *and* (5.89) *are satisfied, then there exists a constant* $\sigma^{\dagger} > 0$*, such that,*

$$\dot{W}(t) \leq -\sigma^{\dagger} W\left(X_1(t), X_{3t}\right), \quad \textbf{\textit{for almost all}} \ t \geq 0. \tag{5.90}$$

Therefore, by integrating the previous inequality, we conclude that ***for all*** $t \geq 0$*,*

$$W\left(X_1(t), X_{3t}\right) \leq e^{-\sigma^{\dagger} t} W\left(\varphi_{X_1}(0), \varphi_{X_{3t}}\right). \tag{5.91}$$

Bearing in mind the formula of the functional W*, if follows that the solutions of the model* (5.74) *are such that* $X_1(t)$ *and* $\int_{t-\tau}^{t} X_3(\ell)d\ell$ ***converge exponentially*** *to the origin, with a decay rate smaller or equal to* $\sigma^{\dagger}$*. Therefore, we deduce from the second equation in* (5.73) *that* $X_2(t)$ *converges* ***exponentially*** *to zero. Finally, using the third equation in* (5.73)*, together with Lemma* (1) *(by putting* $\xi(t) = B^s(t)X_2(t)$*, for all* $t \geq 0$*), we readily conclude that* $X_3(t)$ *converges* ***exponentially*** *to zero. Next, from the definition of* X_1*,* X_2 *and* X_3*, we deduce that the* ***positive*** *trajectories* $\left(\xi, \tilde{x}, \tilde{u}, \psi, \tilde{z}, \tilde{y}\right)$ *of* (5.68) *are exponentially stable on the positive orthant. Therefore they are globally exponentially stable and it follows that the solution of* (5.64) *(or, equivalently,* (5.65)*) are globally exponentially stable to their origin. We conclude that the solutions of* (5.58) *are globally exponentially stable, on their domain of definition, i.e.* $\tilde{x} \in (-x_e, +\infty)$*, and,* $\tilde{u} \in (-u_e, +\infty)$*. Therefore, we conclude that* ***all the positive trajectories*** *of the system* (6.8) *converge* ***exponentially*** *to the strictly positive steady state* $E = (x_e, u_e)$*,* $x_e > 0$*,* $u_e > 0$*.*

The theory summarized in Remark 33, above, is derived without any consideration for the nature of the nonlinearity in the system describing hematopoiesis, with the exception of the boundedness condition, i.e. $\exists z_2 > 0$ such that $\left|J(t)\right| < z_2$. On some numerical examples, we are going to translate the latter findings in our case.

5.4.1.4 Numerical results and interpretations

Let us consider the biological parameters and functions given in Table 5.1. In fact, in these parameters only the apoptosis rate γ is varying from one system to another. These sets of parameters define four different systems that we denote **Sys.1**, ..., **Sys.4**. All these systems satisfy the conditions of existence of a strictly positive steady state, $E = (x_e, u_e)$, which is given for each system in Table 5.1.

	γ	$\beta(m)$	τ	K	δ	x_e	u_e
Sys.1	0.1	$\frac{1.33}{1+m^2}$	0.2	0.1	0.75	1.057541503	0.82586247
Sys.2	0.2	$\frac{1.33}{1+m^2}$	0.2	0.1	0.75	1.01143581	0.82312744
Sys.3	0.3	$\frac{1.33}{1+m^2}$	0.2	0.1	0.75	0.96456477	0.81878866
Sys.4	0.4	$\frac{1.33}{1+m^2}$	0.2	0.1	0.75	0.91675560	0.81250312

Table 5.1 The biological paremeters of the systems **Sys.1**,..., **Sys.4** satisfy the conditions of existence of $E = (x_e, u_e)$.

Let us focus on **Sys.1**, first. In Figure 5.4, the function $x \to \left|\frac{\beta(x)x - \beta(x_e)x_e - \theta(x-x_e)}{x-x_e}\right|$, for all $x \in [0, 500]$, is illustrated. The same function, but restricted to the interval $x \in [0, 15]$, is represented in Figure 5.5, where the intersection between the vertical red line and the x-axis gives the strictly positive equilibrium point $x_e = 1.057541503$. In this case (i.e. **Sys.1**), we have $\theta = -0.03508875$. We notice that on the positive orthant, i.e. $x \in (0, +\infty)$, the global z_2-value is greater than 0.65. Unfortunately, for that global z_2-value, the global (sufficient) decay conditions (5.84) and (5.89) are not satisfied.

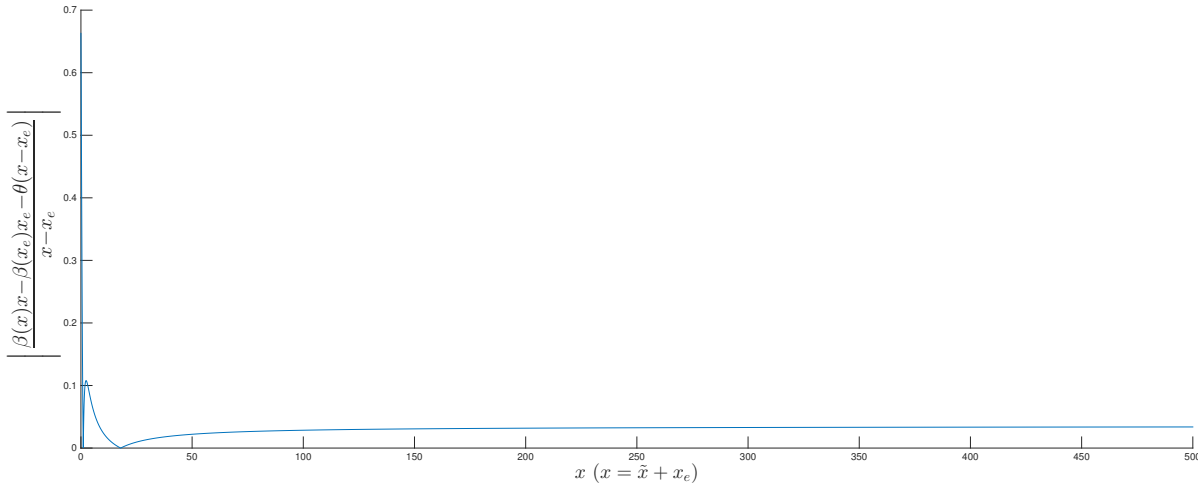

Fig. 5.4 The pattern of the curve $x \to \left|\frac{\beta(x)x - \beta(x_e)x_e - \theta(x-x_e)}{x}\right|$ in **Sys.1**, for $x \in [0, 500]$.

On the other hand, we notice from Figure 5.4 (without loss of generality) that the high value of z_2 for which, in this example, the decay conditions cannot be satisfied, is specific to a certain interval in the x-domain. Otherwise, we can see for instance that if $z_2 = 0.15$ (which is in fact the value indicated in Figure 5.5 by the horizontal red line) then, according to the Figure 5.5, the blue curve is always under the horizontal red line, except for the interval $x \in [0, 0.68]$. In addition, after simple calculations, we can check that for $z_2 = 0.15$, the global decay conditions (5.84) and (5.89) are satisfied for all the systems **Sys.1**,..., **Sys.4**, as shown in Table 5.2.

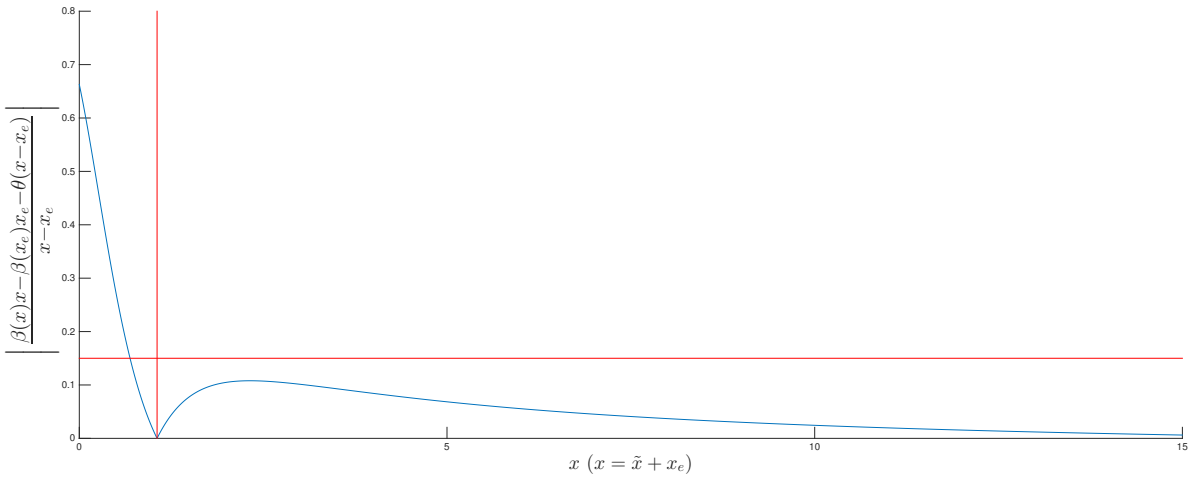

Fig. 5.5 The pattern of the curve $x \to \left|\frac{\beta(x)x-\beta(x_e)x_e-\theta(x-x_e)}{x}\right|$ in **Sys.1**, for $x \in [0, 15]$.

	$\frac{\alpha_0\tau}{\sigma_1^2}\left[S+\sigma_1(\sigma_1+1)(\lvert\theta\rvert+z_2)\right]$	$\delta-\left(\frac{2e^{-\gamma\tau}-1}{1-2Ke^{-\gamma\tau}}+\sigma_1(\sigma_1+1)\right)(\lvert\theta\rvert+z_2)$
Sys.1	0.3923	0.1445
Sys.2	0.3637	0.2308
Sys.3	0.3523	0.1683
Sys.4	0.3509	0.0352

Table 5.2 The global decay conditions computed for $z_2 = 0.15$ for the four systems of Table 5.1

We recall that the decay conditions require that

$$\frac{\alpha_0\tau}{\sigma_1^2}\left[S+\sigma_1(\sigma_1+1)(|\theta|+z_2)\right] < 1, \text{ and, } \delta-\left(\frac{2e^{-\gamma\tau}-1}{1-2Ke^{-\gamma\tau}}+\sigma_1(\sigma_1+1)\right)(|\theta|+z_2) > 0,$$

which are satisfied for the four systems in Table 5.2.

Consequently, we conclude that for all initial conditions $\varphi_x(0) \in (0.68, +\infty)$ associated to the systems **Sys.1**,..., **Sys.4**, their respective strictly positive steady states given in Table 5.1 are globally exponentially stable. The decay feature is lost if the system trajectory $x(t)$ enters, at a given time instant $t \geq 0$, in the interval $x \in (0, 68]$, where the sufficient decay conditions are violated. Nothing can be said about the behavior of the system in the region $x \in (0, 0.68]$, since the provided decay conditions are only sufficient. One can notice that the threshold z_2 which ensures the feasibility of the decay conditions (5.84) and (5.89)

is entirely dependent on the x-values, according to the nonlinear characteristic patterns as in Figure 5.4. However, the initial condition $\varphi_u(m)$, for $m \in [-\tau, 0]$, plays an implicit role to fulfill the sufficient decay conditions. It can be seen for instance in the Figures 5.8-5.9 that according to $\varphi_u(m)$, for $m \in [-\tau, 0]$, the trajectory $x(t)$ for all $t \geq 0$, may evolve in a x-domain where the sufficient decay conditions are satisfied or not. It is worth mentioning that restricting x to the domain $\mathbb{R}^+ - (0, 0.68]$ does not mean that the decay conditions (5.84) and (5.89), as well as the estimate of the decay rate of the solutions $\sigma^\dagger > 0$, are dependent on the fixed trajectory $x_0(t)$ used in the definition of $J(t)$, for all $t \geq 0$. Indeed, as we see in the Figure 5.4 for instance, $\left|J(t)\right| < z_2 = 0.15$, is satisfied for any fixed trajectory $x_0(t)$ of the system when it belongs to $\mathbb{R}^+ - [0, 0.68]$[3]. More precisely, the characteristic nonlinear patters as in Figures 5.4-5.5 are standard profiles as long as we keep the same form of the nonlinearity β (the Hill function). Thus, some fixed trajectories $x_0(t)$ may evolve for all $t \geq 0$ in a x-domain where the global decay conditions are always satisfied. This is for instance the case of the trajectories $x(t)$ of **Sys.1**, represented in red color in the Figures 5.6 and 5.7, for large positive initial conditions $\varphi_x(0)$. While some other fixed trajectories go through the x-region where the sufficient decay conditions are not satisfied. This is the case for instance of the trajectories $x(t)$ that starts from small initial conditions, as in the Figure 5.8. One notices that the global value of z_2 is directly related to the value of $\beta(0)$. More importantly, we notice that for the large values of x, the decay conditions are more likely to be satisfied, which is an interesting feature of the studied model. This is unusual since for nonlinear systems it is generally expected that the stability property of an equilibrium point is more likely to be lost when the trajectories go away from the equilibrium of interest. However, in our case, the sufficient decay conditions are no longer valid for small values of x, since the corresponding *local*-value z_2 is large in that domain. On the other hand z_2 becomes *locally* smaller for large values of x, as it can be deduced from Figure 5.4.

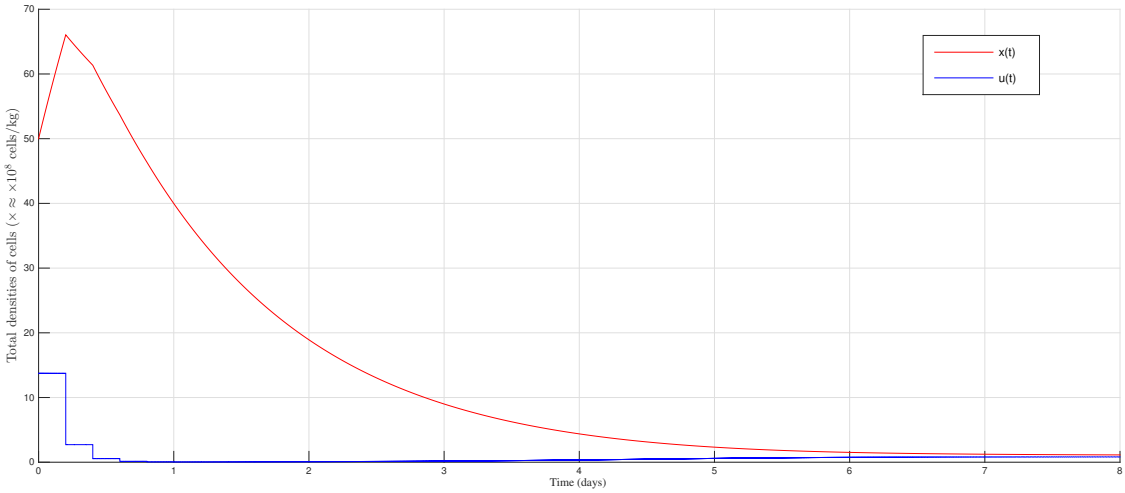

Fig. 5.6 Example of the trajectories of **Sys.1** for a large initial condition $\varphi_x(0)$ and a large initial condition $\varphi_u(m)$, for $m \in [-\tau, 0]$.

Finally, it appears clear that even for a fixed nonlinear function β (as for **Sys.1**,..., **Sys.4**), the threshold where the decay conditions (5.84) and (5.89) are no longer satisfied depends on the different biological

[3] Or, equivalently, for all fixed shifted trajectory $\tilde{x}_0(t)$ belonging to $(-x_e, +\infty) - (-x_e, 0.3775] = (-0.3775, +\infty)$.

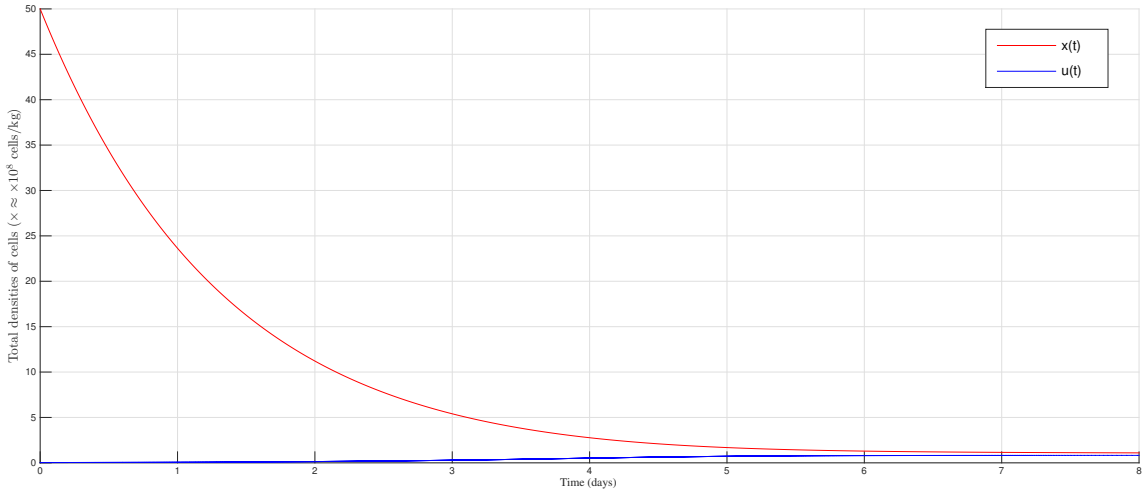

Fig. 5.7 Example of the trajectories of **Sys.1** for a large initial condition $\varphi_x(0)$ and a small initial condition $\varphi_u(m)$, for $m \in [-\tau, 0]$.

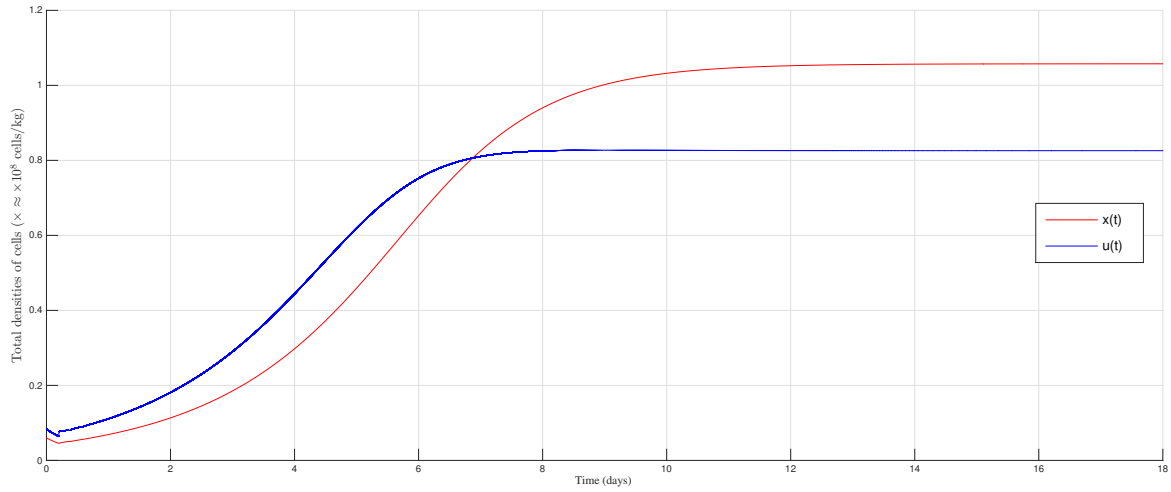

Fig. 5.8 Example of the trajectories of **Sys.1** for a small initial condition $\varphi_x(0)$ and a small initial condition $\varphi_u(m)$, for $m \in [-\tau, 0]$.

parameters involved in the model (and, consequently, on the value of x_e). Thus, we observe that for $z_2 = 0.2$, the decay conditions for the considered systems are given in Table 5.3.

	$\frac{\alpha_0 \tau}{\sigma_1^2}\left[S+\sigma_1(\sigma_1+1)(\lvert\theta\rvert+z_2)\right]$	$\delta-\left(\frac{2e^{-\gamma\tau}-1}{1-2Ke^{-\gamma\tau}}+\sigma_1(\sigma_1+1)\right)(\lvert\theta\rvert+z_2)$
Sys.1	0.409	−0.0189
Sys.2	0.3822	0.066
Sys.3	0.3720	0.002
Sys.4	0.3715	−0.1327

Table 5.3 The global decay conditions computed for $z_2 = 0.2$ for the four systems of Table 5.1

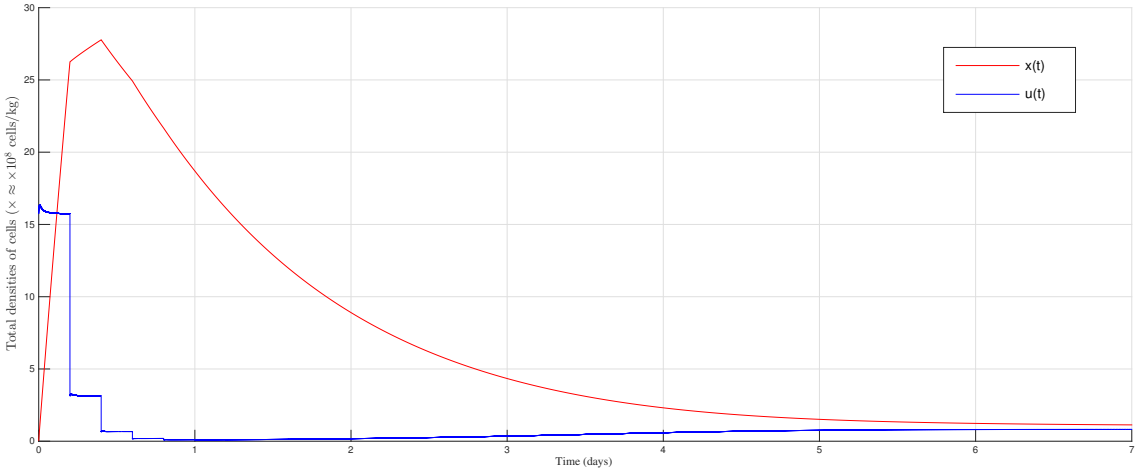

Fig. 5.9 Example of the trajectories of **Sys.1** for a small initial condition $\varphi_x(0)$ and a large initial condition $\varphi_u(m)$, for $m \in [-\tau, 0]$.

We notice that the second sufficient decay condition (5.89) is no longer verified for **Sys.1** and **Sys.4** when $z_2 = 0.2$. In fact, numerically we determine that the threshold for **Sys.3** is around $z_2 = 0.21$, while it is approximately $z_2 = 0.23$ for **Sys.2**.

What we retain from this first part of the analysis, of the strictly positive steady state, are the sufficient global conditions of global exponential stability. These decay conditions are less restrictive for large initial conditions associated to the system, which is a nice point of the study since it is not covered by local results (i.e. no local analysis may provide such a statement). In the next section, we perform a complementary (more classical) regional study, i.e. in the neighborhood of the strictly positive steady state. The analysis will be performed using quadratic functionals that provide sufficient local exponential stability conditions and an estimate of the basin of attraction of the strictly positive steady state.

5.4.2 An alternative analysis through quadratic Lyapunov functionals

In the present chapter, without extra assumptions on the system (5.38) -that may admit piecewise-continuous solutions- we prove under suitable sufficient conditions that E is locally exponentially stable by a direct Lyapunov approach, which allows us to determine an approximation of its basin of attraction.

Observe that, due to the shifting, the trajectories are no longer positive ($\tilde{x} > -x_e$, $\tilde{u} > -u_e$, where $x_e > 0$ and $u_e > 0$). To analyze the model (5.43), we introduce the following function and functionals

$$Q(a) = \frac{1}{2}a^2, \tag{5.92}$$

$$\Theta(\tilde{u}_t) = \int_{t-\tau}^{t} Q(\tilde{u}(\ell))d\ell, \tag{5.93}$$

$$\Lambda(\tilde{u}_t) = \int_{t-\tau}^{t}\int_{m}^{t} e^{\ell-t} Q(\tilde{u}(\ell))d\ell dm. \tag{5.94}$$

Next, let us define the following constants which depend on the biological parameters:

$$\xi = \theta^2 + 2K|\theta|e^{-\gamma\tau}, \tag{5.95}$$

$$\Re = \left(2Ke^{-\gamma\tau}\right)^2 + 2K|\theta|e^{-\gamma\tau} - 1, \tag{5.96}$$

$$\overline{\omega} = \frac{2\left(\delta + \theta - Le^{-\gamma\tau}\right)}{\xi}, \tag{5.97}$$

and

$$\underline{\omega} = -\frac{2Le^{-\gamma\tau}}{\Re}, \quad \text{for } \Re \neq 0. \tag{5.98}$$

Now we are ready to prove the following result:

Theorem 12. *If the conditions*

$$0 < \underline{\omega} < \overline{\omega}, \tag{5.99}$$

are satisfied, then the positive equilibrium E of the nonlinear system (6.8) *is locally exponentially stable. Moreover, an open subset of the basin of attraction that contains E can be determined.*

Proof. The derivative of the functional $Q(\tilde{x}(t))$ along the trajectories of (5.43) satisfies

$$\begin{aligned}\dot{Q}(t) &= -2\left(\delta+\theta\right)Q(\tilde{x}(t)) - \tilde{x}(t)I(\tilde{x}(t)) + 2Le^{-\gamma\tau}\tilde{x}(t)\tilde{u}(t-\tau)\\ &\leq -2\left(\delta+\theta\right)Q(\tilde{x}(t)) + z_1|\tilde{x}(t)|Q(\tilde{x}(t)) + 2Le^{-\gamma\tau}\tilde{x}(t)\tilde{u}(t-\tau),\end{aligned} \tag{5.100}$$

where the last inequality is a consequence of (5.44). Using the inequality $\tilde{x}(t)\tilde{u}(t-\tau) \leq Q(\tilde{x}(t)) + Q(\tilde{u}(t-\tau))$, it follows that

$$\dot{Q}(t) \leq -2\left(\delta+\theta-Le^{-\gamma\tau}\right)Q(\tilde{x}(t)) + z_1|\tilde{x}(t)|Q(\tilde{x}(t)) + 2Le^{-\gamma\tau}Q(\tilde{u}(t-\tau)). \tag{5.101}$$

On the other hand, through lengthy but simple calculations, we can prove that $Q(\tilde{u}(t))$ satisfies,

$$\begin{aligned}Q(\tilde{u}(t)) \leq& \xi Q(\tilde{x}(t)) + (\Re+1)Q(\tilde{u}(t-\tau)) + \frac{z_1z_2}{2}|\tilde{x}(t)|Q(\tilde{x}(t)) + |\theta|z_1|\tilde{x}(t)|Q(\tilde{x}(t))\\ &+ 2Ke^{-\gamma\tau}z_1|\tilde{u}(t-\tau)|Q(\tilde{x}(t))\\ \leq& \xi Q(\tilde{x}(t)) + (\Re+1)Q(\tilde{u}(t-\tau)) + \frac{z_1\left(z_2+2|\theta|\right)}{2}|\tilde{x}(t)|Q(\tilde{x}(t))\\ &+ Ke^{-\gamma\tau}z_1|\tilde{x}(t)|\left[Q(\tilde{u}(t-\tau)+Q(\tilde{x}(t))\right],\end{aligned}$$

where the last inequality is a consequence of the inequalities,

$$\begin{aligned}&I(\tilde{x}(t))^2 \leq z_1z_2|\tilde{x}(t)|Q(\tilde{x}(t)),\ \ \left|\tilde{u}(t-\tau)I(\tilde{x}(t))\right| \leq z_1\left|\tilde{u}(t-\tau)\right|Q\left(\tilde{x}(t)\right),\\ &\left|\tilde{u}(t-\tau)\right|Q(\tilde{x}(t)) = \frac{1}{2}|\tilde{x}(t)|\left|\tilde{u}(t-\tau)\tilde{x}(t)\right| \leq \frac{1}{2}|\tilde{x}(t)|\left[Q(\tilde{u}(t-\tau)) + Q(\tilde{x}(t))\right].\end{aligned} \tag{5.102}$$

By grouping the terms we obtain:

$$Q(\tilde{u}(t)) \leq \xi Q(\tilde{x}(t)) + (\Re + 1) Q(\tilde{u}(t-\tau)) + a_1 |\tilde{x}(t)| Q(\tilde{x}(t)) + a_2 |\tilde{x}(t)| Q(\tilde{u}(t-\tau)), \tag{5.103}$$

where, $a_1 = \frac{z_1\left(z_2 + 2|\theta| + 2Ke^{-\gamma\tau}\right)}{2}$, $a_2 = Ke^{-\gamma\tau} z_1$, and, ξ and $\Re$ are the constants defined respectively in (5.95) and (5.96). A direct consequence of (5.103) is that the derivative of the functional Θ, defined in (5.93), along the trajectories of (5.43), satisfies,

$$\dot{\Theta}(t) \leq \xi Q(\tilde{x}(t)) + \Re Q(\tilde{u}(t-\tau)) + a_1 |\tilde{x}(t)| Q(\tilde{x}(t)) + a_2 |\tilde{x}(t)| Q(\tilde{u}(t-\tau)). \tag{5.104}$$

Now, let us assume that the condition (5.99), i.e., the decay condition, is satisfied. First, we notice that $\Re < 0$. In addition, we introduce the strictly positive constant:

$$\omega = \frac{\overline{\omega} + \underline{\omega}}{2}, \quad (\omega > 0). \tag{5.105}$$

By combining (6.53) and (5.104), we conclude that, since $\Re \neq 0$, the derivative of the functional,

$$V(\tilde{x}(t), \tilde{u}_t) = Q(\tilde{x}(t)) + \omega \Theta(\tilde{u}_t), \tag{5.106}$$

along the trajectories of (5.43), satisfies the inequality,

$$\begin{aligned} \dot{V}(t) \leq & -\xi \left[\overline{\omega} + \omega\right] Q(\tilde{x}(t)) + \Re \left[\omega - \underline{\omega}\right] Q(\tilde{u}(t-\tau)) \\ & + \left(a_1 \omega + z_1\right) |\tilde{x}(t)| Q(\tilde{x}(t)) + a_2 \omega |\tilde{x}(t)| Q(\tilde{u}(t-\tau)), \end{aligned} \tag{5.107}$$

with $\xi > 0$ and $\Re < 0$. From (5.105), we conclude that

$$\dot{V}(t) \leq -\mathfrak{q} \left[Q(\tilde{x}(t)) + Q(\tilde{u}(t-\tau))\right] + \left(a_1 \omega + z_1\right) |\tilde{x}(t)| Q(\tilde{x}(t)) + a_2 \omega |\tilde{x}(t)| Q(\tilde{u}(t-\tau)), \tag{5.108}$$

where $\mathfrak{q} = \min\left\{\xi\left(\overline{\omega} - \omega\right), -\Re\left(\omega - \underline{\omega}\right)\right\} > 0$. Now, we turn our attention on the functional Λ, introduced in (5.94). We notice that its derivative along the trajectories of (5.43) satisfies,

$$\begin{aligned} \dot{\Lambda}(t) = & \tau Q(\tilde{u}(t)) - \int_{t-\tau}^{t} e^{\ell - t} Q(\tilde{u}(\ell)) d\ell - \Lambda(\tilde{u}_t) \\ \leq & \tau Q(\tilde{u}(t)) - e^{-\tau} \Theta(\tilde{u}_t) - \Lambda(\tilde{u}_t) \\ \leq & \tau \xi Q(\tilde{x}(t)) + \tau(\Re + 1) Q(\tilde{u}(t-\tau)) + \tau a_1 |\tilde{x}(t)| Q(\tilde{x}(t)) \\ & + \tau a_2 |\tilde{x}(t)| Q\left(\tilde{u}(t-\tau)\right) - e^{-\tau} \Theta(\tilde{u}_t) - \Lambda(\tilde{u}_t), \end{aligned} \tag{5.109}$$

where the last inequality is a consequence of (5.103). Now, by combining (5.109) and (5.108), we straightforwardly conclude that the derivative of the functional,

$$\mathscr{U}(\tilde{x}(t), \tilde{u}_t) = V(\tilde{x}(t), \tilde{u}_t) + \mathfrak{p} \Lambda(\tilde{u}_t), \tag{5.110}$$

where, $\mathfrak{p} = \frac{\mathfrak{q}}{2\tau\max\{\xi,\Re+1\}}$, along the trajectories of (5.43), satisfies,

$$\begin{aligned}\dot{\mathscr{U}}(t) \leq &-\frac{\mathfrak{q}}{2}Q(\tilde{x}(t)) - \frac{\mathfrak{q}}{2}Q(\tilde{u}(t-\tau)) + \left[a_1(\omega+\tau\mathfrak{p})+z_1\right]|\tilde{x}(t)|Q(\tilde{x}(t)) \\ &+ a_2(\omega+\tau\mathfrak{p})|\tilde{x}(t)|Q(\tilde{u}(t-\tau)) - \mathfrak{p}e^{-\tau}\Theta(\tilde{u}_t) - \mathfrak{p}\Lambda(\tilde{u}_t).\end{aligned} \tag{5.111}$$

Since $|\tilde{x}(t)| \leq \sqrt{2\mathscr{U}(\tilde{x}(t),\tilde{u}_t)}$, we deduce that,

$$\begin{aligned}\dot{\mathscr{U}}(t) \leq &-\left[\frac{\mathfrak{q}}{2} - \left[a_1(\omega+\tau\mathfrak{p})+z_1\right]\sqrt{2\mathscr{U}(\tilde{x}(t),\tilde{u}_t)}\right]Q(\tilde{x}(t)) \\ &-\left[\frac{\mathfrak{q}}{2} - a_2(\omega+\tau\mathfrak{p})\sqrt{2\mathscr{U}(\tilde{x}(t),\tilde{u}_t)}\right]Q(\tilde{u}(t-\tau)) \\ &-\mathfrak{p}e^{-\tau}\Theta(\tilde{u}_t) - \mathfrak{p}\Lambda(\tilde{u}_t).\end{aligned} \tag{5.112}$$

Therefore, for all initial conditions $\tilde{x}(0)$ and $\tilde{\varphi}_u$, satisfying

$$\mathscr{U}(\tilde{x}(0),\tilde{\varphi}_u) < \overline{\mathscr{U}}, \tag{5.113}$$

where,

$$\overline{\mathscr{U}} = \min\left\{\left(\frac{\mathfrak{q}}{4\sqrt{2}\left[a_1(\omega+\tau\mathfrak{p})+z_1\right]}\right)^2, \left(\frac{\mathfrak{q}}{4\sqrt{2}a_2(\omega+\tau\mathfrak{q})}\right)^2\right\}, \tag{5.114}$$

the derivative of the functional $\mathscr{U}$ satisfies:

$$\dot{\mathscr{U}}(t) \leq -\frac{\mathfrak{q}}{4}Q(\tilde{x}(t)) - \mathfrak{p}e^{-\tau}\Theta(\tilde{u}_t) - \mathfrak{p}\Lambda(\tilde{u}_t). \tag{5.115}$$

Finally, we conclude that:

$$\dot{\mathscr{U}}(t) \leq -\mathfrak{r}\mathscr{U}(\tilde{x}(t),\tilde{u}_t), \quad \text{where,} \quad \mathfrak{r} = \min\left\{1, \frac{\mathfrak{p}e^{-\tau}}{\omega}, \frac{\mathfrak{q}}{4}\right\}. \tag{5.116}$$

By virtue of the Lyapunov-like functional, $\mathscr{U}$, we conclude that $\tilde{x}$ converges **exponentially** to its origin with a **decay rate** smaller or equal to $\frac{\mathfrak{r}}{2}$.
Moreover, using the second equation in (5.43), we see from Lemma 1 that $\tilde{u}$ converges exponentially to its origin, since the condition $\underline{\omega} > 0$ (i.e., $\Re < 0$) implies that $2Ke^{-\gamma\tau} < 1$.
Finally, notice that the set of all initial conditions satisfying the condition (5.113) provides an estimate of the **basin of attraction** of the origin of the shifted system (5.43). Therefore, the set

$$\mathscr{A} = \left\{x(0) \in \mathbb{R}^+, \varphi_u \in \mathscr{PC}\left([-\tau,0],\mathbb{R}^+\right), \mathscr{U}\left(x(0)-x_e, \varphi_u - u_e\right) < \overline{\mathscr{U}}\right\}, \tag{5.117}$$

where the sublevel $\overline{\mathscr{U}} > 0$ is given in (5.114), is a subset of **the basin of attraction of the strictly positive equilibrium E of the positive system** (6.8).

□

Example 8. *Here we give a numerical example that satisfies the conditions of existence of E (i.e. Proposition 4) and also the decay conditions provided in Theorem 12. We consider the following biological parameters and functions:* $\tau = 1$, $\beta(m) = \frac{2.78}{1+m^3}$, $\delta = 0.9$, $\gamma = 0.4$, *and where the rate of permanently proliferating cells is* $K = 0.2$.

After simple calculations we get,

$$\mu = \frac{\beta(0)}{\delta} = 3.088888,\ \overline{K} = \frac{1}{2}e^{\gamma\tau} = 0.745912,\ \underline{K} = (\mu+1)\overline{K} - \mu = -0.038936, \tag{5.118}$$

and, $s = \underline{K} - K = -0.238936$. *It follows that the origin is not attractive.*

Next, the first condition in Proposition 4 is satisfied, i.e.,

$$0 < \underbrace{K}_{0.2} < \underbrace{\overline{K}}_{0.745912} < \underbrace{\frac{\mu}{\mu+1}}_{0.755434}, \tag{5.119}$$

and, consequently, a unique strictly positive steady state exists. This equilibrium is given by:

$$E = (x_e, u_e),\ \textit{where},\ x_e = 0.7592526,\ \textit{and},\ u_e = 2.006009. \tag{5.120}$$

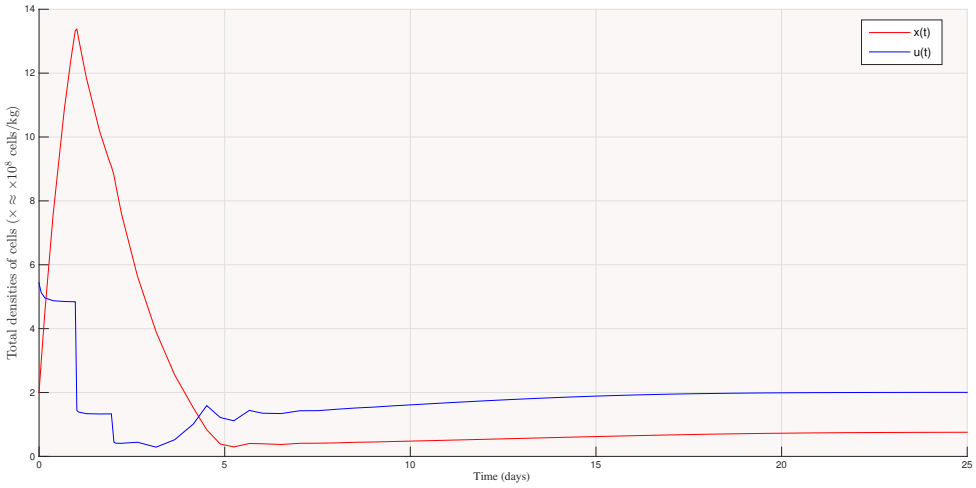

Fig. 5.10 The trajectories of the differential-difference nonlinear system (6.8), for the model paramaters given in Example 8.

Simple calculations give:

$$\begin{aligned}
&\theta = \beta(x_e) + x_e\beta'(x_e) = 0.167633, \quad \xi = \theta^2 + 2K|\theta|e^{-\gamma\tau} = 0.073048,\\
&\mathfrak{K} = \left(2Ke^{-\gamma\tau}\right)^2 + 2K|\theta|e^{-\gamma\tau} - 1 = -0,883160,\\
&\overline{\omega} = \frac{2\left(\delta + \theta - Le^{-\gamma\tau}\right)}{\xi} = 14.548691, \quad \underline{\omega} = -\frac{2Le^{-\gamma\tau}}{\mathfrak{K}} = 1.214402.
\end{aligned} \tag{5.121}$$

We conclude that the decay condition $0 < \underline{\omega} < \overline{\omega}$ is satisfied, and therefore E is regionally exponential stable. It is worth mentioning that in simulations, the region of attraction seems to be the entire positive orthant, i.e. the estimate provided in Theorem 12 is conservative, as it is generally the case with Lyapunov approaches. For an arbitrary initial condition, the trajectories of the corresponding system are shown in the Figure 5.10.

5.5 Concluding remarks and discussion

In this chapter, we revisited the analysis of a recent biological differential-difference system ([4]), describing the stem cell dynamics. The feature of the proposed approach is that it is based on Lyapunov-like techniques. This corresponds with our aim of extending the analysis and the modeling aspects of the hematopoietic system. Indeed, the studied model has the interesting feature of allowing a sub-population of stem cells to be permanently active in the proliferating phase. Two steady states may exist: the 0-equilibrium, and, under some conditions on the biological parameters, a strictly positive steady state.

We revisited the stability properties of the 0-equilibrium by extending the Lyapunov construction of [4], in order to establish global exponential stability of the trajectories. The positivity of the studied system is an asset that allows its analysis through linear Lyapunov functionals ([124]). Since linear functionals are more convenient for the analysis and the computations, we focused on the second part on whether it was possible to define a framework to study the stability properties of the strictly positive equilibrium point using a linear Lyapunov functionals (knowing that the trajectories we are interested in are no longer all positive when studying the positive equilibrium point, after a classical change of coordinates). For that purpose, the first step that we performed was the determination of a linear *Comparative System* ([250]). The origin of the latter system has the particularity of being globally exponentially stable if it is exponentially stable on only the positive orthant ([196]). Then, some global decay conditions were derived via a construction of a suitable linear functional. Exploitation of that study in the case of our hematopoietic system, together with the feasibility of the global results, were discussed through numerical applications. The characteristic nonlinear patterns for the specific studied model made the global decay conditions less conservative for large initial conditions. For the local study (i.e. in the neighborhood of the positive steady state), a more classical analysis was performed, via a quadratic Lyapunov-like construction. Sufficient conditions for the regional exponential stability of the positive equilibrium were provided, with a subset of its basin of attraction.

Chapter 6

A coupled model between healthy and mutated stem cells: cancer dormancy and eradication of cancer stem cells

Synopsis. An age-structured McKendrick model describing the coexistence between tumor and ordinary stem cells is developed and explored. Firstly, the model is transformed into a nonlinear time-delay system that describes the dynamics of healthy cells, coupled to a nonlinear differential-difference system governing the dynamics of unhealthy cells. Then, its main features are highlighted and an advanced stability analysis of several coexisting steady states is performed, through a Lyapunov-like approach for descriptor-type systems. We pursue an analysis that provides a theoretical treatment framework following different medical orientations, among which: i) the case where therapy aims to eradicate cancer cells while preserving healthy cells, ii) a less demanding, more realistic, scenario that consists in maintaining healthy and unhealthy cells in a controlled stable steady-state (cancer dormancy). Biological interpretations and therapeutic strategies are discussed according to our findings throughout the chapter.

6.1 Overview of the chapter

We recall that sometimes a pathological population of cells, that does not initially necessarily belong to the SC family, acquires self-renewing and proliferating capabilities similar to those of SCs ([93], [94], [230]). These stem-like cells are very often out of control [247] and they are capable of initiating, developing and regenerating cancers [93], hence their designation as cancer stem cells (CSCs) [150].

Very often, CSCs are characterized by unhealthy behaviors such as excessive proliferation and abnormal loss of their differentiation faculties (this is what we observe in leukemia [147], for instance). On the other hand, it cannot be disregarded that in some cases (as in breast cancer and leukemia [88], [18]) CSCs do not overproliferate (cancer without disease [102], or, *in situ* tumor). However, even during

their non-overproliferating states, CSCs remain in general distinguishable through specific markers on their surface[1] [247].

Strong evidence about the existence of this stalled growth (i.e. tumor dormancy), has been established many years ago when microscopic tumors were frequently encountered during autopsy examinations ([220], [102]). More details are given in Chapter 2, however, the most likely explanations (see [15], and also [261] and [102]) of CSCs dormancy state are: i) blood and nutrient supply issues that prevent tumor growth, or at least delay its clinical manifestation [213], and ii) vigilance of the immune system which, in some rare cases, suffices to stop tumor development (see [98, 261, 213, 299, 291] and the references therein). In fact, there has been a lengthy debate on the role of the immune system in the defense against cancer: a process called *cancer immunosurveillance* [291]. The ambiguity about the immunosurveillance concept stems from the fact that often the immune system favors the development of the tumor instead of trying to eliminate it. The concept that attempts to integrate the diverse effects of the immune system on tumor progression is known as *cancer immunoediting* (see the review articles [261] and [291]). However, even if it appears as an unsystematic process, the immune response remains one of the most likely justifications for cancer dormancy.

Not surprisingly, an interest arises for cancer therapies that are oriented on the immune system, bearing the name of *immunotherapy*[2]. In a similar spirit, monoclonal antibodies, e.g. gemtuzumab ozogamicin, have been approved in the treatment protocols of some cancers (as in acute myeloid leukemia [115]), even if more trials are still needed to identify their exact benefits [253, 115]. Other cancer therapies, sometimes assimilated to immunotherapy, are using some *immune checkpoint inhibitors* (see for instance, [228], [169] and [44]). In the last part of our work, we will be shortly adopting some of these immuno-oriented concepts, associated with classical chemotherapy, as it is frequently adopted in practice.

In a general perspective, apart from the interpretation of tumor dormancy as an observed natural phenomenon in human cancers, the idea to transform cancer into a chronic disease is in the voices of many people in the medical world nowadays [111], [14]. Indeed, the interesting issue here is about: *how can we bring CSCs from an overproliferating activity to a dormant state?* More precisely, since cancer treatments most often consist of delivering the maximum tolerable doses of drugs in order to kill diagnosed tumors, and knowing that a non-completely eradicated tumor frequently grows again, even more aggressively than the initial one [93], the option of maintaining the tumor in dormancy is more appealing than trying to eradicate it [147]. Further discussions on the opportunities offered by cancer dormancy in therapeutics can be found for instance in [14], [289], [111], and the references therein.

The development of a relevant mathematical framework appears as a necessary tool to apprehend tumor dormancy as a biological mechanism [154], with the ultimate goal to apply it in therapeutic settings. However, the task of mastering CSCs, i.e. bringing them into a dormant state, seems to be difficult to conduct. Indeed, one of the first dormancy-oriented therapeutic approaches has not been very fruitful. It was based on the use of *angiogenesis inhibitors* (substances that inhibit the growth of new blood vessels [102]) as drugs that choke off the blood supply of the tumor, in order to maintain it in dormancy. However,

[1] For instance, stems cells in acute myeloid leukemia have some *interleukin-3–receptor α chain* surface markers, which are not found in normal hematopoietic stems cells (see [150, 99]).

[2] Immunotherapy aims to help the immune system destroy cancer cells. It is given after -or at the same time as- another cancer treatment such as chemotherapy. (`http://www.cancer.net/`) - See also Chapter 2 for related facts related to tumor dormancy.

unexpected effects occurred in practice, in some situations, where targeting the blood vessels that feed tumors actually accelerated the spread of cancer [134], [248].

In the clinic of cancers today, eradication of CSCs remains the predominant treatment approach (although there is still a long way to improve the existing eradication treatment strategies [277]). In light of the previously mentioned observations, one can say that dormancy has actually generated more issues than answers, in the process of understanding cancer. Among the open issues, we emphasize the following ones: *when a treatment protocol is elaborated for CSCs eradication with a given rate of success, how can we actually administer it (or a part of it) in order to achieve dormancy?* In addition, since eradication techniques may generate some surviving tumors which become even more aggressive than the initial ones, a key question is to determine *whether it is effective to consider the same targets and drugs, as for CSCs eradication, in order to achieve dormancy?* One can already figure out the utility of mathematical studies in such a context.

Objectives of the chapter

We aim to provide a consistent theoretical framework for the modeling and the analysis of healthy and unhealthy cell dynamics, following different medical orientations, among which: the case where therapy aims to eradicate cancer cells while preserving healthy ones, and the scenario that consists in maintaining healthy and unhealthy cells in a controlled stable steady-state (i.e. cancer dormancy). To that purpose, a model of cohabitation between ordinary and mutated cells is introduced and analyzed. Firstly, we investigate the stability properties of the origin of the resulting model: this is equivalent to the radical case in which all the cells are eradicated. Then, we perform a stability analysis that applies to cases of cancer dormancy and unhealthy cell eradication (while healthy cells survive). For the biological motivations stated here and in Chapter 2, we focus more on the study of cancer dormancy throughout the chapter.

As it is the case throughout the thesis, we emphasize in the current study the particular case of hematopoietic SCs, which are at the root of the hematopoietic system (Chapter 2). We recall that hematopoiesis is a complex process in which the number of hematopoietic SCs involved in proliferation, together with their frequency of division, have to be well controlled [138] in order to avoid a wide range of blood disorders[3]. Currently, AML treatment still relies on heavy chemotherapy with a high toxicity level and a low rate of success [85]. In fact, the only certain AML cure being not the result of chemotherapy, but of total bone marrow transplant (that induces nearly $10-20\%$ of mortality during the manipulation and due to severe reaction, GVH, of the graft versus the host).

In this chapter, a better understanding of the behavior of CSCs (leukemic cells in AML) should allow us to propose some selective combined targeted therapies that lead, theoretically, to cancer dormancy. In particular, our ambition is to provide a relevant theoretical framework, taking into account observations made by hematologists, and allowing for the suggestion of new treatments insights. It is in this light that we propose in this chapter a model of cohabitation between ordinary and mutated cells in the case of the hematopoietic system.

[3] In particular, periodic diseases, such as cyclic neutropenia and some cases of chronic acute leukemia ([184], [37], [66], [180], and the references therein), but also overproliferating malignant hemopathies, such as acute myeloid leukemia (see the definitions in Chapter 2, and the models in [8], [225], [80]).

This model follows recent observations (made in [137] and in many other works) that associate the emergence of leukemic cells to an accumulation of several mutations, most often occurring in a standard chronological order, in the SC compartment. Thus, we analyze here two categories of heterogeneous cells as illustrated in Figure 6.1, where the addition of mutations (TET2, NPM1, FLT3) that we have consider had been established in [137].

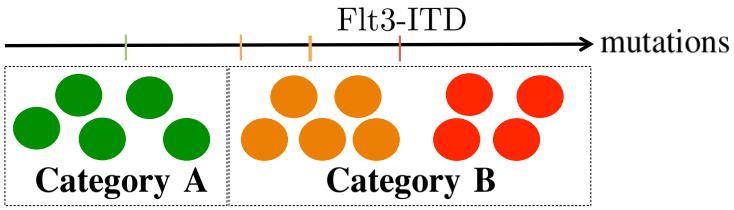

Fig. 6.1 **Category A:** healthy stem cells. **Category B:** unhealthy stem cells. The latter class (B) has a first mutation in some genes encoding enzymes in epigenetics (e.g. TET2, DNMT3A [74, 239]), that increases the self-renewing activity of the affected cells. A more serious pathological situation arises when a second mutation, affecting this time the pathways regulating the differentiation process such as NPM1 or transcription factors, appears on some of the cells. The superposition of these two events yields a blockade in differentiation (the subpopulation in orange color). Finally, a subsequent mutation impairing proliferation control (e.g. FLT3) appears in a subpopulation of cells that have already accumulated one or more of the previously mentioned mutations. The latter event activates an uncontrolled overproliferation of a subpopulation of cells, CSCs (in red), and thereby causes AML [137].

The study that we perform in this chapter generalizes the one that we proposed in a series of works: [4], [23], [25], (but see also [241], [189], [101], [276], [275], [8], [225], [81]). It is worth mentioning that the model in [25], [23] can neither model dormancy nor the abnormal overproliferation (e.g. invasion of the bone marrow by blasts). The latter point is improved by adopting a different form of fast self-renewing process, which has been recently introduced in [4], and where a subpopulation of cells is considered to be always active in proliferation. In fact, cancer dormancy has not been considered in all the previously mentioned works[4].

Organization of the chapter

In light of the above mentioned remarks, the coupled model (between healthy and mutated cells as in Figures 6.1-6.2) of interest is presented in Section 6.2.

Next, some features of the resulting coupled differential-difference model, together with the conditions of existence of our favourable steady states (reflecting dormancy and CSCs eradication), are discussed in Section 6.3. Then, in Section 6.4, the stability analysis of the case of all-cell extinction, via a construction of a linear Lyapunov-like functional, is performed (here we provide conditions for global exponential stability of the origin of the coupled model).

Then, afterwards, we address in Section **??** the stability analysis, in the time-domain framework, of the cases describing cancer dormancy or unhealthy cells eradication (while healthy cells survive). The latter study goes through quadratic Lyapunov-like constructions (i.e. suitable degenerate functionals for the class of differential-difference systems).

[4] See also [154] for a different approach of modeling and analysis, where an ODE system describing dormancy is discussed, but without considering the coexistence between healthy and unhealthy cells.

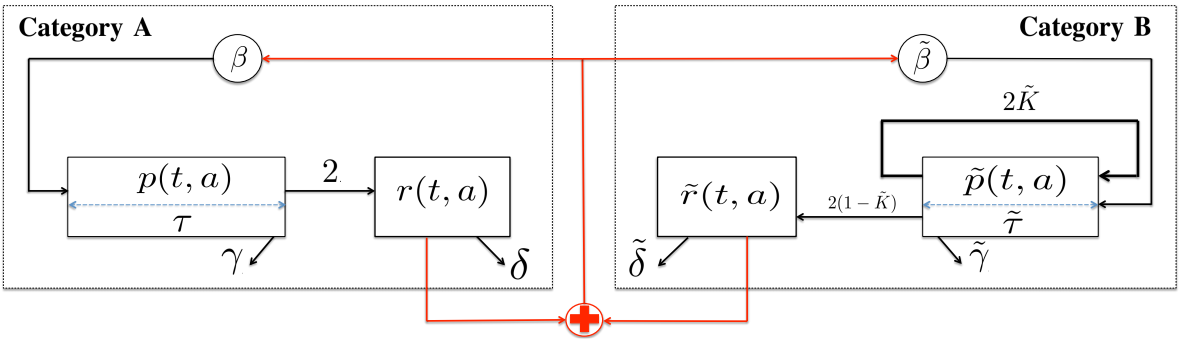

Fig. 6.2 Schematic representation of the coupled model of interest, involving a healthy SCs compartment (on the left) and an unhealthy compartment (on the right). For the sake of simplicity, we assume that unhealthy cells are those presenting mutations that lead to cancer (cells in orange and cells in red in Figure 6.1). Thus, with an abuse of notation, we use equivalently the designations: unhealthy cells, mutated cells, and CSCs. Similarly, healthy cells, or ordinary cells, represented on the left of the figure, are those which do not have any abnormal mutation, or those presenting some abnormalities but are not related with cancer. The definition of the biological parameters given in this figure is provided in Section 6.2.

In fact, we are going to use two slightly different constructions: the first one is more general and relies on LMI conditions derived via the *descriptor* method [106], applied to the linear approximation of the model around its nontrivial steady state of interest. This approach aims to provide a theoretical (sufficient) stability criterion, in the LMI form, to establish whether the steady state of a specific biological system is locally stable. The latter technique is followed by a second Lyapunov-type construction that allows us to determine *explicit* decay conditions (not in the LMI form) as well as an estimate of the decay rate of solutions and an approximation of the basin of attraction of the studied steady state. These sufficient stability conditions may be more restrictive than the LMI ones, however, they have the advantage of being easier to handle and, therefore, make it possible to interpret them biologically, from medical and therapeutic standpoints.

Finally, numerical illustrations are provided and concluding discussions (including biological interpretations of the findings) are outlined in Section 6.5.

6.2 A new mathematical model involving coexistence between healthy and cancer stem cells

Our objective is to introduce a more general model than the existing ones, with regard to the recent biological features of interest, that are: mutations accumulation [137], cancer dormancy [93] ,[88], control and eradication of CSCs [147]. In particular, the model that we want has to take into account the cohabitation between healthy and unhealthy cells, to reproduce and interpret the case of cancer dormancy, with the ultimate goal of providing theoretical stability conditions, along with therapeutic insights, that lead to stable dormant CSCs.

6.2.1 A multi-compartmental model for healthy and unhealthy cells

We focus on the model illustrated in Figure 6.2, where CSCs are characterized by an over-proliferating ability represented by the parameter $\tilde{K}$, as considered in [4], and previously envisaged in [25, 23] in a different configuration. One notices that the model in [80] is similar to the one in Figure 6.2, however, the models of healthy and unhealthy cells studied in [25, 80, 23] do not admit a stable steady state that describes cancer dormancy. In fact, this issue is overcome by considering a more general manner of coupling healthy and unhealthy SCs, while retaining the same model structure as in [80] (Figure 6.2). Finally, we mention that as many other works (see [180, 241, 8], among others), we are considering a compartmental model in which each cell can be in a resting phase or in a proliferating one.

We notice in Figure 6.2 that a sub-population of unhealthy cells is in a permanent dividing state, i.e. the portion $2\tilde{K}$, where, $0 < \tilde{K} < 1$, as in [4] for a non-coupled model. This is different from the healthy SCs behavior (Figure 6.2, on the left) where daughter cells, that arise from mother-cells division, leave the proliferating compartment and join necessarily the resting one, where they can stay until their death, differentiate, or start a new proliferating cycle by passing through the reintroduction function β. Next, we denote by δ (resp. $\tilde{\delta}$) the rate of resting cells which is lost either by differentiation or natural cell death for healthy SCs (resp. CSCs). A resting cell may start a cell cycle by entering in the proliferating phase during which each proliferating SC (resp. CSC) may die by apoptosis at a rate γ (resp. $\tilde{\gamma}$), or complete its mitosis and become two daughter cells at the end of the proliferating phase. We denote τ (resp. $\tilde{\tau}$) the average time taken to complete mitosis in the healthy (resp. unhealthy) proliferating compartment.

For proliferation, the mechanisms regulating the entry into the cell cycle -at the cellular level- rely on some regulatory molecules that can play the role of growth-factors (by stimulating the entry into proliferation of resting healthy and unhealthy cells), or, they can play the role of mitotic inhibitor ligands (meaning that mitosis proceeds normally if inhibitors are not combined with cell receptors, while it is stalled when they bind them). Consequently, we consider in our model that the passing from the resting to the proliferating states is controlled by some reintroduction functions (as in [180, 241] and the majority of earlier works). More precisely, we let β (resp. $\tilde{\beta}$) be the reintroduction function from the healthy (resp. unhealthy) resting phase to the healthy (resp. unhealthy) proliferating phase.

In addition, since healthy and unhealthy cells share the same environment (called *niches* [69] in hematopoiesis), we consider that each of the two functions β and $\tilde{\beta}$ depend simultaneously on both: the total density of resting healthy cells, $x(t) = \int_0^\infty r(t,a)da$, and, the total density of unhealthy resting cells, $\tilde{x}(t) = \int_0^\infty \tilde{r}(t,a)da$, where $r(t,a)$ and $\tilde{r}(t,a)$ are, respectively, the densities of resting healthy cells and resting unhealthy cells, of age $a \geq 0$, at time $t \geq 0$ [80]. This modeling approach reflects cohabitation between healthy and unhealthy cells: by considering that the entry into proliferation of healthy cells (resp. unhealthy cells) is also dependent on the total density of unhealthy cells (resp. healthy cells), the dynamics of the left and the right sub-populations in Figure 6.2 become thus strongly coupled (linked in red color in Figure 6.2).

In summary, we consider that the reintroduction functions β and $\tilde{\beta}$ are controlled by some mitotic regulatory molecules (that are either secreted by the body or administrated as drug doses), which are in turn assumed to be related to the cell densities x and $\tilde{x}$ (i.e. the concentration of the regulatory molecules is

proportional to the cell density, as developed in [180] for a non-coupled model). More details are provided in the next section.

6.2.2 The coupling form between ordinary and mutated cells

Now, the remaining issue regarding the functions β and $\tilde{\beta}$ is to select the coupling function between the total density of healthy resting cells x and the total density of mutated resting cells $\tilde{x}$ (i.e. specifying how β and $\tilde{\beta}$ actually depend on x and $\tilde{x}$). It appears that the simplest choice is to consider that both β and $\tilde{\beta}$ depend on the sum $x+\tilde{x}$, as previously considered in [25] and [80]. The latter scheme expresses a kind of absence of dominance between the populations x and $\tilde{x}$, since they show equal influence on β and $\tilde{\beta}$. However, differences actually exist between x and $\tilde{x}$ in their shared host environment, mainly due to the mutations acquired by abnormal cells [139]. Changes that occur in mutated cell behavior may enhance the growth of cancer and result in cachexia and death [33] (see also [91, 237] and the references therein, for biological observations and modeling of the interaction between unhealthy cells and their host environment).

We might be tempted to argue that, in our particular context, considering a coupling in the form $x+\tilde{x}$ may be a result of an homogeneous sensitivity[5] expressed by the resting ordinary and mutated populations to the concentration of mitotic regulatory molecules, that act on the reintroduction mechanisms of resting cells into proliferation. This is in fact a particular situation (considered in [23], [26]), which corresponds to the cases (b)-(c) in Figure 6.3, where we notice that mutated resting cells in orange (c), and ordinary resting cells in green (b), are reacting with (or, sensitive to) the same concentration of regulatory molecules (small molecules represented in blue).

In turn, by generalizing the arguments used in [180] for a non-coupled model by assuming that the concentration of the mitotic regulatory molecules (in blue) is proportional to the total density $\tilde{x}+x$ (green and orange cells). Thus, homogeneity between $\tilde{x}$ and x in that case means that healthy cells (green cells (b)) and unhealthy resting cells (in orange (c)) have a common interpretation of their shared host environment. We aim in the present work (in contrast with [23]) to extend the modeling aspects by considering a more general form of coupling functions, so that one subpopulation may dominate the other one. For that purpose, we consider that β depends on a function $C(x,\tilde{x})$, while $\tilde{\beta}$ depends at the same time on a different combination $\tilde{C}(x,\tilde{x})$. In particular, we are interested in the case of linear functions in the forms: $C=\alpha x+\tilde{x}$ and $\tilde{C}(x,\tilde{x})=x+\tilde{\alpha}\tilde{x}$, where, α and $\tilde{\alpha}$ are some positive weighted constants. In that framework, the previous situation expressing a homogeneous sensitivity $C=\tilde{C}$ (i.e. as in [23, 26]), becomes a particular case characterized by $\alpha=\tilde{\alpha}=1$.

[5] **Sensitivity** here is related to the **dominance** property that healthy or unhealthy resting sub-populations may express. More precisely, it refers to the different perception carried on the same common host environment of healthy and unhealthy cells, while some of them are more sensitive to certain molecules (e.g. ligands) and less sensitive to the others. For example, due to epigenetic mutations, unhealthy cells become **less sensitive** than healthy ones to the regulatory molecules secreted by the body, while healthy cells are **less sensitive** to drugs since they are designed to target unhealthy cells. These situations show how healthy and unhealthy cells may react differently to their shared host environment in which they live (see Figure 6.3), which later results in the dominance of one subpopulation. For further information, notice that in biological systems and enzyme kinetics, *sensitivity* has different meanings. The most used one refers to the sigmoidally shaped response behavior (*responsiveness*, see [**?**]-Section 6). In our application, it is worth mentioning that the reintroduction functions β and $\tilde{\beta}$ behave in a sigmoidal manner (Hill functions, see [**?**]), but it is not our intended meaning of sensitivity here, which is rather related to the concept of dominance, as explained above.

In fact, to ease the notation, we can normalize without loss of generality the value of α, i.e. $\alpha = 1$, that becomes a reference (6.3-(b)) describing a healthy case. It follows that the free-parameter $\tilde{\alpha}$ varies relatively to that reference: $\tilde{\alpha} < 1$ (Figure 6.3-(d)), $\tilde{\alpha} > 1$ (Figure 6.3-(e)), or $\tilde{\alpha} = 1$ (Figure 6.3-(c)). Thus, throughout the paper, we focus on the situation where α is normalized and $\tilde{\alpha} > 0$ is a free parameter, i.e. $(\alpha, \tilde{\alpha}) = (1, \tilde{\alpha})$. We will prove later in Section 6.3 that actually dormancy may exist only if $\tilde{\alpha} \neq 1$.

In illustrative manner, we observe that Figure 6.3-(d) provides a cartoon representation of the case $\tilde{C}(x, \tilde{x}) = x + \tilde{\alpha}\tilde{x}$, when $\tilde{\alpha} < 1$, compared to the neutral case (without dominance), $C(x, \tilde{x}) = \tilde{C}(x, \tilde{x}) = x + \tilde{x}$, described by the couple of Figures 6.3-(b)-(c), where regulatory molecules are equal. The case of Figure 6.3-(d) means that even if ordinary and mutated cells are sharing the same environment, the mutated ones indicated in orange 6.3-(d) are less sensitive to the regulatory molecules, present in the host environment, that we consider to be inhibitors which decrease cell proliferation (as previously envisaged in [180]).

This appears to be in line with medical practice, since the unhealthy behavior is mainly due to epigenetic mutations that make cells partially unresponsive to the regulating system. Therefore, the case $\tilde{\alpha} < 1$ suits well the untreated unhealthy behavior, in which cells get out of control. Indirectly, the sensitivity parameter $\tilde{\alpha}$ that we introduced, led to a concept of dominance between the healthy and mutated cells x and $\tilde{x}$.

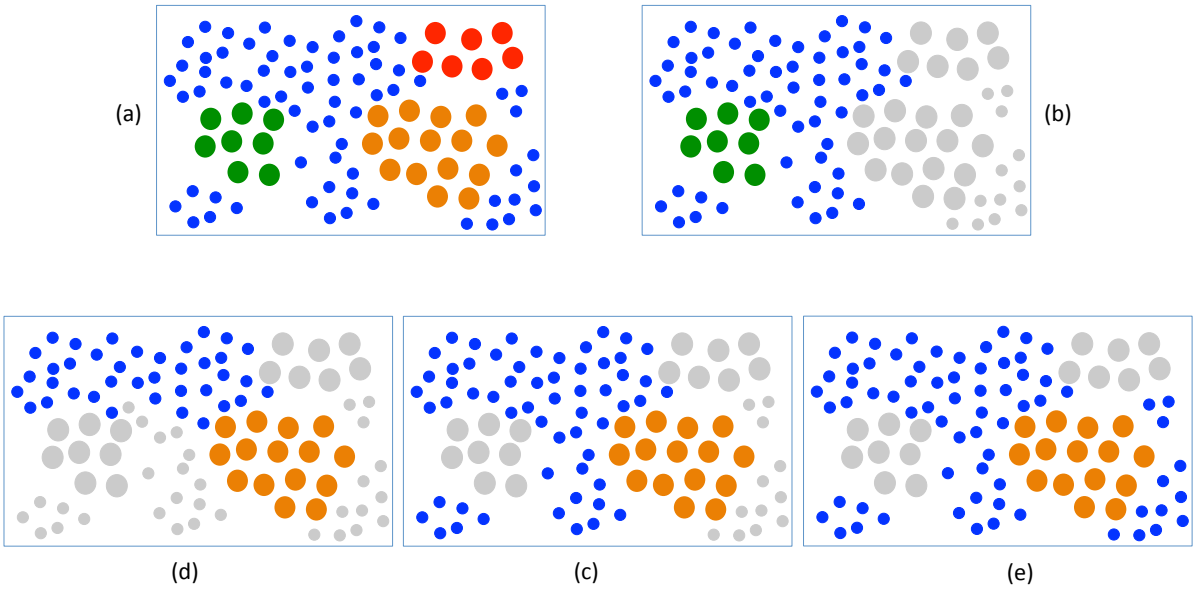

Fig. 6.3 Cartoon illustration of healthy and unhealthy cells in their shared environment. In **(a)**, red cells are the subpopulation of cells which is constantly active in proliferation, orange cells are unhealthy mutated cells that go through quiescence to re-start a cell-cyle, green cells are ordinary cells with normal behavior, while blue molecules represent natural mitotic regulatory molecules (inhibitor ligands), or drug molecules. The representation **(b)** gives a reference, which is the shared environment as regarded by healthy cells (the density of blue molecules is proportional to $x + \tilde{x}$. On their part, unhealthy cells perceive the same environment in the case where $\tilde{\alpha} = 1$, as illustrated in **(c)**. However, cells are expected to be different from healthy cells due to epigenitic mutations. The latter case in which unhealthy cells are out of control of a part of regulatory molecules is illustrated in **(d)** ($\tilde{\alpha} < 1$). Finally, the case where unhealthy cells are targeted by administrated drugs and by the body immune reaction (while healthy cells (**(b)** are spared) is illustrated in **(e)** ($\tilde{\alpha} > 1$).

On the other hand, the reverse situation corresponding to $\tilde{\alpha} > 1$, as illustrated in Figure 6.3-(e), describes an environment where unhealthy cells are more affected by the regulatory molecules than the

healthy population. This may be partially due to the immune system response (*cancer immunosurveillance* [291]) which may explain the dormancy phenomenon as a result of an effective immune action that contains cancer [299]. However, it can be effectively argued that the case $\tilde{\alpha} > 1$ relies on the use of drugs (chemotherapy, immunotherapy, etc.) that specifically target unhealthy cells. Indeed, we recall that recent drug molecules are increasingly more accurate due to their overexpression of cancer receptors, which allow them to target unhealthy cells while the majority of healthy cells are spared (Figures (b) and (e)). Therefore, it becomes reasonable to consider that during treatments, unhealthy cells are likely to be more sensitive (i.e. $\tilde{\alpha} > 1$) than healthy cells to the whole regulatory molecules in the host environment (Figures 6.3 -(e)-(b)).

Finally, it is worth mentioning that the introduction of the above considerations related to the coupling functions between x and $\tilde{x}$ will make the dynamics of the resulting model richer than earlier models, as discussed in the next sections (see Section 6.3). To the authors' knowledge, no equivalent model exists in the literature.

Next, as conventionally considered, we assume that $\tilde{\beta}$ and β are nonlinear continuous decreasing functions, and, $\lim_{\ell\to\infty}\tilde{\beta}(\ell) = \lim_{\ell\to\infty}\beta(\ell) = 0$. As in [180], [241], and all subsequent works for non-coupled models, we consider the typical Hill forms, belonging to the family of functions with negative Schwarzian derivatives (see [17], Chap. 3),

$$\tilde{\beta}(\ell) = \frac{\tilde{\beta}(0)}{1+\tilde{b}\ell^{\tilde{n}}},\ \beta(\ell) = \frac{\beta(0)}{1+b\ell^{n}} \tag{6.1}$$

where $\tilde{b}$, b, $\tilde{\beta}(0)$ and $\beta(0)$ are strictly positive real numbers and, $\tilde{n} \geq 2$ and $n \geq 2$. In our case, classical arguments on cooperativity of enzyme inhibition kinetics (see [156], and [242]), allow to determine the Hill-type expressions (6.1). The cooperative effect in our case results from the fact that the binding of one regulatory molecule on one extracellular -surface- receptor of one cell will affect the binding of subsequent regulatory molecules on other receptors of the same cell. Due to the above considerations on the heterogeneous sensitivity between healthy and unhealthy cells in the niches, we can readily deduce that for a given total densities x and $\tilde{x}$, the associated reintroduction functions β and $\tilde{\beta}$ actually operate according to:

$$\tilde{\beta}\left(x+\tilde{\alpha}\tilde{x}\right) = \frac{\tilde{\beta}(0)}{1+\tilde{b}\left(x+\tilde{\alpha}\tilde{x}\right)^{\tilde{n}}},\ \beta\left(x+\tilde{x}\right) = \frac{\beta(0)}{1+b\left(x+\tilde{x}\right)^{n}} \tag{6.2}$$

where we recognize $C(x,\tilde{x}) = x+\tilde{x}$ and $\tilde{C}(x,\tilde{x}) = x+\tilde{\alpha}\tilde{x}$, in the definition of the functions (Figure 6.4).

6.2.3 Equations describing the dynamics of coupled cell populations

After the description of the particular case of the reintroduction functions β and $\tilde{\beta}$ according to the variation of the cell densities x and $\tilde{x}$ (as in Figure 6.4), we now focus on the dynamical equations describing the populations of cells. Similarly to x and $\tilde{x}$, we denote by y and $\tilde{y}$, respectively, the total densities of proliferating healthy and unhealthy cells: $y(t) = \int_0^{\tau} p(t,a)da$, and, $\tilde{y}(t) = \int_0^{\tilde{\tau}} \tilde{p}(t,a)da$. The

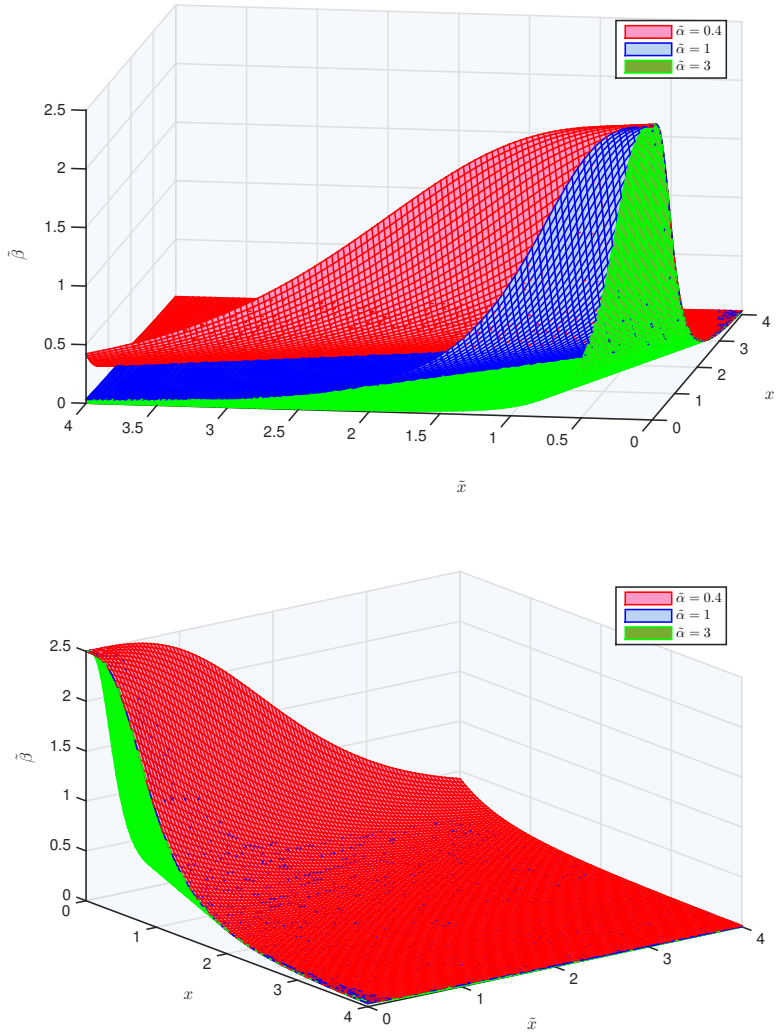

Fig. 6.4 Illustrative example of variations of a typical $\tilde{\beta}$-surface with respect to $\tilde{x}$ and x, for different values of $\tilde{\alpha}$ (i.e. in the three possible situations: $\tilde{\alpha} > 1$, $\tilde{\alpha} = 1$, and $\tilde{\alpha} < 1$).

age-structured PDEs describing the coupled model in Figure 6.2, are given for all $t > 0$ by:

$$\begin{cases} \partial_t \tilde{r}(t,a) + \partial_a \tilde{r}(t,a) = -\left[\tilde{\delta} + \tilde{\beta}\left(\tilde{C}(t)\right)\right] \tilde{r}(t,a), \quad a > 0, \\ \partial_t \tilde{p}(t,a) + \partial_a \tilde{p}(t,a) = -\tilde{\gamma}\tilde{p}(t,a), \quad 0 < a < \tilde{\tau}, \\ \partial_t r(t,a) + \partial_a r(t,a) = -\left[\delta + \beta\left(C(t)\right)\right] r(t,a), \quad a > 0, \\ \partial_t p(t,a) + \partial_a p(t,a) = -\gamma p(t,a), \quad 0 < a < \tau, \end{cases} \tag{6.3}$$

where, by abuse of notation, we set, $\tilde{C}(t) = x(t) + \tilde{\alpha}\tilde{x}(t)$, and, $C(t) = \tilde{x}(t) + x(t)$. As for all the McKendrick-type models, we recall that only the death rates (δ, $\tilde{\delta}$, γ and $\tilde{\gamma}$), and the removal terms (β and $\tilde{\beta}$, since the reintroduction functions are considered as cell loss from resting cells) appear in the PDE system (6.3). On the other hand, the new births, which are the renewal conditions at the age $a = 0$, for resting and

proliferating cells, are introduced through the following boundary conditions:

$$\begin{cases} \tilde{r}(t,0) = 2(1-\tilde{K})\tilde{p}(t,\tilde{\tau}), \\ \tilde{p}(t,0) = \tilde{\beta}(\tilde{C}(t))\tilde{x}(t) + 2\tilde{K}\tilde{p}(t,\tilde{\tau}) \stackrel{\Delta}{=} \tilde{u}(t), \\ r(t,0) = 2p(t,\tau), \\ p(t,0) = \beta(C(t))x(t), \end{cases} \tag{6.4}$$

for all $t > 0$. Finally, the initial age-distributions, respectively, $\tilde{r}(0,a) = \tilde{r}_0(a)$, for $a > 0$, $\tilde{p}(0,a) = \tilde{p}_0(a)$, for $0 < a < \tilde{\tau}$, $r(0,a) = r_0(a)$, for $a > 0$, and $p(0,a) = p_0(a)$, for $0 < a < \tilde{\tau}$, are assumed to be L^1-functions. Using the classical method of characteristics, we determine that:

$$\tilde{p}(t,a) = \begin{cases} e^{-\tilde{\gamma}t}\tilde{p}_0(a-t), & 0 \le t \le a \\ e^{-\tilde{\gamma}a}\tilde{p}(t-a,0), & t > a. \end{cases} \tag{6.5}$$

Consequently, the first equation in (6.4) is then equivalent to

$$\tilde{r}(t,0) = \begin{cases} 2(1-\tilde{K})e^{-\tilde{\gamma}t}\tilde{p}_0(\tilde{\tau}-t), & 0 \le t \le \tilde{\tau}, \\ 2(1-\tilde{K})e^{-\tilde{\gamma}\tilde{\tau}}\tilde{p}(t-\tilde{\tau},0), & t > \tilde{\tau}. \end{cases} \tag{6.6}$$

From biological considerations we set, $\lim_{a\to\infty}\tilde{r}(t,a) = \lim_{a\to\infty} r(t,a) = 0$, for all fixed value of $t \ge 0$.

Then, using (6.6), and by integrating the first equation in (6.3) with respect to a between 0 and $+\infty$, we determine that the long time behavior ([31]) of $\tilde{x}$ is given by

$$\dot{\tilde{x}}(t) = -\left(\tilde{\delta} + \tilde{\beta}\left(\tilde{C}(t)\right)\right)\tilde{x}(t) + 2(1-\tilde{K})e^{-\tilde{\gamma}\tilde{\tau}}\tilde{u}(t-\tilde{\tau}),$$

where, $\tilde{u}(t)$, as defined in (6.4), represents for all $t > 0$ the density of new unhealthy proliferating cells. Similarly, by integrating the second equation in (6.3) over the variable a, between 0 and $\tilde{\tau}$, and using $\tilde{p}(t,\tilde{\tau}) = \tilde{u}(t-\tilde{\tau})$, we get,

$$\dot{\tilde{y}}(t) = -\tilde{\gamma}\tilde{y}(t) + \tilde{\beta}\left(\tilde{C}(t)\right)\tilde{x}(t) - (1-2\tilde{K})e^{-\tilde{\gamma}\tilde{\tau}}\tilde{u}(t-\tilde{\tau}).$$

Using similar arguments for the healthy compartment, we obtain for all $t > 0$ the following overall-system,

$$\begin{cases} \dot{\tilde{x}}(t) &= -\left[\tilde{\delta} + \tilde{\beta}\left(\tilde{C}(t)\right)\right]\tilde{x}(t) + 2(1-\tilde{K})e^{-\tilde{\gamma}\tilde{\tau}}\tilde{u}(t-\tilde{\tau}), \\ \dot{\tilde{y}}(t) &= -\tilde{\gamma}\tilde{y}(t) + \tilde{\beta}\left(\tilde{C}(t)\right)\tilde{x}(t) - (1-2\tilde{K})e^{-\tilde{\gamma}\tilde{\tau}}\tilde{u}(t-\tilde{\tau}), \\ \tilde{u}(t) &= \tilde{\beta}\left(\tilde{C}(t)\right)\tilde{x}(t) + 2\tilde{K}e^{-\tilde{\gamma}\tilde{\tau}}\tilde{u}(t-\tilde{\tau}), \\ \dot{x}(t) &= -\left[\delta + \beta(C(t))\right]x(t) + 2e^{-\gamma\tau}\beta(C(t-\tau))x(t-\tau), \\ \dot{y}(t) &= -\gamma y(t) + \beta(C(t))x(t) - e^{-\gamma\tau}\beta(C(t-\tau))x(t-\tau). \end{cases} \tag{6.7}$$

The triangular structure of the previous system leads us to study first:

$$\begin{cases} \dot{\tilde{x}}(t) = -\left[\tilde{\delta} + \tilde{\beta}\left(x(t) + \tilde{\alpha}\tilde{x}(t)\right)\right]\tilde{x}(t) + 2(1-\tilde{K})e^{-\tilde{\gamma}\tilde{\tau}}\tilde{u}(t-\tilde{\tau}), \\ \tilde{u}(t) = \tilde{\beta}\left(x(t) + \tilde{\alpha}\tilde{x}(t)\right)\tilde{x}(t) + 2\tilde{K}e^{-\tilde{\gamma}\tilde{\tau}}\tilde{u}(t-\tilde{\tau}), \\ \dot{x}(t) = -\left[\delta + \beta\left(x(t) + \tilde{x}(t)\right)\right]x(t) + 2e^{-\gamma\tau}\beta\left(x(t-\tau) + \tilde{x}(t-\tau)\right)x(t-\tau). \end{cases} \tag{6.8}$$

We can prove that a unique piecewise continuous solution, $\left(\tilde{x}(t), \tilde{u}(t), x(t)\right)$, exists for all $t \geq 0$, when system (6.8) is associated with appropriate initial conditions $(\varphi_{\tilde{x}}, \varphi_{\tilde{u}}, \varphi_x)$, where, $\varphi_{\tilde{x}} \in \mathscr{C}\left([-\tau, 0], \mathbb{R}\right)$, $\varphi_x \in \mathscr{C}\left([-\tau, 0], \mathbb{R}\right)$, and, $\varphi_{\tilde{u}} \in \mathscr{C}\left([-\tilde{\tau}, 0], \mathbb{R}\right)$. Moreover, we can show that the system (6.8) is positive, since $\tilde{K} \in (0,1)$. Throughout this work, only positive solutions of (6.8) are considered.

6.3 Notable features of the coupled model

In this section, we point out some properties of the model (6.8) that highlight its rich dynamics, according to the following possibly existing cases[6]:

Point of interest of $\tilde{x}$	0	$\tilde{x}_e$	0	$\tilde{x}_e$	∞
Point of interest of $\tilde{u}$	0	$\tilde{u}_e$	0	$\tilde{u}_e$	∞
Point of interest of x	0	0	x_e	x_e	*

❑ **Cell extinction:** Clearly, $(0,0,0)$, is an equilibrium point of model (6.8). Biologically, convergence to the origin is synonymous of the extinction of all the cells (both healthy and unhealthy populations). From a therapeutic standpoint, we said that we aim to address theoretical studies for the case of unhealthy cells eradication (while ensuring that healthy cells survive), and also for a dormancy steady state (where all the cells are at a stable steady state). In both situations we do not consider that healthy cells may vanish. However, at this juncture, an interesting question may arise: *Does chemotherapy affect healthy cells?* In fact, side-effects of recent chemotherapy treatments are fewer than those of the drugs used in the past, since novel molecules are designed for over-expressed receptors (i.e. drugs are more accurate since they attack cells with accurate extracellular receptors expressed only on mutated cells). In addition, medications are mainly acting on cells during their phase of proliferation, while it appears that most of the healthy cells are in quiescence. Therefore, we consider that only a *radical* therapy will lead to total cell eradication, and this is a situation that we want to avoid. Nevertheless, the theoretical conditions (depending on the biological functions and parameter involved in our model) that cause total cell eradication are discussed in the next section.

❑ **Escape from dormancy in diseased cells:** One of the main concerns related to dormancy is to explain how escape from tumor dormancy can emerge (see [154], but also the non-coupled model in [4] that admits unbounded solutions).

Similarly, we notice in the coupled model (6.8) that the CSC compartment may have unbounded solutions that reproduce the unlimited cell proliferation in cancer. Indeed, from the second equation in (6.8) it is obvious that $2\tilde{K}e^{-\tilde{\gamma}\tilde{\tau}} > 1$, implies that, $\lim_{t\to+\infty}\tilde{u}(t) = +\infty$. It follows from the the first equation

[6] We recall that $\tilde{x}_e = 0$ implies that $\tilde{u}_e = 0$, and vice versa.

in (6.8) that $\lim_{t\to+\infty}\tilde{x}(t)=+\infty$. This situation may reflect the escape from tumor dormancy, or the invasion of the bone marrow by the blasts in AML ([4]).

❑ **Existence of the desired steady states $\mathfrak{D}$ and $\mathfrak{E}$:** Let us start from the general case in which the nonnegative point $(\tilde{x}_e,\tilde{u}_e,x_e)$ is a steady state of (6.8). Therefore, it follows that this equilibrium point satisfies:

$$\begin{cases} \left[\tilde{\delta}+\tilde{\beta}(x_e+\tilde{\alpha}\tilde{x}_e)\right]\tilde{x}_e=2(1-\tilde{K})e^{-\tilde{\gamma}\tilde{\tau}}\tilde{u}_e,\\ \tilde{\beta}(x_e+\tilde{\alpha}\tilde{x}_e)\tilde{x}_e=\left(1-2\tilde{K}e^{-\tilde{\gamma}\tilde{\tau}}\right)\tilde{u}_e,\\ \left[\delta-\left(2e^{-\gamma\tau}-1\right)\beta(x_e+\tilde{x}_e)\right]x_e=0, \end{cases} \tag{6.9}$$

where we exclude the previously discussed case of unbounded solutions by assuming that: $2\tilde{K}e^{-\tilde{\gamma}\tilde{\tau}}<1$. Indeed, our main objective here is to determine necessary and sufficient conditions for the existence of $\mathfrak{D}=(\tilde{x}_e,\tilde{u}_e,x_e)$, where $x_e>0$, $\tilde{x}_e>0$ and $\tilde{u}_e>0$, and for the existence of $\mathfrak{E}=(0,0,x_e)$, where $x_e>0$.

First, since β is continuous and decreasing from $\beta(0)$ to zero, we deduce from the third equation in (6.9) that,

$$\delta<\left[2e^{-\gamma\tau}-1\right]\beta(0), \tag{6.10}$$

is a necessary and sufficient condition for the existence of x_e and $\tilde{x}_e$ such that, $x_e+\tilde{x}_e>0$, and, $\delta-\left(2e^{-\gamma\tau}-1\right)\beta(x_e+\tilde{x}_e)=0$. In fact, the inequality (6.10) is a necessary and sufficient condition for the existence of $\mathfrak{E}$ (but not $\mathfrak{D}$).

Next, from the second equation in (6.9), we obtain that $\tilde{u}_e=\frac{\tilde{\beta}(x_e+\tilde{\alpha}\tilde{x}_e)\tilde{x}_e}{1-2\tilde{K}e^{-\tilde{\gamma}\tilde{\tau}}}$.

By substituting $\tilde{u}_e$ in the first equation of (6.9), we get:

$$\left[\tilde{\delta}-\frac{2e^{-\tilde{\gamma}\tilde{\tau}}-1}{1-2\tilde{K}e^{-\tilde{\gamma}\tilde{\tau}}}\tilde{\beta}(x_e+\tilde{\alpha}\tilde{x}_e)\right]\tilde{x}_e=0. \tag{6.11}$$

The fact that $\tilde{\beta}$ is continuous and decreasing implies that the condition,

$$\tilde{\delta}<\left[\frac{2e^{-\tilde{\gamma}\tilde{\tau}}-1}{1-2\tilde{K}e^{-\tilde{\gamma}\tilde{\tau}}}\right]\tilde{\beta}(0), \tag{6.12}$$

is necessary and sufficient for the existence of x_e and $\tilde{x}_e$, such that, $x_e+\tilde{\alpha}\tilde{x}_e>0$, and, $\tilde{\delta}-\frac{2e^{-\tilde{\gamma}\tilde{\tau}}-1}{1-2\tilde{K}e^{-\tilde{\gamma}\tilde{\tau}}}\tilde{\beta}(x_e+\tilde{\alpha}\tilde{x}_e)=0$. Obviously, we notice that, $2\tilde{K}e^{-\tilde{\gamma}\tilde{\tau}}<1<2e^{-\tilde{\gamma}\tilde{\tau}}$. In fact, the condition (6.12) is a necessary and sufficient condition for the existence of $(\tilde{x}_e,\tilde{u}_e,0)$, where $\tilde{x}_e>0$ and $\tilde{u}_e>0$.

It is worth mentioning that, if the condition (6.10) is satisfied (i.e. the necessary and sufficient condition for the existence of $\mathfrak{E}$), together with the condition

$$\tilde{\delta}>\left[\frac{2e^{-\tilde{\gamma}\tilde{\tau}}-1}{1-2\tilde{K}e^{-\tilde{\gamma}\tilde{\tau}}}\right]\tilde{\beta}(0), \tag{6.13}$$

then $(0,0,0)$ and $\mathfrak{E}$ are the unique existing steady states of the studied model. Let us now focus on the case where both x_e and $\tilde{x}_e$ are simultaneously strictly positive (and then $\tilde{u}_e$ is strictly positive). In the latter

situation, we get,

$$\begin{cases} x_e + \tilde{\alpha}\tilde{x}_e = \tilde{\beta}^{-1}(\tilde{\mu}), \\ x_e + \tilde{x}_e = \beta^{-1}(\mu), \end{cases} \tag{6.14}$$

where, $\mu = \frac{\delta}{2e^{-\gamma\tau}-1}$, and, $\tilde{\mu} = \frac{\tilde{\delta}\left(1-2\tilde{K}e^{-\tilde{\gamma}\tilde{\tau}}\right)}{2e^{-\tilde{\gamma}\tilde{\tau}}-1}$. Consequently, we get,

$$\begin{cases} x_e = \frac{1}{\tilde{\alpha}-1}\left[\tilde{\alpha}\beta^{-1}(\mu) - \tilde{\beta}^{-1}(\tilde{\mu})\right], \\ \tilde{x}_e = \frac{1}{\tilde{\alpha}-1}\left[\tilde{\beta}^{-1}(\tilde{\mu}) - \beta^{-1}(\mu)\right], \\ \tilde{u}_e = \frac{\tilde{\delta}}{2e^{-\tilde{\gamma}\tilde{\tau}}-1}\tilde{x}_e. \end{cases} \tag{6.15}$$

Now, we distinguish between the following two situations:
The case $\tilde{\alpha} = 1$: Here we notice that,

$$\begin{cases} x_e + \tilde{x}_e = \tilde{\beta}^{-1}(\tilde{\mu}) = \beta^{-1}(\mu), \\ \tilde{u}_e = \frac{\tilde{\delta}}{2e^{-\tilde{\gamma}\tilde{\tau}}-1}\tilde{x}_e, \end{cases} \tag{6.16}$$

which is either an impossible case if the biological parameters are such that $\tilde{\beta}^{-1}(\tilde{\mu}) \neq \beta^{-1}(\mu)$, or, when $\tilde{\beta}^{-1}(\tilde{\mu}) = \beta^{-1}(\mu)$, it corresponds to a *continuum* equilibrium point (the infinite possible values of x_e and $\tilde{x}_e$ that satisfy the first equation in (6.16)). We want to avoid the latter continuum equilibrium points since that case has no concrete biological signification.
The case $\tilde{\alpha} > 1$ or $0 < \tilde{\alpha} < 1$: First, we focus on the case $0 < \tilde{\alpha} < 1$. We recall from earlier discussion that, biologically, $0 < \tilde{\alpha} < 1$ means that CSCs are less sensitive than ordinary cells to their shared environment composed by regulatory mitotic molecules (due to epigenetic mutations for instance, unhealthy cells no longer respond to inhibitory signals and continue to proliferate). More generally, $\tilde{\alpha} < 1$ plays the role of a mitigating factor of the effect of regulatory molecules that attenuate the entrance frequency into proliferation. Now, from (6.15), we deduce that a sufficient condition for the existence of $\mathfrak{D}$ when $\tilde{\alpha} < 1$, is given by: $\tilde{\alpha}\beta^{-1}(\mu) < \tilde{\beta}^{-1}(\tilde{\mu}) < \beta^{-1}(\mu)$.

On the other hand, we observe that when $\tilde{\alpha} > 1$, then, from (6.15), we deduce that a sufficient condition for the existence of $\mathfrak{D}$ is given by: $\beta^{-1}(\mu) < \tilde{\beta}^{-1}(\tilde{\mu}) < \tilde{\alpha}\beta^{-1}(\mu)$. We summarize the overall discussion in the following result:

Proposition 6. ***(i)*** *For all $\tilde{\alpha} > 0$, if the conditions*

$$\tilde{\delta} > \left[\frac{2e^{-\tilde{\gamma}\tilde{\tau}}-1}{1-2\tilde{K}e^{-\tilde{\gamma}\tilde{\tau}}}\right]\tilde{\beta}(0), \text{ and, } \delta > \left[2e^{-\gamma\tau}-1\right]\beta(0), \tag{6.17}$$

are satisfied, then $(0,0,0)$ is the unique equilibrium point of the system (6.8)*. Note that in fact $(0,0,0)$ is always a steady state of the system* (6.8)*.*

(ii) *For all $\tilde{\alpha} > 0$, the condition*

$$\delta < \left[2e^{-\gamma\tau}-1\right]\beta(0), \tag{6.18}$$

is a necessary and sufficient conditions for the existence of the steady state, $\mathfrak{E} = (0,0,x_e)$, where $x_e > 0$, for the system (6.8)*.*

(iii) *For all $\tilde{\alpha} > 0$, if the conditions*

$$\tilde{\delta} > \left[\frac{2e^{-\tilde{\gamma}\tilde{\tau}} - 1}{1 - 2\tilde{K}e^{-\tilde{\gamma}\tilde{\tau}}}\right]\tilde{\beta}(0), \text{ and, } \delta < \left[2e^{-\gamma\tau} - 1\right]\beta(0), \tag{6.19}$$

are satisfied, then $(0,0,0)$ and $\mathfrak{E} = (0,0,x_e)$ are the unique steady states of system (6.8).

(iv) *For all $\tilde{\alpha} > 0$, the condition*

$$\tilde{\delta} < \left[\frac{2e^{-\tilde{\gamma}\tilde{\tau}} - 1}{1 - 2\tilde{K}e^{-\tilde{\gamma}\tilde{\tau}}}\right]\tilde{\beta}(0), \tag{6.20}$$

is a necessary and sufficient condition for the existence of the steady state $(\tilde{x}_e, \tilde{u}_e, 0)$ where, $\tilde{x}_e > 0$ and $\tilde{u} > 0$, for the system (6.8).

(v) *For all $\tilde{\alpha} > 0$, if the conditions*

$$\tilde{\delta} < \left[\frac{2e^{-\tilde{\gamma}\tilde{\tau}} - 1}{1 - 2\tilde{K}e^{-\tilde{\gamma}\tilde{\tau}}}\right]\tilde{\beta}(0), \text{ and, } \delta > \left[2e^{-\gamma\tau} - 1\right]\beta(0), \tag{6.21}$$

are satisfied, then $(0,0,0)$ and $(\tilde{x}_e, \tilde{u}_e, 0)$ are the unique steady states of system (6.8).

(vi) *For all $\tilde{\alpha} > 0$, the conditions*

$$\alpha \neq 1, \ \tilde{\delta} < \left[\frac{2e^{-\tilde{\gamma}\tilde{\tau}} - 1}{1 - 2\tilde{K}e^{-\tilde{\gamma}\tilde{\tau}}}\right]\tilde{\beta}(0), \text{ and, } \delta < \left[2e^{-\gamma\tau} - 1\right]\beta(0), \tag{6.22}$$

are necessary, but not sufficient, for the existence of $\mathfrak{D} = (\tilde{x}_e, \tilde{u}_e, x_e)$.

(vii) *We denote $\mu = \frac{\delta}{2e^{-\gamma\tau}-1}$, and, $\tilde{\mu} = \frac{\tilde{\delta}\left(1-2\tilde{K}e^{-\tilde{\gamma}\tilde{\tau}}\right)}{2e^{-\tilde{\gamma}\tilde{\tau}}-1}$. If the conditions,*

$$\begin{cases} 0 < \tilde{\alpha} < 1, \ \mu < \beta(0), \ \tilde{\mu} < \tilde{\beta}(0), \\ \tilde{\alpha}\beta^{-1}(\mu) < \tilde{\beta}^{-1}(\tilde{\mu}) < \beta^{-1}(\mu), \\ 2\tilde{K}e^{-\tilde{\gamma}\tilde{\tau}} < 1 < 2e^{-\tilde{\gamma}\tilde{\tau}}, \end{cases} \tag{6.23}$$

or,

$$\begin{cases} \tilde{\alpha} > 1, \ \mu < \beta(0), \ \tilde{\mu} < \tilde{\beta}(0), \\ \beta^{-1}(\mu) < \tilde{\beta}^{-1}(\tilde{\mu}) < \tilde{\alpha}\beta^{-1}(\mu), \\ 2\tilde{K}e^{-\tilde{\gamma}\tilde{\tau}} < 1 < 2e^{-\tilde{\gamma}\tilde{\tau}}, \end{cases} \tag{6.24}$$

are satisfied, then a unique strictly positive dormancy steady state $\mathfrak{D} = (\tilde{x}_e, \tilde{u}_e, x_e)$, exists and is given by (6.15).

Remark 34. ***1)*** *Obviously, uniqueness in Proposition 6-**(vii)** means the existence of a unique isolated strictly positive equilibrium point $\mathfrak{D}$, but the origin and the points $\mathfrak{E} = (0,0,x_e)$, $(\tilde{x}_e, \tilde{u}_e, 0)$ are also steady states of system* (6.8).

2) *The third condition in* (6.23)-(6.24) *expresses an interesting relationship between the fast-self renewing ability $\tilde{K}$, the apoptosis rate of malignant cancer cells $\tilde{\gamma}$, and their average cell-cycle duration $\tilde{\tau}$. We notice that even if $\tilde{K}$ is relatively important (and knowing that it is not easy to act on $\tilde{K}$ by drugs*

infusion since its high value is due to FLT3 mutation) it is still possible to guarantee the existence of a dormancy state by increasing $\tilde{\tau}\tilde{\gamma}$. However, the increase must be moderate to not exceed the upper-bound $\tilde{\gamma}\tilde{\tau} < \ln(2)$.

***3)** Finally, we notice that other cases can be discussed if biologically needed. For instance, by adding the following restriction: $2\tilde{\beta}^{-1}(\tilde{\mu}) < (1+\tilde{\alpha})\beta^{-1}(\mu)$, to the conditions in* (6.23)-(6.24)*, we ensure that $x_e > \tilde{x}_e$, which is the expected situation of existing (dormant) tumors, without forming a clinically apparent cancer.*

Now, we motivate our stability analysis through some preliminary numerical observations that highlight the rich dynamics of the model that we introduced in this work. In particular, we point out the different possible behaviors of the nonlinear differential-difference system (6.8) according to its associated initial conditions. The latter fact emphasizes the importance of determining mathematically an estimate of the region of attraction of each steady state of interest.

Example 9. *Let us consider the following biological functions and parameters for cells in Category A and Category B:*

Category A:	$\tau = 1.11$	$\delta = 0.1$	$\gamma = 0.1$	$\beta(m) = \frac{3}{1+m^4}$	$\alpha = 1$	
Category B:	$\tilde{\tau} = 0.9$	$\tilde{\delta} = 0.36$	$\tilde{\gamma} = 0.32$	$\tilde{\beta}(m) = \frac{2}{1+m^4}$	$\tilde{\alpha} = 0.6$	$\tilde{K} = 0.54$

For the considered set of parameters and functions, a unique dormancy steady state $\mathfrak{D}$ exists and is given by $\mathfrak{D} = (\tilde{x}_e, \tilde{u}_e, x_e)$, where $\tilde{x}_e = 0.6573$, $\tilde{u}_e = 0.4737$ and $x_e = 1.5255$. This steady state is shown in Figure 6.5. However, the latter point is not the unique equilibrium point of the system. Indeed, the 0-equilibrium $(0,0,0)$, and the points: $\mathfrak{E} = (0,0,2.1826)$ and $(3.1998, 2.3060, 0)$, also exist[7]*. When we select the constant initial conditions $\varphi_x(t) = \varphi_{\tilde{x}}(t) = 2$, for all $t \in [-\tau, 0]$, and $\varphi_{\tilde{u}}(t) = 1$, for all $t \in [-\tilde{\tau}, 0]$, we observe that the trajectories converge to $(3.1998, 2.3060, 0)$, as illustrated in Figure 6.6, where unhealthy cells survive (the attractive point seems to be stable), while the healthy cells vanish (converge to zero).*

By changing the initial condition of $\tilde{u}$, from the previous value to $\varphi_{\tilde{u}}(t) = 0.1$, for all $t \in [-\tilde{\tau}, 0]$, we observe that the trajectories converge to $\mathfrak{E}$, as illustrated in Figure 6.7. Moreover, the steady states in Figures 6.6 and 6.7 seem to be stable (each one has its region of attraction). Lyapunov theory offers strong tools to establish the regional stability properties of the steady states of interest, provided that a suitable Lyapunov functional is found for the studied model.

Now, let us modify the value of $\tilde{K}$ by increasing it to $\tilde{K} = 0.6680$. It follows that $2\tilde{K}e^{-\tilde{\gamma}\tilde{\tau}} - 1 = 0.017$, which implies that the trajectories of the unhealthy compartment are unbounded (similarly to [4]). Numerical simulations in that case, for arbitrary initial conditions, are given in Figure 6.8.

[7] One may notice the relationship that exists between the three different non-trivial steady states. In fact, the x_e-value in $\mathfrak{E}$ corresponds to the sum $x_e + \tilde{x}_e$ of the dormancy steady state $\mathfrak{D}$, while the $\tilde{x}_e$-value in the steady state $(\tilde{x}_e, \tilde{u}_e, 0)$ corresponds to the value $\frac{x_e + \tilde{\alpha}\tilde{x}_e}{\tilde{\alpha}}$, where x_e and $\tilde{x}_e$ in the latter fraction are the corresponding values in the dormancy steady state $\mathfrak{D}$.

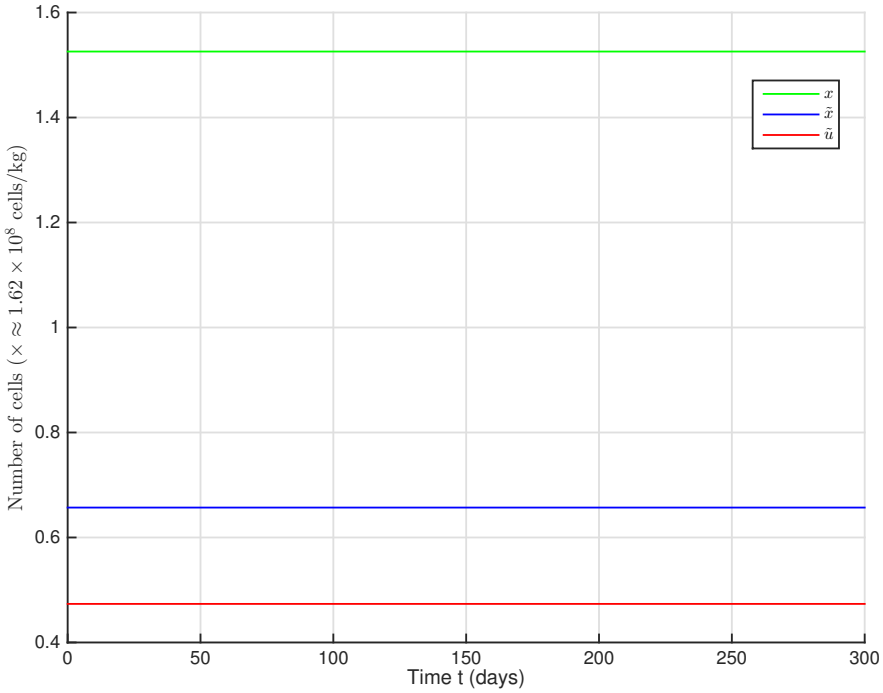

Fig. 6.5 Convergence to $\mathfrak{D}$.

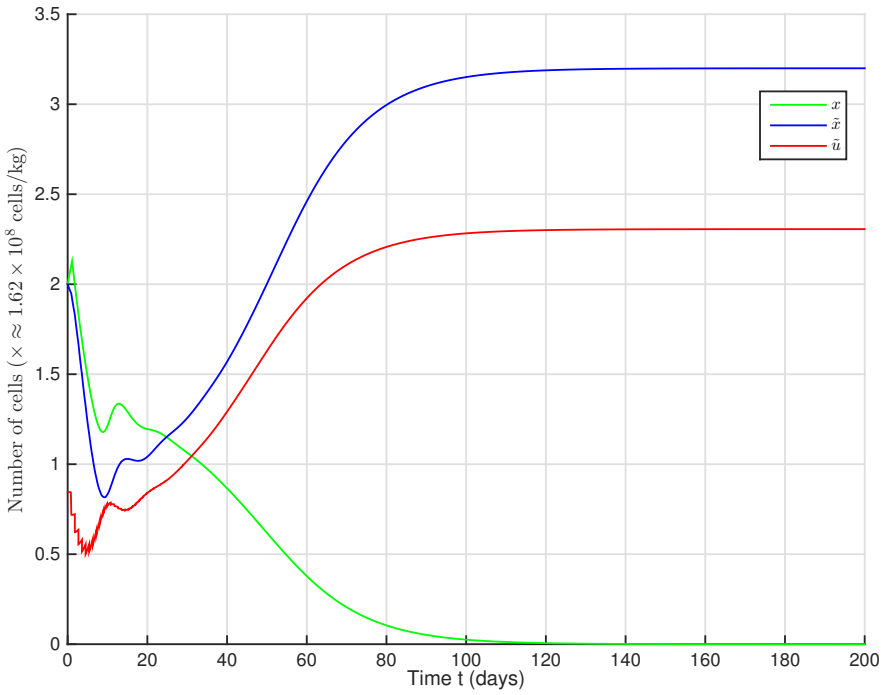

Fig. 6.6 Convergence to $(\tilde{x}_e, \tilde{u}_e, 0)$.

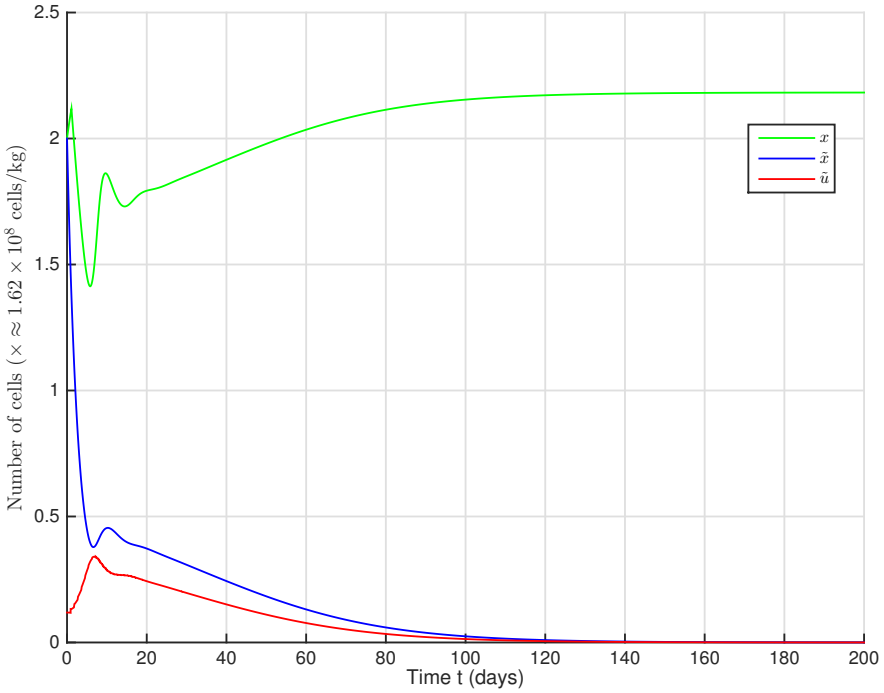

Fig. 6.7 Convergence to $\mathfrak{E}$.

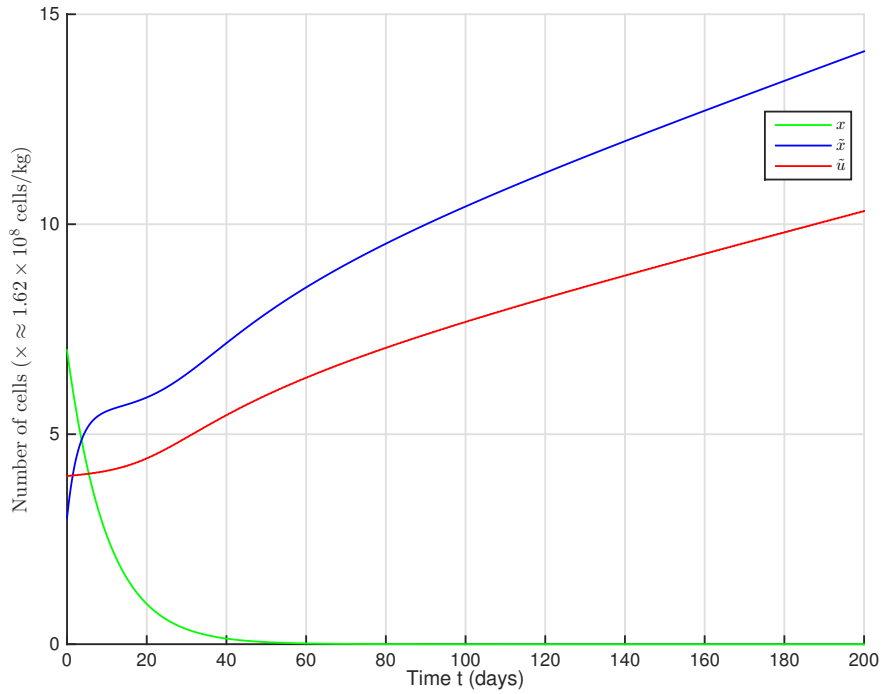

Fig. 6.8 Unbounded CSCs behavior.

Example 10. *Now, let us consider the following functions and parameters:*

Category A:	$\tau = 1.25$	$\delta = 0.2$	$\gamma = 0.2$	$\beta(m) = \frac{1}{1+m^2}$	$\alpha = 1$	
Category B:	$\tilde{\tau} = 1.66$	$\tilde{\delta} = 0.1$	$\tilde{\gamma} = 0.2$	$\tilde{\beta}(m) = \frac{1.2}{1+5m^4}$	$\tilde{\alpha} = 0.4$	$\tilde{K} = 0.3$

The steady states $(0,0,0)$, $\mathfrak{E} = (0,0,x_e)$, $(\tilde{x}_e, \tilde{u}_e, 0)$ *and* $\mathfrak{D} = (\tilde{x}_e, \tilde{u}_e, x_e)$, *of the corresponding system, exist.*

If we select the constant initial conditions $\varphi_x(t) = 1.55$, *and* $\varphi_{\tilde{x}}(t) = 1$, *for all* $t \in [-\tau, 0]$, *and* $\varphi_{\tilde{u}}(t) = 0.3$, *for all* $t \in [-\tilde{\tau}, 0]$, *we observe that the trajectories are unstable as illustrated in Figure 6.9, knowing that the dormancy steady state here is* $\mathfrak{D} = (0.3445, 0.0792, 0.9926)$. *We recall that oscillations in hematopoietic systems are associated to many periodic diseases (e.g. cyclic neutropenia [37], [241], or some types of chronic myeloid leukemia).*

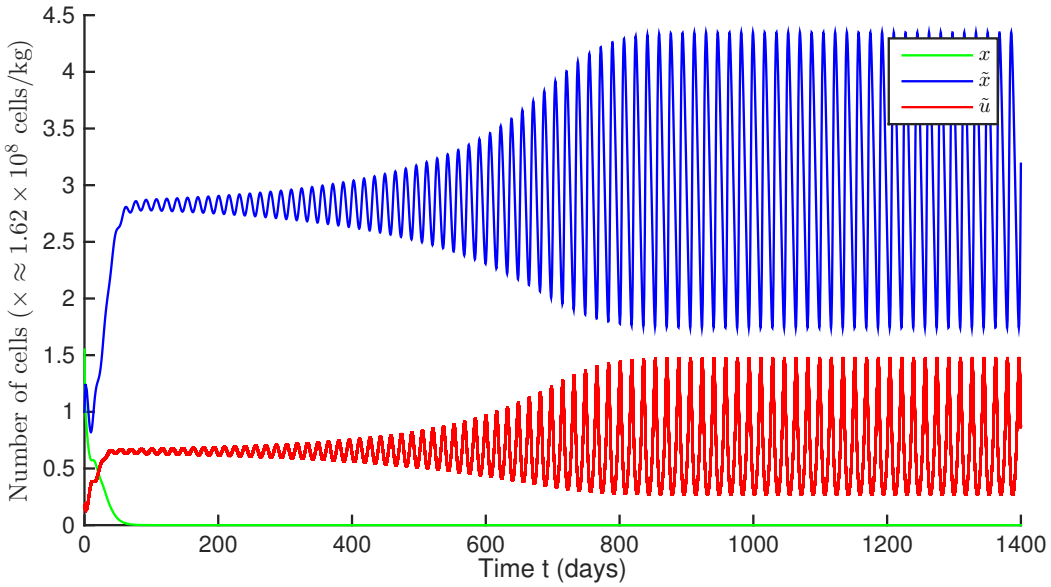

Fig. 6.9 Unstable (oscillatory) solutions.

Now, let us consider random constant initial conditions and let us keep constant all the biological parameters except the value of $\tilde{\alpha}$, *that we consider to be ranging between* 0.1 *and* 0.6. *As shown in Figure 6.10, we note that by increasing the value of* $\tilde{\alpha}$, *the trajectories of the corresponding system become stable when* $\tilde{\alpha}$ *increases. Thus, it appears that* $\tilde{\alpha}$ *may have, at least in this example, a stabilizing (or destabilizing) effect on the trajectories of the system* (6.8).

Example 11. *Finally, let us consider the following functions and parameters:*

Category A:	$\tau = 1.25$	$\delta = 0.1$	$\gamma = 0.2$	$\beta(m) = \frac{1}{1+m^2}$	$\alpha = 1$	
Category B:	$\tilde{\tau} = 0.7$	$\tilde{\delta} = 0.2$	$\tilde{\gamma} = 0.1$	$\tilde{\beta}(m) = \frac{2}{1+2m^4}$	$\tilde{\alpha} = 2$	$\tilde{K} = 0.5$

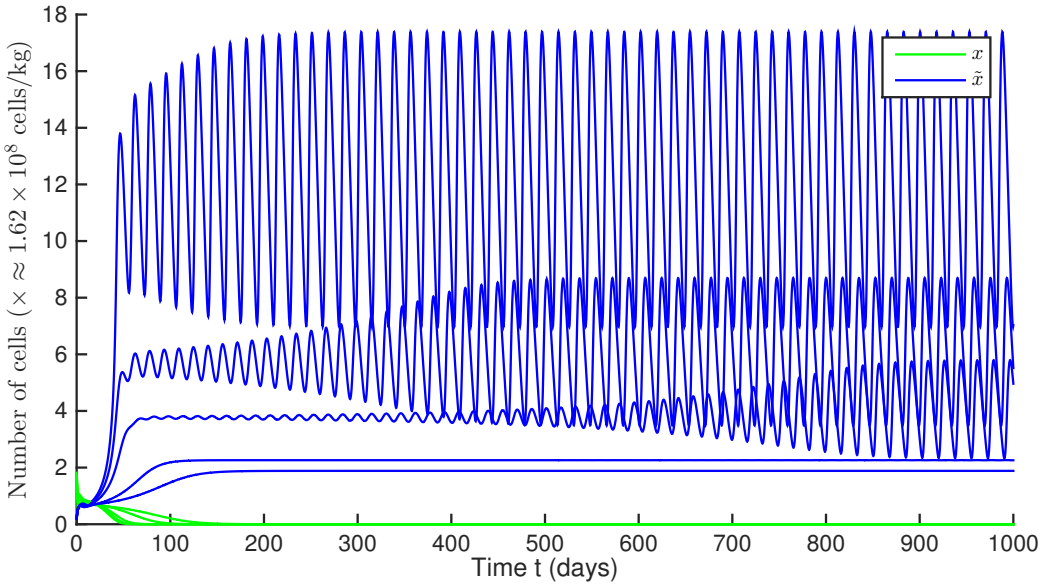

Fig. 6.10 Stabilizing effect of $\tilde{\alpha}$.

The conditions of existence of $\mathfrak{D} = (\tilde{x}_e, \tilde{u}_e, x_e)$ *are satisfied, and in this case we obtain:* $\tilde{x}_e = 0.6833$, $\tilde{u}_e = 0.1580$ *and* $x_e = 1.45599$. *For the constant initial conditions* $\varphi_x(t) = 0.1$ *and* $\varphi_{\tilde{x}}(t) = 1.5$, *for all* $t \in [-\tau, 0]$, *and* $\varphi_{\tilde{u}}(t) = 1.5$ *for all* $t \in [-\tilde{\tau}, 0]$, *it appears that* $\mathfrak{D}$ *is stable as illustrated in Figure 6.11.*

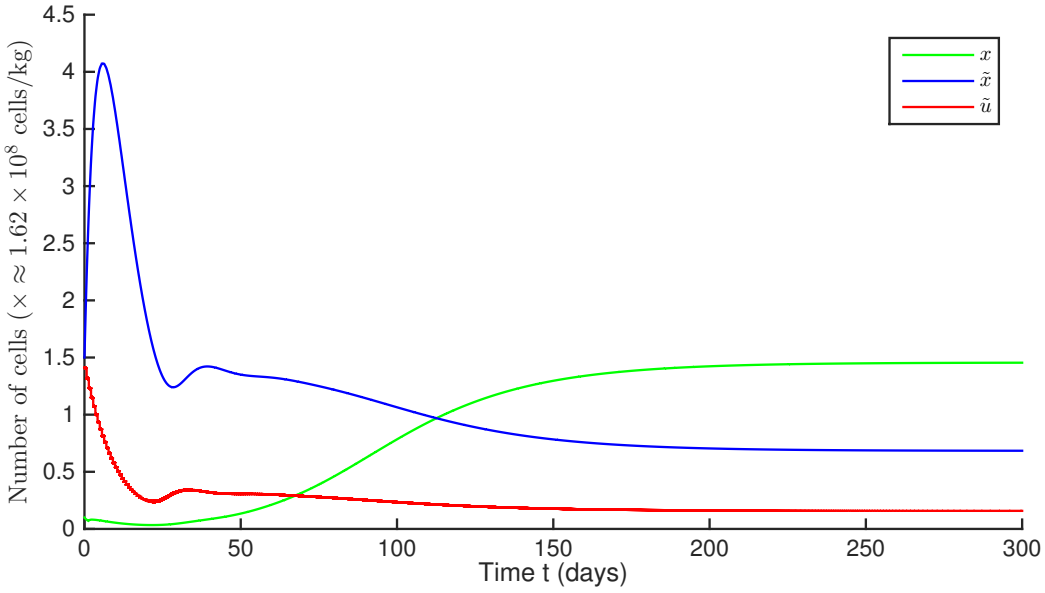

Fig. 6.11 Convergence to the dormancy steady state $\mathfrak{D}$.

At this juncture, we deduce that the coupled system (6.8) under study has richer dynamical features than the earlier models. Firstly, we saw that the solutions of the coupled system can be bounded or unbounded. In the former case, several steady states may exist and their values depend on the different biological parameters of the model. The existence of the steady states of interest ($\mathfrak{D}$ and $\mathfrak{E}$) are governed

by some non-intuitive conditions on the biological parameters involved in the system (see Proposition 6). In addition, we saw that according to the initial conditions associated with the model trajectories, the bounded solutions may converge to one among several possible steady states, meaning that stability of each steady state is regional (local). Moreover, in the general case, the steady states of the system (6.8) are not always stable, but on the contrary, we noticed that oscillations may emerge, as in Example 10). Our objective in the sequel is to determine exponential stability conditions for the steady states of interest (all-cell extinction $(0,0,0)$, unhealthy cell eradication $\mathfrak{E}$, and cancer dormancy $\mathfrak{D}$).

6.4 Stability analysis of the extinction of all the cells

In this section, we perform a stability analysis of the 0-equilibrium of the system (6.8). From a biological standpoint, this is a case that we want to avoid, as discussed in the previous section (see the first point, *Cell extinction*), since it is synonymous of an excessive therapy that not only alters unhealthy populations, but also leads to the extinction of healthy cells in the coupled model.

Here we introduce the following functional:

$$\begin{aligned}\mathscr{W}(\tilde{x}_t,\tilde{u}_t,x_t) =& \tilde{x}(t)+x(t)+\psi_1\int_{t-\tilde{\tau}}^{t} e^{\rho_1(\ell-t)}\tilde{u}(\ell)d\ell \\ &+\psi_2\int_{t-\tau}^{t} e^{\rho_2(\ell-t)}\beta\left(x(\ell)+\tilde{x}(\ell)\right)x(\ell)d\ell,\end{aligned} \tag{6.25}$$

where, $\psi_1=\psi_{11}+\psi_{12}$, $\psi_{11}=1+\frac{\tilde{\delta}}{\tilde{\beta}(0)}$, $\psi_{12}=-\frac{\psi^*}{3\left(\overline{K}-\tilde{K}\right)\tilde{\beta}(0)}$, $\overline{K}=\frac{1}{2}e^{\tilde{\gamma}\tilde{\tau}}$, $\psi^*=\left(\tilde{\beta}(0)+\tilde{\delta}\right)\overline{K}-\tilde{\beta}(0)-\tilde{K}\tilde{\delta}$, and, $\psi_2=2\psi_3 e^{-\gamma\tau}$, where, ψ_3, together with ρ_1 and ρ_2, are strictly positive constants that we choose later.

We can readily check that if $2\tilde{K}e^{-\tilde{\gamma}\tilde{\tau}}<1$ (that we can rewrite as $\tilde{K}<\overline{K}$), and $\psi^*>0$, (i.e. $\psi_{12}<0$), we obtain $\psi_1>0$. It follows that the functional $\mathscr{W}$ is nonnegative. We notice also that $\mathscr{W}$ is an unusual LKF candidate, since it can be used only because the system (6.8) is positive. In addition, it is a *degenerate* LKF candidate (since $\mathscr{W}=0$ does not imply $\tilde{u}=0$) which is usually the case for differential-difference systems. This will also be the case when we investigate the stability properties of the dormancy steady state, where we will construct a quadratic degenerate LKF.

Thanks to the functional $\mathscr{W}$, we prove the following result:

Theorem 13. *If the conditions*

$$\left(2e^{-\gamma\tau}-1\right)\beta(0)<\delta,\quad 0<\psi^*,\quad \textit{and,}\quad 2\tilde{K}e^{-\tilde{\gamma}\tilde{\tau}}<1, \tag{6.26}$$

are satisfied, then the origin of system (6.8) *is globally exponentially stable with a decay rate smaller or equal to* $\psi_4>0$ *that we estimate.*

Proof. Simple calculations show that the derivative of $\mathscr{W}$, defined in (6.25), along the trajectories of (6.8), satisfies, for almost all $t \geq 0$,

$$\begin{aligned}
\dot{\mathscr{W}}(t) = & \left[-\tilde{\delta} + (\psi_1 - 1)\,\tilde{\beta}\left(x(t) + \tilde{\alpha}\tilde{x}(t)\right)\right]\tilde{x}(t) \\
& - \left[\psi_1\left(e^{-\rho_1\tilde{\tau}} - 2\tilde{K}e^{-\tilde{\gamma}\tilde{\tau}}\right) - 2(1-\tilde{K})e^{-\tilde{\gamma}\tilde{\tau}}\right]\tilde{u}(t-\tilde{\tau}) \\
& - \left[\delta + (1-\psi_2)\,\beta\left(x(t) + \tilde{x}(t)\right)\right]x(t) - \psi_1\rho_1\int_{t-\tilde{\tau}}^{t} e^{\rho_1(\ell-t)}\tilde{u}(\ell)d\ell \\
& - \left(\psi_3 e^{-\rho_2\tau} - 1\right)2e^{-\gamma\tau}\beta\left(x(t-\tau) + \tilde{x}(t-\tau)\right)x(t-\tau) \\
& - \psi_2\rho_2\int_{t-\tau}^{t} e^{\rho_2(\ell-t)}\beta\left(x(\ell) + \tilde{x}(\ell)\right)x(\ell)d\ell.
\end{aligned} \tag{6.27}$$

Now, according to 6.26, the conditions $2\tilde{K}e^{-\tilde{\gamma}\tilde{\tau}} < 1$ and $\psi^* > 0$ are satisfied. It follows that for all $\rho_1 \in \left(0, \frac{1}{\tilde{\tau}}\ln\left(\frac{k}{1+2(k-1)\tilde{K}e^{-\tilde{\gamma}\tilde{\tau}}}\right)\right)$, where $k > 1$ is a constant that we will select later, we have,

$$0 < \frac{1 - 2\tilde{K}e^{-\tilde{\gamma}\tilde{\tau}}}{k} < e^{-\rho_1\tilde{\tau}} - 2\tilde{K}e^{-\tilde{\gamma}\tilde{\tau}} < 1 - 2\tilde{K}e^{-\tilde{\gamma}\tilde{\tau}}.$$

On the other hand, using the definition of ψ_1, we can readily check that:

$$\psi_1\left(1 - 2\tilde{K}e^{-\tilde{\gamma}\tilde{\tau}}\right) - 2\left(1-\tilde{K}\right)e^{-\tilde{\gamma}\tilde{\tau}} > 0.$$

Therefore, we can notice that for all $k \in \left(1, \frac{\left(1-2\tilde{K}e^{-\tilde{\gamma}\tilde{\tau}}\right)\psi_1}{2(1-\tilde{K})e^{-\tilde{\gamma}\tilde{\tau}}}\right)$,

$$\bar{k} = \psi_1\left(\frac{1 - 2\tilde{K}e^{-\tilde{\gamma}\tilde{\tau}}}{k}\right) - 2\left(1-\tilde{K}\right)e^{-\tilde{\gamma}\tilde{\tau}},$$

is a strictly positive constant. Next, since $\tilde{\beta}$ is decreasing, and using the fact that $\psi_{11} > 1$, it follows that $(\psi_{11} - 1)\,\tilde{\beta}\left(x(t) + \tilde{\alpha}\tilde{x}(t)\right) \leq (\psi_{11} - 1)\,\tilde{\beta}(0)$.

From the previous intermediate results, we conclude that for all $t \geq 0$,

$$-\tilde{\delta} + (\psi_1 - 1)\,\tilde{\beta}\left(x(t) + \tilde{\alpha}\tilde{x}(t)\right) \leq \psi_{12}\tilde{\beta}\left(x(t) + \tilde{\alpha}\tilde{x}(t)\right),$$

where, $\psi_{12} < 0$.

Now, let us assume that the third decay condition, $\delta > \left(2e^{-\gamma\tau} - 1\right)\beta(0)$, is satisfied. Then we choose $\psi_3 = \frac{2\beta(0) + \left(\delta + \beta(0)\right)e^{\gamma\tau}}{4\beta(0)}$. Therefore, it is easy to check that, in the case, we have $\psi_3 \in \left(1, \frac{\delta+\beta(0)}{2\beta(0)}e^{\gamma\tau}\right)$.

It follows that $\delta + (1-\psi_2)\,\beta(0)$ is positive.

For later use we denote $\delta^* = \delta + (1-\psi_2)\,\beta(0)$.Next, by selecting $\rho_2 = \frac{1}{2\tau}\ln\left(\frac{2\psi_3}{\psi_3+1}\right) > 0$, we deduce that $\psi_3 e^{-\rho_2\tau} - 1$ is positive. For later use we denote $\rho^* = \psi_3 e^{-\rho_2\tau} - 1$.

We conclude that $\dot{\mathscr{W}}(t)$ satisfies, for almost all $t \geq 0$,

$$\begin{aligned}\dot{\mathscr{W}}(t) \leq & \psi_{12}\tilde{\beta}\left(x(t)+\tilde{\alpha}\tilde{x}(t)\right)\tilde{x}(t) - \psi_1\rho_1\int_{t-\tilde{\tau}}^{t} e^{\rho_1(\ell-t)}\tilde{u}(\ell)d\ell \\ & -\bar{k}\tilde{u}(t-\tilde{\tau}) - 2\rho^* e^{-\gamma\tau}\beta\left(x(t-\tau)+\tilde{x}(t-\tau)\right)x(t-\tau) \\ & -\delta^* x(t) - \psi_2\rho_2\int_{t-\tau}^{t} e^{\rho_2(\ell-t)}\beta\left(x(\ell)+\tilde{x}(\ell)\right)x(\ell)d\ell,\end{aligned} \tag{6.28}$$

where, $\psi_{12} < 0$, $\bar{k} > 0$, $\delta^* > 0$, and, $\rho^* > 0$. By integrating the previous inequality (6.28), we deduce that the functional $\mathscr{W}$ is bounded over $[0,+\infty)$. From the definition of $\mathscr{W}$, it follows that for all $t \geq 0$, the trajectories $\tilde{x}(t)$ and $x(t)$ are bounded by, respectively, the positive constants $\tilde{x}_s$ and x_s.

A direct consequence is that for almost all $t \geq 0$,

$$\begin{aligned}\dot{\mathscr{W}}(t) \leq & \psi_{12}\tilde{\beta}\left(x_s+\tilde{\alpha}\tilde{x}_s\right)\tilde{x}(t) - \psi_1\rho_1\int_{t-\tilde{\tau}}^{t} e^{\rho_1(\ell-t)}\tilde{u}(\ell)d\ell \\ & -\delta^* x(t) - \psi_2\rho_2\int_{t-\tau}^{t} e^{\rho_2(\ell-t)}\beta\left(x(\ell)+\tilde{x}(\ell)\right)x(\ell)d\ell.\end{aligned} \tag{6.29}$$

We conclude that for almost all $t \geq 0$, we have,

$$\dot{\mathscr{W}}(t) \leq -\psi_4\mathscr{W}\left(\tilde{x}_t,\tilde{u}_t,x_t\right), \tag{6.30}$$

where $\psi_4 = \min\left\{-\psi_{12}\tilde{\beta}(x_s+\tilde{\alpha}\tilde{x}_s), \delta^*, \rho_1, \rho_2\right\} > 0$.

Now, by integrating the inequality (6.30), we deduce that for all $t \geq 0$,

$$\mathscr{W}\left(\tilde{x}_t,\tilde{u}_t,x_t\right) \leq e^{-\psi_4 t}\mathscr{W}\left(\varphi_{\tilde{x}},\varphi_{\tilde{u}},\varphi_x\right). \tag{6.31}$$

It follows from the definition of $\mathscr{W}$ that $\tilde{x}$ and x converge exponentially to zero with a decay rate greater or equal to ψ_4. From the second equation in (6.8), we note that the linearity in $\tilde{u}$ and the fact that $2\tilde{K}e^{-\tilde{\gamma}\tilde{\tau}} < 1$, imply that $\tilde{u}$ converges exponentially to the origin when $\tilde{x}$ and x also converge exponentially to the origin. This concludes the proof of Theorem 13. □

Remark 35. ***i)*** *The conditions* (6.26) *exclude the existence of any steady state different from the origin.*

ii) *We can interpret the cell extinction as a result of an excessive therapy that affects also healthy cells so that their apoptosis rate, γ, increases until becoming greater than the ratio $\frac{\ln(2)}{\tau}$, or, until the death rate and differentiation rate, i.e. δ, becomes greater than $\left(2e^{-\gamma\tau}-1\right)\beta(0)$ (which is a less demanding condition in comparison to $\gamma > \frac{\ln(2)}{\tau}$).*

iii) *Arguing as in Chapter 4 and in [4], we can prove that the conditions* (6.26) *are also necessary for the asymptotic stability of the origin.*

iv) *Finally, we deduce from Theorem 13 that all-cell extension results from uncorrelated conditions between the healthy and unhealthy compartments. Indeed, we note that the last two conditions in* (6.26) *relate to the unhealthy compartment, since only unhealthy parameters are involved. Moreover, these conditions are similar to those giving global asymptotic stability in [4] for a non-coupled model. The biological interpretation is that cell extension occurs if and only if both the healthy and unhealthy compartments are enable to regenerate themselves autonomously. In other words, it appears that the*

coupling has no effect on the stability of the 0-equilibrium since the conditions for total-cell eradication imply extinction of the unhealthy and healthy compartments separately. This observation will not hold when we study dormancy.

Here we will emphasize on the dormancy steady state $\mathfrak{D} = (\tilde{x}_e, \tilde{u}_e, x_e)$, where all the components of the steady state are different from zero (i.e. $\tilde{x}_e > 0$, $\tilde{u}_e > 0$, $x_e > 0$). In fact, we will highlight the case of dormancy $\mathfrak{D}$, since it is clearly the most general one. Indeed, from the analysis of $\mathfrak{D}$, it becomes possible to evaluate the regional stability properties of $\mathfrak{E} = (0,0,x_e)$ (which are partially investigated in [**?**], when $\tilde{\alpha} = 1$), and also of the steady state $(\tilde{x}_e, \tilde{u}_e, 0)$.

6.4.1 A new representation of the system

Now, we want to investigate the stability properties of $\mathfrak{D}$ when it exists. Thus, we assume that the conditions given in *Proposition 6*-**(vii)** are satisfied and we perform the classical changes of coordinates: $\tilde{X} = \tilde{x} - \tilde{x}_e$, $\tilde{U} = \tilde{u} - \tilde{u}_e$, and $X = x - x_e$. Therefore, from (6.8), it follows that for all $t \geq 0$,

$$\begin{cases} \dot{\tilde{X}}(t) = -\left[\tilde{\delta} + \tilde{\beta}(X(t) + \tilde{\alpha}\tilde{X}(t) + x_e + \tilde{\alpha}\tilde{x}_e)\right](\tilde{X}(t) + \tilde{x}_e) \\ \qquad\quad +2(1-\tilde{K})e^{-\tilde{\gamma}\tilde{\tau}}(\tilde{U}(t-\tilde{\tau}) + \tilde{u}_e), \\ \tilde{U}(t) + \tilde{u}_e = \tilde{\beta}(X(t) + \tilde{\alpha}\tilde{X}(t) + x_e + \tilde{\alpha}\tilde{x}_e)(\tilde{X}(t) + \tilde{x}_e) \\ \qquad\quad +2\tilde{K}e^{-\tilde{\gamma}\tilde{\tau}}(\tilde{U}(t-\tilde{\tau}) + \tilde{u}_e), \\ \dot{X}(t) = -\left[\delta + \beta(X(t) + \tilde{X}(t) + x_e + \tilde{x}_e)\right](X(t) + x_e) \\ \qquad +2e^{-\gamma\tau}\beta(X(t-\tau) + \tilde{X}(t-\tau) + x_e + \tilde{x}_e)(X(t-\tau) + x_e). \end{cases} \tag{6.32}$$

To ease the analysis of the above system, we rewrite it in a more convenient form. Observe that for all $\mathfrak{z} > -\mathfrak{e}$, $\mathfrak{e} > 0$, where, $\mathfrak{z} = X + \tilde{X}$ and $\mathfrak{e} = x_e + \tilde{x}_e$, we have, with an abuse of notation,

$$\beta(\mathfrak{z} + \mathfrak{e}) = \beta(\mathfrak{e}) + \theta\mathfrak{z} + R(\mathfrak{z}), \tag{6.33}$$

where β is the Hill-function defined in (6.1), $\theta = \beta'(\mathfrak{e})$, and, $R(\mathfrak{z}) = \int_{\mathfrak{e}}^{\mathfrak{e}+\mathfrak{z}} (\mathfrak{z} + \mathfrak{e} - \ell)\beta^{(2)}(\ell)d\ell$. Next, for all $\tilde{\mathfrak{z}} > -\tilde{\mathfrak{e}}$, $\tilde{\mathfrak{e}} > 0$, where, $\tilde{\mathfrak{z}} = X + \tilde{\alpha}\tilde{X}$, and, $\tilde{\mathfrak{e}} = x_e + \tilde{\alpha}\tilde{x}_e$, we get similarly to (6.33),

$$\tilde{\beta}(\tilde{\mathfrak{z}} + \tilde{\mathfrak{e}}) = \tilde{\beta}(\tilde{\mathfrak{e}}) + \tilde{\theta}\tilde{\mathfrak{z}} + \tilde{R}(\tilde{\mathfrak{z}}), \tag{6.34}$$

where, $\tilde{\theta} = \tilde{\beta}'(\tilde{\mathfrak{e}})$, and, $\tilde{R}(\tilde{\mathfrak{z}}) = \int_{\tilde{\mathfrak{e}}}^{\tilde{\mathfrak{e}}+\tilde{\mathfrak{z}}} (\tilde{\mathfrak{z}} + \tilde{\mathfrak{e}} - \ell)\tilde{\beta}^{(2)}(\ell)d\ell$. Therefore, using (6.33)-(6.34), and by simplifying some terms using (6.9), we get the system,

$$\begin{cases} \dot{\tilde{X}}(t) = -\mathfrak{a}_1\tilde{X}(t) - \mathfrak{a}_2 X(t) + \mathfrak{a}_3\tilde{U}(t-\tilde{\tau}) + F(X(t), \tilde{X}(t)), \\ \tilde{U}(t) = \mathfrak{a}_4\tilde{X}(t) + \mathfrak{a}_2 X(t) + \mathfrak{a}_5\tilde{U}(t-\tilde{\tau}) - F(X(t), \tilde{X}(t)), \\ \dot{X}(t) = -\mathfrak{a}_6 X(t) - \mathfrak{a}_7\tilde{X}(t) + \mathfrak{a}_8 X(t-\tau) + \mathfrak{a}_9\tilde{X}(t-\tau) + G(X_t, \tilde{X}_t), \end{cases} \tag{6.35}$$

$$\begin{aligned} \text{where,} \quad F(X(t), \tilde{X}(t)) = &-\tilde{\theta}\left[\tilde{\alpha}\tilde{X}^2(t)) + X(t)\tilde{X}(t)\right] \\ &- \tilde{R}(X(t) + \tilde{\alpha}\tilde{X}(t))(\tilde{X}(t) + \tilde{x}_e), \end{aligned} \tag{6.36}$$

$$\begin{aligned} G(X_t,\tilde{X}_t) =& -\theta\left[X^2(t)+X(t)\tilde{X}(t)\right]-R(X(t)+\tilde{X}(t))(X(t)+x_e)\\ &+2e^{-\gamma\tau}\theta\left[X^2(t-\tau)+X(t-\tau)\tilde{X}(t-\tau)\right]\\ &+2e^{-\gamma\tau}R(X(t-\tau)+\tilde{X}(t-\tau))(X(t-\tau)+x_e), \end{aligned} \tag{6.37}$$

and where the constant parameters $\mathfrak{a}_i$ are given by:

$$\begin{cases} \mathfrak{a}_1=\tilde{\delta}+\tilde{\beta}(x_e+\tilde{\alpha}\tilde{x}_e)+\tilde{\alpha}\tilde{\theta}\tilde{x}_e,\ \mathfrak{a}_2=\tilde{\theta}\tilde{x}_e,\ \mathfrak{a}_3=2(1-\tilde{K})e^{-\tilde{\gamma}\tilde{\tau}},\\ \mathfrak{a}_4=\tilde{\beta}(x_e+\tilde{\alpha}\tilde{x}_e)+\tilde{\alpha}\tilde{\theta}\tilde{x}_e,\mathfrak{a}_5=2\tilde{K}e^{-\tilde{\gamma}\tilde{\tau}},\ \mathfrak{a}_6=\delta+\beta\,(x_e+\tilde{x}_e)+\theta x_e,\\ \mathfrak{a}_7=\theta x_e,\ \mathfrak{a}_8=2e^{-\gamma\tau}\left[\beta\,(x_e+\tilde{x}_e)+\theta x_e\right],\ \mathfrak{a}_9=2e^{-\gamma\tau}\theta x_e. \end{cases} \tag{6.38}$$

We notice that if the trajectories of (6.35) converge exponentially to the 0-equilibrium, then the positive trajectories of the system (6.8) converge exponentially to $\mathfrak{D}$. Now, we are going to state and prove some sector conditions on the nonlinear terms R and $\tilde{R}$. Then, we deduce some upper-bounds on the nonlinear terms F and G. For that purpose, we prove in **??** through lengthy calculations that there exist strictly positive constants $\mathfrak{s}$, $\tilde{\mathfrak{s}}$, $\mathfrak{m}$ and $\tilde{\mathfrak{m}}$, satisfying:

$$|R(\mathfrak{z})|\leq\mathfrak{s}|\mathfrak{z}|,\ \text{ and }\ |\tilde{R}(\tilde{\mathfrak{z}})|\leq\tilde{\mathfrak{s}}|\tilde{\mathfrak{z}}|, \tag{6.39}$$

$$|R(\mathfrak{z})|\leq\mathfrak{m}\mathfrak{z}^2,\ \text{ and }\ |\tilde{R}(\tilde{\mathfrak{z}})|\leq\tilde{\mathfrak{m}}\tilde{\mathfrak{z}}^2, \tag{6.40}$$

for all $\mathfrak{z}>-\mathfrak{e}$ ($\mathfrak{z}$ and $\mathfrak{e}$ are defined before (6.33)), and for all $\tilde{\mathfrak{z}}>-\tilde{\mathfrak{e}}$ ($\tilde{\mathfrak{z}}$ and $\tilde{\mathfrak{e}}$ are defined before (6.34)). Moreover, using (6.39) and (6.40), we can determine strictly positive constants $\mathfrak{c}_i$, $i=\{1,\ldots,6\}$, such that the following quadratic upper bounds hold true:

$$\left|F(X,\tilde{X})\right|\leq\mathfrak{c}_1Q(X)+\mathfrak{c}_2Q(\tilde{X}), \tag{6.41}$$

$$\left|G(X_t,\tilde{X}_t)\right|\leq\mathfrak{c}_3Q(X(t))+\mathfrak{c}_4Q(\tilde{X}(t))+\mathfrak{c}_5Q(X(t-\tau))+\mathfrak{c}_6Q(\tilde{X}(t-\tau)). \tag{6.42}$$

Remark 36. ***(1)*** *The upper-bounds given in* (6.39), (6.40), (6.41), *and,* (6.42), *will not intervene when we determine the decay conditions and the decay rate of the solutions. However, their effect appears in the size of the basin of attraction that we will provide. Actually, if the constants* $\mathfrak{s}$, $\tilde{\mathfrak{s}}$, $\mathfrak{m}$, $\tilde{\mathfrak{m}}$, *in* (6.39)-(6.40), *as well as the constants* $\mathfrak{c}_i$ *in* (6.41)-(6.42), *are large, then the size of the basin of attraction shrinks accordingly.* ***(2)*** *By comparing the present study with [***?** *], we notice that [***?** *] was devoted to the study of a model which was simpler than the system* (6.35) *under study in this paper. Indeed, the model in [***?** *] can be obtained by putting* $\tilde{\alpha}=1$ *and by eliminating all the terms where* $\tilde{x}_e$ *is present in equations* (6.35), (6.38), (6.36) *and* (6.37). ***(3)*** *It is worth mentioning that the stability results that we will determine later apply for a wide range of functions* β *and* $\tilde{\beta}$, *as long as the sector conditions* (6.39) *and* (6.40) *are satisfied.*

Now, we want to perform a stability analysis of the trivial steady state of the (shifted) model using its representation in (6.35): we recall that the 0-equilibrium of (6.35) can be $\mathfrak{D}$ or $\mathfrak{E}$ of (6.8). For meeting such a purpose, strong tools are provided by Lyapunov theory, in the analysis of nonlinear differential-

difference systems with possibly piecewise continuous solutions (see e.g. [121], [152], [232], and the references therein). However, finding a suitable LKF is not an easy task. In addition, the provided stability conditions can be conservative. So, we adopt the following strategy that highlights our biological aims:

① Firstly, we use the *descriptor method* [106] that allows us to provide a local (Lyapunov-based) stability result for our biological model. The advantage of this approach is that it provides an effective tool (formulated as an LMI condition) to check if a steady state of a specific biological model (defined by its set of parameters) is locally stable.

② In order to address the following issue: *How can we provide realistic stability conditions that can be interpreted and satisfied under the effect of drugs?*, the first approach will be slightly modified in a second time. Thus, we establish a different result (that can be seen as a particular formulation of the first approach) which relies on the analytic construction of a suitable Lyapunov-like functional, specific for the studied biological system. The latter approach allows us to provide more explicit decay conditions than the common LMI-type approaches. We point out that even if the second construction provides more conservative conditions than the LMI ones, they have the advantage of being more easily (biologically) understandable. It is to this end that, in the last section, we show how the decay conditions can be interpreted, in practice, according to the biological context of hematopoiesis and leukemia.

In summary, we determine throughout this section some exponential decay conditions (along with an estimate of the decay rate of the solutions and a region of attraction of the favourable steady states), via two complementary approaches: the descriptor method that provides local stability results for the general structure of the studied system, and, a suitable explicit Lyapunov-like construction that allows us to address the regional stability properties of the dormancy steady state. The latter decay conditions lend themselves more easily than the LMI ones to medical interpretations.

6.4.2 Stability analysis using the *descriptor* method

In this section, we consider as a first step only continuous solutions of the system in (6.35) and we study the linear approximation of the state $col\left\{X,\tilde{X}\right\}$, that we denote $Z = col\left\{Z_1,Z_2\right\}$. Then, by neglecting the nonlinear terms F and G in (6.35), we rewrite the studied system in the following compact form:

$$\begin{cases} \dot{Z}(t) = B_0 Z(t) + B_1 Z(t-\tau) + B_2 \tilde{U}\left(t-\tilde{\tau}\right), \\ \tilde{U}(t) = B_3 Z(t) + B_4 \tilde{U}\left(t-\tilde{\tau}\right), \end{cases} \tag{6.43}$$

for all $t \geq 0$, where B_i are given by (we recall that $\mathfrak{a}_i$ are defined in (6.38)),

$$\begin{array}{l} B_0 = -\begin{pmatrix} \mathfrak{a}_6 & \mathfrak{a}_7 \\ \mathfrak{a}_2 & \mathfrak{a}_1 \end{pmatrix},\ B_1 = \begin{pmatrix} \mathfrak{a}_8 & \mathfrak{a}_9 \\ 0 & 0 \end{pmatrix}, B_2 = \begin{pmatrix} 0 \\ \mathfrak{a}_3 \end{pmatrix}, \\ B_3 = \begin{pmatrix} \mathfrak{a}_2 & \mathfrak{a}_4 \end{pmatrix},\ \text{and},\ B_4 = \mathfrak{a}_5 = 2\tilde{K}e^{-\tilde{\gamma}\tilde{\tau}}. \end{array} \tag{6.44}$$

Next, we consider some symmetric positive definite matrices $P>0$, $S>0$, $J>0$, of appropriate dimension, together with a strictly positive constant $\tilde{\mathfrak{a}}$, and we verify that the derivative of the functional,

$$V\left(Z_t,\tilde{U}_t\right)=Z(t)^TPZ(t)+\int_{t-\tau}^{t}Z^T(\ell)SZ(\ell)d\ell+\tilde{\mathfrak{a}}\int_{t-\tilde{\tau}}^{t}\tilde{U}^2(\ell)d\ell+\tau\int_{t-\tau}^{t}(\ell+\tau-t)\dot{Z}^T(\ell)J\dot{Z}(\ell)d\ell, \tag{6.45}$$

along the trajectories of (6.43), is given by,

$$\begin{aligned}\dot{V}(t)=&Z^T(t)\left[P+P^T\right]\dot{Z}(t)+Z^T(t)SZ(t)-Z^T(t-\tau)SZ(t-\tau)\\&-\tau\textstyle\int_{t-\tau}^{t}\dot{Z}^T(\ell)J\dot{Z}(\ell)d\ell+\tau^2\dot{Z}^T(t)J\dot{Z}(t)+\tilde{\mathfrak{a}}\left(\tilde{U}^2(t)-\tilde{U}^2(t-\tilde{\tau})\right).\end{aligned}$$

First, we notice that an upper-bound of $\dot{V}$ is given by,

$$\begin{aligned}\dot{V}(t)\leq&Z^T(t)\left[P+P^T\right]\dot{Z}(t)+Z^T(t)SZ(t)-Z^T(t-\tau)SZ(t-\tau)\\&+\tau^2\dot{Z}^T(t)J\dot{Z}(t)-Z^T(t)JZ(t)+Z^T(t)JZ(t-\tau)\\&+Z^T(t-\tau)JZ(t)-Z^T(t-\tau)JZ(t-\tau)+\tilde{\mathfrak{a}}\tilde{U}^2(t)-\tilde{\mathfrak{a}}\tilde{U}^2(t-\tilde{\tau})\\&+2\left[Z^T(t)\overline{P}^T+\dot{Z}^T(t)\overline{\overline{P}}^T\right]\underbrace{\left[B_0Z(t)+B_1Z(t-\tau)+B_2\tilde{U}\left(t-\tilde{\tau}\right)-\dot{Z}(t)\right]}_{=0},\end{aligned} \tag{6.46}$$

which, in fact, directly follows from the Jensen's Inequality given by,

$$\begin{aligned}-\tau\int_{t-\tau}^{t}\dot{Z}^T(\ell)J\dot{Z}(\ell)d\ell\leq&-\int_{t-\tau}^{t}\dot{Z}^T(\ell)d\ell J\int_{t-\tau}^{t}\dot{Z}(\ell)d\ell\\=&-\left[Z(t)-Z(t-\tau)\right]^TJ\left[Z(t)-Z(t-\tau)\right],\end{aligned}$$

and where $\overline{P}$ and $\overline{\overline{P}}$ that appear in (6.46) are some free-weighting matrices of appropriate dimension. Then, it follows that,

$$\dot{V}(t)\leq\eta^T(t)\Phi\eta(t)+\tilde{\mathfrak{a}}\tilde{U}^2(t),$$

where η is an augmented state defined by,

$$\eta^T(t)=\left[\begin{array}{cccc}Z(t) & \dot{Z}(t) & Z(t-\tau) & \tilde{U}(t-\tilde{\tau})\end{array}\right], \tag{6.47}$$

and the matrix Φ is given by,

$$\Phi=\begin{pmatrix}S-J+\overline{p}^TB_0+B_0^T\overline{P} & P-\overline{P}^T+B_0^T\overline{\overline{P}} & J+\overline{P}^TB_1 & \overline{P}^TB_2\\ * & \tau^2J-\overline{\overline{P}}^T-\overline{\overline{P}} & \overline{\overline{P}}^TB_1 & \overline{\overline{P}}^TB_2\\ * & * & -S-J & 0\\ * & * & * & -\tilde{\mathfrak{a}}\end{pmatrix}. \tag{6.48}$$

Noticing that, $\tilde{U}(t)=\left[\begin{array}{cccc}B_3 & 0 & 0 & B_4\end{array}\right]\eta(t)$, it follows that,

$$\tilde{\mathfrak{a}}\tilde{U}^2(t)=\eta^T(t)E\eta(t),\ \text{where,}\ E=\left[\begin{array}{cccc}B_3 & 0 & 0 & B_4\end{array}\right]^T\tilde{\mathfrak{a}}\left[\begin{array}{cccc}B_3 & 0 & 0 & B_4\end{array}\right].$$

Therefore, by applying Schur complement, we conclude that $\dot{V}(t) < 0$ is satisfied provided that the following LMI:

$$\Psi = \begin{pmatrix} S-J+\overline{P}^T B_0 + B_0^T \overline{P} & P-\overline{P}^T + B_0^T \overline{\overline{P}} & J+\overline{P}^T B_1 & \overline{P}^T B_2 & B_3^T \tilde{\mathfrak{a}} \\ * & \tau^2 J - \overline{\overline{P}}^T - \overline{\overline{P}} & \overline{\overline{P}}^T B_1 & \overline{\overline{P}}^T B_2 & 0 \\ * & * & -S-J & 0 & 0 \\ * & * & * & -\tilde{\mathfrak{a}} & B_4^T \tilde{\mathfrak{a}} \\ * & * & * & * & -\tilde{\mathfrak{a}} \end{pmatrix} < 0, \tag{6.49}$$

holds. Next, by following arguments of [105, 106], we deduce from $\Psi < 0$ that the last block in (6.49) satisfies $\begin{pmatrix} -\tilde{\mathfrak{a}} & B_4^T \tilde{\mathfrak{a}} \\ * & -\tilde{\mathfrak{a}} \end{pmatrix} < 0$. The latter implies by Schur complement that $-I + B_4^T B_4 < 0$. Hence, the eigenvalues of B_4 are inside the unit circle, i.e. the difference equation $\tilde{U}(t) = B_4 \tilde{U}(t-\tilde{\tau})$ is stable for all $\tilde{\tau} > 0$. The latter, together with $\dot{V} < 0$, guarantees the asymptotic stability of the system (6.43). We mention that it is possible to extend the stability result to the nonlinear system (6.35), using the functional V (i.e. providing some conditions on the nonlinear terms F and G as in [106], Section 3.11). However, since it seems actually difficult to interpret the LMI (6.49) as a combined targeted therapy for the studied biological system, we slightly modify our Lyapunov approach by designing, in the next section, a suitable specific LKF for the studied system that provides explicit (sufficient) stability conditions for the dormancy steady state of the nonlinear system (6.35). The functional that we are going to propose has some similarities with the functional V. Actually, in the next section, we are going to select some matrices P, S and J, together with the constant $\tilde{\mathfrak{a}}$, involved in the above construction. Thus, we will determine analytically some upper-bounds on $\dot{V}$, through classical inequalities. Not surprisingly, the latter approach increases the *conservatism* of the sufficient stability condition in the LMI form (the LMI condition is given by (6.49)). That is the price of determining more biologically exploitable results (i.e. explicit exponential decay conditions with an estimate on the decay rate of the solution and a subset of the basin of attraction of the trivial steady state of the nonlinear system (6.35)).

6.4.3 Obtaining Explicit *Exponential* Decay Conditions

We focus on the coupled system using its representation in (6.35), with possibly piecewise continuous solutions. Firstly, let us introduce the quadratic function:

$$\mathfrak{Q}(X,\tilde{X}) = Q(X) + \lambda_1 Q(\tilde{X}), \text{ where, } Q(\ell) = \tfrac{1}{2}\ell^2, \tag{6.50}$$

and $\lambda_1 = 2$. This is equivalent to put $P = diag\{1/2, 1\}$ in V of the previous section. Next, we consider the following operators,

$$\mathscr{Y}(\tilde{\varphi}) = \int_{-\tilde{\tau}}^{0} e^{\rho_1 \ell} Q(\tilde{\varphi}(\ell)) d\ell, \text{ and,} \tag{6.51}$$

$$\mathscr{S}(\varphi) = \int_{-\tau}^{0} e^{\rho_2 \ell} Q(\varphi(\ell)) d\ell, \tag{6.52}$$

where, $\varphi \in \mathscr{C}\left([-\tau,0],\mathbb{R}\right)$, $\tilde{\varphi} \in \mathscr{C}\left([-\tilde{\tau},0],\mathbb{R}\right)$, and ρ_1, ρ_2, are strictly positive constants that we determine later. In fact, observe that, compared to the integral terms in V of the previous section, $\mathscr{S}$ and $\mathscr{Y}$ have exponential functions -in the integral terms- that make it possible to get a lower-bound on the exponential decay of the solutions. Next, in the quest for explicit decay conditions, we are going to substitute $\dot{X}$ and $\dot{\tilde{X}}$ when computing the derivative of $\mathfrak{Q}$ (which is not the approach adopted in the descriptor method, where $\dot{X}$ and $\dot{\tilde{X}}$ were not replaced). Thus, the derivative of $\mathfrak{Q}$ along the trajectories of (6.35), satisfies

$$\begin{aligned}\dot{\mathfrak{Q}}(t) =& -2\mathfrak{a}_1\lambda_1 Q(\tilde{X}(t)) - 2\mathfrak{a}_6 Q(X(t)) - (\mathfrak{a}_2\lambda_1+\mathfrak{a}_7)X(t)\tilde{X}(t)\\ &+\mathfrak{a}_3\lambda_1\tilde{X}(t)\tilde{U}(t-\tilde{\tau}) + \mathfrak{a}_8 X(t)X(t-\tau) + \mathfrak{a}_9 X(t)\tilde{X}(t-\tau)\\ &+\lambda_1\tilde{X}(t)F(X(t),\tilde{X}(t)) + X(t)G(X_t,\tilde{X}_t).\end{aligned} \tag{6.53}$$

Notice that the derivative of $\mathscr{Y}(\tilde{U}_t)$, for almost all $t \geq 0$, is

$$\dot{\mathscr{Y}}(t) = Q(\tilde{U}(t)) - e^{-\rho_1\tilde{\tau}}Q(\tilde{U}(t-\tilde{\tau})) - \rho_1\mathscr{Y}(\tilde{U}_t). \tag{6.54}$$

Now, using the second equation in (6.35), we obtain

$$\begin{aligned}\dot{\mathscr{Y}}(t) =& -\rho_1\mathscr{Y}(\tilde{U}_t) + \mathfrak{a}_4^2 Q(\tilde{X}(t)) + \mathfrak{a}_2^2 Q(X(t)) - (e^{-\rho_1\tilde{\tau}} - \mathfrak{a}_5^2)Q(\tilde{U}(t-\tilde{\tau}))\\ &+\mathfrak{a}_2\mathfrak{a}_4 X(t)\tilde{X}(t) + \mathfrak{a}_2\mathfrak{a}_5 X(t)\tilde{U}(t-\tilde{\tau}) + \mathfrak{a}_4\mathfrak{a}_5\tilde{X}(t)\tilde{U}(t-\tilde{\tau})\\ &+Q(F(\tilde{X}(t),X(t))) - F(X(t),\tilde{X}(t))\left[\mathfrak{a}_4\tilde{X}(t) + \mathfrak{a}_2 X(t) + \mathfrak{a}_5\tilde{U}(t-\tilde{\tau})\right],\end{aligned}$$

where the $\mathfrak{a}_i$'s and F are defined after (6.35). Similarly, we compute the derivatives of the functionals $\mathscr{S}(X_t)$ and $\mathscr{S}(\tilde{X}_t)$. By combining the previous intermediate results (i.e. $\dot{\mathfrak{Q}}$, $\dot{\mathscr{Y}}$ and $\dot{\mathscr{S}}$), we deduce that the time derivative of the functional,

$$V^{\dagger}(X_t,\tilde{X}_t,\tilde{U}_t) = \mathfrak{Q}(X(t),\tilde{X}(t)) + \lambda_2\mathscr{S}(X_t) + \lambda_3\mathscr{S}(\tilde{X}_t) + \lambda_4\mathscr{Y}(\tilde{U}_t), \tag{6.55}$$

where λ_2, λ_3 and λ_4 are positive constants to be chosen later, along the trajectories of (6.35) is given, for almost all $t \geq 0$, by:

$$\begin{aligned}\dot{V}^{\dagger}(t) =& -\left[2\lambda_1\mathfrak{a}_1 - \lambda_3 - \lambda_4\mathfrak{a}_4^2\right]Q(\tilde{X}(t)) - \left[2\mathfrak{a}_6 - \lambda_2 - \lambda_4\mathfrak{a}_2^2\right]Q(X(t))\\ &-\rho_2\lambda_3\mathscr{S}(\tilde{X}_t) - \rho_2\lambda_2\mathscr{S}(X_t) - \rho_1\lambda_4\mathscr{Y}(\tilde{U}_t) - \lambda_4\left[e^{-\rho_1\tilde{\tau}} - \mathfrak{a}_5^2\right]Q(\tilde{U}(t-\tilde{\tau}))\\ &-\lambda_2 e^{-\rho_2\tau}Q\left(X(t-\tau)\right) - \lambda_3 e^{-\rho_2\tau}Q(\tilde{X}(t-\tau)) + \mathfrak{a}_2\mathfrak{a}_5\lambda_4 X(t)\tilde{U}(t-\tilde{\tau})\\ &-[\mathfrak{a}_2\lambda_1 + \mathfrak{a}_7 - \lambda_4\mathfrak{a}_2\mathfrak{a}_4]X(t)\tilde{X}(t) + \mathfrak{a}_8 X(t)X(t-\tau) + \mathfrak{a}_9 X(t)\tilde{X}(t-\tau)\\ &+[\mathfrak{a}_3\lambda_1 + \mathfrak{a}_4\mathfrak{a}_5\lambda_4]\tilde{X}(t)\tilde{U}(t-\tilde{\tau}) - \mathfrak{a}_5\lambda_4 F(X(t),\tilde{X}(t))\tilde{U}(t-\tilde{\tau})\\ &+X(t)G(X_t,\tilde{X}_t) + \lambda_4 Q(F(\tilde{X}(t),X(t))) - \lambda_4 F(X(t),\tilde{X}(t))\left[\mathfrak{a}_4\tilde{X}(t) + \mathfrak{a}_2 X(t)\right].\end{aligned}$$

Next, we recall that for strictly positive constants, $\nu_i > 0$, $i = 1$ to 5, (that we will choose later), we have the following inequalities: $\left|X\tilde{X}\right| \leq \frac{1}{\nu_1}Q(X) + \nu_1 Q(\tilde{X})$, $\left|X(t)X(t-\tau)\right| \leq \frac{1}{\nu_2}Q(X(t)) + \nu_2 Q(X(t-\tau))$, $\left|X(t)\tilde{X}(t-\tau)\right| \leq \frac{1}{\nu_3}Q(X(t)) + \nu_3 Q(\tilde{X}(t-\tau))$, $\left|\tilde{X}(t)\tilde{U}(t-\tilde{\tau})\right| \leq \frac{1}{\nu_4}Q(\tilde{X}(t)) + \nu_4 Q(\tilde{U}(t-\tilde{\tau}))$, $\left|X(t)\tilde{U}(t-\tilde{\tau})\right| \leq \frac{1}{\nu_5}Q(X(t)) + \nu_5 Q(\tilde{U}(t-\tilde{\tau}))$. Therefore, it follows that the derivative $\dot{V}^{\dagger}(t)$ satisfies, for almost all $t \geq 0$,

the following inequality:

$$\begin{aligned}\dot{V}^{\dagger}(t) \leq & -\left[2\lambda_1\mathfrak{a}_1-\mathfrak{b}_1\right]Q(\tilde{X}(t))-\left[2\mathfrak{a}_6-\mathfrak{b}_2\right]Q(X(t))-\rho_2\lambda_3\mathscr{S}(\tilde{X}_t)\\ & -\rho_2\lambda_2\mathscr{S}(X_t)-\rho_1\lambda_4\mathscr{Y}(\tilde{U}_t)-\left[\lambda_4e^{-\rho_1\tilde{\tau}}-\mathfrak{b}_3\right]Q(\tilde{U}(t-\tilde{\tau}))\\ & -\left[\lambda_2e^{-\rho_2\tau}-\mathfrak{b}_4\right]Q\left(X(t-\tau)\right)-\left[\lambda_3e^{-\rho_2\tau}-\mathfrak{b}_5\right]Q(\tilde{X}(t-\tau))\\ & +\lambda_4Q(F(\tilde{X}(t),X(t)))-\mathfrak{a}_5\lambda_4F(X(t),\tilde{X}(t))\tilde{U}(t-\tilde{\tau})\\ & +X(t)G(X_t,\tilde{X}_t)-\lambda_4F(X(t),\tilde{X}(t))\left[\mathfrak{a}_4\tilde{X}(t)+\mathfrak{a}_2X(t)\right],\end{aligned} \tag{6.56}$$

where,

$$\begin{cases}\mathfrak{b}_1 = & \lambda_3+\lambda_4\mathfrak{a}_4^2+\nu_1\left|\mathfrak{a}_2\lambda_1+\mathfrak{a}_7-\lambda_4\mathfrak{a}_2\mathfrak{a}_4\right|,\\ \mathfrak{b}_2 = & \lambda_2+\lambda_4\mathfrak{a}_2^2+\frac{\left|\mathfrak{a}_2\lambda_1+\mathfrak{a}_7-\lambda_4\mathfrak{a}_2\mathfrak{a}_4\right|}{\nu_1}+\frac{|\mathfrak{a}_8|}{\nu_2}+\frac{|\mathfrak{a}_9|}{\nu_3}+\frac{|\mathfrak{a}_2\mathfrak{a}_5|\lambda_4}{\nu_5},\\ \mathfrak{b}_3 = & \lambda_4\mathfrak{a}_5^2+\nu_4\left|\mathfrak{a}_3\lambda_1+\mathfrak{a}_4\mathfrak{a}_5\lambda_4\right|+\nu_5\lambda_4\left|\mathfrak{a}_2\mathfrak{a}_5\right|,\\ \mathfrak{b}_4 = & \nu_2|\mathfrak{a}_8|,\ \text{ and, }\ \mathfrak{b}_5=\nu_3|\mathfrak{a}_9|.\end{cases} \tag{6.57}$$

Now we are ready to determine decay conditions that ensure the regional exponential stability of the trivial steady state of the system (6.35). The terms where F and G are involved in (6.56) will be used only to determine a subset of the basin of attraction of the trivial steady state of the system (6.35).

Let us focus on the constant which is multiplied by $Q(\tilde{U}(t-\tilde{\tau}))$ in (6.56). Using the inequality $|\mathfrak{a}_3\lambda_1+\mathfrak{a}_4\mathfrak{a}_5\lambda_4|\leq\lambda_1|\mathfrak{a}_3|+\lambda_4|\mathfrak{a}_4\mathfrak{a}_5|$, we notice that the inequality $\lambda_4e^{-\rho_1\tilde{\tau}}-\mathfrak{b}_3>0$ is verified if

$$\lambda_4\left(e^{-\rho_1\tilde{\tau}}-\mathfrak{a}_5^2-\nu_4|\mathfrak{a}_4\mathfrak{a}_5|-\nu_5|\mathfrak{a}_2\mathfrak{a}_5|\right)-\nu_4\lambda_1|\mathfrak{a}_3|>0. \tag{6.58}$$

For later use, we set $\mathfrak{d}_1\triangleq\lambda_4\left(e^{-\rho_1\tilde{\tau}}-\mathfrak{a}_5^2-\nu_4|\mathfrak{a}_4\mathfrak{a}_5|-\nu_5|\mathfrak{a}_2\mathfrak{a}_5|\right)-\nu_4\lambda_1|\mathfrak{a}_3|$.

We deduce that the first decay condition is given by:

$$\mathfrak{a}_5^2+\nu_4|\mathfrak{a}_4\mathfrak{a}_5|+\nu_5|\mathfrak{a}_2\mathfrak{a}_5|<1. \tag{6.59}$$

Indeed, the previous condition is necessary to guarantee that (6.58) is satisfied. Now, let us select $\nu_4=\frac{1}{2}|\mathfrak{a}_4|^{-1}$, and $\nu_5=\frac{1}{2}|\mathfrak{a}_2|^{-1}$, for $\mathfrak{a}_4\neq0$ and $\mathfrak{a}_2\neq0$. Using the definitions of $\mathfrak{a}_i$'s, ν_4 and ν_5, it follows that the first decay condition (6.59) is equivalent to

$$(2\tilde{K}e^{-\tilde{\gamma}\tilde{\tau}})^2+2\tilde{K}e^{-\tilde{\gamma}\tilde{\tau}}<1. \tag{6.60}$$

Remark 37. *One notices that we have deliberately chosen $\nu_4=\frac{1}{2}|\mathfrak{a}_4|^{-1}$, and, $\nu_5=\frac{1}{2}|\mathfrak{a}_2|^{-1}$, and that these choices are not unique. Indeed, our objective here is to determine a sufficient decay condition that involves only the unhealthy parameters of the permanently dividing subpopulation (for instance, the subpopulation with FLT3-type mutations in AML) which are, $\tilde{K}$, $\tilde{\tau}$ and $\tilde{\gamma}$. For that purpose, we derive a decay condition involving only the parameter $\mathfrak{a}_5$. Therefore, ν_4 and ν_5 are used in order to compensate $\mathfrak{a}_4$ and $\mathfrak{a}_2$. A more general form is given by $\nu_4=\tilde{\nu}_4|\mathfrak{a}_4|^{-1}$, $\nu_5=\tilde{\nu}_5|\mathfrak{a}_2|^{-1}$, where $\tilde{\nu}_4>0$, and, $\tilde{\nu}_5>0$. In this case, the decay condition* (6.60) *rewrites as, $(2\tilde{K}e^{-\tilde{\gamma}\tilde{\tau}})^2+2\left(\tilde{\nu}_4+\tilde{\nu}_5\right)\tilde{K}e^{-\tilde{\gamma}\tilde{\tau}}<1$.*

Now, notice that a direct consequence of the inequality (6.60) is that for all $\rho_1 \in \left(0, \frac{1}{\tilde{\tau}} \ln\left(\frac{5}{1+4\left[\mathfrak{a}_5^2+\mathfrak{a}_5\right]}\right)\right)$, we get $e^{-\rho_1\tilde{\tau}} - \left[\mathfrak{a}_5^2+\mathfrak{a}_5\right] > \frac{1-\left[\mathfrak{a}_5^2+\mathfrak{a}_5\right]}{5} > 0$. Consequently, we deduce that $\mathfrak{d}_1$, which is defined right after (6.58), and which is now equal to: $\mathfrak{d}_1 = \lambda_4\left(e^{-\rho_1\tilde{\tau}} - \left[\mathfrak{a}_5^2+\mathfrak{a}_5\right]\right) - \nu_4\lambda_1|\mathfrak{a}_3|$, satisfies the inequality, $\mathfrak{d}_1 > 0$, for all $\lambda_4 = \frac{\tilde{\lambda}_4\lambda_1\nu_4|\mathfrak{a}_3|}{e^{-\rho_1\tilde{\tau}}-\left[\mathfrak{a}_5^2+\mathfrak{a}_5\right]} > 0$, where $\tilde{\lambda}_4 > 1$. Next, using the inequality,

$$\left|F(X(t),\tilde{X}(t))\tilde{U}(t-\tilde{\tau})\right| \leq \frac{2|\mathfrak{a}_5|\lambda_4}{\mathfrak{d}_1}Q(F(X(t),\tilde{X}(t))) + \frac{\mathfrak{d}_1}{2|\mathfrak{a}_5|\lambda_4}Q(\tilde{U}(t-\tilde{\tau}),$$

it follows from (6.56) that,

$$\begin{aligned}\dot{V}^{\dagger}(t) \leq & -\left[2\lambda_1\mathfrak{a}_1 - \mathfrak{b}_1\right]Q(\tilde{X}(t)) - \left[2\mathfrak{a}_6 - \mathfrak{b}_2\right]Q(X(t)) - \frac{\mathfrak{d}_1}{2}Q(\tilde{U}(t-\tilde{\tau})) \\ & - \rho_2\lambda_2\mathscr{S}(X_t) - \rho_2\lambda_3\mathscr{S}(\tilde{X}_t) - \left[\lambda_2 e^{-\rho_2\tau} - \mathfrak{b}_4\right]Q(X(t-\tau)) \\ & - \left[\lambda_3 e^{-\rho_2\tau} - \mathfrak{b}_5\right]Q(\tilde{X}(t-\tau)) - \rho_1\lambda_4\mathscr{V}(\tilde{U}_t) + H(X_t,\tilde{X}_t),\end{aligned} \tag{6.61}$$

where,

$$\begin{aligned}H\left(X_t,\tilde{X}_t\right) = & \left(\lambda_4 + \frac{2\left(\mathfrak{a}_5\lambda_4\right)^2}{\mathfrak{d}_1}\right)Q(F(X(t),\tilde{X}(t))) + X(t)G(X_t,\tilde{X}_t) \\ & - \lambda_4 F(X(t),\tilde{X}(t))\left[\mathfrak{a}_4\tilde{X}(t) + \mathfrak{a}_2X(t)\right].\end{aligned} \tag{6.62}$$

Arguing similarly, we select ν_2 and ν_3 that compensate the terms $\mathfrak{a}_8$ and $\mathfrak{a}_9$ (for $|\mathfrak{a}_8| \neq 0$, and $|\mathfrak{a}_9| \neq 0$). For instance, we can consider $\nu_2 = \frac{1}{6|\mathfrak{a}_8|}$ and $\nu_3 = \frac{1}{6|\mathfrak{a}_9|}$. Then, we put, for instance, $\lambda_2 = \lambda_3 = \frac{1}{3}$. We notice that our choices of ν_2 and ν_3 in this case are equivalent to $\mathfrak{b}_4 = \mathfrak{b}_5 = \frac{1}{6}$, and it follows that for all $\rho_2 \in \left(0, \frac{1}{\tau}\ln\left(\frac{\lambda_2}{\mathfrak{b}_4}\right)\right)$, we obtain in this case $e^{-\rho_2\tau} > \frac{2}{3}$. Thus, we end up with[8]

$$\begin{aligned}\mathfrak{d}_2 &\triangleq \lambda_2 e^{-\rho_2\tau} - \mathfrak{b}_4 = \tfrac{1}{3}\left(e^{-\rho_2\tau} - \tfrac{1}{2}\right) > \tfrac{1}{18}, \\ \mathfrak{d}_3 &\triangleq \lambda_3 e^{-\rho_2\tau} - \mathfrak{b}_5 = \tfrac{1}{3}\left(e^{-\rho_2\tau} - \tfrac{1}{2}\right) > \tfrac{1}{18}.\end{aligned} \tag{6.63}$$

Finally, by selecting $\nu_1 = \lambda_1 = 2$, all the setting parameters involved in the functional $V^{\dagger}$ are now chosen. We conclude that if the decay conditions $\mathfrak{d}_4 \triangleq 2\lambda_1\mathfrak{a}_1 - \mathfrak{b}_1 > 0$, and $\mathfrak{d}_5 \triangleq 2\mathfrak{a}_6 - \mathfrak{b}_2 > 0$, are satisfied, then (6.61) satisfies for almost all $t \geq 0$,

$$\begin{aligned}\dot{V}^{\dagger}(t) \leq & -3\overline{\mathfrak{d}}V^{\dagger}(X_t,\tilde{X}_t,\tilde{U}_t) - \frac{\mathfrak{d}_4}{2}Q(\tilde{X}(t)) - \frac{\mathfrak{d}_5}{2}Q(X(t)) - \frac{\mathfrak{d}_1}{2}Q(\tilde{U}(t-\tilde{\tau})) \\ & - \mathfrak{d}_2 Q(X(t-\tau)) - \mathfrak{d}_3 Q(\tilde{X}(t-\tau)) + H(X_t,\tilde{X}_t),\end{aligned}$$

where $\overline{\mathfrak{d}} = \frac{1}{3}\min\left\{\frac{\mathfrak{d}_4}{2\lambda_1}, \frac{\mathfrak{d}_5}{2}, \rho_1, \rho_2\right\}$.

[8] Similarly to ν_4 and ν_5 in Remark 37, the choices of ν_2 and ν_3 are not unique (and, similarly, those of λ_2 and λ_3 either). In Example 12, we are going to use different numerical values that also satisfy $\mathfrak{d}_2 > 0$ and $\mathfrak{d}_3 > 0$.

Now, we focus on the function H, defined after (6.61), in order to define a subset of the basin of attraction of the trivial steady state of system (6.35). We recall that there exist $\mathfrak{c}_i > 0$, $i = 1,\dots,6$ such that (6.41) and (6.42) are satisfied. In addition, from the expression of $V^\dagger$, defined in (6.55), we notice that since $\lambda_1 = 2$, we get,

$$V^\dagger(X_t,\tilde{X}_t,\tilde{U}_t) \geq \frac{\mathfrak{c}_1}{\max\{\mathfrak{c}_1,\mathfrak{c}_2\}}Q(X(t)) + \frac{\mathfrak{c}_2}{\max\{\mathfrak{c}_1,\mathfrak{c}_2\}}Q(\tilde{X}(t),$$

$$\left|\tilde{X}(t)\right| \leq \sqrt{V^\dagger(X_t,\tilde{X}_t,\tilde{U}_t)}, \text{ and, } \left|X(t)\right| \leq \sqrt{2V^\dagger(X_t,\tilde{X}_t,\tilde{U}_t)}.$$

By combining the previous inequalities, we get the following upper bound:

$$\begin{aligned}\left|H(X_t,\tilde{X}_t)\right| \leq\ & \nu {V^\dagger}^2(X_t,\tilde{X}_t,\tilde{U}_t) + \mathfrak{c}_5\sqrt{2V^\dagger(X_t,\tilde{X}_t,\tilde{U}_t)}Q(X(t-\tau)) \\ & + \left[\lambda_4\mathfrak{c}_1(\mathfrak{a}_4+\mathfrak{a}_2)+\mathfrak{c}_3\right]\sqrt{2V^\dagger(X_t,\tilde{X}_t,\tilde{U}_t)}Q(X(t)) \\ & + \left[\lambda_4\mathfrak{c}_2(\mathfrak{a}_4+\mathfrak{a}_2)+\mathfrak{c}_4\right]\sqrt{2V^\dagger(X_t,\tilde{X}_t,\tilde{U}_t)}Q(\tilde{X}(t)) \\ & + \mathfrak{c}_6\sqrt{2V^\dagger(X_t,\tilde{X}_t,\tilde{U}_t)}Q(\tilde{X}(t-\tau)),\end{aligned} \tag{6.64}$$

where, $\nu = \frac{\left(\mathfrak{d}_1\lambda_4+2(\mathfrak{a}_5\lambda_4)^2\right)\max\{\mathfrak{c}_1,\mathfrak{c}_2\}^2}{2\mathfrak{d}_1}$. A direct consequence is that the time derivative of $V^\dagger$ satisfies for almost all $t \geq 0$,

$$\begin{aligned}\dot{V}^\dagger(t) \leq & -2\overline{\mathfrak{d}}V^\dagger(X_t,\tilde{X}_t,\tilde{U}_t) - \frac{\mathfrak{d}_1}{2}Q(\tilde{U}(t-\tilde{\tau})) \\ & - \left[\overline{\mathfrak{d}} - \nu V^\dagger(X_t,\tilde{X}_t,\tilde{U}_t)\right]V^\dagger(X_t,\tilde{X}_t,\tilde{U}_t) \\ & - \left[\frac{\mathfrak{d}_4}{2} - \left(\lambda_4\mathfrak{c}_2(\mathfrak{a}_4+\mathfrak{a}_2)+\mathfrak{c}_4\right)\sqrt{2V^\dagger(X_t,\tilde{X}_t,\tilde{U}_t)}\right]Q(\tilde{X}(t)) \\ & - \left[\mathfrak{d}_2 - \mathfrak{c}_5\sqrt{2V^\dagger(X_t,\tilde{X}_t,\tilde{U}_t)}\right]Q(X(t-\tau)) \\ & - \left[\frac{\mathfrak{d}_5}{2} - \left(\lambda_4\mathfrak{c}_1(\mathfrak{a}_4+\mathfrak{a}_2)+\mathfrak{c}_3\right)\sqrt{2V^\dagger(X_t,\tilde{X}_t,\tilde{U}_t)}\right]Q(X(t)) \\ & - \left[\mathfrak{d}_3 - \mathfrak{c}_6\sqrt{2V^\dagger(X_t,\tilde{X}_t,\tilde{U}_t)}\right]Q(\tilde{X}(t-\tau)).\end{aligned} \tag{6.65}$$

Consequently, for all initial conditions belonging to the set

$$\mathscr{B} = \left\{\left(\varphi_X,\varphi_{\tilde{X}},\varphi_{\tilde{U}}\right) \in \mathscr{C}_\tau \times \tilde{\mathscr{C}}_\tau \times \tilde{\mathscr{C}}_{\tilde{\tau}} \;\middle|\; V^\dagger\left(\varphi_X,\varphi_{\tilde{X}},\varphi_{\tilde{U}}\right) < \overline{V}^\dagger\right\}, \tag{6.66}$$

where, with an abuse of notation, we consider the spaces of continuous functions: $\mathscr{C}_\tau = \mathscr{C}\left([-\tau,0],(-x_e,+\infty)\right)$, $\tilde{\mathscr{C}}_\tau = \mathscr{C}\left([-\tau,0],(-\tilde{x}_e,+\infty)\right)$, and, $\tilde{\mathscr{C}}_{\tilde{\tau}} = \mathscr{C}\left([-\tilde{\tau},0],(-\tilde{u}_e,+\infty)\right)$, as well as the upper bound: $\overline{V}^\dagger = \min\{\frac{\overline{\mathfrak{d}}}{\nu},u_1^2,u_2^2,u_3^2,u_4^2\}$, where, $u_1 = \frac{\mathfrak{d}_4}{8\left(\lambda_4\mathfrak{c}_2(\mathfrak{a}_4+\mathfrak{a}_2)+\mathfrak{c}_4\right)}$, $u_2 = \frac{\mathfrak{d}_5}{8\left(\lambda_4\mathfrak{c}_1(\mathfrak{a}_4+\mathfrak{a}_2)+\mathfrak{c}_3\right)}$, $u_3 = \frac{\mathfrak{d}_4}{4\mathfrak{c}_5}$, and, $u_4 = \frac{\mathfrak{d}_3}{4\mathfrak{c}_6}$, we finally find that the derivative of the functional $V^\dagger$ satisfies:

$$\dot{V}^\dagger(t) \leq -2\overline{\mathfrak{d}}V^\dagger(X_t,\tilde{X}_t,\tilde{U}_t), \text{ where } \overline{\mathfrak{d}} > 0, \text{ for almost all } t \geq 0.$$

We integrate this inequality and we obtain for all $t \geq 0$,

$$V^{\dagger}(X_t, \tilde{X}_t, \tilde{U}_t) \leq e^{-2\overline{\mathfrak{d}}t} V^{\dagger}\left(\varphi_{X_t}, \varphi_{\tilde{X}_t}, \varphi_{\tilde{U}_t}\right). \tag{6.67}$$

Consequently, we get for all $t \geq 0$, $X^2(t) + \lambda_1 \tilde{X}^2(t) \leq 2e^{-2\overline{\mathfrak{d}}t} V^{\dagger}\left(\varphi_X, \varphi_{\tilde{X}}, \varphi_{\tilde{U}}\right)$. We conclude that the trajectories $X(t)$ and $\tilde{X}(t)$ converge exponentially to the trivial steady state of the shifted system, with a decay rate larger than, or equal to, $\overline{\mathfrak{d}}$. By classical arguments, we observe from the second equation in (6.35) that, since $2\tilde{K}e^{-\tilde{\gamma}\tilde{\tau}} < 1$, $\tilde{U}(t)$ converges exponentially to zero when $X(t)$ and $\tilde{X}(t)$ converge exponentially to the zero.

To summarize, we considered that $\mathfrak{D}$ (or $\mathfrak{E}$) exists and we rewrote the studied system (6.8) in the form (6.35). Next, we proved that if the decay conditions ((6.60), $\mathfrak{d}_4 > 0$, $\mathfrak{d}_5 > 0$) are satisfied, then the trajectories of (6.35) associated with initial conditions belonging to the set $\mathscr{B}$, converge exponentially to 0-equilibrium of the shifted system (6.35), with a decay rate larger than, or equal to, $\overline{\mathfrak{d}}$. By explicitly rewriting the decay conditions, we summarize our findings as follows:

Theorem 14. ***(A)*** *Assume that $\mathfrak{D}$ (resp. $\mathfrak{E}$) exists, then consider the shifted system* (6.35)*, such that its trivial steady state corresponds to $\mathfrak{D}$ (resp. $\mathfrak{E}$) of* (6.8)*. If there exist matrices P, S, J, $\overline{P}$ and $\overline{\overline{P}}$, of appropriate dimension, and a positive constant $\tilde{\mathfrak{a}}$, that satisfy the LMI* (6.49)*, then the trivial steady state of the shifted system* (6.35)*, which is $\mathfrak{D}$ (resp. $\mathfrak{E}$) of* (6.8)*, is locally asymptotically stable.*

(B) *Assume that system* (6.8) *admits a positive steady state $\mathfrak{D}$ (i.e.* (6.23) *or* (6.24) *in Proposition 6-**(vii)** hold). If*

$$\begin{array}{ll} i) & \left(2\tilde{K}e^{-\tilde{\gamma}\tilde{\tau}}\right)^2 + 2\tilde{K}e^{-\tilde{\gamma}\tilde{\tau}} < 1, \\ ii) & \frac{\mathfrak{b}_1}{4} - \tilde{\alpha}\tilde{\theta}\tilde{x}_e < \tilde{\beta}\left(x_e + \tilde{\alpha}\tilde{x}_e\right) + \tilde{\delta}, \\ iii) & \frac{\mathfrak{b}_2}{2} - \theta x_e < \beta\left(x_e + \tilde{x}_e\right) + \delta, \end{array} \tag{6.68}$$

are satisfied, ensuring also that $\mathfrak{d}_2 > 0$ and $\mathfrak{d}_3 > 0$, then $\mathfrak{D}$ is regionally exponentially stable with a decay rate larger than, or equal to, $\overline{\mathfrak{d}}$, and with basin of attraction defined by:

$$\begin{aligned} \mathscr{B}^{\dagger} = \Bigg\{ & \varphi_x \in \mathscr{C}\left([-\tau, 0], \mathbb{R}^+\right), \varphi_{\tilde{x}} \in \mathscr{C}\left([-\tau, 0], \mathbb{R}^+\right), \varphi_{\tilde{u}} \in \mathscr{C}\left([-\tilde{\tau}, 0], \mathbb{R}^+\right) \Big| \\ & V^{\dagger}\left(\varphi_x - x_e, \varphi_{\tilde{x}} - \tilde{x}_e, \varphi_{\tilde{u}} - \tilde{u}_e\right) < \overline{V}^{\dagger} \Bigg\}. \end{aligned} \tag{6.69}$$

(C) *Assume that $\mathfrak{E}$ exists (Proposition 6-**(ii)**), and consider that $\tilde{x}_e = 0$ in* (6.68)*. If the conditions* (6.68) *are satisfied (for $\tilde{x}_e = 0$), then $\mathfrak{E}$ of* (6.8) *is regionally exponentially stable with a decay rate $\mathfrak{d}$ and basin of attraction defined by* (6.69)*, where we consider now that $\tilde{x}_e = \tilde{u}_e = 0$ in* (6.69)*.*

Example 12. *In this example, we assume that $\tilde{\alpha} = 5$. For the unhealthy compartment, we consider the parameters given in Table 6.1, while for the healthy case we consider the parameters of Table 6.2.*

We want to investigate the stability properties of the dormancy steady state: $\mathfrak{D} = (\tilde{x}_e, \tilde{u}_e, x_e)$, where, $\tilde{x}_e = 0.0217$, $\tilde{u}_e = 0.0593$, and $x_e = 0.2535$. Obviously, if the decay conditions (6.68) *are satisfied, then the LMI* (6.49) *admits a solution.*

$\tilde{\delta}$	$\tilde{\gamma}$	$\tilde{\tau}$	$\tilde{\beta}(m)$	$\tilde{K}$	$\tilde{u}_e$	$\tilde{x}_e$
0.928	0.4	1	$\frac{2.78}{1+3m^2}$	0.2	0.05938567	0.02179864

Table 6.1 Parameters of the unhealthy compartment, and the values of $\tilde{x}_e$ and $\tilde{u}_e$.

δ	γ	τ	$\beta(m)$	x_e
0.168	0.001	0.12	$\frac{0.219}{1+4m^2}$	0.25354595

Table 6.2 Parameters of the healthy hematopoetic stem cell compartment, and the value of x_e.

We check that the decay conditions (6.68) *are verified:*

$$\begin{aligned}
&\textbf{\textit{(i)}} \quad 1-2\tilde{K}e^{-\tilde{\gamma}\tilde{\tau}}-\left(2\tilde{K}e^{-\tilde{\gamma}\tilde{\tau}}\right)^2 = 0.659979347 > 0,\\
&\textbf{\textit{(ii)}} \quad \tilde{\beta}\left(x_e+\tilde{\alpha}\tilde{x}_e\right)+\tilde{\delta}-\left(\frac{\mathfrak{b}_1}{4}-\tilde{\alpha}\tilde{\theta}\tilde{x}_e\right) = 0.987350196 > 0,\\
&\textbf{\textit{(iii)}} \quad \beta\left(x_e+\tilde{x}_e\right)+\delta-\left(\frac{\mathfrak{b}_2}{2}-\theta x_e\right) = 0.000149333 > 0,
\end{aligned} \tag{6.70}$$

where we consider: $\lambda_1 = 2$, $\lambda_2 = \lambda_3 = 0.261780$, $\lambda_4 = 2.205796$, $\tilde{\lambda}_4 = 2$, $\nu_1 = 2$, $\nu_2 = \frac{1}{4|\mathfrak{a}_8|} = 1.301858$, $\nu_3 = \frac{1}{4|\mathfrak{a}_9|} = 1.736024$, $\nu_4 = \frac{1}{2|\mathfrak{a}_4|} = 0.302151$, $\nu_5 = \frac{1}{2|\mathfrak{a}_2|} = 7.374022$, $\rho_1 = \frac{1}{10\tilde{\tau}}\ln\left(\frac{5}{1+4(\mathfrak{a}_5^2+\mathfrak{a}_5)}\right) = 0.075074$ *and* $\rho_2 = \frac{1}{10\tau}\ln\left(\frac{\lambda_2}{\mathfrak{b}_4}\right) = 0.038369$. *For these numerical values, we check that* $\mathfrak{d}_1 = \mathfrak{d}_2 = 0.010577 > 0$. *Therefore, according to Theorem 14, the dormancy steady state,* $\mathfrak{D} = (0.0217, 0.0593, 0.2535)$, *is regionally exponentially stable, as illustrated in Figure 12. This example will be revisited in the next section, in the practical situation of therapeutic strategies.*

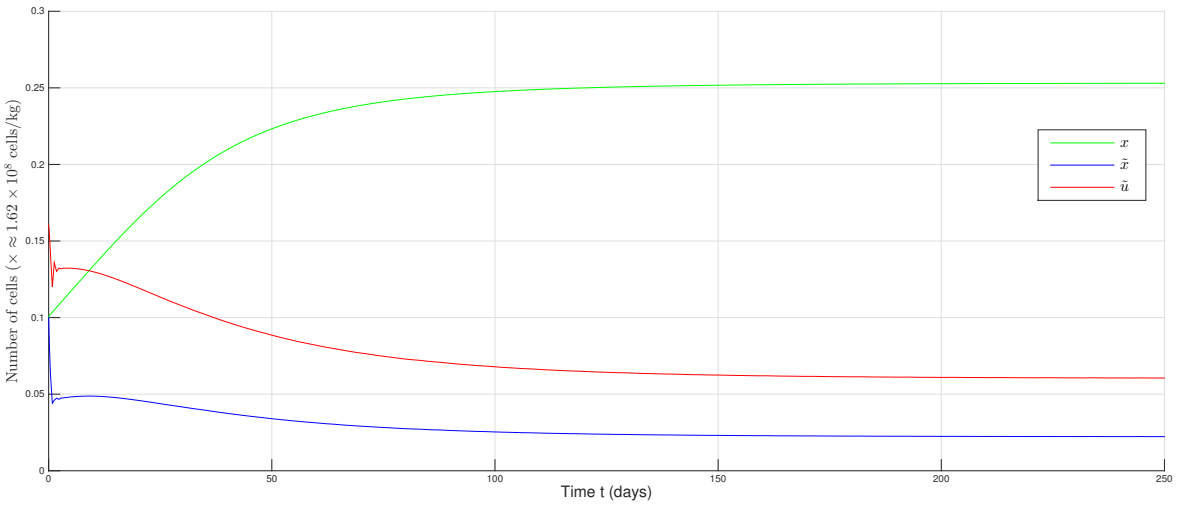

Fig. 6.12 Trajectories of the system of the numerical example 12 (Tables 6.1-6.2). In this case, the dormancy steady state $\mathfrak{D}$ exists, such that $\tilde{x}_e = 0.0217$, $\tilde{u}_e = 0.0593$. The sufficient local stability conditions given in *Theorem 14-(B)* are satisfied, as shown in (6.70), and the trajectories of the system converge exponentially to $\mathfrak{D}$.

6.5 Concluding comments on the findings and possible therapeutic strategies oriented towards cancer dormancy

A first remark is that CSC dormancy probably results from complex relationships between the different biological parameters involved in this process, that are difficult to elicit, let alone to be understood. This observation concerns the stability properties (decay conditions in Theorem 14), but also the conditions of existence of dormancy (Proposition 6-**(vii)**), along with the role of the sensitivity parameter $\tilde{\alpha}$. This should lead us to develop further the mathematical framework sketched here, in order to help us understand the mechanisms behind dormancy.

Nevertheless, as a first step, the analysis that we performed throughout this paper reveals that our theoretical results may suggest some therapeutic guidelines to eradicate aggressive CSCs ($\mathfrak{E}$), or to bring them to dormancy ($\mathfrak{D}$), as discussed in the sequel.

1) Towards the adoption of a common therapeutic strategy to yield states $\mathfrak{D}$ and $\mathfrak{E}$? It cannot be claimed that convergence to the steady state $\mathfrak{D}$ and the steady state $\mathfrak{E}$ should share the same therapeutic roadmap, since a crucial difference lies in their conditions of existence. For instance, $\mathfrak{E}$ exists even if $\tilde{\delta} > \frac{2e^{-\tilde{\gamma}\tilde{\tau}}-1}{1-2\tilde{K}e^{-\tilde{\gamma}\tilde{\tau}}}\tilde{\beta}(0)$ (see Proposition 6), while the reverse situation is required in order to allow for the existence of dormancy $\mathfrak{D}$, in addition to other conditions. We recall that in our system, the conditions of existence of the steady states of interest are a type of *red lines*, that must not be crossed when elaborating a treatment strategy.

On the other hand, when we focus on the stability conditions, wondering how therapeutic actions can make the biological system go into the direction of the decay conditions (6.68), we realize that the respective decay conditions of $\mathfrak{D}$ and $\mathfrak{E}$ are substantially similar. More precisely, our sufficient stability conditions suggest that the biological parameters that can be targeted in order to satisfy (6.68), in either of the two states $\mathfrak{D}$ or $\mathfrak{E}$, are similar (but not identical). In this sense, we can state that a common therapeutic strategy for $\mathfrak{D}$ and $\mathfrak{E}$ can be proposed. So, in light of the existing therapies and recent clinical trials that highlight novel effective molecules as potential drugs in AML, we briefly discuss how a combined therapy may satisfy the theoretical conditions (6.68).

First, we observe that the condition **(B-i)** in Theorem 14 provides a restriction on the dynamics of over-proliferating cells, since $\tilde{K}$, $\tilde{\gamma}$ and $\tilde{\tau}$ are involved. Satisfying the previous condition relies in increasing the product $\tilde{\gamma}\tilde{\tau}$, and decreasing $\tilde{K}$. Increasing $\tilde{\gamma}\tilde{\tau}$ means that we extend the average duration of the cell cycle $\tilde{\tau}$ and/or increase the apoptosis rate $\tilde{\gamma}$ in the population of unhealthy cells. Leukemic cells may be targeted by drugs such as quizartinib (AC220 [305]) or erlotinib [167] to increase $\tilde{\tau}$, while cytosine arabinoside can be used to increase the apoptosis rate $\tilde{\gamma}$. Moreover, quizartinib can be used to decrease the fast self-renewal rate $\tilde{K}$. In fact, $\tilde{K}$ is expected to be the hardest parameters to modify in practice, due to preexisting mutations in epigenetic control genes (DNMT3A, TET2). However, new *FLT3 inhibitors*, such as midostaurin[9], have achieved good performance (see the recent quantitative results provided in [277]) and are now approved for use along with chemotherapy to target leukemic cells in AML.

[9]Midostaurin is a multi-targeted protein kinase inhibitor, which can be active against oncogenic CD135 (FMS-like tyrosine kinase 3 receptor, FLT3). [85, 277]. See also some other comments in Chapter 2.
Basic information on midostaurin can be found in the *American Cancer Society* website:
`https://www.cancer.org/cancer/acute-myeloid-leukemia/treating/targeted-therapy.html`

Next, in the conditions **(B-ii)** and **(B-iii)** of Theorem 14, the targets can be the parameters δ and $\tilde{\delta}$ (mainly $\tilde{\delta}$, since it is the unhealthy parameter) that appear in the right hand sides of the corresponding inequalities. We recall that $\tilde{\delta}$ includes the death rate and the differentiation rate of unhealthy resting cells. In practice, increasing $\tilde{\delta}$ means that we should increase the differentiation rates, which can be achieved in the case of leukemia by infusing dasatinib [167], that targets most of the tyrosine kinases including the c-KIT gene. In fact, it was thought that drugs promoting re-differentiation of CSCs in many cancers are not effective in the specific case of AML. However, this therapeutic option has been relaunched recently after successful clinical trials, where *dihydroorotate dehydrogenase (DHODH) inhibitors* restored differentiation of leukemic cells in AML [278]. Finally, increasing $\beta(0)$ and $\tilde{\beta}(0)$ can be performed by using G-CSF molecules [100]. These are the main common targets shared by $\mathfrak{D}$ and $\mathfrak{E}$.

2) Constraints and spillover risks of CSCs eradication: Increasing the parameters $\tilde{\delta}$, $\tilde{\gamma}$ and $\tilde{\tau}$ (using some of the previously mentioned molecules or their equivalent), promotes the existence of the state $\mathfrak{E}$, together with its stability. However, it may exclude the steady state $\mathfrak{D}$, by violating its conditions of existence. Furthermore, an excessive therapy that affects also healthy cells leads, theoretically, to the extinction of all the cells (*Theorem 13*). At the other extreme, an insufficient dose of drugs leads to CSCs overproliferation (when $2\tilde{K}e^{-\tilde{\gamma}\tilde{\tau}} > 1$). The overproliferating behavior may be worsened by CSC resistance to drugs. Therefore, the dormancy steady state $\mathfrak{D}$ appears as a delicate intermediate equilibrium between the cancer progression and CSC eradication.

3) Specific constraints related to dormancy: In the *common strategy* that aims to satisfy the condition (6.68), we noticed that drugs have to increase the product $\tilde{\gamma}\tilde{\tau}$. On the other hand, we recall from Proposition 6-**(vii)** that the condition $1 < 2e^{-\tilde{\gamma}\tilde{\tau}}$ is necessary for the existence of $\mathfrak{D}$. Thus, the therapy action in this case has to take into account this supplementary condition. We infer from this remark that the probability to achieve the dormancy steady state $\mathfrak{D}$ by using the classical strategies that consist in giving the maximum tolerated dose of drugs during the treatment period [93], is therefore very low. Indeed, since a high dose is expected to yield $1 > 2e^{-\tilde{\gamma}\tilde{\tau}}$, the condition of existence of $\mathfrak{D}$ is then violated.

The multiple restrictions on the biological parameters listed in *Proposition 1* show that the existence of $\mathfrak{D}$ is more difficult to achieve than the existence of $\mathfrak{E}$. However, we suggest that infusing G-CSF molecules appears to favour the existence of a dormancy steady state, since increasing (relatively) $\beta(0)$ seems to go in the right direction in order to satisfy both the existence and the stability conditions of $\mathfrak{D}$.

4) The suggestion of therapeutic strategies that achieve dormancy: In light of the above discussion, we propose to implement what can be considered as a simple theoretical therapeutic strategy that aims to achieve a stable dormancy steady state. More precisely, we consider an hematopoietic system with the clinical symptoms that we expect when facing some overproliferating malignant hemopathies. This ranges from a blockade in differentiation mechanisms to the survival of abnormal cells, along with a high rate of self-renewal activity. We will in fact check that in the absence of adequate treatment, the unhealthy population will proliferate abundantly. Then, in a second time, our objective is to stabilize the total cell density, through multiple drug infusions of a combined therapy that is in line with our theoretical results (i.e. the decay conditions in *Theorem 14*). In other words, we aim to bring the hematopoietic system from an initial abnormal overproliferating state into a dormant stable steady state. For that purpose, let us assume that the initial parameters of the unhealthy compartment are those given in Table 6.3. In

fact, we have deliberately chosen an intuitive set of parameters that matches specific dysfunctions in overproliferating malignant hemopathies (particularly the condition $2\tilde{K}e^{-\tilde{\gamma}\tilde{\tau}} > 1$).

$\tilde{\delta}$	$\tilde{\gamma}$	$\tilde{\tau}$	$\tilde{\beta}(m)$	$\tilde{K}$	$\tilde{\alpha}$
0.25	0.1	0.2	$\frac{2.78}{1+m^3}$	0.55	0.8

Table 6.3 The set of initial (i.e. before treatment) parameters of the unhealthy compartment.

On the other hand, we assume that the parameters of the healthy compartment are those given in Example 12, and we consider that the therapy to be administrated has a negligible effect on ordinary cells.

In medical practice, usually the hematopoietic system is targeted through chemotherapy (a combination of two or three drugs), sometimes infused along with a complementary treatment. All these drugs have molecular targets (e.g. dasatinib targets BCR/Abl, Src, ephrin receptors, c-Kit and many other tyrosine kinases), that result in a modification of some biological mechanisms (e.g. generally, dasatinib increases proliferation, and differentiation in AML [96]).

It should be borne in mind that the functional effect resulting from the molecular action of the infused drugs, varies in practice according to several facts (for instance, the buildup of many types of mutations by some individuals). However, when we put aside all the intermediate complications that may exist in practice, we can take a shortcut that associates to each infused drug its most likely action on one or several biological functions (that are: differentiation, apoptotis, and so on), with a certain amount of confidence. Thus, we can roughly state from medical practice some major families of molecules that can be used in the case of AML or other cancers, according to their expected effect on the biological functionalities.

Fast self-renewing ($\tilde{K}$)	Quizartinib, midostaurin Dihydroorotate dehydrogenase (DHODH) inhibitors
Apoptosis ($\tilde{\gamma}$)	Daunorubicin, cytosine arabinoside, volasertib
Differentiation ($\tilde{\delta}$)	Dihydroorotate dehydrogenase (DHODH) inhibitors
Cell cylce dur. ($\tilde{\tau}$)	Quizartinib, erlotinib, volasertib

Table 6.4 Here we associate the most likely (clinically established) effect of some advanced drugs/molecules on the biological features of the hematopoietic system, in the specific case of AML (without focussing neither on the molecular mechanisms behind each drug action, or on the possible mutual interactions that may exist between drugs within some combinations).

Remark 38. ***(i)*** *One notices that some molecules in Table 6.4 are expected to modify more than one model parameter. For instance, the DHODH inhibitor, which is a differentiation re-activator, may decrease $\tilde{K}$ and increase $\tilde{\delta}$, since both actions seem to promote a return into normal differentiation.*

(ii) *The volasertib (recognized as orphan drug for AML since 2014), belongs to the family of Polo-like kinase (Plk) inhibitors. It can be used in the treatment of AML to promote apoptosis and cell cycle arrest (see for instance [45]). In fact, the list of drugs given in Table 6.4 is not exhaustive and can be enlarged, for instance, to: histone deacetylase (HDAC) inhibitors (vorinostat and panobinostat), and the family of aurora kinase inhibitors (AZD115).*

(iii) *According to the description of the dominance measure $\tilde{\alpha}$, and its acting modes as a sensitivity parameter to mitotic inhibitors (as discussed in Section 6.2.2), we can reasonably suggest some drug infusion ways to change its behavior. It appears that molecules such as vincristine (a mitotic inhibitor), or monoclonal antibodies (e.g. gemtuzumab ozogamicin) and other immuno-oriented therapies, can be more likely expected to act on the parameter $\tilde{\alpha}$.*

Now, we observe that the biological parameters considered in Table 6.3 imply that $2\tilde{K}e^{-\tilde{\gamma}\tilde{\tau}} = 1.078$. It follows that, theoretically, if AML is not treated, unhealthy cells will invade the bone marrow and possibly the bloodstream. In Figure 6.13, we illustrate the evolution of cell densities for the selected model parameters, where we observe the unbounded proliferation of unhealthy cells.

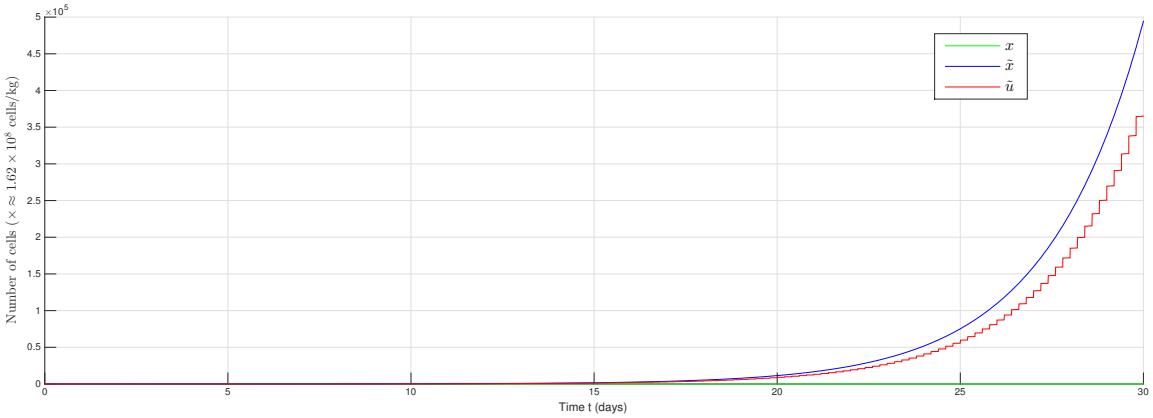

Fig. 6.13 Trajectories of the system for the (non-treated) model parameters of Table 6.3.

Actually, the elaboration of an *optimal* therapeutic strategy[10] is beyond the scope of this chapter. Here, we are suggesting a theoretical therapeutic strategy, that can be based on some suitable combination of drugs (listed in Table 6.4, or others similar ones). We assume that the resulting evolution patterns of the biological model parameters are those illustrated in Figure 7.22. In fact, we can distinguish between two evolution trends, nested within one another as follows:

1) The first series of infusions aims to decrease $\tilde{K}$ (fast self-renewing rate), to increase $\tilde{\tau}$ (cell-cycle duration), and to increase $\tilde{\gamma}$ (apoptosis rate). It is worth mentioning that the direction of the change in the model parameters (i.e. by increasing/decreasing the model parameters values) is in line with the observed effect of the drugs listed in Table 6.3. This treatment phase is expected to limit the expansion of CSCs. We also assume that the first treatment phase is accompanied by a slight increase of the value of $\tilde{\alpha}$, under the effect of the drugs that target unhealthy cells[11].

2) The second phase of the treatment aims, on the one hand, to maintain the trend given for the parameters ($\tilde{K}$, $\tilde{\tau}$, $\tilde{\gamma}$), and on the other hand, to reactivate the differentiation of unhealthy cells (using

[10] The optimal therapy requires the determination of the best infusion planning, that takes into account drug toxicity and other practical considerations (e.g. how the doses of each drug type are spread over the duration of the therapy). These points deserve a separated study. An approach to deal with this issue is proposed in the next chapter (Part III. Chapter 7).

[11] Before therapy, it is expected that $\tilde{\alpha} < 1$, meaning that unhealthy cells are less sensitive than healthy cells to the natural mitotic regulatory molecules that are secreted by the body. Then, we consider that $\tilde{\alpha}$ increases when selected therapy targets unhealthy cells, thus reversing the trend since unhealthy cells become progressively sensitive to more and more regulatory molecules (i.e. drugs) when therapy is in progression.

DHODH inhibitors, for instance) and to increase the sensitivity parameter $\tilde{\alpha}$ with more virulence than in the first series of infusions (by administrating some mitotic regulatory molecules that target unhealthy cells, such as immunotherapy).

Remark 39. *It seems legitimate to wonder whether the reactivation of differentiation of CSCs is a good strategy to fight cancer. The answer is argued for instance in [93], where it is explained how CSCs can initiate and regenerate cancers, while differentiated cancer cells (called CCs [93]) will inevitably die out (see the section "Cancer stem cells and non-stem cancer cells", [93]). Thus, promoting the differentiation of CSCs into CCs appears as a sustainable way to both limit cancer progression, and avoid the escape from cancer dormancy.*

Now, let us assume that an adequate combination of drugs has been fixed. We can highlight one suggestion among other possibilities, in which we propose:

① a shock treatment through chemotherapy promoting apoptosis $\tilde{\gamma}$, cell arrest $\tilde{\tau}$ (e.g. through volasertib for both objectives), and targeting $\tilde{K}$ using AC220 (which may in addition have a suitable effect on cell arrest, i.e. increasing $\tilde{\tau}$),

② followed by a more differentiation-oriented treatment (e.g. using drugs that are based on DHODH inhibitors) and mitotic inhibition of unhealthy cells (possibly using some immunotherapy-based drugs, or vincristine, see also [258]).

We aim through the selected therapy to achieve an evolution pattern of the model parameters as close as possible to the idealistic ones given in Figure 7.22.

Remark 40. *The treatment protocol that we suggest have many similarities with classical methods in AML therapeutics [258]. We can mention in particular the **3+7** most famous strategy, which is also based on two main separated phases (7 days of intensive induction through cytarabine, plus 3 days of an anthracycline [258]), and then possibly followed by consolidation chemotherapy and hematopoietic cell transplant [85, 258].*

Next, we apply the therapeutic strategy given in Figure 7.22 to our model, starting the first infusion at $t = 1$ day, and considering a fixed treatment step of 1 day between successive infusions (another choice may be envisaged if needed). One notices that the model parameters after *Infusion* 9 are those given in Example 12, for which the decay conditions (6.68) of Theorem 14 are satisfied.
The evolution of the ordinary and mutated cell densities is shown in Figure 6.15.

It is worth mentioning that in practice, the treatment of AML is spread over several separated phases. For instance, in the recent experimental work [277], an AML (FLT3-type) therapy based on midostaurin and chemotherapy, has been separated into two *induction phases*, a *consolidating phase* and *maintenance phase* (59% of patients that have undergone the previously mentioned therapeutic protocol, then underwent bone marrow transplant, have reached the complete remission state [277]). Similarly, in our example, we assume that after *Infusion* 9, a consolidating and a maintenance phases continue so as to correct, adjust, strengthen, and fortify the desired dormancy state of the hematopoietic system (which is the state described by the set of parameters of *Infusion* 9).

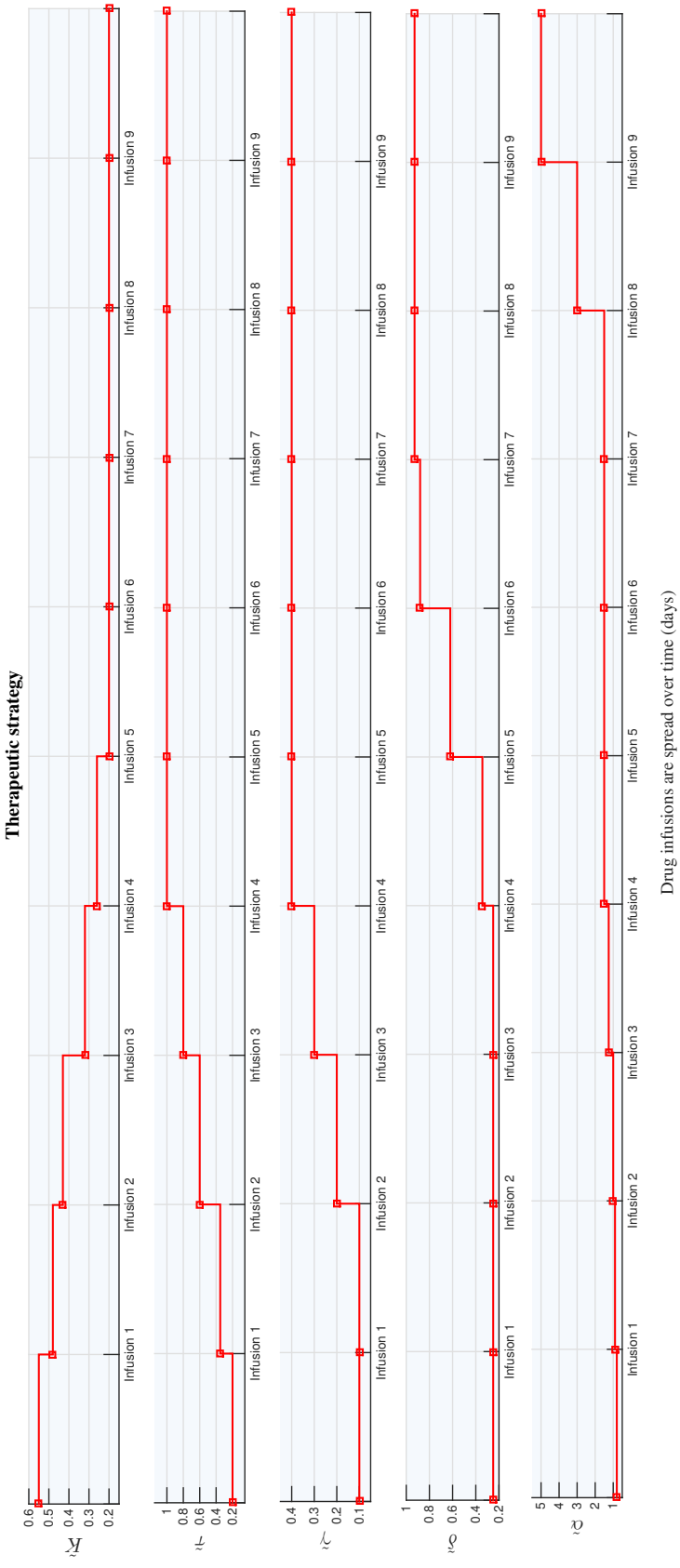

Fig. 6.14 An illustrative therapeutic strategy that gradually modifies five model parameters, using adequates drugs (a mixture of chemotherapy along with complementary molecules).

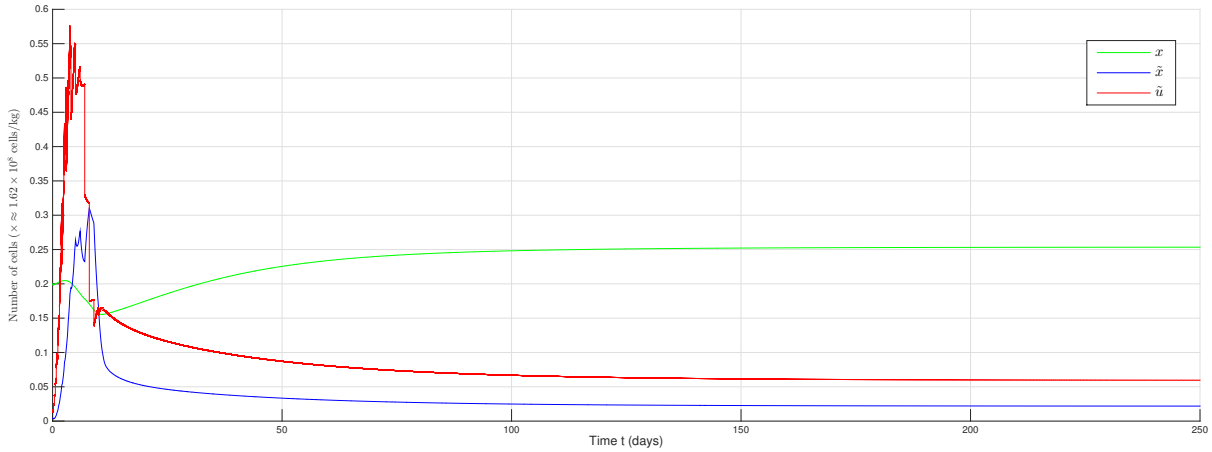

Fig. 6.15 The evolution of the total densities of healthy and unhealthy cells (resp. $x(t)$ and $\tilde{x}(t)$) and $\tilde{u}(t)$, in the mathematical model. The trajectories converge from a leukemic overproliferating behavior to a dormancy stable steady state under the effect of the therapy in Figure 7.22.

We conclude this work by referring to Table 1 in [258], which summarizes a number of emerging promising AML therapies, that open up other possibilities to act on cancerous hematopoietic systems. Many of these strategies can in fact be implemented and discussed within the modeling and analysis framework that we introduced in our current work. It is worth mentioning that the addition of midostaurin to chemotherapy resulted in a 22% lower risk of death among patients, in comparison to another more classical treatment (see [277]). Notice that, most of the molecules listed in [258] (and the references therein) are in early phases of development and trials, but they participate greatly, as well as many multidisciplinary works, to nourish this hope of moving towards systematic treatments for cancer, in general, and leukemia, in particular.

Part III

Nonlinear systems involving growth factors and drugs

Chapter 7

Stabilization of blood cell counts through growth-factors and drugs switching

Synopsis. **Trying to deepen the mathematical modeling of cell dynamics has a cost and may be highly demanding in terms of mathematical analysis. The present work is a step-forward in refining the analysis presented in the previous chapters. First, we start from a description of cell proliferation and quiescence where almost all the involved parameters and functions are affected by multiple growth-factor concentrations. For the first time, we interpret the resulting system as a possibly switching one. This work launches the modeling of hematopoietic systems through switching and event-triggered ones, resulting from drug infusions or from practical situations where the body requires to adapt efficiently its blood cell count (e.g. for combating an infection). The key point consists in the original complete-type formulation of the *stabilization* issues that we propose through artificial intelligence planning tools. In that framework, an optimal solution is discovered via classical planning and scheduling algorithms. We show the large spectrum of application of our method: in the unhealthy hematopoiesis, we address the treatment issue through multiple drug infusions. In that case, we determine the *best* therapeutic strategy that might restore an ordinary hematopoietic system. Next, the healthy hematopoiesis is considered as an *intelligent agent* able to set objectives - that correspond to body requirements - and to achieve them in an optimal way. Biological interpretations and numerical simulations are provided throughout the chapter.**

7.1 General overview and description of the findings

In this work, we will address some open issues, mainly related to the idea of *stabilization* or *regulation* of the hematopoietic process in healthy and unhealthy situations. Knowing that, until now, research efforts were particularly focusing on continually improving the existing models of hematopoietic cell dynamics and on their stability properties. Most of the time, these models involve fixed parameters and functions (representing differentiation, self-renewing, proliferation, death rates, apoptosis rates etc), which are assumed not to depend on growth factors (hormone-like molecules, Chapter 2). In fact, despite their paramount importance, growth factors are evoked in only few works among a large list of papers dedicated to this subject. The reason behind that is quite simple: including growth-factor dynamics notably

complicates the resulting models, as well as their analysis. Not surprisingly, growth-factor dependent parameters are usually avoided.

Moreover, the majority of the mathematical models of hematopoietic systems (at least those studied in [49], [180], [31], [100], [185], [6], [7], [8], [20], [4], [3], [189], [275], [224], [225], [37], [39], [23], [107], [81], [154], and, [170]) share in common the fact that they can admit a *unique* strictly positive steady state, which has been less studied in the models involving growth-factor dependent parameters since it is more demanding in terms of mathematical analysis (refer to the Section 7 of the most recent work [3]).

We want to go a step further in the analysis of the behavior of population dynamical systems. For that purpose, a first step consists in considering a model where almost all the biological functions and parameters are growth-factor dependent. This is in line with the previous works ([31], [185], [6] and [3]) insofar as we will continue their efforts to improve and refine the hematopoietic models. For instance, we consider several discrete maturity stages, where biological parameters of the overall system are controlled by five different growth-factors. We consider that cells may divide with a high degree of freedom[1] during their cell-cycle, exactly like the models discussed in Part I of the thesis (Chapters 3 and 4, in models which are not growth-factor dependent).

In the first part of the chapter, we discuss some modeling features and we revisit the description given to growth-factor dynamics. In fact, we note that the characteristic patterns that describe how a model parameter may vary according to a growth-factor concentration is a fundamental issue when addressing the stabilization of the hematopoietic system. Thus, we are going to introduce a different formulation of how growth-factor concentrations are acting on the biological features of the model, no matter the number of the controlled parameters. For that purpose, we employ the time-scaling heterogeneity in the overall system that regroups the cell population dynamics and the variation of the hormone-like molecule concentrations. It is agreed that the secretion of growth factors is very fast in comparison to population cell response and cell proliferation. This assertion is actually behind the models of cell dynamics that consider static biological parameters. More importantly, this time-scaling heterogeneity had allowed the study of models where parameters depend on growth-factors that are in quasi-steady states (see [189]). For instance, since the half-life of erythropoirtins (which are the EPO hormones that regulate erythropoiesis -Chapter 2) is very short compared to the hematopoietic cell proliferation, a quasi-steady state approximation of growth-factor dynamics was considered in [31].

In fact, we noted that the models involving growth-factor dynamics were considering that the total density of mature cells is exerting a form of control on the growth-factor concentrations, through a specific evolution equation. This is a differential equation suggesting that hormone-like molecules may evolve in the same time-scaling as population dynamics. In this modeling approach, it appears from a practical point of view that actually mature cells are directly controlling the secretion of growth factors, however, the evolution of growth-factor concentrations as considered in previous models could be considered in a different way. More precisely, the evolution equation of growth-factor concentrations have to take into account the heterogeneous time-scaling between growth-factor secretion and cell proliferation. The issue of determining an alternative and effective approximate representation of growth-factor (or drug)

[1] In other words, we do not assume that mitosis occurs at a fixed age, as usually done in models that take into account growth-factor dynamics

dynamics, which can be convenient for blood cell regulation, is discussed in detail in Section 7.3 (see also Section 7.6 for numerical applications).

The key point we see in Section 7.3 is that we can interpret the hematopoietic mechanisms from a different perspective: we suggest that the hematopoietic system is a possibly **switching** one, in the sense that growth-factor concentrations exert a form of **event-triggered control** on the different biological features and parameters involved in the model. The latter approach shows -throughout the second part of the chapter (see in particular Section 7.6)- its efficiency to describe both the unhealthy[2] and healthy hematopoiesis. One of the fundamental issues that guided our modeling research relies on the elaboration of an unified framework that allows -in some sense- the existence of several strictly positive steady states in one overall model describing hematopoiesis. As far as we know, all the mathematical models of hematopoiesis admit a unique strictly positive steady state. This fact is even more frustrating for models involving growth factors, since their introduction should allow more flexibility in the system. In other words, the resulting hematopoietic system should be able to change its operating mode, by changing the levels of the growth-factors secreted by the body, or through drug therapy if infused.

Many evidences support the hypothesis under which the hematopoietic system admits multiple operating points. For instance, in normal hematopoiesis, the body adapts its blood count to face some frequent situations such as seasonal allergies, or when dealing with asthma, eczema, and infections. Some frequently encountered examples are evoked in Section 7.2, but here we briefly mention the well-known case of *eosinophil*[3] ***normal*** count, that ***moves*** from one value to another one, depending on body requirements when facing many types of allergy. We also know from the works of the anatomist François-Gilbert Viault (1890) that high altitude dwellers have higher hematocrits than sea-level residents. The same is observed for persons suffering from pulmonary insufficiency.

In light of all the previously mentioned considerations, we are going to present in Section 7.4.1 a coupled PDE-system of McKendrick-type, that describes the dynamics of gradually immature cell subpopulations residing inside the bone marrow, together with one type of mature cells that are active in the bloodstream. Almost all the biological parameters and functions involved in the PDEs and their associated boundary conditions are growth-factor dependent. We approximate the relationship between the growth-factor concentrations and the values of their corresponding parameters by some step-like functions, as indicated in Section 7.3. That is precisely a triggered-event operating mode, where at different thresholds of the growth-factor concentrations, the corresponding controlled biological parameter jumps from one level to another one (Section 7.3). Roughly speaking, one can observe that by changing the value of a specific growth-factor concentration in a way that makes it crossing a predefined threshold, we will be able -as a consequence- to move the value of the corresponding controlled parameter from its initial state to a new one. The latter idea achieves a consistent representation where, actually, the hematopoeitic system is able to change its steady state and operating mode, as illustrated throughout our work. Of course, the question remains of how growth factors are changing with respect to time in order to drive the event leading to the described parameter-switching: this is the issue that we address through some planning tools as in Sections 7.5-7.6.

[2]By assuming that drug concentrations act as growth factors when therapeutic control is envisaged

[3]This is a type of mature white blood cells.

In fact, we will go through several representations until achieving the one that interests us, which is given by a nonlinear switching system with distributed delays, that we obtain in Section 7.4.2 and link to the models in Part I. In summary, we say that by exploiting the event-triggered operating mode that growth-factor exert on the biological functionalities, together with the McKendrick-type model of mature and immature cells populations, we achieve a representation of the complete-type hematopoietic system, which is composed by **a family of nonlinear switching subsystems with distributed delays**. However, the resulting system is a complicated one, and can operate only under reasonable assumptions. Finally, in our model, the family of subsystems, generated from the complete-type switching system, achieves the objective of admitting several positive steady states. So comes the issue of determining how growth factors or drugs are managing to make the system moving between the possible subsystems, in order to activate, restore, or achieve new operating modes. As previously mentioned, that concept is related to the stabilization issue in our context. In some sense, we need to elaborate a systematic strategy to pursue, in order to provide the suitable switching signal managing the optimal succession of transitions, from an initial operating mode until reaching a desired new one. To put the concepts into perspective, we distinguish between two situations: healthy and unhealthy hematopoiesis. The common characteristics and the differences between these two cases are detailed in Section 7.5.

When reflecting on the meaning of *stabilization* in healthy and unhealthy contexts, we were not expecting that this could bring us into the fundamental field of *automated planning and scheduling*, which belongs to the branch of *artificial intelligence* (AI) [254]. Mainly it concerns the elaboration and the realization of strategies and action sequences, in order to set goals and achieve them (see [151]). This theory is used when the solutions are complex and must be **discovered** and **optimized** in multidimensional space. Thus, **our issue is to clearly specify how the switching occur between the appropriate subsystems in order to achieve a final goal** (that depends on whether it is a healthy or unhealthy hematopoiesis).

It is interesting to notice that the strategy to be developed operates under strict conditions, some of them stem from our specific model (mathematical constraints), while others are related to the application (biological constraints). Let say for instance that we need to move the total density of a type of mature cells from an initial value $M^{(0)}$ to a new value that we assume to be the required density M^* to confront an infection. Then, it is necessary to realize that among a large number of possible subsystems candidates, where each one is actually defined through a unique biological parameter combination, only a few of them can be validated. This is because many times, when switching from a subsystem to its neighbor[4], the strictly positive steady state of the latter subsystem can be: *mathematically* non-existent, or it can exist but it turns out later that it is unstable (which is recommended to avoid), or it can be stable but *biologically* insignificant (too high or too low), etc. Therefore, the question here is: how can we choose between the succession of subsystems, the *best path* to move from $M^{(0)}$ to M^*. So, to deal with these situations, we provide a well-established framework adapted to our main concerns (see Section 7.5). Then, we formulate and solve our issues by proposing a series of algorithms that we adapt to the healthy cells and to the unhealthy ones. Our approach implicitly uses an A^* *Replanner algorithm* (see [130], [273]). A step-by-step implementation, together with numerical results, are presented through the Sections 7.5-7.6.

[4]two subsystems are each in the vicinity of each other, if at most one switching action in each of the controlled parameters involved in the model, is sufficient to pass directly from one subsystem to the other one, and vice versa.

7.2 Open challenges in population cell dynamics involving growth-factor regulation

Extending the modeling aspects are essential steps towards consolidating the common knowledge about mechanisms behind blood cells regulation. On the other hand, these improvements have a cost and may be highly demanding in terms of mathematical analysis. Ideally, growth factors manage to maintain almost quasi-constant level of production and replenishment of cells in a healthy situation: for instance, growth factors stimulate the production of cells to replace the diminution of their number by natural death, after an hemorrhage, or due to blood donation. In other situations, the body needs to react in an effective manner to deal with changes in body health.

Before going further we need to clarify what we mean by healthy and unhealthy hematopoiesis, in order to avoid confusion. So, healthy hematopoiesis includes all the normal behaviors and reactions preformed by the hematopoietic system for a specific objective. This covers the case in which the body reacts to parasitic worms, infections, eczema, asthma, seasonal allergies, fever, etc. These are abnormal but frequent situations that require a change in some blood type counts (e.g. eosinophil), and which are considered as healthy or ordinary reactions. The intermediate inference that may be drawn here is that the body properly controls its steady states and regulates its operating modes according to its requirements: this task is achieved through a suitable adaptation of growth-factors concentrations. On the other hand, unhealthy hematopoiesis is the one that displays abnormal behaviors that emerge from the hematopoietic compartments themselves. We can mention some serious diagnosis as acute myeloid leukemia or blood periodic disorders like cyclical neutropenia (see Chapter 2).

The phenomenon of red blood cells creation and regulation -erythropoiesis- is the best known feedback control system in hematopoiesis. Basically, erythropoietin (EPO) hormones are secreted to promote the production of red blood cells if required. However, several aspects in that regulation remain mysterious. The Figure 7.1-[A], which is taken from [148], illustrates in a simplified manner the erythropoiesis control principle. In the latter reference, we are particularly interested by two facts, pointed out by the author: «*Lack of O_2 (hypoxia) is a stimulus for the synthesis of erythropoietin (EPO), primarily in the kidneys. EPO is a survival, proliferation and differentiation factor for the erythrocytic progenitors, particularly the colony-forming units-erythroid (CFU-Es). The O_2 capacity of the blood increases with the enhanced release of reticulocytes. The role of extra-renal sites (brain, skin) in the control of the renal EPO synthesis is still incompletely understood* » [148]. So, first, the role of brain in the feedback control system is admitted to be unclear (see Figure 7.1-[A]). However, it has been proved in the literature that brain affects renal-EPO secretion. There are even cases of local hypoxia[5] in brain that yields to an increasing renal-EPO [294]. It appears also that brain-derived EPO exists but its action is local and cannot replace the renal-derived one in kidney-failure. The highly complicated mechanism behind the neural activity in the bone marrow niche (see Figure 7.1-[B]), which is managed by the *sympathetic nervous system* (SNS), is nicely described in [129]. The second point that we reiterate here, from the above quoted passage of [148] is about the EPO-targets. Indeed, this growth factor decreases **apoptosis rates**, while promoting **proliferation** and **differentiation** of erythrocytic progenitors. These EPO targets (the three

[5] Deficiency in the amount of oxygen reaching the tissues.

biological features) are also emphasized in [129]. **Later in our model, these three biological processes (in addition to the self-renewing activity of HSCs) will be the focus of our stabilization analysis**.

At this juncture, while we strive to identify the complex mechanisms and signals responsible of blood cell regulation, an issue draws our attention. Indeed, it is also impressive to realize how the body estimates the extend of its requirements, and then reacts reasonably. This is a strong motivation for suggesting a mathematical framework in which the hematopoietic system is formulated as an *intelligent agent* able to -sequentially- performs a real-time diagnosis, sets new objectives according to its current requirements, analyzes the costs and investigates diverse possibilities to achieve its objectives, then establishes the best strategy of self-regulation and applies it. We will suggest an approach that uses some planning tools derived from the artificial intelligence theory, in order to propose an implementation of a convenient framework for the previously mentioned issues. To our knowledge, this is a new approach that has never been envisaged in the study of blood cells dynamics, during the past decades.

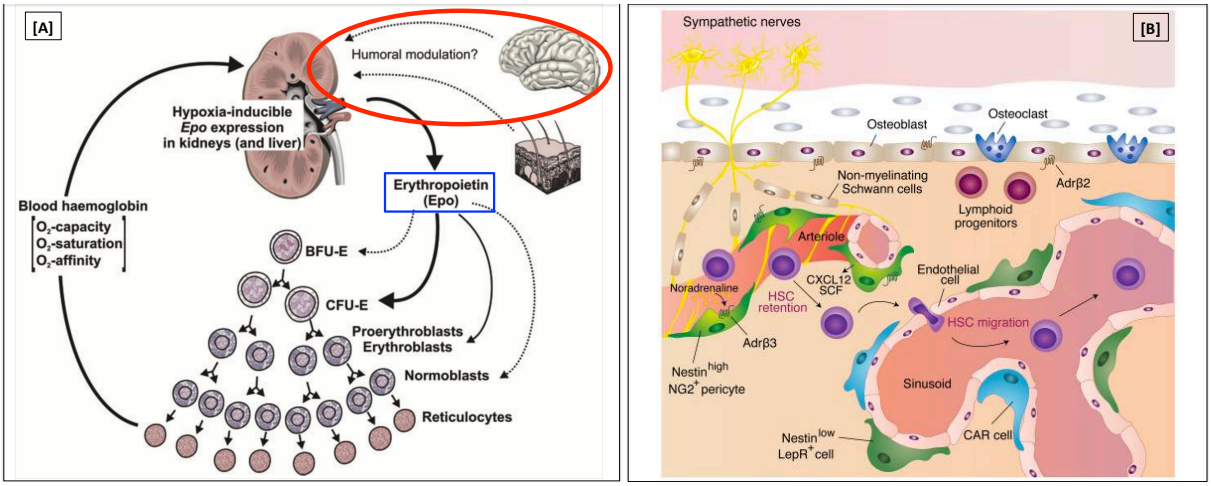

Fig. 7.1 **[A] The figure is taken from** [148]. It shows the regulation of erythropoiesis, which designates the hematopoietic lineage responsible of red blood cells production. When the body detects that cells are not getting enough oxygen, kidney responds by releasing erythropoietin (EPO), that catalyzes the development of proerythroblasts into reticulocyte. Brain reaction in EPO secretion remains ambiguous. **[B] The figure is taken from** [129]. It shows the autonomic signals that modulate steady-state hematopoiesis. Stromal cells of different types regulate HSC maintenance and regulation. The neuronal components of the HSC niche comprise peripheral sympathetic neurons and circadian noradrenaline secretion from sympathetic nerves leads in rhythmic release of HSCs to the periphery. The figure is from [129]. See Chapter 2 for regulation of hematopoietic niches.

Now, let us come back to the existing mathematical modeling of hemetopoietic systems. It is worth mentioning that relatively few works are considering growth-factor supervision of the biological functionalities involved in the hematopoietic system. As previously mentioned, including growth factor dynamics notably complicates the resulting models and that is why they are usually neglected. First, we put the spotlight on the series of works that emphasize on growth-factor dynamics and we quote in a chronological order the following papers that deal with hematopoietic systems involving growth factor-dependent parameters: [31], [185], [12], [6], [7], and, [3]. The pioneering paper by [31] is very important (this work was improved by the same authors in [185], where they considered a possible controlled apoptosis in mature cells compartment). These papers introduced and analyzed a maturity structured model, which was reduced to a time-delay system using the method of characteristics. An

important feature in their systems is that they considered a maturity velocity controlled by a growth factor. This velocity was then neglected in order to simplify the mathematical analysis of their resulting system. Following them, we will obtain the distributed time-delay system that we study in the present contribution. Moreover, the maturity velocity of [31] is, in some sense, equivalent to the several aging velocities that we consider here, in a model with discrete maturity stages. The second generation of papers, by Adimy and his co-authors, continues the effort of gradually refining the hematopoiesis models. In their most recent contribution ([3]), they focused on a model in which differentiation, proliferation and apoptosis rates are governed by growth factors. One immature stage was considered, without aging velocity, and under the assumption that cells divide (mitosis occurs) after they reach a fixed age during their cell-cycle. When it comes to discuss the stabilization technique in our work (Section 7.5), we will also consider that the aging velocity is fixed, and to ease the study, we focus on the HSCs compartment for immature cells. However, in the first part of the work, and owing a great deal to the previously mentioned works, we establish a generalized multi-stage model of hematopoiesis that includes multiple growth-factor types. Then, we complement early works in the following way:

❍ We consider a model with several discrete maturity stages, where all the biological parameters, and aging velocities, are affected by different growth factors. In addition, we consider that cells may divide at any moment during their cell-cycle.

❍ Regarding mathematical analysis, we focus on the stability properties of positive steady states, which were less studied in the literature. For that, we interpret hematopoiesis mechanisms from a different perspective: we consider the hematopoietic system as a possibly switching one, in the sense that growth-factors concentrations exert a form of event-triggered control on different biological features involved in the model. In a broader context, interpreting cell dynamics using switching systems leads to a good compromise between complexity of realistic models and their mathematical analysis.

❍ We also mention that the stabilization techniques we are going to discuss later in the chapter may (under some conditions) apply to the case of switching aging-velocities or any other switching parameter in the model. Indeed, we discuss **a general framework where any model parameter can be switching -reasonably- between several levels**: a behavior that results from a significant change in their corresponding growth-factor concentration.

Thus, we end up with a large family of subsystems that constitute one overall nonlinear switching system with distributed delays. The subsystems share in common some fixed biological parameters while they are distinguishable according to the possible combination taken by the switching ones. Each possibly switching parameters has a characteristic pattern that connects the concentration of its respective growth factor to its current value. These characteristics are in the form of monotonic step-like evolution functions (see for instance, Figure 7.4).

Based on earlier results ([81], [225]), we will be able to address the stability issue of each subsystem, followed by the stability property when switching from one subsystem to any other one in its neighborhood. The remaining questions to be addressed, in Section 7.5, are related to how the switching-instructions are **quantified** and **scheduled** both in: i) the healthy case where we focus on the role of mature cells in the control exerted on growth-factors, and, ii) in the unhealthy case where an optimal therapeutic strategy has to be determined, taking into account drugs toxicity, as well as other practical considerations.

Henceforth, each subsystem -which is actually fully defined by a unique combination of the switching parameters among all the possibly existing ones- is considered as a node or vertices, in a network representing all the existing and admissible subsystems. We will define the rules and the possibilities for the transitions permissions between the nodes (i.e. edges costs, when switching between the subsystems is allowed). That is our suitable framework for the optimal strategy planning. Then, the final solution is provided as an assembly of algorithms to solve the stabilization issues in healthy and unhealthy situations, through simple planning tools.

7.3 On the modeling of growth-factor dynamics

In the starting part, we revisit the description given to growth-factor dynamics. Indeed, we are going to improve the formulation of how growth-factor concentrations evolve. We employ the feature about the time-scaling heterogeneity in the overall system, which is composed by population cell dynamics and growth-factor evolution characteristics.

We recall that the secretion of growth factors is much faster than the dynamics of cell populations, which means that levels of growth-factor concentrations converge very quickly to their steady states. Hence, if quasi-fixed growth-factor concentrations are considered, the corresponding controlled parameters are frozen. We also pointed out that models involving growth-factor dynamics were considering the control exerted by the total density of mature cells on growth-factor concentrations through an evolution equation. Their formulation was suggesting that hormone-like molecules may evolve in the same time-scaling as population dynamics. It is indeed well-known that mature cells are directly controlling the secretion of growth factors.

More precisely, in [31] and in almost all the subsequent works (see the recent paper [3]), the dynamics of growth factors are governed by a differential equation of the form:

$$\dot{\mathfrak{e}}_j(t) = -\alpha_j \mathfrak{e}_j(t) + \mathfrak{f}_j\left(M(t)\right), \tag{7.1}$$

where $\mathfrak{e}_j$ is the concentration of a growth factor j, $\alpha_j > 0$, $M(t)$ is the total density of mature cells, the functions $\mathfrak{f}_j$ are positive decreasing functions, and $\lim_{\ell\to+\infty} \mathfrak{f}_j(\ell) = 0$. However, what does this equation mean? In fact, this is a basic representation that can be qualitatively interpreted in the following way: if we assume that the total density of mature cells $M(t)$ at time $t \geq 0$ is too high, then $\mathfrak{f}_j(M(t)) \to 0$, and it follows that $\dot{\mathfrak{e}}_j(t) < 0$, since $\alpha_j > 0$. Therefore, the growth-factor concentration $\mathfrak{e}_j$ will decrease, and $M(t)$ will also decrease for all the future time. Indeed, when $\mathfrak{e}_j$ decreases, the model parameters are affected in such a way as to discourage cell production. The opposite situation (i.e. $M(t)$ very low) is interpreted in a similar way. Unfortunately, the resulting framework cannot represent how the change in growth factor concentration may induce to a different steady state in the model (i.e. to change the operating mode), since only one positive steady state does exist. Moreover, $\mathfrak{e}_j(t)$ approaches its unique steady state $\mathfrak{e}_j^* = \frac{\mathfrak{f}(M^*)}{\alpha}$ when $M(t)$ approaches its steady state M^* (i.e. e_j and M evolve in the same time-scaling). The latter two points might be improved in order to become more consistent with the general understanding we have. Thus, we do not consider the equation (7.1).

Let us now observe the following introductory example:

Example 13. *Let us consider that an infection forces the body to set a new objective, which is to increase the total density of white blood cells to a novel reference-density M^*. We assume that the body is able to act through three distinct growth factors, that promote differentiation, proliferation and decrease apoptosis rates (death rates of proliferating cells). For the time being, we consider that the body knows how to recognize the triplet value of the model parameters $\left(\beta^*(0),\gamma^*,K^*\right)$ that leads to the hematopoietic system which admits M^* as a stable steady state. Therefore, we expect that the growth-factor concentrations corresponding to that suitable triplet are immediately secreted. However, it will certainly take more time for the overall system to reach the required steady state M^*. Indeed, the cell population in the bone marrow will be instigated by the secreted growth factors, then immature hematopoietic stem cells (HSCs) will be recruited to enter a cell-cycle for a non-negligible duration, and then differentiate.*

That is exactly what we want to achieve through this work (at the end, Section 7.6). Some major questions are in fact barely veiled in the statement of Example 13. For instance, it is assumed that the body *moves* its triplet of parameters from an initial state $\left(\beta^{(0)}(0),\gamma^{(0)},K^{(0)}\right)$, to a suitable triplet $\left(\beta^*(0),\gamma^*,K^*\right)$, through growth-factor secretions. But how does it occur? How does the body determine the $\left(\beta^*(0),\gamma^*,K^*\right)$ that corresponds to M^*? In order to move from $\left(\beta^{(0)}(0),\gamma^{(0)},K^{(0)}\right)$ to $\left(\beta^*(0),\gamma^*,K^*\right)$, do we have to target (by increasing or by decreasing) all the involved biological parameters? Is it possible to achieve this objective through only one growth-factor secretion or several steps are required? Similarly for the unhealthy case: imagine that we are dealing with a blood disorder that we want to cure through drug infusions. Thus, we certainly need to recognize the objective parameters $\left(\beta^*(0),\gamma^*,K^*\right)$ of the therapy, that correspond to the reference M^* prescribed by health professionals. Then, we have to identify the parameters to be targeted and establish the therapy protocol. Is it a one dose therapy? Are there any optimal and systematic strategy to follow in order to restore the healthy hematopoiesis? These are in fact the open questions that we are going to answer in this work.

We will not get to these issues as early. We need first to go through a certain number of steps. As regards the dynamics of growth factors, we consider a more general expressions than (7.1), that may cover for instance the option of therapeutic action and the feedback from mature cells. The general form can be expressed by:

$$\dot{\mathfrak{e}}_j(t) = \mathfrak{g}_j(t,\mathfrak{e}_j,M(t)), \tag{7.2}$$

where $\mathfrak{g}_j$ is a function that depends also on time. In this case, a time-triggered switching can be modeled, by infusing periodic doses of drugs for instance. Next, in this work, we consider five different growth factors (i.e., $j \in \{1,\ldots,5\}$), each one is acting on a specific biological function.

In the general description of the hematopoietic system, the growth factors are stimulating proliferation, differentiation rates and aging velocities; while they are blocking apoptosis, that is death rate of proliferating cells (this is a negative feedback, meaning that apoptosis rate decreases when the corresponding growth-factor concentration increases [3]). Generally speaking, growth factors are increasing the effect of the biological feature that are favorable to cell prosperity.

In addition, we introduce a general model where growth-factors concentrations are governed by (7.2), without wondering about time-scaling in growth-factor evolution. The latter consideration will be used,

subsequently, to introduce a new interpretation when it comes to investigate the stability properties of the resulting mathematical model.

Differently from those who consider constant biological parameters for all the time, we study the case in which growth factors are active, moving their quasi-steady states to new ones when it is needed. Such a behavior is representative of actions initiated by the body itself to meet its requirement in healthy hematapoiesis, or due to sudden therapeutic measures (drug infusions, bone marrow transplantation etc) when facing some blood disorders. That kind of evolution is well-approximated by step-like functions as illustrated in Figure 7.2. Thus, by relying on that characteristic, a first approach consists in inferring how the behavior of the different biological parameters will be (see Figure 7.3).

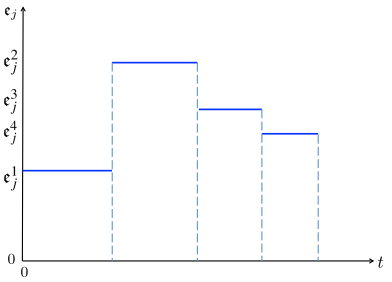

Fig. 7.2 Qualitative behavior of e_j in the time-scale of cell dynamics (in hours or in days).

Figure 7.3 gives an illustration for the expected evolution of the aging velocity (v), and of a differentiation rate (K), with respect to their growth-factor concentrations, when they behave as in Figure 7.2.

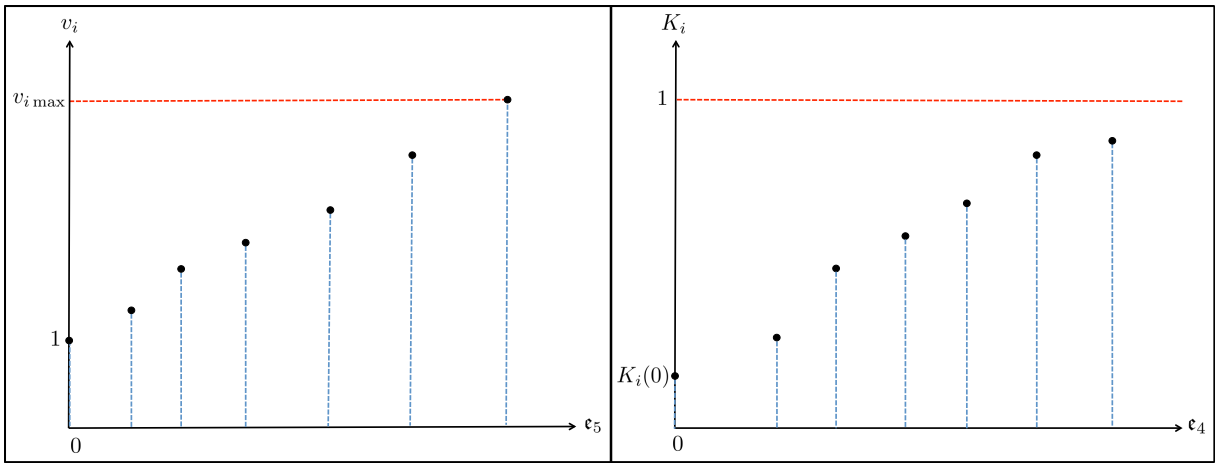

Fig. 7.3 Qualitative behavior of v_i and K_i with respect to their growth-factors concentration.

For $\mathfrak{p}$ values taken by $\mathfrak{e}_j$, i.e. $\left\{\mathfrak{e}_j^1, \mathfrak{e}_j^2, \mathfrak{e}_j^3, \ldots, \mathfrak{e}_j^{\mathfrak{p}}\right\}$, in Figure 7.2, where $\mathfrak{p}$ is arbitrary large, it follows that the characteristic patterns illustrated in Figure 7.3 will approach continuous monotonic[6] curves. It is hard to imagine how such a characteristic pattern can be obtained in practice. What we could rather expect to determine (at least approximately) is the effect of a molecule or a drug on a given biological functionality, that we approximate using a step-like pattern as in Figure 7.4. That representation is convenient because it allows us to approximate the real cell-population dynamics via a model involving parameters that remain constant over a certain period of time. During that time-interval, the growth factor concentration varies slightly, until it crosses a given threshold, that triggers a switch in the parameter value.

A characteristic as in Figure 7.4 has to be determined experimentally and may vary from one individual to another, because the effect of a molecule on the hematopoietic system is strongly dependent on the

[6]Later we will state that the step-like functions used to describe the biological parameters are either entirely nonincreasing or nondecreasing with respect to increasing growth-factor concentrations.

genetic and epigenetic levels (e.g. presence and accumulation of diverse main and auxiliary mutations). This is for the quantitative aspect, but fortunately the qualitative aspect of the variation of a parameter, with respect to its growth factor, remains unchanged as described for each of the parameters in the following paragraph.

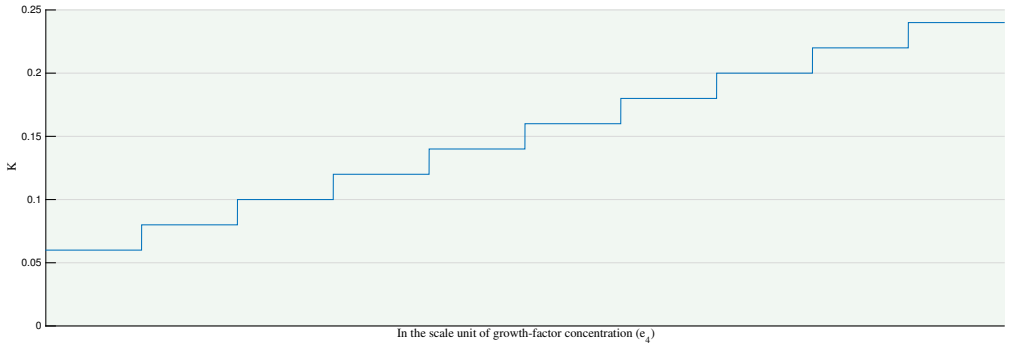

Fig. 7.4 An example of the approximate variation of the differentiation rate for a given maturity stage (denoted K) with respect to the concentration of its growth factor ($\mathfrak{e}_4$).

In Figure 7.5, we have n different (discrete) maturity stages as introduced in [8] for a model without growth factors. The first stage in Figure 7.5, i.e. for $i = 1$, is the compartment of hematopoietic stem cells (HSCs), that are found in the bone marrow. For all $i \in I_n = \{1,\dots,n\}$, $R_i(t)$ is the total density of resting cells of the i-th generation of immature cells, while $M(t)$, as mentioned previously, is the total density of one type of mature cells (e.g. one among the five types of white blood cells) in the blood circulation. Resting cells may die or differentiate to other lineages at a rate $0 < \delta_i < 1$. They can also re-enter to the proliferating stage, in order to start a dividing-cycle, according to a particular function that we denote β_i. During their cell-cycle, cells may die with a death rate (apoptosis rate) γ_i, or they can complete their mitosis, i.e. each mother-cell divides into two daughter-cells, before reaching a maximal age τ_i. At each division, a proportion $0 < K_i < 1$ of new daughter cells will differentiate (i.e. join the next *more mature* stage $i+1$, in the cascade of immature stages, as illustrated in Figure 7.5). The remaining portion, i.e. $0 < 1-K_i < 1$, will join the same maturity level as the one of mother cells: this is a self-renewing process that we denote L_i ($L_i = 1-K_i$). In addition, we consider an aging velocity v_i, in the proliferating phases as illustrated in Figure 7.5. After n immature stages, cells are ready to leave the bone marrow and join the blood circulation.

Next, and this is the key point, we consider that the five different growth factors concentrations ($\mathfrak{e}_j$, $j \in \{1,\dots,5\}$) are acting on the biological functionalities as follows:

- $\delta_i(\cdot)$ depends on $\mathfrak{e}_1$. Increasing $\mathfrak{e}_1$ yields to increase δ_i, across all maturity levels, similarly to what is shown in Figure 7.3 for K_i and v_i. We also consider that $\lim_{\mathfrak{e}_1\to\infty}\delta_i(\mathfrak{e}_1) = \overline{\delta_i} < 1$, for all $i \in I_n$.
- $\beta_i(\cdot,\cdot)$ is a function that depends on $\mathfrak{e}_2$ and on the total density of resting cells, R_i for all $i \in I_n$. We consider that for each fixed $\mathfrak{e}_2$, the mapping $\beta_i(\mathfrak{e}_2, R_i)$ is *continuously* decreasing with respect to R_i, and $\lim_{R_i\to\infty}\beta_i(\cdot,R_i) = 0$ (see [180]). On the other hand, for a fixed R_i, the mapping $\beta_i(\mathfrak{e}_2,R_i)$ is increasing when $\mathfrak{e}_2$ increases, in a similar form as in Figure 7.3, where $\beta_i(0,R_i) \approx 0$, and, $\lim_{\mathfrak{e}_2\to\infty}\beta_i(\mathfrak{e}_2,R_i) = \overline{\beta_i} > 0$.
- The apoptosis rates, $\gamma_i(\cdot)$, depend on the concentration $\mathfrak{e}_3$. Since, by convention, a growth factor stimulates the production of cells, we consider that the mapping $\gamma_i(\mathfrak{e}_3)$ is decreasing with respect to $\mathfrak{e}_3$.

- Differentiation, $K_i(\cdot)$, increases with respect to $\mathfrak{e}_4$ as illustrated in Figure 7.3, and $\lim_{\mathfrak{e}_4\to\infty} K_i(\mathfrak{e}_4) = K_{i\max} < 1$.
- Similarly, the aging-velocities v_i, which are affected by the concentration $\mathfrak{e}_5$, for all $i \in I_n$, are increasing from a normal velocity-values (normalized to 1), until reaching a maximum velocity, as shown by Figure 7.3.

Remark 41. *To summarize, at this stage we have already discussed the evolution of growth-factor concentrations with respect to time (as step-like functions, in the time-scale of cell dynamics), then, we described how parameters of the model may vary with respect to growth-factor concentrations (also approximated by step-like functions). Therefore, we deduce that changes in growth-factor concentrations with respect to time exert a kind of triggered-event control on the different biological functionalities, i.e. a jump in model parameter occurs each time the growth-factor concentration crosses a threshold. We retain that by knowing the evolution of growth-factor concentrations (e.g. predefined therapeutic protocols) we can determine how the biological parameters evolve with respect to time, as illustrated for instance in the Figures (a),(b)-Table 7.3 for γ_i and v_i.*

7.4 From a model of dynamical equations to a network representation

In this part we will go through several stages, starting with a PDE system that describes cell population dynamics (Section 7.4.1), which will be reduced to a nonlinear system with distributed delays (Section 7.4.2). The latter system will be presented as a nonlinear switching systems with distributed delays (Section 7.4.3), through the arguments provided in Section 7.3.

In order to be brief and to focus more on the stabilization issues, we will show in Section 7.4.4 that the study of each subsystem[7] can be performed thanks to some earlier work. More precisely, we employ our results on the global stability properties of the strictly positive steady state of the nonlinear model in [8], which was widely analyzed in [225] via Input/Output approaches, and more recently in [81] through Lyapunov-Krasovskii functionals constructions. Through that formulation, we will not dwell on the stability issue of each subsystem (Section 7.4.4). Then, we establish the stability properties when switching from one stable subsystem to another one. Once this step is done, we formulate the stabilization issue as the problem of how finding the adequate switching law (or signal) between the different subsystems, in order to reach a desired operating mode. The targeted reference that we set is the favorable total density of mature cells in the bloodstream.

Finally, once we address the stability of each subsystem, and once we establish the stability properties of a switching between one subsystem to any other one in its neighborhood, we will be ready to represent each subsystem as a node in a network representing all the possible subsystems constituting the overall system. The latter representation and its aims will be widely discussed in Section 7.5.

[7]The subsystem here is a system that belongs to the family of systems constituting the overall switching model. Each subsystem can be written on a time interval $[t_{s1}+\tau_i, t_{s2}]$, where t_{s1} and t_{s2} are two consecutive switching time-instants, as a system without any switching parameter (all the parameters are constants during that interval), and it involves one or more switching on the time interval $[t_{s1}, t_{s1}+\tau_i]$, i.e. the length of the cell-cycle τ_i.

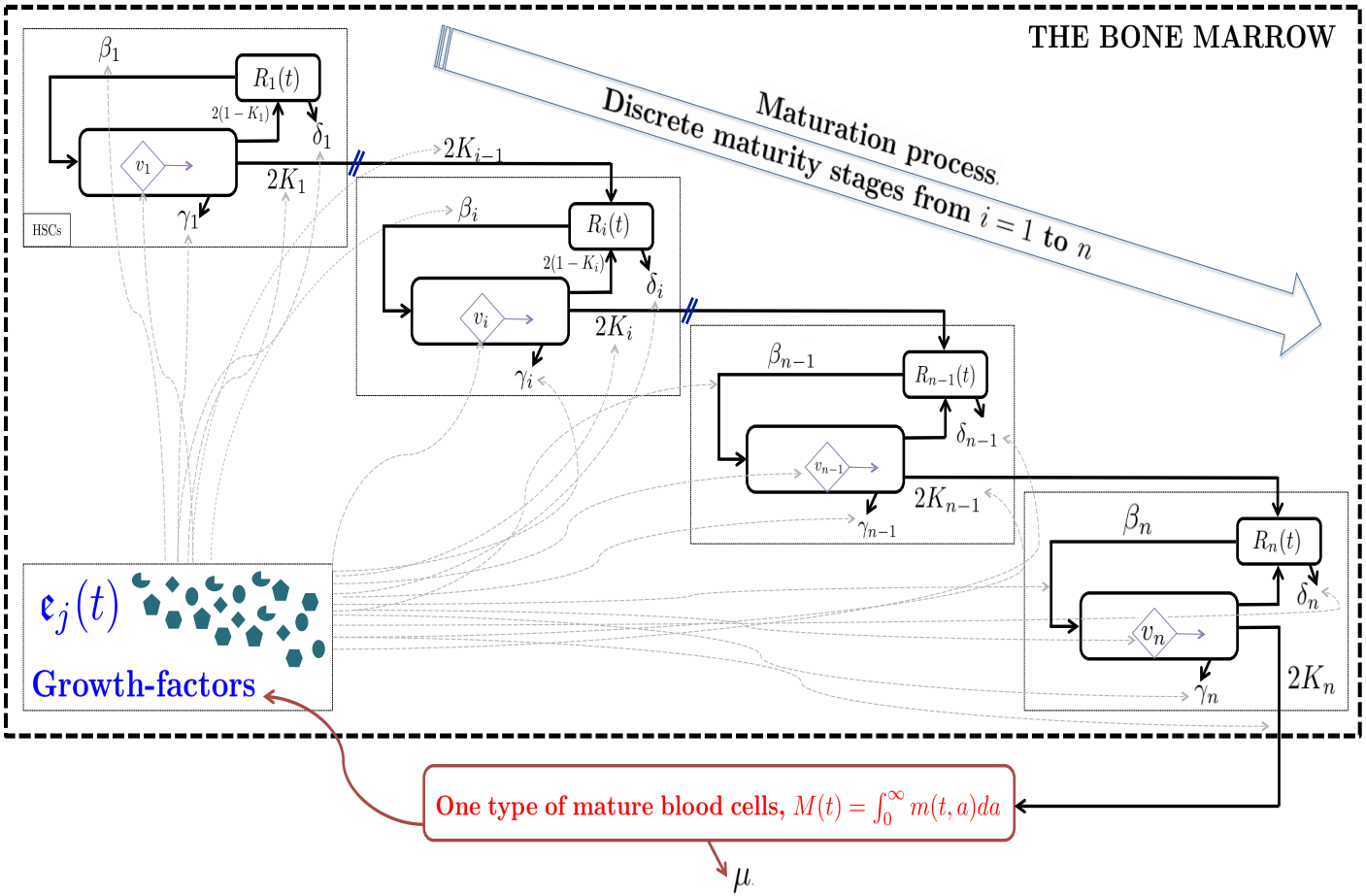

Fig. 7.5 Schematic representation of the model studied in Sections 7.3, 7.4.1, 7.4.2, 7.4.3. As a general and unified framework, we are considering growth-factor concentrations and drug doses to act similarly on the different biological parameters involved in hematopoiesis. In other words the growth factors $\mathfrak{e}_j$, represented in blue, may include the drug molecules. For instance, in the process of erythropoiesis evoked in Section 7.2, usually regulation is done through renal-EPO secretion (normal growth factor), however, sometimes, this control fails and a low blood cell production causes anemia (e.g. in advanced chronic kidney disease). In this case, the ***erythropoiesis-stimulating*** (ESA), which is a medicine similar to EPO, is prescribed. Structurally and biologically, ESA and EPO are similar. On the other hand, when we will address the stabilization issues, some differences will be taken into account according to the healthy or unhealthy contexts (Section 7.5). For instance, in the unhealthy case, the feedback control from mature cells (in red) is broken, i.e. the biological parameters representing differentiation, apoptosis and proliferation, no longer react to body requirement due to kideny failure for instance. Thus, in that case, the model parameters obey only to the doses and frequences of drug infusions.

7.4.1 An age-structured model describing cells population dynamics including growth-factor depending parameters

We have already described in Section 7.3 the biological functionalities and parameters (differentiation, self-renewing, death-rates etc) involved in our model, as illustrated in Figure 7.5. Now, what we are interested in, is the model governing the dynamics of mature and immature cell populations. We recall that the n first generations of cells in Figure 7.5 represent the immature cells, at different maturity stages, inside the bone marrow. So, we defined $R_i(t)$, for all $t \geq 0$ and $i \in I_n$, that represents the total density of resting cells of the i-th generation of immature cells. We recall that $M(t)$, for all $t \geq 0$, represents the total density of one type of mature cells in the bloodstream. In fact, $R_i(t) = \int_0^{+\infty} r_i(t,a)da$, where $r_i(t,a)$ is the density of resting cells at time $t \geq 0$ and age $a \geq 0$, for all $i \in I_n$. Similarly, $p_i(t,a)$ is the density of proliferating cells at time t and age a during their cell-cycle (the proliferating stage, Figure 7.5), along with the density $m(t,a)$, of mature cells at time t and age a, and $M(t) = \int_0^{+\infty} m(t,a)da$, for all $t \geq 0$. The PDE system that describes the dynamics of the densities $r_i(t,a)$, $p_i(t,a)$, for all $i \in I_n$, and $m(t,a)$, for all $t > 0$ and $a > 0$, is formed by the following age-structured McKendrick model,

$$\begin{cases} \frac{\partial r_i(t,a)}{\partial t} + \frac{\partial r_i(t,a)}{\partial a} = -\Big[\delta_i(\mathfrak{e}_1(t)) + \beta_i\left(\mathfrak{e}_2(t), R_i(t)\right)\Big] r_i(t,a), \quad \text{for all } a > 0, \\ \frac{\partial p_i(t,a)}{\partial t} + v_i(\mathfrak{e}_5(t))\frac{\partial p_i(t,a)}{\partial a} = -\left[\gamma_i(\mathfrak{e}_3(t)) + h_i(a)\right] p_i(t,a), \quad \text{for all } 0 < a < \tau_i, \text{ and,} \\ \frac{\partial m(t,a)}{\partial t} + \frac{\partial m(t,a)}{\partial a} = -\mu m(t,a), \quad \text{for all } a > 0, \end{cases} \tag{7.3}$$

in which the new births, i.e. at age $a = 0$, in the proliferating and resting phases are introduced through the following boundary conditions:

$$\begin{cases} r_1(t,0) = 2\left(1 - K_1(\mathfrak{e}_4(t))\right) \int_0^{\tau_1} h_1(a) p_1(t,a)da, \quad \text{and, for all } i > 1, \\ r_i(t,0) = 2\left(1 - K_i(\mathfrak{e}_4(t))\right) \int_0^{\tau_i} h_1(a) p_i(t,a)da \\ \qquad\qquad + 2K_{i-1}(\mathfrak{e}_4(t)) \int_0^{\tau_{i-1}} h_{i-1}(a) p_{i-1}(t,a)da, \quad \text{and, for all } i \in I_n, \\ p_i(t,0) = \beta_i(\mathfrak{e}_2(t), R_i(t)) R_i(t), \quad \text{and,} \\ m(t,0) = 2K_n(\mathfrak{e}_4(t)) \int_0^{\tau_n} h_n(a) p_n(t,a)da. \end{cases} \tag{7.4}$$

We consider that the initial conditions at $t = 0$, associated with the PDE system (7.3), namely $r_i^0(a) = r_i(0,a)$ for $a > 0$, and $p_i^0(a) = p_i(0,a)$, for $0 < a < \tau_i$, for all $i \in I_n$, and $m^0(a) = m(0,a)$, for $a > 0$, are some appropriate positive L^1-functions. Next, we will follow [31], (see also [101], [201], and the references therein), who themselves were inspired by techniques of [267], in order to reduce the age-structured system (7.3)-(7.4) to a time-delay system, using the classical method of characteristics.

7.4.2 A nonlinear time-delay system involving growth-factor dependent parameters

We use the classical method of characteristics, by applying to our model the arguments developed in [31] and [101], starting by the introduction of a parametrization z in the $(t-a)$ space where $t > 0$, and $0 < a < \tau_i$. Therefore, we can write (with an abuse of notation), $p_i(z) = p_i(t(z), a(z))$.

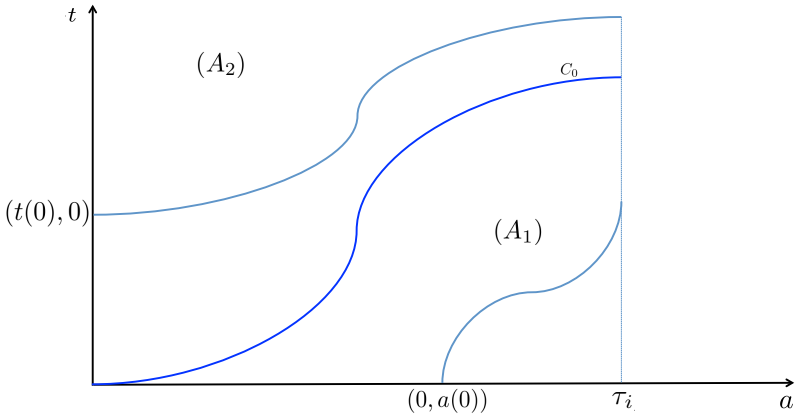

Fig. 7.6 The illustrative curve C_0, that emanates from the point $\big(t(0),a(0)\big)=(0,0)$, separates the $t-a$ plane into two regions ([31], [101]).

It follows that: $\frac{dp_i(z)}{dz}=\frac{\partial p_i(t,a)}{\partial t}\frac{dt}{dz}+\frac{\partial p_i(t,a)}{\partial a}\frac{da}{dz}$. The parameter z follows a characteristic curve for the second equation in (7.3), characterized by the ODEs, $\frac{dt}{dz}=1$, and, $\frac{da}{dz}=v_i(\mathfrak{e}_5(t))$, for all $t>0$, and $a\in[0,\tau_i]$ ([31, 101]). In fact, the characteristic curves are described by [31],

$$\begin{cases} t(z)-t(0)=z, \text{ and,} \\ a(z)-a(0)=\int_0^z v_i\left(\mathfrak{e}_5(t(\ell))\right)d\ell. \end{cases} \tag{7.5}$$

Next, we notice that along the characteristics (7.5), the second equation in (7.3) is written as

$$\frac{dp_i(z)}{dz}=-\left[\gamma_i(\mathfrak{e}_3(t(z)))+h_i(a(z))\right]p_i(z), \tag{7.6}$$

and its general solution is given by

$$p_i(z)=p_i(0)e^{-\int_0^z\left[\gamma_i(\mathfrak{e}_3(t(\ell)))+h_i(a(\ell))\right]d\ell}. \tag{7.7}$$

Now, what we need to determine is an expression for z and $p_i(0)$, in function of t and a, in order to obtain $p_i(t,a)$. Naturally, the solution has different forms depending on which region we are (i.e. (A_1) or (A_2), illustrated in Figure 7.6).

First, the region (A_1) is characterized by $t(z)=z$ and $a(z)=a(0)+\int_0^z v_i(\mathfrak{e}_5(t(\ell)))d\ell$. Moreover, using $a(\ell)=a-\int_\ell^t v_i(\mathfrak{e}_i(w))dw$, we conclude that for all $(t,a)\in(A_1)$,

$$p_i(t,a)=p_i^0\left(a-\int_0^t v_i(\mathfrak{e}_5(\ell))d\ell\right)e^{-\int_0^z\left[\gamma_i(\mathfrak{e}_3(\ell))+h_i\left(a-\int_\ell^t v_i(\mathfrak{e}_i(w))dw\right)\right]d\ell}. \tag{7.8}$$

Secondly, we are looking for the solutions $p_i(t,a)$ in (A_2). In that region, the characteristic curves (7.5) intersect the time-axis. Therefore, using (7.5), we notice that this region is characterized by $t(z)=t(0)+z$ and $a(z)=\int_0^z v_i(\mathfrak{e}_5(t(\ell)))d\ell$. Thus,

$$a(z)=\int_0^z v_i(\mathfrak{e}_5(t(0)+\ell))d\ell=\int_{t(0)}^{t(0)+z} v_i(\mathfrak{e}_5(\ell))d\ell. \tag{7.9}$$

Thanks to the boundary conditions (7.4), we get,

$$p_i(0) = p_i(t(0),a(0)) = p_i(t-z,0). \tag{7.10}$$

At this juncture, we need to give an expression for z. As previously encountered in [31] and [101], we realize that the z variable is implicitly defined by the expression of $a(z)$. Knowing that z is the *time* required for the *age* a to increase from 0 to $a(z)$, and using (7.9), we obtain ([31, 101]): $a = \int_{t-z}^{t} v_i(\mathfrak{e}_5(\ell))d\ell$. Here we are interested in all age-values between 0 and the maximum age value τ_i (this is a fact that complicates our problem, in comparison with [31]). Thus, we notice that if T_a is the *time* (i.e. z), necessary to grow from the *age* 0 to $a \leq \tau_i$, then, $a = \int_{t-T_a}^{t} v_i(\mathfrak{e}_5(\ell))d\ell$. Therefore, we obtain

$$\begin{aligned} p_i(t,a) &= p_i(t-T_a,0)e^{-\int_0^{T_a}\left[\gamma_i\left(t(0)+\ell\right)+h_i(a(\ell))\right]d\ell} \\ &= p_i(t-T_a,0)e^{-\int_0^{T_a}\left[\gamma_i(t-z+\ell)+h_i\left(\int_0^{\ell} v_i(\mathfrak{e}_5(w))dw\right)\right]d\ell} \\ &= p_i(t-T_a,0)e^{-\int_0^{T_a}\left[\gamma_i(t-T_a+\ell)+h_i\left(\int_0^{\ell} v_i(\mathfrak{e}_5(w))dw\right)\right]d\ell}. \end{aligned}$$

We conclude that in the $t-a$ plane the solutions $p_i(t,a)$ for all $i \in I_n$, along the characteristic curves (7.5), are given by:

$$p_i(t,a) = \begin{cases} p_i^0\left(a - \int_0^t v_i(\mathfrak{e}_5(\ell))d\ell\right) e^{-\int_0^z\left[\gamma_i(\mathfrak{e}_3(\ell))+h_i\left(a-\int_\ell^t v_i(\mathfrak{e}_i(w))dw\right)\right]d\ell}, \\ \qquad \text{for all } (t,a) \in (A_1), \text{ and;} \\ p_i(t-T_a,0)e^{-\int_0^{T_a}\left[\gamma_i(t-T_a+\ell)+h_i\left(\int_0^{\ell} v_i(\mathfrak{e}_5(w))dw\right)\right]d\ell}, \text{ for all } (t,a) \in (A_2), \\ \qquad \text{where, } a \in [0,\tau_i], \text{ and, } a = \int_{t-T_a}^{t} v_i(\mathfrak{e}_5(\ell))d\ell. \end{cases} \tag{7.11}$$

Remark 42. *In view of the solutions obtained in* (7.11)*, we notice that if we consider* $v_i \equiv 1$ *then,* $\forall i \in I_n$ *and* $t > 0$*,*

$$p_i(t,a) = \begin{cases} p_i(t-a,0)e^{-\int_0^a \gamma_i\left(\mathfrak{e}_3(\ell+t-a)\right)+h_i(\ell)d\ell}, \ t > a, \\ p_i^0(a-t)e^{-\int_0^t \gamma_i\left(\mathfrak{e}_3(\ell)\right)+h_i(\ell+a-t)d\ell}, \ a > t. \end{cases}$$

Even this simpler case was not studied in the past, for model with growth-factor dependent parameters. Only its version with constant ones was analyzed in ([8], [225], and, [81]).

As explained in [31] (and also in [101]) we are interested in long-time behavior of our system. Hence, we do not focus on the solution in (A_1) since it is related to the initial conditions p_i^0. In the sequel, we consider the solution on the region (A_2), which is related to the boundary conditions (that express long time behavior). By integrating the first equation in (7.3), with respect to the age-variable a between 0 and ∞, we get,

$$\dot{R}_i(t) = r_i(t,0) - \left[\delta_i(\mathfrak{e}_1(t)) + \beta_i(\mathfrak{e}_2(t),R_i(t))\right]R_i(t). \tag{7.12}$$

Using the boundary condition (7.4), we obtain for all $i > 1$,

$$\begin{aligned}\dot{R}_i(t) = &- \left[\delta_i(\mathfrak{e}_1(t)) + \beta_i(\mathfrak{e}_2(t), R_i(t))\right] R_i(t) + 2\left(1 - K_i(\mathfrak{e}_4(t))\right) \int_0^{\tau_i} h_i(a) p_i(t,a) da \\ &+ 2K_{i-1}(\mathfrak{e}_4(t)) \int_0^{\tau_{i-1}} h_{i-1}(a) p_{i-1}(t,a) da.\end{aligned}$$

Similarly, if we integrate the third equation in (7.3) with respect to the age-variable, we get,

$$\dot{M}(t) = -\mu M(t) + 2K_n(\mathfrak{e}_4(t)) \int_0^{\tau_n} h_n(a) p_i(t,a) da. \tag{7.13}$$

Next, substituting $p_i(t,a)$ by its expression (given in (7.11), for $(t,a) \in (A_2)$) leads to the system exposed in Table 7.1. That is the general time-delay form that we obtain for our PDE system, when five distinct growth-factors are acting on model parameters, and which are governed by the general form of their dynamics (7.1). Next, we incorporate the growth-factor effect as described in (7.3), in order to give a specific form to the system in Table 7.1.

7.4.3 The model equations under event-triggered parameters

A first observation is that exploitation of our mathematical model in its general form as presented in Table 7.1 is not an easy task. Indeed, the implicitly defined variable T_a (the same observation occurred in [31]), and the state variables that appear in the distributed delay terms (which are the total densities R_i, and the growth-factor concentrations $\mathfrak{e}_2$, $\mathfrak{e}_3$, and, $\mathfrak{e}_5$), cannot be easily manipulated in order to investigate the existence and the stability properties of the positive steady states. For that reason, we are looking for a new representation of the model given in Table 7.1. A key feature that helps us at this stage is the behavior of the growth factors, as explained in Section 7.3, and their triggering-effects on the biological functionalites involved in the model.

❑ First, we start by assuming that the fourth equation in Table 7.1 has a unique piecewise continuous solution for all $j \in \{1,\ldots,5\}$. Whatever the behavior of the states $\mathfrak{e}_j(t)$, for all $t \geq 0$, (whether driven by a body requirement or resulting from drug infusions), their effect on the biological functions (δ_i, β_i, γ_i, K_i and v_i) is the same. We recall from Section 7.3 that knowing the solutions $\mathfrak{e}_j$ allows us to determine the variation of the biological parameters with respect to time. An illustration is provided in Figures (a-b)-Table 7.3, in which we give a qualitative example with two parameters, v_i and γ_i (see also Figure 7.4 for variations of K). The remaining biological parameters can be represented in a similar way.

Now, we define for all $t \geq 0$, the time duration $\mathfrak{h}$ that corresponds to the smallest[8] time-interval during which all the biological parameters (not only those represented in the corresponding Figures (a-b)-Table 7.3) are invariant with respect to the possible change in their respective growth-factor concentrations. Therefore, we can distinguish two interesting situations:

① The case $\mathfrak{h} < \tau_i$: A simplified version of the resulting model obtained in this situation is given in Table 7.2. This case is not easy to be studied without strong extra assumptions on the model. The difficulty comes mainly from the distributed delay terms that can cover -in the general case- a large period of time, and which involves several switching as illustrated in Table 7.2 (the distributed delay terms are denoted $\Im_i$, with an abuse of notation). This scenario is shown in Figure (a)-Table 7.3.

[8] In the classical theory of switching systems, $\mathfrak{h}$ is called the ***dwell-time***.

② The case $\mathfrak{h} >> \tau_i$: This is a more suitable situation for analysis purposes (see Figure (b)-Table 7.3). Indeed, since the biological parameters do not vary during a sufficiently large period of time, we can rewrite the system presented in Table 7.1 in a more convenient form, especially in the region $(\mathfrak{D}_3)$ which is illustrated in Figure (b)-Table 7.3. That region coincides with the time interval $[t_{s1} + \tau_i, t_{s2}]$, where t_{s1} and t_{s2} are assumed to be two consecutive switching time-instants. The particularity of $(\mathfrak{D}_3)$ is that the model in Table 7.1 can be rewritten as a system without switching dynamics, even inside its distributed delay terms (the corresponding model equations are given in Table 7.4). If a switching (in at least one of the model parameters) occurs at a time instant $t_{s1} > 0$, then, by definition of the dwell-time, the next switching instant will not occur before $t_{s1} + \mathfrak{h}$.

We use the following abuse of notation: the parameter $\sigma \in \mathbb{N}$ identifies which subsystem is activated at any time instant[9] $t \geq 0$ (e.g. when at least one parameter changes at $t_{s1} > 0$, then the system in Table 7.4 switches from a subsystem $\sigma = 1$, to a sub-system $\sigma = 2$). In the region $(\mathfrak{D}_3)$, the system is exclusively defined by specifying σ. However, it is not the case in the region $(\mathfrak{D}_2)$ since the distributed delay terms appeal the history of the system in the region $(\mathfrak{D}_1)$, which complicates its analysis. Without loss of generality, we select in Table 3 the non-switching dynamical subsystem defined by $\sigma = 1$ to be activated during the $(\mathfrak{D}_2)$-$(\mathfrak{D}_3)$- time-period, between two consecutive switching time-instants t_{s1} and t_{s2}.

❑ At this juncture, from the previous discussion, we assume in our model that $\mathfrak{h} >> \tau_i$ (case ②, even if the numerical simulations that we will perform (Section 7.6) show that this restriction is not necessary). In the sequel, stability properties of our model are discussed. An interesting observation is that, by focusing on the behavior of the fixed subsystem on $(\mathfrak{D}_3)$, the portion on $(\mathfrak{D}_2)$ appears as nothing more than the initial condition associated to the studied subsystem. That feature will be the subject of the next section, in which the stability properties when switching from one subsystem to its neighbor are discussed. Thus, the issue of stable *jump* between a given subsystem and any other subsystem present in its vicinity (subsystems are illustrated by the set of blues points in the Figure (d)-Table 7.3) is the next crucial step towards stabilization. More precisely, stabilization tools focus on searching the *best neighbor* (also called a *successor*) to which the initial system will move, then iterate the process until reaching the desired operating mode[10] (the reference), represented by the red point in Figure (d)-Table 7.3.

[9] Actually, σ depends on time. It is the ***switching signal***, that determines which subsystem is activated at $t \geq 0$. However, in our application, it is more convenient to write σ instead of $\sigma(t)$, for more clarity in the system equations. We recall from Section 7.3 that the switching signal $\sigma(t)$ is triggered when the growth-factor concentrations cross a specific thresholds. Therefore, the issue of how the switching signal σ evolves with respect to time is a problem-specific. It will be separately addressed in Section 7.5, since the switching signal is actually governed by the stabilization algorithm that we will propose later.

[10] The ordered list of *successors* from the initial activated subsystem until the goal is the optimal path, which thereby defines the switching signal $\sigma(t)$.

$$
\begin{cases}
\dot{R}_1(t) = -\left[\delta_1(\mathfrak{e}_1(t)) + \beta_1\left(\mathfrak{e}_2(t), R_1(t)\right)\right] R_1(t) + 2\left(1 - K_1(\mathfrak{e}_4(t))\right) \mathfrak{I}_1\left(R_{1t}, \mathfrak{e}_{2t}, \mathfrak{e}_{3t}, \mathfrak{e}_{5t}\right), \quad \text{and, for all } i \geq 2, \\
\dot{R}_i(t) = -\left[\delta_i(\mathfrak{e}_1(t)) + \beta_i\left(\mathfrak{e}_2(t), R_i(t)\right)\right] R_i(t) + 2\left(1 - K_i(\mathfrak{e}_4(t))\right) \mathfrak{I}_i\left(R_{it}, \mathfrak{e}_{2t}, \mathfrak{e}_{3t}, \mathfrak{e}_{5t}\right) + 2K_{i-1}(\mathfrak{e}_4(t)) \mathfrak{I}_{i-1}\left(R_{i-1t}, \mathfrak{e}_{2t}, \mathfrak{e}_{3t}, \mathfrak{e}_{5t}\right), \\
\dot{M}(t) = -\mu M(t) + 2K_n\left(\mathfrak{e}_4(t)\right) \mathfrak{I}_n\left(R_{nt}, \mathfrak{e}_{2t}, \mathfrak{e}_{3t}, \mathfrak{e}_{5t}\right), \\
\dot{\mathfrak{e}}_j(t) = -\mathfrak{g}_j\left(t, \mathfrak{e}_j(t), M(t)\right), \quad \text{for all } j \in \{1, \ldots, 5\},
\end{cases}
$$

where,

$$
\mathfrak{I}_i\left(R_{it}, \mathfrak{e}_{2t}, \mathfrak{e}_{3t}, \mathfrak{e}_{5t}\right) = \int_0^{\tau_i} h_i(a) e^{-\int_0^{T_a} h_i\left(\int_0^{\ell} v_i(\mathfrak{e}_5(w))dw\right) - \gamma_i\left(\mathfrak{e}_3\left(t - T_a + \ell\right)\right) d\ell} \beta_i\left(\mathfrak{e}_2(t - T_a), R_i(t - T_a)\right) R_i\left(t - T_a\right) da,
$$

and, T_a is implictly defined by, $a = \int_{t - T_a}^{t} v_i(\mathfrak{e}_5(\ell)) d\ell$, for all $a \in [0, \tau_i]$.

Table 7.1 The resulting nonlinear system with distributed delays obtained after reducing the PDEs system (7.3), associated with the boundary conditions (7.4), using the method of characteristics (Section 7.4.2).

$$
\begin{cases}
\dot{R}_1(t) = -\left[\delta_1^{\sigma} + \beta_1^{\sigma}(R_1(t))\right] R_1(t) + 2\left(1 - K_1^{\sigma}\right) \mathfrak{I}_1^{\tilde{\sigma}}\left(R_{1t}\right), \quad \text{and, for all } i \geq 2, \\
\dot{R}_i(t) = -\left[\delta_i^{\sigma} + \beta_i^{\sigma}(R_i(t))\right] R_i(t) + 2\left(1 - K_i^{\sigma}\right) \mathfrak{I}_i^{\tilde{\sigma}}\left(R_{it}\right) + 2K_{i-1}^{\sigma} \mathfrak{I}_{i-1}^{\tilde{\sigma}}\left(R_{i-1t}\right), \\
\dot{M}(t) = -\mu M(t) + 2K_n^{\sigma} \mathfrak{I}_n^{\tilde{\sigma}}\left(R_{nt}\right), \\
\dot{\mathfrak{e}}_j(t) = -\mathfrak{g}_j\left(t, \mathfrak{e}_j(t), M(t)\right), \quad \text{for all } j \in \{1, \ldots, 5\},
\end{cases}
$$

where, $\sigma \in \mathbb{N}$ is implicitly controled by the dynamics of $\mathfrak{e}_j$, and, the distributed delay terms are rewritten as:

$$
\mathfrak{I}_i^{\tilde{\sigma}}\left(R_{it}\right) = \sum_{\mathfrak{s}=0}^{k} \int_{\mathfrak{s}\mathfrak{h}}^{(\mathfrak{s}+1)\mathfrak{h}} h_i(a) e^{-\int_0^{\frac{a}{v_i^{\tilde{\sigma}^{\mathfrak{s}}}}} h_i\left(v_i^{\tilde{\sigma}^{\mathfrak{s}}} \ell\right) d\ell} e^{-\frac{a\gamma_i^{\tilde{\sigma}^{\mathfrak{s}}}}{v_i^{\tilde{\sigma}^{\mathfrak{s}}}}} \beta_i^{\tilde{\sigma}^{\mathfrak{s}}}\left(R_i\left(t - \frac{a}{v_i^{\tilde{\sigma}^{\mathfrak{s}}}}\right)\right) R_i\left(t - \frac{a}{v_i^{\tilde{\sigma}^{\mathfrak{s}}}}\right) da,
$$

where, with an abuse of notation, we denote by $\tilde{\sigma}$ a family of indices $\tilde{\sigma}^{\mathfrak{s}}$, with $\mathfrak{s} \in \{1, \ldots, k\}$, $\tau_i = k\mathfrak{h}$, $k \in \mathbb{N}$, such that, $\tilde{\sigma}^{\mathfrak{s}} \neq \sigma$, almost all the time.

Table 7.2 The new representation of the studied system when $\mathfrak{h} < \tau_i$ (case ①). For convenience, we illustrate the case where $\tau_i = k\mathfrak{h}$, $k \in \mathbb{N}$, for all $i \in I_n$.

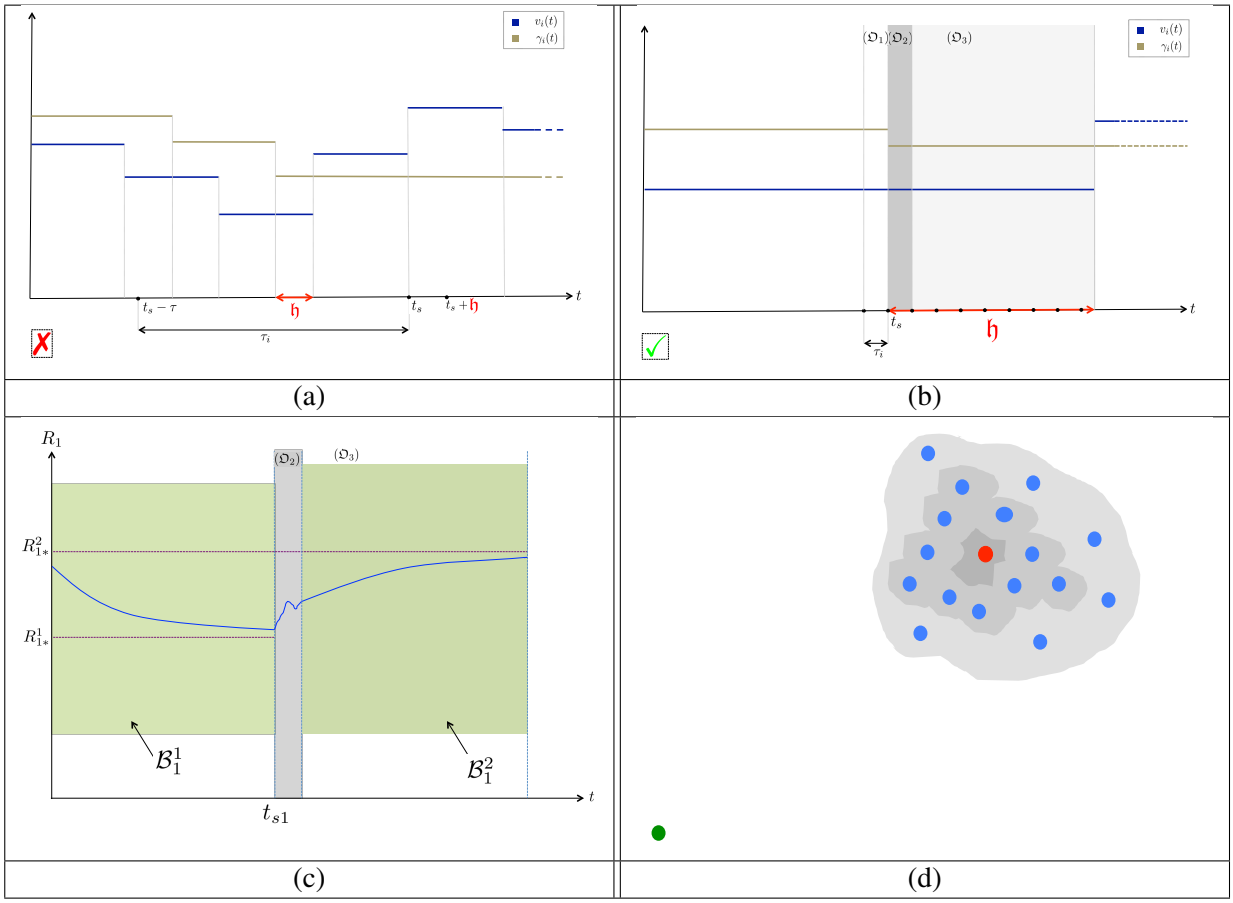

Table 7.3 **(a)** The case ①, where $\mathfrak{h} < \tau_i$. **(b)** The case ②, where $\mathfrak{h} >> \tau_i$. **(c)** Illustration of the trajectory $R_1(t)$. The values R^1_{1*} and R^2_{2*} represent, respectively, the positive steady states of the subsystems $\sigma = 1$ and $\sigma = 2$. The green regions $\mathscr{B}^1_1$ and $\mathscr{B}^2_1$ illustrate the plausible regions of attraction of, respectively, R^1_{1*} and R^2_{2*}. **(d)** The steady states (of interest) of the studied overall-system. The green point represents the origin (zero) of the studied model, which is always an equilibrium point, while the blue points and the red one represent the different positive steady states, for the different possible subsystems ($\sigma = 1$, $\sigma = 2$, ...). Actually, the red point is assumed to represent the favourable steady state that the hematopoiesis process achieves after a series of switching: it can be for instance the objective of a therapy.

for all $t \in [t_{s1}+\tau_i, t_{s2}] \cup [t_{s2}+\tau_i, t_{s2}] \cup \dots$

$$\begin{cases} \dot{R}_1(t) = -\left[\delta_1^\sigma + \beta_1^\sigma(R_1(t))\right] R_1(t) + 2\left(1-K_1^\sigma\right)\Im_1^\sigma(R_{1t}), \quad \text{and, for all } i \geq 2, \\ \dot{R}_i(t) = -\left[\delta_i^\sigma + \beta_i^\sigma(R_i(t))\right] R_i(t) + 2\left(1-K_i^\sigma\right)\Im_i^\sigma(R_{it}) + 2K_{i-1}^\sigma \Im_{i-1}^\sigma(R_{i-1t}), \\ \dot{M}(t) = -\mu M(t) + 2K_n^\sigma \Im_n^\sigma(R_{nt}), \\ \dot{\mathfrak{e}}_j(t) = 0, \quad \text{for all } j \in \{1,\dots,5\}, \quad \text{and for almost all } t \in [t_{s1}+\tau_i, t_{s2}] \cup [t_{s2}+\tau_i, t_{s2}] \cup \dots, \end{cases}$$

where, $\sigma \in \mathbb{N}$ is implicitly controled by the dynamics of $\mathfrak{e}_j$. For instance, if we consider that, $\forall t \in [t_{s1}+\tau_i, t_{s1}+\mathfrak{h}] \subseteq [t_{s1}+\tau_i, t_{s2}]$, we have $\sigma = 1$, then, the distributed delay terms are rewritten as

$$\Im_i^1(R_{it}) = \int_0^{\tau_i} h_i(a) e^{-\int_0^{\frac{a}{v_i^1}} h_i\left(v_i^1 \ell\right) d\ell} e^{-\frac{a\gamma_i^1}{v_i^1}} \beta_i^1\left(R_i\left(t-\frac{a}{v_i^1}\right)\right) R_i\left(t-\frac{a}{v_i^1}\right) da.$$

Table 7.4 The new representation of the studied system when $\mathfrak{h} >> \tau_i$ (case ②), on the time-intervals $t \in [t_{s\ell}+\tau_i, t_{s(\ell+1)}]$, $\ell \in \mathbb{N}$.

Remark 43. *Since we are dealing with an interesting nested biological process, we want to say few words about the mechanisms that interweave in order to accomplish the representation that we aim to achieve. Let us return to the title given to the current section, and particularly the part «event-triggered parameters». Is it equivalent to change event-triggered by switching in this context? The answer is that it depends. In fact, the appellation switching is a shortcut that describes the evolution of the biological parameter with respect to time. However, it conceals the fact that the parameters are actually dependent on specific growth-factor concentrations -which evolve with respect to time-, and that the switching actually occurs in the growth-factor concentration. To recall what we said in Section 7.3, the switching in the growth-factor concentration is due to the difference in the time-scaling between hormone secretion and cell-populations dynamics. So, one may think that in fact it is a double-switching mechanism: the first one occurs in the growth-factor concentration with respect to time, while the second one occurs in the model parameter with respect to its growth-factor concentration. This is true, but it is crucial to mention that we assume that it is possible that some switching occurring in the growth-factor concentrations may not cause a switching in the model parameters. Indeed, as represented in the characteristic patterns, given for instance in Figure 7.4, we see that the model parameter jumps occur if and only if the growth-factor concentration is actually crossing some thresholds, otherwise nothing will happen. Hence the appellation* ***event-triggered*** *process. However, having said that, we can shorten the description and use, in the sequel, «switching system»to refer to the resulting time-delay model presented in Table 7.4.*

7.4.4 On the stability properties of the individual nodes

For a long time, we saw that many works ([180], [8], [9], [226], [225], [78], [4], [189], [3], [107], and [81]) focused on the stability issues of some hematopoietic systems whose parameters are frozen, or growth factor-dependent but with limiting considerations. Unlike all the previous works in this field, we propose here a description of the parameters involved in a complete-type model as an event-triggered process, which leads to dynamical systems formulated in the framework of switching nonlinear systems with distributed delays. We can see that actually the switching occurs between a wide variety of subsystems, and merely some of them can be put in the form of some previously studied models.

Therefore, since we do not intend to dwell upon technical issues that are not necessary for the stabilization problem[11], we consider without loss of generality that the considered growth-factors are effectively acting on proliferation, apoptosis rates, differentiation and self-renewing rates, while their variations are not significant for the other biological features (i.e. their growth factors may vary but without crossing the thresholds that trigger a switching in their corresponding model parameter (see Remark 43). As we remember, the role of EPO hormones is the regulation of proliferation, apoptosis and differentiation, during erythropoiesis (see Section 7.2). More generally, these biological parameters are in fact affected by many molecules, which are effectively tested and used as drugs. The best known examples are the cytotoxic drugs, which increase the apoptosis rates. In particular, in the case of hematopoiesis, the cytosine arabinoside has a well-known effect on apoptosis rates. The anthracyclines (idarubicin and daunorubicin) can also be used to increase apoptosis in some blood disorders. Next, for promoting re-differentiation, the dihydroorotate dehydrogenase inhibitors gave very recently encouraging results, even in the very severe case of acute myeloid leukemia [278]. The dasatinib molecules [167] can also be used to increase differentiation in hematopoietic systems. Finally, proliferation is classically targeted using G-CSF molecules [141].

We focus on the new representation of the model as in Table 7.4, where $\sigma = 1$, on the time interval $t \in [t_{s1}, t_{s1} + \mathfrak{h}] \subseteq [t_{s1}, t_{s2}]$. In order to determine the asymptotic behavior of this system, we start by assuming that no switching will occur (i.e. $t_{s2} \to \infty$). Then, one may investigate the existence of a strictly positive steady state, $E^{\sigma=1} = \left(R^1_{1*}, \ldots, R^1_{n*}, M^1_*\right)$, of the studied system. We notice also that the origin of the system described in Tables 7.1-7.4 is always an equilibrium point. In our work, we are only focusing on strictly positive steady states. For a given subsystem in the overall system (i.e. for a fixed σ), when the strictly positive equilibrium points exists, the 0-equilibrium is unstable. We refer to [8] for a complete discussion on the existence of equilibrium points for a similar model (when $v_i = 1$ and a fixed σ). Of course, by changing σ, the positive equilibrium point $E^\sigma = \left(R^\sigma_{1*}, \ldots, R^\sigma_{n*}, M^\sigma_*\right)$ will change. Whether through medication or by an action of the body, we expect that the dynamics $\mathfrak{e}_j$ (Eq.(7.2)) converge to a favourable state $\mathfrak{e}^f_j$. The corresponding positive equilibrium point (i.e. E^σ_f for a fixed desired σ_f), is then the red point in Figure(d)-Table 7.3. The determination of the optimal strategy to converge to the favourable state will be the subject of the next section. Let us come-back to the subsystem ($\sigma = 1$) in Table 7.4. We assume that its positive equilibrium, $E^{\sigma=1}$, exists. By classical arguments, one can study the local stability properties of $E^{\sigma=1}$. We refer to [225], for the stability analysis of a similar system, based on Input-Output approaches. Then, in Chapter 3 of the thesis, we derived slightly more restrictive

[11] That assertion is argued in Remark 44, at the end of the current section.

results using a Lyapunov approach. The size of the region of attraction of the positive equilibrium, for a typical form of the functions β_i (Hill functions, see [180]), was also estimated. We recall that this region of attraction is expressed as a sublevel of a suitable Lyapunov-Krasovskii functional (see [126] and [165]). More precisely, the estimate of the region of attraction quantifies the set of all initial conditions such that the states R_{it} and M_t converge to the positive steady state.

In the case of the present chapter, we use the previously mentioned constructions and we only focus on the novelty, which is the issue of switching between several subsystems. This situation is represented in Figure(c)-Table 7.3, where a possible trajectory $R_1(t)$ is illustrated. Let us observe the positive equilibrium R^2_{1*}, for the subsystem $\sigma = 2$, and the region $\mathscr{B}^2_1$ which qualitatively represents the region of attraction of R^2_{1*}. A first remark is that if the portion of the trajectory R_{1t}, for $t \in (\mathfrak{D}_2)$, satisfies the LKF-sublevel condition defining the region of attraction of R^2_{1*}, then the trajectory $R_1(t)$ converges exponentially to its positive equilibrium point. Extra-assumptions on the overall model ensure that these conditions always happen, using the fact that the trajectories of the studied system are bounded, and assuming that the successive R^σ_{i*} are sufficiently close. Moreover, in [225], the following conjuncture was stated from numerical simulations: the systems of the studied class (i.e. for each fixed σ for all $t \geq 0$) have a region of attraction which is much bigger than the one rigorously provided by the LKF-approach (i.e. the results provided by the Lyapunov approach are more conservative). Consequently, and without extra-assumptions on the model, we confirm that the behavior of the trajectories during the $(\mathfrak{D}_2)$-periods does not impact the $(\mathfrak{D}_3)$ phases.

To summarize the previous key points, we retain that we have a large family of subsystems that constitute one overall nonlinear switching system with distributed delays, which is in fact the switching version of the general model obtained in Table (7.1). The subsystems share in common some fixed biological parameters (δ_i, τ_i) while they are distinguishable according to the possible combination taken by the three switching parameters, that we denote by the *triplet* $\big(\beta_i(0), \gamma_i, K_i\big)$, representing respectively the proliferation maximum recruitment rate, the apoptosis rate, and the differentiation rate of the i-th generation. Each of these three parameters has a characteristic pattern that connects the concentration of its respective growth-factor to its current value; in the form of a monotonic step-like evolution function, as the one shown by Figure 7.4. In other words, a typical growth-factor is exercising over each model parameter an event-triggered control.
Let us assume for instance that initially, a triplet of parameters is activated, then at a time instant $t_0 > 0$, a drug infusion causes a switch in model parameters (at least in one of them), which jump to the triplet $\Big(\beta_i^{(0)}(0), \gamma_i^{(0)}, K_i^{(0)}\Big)$. Based on earlier results (Chapter 3 and [225], [8], [81]), we deduce the following:
i) First, it is possible that the subsystem corresponding to the activated triplet for $t \geq t_0$ does not satisfy the condition of existence of a strictly positive steady state.
ii) If, for the corresponding triplet of parameters, the positive steady state exists, then the latter can be unstable or exponentially stable.
iii) If the condition of its exponential stability is satisfied (we retain the one given in Theorem 3 of [81], or Chapter 3 of the thesis), then the intermediate time-interval, traversed by the trajectory, between t_0 and $t_0 + \tau_i$, can be seen as an initial condition for the model equations written for all $t \geq t_0 + \tau_i$ (where the model equations have no longer any switching parameter, even in their distributed delay terms) has no effect on the dynamics of the system for all $t \geq t_0 + \tau_i$, until the next switching time-instant. The latter assertion is available as long as the overall system is switching between subsystem for which the stability conditions of their positive steady states are satisfied.

7.4.5 Numerical results on a switching hematopoietic systems

At this point, it will be helpful to illustrate the model behavior on some numerical examples. Let us start by the following one, where a switching occurs between three subsystems (we are limiting the frame of possibilities). Each subsystem corresponds to a hematopoietic system which is composed of three generations of immature cells (HSCs, progeny and precursors) and one generation of mature cells (it can be a type of white blood cells or let say red blood cells).

Let us consider the following biological parameters and functions for the three subsystems:

❶ For $\sigma = 1$:

➢ For $i = 1 : K_1 = 0.05$, $\tau_1 = 1.109$, $\gamma_1 = 0.28$, $v_1 = 1$, $\delta_1 = 0.14$, and, $\beta_1(R_1) = \frac{0.5}{1+R_1^2}$.

➢ For $i = 2 : K_2 = 0.05$, $\tau_2 = 1.2$, $\gamma_2 = 0.28$, $v_2 = 1$, $\delta_2 = 0.26$, and, $\beta_2(R_2) = \frac{1}{1+R_2^4}$.

➢ For $i = 3 : K_3 = 0.08$, $\tau_3 = 1.36$, $\gamma_3 = 0.4$, $v_3 = 1$, $\delta_3 = 0.35$, and, $\beta_3(R_3) = \frac{3}{1+R_3^2}$.

➢ For M: $\mu = 0.042$.

After simple calculations, we can prove that the positive steady state is:

$$E^1 = (0.73867, 0.89927, 1.21625, 3.86030)\,.$$

❷ For $\sigma = 2$:

We consider that $\beta_1(R_1) = \frac{0.55}{1+R_1^2}$, $\beta_2(R_2) = \frac{1.13}{1+R_2^4}$, and, $\beta_3(R_3) = \frac{3.15}{1+R_3^2}$. All the other parameters are the same as for $\sigma = 1$. The positive steady state in this case is:

$$E^2 = (0.83677, 0.96778, 1.26532, 4.01943)\,.$$

❸ For $\sigma = 3$:

We consider that the functions β_1, β_2, and β_3, and the parameters δ_1, δ_2 and δ_3 are similar to those considered in $\sigma = 2$. On the other hand, we assume that in this case we have: $\gamma_1 = 0.18$, $K_1 = 0.06$, $\gamma_2 = 0.18$, $K_2 = 0.045$, $\gamma_3 = 0.3$, and, $K_3 = 0.055$. The positive steady state is:

$$E^3 = (1.10952, 1.14432, 1.72306, 2.70245)$$

Now, we consider that a first switching from the subsystem $\sigma = 1$ to the subsystem $\sigma = 2$, occurs at $t = 90$. Then, a second switching from the subsystem $\sigma = 2$ to the subsystem $\sigma = 3$ occurs at $t = 160$. The trajectories of the system are given in Figure 7.7.

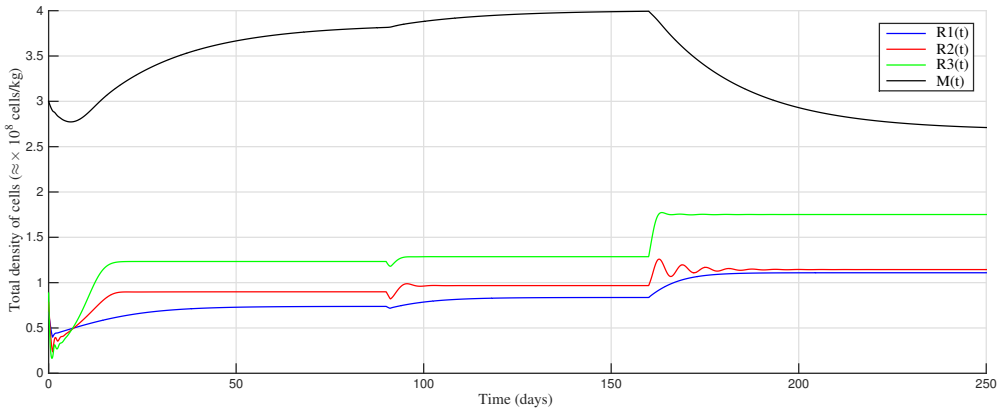

Fig. 7.7 Trajectories of the switching system of the numerical example in Section 7.4.5.

Remark 44. *At this juncture, it is worth mentioning that the part of the work presented throughout the previous sections is already a step-forward in refining the analysis of healthy and unhealthy hematopoiesis. Indeed, here we introduced the basics of a new representation of hematopoietic processes as a switching system, through event-triggered parameters. The Example 7.4.5 emphasizes on a particular case in which it is assumed that the behavior of the growth factors is known. It is representative of a well-defined therapeutic protocol in which drugs are administrated at two time-instants decided for instance by the health professionals. Now, the issues that remain to be addressed are related to precisely how these switching instructions are* ***quantified*** *and* ***scheduled****, both in: i) the healthy case where we focus on the role of mature cells (in Eq* (7.2)*) in the control exerted on growth-factors, and, ii) in the unhealthy cases where an optimal therapeutic strategy have to be determined (and which takes into account drugs toxicity and other factors). Henceforth, each subsystem, which is actually fully defined by a unique triplet of parameters among the possible triplet-combinations of the switching parameters* $\left(\beta_i(0), \gamma_i, K_i\right)$*, is considered as a node or vertices, in a network representing all the possible subsystems. We will define the rules and the possibilities for the transitions between the nodes (i.e. switching between the subsystems). Through numerical illustrations (Section 7.6) we will prove that this is a suitable representative framework for optimal strategies planning.*

Finally, the characteristics concerning each node (each subsystem) which are fundamental and that we retain for the next steps are: ***i) Existence of*** M_e***:*** *if the positive steady state* M_e*, of mature cells, exists or not, for each subsystem and,* ***ii) Stability of*** M_e***:*** *if the existing positive steady state* M_e *is stable or not*[a]*. This justifies our assertion at the beginning of this section, when we claimed that without loss of generality we focus on only three parameters (actually, they are four, because self-renewal rates depend on differentiation). In other words, even if we add other switching parameters, or even if we slightly modify the studied model, all what we need to provide is: the existence and the stability properties (points (i) and (ii)) of each node in the resulting network. Then, the planning algorithms for the stabilization issues that we will discuss in the next section remain exploitable.*

[a] This is an abuse of notation. We are considering that the strictly positive steady state M_e of a specific subsystem (i.e. fixed σ) is unstable, if it does not satisfy the exponential stability condition in Chapter 3 - even if the latter condition is just sufficient-.

7.5 Stabilization through drug infusions and regulation via proper means of the body

Several times throughout this work, we had mentioned that when searching the best stabilization strategy for an hematopoietic system, some nuances exist between the healthy and the unhealthy cases. In this section, we set the appropriate rules that the strategy-finding algorithm takes into account in order to establish the optimal strategy in each case. In fact, these are, for the most part, practical constraints and instructions. However, it is worth mentioning that our algorithms remain flexible and easily modifiable if one wants to enrich or change the set of initial rules.

We start here by the statement of common rules, which are available for both the healthy and the unhealthy cases. It is worth mentioning that for the sake of clarity, the stabilization theory is formulated for the case where the model involves only one immature compartment (HSCs, in the bone marrow) and one mature-type compartment (e.g. white or red blood cells, in the bloodstream). This is particularly convenient for the implementation of the algorithms that we provide. A further worthwhile clarification: we denote by ***stable node***, or ***stable subsystem***, a subsystem belonging to the set of possible subsystems (that constitute the overall hematopoietic model) which has a stable strictly positive equilibrium point. The stable steady state is in fact the point (R_e, M_e), where R_e is the steady state of HSCs and M_e is the steady state in the mature compartment. However, for clarity, we focus only on M_e, since both M_e and R_e have the same properties (i.e. existence and stability properties, see Remark 44). This is convenient in practice because the reference is usually given in terms of active mature cells in the bloodstream. Therefore, we can say that the ***stable node*** in our network is completely defined by its associated M_e. In addition, when we determine the network of all the possible existing nodes, we define the domain that we call «`Limit_area`», that contains only the biologically significant values of M_e, i.e. the values which are too high or too low, at the point of becoming impossible nodes, are excluded. Having said that, we state the first fundamental rule in our networks:

Rule 1. *The **neighbors** of a given node are those which can be directly reached from it through **one** transition, which requires no more than one **switching** in each possibly switching parameter.*

We recall the form of the characteristic pattern given for instance in Figure 7.4. In that step-like function, the parameter K is switching by ± 0.02 from its previous value at each time it changes (continuously) with respect to its growth-factor concentration $\mathfrak{e}_4$ (e.g. the K-value is increasing or decreasing by a step of 0.02, each time it changes to a new level). However, we have three switching parameters in our model. Thus, Rule 1 allows one **elementary switching** in each possibly switching parameter, through one transition. For instance, if we consider the initial node to be $M_e^{(0,0,0)}$, meaning that the activated initial subsystem has the parameters $\left(\beta^{(0)}, \gamma^{(0)}, K^{(0)}\right)$, then the point denoted[12] $M_e^{(+1,0,+1)}$ belongs to the neighborhood of the initial node, however, it is not possible to make a **direct** transition between $M_e^{(0,0,0)}$ and $M_e^{(0,0,+2)}$, because the latter action requires a double jump in K-value. Rule 1 avoids giving more than one dose of one-type drug at the same moment. That situation is banned because the elementary switching-step is to be understood as the maximum tolerable dose of the used-type molecule at one dose.

[12] That is a compact form that means that, in comparison to the parameters of $M_e^{(0,0,0)}$, the $\beta(0)$ increases by one jump, apoptosis remains unchanged, while differentiation increases by one jump.

Therefore, giving a double dose of one-type drug at the same moment is considered to be highly toxic. Moreover, if the drug infusions are not well-spread over time, their effect is expected to be saturated. On the other hand, Rule 1 allows the infusion of different drugs, if they are targeting different parameters, at the same time[13] (however, possible does not mean that it is the best choice, as described in the next section). Now, we set the rules which are specific to healthy and unhealthy cases. Starting with the latter one.

7.5.1 Procedures and constraints of the stabilization through drug-infusions

If we want to cure the hematopoietic system, it is because, without drugs, it shows some malfunctions. We can distinguish between two situations: on the one hand, before treatment, the initial state of the system is stable, but diagnosed with an abnormal blood cell count (e.g. a severe low blood count in a type of mature cells, as it is the case in many diseases). On the other hand, the initial system can show an oscillatory behavior as in cyclic and periodic blood disorders (e.g. cyclical neutropenia). The latter case is equivalent to say that the initial node in the network corresponding to the overall model is unstable. Next, when constructing the effective network regrouping only the *allowed* nodes, we can decide that switching can occur only between stable nodes, or we can admit some transitions through few unstable nodes. This issue does not even arise in the healthy case, in which we exclude at early stage all the unstable nodes from the set of possible transitions[14]. But the answer is not as obvious for the unhealthy case. Then, on the basis of the most reasonable option, we set the following rule:

Rule 2. *When the initial system starts from an unstable node, the first therapeutic step is to drive it to the* ***most quickly reachable*** *stable node, even if the latter subsystem is not the* ***best successor*** *in the chain of successors leading to the ultimate goal of the therapy.*

The example shown in Figure 7.8 highlights the fact that in a general construction, it may be possible that the optimal pathway (or the unique one) towards the objective M^* is the one that passes through some unstable nodes. However, to avoid drowning in the details that lengthen the description, we limit ourselves to the application of Rule 2, and we emphasize the case of networks formed by stable nodes.

Since the starting point itself may be unstable, one might be tempted to consider the paths through some unstable points. However, this option is banned by Rule 2 because we notice that important oscillations in blood counts may emerge from unstable nodes, creating the risk of significantly exceeding the tolerable limit (i.e. `Limit_area`), which is prohibited. An illustration of the oscillatory behavior is given in the following example.

Example 14. *Let us consider the following biological parameters for what we assume to be an arbitrary subsystem of an overall switching system describing hematopoiesis:*
***For HSCs**: $K = 0.05$, $\gamma = 0.03$, $\tau = 2.81165$, $\delta = 0.85$, $f(a) = \frac{e^a}{e^\tau - 1}$, and, $\beta(R) = \frac{8}{1+R^3}$.*
***For mature cells:** $\mu = 0.025$. The trajectories of the total density of resting HSCs $R(t)$ and the total density of the mature-type cells $M(t)$ are given in Figure 7.9. It shows an oscillatory behavior of important*

[13] This is called a combined-targeted therapy.

[14] It is hard to believe that when the body wants to adapt its operating mode from one state to another one, it expresses unstable or unhealthy behavior between the two.

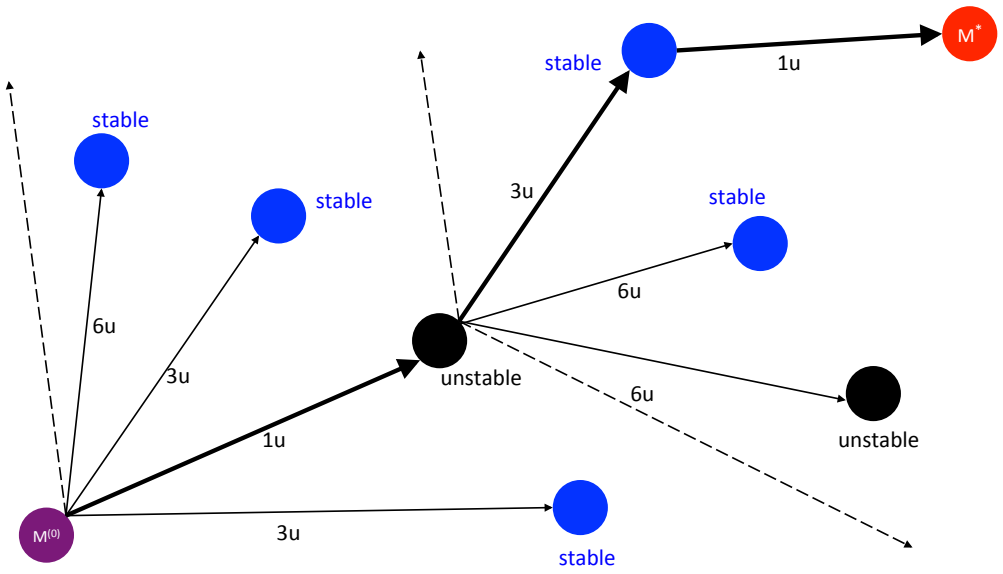

Fig. 7.8 Stabilization through drug infusions: the transitions and their costs.

amplitudes, in particular in the HSCs compartment. If the values of the steady states associated with a specific subsystem are close to the boundaries specified by the `Limit_area`*, then the oscillatory behavior can become problematic because it leads to a clear overrun of the tolerable limits. Thus, we tend to avoid such a compromising situation.*

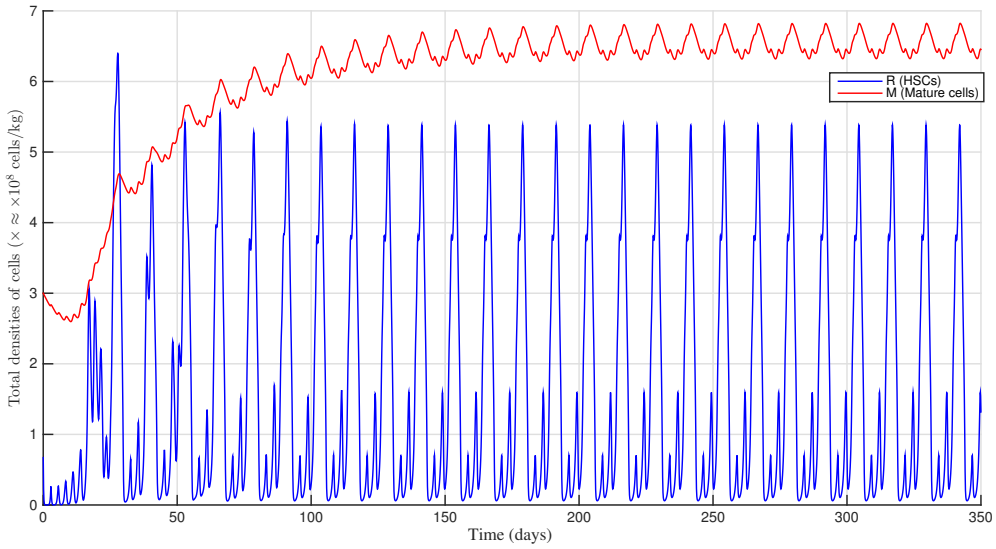

Fig. 7.9 An example of the oscillatory behavior of an unstable node representing one subsystem in the overall hematopoietic system. The trajectories correspond to the subsystem-parameters of Example 14.

Moreover, because of the high toxicity levels caused by the drugs (in particular, chemotherapy and its severe side-effects), **priority must be given to any therapy strategy that requires the minimum quantity of drugs at each infusion**. Therefore, one possible consideration is as follows:

Rule 3. *i) The cost of a one-step transition that requires targeting the three biological parameters in one dose is* 6*u. ii) The cost of a one-step transition that requires targeting two biological parameters in one dose is* 3*u. iii) The cost of a one-step transition that requires targeting only one biological parameter in one dose is* 1*u.*

In Rule 3, the u indicates a normalized unit associated to the *cost* in our context. The lowest cost is $1u$ and it is associated to the simplest transition from one node to another one, that requires exactly one switching in only one of the possible parameters. For later use, we mention that when elaborating the decision function in the search algorithm, it is important to associate to the heuristic function the same scaling-unit as the one for the cost.

7.5.2 Procedures and constraints in the regulation of mature cell density through self-tuning switching mediated by growth-factors

In the case of a healthy well-regulated hematopoiesis, some features are to be pointed. First, in contrast to what has been precised for the unhealthy case, here the starting node represents a healthy subsystem (i.e. the node is stable). When the body requires to move from that initial state in order to reach a desired state M^*, as in Figure 7.10, only stable subsystems are investigated.

Rule 4. *Among all the subsystems (or, equivalently, the nodes) generated from the set of combinations between the possible values of the switching parameters, the selected nodes-network is entirely formed by the subsystems verifying the constraints of* ***existence***, ***stability*** *(i-ii in Remark 44), and the* `Limit_area` *requirement.*

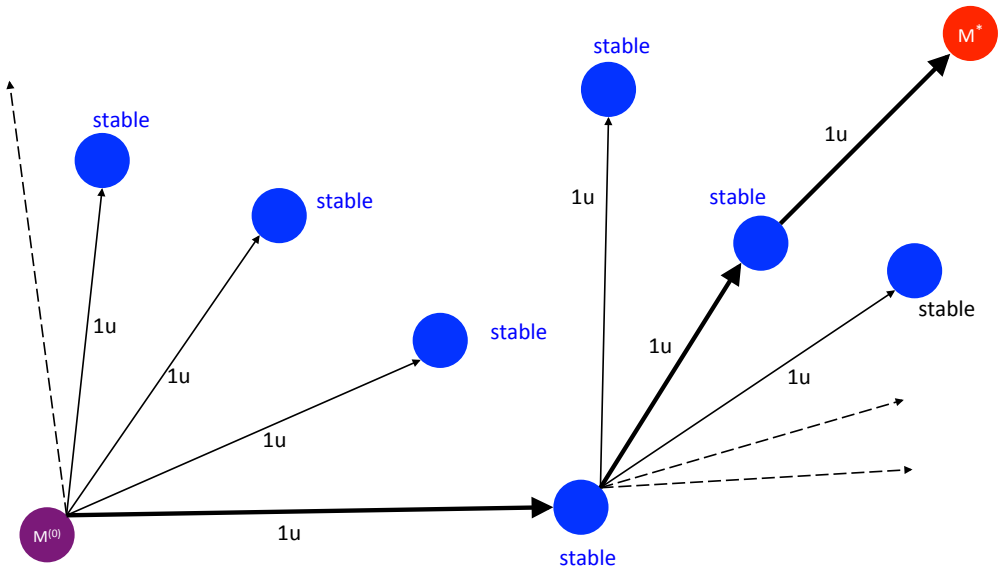

Fig. 7.10 Body regulation: Transitions, rules, and instructions. The newtork is exclusively composed by stable nodes. The cost of $1u$ is associated to all the elementary transitions.

In the previous section, we have considered that the use of drugs is toxic and expensive. However, the growth-factor secretion is a natural phenomenon that does not imply notable costs or side-effects,

compared to chemotherapy for instance. Therefore, there is no reason to consider that according to the number of switching executed by the parameters, different costs are attributed to the elementary transitions. In other words, we do not consider that a growth-factor secretion has a cost for the body, when moving from one node to its neighbor.

Rule 5. *The cost of a one-step transition (i.e. elementary switching) between one node and any available node in its neighborhood, is the same and it is worth* $1u$.

Remark 45. *The previously mentioned rules offer a reasonable framework that allow us to provide a consistent framework, by taking into account some practical constraints. Changing or adding the rules can be done without a major difficulty (e.g. adding rules that include multiple costs for different drugs, due to a difference in toxicity levels, price or a shortage of some molecules). It is precisely this flexibility that we will highlight in the sequel, by providing two different implementations: one for the healthy case and another one for the unhealthy case.*

7.5.3 Where does the interest for *planning* come from?

When reflecting on the meaning of *stabilization* in healthy and unhealthy contexts, we were not suspecting that this could bring us into the fundamental field of *automated planning and scheduling*, which is a fully inserted branch of *artificial intelligence* (AI) [254] and *decision theory*. Mainly it concerns the elaboration and the realization of strategies and action sequences, in order to set goals and achieve them (see [151]). This theory is used when the solutions are complex and must be **discovered** and **optimized** in multidimensional spaces. As an example, here we can evoke robotics and the pathfinding issue for autonomous vehicles, where the latter theory is widespread. In this regard, we are going to take the similarities between our application and the pathfinding issues to illustrate the interest that we have in *planning*.

So, on the one hand, we consider the issue of searching an optimal path (see [151], Chapters 5 and 7) for physical objects (e.g. a mobile robot) in a known, partially known, or unknown environment. We can think about a $2D$ surface on which a robot is looking for the optimal trajectory to join two points S (Start) and G (Goal). During its journey, the robot seeks to avoid the static or dynamic obstacles that appear on its way, while discovering new scenes during its movement. It is also possible that the point G is also moving.

On the other hand, we have achieved a description of the hematopoietic system as a switching one. Thus, the question is clearly how to move, or switch, between the appropriate subsystems in order to achieve a final objective (which turns out to be different if it is healthy or unhealthy hematopoiesis). It is interesting to notice that the strategy to be developed operates under strict conditions that come from our specific model (mathematical constraints) and are also related to the application (biological constraints). More precisely, let us assume that one wishes to switch between several subsystems before reaching a fixed objective: this is for instance a behavior which is similar to the one described in Example 7.4.5 and Figure 7.7. Then, it is necessary to know that among a large number of possible subsystems candidates, where each one is actually defined through a unique biological parameter combination, only a few of them

can be validated. This is because many times, when switching from a subsystem to its neighbor[15], the strictly positive steady state of the latter subsystem can be *mathematically* non-existent, or it can exist but it turns out later that it is an unstable steady state to be avoided (Rule 4), or it can be stable but biologically insignificant (outside the `Limit_area`), etc.

Consequently, if we return to the robot illustration, we deduce the following parallels:

> The set of all the possible hematopoietic subsystems is equivalent to the virgin scene that is in front of the robot. In particular, each subsystem is in some sense equivalent to a unit of space (e.g. $1m^2$) that the robot can occupy at a given time instant. So, it appears clear that the units of space that the robot cannot borrow because of the presence of obstacles, are equivalent for us to the hematopoietic subsystems that are rejected because of one of the previously stated reasons. Next, the departure point S of the robot is similar to the initial hematopoietic subsystem, while the goal G can be set by body requirements in order increase or decrease its blood counts (see Introduction), or, in the unhealthy case, it can be a reference prescribed by health professionals (i.e. therapeutic objectives).

That said, now we give a glimpse on few well-known techniques bequeathed from AI. We only mention some flagship works that are related to our objectives, starting from 1968, when three researchers from the Stanford Research Institute provided a strong conceptual framework for pathfinding issues. In their famous paper [130], they presented the A^* *algorithm* which uses a heuristic approach. Generally speaking, there are two main ways to solve the optimal planning problems: dynamic programming and greedy approaches. The former one is based on the idea that the whole problem should be divided in several subproblems, then by combining the individual solutions of the subproblems, we can determine the optimal solution of the overall problem. On the other hand, the greedy approach, which is an algorithmic paradigm that follows the problem solving heuristic of making the locally optimal choice at each stage (by making one greedy choice after another until finding the optimal global solution). All the conditions of consistency, admissibility and optimality of A^* -that allow it to find the optimal path- are rigorously established in [130]. We will revisit in detail the most important point about the heuristics in our context. But here we continue with some generalities about the incremental search algorithms, that are useful for us. It is worth mentioning, however, that our application creates more issues than the basic example of the 2D robot pathfinding as illustrated in the following sections. Next, the D^* *algorithm*, which is an informed incremental search algorithm for dynamical partially known environment, appears in [273]. The latter algorithm is proved to be efficient and optimal, with a high ability to deal with changing environments. Many versions of D^* followed, with always the aim of extending the field of application and improving the computational aspects. That is how the *Focused* D^* appears in [274], followed by the D^* *Lite* in [162]. Finally, we mention the recent work in [186], where a *3D-*D^* *algorithm* was introduced. The latter method is approaching what we are going to do, because it considers the pathfinding issues in a three-dimensional space *xyz* (e.g. for a drone). The *xyz* space in our application is the space $\beta(0)$-γ-K where each axis admits a set of finite discrete values defined according to the evolution patterns (as in

[15] We recall that two subsystems are each in the vicinity of each other, if at most one switching action in each of the controlled parameters involved in the model, is sufficient to pass from one subsystem to the other one, and vice versa.

Figure 7.4). The resulting set of nodes in the 3D space is illustrated in the Figure 7.11, where the $M^{(0)}$ node (or, equivalently, $M^{(0,0,0)}$) is represented in purple color.

The 3D-representation of our network is painful and does not bring any information about the features of the network (it may even be misleading, because some nodes in the center of the 3D construction can represent values outside the `Limit_area`, for instance). The only benefit of the latter representation is that each node is placed near its possible neighbors (26 neighbors, if all of them satisfy all the fundamental requirements). Therefore, we prefer a more convenient representation, in a 2D graph, as sketched in the previous section (Figures 7.8-7.10). More precisely, we set a more intuitive representation where the flat space incorporates all the admissible nodes and marginalizes those outside the `Limit_area`, as illustrated in Figure 7.12 in which the `Confidence_area` contains the so-called `Goal`-nodes, which are the objective, or, the reference nodes.

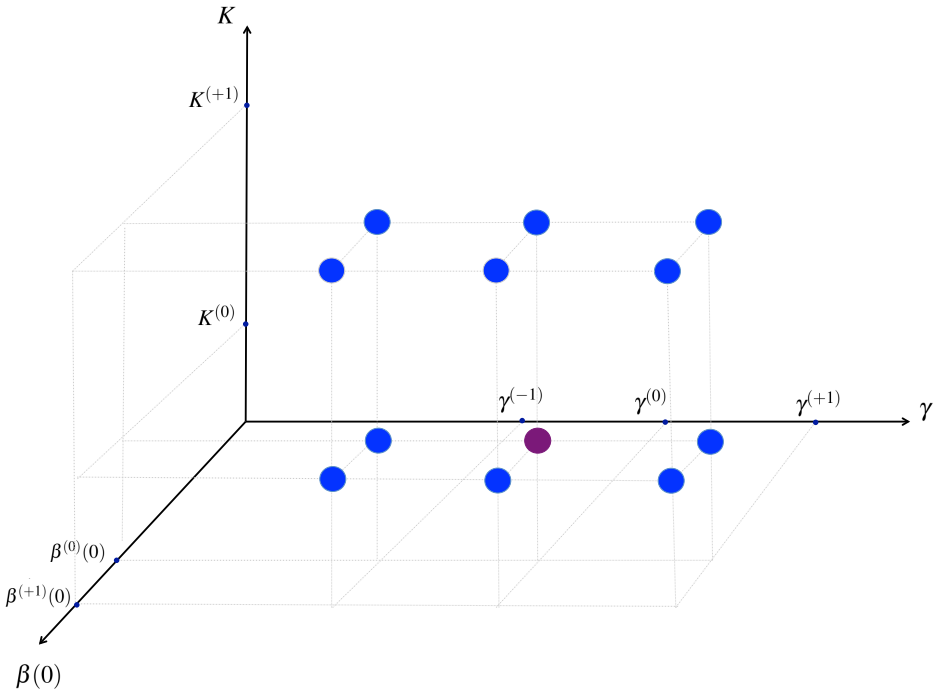

Fig. 7.11 A selected part of the hematopoietic network in the 3D space. The connections between the nodes are not represented. Notice that, in fact, some of the nodes may not exist if the corresponding triplet does not satisfy one of the fundamental requirements. Other nodes can be unstable or stable but insignifiant (outside the `Limit_area`). However, all these information cannot be deduced directly from the 3D representation, so we are looking for a better representation (a suitable 2D projection).

7.5.4 Pseudo-Codes and main features of the hematopoietic system network

In relation with what we have said in the previous section, we want to point out a fundamental feature that characterizes our hematopoietic system network. The concepts that we are going to discuss here are related to the meaning of *optimal* strategy.

Remark 46. *A further worthwhile clarification, useful in this section, is: for notational convenience, we employ equivalently the forms* $M_e^{(0,0,0)}$ *and* $M_e^{(0)}$. *The former one is used most of the time, while the latter compact one is employed when no confusion is possible.*

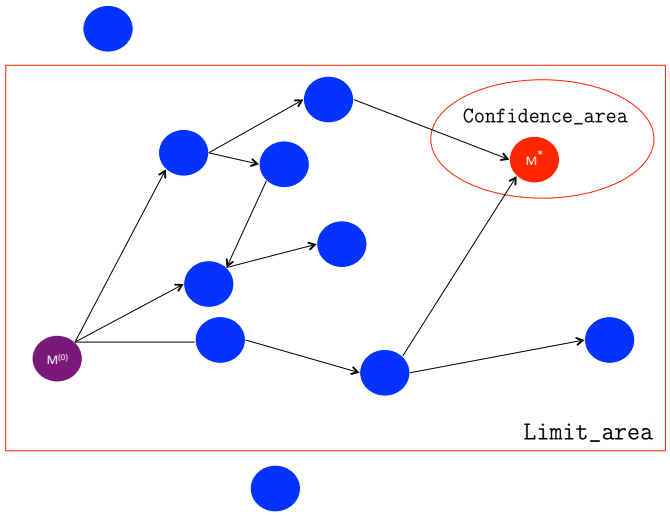

Fig. 7.12 The 2D representation of the network, with some illustrative nodes and connections between them. The costs of the transitions are not mentioned. The nodes outside the `Limit_area` are not taking into account when searching the optimal path to the objective. The optimal path is the cheapest possible path from the purple node (initial point) until one of the nodes satisfying the `Confidence_area` requirements (the goal). Each of the blue nodes is defined by the value of the positive steady state of the mature cells and its corresponding triplet of parameters, i.e. $M_e^{(\texttt{attribute}_1,\texttt{attribute}_2,\texttt{attribute}_3)}$.

First, let us further the comparison between our hematopoietic system strategy and more practical fields that usually implement the pathfinding techniques. The case of a moving object in a 2D scene is the most classical one. In Figure 7.13, three scenes are proposed. We consider the general case in which the moving object can perform lateral and front movements (cost $1u$ for white squares, and $2u$ for the gray ones) and also diagonal movements (cost $1.4u$ for the white squares and $2.8u$ for the gray ones). These costs are not coincidental: they are actually proportional to the distance traveled by the moving object. If we consider that a lateral or frontal movement represents a unit (1) distance, then the length of the diagonal is $(\sqrt{2})$, which gives the cost $1.4u$ for the corresponding progress. Moreover, observe that in Figure 7.13 (**(b)**-**(c)**), whether one decides to move between S and its diagonal successor, or between N_1 and N_2, the costs and the traveled distances of these movements are the same. In this case, we say that for **the one-step transition**, we have **coordinates-free traveled distances and costs**.

Thus, in the latter situation, we highlight the fact that the concept of *distance* plays a *dual* role:
(use-i) First, at each progress-step, the cost of the transition between the current node (or, square) and its successor is proportional to the distance between the two nodes (or, squares).
(use-ii) The progress towards the final objective is also measured (or, estimated) through the distance separating the current position and the final objective: the mission is accomplished if this distance is zero.

Consequently, since the same notion of *distance* is considered in the two points **(use-i)** and **(use-ii)**, the problem of optimal pathfinding is readily formulated and solved, by choosing the *shortest distance* between any two squares (i.e. the straight line between them) as a **consistent** and **admissible heuristic** in the search algorithm [130]. However, things are slightly more complicated in our hematopoietic system network. Indeed, in our application, three variables are switching (or, moving). A 3D space is then considered, which is in fact the $\beta(0)$-γ-K-space, as illustrated in Figure 7.14-**(a)**. That representation is discretized, such that each volume-unit is a cube (equivalent to the squares in 2D, Figure 7.13), such that

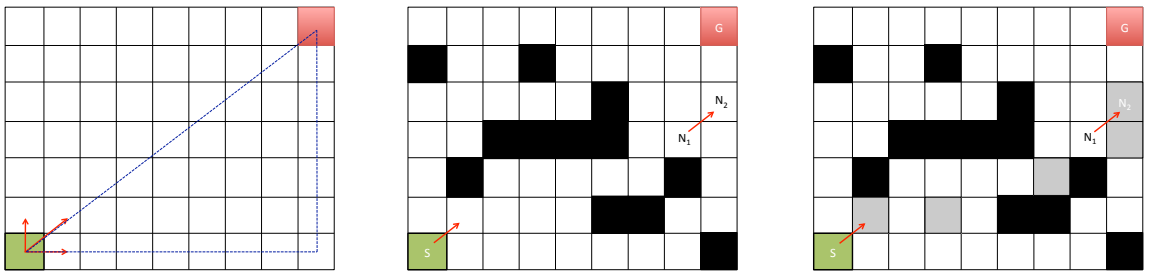

Fig. 7.13 In green the starting point and in red the objective point. **(a)** A scene without obstacles: the white squares are accessible for the robot. **(b)** a scene with obstacles: the black squares are forbidden for the robot, which has to avoid them. **(c)** A heterogeneous scene that contains white squares and black squares, but also some gray squares for "*damaged land*", that the moving object can borrow but they are more costly than the white ones, as they represent a perilous path.

each cube is defined by its coordinates, i.e. its triplet of parameters $(\beta(0), \gamma, K)$. We consider that the nodes M_e - when they exist for the specific triplets - are placed in the center of each cube.

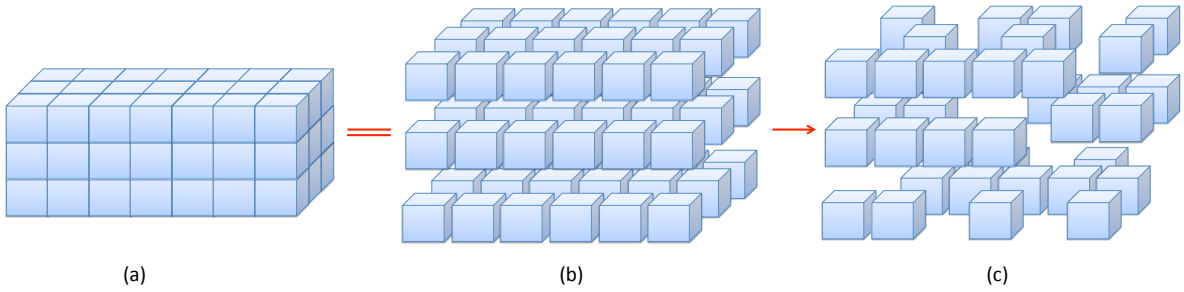

Fig. 7.14 Representation of the 3D-space $\beta(0)$-γ-K.

In order to visualize the space inside the 3D-construction, we separate the cubes as shown in Figure 7.14-**(b)**. That representation is admitted to be completely equivalent to the previous one (Figures 7.14-**(a)**). Similarly to the black squares (i.e. the obstacles) in the 2D example (Figure 7.13-**(b)**-**(c)**), the hematopoietic network may contain many triplets of parameters that are inadmissible (non-existent M_e-points, unstable M_e, or M_e-values outside the `Limit_area`). For the sake of clarity, we choose to simply remove the inadmissible nodes from the 3D-representation (Figure 7.14-**(c)**), instead of putting them in black color. Now, let us consider an arbitrary node to be the initial node (represented in green in Figure 7.15). We focus on the more interesting case of unhealthy hematopoiesis, since different transition-costs are involved (Rule 3). Therefore, in the general case when all the neighbors of the green node exist, the transitions and their associated costs are those illustrated in the Figure 7.15.

Similarly to the moving-object situation discussed previously, the concept of *distance* plays an important role in the hematopoietic system network. Indeed, the stabilization objective behind the therapy (or the body regulation) is a reference M^* that gives the desired mature blood cells density, and we can use a norm that measures the **distance** between $M(t)$ and its objective M^* (see the algorithms in Appendix). In practice, we cannot expect that the body cell count is stabilized to an exact mathematical

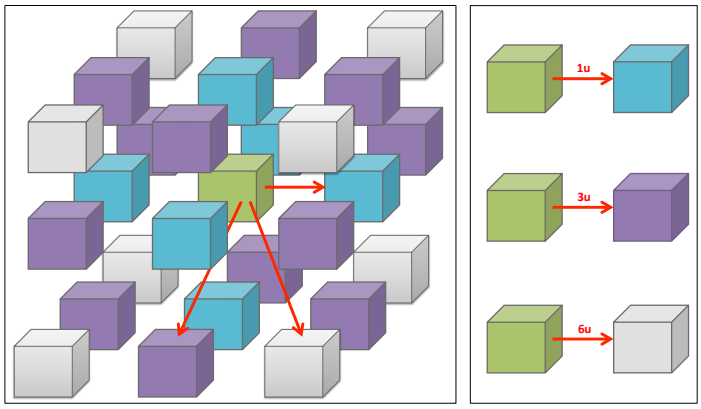

Fig. 7.15 3D representation in the $\beta(0)$-γ-K-space. In the case of unhealthy hematopoiesis, the transistions and their costs are given by the Rule 3.

value. Therefore, we admit that the exact value M^* is associated to a `Confidence_area`, which is a safety-distance threshold around the exact value M^*. For instance, for the red blood cells, we can for instance consider that the therapy objective is to guarantee a stable steady state between 38%-42% of the total blood volume in the bloodstream (M^* is given as number of cells/kg of blood). At first glance, we may think that the difference between the cell-densities of each current value M_e -of one activated hematopoietic subsystem- and the prescribed reference M^*, is a heuristic candidate in our application. That is because, starting -for instance- from an unhealthy state (e.g. a low stable blood cell density $M_e^{(0)}$), we can observe the evolution of blood count and the progress through therapy until its stops when the distance -i.e. the difference- between one reached stable steady state M_e, and the objective M^*, satisfies the requirement given by the `Confidence_area`. One can make the parallel between the case described above, and the point **(use-ii)** previously illustrated in the example of the moving-object. Unfortunately, that concept of *distance* does not satisfy the dual conditions of the example of the moving-object. More precisely, if we compare our network with the point **(use-i)**, we notice that, in our application, the **cost of a transition** between the current node that we consider for instance to be $M_e^{(0)}$, and its neighbors (Figure 7.15) is **not proportional to the distance** between the two concerned nodes, if the distance is considered as the difference between the current blood cell density and the one set as an objective. The latter remark results from the complex relationship between the biological parameters and the M_e-values. In other words, we can get a considerable jump in the M_e-value by a one-step transition in which only one model parameter changes (i.e. the cheapest cost - Rule 3), while a timid advance in the M_e-value is achieved through a more costly one-step transition (involving two or three jumps in the switching parameters). In addition, this is a coordinate-dependent problem[16], since by applying a one-step transition to two different initial nodes, the result in terms of distance in the M_e-values is not the same. More precisely, we can expect that the first node jumps to a value M_e which is far from its initial value, while the second node, of different coordinates, jumps to a closer point, even if the applied one-step transition type is the same. To make it clear, we provide the following numerical example.

[16]The opposite of the free-coordinates distances and costs described in the moving-object comparative example.

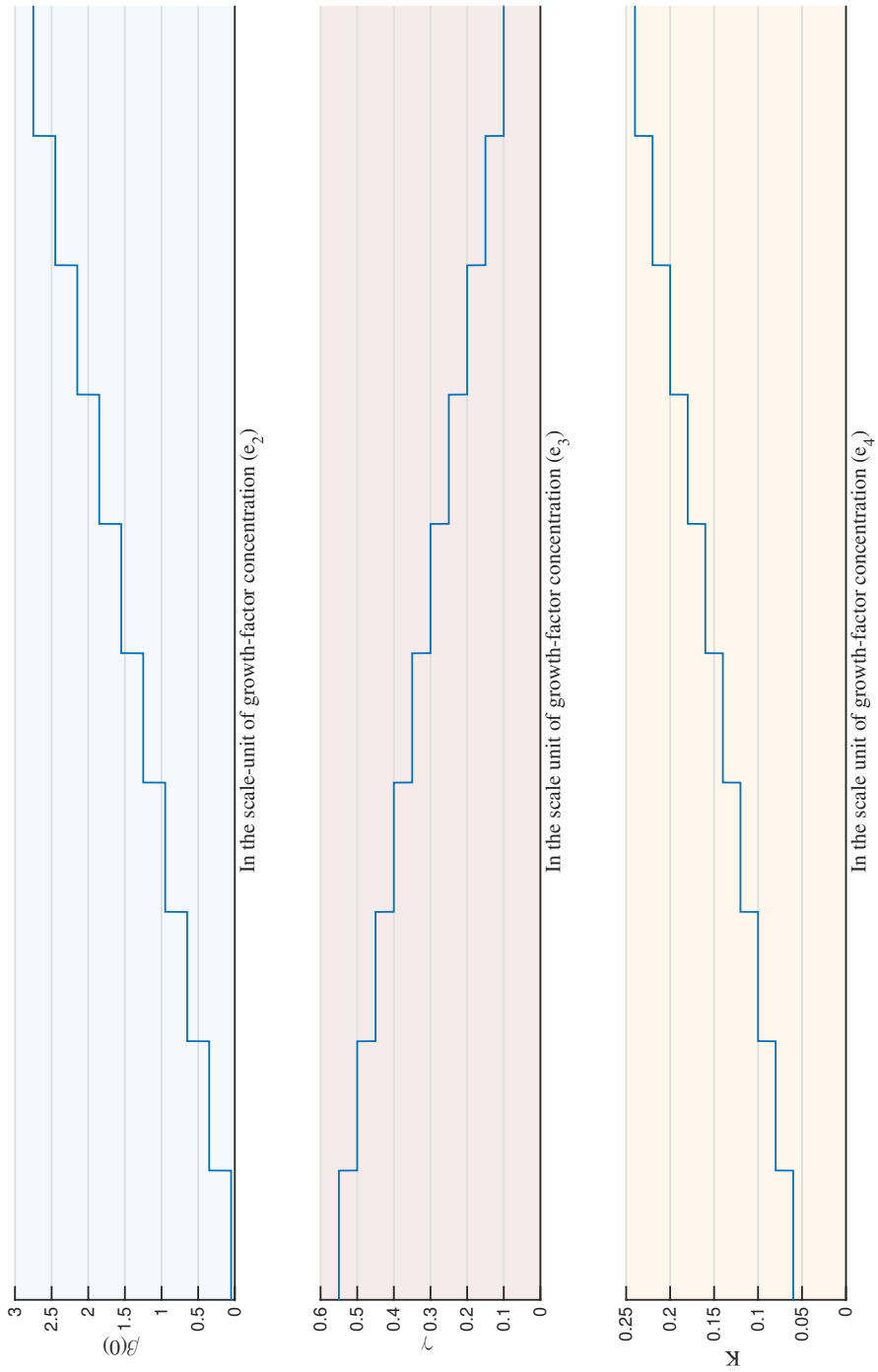

Fig. 7.16 A numerical example of the step-like functions modeling the behavior of the system parameters according to their growth-factor concentrations (recall that L, the self-renewing parameter, is implicitely varying according to $L = 1 - K$).

Example 15. *Let us consider the following fixed biological parameters and functions:*

For the HSCs compartment: $\tau = 1.25$ *(actual cell-cycle duration),* $\delta = 0.14$ *(death rate),* $f(a) = \frac{me^{ma}}{e^{m\tau}-1}$ *(the mitosis function), where* $m = 10$*, and,* $\beta(\mathfrak{e}_2, R) = \frac{\beta(\mathfrak{e}_2,0)}{1+bR^n}$ *(the re-introduction function from resting to proliferating phases), where* $b = 1$*, and* $n = 4$*.*

For mature cells: $\mu = 0.05$ *(the degradation rate).*

We continue to refer to the parameters, of each subsystem of the overall system, that depend on growth factor concentrations by $\beta(0)$*,* γ *and* K*, instead of* $\beta(\mathfrak{e}_2,0)$*,* $\gamma(\mathfrak{e}_3)$ *and* $K(\mathfrak{e}_4)$*. In particular, here we want to investigate the case where the previously mentioned parameters vary, with respect to their corresponding growth-factor (or drug) concentrations, as described in Figure 7.16.*

Let us suppose that at $t = 0$ *the initial parameter values are:* $B^{(0)}(0) = 0.95$*,* $\gamma^{(0)} = 0.25$*, and,* $K^{(0)} = 0.08$*. We recall from Chapter 3 (or, [8, 225, 81]) that the strictly positive steady states* $R_e^{(0)}$ *(for HSCs) and* $M_e^{(0)}$ *(or, equivalently in this case,* $M_e^{(0,0,0)}$*),* ***when they exist****, satisfy:*

$$\begin{aligned} R_e^{(0)} &= \beta^{-1}\left(\frac{\delta}{2(1-K^{(0)})\int_0^\tau f(\ell)e^{-\gamma^{(0)}\ell}d\ell}\right), \\ M_e^{(0)} &= \frac{1}{\mu}\left(\frac{2K\beta^{(0)}(0)R_e^{(0)}}{1+b\left(R_e^{(0)}\right)^n}\int_0^\tau f(\ell)e^{-\gamma^{(0)}\ell}d\ell\right). \end{aligned} \tag{7.14}$$

After calculation, using the previous numerical values, we obtain: $M_e^{(0,0,0)} = 0.99054255$*.*

Now, we notice that moving from $M_e^{(0,0,0)}$ *to* $M_e^{(0,+1,0)}$ *requires one dose of one type of drug in order to decrease the apoptosis rate. Therefore, using the characteristics given in Figure 7.16 (the second one is for* $\mathfrak{e}_3 \to \gamma(\mathfrak{e}_3)$*), we observe that the previous action needs to decrease the apoptosis rate from* 0.25 *to* 0.2*. We recall that the overscript* $+1$ *in* $M_e^{(0,+1,0)}$ *means that we increase the value of the growth factor corresponding to the apoptosis rates, which consequently decreases the apoptosis since it has a negative feedback on that parameter. Then, after calculation, we get:* $M_e^{(0,+1,0)} = 0.93120333$*.*

On the other hand, let us observe for instance the transition $M_e^{(0,0,0)} \to M_e^{(+1,+1,+1)}$*, which means that all the controlled parameters are changing their initial values. Clearly, a combined-chemotherapy is required, and by definition a higher cost is set, due to the toxicity risks (Rule 3). In our numerical example, the transition of interest leads to the following parameters:* $\beta(0) = 1.25$*,* $\gamma = 0.2$*,* $K = 0.1$*. It follows that:* $M_e^{(+1,+1,+1)} = 1.34252268$*. Finally, we can observe that the transition* $M_e^{(0,0,0)} \to M_e^{(-1,+1,+1)}$*, which also commits a high cost, consists in moving model parameters to* $\beta(0) = 0.65$*,* $\gamma = 0.2$*, and,* $K = 0.1$*. This transition yields to:* $M_e^{(-1,+1,+1)} = 1.033486086$*.*

It should be noted that at this level, we give the values of the existing positive steady state but we do not check whether these equilibria are stable or not (it will be done in Section 7.6). But now, we are focusing on the previous obtained steady states and we are comparing how far away they are from the initial point $M^{(0,0,0)}$*. We notice clearly that the cost of the action from which a transition emerges is not proportional to the change in mature cell count (see the approximate representation* ***A****-Figure 7.17). This is of course a direct consequence of the equations in* (7.14)*. But recall that the requirements of the body*

and the aims of the drug therapy is to reach a stable cell count M^*. Therefore, the concept of distance towards the final desired steady state is important to be measured. Finally, let us consider for instance that the steady state $M_e^{(+1,+1,+1)}$ is close to M^* and satisfies the `Confidence_area` *condition, associated to the therapy objective. In other words, that means that -if this equilibrium point is stable- convergence to it is satisfactory for the therapy (Figure 7.17). Here we have explored a very small field of possibilities, and by expanding the network, some other M_e-values, corresponding to other triplet of parameters, can be discovered inside the* `Confidence_area`*, thus forming the set* `Goal` *of potential objectives.*

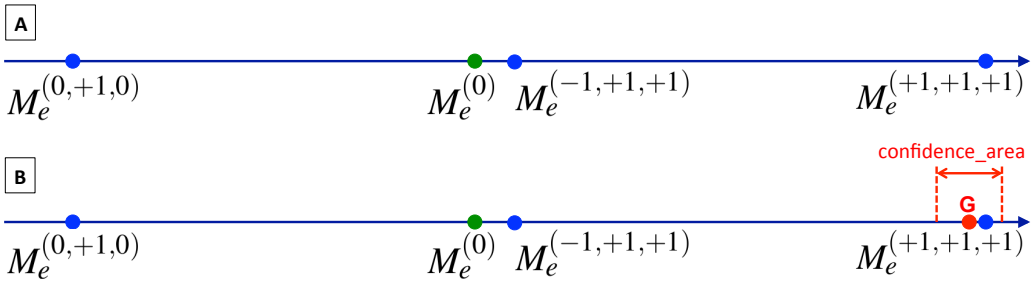

Fig. 7.17 Cartoon illustration - using approximate distances - of the positive steady states of Example 15.

Nevertheless, in the case where we consider that $M_e^{(+1,+1,+1)}$ is the unique objective, we notice that if all the nodes are stable, then the path:

$$M_e^{(0,0,0)} \to M_e^{(0,0,+1)} \to M_e^{(0,+1,+1)} \to M_e^{(+1,+1,+1)}, \tag{7.15}$$

is certainly ***the cheapest one****. We can see the similarity with the moving object, for which the cheapest path is the straight line, if it exists (i.e. no obstacle on this way). That is exactly what the heuristics serve for: estimating the cheapest paths, as discussed in the sequel.*

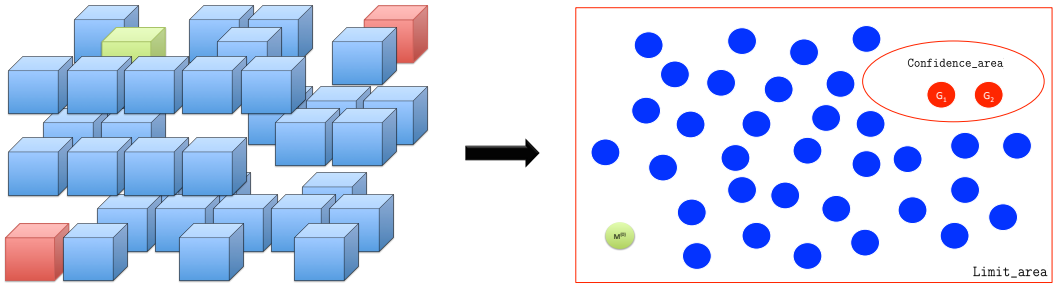

Fig. 7.18 On the left, an example of a 3D-representation of the hematopoietic network of 35 retained nodes in the $\beta(0)$-γ-K-space. In the right, the equivalent 2-D projection of the same hematopoietic network, presented in a suitable form that highlights the therapy objectives (`Confidence_area`, `Goal`, `Limit_area`). The connections between the nodes are not represented. We notice that the red nodes belonging to `Goal` in the right, are close to each other. However, nothing prevents the fact that their corresponding parameters are far from each other, as represented by red cubes on the left.

We conclude that our hematopoietic network have some particularities, when it is compared to classical applications of pathfinding algorithms. Specifically, we need to make a difference between:
i) on the one hand, the 3D-hematopoietic network represented according to its **switching parameters**, in the $\beta(0)$-γ-K-space.
i) and on the one hand, the **apparent objectives**, which are dependent on the measurements related to the **total density of mature cells and its features:** the nodes are the stable M_e points, the `Limit_area` defined for the mature cell density, the therapy objectives defined by the prescribed M^* density and its `Confidence_area` (which allow to determine the `Goal` set). All these elements are defined according to the distance separating the current nodes from the therapy-objective M^*, as illustrated in Figure 7.18- on the right.
To illustrate a typical situation that can be encountered in the hematopoietic network system, we can consider the case where two nodes belong to the `Goal` set[a], and we notice that actually they can be distant from each another in the parameter-space representation (see Figure 7.18 on the left).
Such a situation cannot occur in the example of the moving object. Indeed, if a `Confidence_area` is considered in that case, then any additional goal-square in Figure 7.13 will be in the neighborhood of the initial one in red (i.e. they are directly connected).
To summarize, we say that with the aim of prioritizing the representation that highlights our final objectives, we continue to use the representation in 2D-projection as in the Figure 7.18-on the right. However, for the implementation issues of the heuristic function (using A^*-like algorithm for instance), the 3D-representation on the left is fundamental.

[a] Both of them are close to M^* -in terms of distance- and satisfy the `Confidence_area` requirement (e.g. G_1 and G_2 in the Figure 7.18)

What can the heuristic function be in the hematopoietic network?

Let us begin by examining the fundamental definition of the heuristic function:

Definition 14. *At a node M_e, $H(M_e)$ is a **heuristic** that estimates the cost of the **cheapest** path from the node M_e to the considered objective node M^* (i.e. $M^* \in$ `Goal`).*

The concept of heuristics is problem-specific. For instance, in our application, the nonlinear relationship between the controlled parameters and the steady states (i.e. $\left(\beta(0),\gamma,K\right) \rightarrow M_e\left(\beta(0),\gamma,K\right)$), and the previously mentioned rules (Rules 1, 2,...,5) imply that even if the progress towards the objective (M^*) is measured by the difference between the cell total densities at M^* and a given node M_e in the network, it is an illusion to think that the *closest* point to M^* (in terms of blood cell count) has necessary the *cheapest cost* to reach the goal M^*. The previous idea has been illustrated and discussed above.

We conclude that, in the unhealthy case, the heuristic associated to any node $M_e^{\left(\texttt{attribute}_\beta,\texttt{attribute}_\gamma,\texttt{attribute}_K\right)}$ in the effective hematopoietic network which has $G \in$ `Goal` and $G^{\left(\texttt{attribute}_\beta^G,\texttt{attribute}_\gamma^G,\texttt{attribute}_K^G\right)}$, is

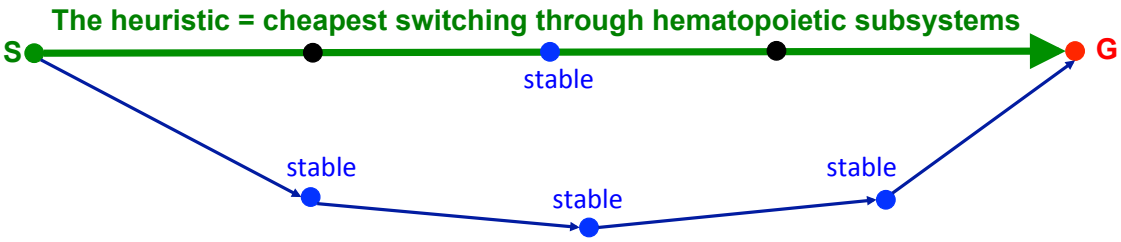

The inadmissible node ● can be:	The heuristic has to be:
• an **unstable** steady state • **non-existing** positive steady state • a point outside the `Limit_area`	• **Admissible:** It must always be lower or equal to the actual path. • **Consistent:** $H(N_1) \leq \text{cost}(N_1,N_2)+H(N_2)$

The **heuristic** does not depend on the distance between a node and the final destination **G**. However, the objective points **G** (belonging to the set `Goal`) are fully-determined through their distance from the prescribed reference M* and satisfy the `Confidence_area` requirement.

Fig. 7.19 In this representation, the *visually closest* points represent the *cheapest costs*, without having to consider the value of the mature cell steady states.

given by

$$\begin{aligned} H\left(M_e^{(\texttt{attribute}_\beta,\texttt{attribute}_\gamma,\texttt{attribute}_K)}\right) = &\frac{1}{\Delta_\beta}\left|\texttt{attribute}_\beta - \texttt{attribute}_\beta^G\right| \\ &+ \frac{1}{\Delta_\gamma}\left|\texttt{attribute}_\gamma - \texttt{attribute}_\gamma^G\right| \\ &+ \frac{1}{\Delta_K}\left|\texttt{attribute}_K - \texttt{attribute}_K^G\right|, \end{aligned} \tag{7.16}$$

where Δ_β, Δ_γ and Δ_K, are respectively the amplitudes of the one-step (an elementary switching) transition in the characteristic step-like patterns $\mathfrak{e}_2 \to \beta\,(\mathfrak{e}_2,0)$, $\mathfrak{e}_3 \to \gamma(\mathfrak{e}_3)$, and, $\mathfrak{e}_4 \to K\,(\mathfrak{e}_4)$. For example, in Figure 7.16, we have $\Delta_\beta = 0.3$, $\Delta_\gamma = 0.05$, and, $\Delta_K = 0.02$.

Now, more details about the implementation issues, where we establish the suitable pseudocodes that describe our techniques, are discussed in Appendix A. That is an adaptation of classical algorithms (such as A*) to our hematopoietic system network. In Appendix A, we particularly focus on the important case of unhealthy hematopoiesis (Algorithm 1, Appendix A), and we discuss also briefly the healthy one. In the next section we provide a numerical illustration.

7.6 Concluding illustrations on the time-delay overall system

This is a first work where we introduce some concepts related to planning and scheduling of regulating strategies in biological contexts. Other works in this direction and others will follow, and we mention particularly that more recent algorithms (such that the D^*) can be employed in the study of the healthy hematopoiesis, for tracking a moving blood cell reference. At the end of this section, we will also mention the interesting case of coupled models between healthy and mutated cells (studied in Part II - Chapter 6).

In this concluding section, we give a numerical illustration that merge all the previously mentioned parts. More precisely, here we combine:

❶ **The dynamics of cell-populations:** The PDE-system (Section 7.4.1), governing the dynamics of hematopoietic stem cells (HSCs) and mature cells. Then, the nonlinear system with distributed delay terms where proliferation, apoptosis, differentiation and self-renewing processes are growth-factor dependent (Section 7.4.2). More precisely, we consider for cell-population dynamics the model given in Table 7.1, where three different growth factors are acting on $\big(\beta(0),\gamma,K\big)$.

❷ **The dynamics of growth-factor concentrations and their effect on cell-dynamics model parameters:** The general growth-factor features are discussed in Section 7.3, and their dynamics are described by (7.2). In the unhealthy case, drugs doses are assumed to act as growth factors. The key feature is the event-triggered property that growth-factors or drugs exert on the model parameters. In the following numerical example, we consider the characteristic patterns (step-like functions) giving the variations of the model parameters with respect to their respective drugs/growth-factor concentrations as in Figure 7.16.

❸ **The switching law defining the stabilization technique:** Given a reference M^* (associated with its `Confidence_area`), which in fact specifies the desired total density of mature blood cells, Algorithm 1 reveals which path (i.e. a succession of subsystems[a]) is optimal to be undertaken in order to achieve the best therapeutic strategy.

[a] From that information, we deduce the suitable step-like functions of the growth-factors with respect to *time*, that yields to the desired switching series, as illustrated in the sequel.

The fixed-parameter system that we consider here are those given in Example 15:

For HSCs: $\tau = 1.25$ (*actual* cell-cycle duration), $\delta = 0.14$ (death rate), $f(a) = \frac{me^{ma}}{e^{m\tau}-1}$ where $m = 10$ (mitosis function), $\beta(\mathfrak{e}_2,R) = \frac{\beta(\mathfrak{e}_2,0)}{1+bR^n}$ (the re-introduction function from resting to proliferating phases), where $b = 1$, $n = 4$.

Finally, the degradation rate of mature cells is $\mu = 0.05$.

Next, using all the possible combinations of the switching parameters given by Figure 7.16, we define 1000 possible hematopoietic subsystem constituting the overall system presented in Table 7.1. However, for half of them the condition of existence of the positive steady state is not verified. Furthermore, only 59 subsystems have a positive steady state that satisfies the exponential stability condition of Chapter 3.

We set `Limit_area` $= 5$ (a normalized value for the total density of mature cells). It follows that the resulting network contains 51 hematopoietic subsystems (the nodes are the positive steady state of each system), i.e. $\texttt{length}\big(\mathscr{M}_{eff}\big) = 51$.

In order to show how the values of the steady states of the total density of mature cells (M_e) spread, we give the following 1D-plot of the 51 points.

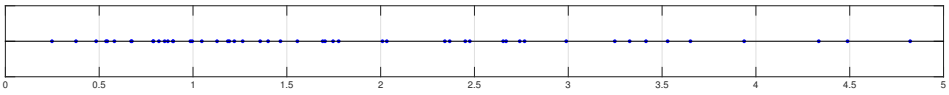

Fig. 7.20 The distribution of the 51 stable steady states, which are inside the `Limit_area` $= (0,5]$.

It suits us to consider some more constraints on the problem in order to reduce the number of nodes in the studied network. We consider that due to the presence of superimposed severe epigenetic mutations [137], it is expected that the drug has only a limited leverage to change the $\beta(0)$-parameter. Then, we can assume, without loss of generality, that this parameter β can vary only between 0.95 and 2.15. It follows that the number of nodes in the network is reduced to 22, i.e. $\texttt{length}\left(\mathscr{M}_{eff}\right) = 22$. However, it is worth mentioning that the complete-type case involving 51 nodes can be addressed exactly in the same way, but detailing it will make the section too long without significant benefits.

Nodes	$\beta(0)$	γ	K	M_e	$M_e^{(0)}$	`Goal` candidates $(M^* \pm 0.5)$
1	0.95	0.40	0.06	0.81808465	✓	
2	0.95	0.40	0.08	0.98614342		
3	0.95	0.35	0.12	1.70355101		
4	0.95	0.35	0.14	1.35798982		
5	0.95	0.30	0.16	2.45099792		
6	0.95	0.30	0.18	2.47511923		
7	0.95	0.25	0.20	3.24792752		
8	0.95	0.25	0.22	3.41423221		
9	1.25	0.45	0.06	0.89302665		
10	1.25	0.40	0.10	1.77626758		
11	1.25	0.35	0.14	2.66862097		
12	1.25	0.35	0.16	2.76695795		
13	1.25	0.30	0.20	3.93743744		
14	1.55	0.45	0.06	1.26462747		
15	1.55	0.45	0.08	1.46594557		
16	1.55	0.40	0.12	2.65308368		
17	1.55	0.35	0.18	3.65098593		
18	1.85	0.45	0.08	2.00965592		
19	1.85	0.40	0.14	3.52953970		
20	1.85	0.30	0.24	4.48839554		✓
21	2.15	0.45	0.10	2.74132806		
22	2.15	0.40	0.14	4.33497547		✓

Table 7.5 The 22 nodes constituing the vector $\mathscr{M}_{eff}$, with their $\beta(0)$-γ-K coordinates. The nodes number 20 and 22 satisfy the `Confidence_area` requirement and thereby are potential therapy objectives.

Remark 47. *if we do not limit the values of $\beta(0)$ to those given in Table 7.5 (i.e., if we consider the* 51 *possible steady states), then a third stable steady state M_e exists in* `Goal`*, having the triplet: $\beta(0) = 2.45$, $\gamma = 0.4$ and $K = 0.16$.*

According to Table (7.5), we set the network system representation (Figure 7.21) corresponding to our overall hematopoietic system.

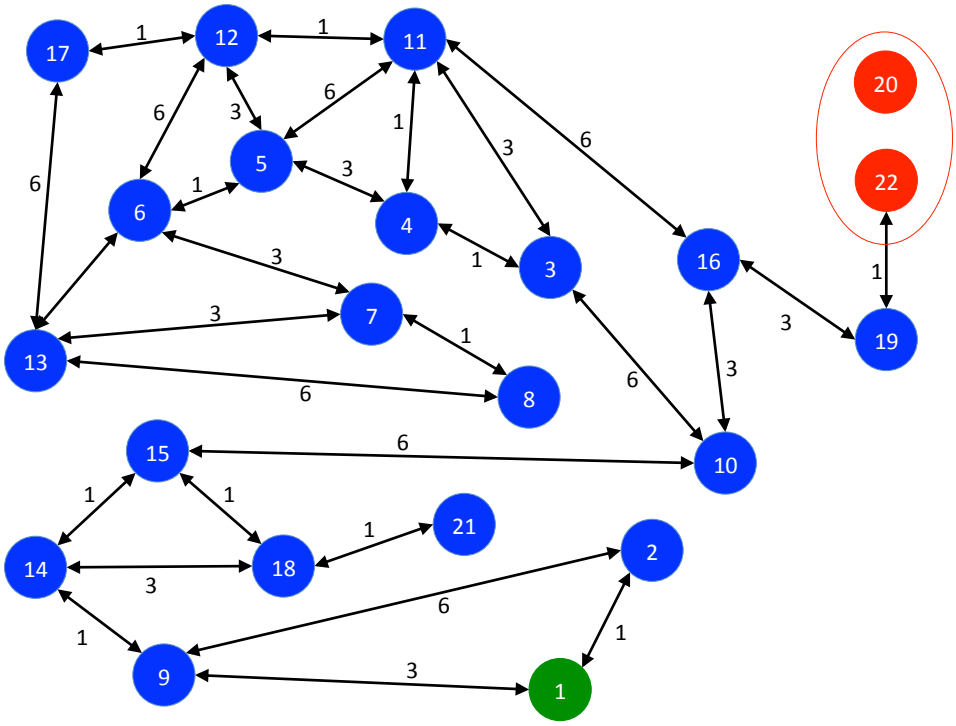

Fig. 7.21 The hematopoetic network corresponding to the example of Table 7.5.

In the `Confidence_area`, only the 22th node is reachable. According to its `attributes` (i.e. coordinates) the heuristic is computed. The results are given in Table 7.6.

Using Table 7.6 and the costs of the edges in Figure 7.21, we easily determine the optimal path from the node initial node to the objective. Indeed, the strategy in this case is given by:

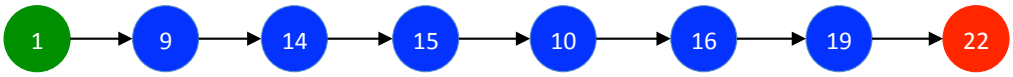

That strategy corresponds exactly to the model parameter evolution in Figure 7.22.

Nodes	$\beta(0)$	γ	K	M_e	$M_e^{(0)}$	`Goal`	Heuristic
1	0.95	0.40	0.06	0.81808465	✓		8
2	0.95	0.40	0.08	0.98614342			7
3	0.95	0.35	0.12	1.70355101			6
4	0.95	0.35	0.14	1.35798982			5
5	0.95	0.30	0.16	2.45099792			7
6	0.95	0.30	0.18	2.47511923			8
7	0.95	0.25	0.20	3.24792752			10
8	0.95	0.25	0.22	3.41423221			11
9	1.25	0.45	0.06	0.89302665			8
10	1.25	0.40	0.10	1.77626758			5
11	1.25	0.35	0.14	2.66862097			4
12	1.25	0.35	0.16	2.76695795			5
13	1.25	0.30	0.20	3.93743744			8
14	1.55	0.45	0.06	1.26462747			7
15	1.55	0.45	0.08	1.46594557			6
16	1.55	0.40	0.12	2.65308368			3
17	1.55	0.35	0.18	3.65098593			5
18	1.85	0.45	0.08	2.00965592			5
19	1.85	0.40	0.14	3.52953970			1
20	1.85	0.30	0.24	4.48839554			8
21	2.15	0.45	0.10	2.74132806			3
22	2.15	0.40	0.14	4.33497547		✓	0

Table 7.6 Nodes, switching parameters, and heuristic measures.

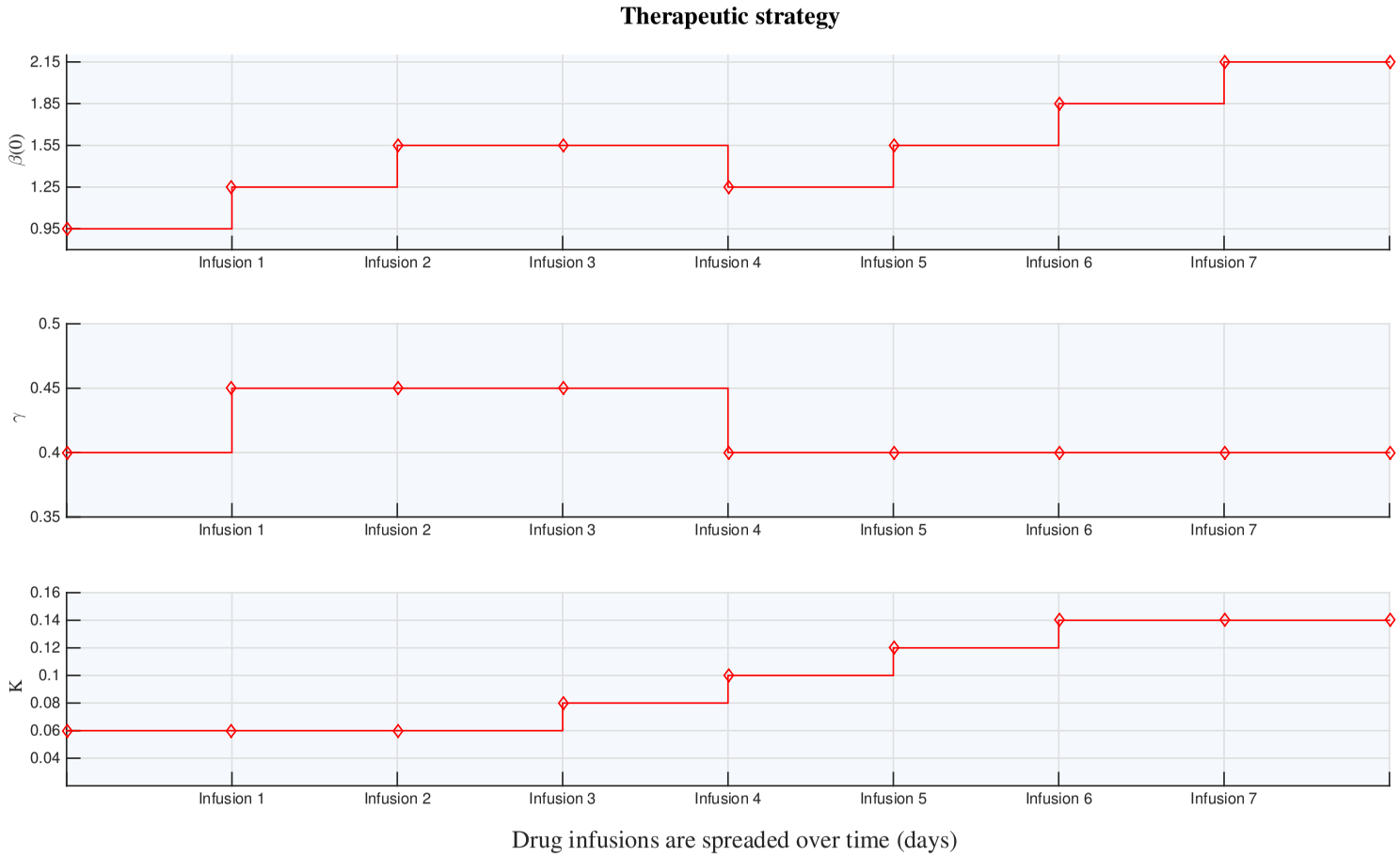

Fig. 7.22 The desired therapeutic strategy in order to achieve an optimal stabilization of the studied hematopoietic overall system, towards the favorable steady state M^*. Therefore, drugs must be infused at each switching-time so that the desired behavior is obtained.

Now we are interested in the time-delay system (Table 7.1) behavior when its parameters are switching through a series of therapeutic drug infusions, following the defined strategy (Figure 7.22). We want to observe the dynamics of HSCs and the total density of mature cells. For that, we need to choose the duration of treatment and the accurate instants for drug infusions (i.e. how infusions are spread over time in Figure 7.22). First, let us select -theoretically- an excessively long-term treatment duration. This allows us to observe the behavior on each node, i.e. each subsystem is activated for sufficient long time in order to check its asymptotic behavior. Therefore, we select $t_{s1} = 200$, $t_{s2} = 400$, $t_{s3} = 600$, $t_{s4} = 800$, $t_{s5} = 1000$, $t_{s6} = 1200$, $t_{s7} = 1400$, where t_{si} is the switching-day corresponding to the i-th infusion. The resulting trajectories are shown in Figure 7.23.

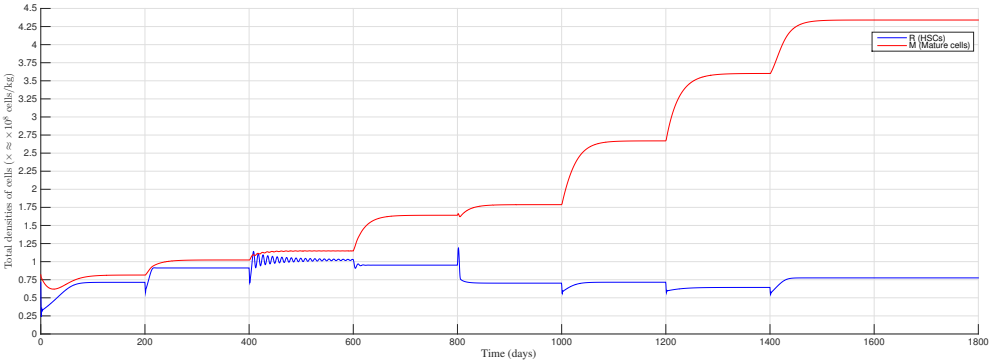

Fig. 7.23 Trajectories of the nonlinear system with distributed delays (Table 7.1), when applying the established therapeutic strategy. The switching-days are sufficiently far apart to allow each of the activated subsystem to show its long-time behavior.

The second switching-days selection is more realistic. Indeed, we consider that the therapy starts at $t_{s1} = 50$, then $t_{s2} = 57$, $t_{s3} = 64$, $t_{s4} = 71$, $t_{s5} = 78$, $t_{s6} = 95$, and finally, $t_{s7} = 102$, i.e. one week between each two successive drugs infusions. The trajectories in that case are illustrated in the Figure 7.24.

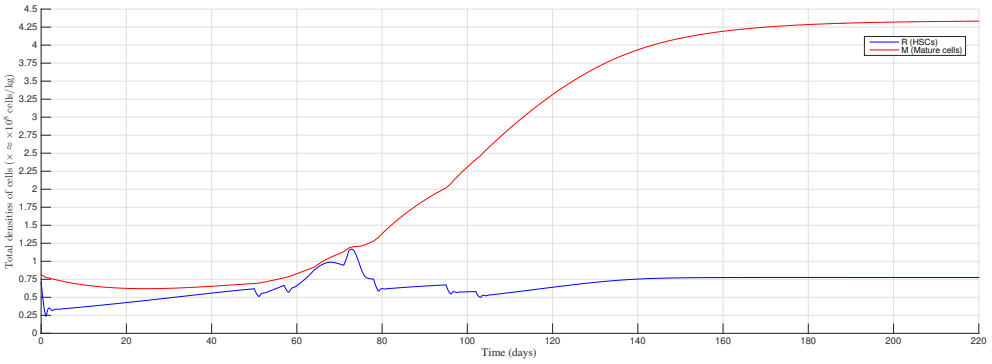

Fig. 7.24 Trajectories of the nonlinear system with distributed delays (Table 7.1), when applying the established therapeutic strategy, where drug infusions are spread over intervals of one week.

One notices that in the case of Figure 7.24, the condition on the dwell-time $\mathfrak{h} > \tau$ (the actual cell-cycle here is nearly one day), discussed in the Sections 7.4.3-7.4.4, is satisfied. However, we observe that even if the latter requirement does not hold, the trajectories are correctly behaving. That point is illustrated

in the last simulation, where we consider that the seven switching-times occur during the length of one distributed delay term. More precisely, we consider that the therapy starts at $t_{s1} = 100$, then $t_{s2} = 100.2$, $t_{s3} = 100.4$, $t_{s4} = 100.6$, $t_{s5} = 100.8$, $t_{s6} = 101$, and, $t_{s7} = 101.2$, while $\tau = 1.25$ in this example. The trajectories in this case are those illustrated in Figure 7.25. The latter case remains of course a theoretical and unrealistic one, because a high toxicity results from such a treatment over a very short period of time.

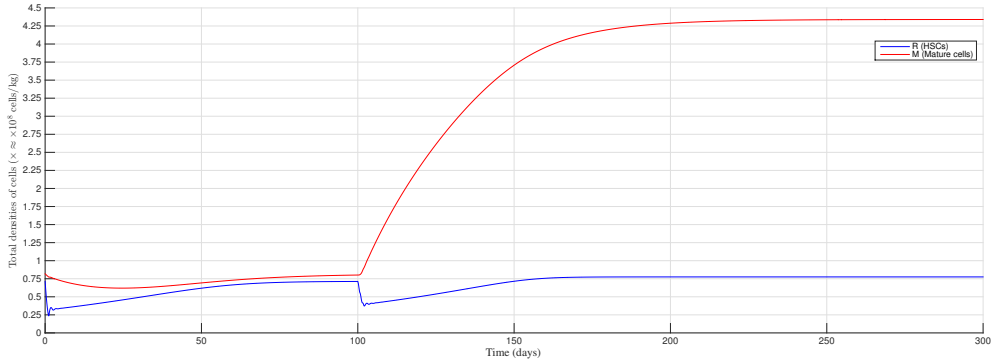

Fig. 7.25 Trajectories of the nonlinear system with distributed delays (Table 7.1), when applying the established therapeutic strategy. In this case, the time between the drug infusions is abnormally very short.

We conclude this last section by evoking an interesting perspective of this work. Our next main focus is to extend both the modeling, the stability/stabilization analysis techniques -together with the use of the search algorithms- to study the case of coupled models (see Figure 7.26). These are models that describe the cohabitation between healthy and cancerous cells, or between healthy and mutated cells from which cancer may emerge. Our idea is as follows:
On the one hand, we notice that the recent anti-cancer drugs contain more and more receptors that allow these molecules to target cancer cells, most of the time. However, a minority of healthy cells is affected by these drugs. On the other hand, abnormal cells that express several mutations, are not completely insensitive to the immune response of the body and its secretions. In conclusion, our next objective is to provide a theoretical framework to study the non-negligible mutual effect between healthy and unhealthy cells. In particular, by enriching the basis of rules as discussed, separately for healthy and unhealthy cases in this work, we aim to provide effective therapeutic strategies for coupled model, that target the unhealthy cells while causing the minimum damage on healthy cells.

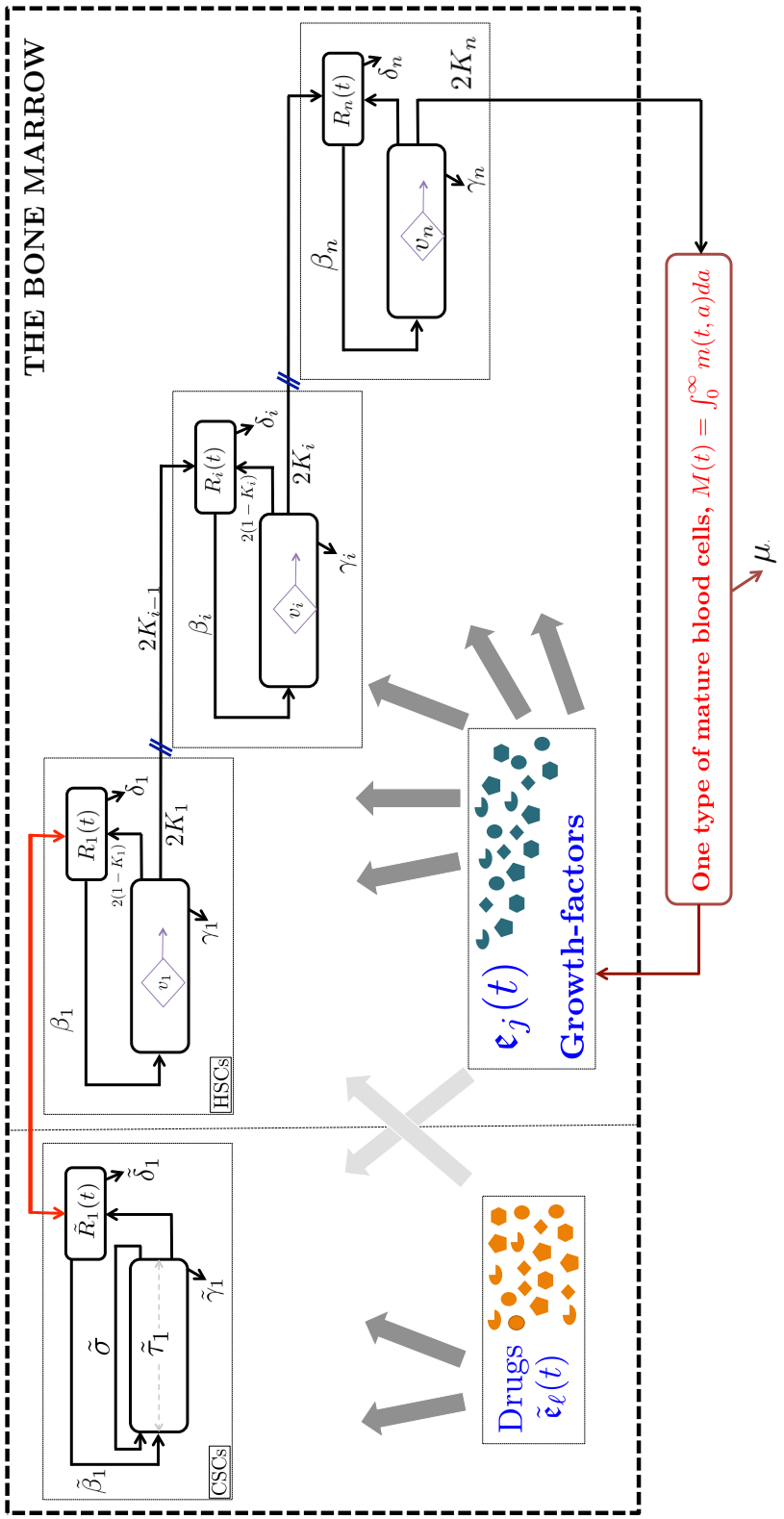

Fig. 7.26 In the coupled model as we conceive it, the drugs are targeting the unhealthy cells thanks to an overexpression of specific receptors (dark arrow). However, some healthy cells can be attacked (light arrow, meaning that the effect is less important). Similarly, the growth-factors act more on healthy cells (dark arrow), but they have a non-negligible effect on unhealthy mutated cells (light arrow).

Conclusion and perspectives

At the end of this dissertation, we want to summarize some key facts in few words. Firstly, understanding cell dynamics and maturation, stem-cell fates, stemness and cancer, is a highly challenging issue that requires strong involvement in theory and practice. In this regard, we wanted to strengthen the analysis theory and take into account the recent medical observations in this field. Thus, efforts have been made to bring back as far as possible some analysis and simulation tools into biology, as well as some biologic concepts into modeling and analysis. From this perspective, we have worked on the analysis of nonlinear delayed biological systems in the time-domain framework, through Lyapunov-like approaches. We mention again that Lyapunov theory has not been widely employed, in the past, in the analysis of the type of models that we emphasized throughout the thesis. Thus, we have been able to diversify and extend some stability analysis aspects[17] through the development of several Lyapunov functional constructions, and we had also brought back some planning algorithms for the interest of the biological application. Similarly, we have emphasized in this thesis the most recent biological evidences to further motivate the mathematical analysis and update models of cell dynamics that we use. In this spirit, we introduced and investigated throughout this work some concepts as: the CSCs-paradigm in a model of cohabitation between mutated cells and ordinary stem cells in their niches, the cell-cycle arrest and cell-plasticity features, as well as emerged chemotherapy treatment of leukemia. Far from being solved, these biological issues remain of paramount interest in future works, both in biologic/medical research and in mathematical modeling, as well as for analysis and simulations techniques.

At this point, we can pay tribute to pioneer and current contributors in the field of modeling of blood cell dynamics (see the review article [240]). Many issues have been addressed during the past five decades by several authors (e.g. Mackey and Adimy), particularly in the case of cyclic blood diseases. To use the wording of Mackey [182], successes of mathematical biology are significant but not growing as fast as it ought to be. One of the recurrent reason is that there still have some barriers to communication between disciplines, but also because there are a lack of corresponding data for stem cells and their progeny [101].

In this thesis, we provided a consistent modeling framework that follows recent medical observations, especially oriented towards overproliferating hematological malignancies from our hematologist collaborators[18]. Our findings, provided through the stability analysis of the resulting models, have been interpreted in the typical case of acute myeloid leukemia (e.g. the last section in Chapter 6).

[17] Analysis of nonlinear systems with finite or infinite distributed delays, possibly with time-varying or switching parameters, analysis of differential-difference coupled systems, exponential stability with estimate of decay rates of solutions, regions of attraction of steady states in nonlinear systems, analysis through positivity and comparative system approaches, robustness, etc).

[18] François Delhommeau and Pierre Hirsch, which are with Groupe de Recherche Clinique sur les Myéloproliferations Aïgues et Chronique, Hôpital Saint-Antoine, Laboratoire d'Hématologie, Paris, France.

In our surroundings, projects are going ahead for the identification of the parameters involved in acute myeloid leukemia. Experiments on fresh blood samples of patients with hyperleukocytosis may allow to identify the apoptosis rate and differentiation rate, however, there is no immediate prospect for estimating the proliferation function β, or the cell-plasticity mechanisms ω_i and ξ_i (Chapter 4).

At the time being, dedifferentiation is admitted as a fully existing biological process, and its possible relation with cancer is often highlighted. However, the current quantitative knowledge on cell-plasticity does not seem sufficient to either arbitrate on cancer origins[19] nor identify the form of dedifferentiation functions in this context. Similarly, data related to how pervasive cancer dormancy is, are not easily traceable. This is mainly due to clinical manifestation of cancer, since generally it becomes detectable only beyond a certain threshold of cancer cell density or tumor size.

Cancer dormancy and cancer plasticity require better understanding, and much remain to be done in biological and mathematical research communities. This is our main line of research in the immediate future. In particular, the study of a coupled model between healthy SCs and CSCs (as in Chapter 6), taking into account several maturity stages with growth-factor dependent functions (as in Chapter 7), along with a dedifferentiation mechanism from cancer (differentiated) cells into the CSCs compartment (as in Chapter 4), would be an interesting case for studying the rise of cancer, since it combines the two hypotheses about CSCs origin. Many other issues remain to be thoroughly investigated, including a more rigorous stability analysis of switching and event-triggering processes that we introduced for cell population dynamical with growth factor dependent parameters (Chapter 7).

Finally we mention that the emergent medical projects which are patient oriented in early leukemic develoment stages offer rich perspectives in terms of disease modelling. The challenge is to predict at first diagnosis the best therapeutic schedule for each patient. This requires to develop models which integrate not only genetic but also epigenetic information and allow the classification of patients into different classes with similar disease evolution and similar response to treatments.

[19] Do cancer stem cells (CSCs) emerge through dedifferentiation of more mature mutated cells, or from abnormalities that occur in the population of stem cells itself? Both hypothesis are investigated.

References

[1] Adam, J. and Bellomo, N. (2012). *A survey of models for tumor-immune system dynamics*. Springer Science & Business Media.

[2] Adimy, M., Angulo, O., Crauste, F., and López-Marcos, J. C. (2008a). Numerical integration of a mathematical model of hematopoietic stem cell dynamics. *Computers & Mathematics with Applications*, 56(3):594–606.

[3] Adimy, M., Bourfia, Y., Hbid, M. L., and Marquet, C. (2016). Age-structured model of hematopoiesis dynamics with growth factor-dependent coefficients. *Electronic Journal of Differential Equations*, page 140.

[4] Adimy, M., Chekroun, A., and Touaoula, T.-M. (2015). Age-structured and delay differential-difference model of hematopoietic stem cell dynamics. *Discrete and Continuous Dynamical Systems-Series B*, 20(9):27.

[5] Adimy, M. and Crauste, F. (2005). Existence, positivity and stability for a nonlinear model of cellular proliferation. *Nonlinear Analysis: Real World Applications*, 6(2):337–366.

[6] Adimy, M. and Crauste, F. (2007). Modelling and asymptotic stability of a growth factor-dependent stem cells dynamics model with distributed delay. *Discrete and Continuous Dynamical Systems-Series B*, 8(1):19–38.

[7] Adimy, M. and Crauste, F. (2009). Mathematical model of hematopoiesis dynamics with growth factor-dependent apoptosis and proliferation regulations. *Mathematical and Computer Modelling*, 49(11):2128–2137.

[8] Adimy, M., Crauste, F., and El Abdllaoui, A. (2008b). Discrete-maturity structured model of cell differentiation with applications to acute myelogenous leukemia. *Journal of Biological Systems*, 16(03):395–424.

[9] Adimy, M., Crauste, F., and El Abdllaoui, A. (2010). Boundedness and lyapunov function for a nonlinear system of hematopoietic stem cell dynamics. *Comptes Rendus Mathematique*, 348(7):373–377.

[10] Adimy, M., Crauste, F., and Pujo-Menjouet, L. (2009). On the stability of a maturity structured model of cellular proliferation. *arXiv preprint arXiv:0904.2492*.

[11] Adimy, M., Crauste, F., and Ruan, S. (2005). A mathematical study of the hematopoiesis process with applications to chronic myelogenous leukemia. *SIAM Journal on Applied Mathematics*, 65(4):1328–1352.

[12] Adimy, M., Crauste, F., and Ruan, S. (2006a). Modelling hematopoiesis mediated by growth factors with applications to periodic hematological diseases. *Bulletin of mathematical biology*, 68(8):2321–2351.

[13] Adimy, M., Crauste, F., and Ruan, S. (2006b). Periodic oscillations in leukopoiesis models with two delays. *Journal of Theoretical Biology*, 242(2):288–299.

[14] Aguirre-Ghiso, J. A. (2006). The problem of cancer dormancy: understanding the basic mechanisms and identifying therapeutic opportunities.

[15] Aguirre-Ghiso, J. A. (2007). Models, mechanisms and clinical evidence for cancer dormancy. *Nature Reviews Cancer*, 7(11):834–846.

[16] Ahmed-Ali, T., Karafyllis, I., Krstic, M., and Lamnabhi-Lagarrigue, F. (2016). Robust stabilization of nonlinear globally lipschitz delay systems. In *Recent Results on Nonlinear Delay Control Systems*, pages 43–60. Springer.

[17] Ahsen, M. E., Özbay, H., and Niculescu, S.-I. (2015). *Analysis of deterministic cyclic gene regulatory network models with delays*. Birkhäuser.

[18] Al-Asadi, M. G., Castellanos, M., May, S. T., Russell, N. H., Seedhouse, C. H., and Pallis, M. (2016). Molecular signature of dormancy in cd34+ cd38-acute myeloid leukaemia cells.

[19] Allman, E. S. and Rhodes, J. A. (2004). *Mathematical models in biology: an introduction*. Cambridge University Press.

[20] Andersen, L. K. and Mackey, M. C. (2001). Resonance in periodic chemotherapy: a case study of acute myelogenous leukemia. *Journal of theoretical biology*, 209(1):113–130.

[21] Arino, O. (1995). A survey of structured cell population dynamics. *Acta Biotheoretica*, 43(1):3–25.

[22] Auger, P., Magal, P., and Ruan, S. (2008). *Structured population models in biology and epidemiology*, volume 1936. Springer.

[23] Avila, J., Bonnet, C., Özbay, H., Clairambault, J., Niculescu, S., Hirsch, P., and Delhommeau, F. (2014a). A coupled model for healthy and cancerous cells dynamics in acute myeloid leukemia. *IFAC Proceedings Volumes*, 47(3):7529–7534.

[24] Avila, J. L., Bonnet, C., Clairambault, J., Özbay, H., Niculescu, S.-I., Merhi, F., Ballesta, A., Tang, R., and Marie, J.-P. (2014b). Analysis of a new model of cell population dynamics in acute myeloid leukemia. In *Delay Systems*, pages 315–328. Springer.

[25] Avila, J. L., Bonnet, C., Clairambault, J., Özbay, H., Niculescu, S.-I., Merhi, F., Tang, R., and Marie, J.-P. (2012). A new model of cell dynamics in acute myeloid leukemia involving distributed delays. *IFAC Proceedings Volumes*, 45(14):55–60.

[26] Avila Alonso, J. L. (2014). *Leucémie aiguë myéoblastique: modélisation et analyse de stabilité*. PhD thesis, Paris 11.

[27] Ballesta, A. and Clairambault, J. (2014). Physiologically based mathematical models to optimize therapies against metastatic colorectal cancer: a mini-review. *Current pharmaceutical design*, 20(1):37–48.

[28] Bao, S., Wu, Q., McLendon, R. E., Hao, Y., Shi, Q., Hjelmeland, A. B., Dewhirst, M. W., Bigner, D. D., and Rich, J. N. (2006). Glioma stem cells promote radioresistance by preferential activation of the dna damage response. *Nature*, 444(7120):756.

[29] Basak, U., Dutta, A., Dutta Chowdhury, D., Bhattacharya, A., Banerjee, S., Khan, P., et al. (2017). Deciphering the cancer puzzle: Cancer stem cells being the pivotal piece. *J Stem Cell Res Transplant*, 4(1):1025.

[30] Bekiaris-Liberis, N. and Krstic, M. (2013). *Nonlinear control under nonconstant delays*. SIAM.

[31] Bélair, J., Mackey, M. C., and Mahaffy, J. M. (1995). Age-structured and two-delay models for erythropoiesis. *Mathematical biosciences*, 128(1):317–346.

[32] Bellman, R. E. and Cooke, K. L. (1963). Differential-difference equations.

[33] Bellomo, N. and Forni, G. (1994). Dynamics of tumor interaction with the host immune system. *Mathematical and computer modelling*, 20(1):107–122.

[34] Bennett, J. M., Catovsky, D., Daniel, M.-T., Flandrin, G., Galton, D. A., Gralnick, H. R., and Sultan, C. (1976). Proposals for the classification of the acute leukaemias french-american-british (fab) co-operative group. *British journal of haematology*, 33(4):451–458.

[35] Beretta, E. and Takeuchi, Y. (1995). Global stability of an sir epidemic model with time delays. *Journal of mathematical biology*, 33(3):250–260.

[36] Berman, A. and Plemmons, R. J. (1994). *Nonnegative matrices in the mathematical sciences*. SIAM.

[37] Bernard, S., Bélair, J., and Mackey, M. C. (2003). Oscillations in cyclical neutropenia: new evidence based on mathematical modeling. *Journal of theoretical biology*, 223(3):283–298.

[38] Bernard, S., Bernard, B. Č., Lévi, F., and Herzel, H. (2010). Tumor growth rate determines the timing of optimal chronomodulated treatment schedules. *PLoS Comput Biol*, 6(3):e1000712.

[39] Billy, F., Clairambault, J., Delaunay, F., Feillet, C., and Robert, N. (2012). Age-structured cell population model to study the influence of growth factors on cell cycle dynamics. *Mathematical Biosciences and Engineering*, page xx.

[40] Birbrair, A. and Frenette, P. S. (2016). Niche heterogeneity in the bone marrow. *Annals of the New York Academy of Sciences*, 1370(1):82–96.

[41] Blau, H. M., Brazelton, T., and Weimann, J. (2001). The evolving concept of a stem cell: entity or function? *Cell*, 105(7):829–841.

[42] Bonnet, D. and Dick, J. E. (1997). Human acute myeloid leukemia is organized as a hierarchy that originates from a primitive hematopoietic cell. *Nature medicine*, 3(7):730–737.

[43] Boyd, S., El Ghaoui, L., Feron, E., and Balakrishnan, V. (1994). *Linear matrix inequalities in system and control theory*. SIAM.

[44] Brahmer, J. R. and Pardoll, D. M. (2013). Immune checkpoint inhibitors: making immunotherapy a reality for the treatment of lung cancer. *Cancer immunology research*, 1(2):85–91.

[45] Brandwein, J. M. (2015). Targeting polo-like kinase 1 in acute myeloid leukemia. *Therapeutic advances in hematology*, 6(2):80–87.

[46] Brikci, F. B., Clairambault, J., and Perthame, B. (2008a). Analysis of a molecular structured population model with possible polynomial growth for the cell division cycle. *Mathematical and Computer Modelling*, 47(7):699–713.

[47] Brikci, F. B., Clairambault, J., Ribba, B., and Perthame, B. (2008b). An age-and-cyclin-structured cell population model for healthy and tumoral tissues. *Journal of mathematical biology*, 57(1):91–110.

[48] Brodal, P. (2004). *The central nervous system: structure and function*. Oxford University Press.

[49] Burns, F. and Tannock, I. (1970). On the existence of a go-phase in the cell cycle. *Cell Proliferation*, 3(4):321–334.

[50] Busłowicz, M. (2010). Robust stability of positive continuous-time linear systems with delays. *International Journal of Applied Mathematics and Computer Science*, 20(4):665–670.

[51] Cacace, F., Germani, A., Manes, C., and Setola, R. (2012). A new approach to the internally positive representation of linear mimo systems. *IEEE Transactions on Automatic Control*, 57(1):119–134.

[52] Cai, S., Fu, X., and Sheng, Z. (2007). Dedifferentiation: a new approach in stem cell research. *Bioscience*, 57(8):655–662.

[53] Castillo, R. E. and Rafeiro, H. (2016). *An introductory course in Lebesgue spaces*. Springer.

[54] Chaffer, C. L., Brueckmann, I., Scheel, C., Kaestli, A. J., Wiggins, P. A., Rodrigues, L. O., Brooks, M., Reinhardt, F., Su, Y., Polyak, K., et al. (2011). Normal and neoplastic nonstem cells can spontaneously convert to a stem-like state. *Proceedings of the National Academy of Sciences*, 108(19):7950–7955.

[55] Chaplygin, S. (1950). A new method of approximate integration of differential equations. *GITTL, Moscow–Leningrad*, 1(950):3–1.

[56] Chekroun, A. (2016). *Contribution à l'analyse mathématique d'équations aux dérivées partielles structurées en âge et en espace modélisant une dynamique de population cellulaire*. PhD thesis, Université Claude Bernard Lyon 1.

[57] Clairambault, J. (2009). Modelling physiological and pharmacological control on cell proliferation to optimise cancer treatments. *Mathematical Modelling of Natural Phenomena*, 4(3):12–67.

[58] Clairambault, J. (2011). Optimizing cancer pharmacotherapeutics using mathematical modeling and a systems biology approach. *Personalized Medicine*, 8(3):271–286.

[59] Clairambault, J. (2014). Deterministic mathematical modelling for cancer chronotherapeutics: Cell population dynamics and treatment optimization. In *Mathematical Oncology 2013*, pages 265–294. Springer.

[60] Clairambault, J. and Fercoq, O. (2012). Physiologically structured cell population dynamic models with applications to combined drug delivery optimisation in oncology.

[61] Clark, S. C. and Kamen, R. (1987). The human hematopoietic colony-stimulating factors. *Science*, 236(4806):1229–1237.

[62] Clarke, F. (2013). *Functional analysis, calculus of variations and optimal control*, volume 264. Springer Science & Business Media.

[63] Clevers, H. (2011). The cancer stem cell: premises, promises and challenges. *Nature medicine*, pages 313–319.

[64] Cobaleda, C., Jochum, W., and Busslinger, M. (2007). Conversion of mature b cells into t cells by dedifferentiation to uncommitted progenitors. *Nature*, 449(7161):473–477.

[65] Cohen, J. E. (2004). Mathematics is biology's next microscope, only better; biology is mathematics' next physics, only better. *PLoS biology*, 2(12):e439.

[66] Colijn, C. and Mackey, M. C. (2005). A mathematical model of hematopoiesis: Ii. cyclical neutropenia. *Journal of theoretical biology*, 237(2):133–146.

[67] Cooper, S. (2003). Reappraisal of serum starvation, the restriction point, g0, and g1 phase arrest points. *The FASEB journal*, 17(3):333–340.

[68] Cozzio, A., Passegué, E., Ayton, P. M., Karsunky, H., Cleary, M. L., and Weissman, I. L. (2003). Similar mll-associated leukemias arising from self-renewing stem cells and short-lived myeloid progenitors. *Genes & development*, 17(24):3029–3035.

[69] Crane, G. M., Jeffery, E., and Morrison, S. J. (2017). Adult haematopoietic stem cell niches. *Nature Reviews Immunology*.

[70] Dahan, P., Gala, J. M., Delmas, C., Monferran, S., Malric, L., Zentkowski, D., Lubrano, V., Toulas, C., Moyal, E. C.-J., and Lemarie, A. (2014). Ionizing radiations sustain glioblastoma cell dedifferentiation to a stem-like phenotype through survivin: possible involvement in radioresistance. *Cell death & disease*, 5(11):e1543.

[71] Dale, D. C. and Mackey, M. C. (2015). Understanding, treating and avoiding hematological disease: Better medicine through mathematics? *Bulletin of mathematical biology*, 77(5):739–757.

[72] Dalerba, P., Cho, R. W., and Clarke, M. F. (2007). Cancer stem cells: models and concepts. *Annu. Rev. Med.*, 58:267–284.

[73] Daley, G. (2008). Common themes of dedifferentiation in somatic cell reprogramming and cancer. In *Cold Spring Harbor symposia on quantitative biology*, pages sqb–2008. Cold Spring Harbor Laboratory Press.

[74] Delhommeau, F., Dupont, S., Valle, V. D., James, C., Trannoy, S., Massé, A., Kosmider, O., Le Couedic, J.-P., Robert, F., Alberdi, A., et al. (2009). Mutation in tet2 in myeloid cancers. *New England Journal of Medicine*, 360(22):2289–2301.

[75] Deotare, U., Al-Dawsari, G., Couban, S., and Lipton, J. (2015). G-csf-primed bone marrow as a source of stem cells for allografting: revisiting the concept. *Bone marrow transplantation*, 50(9):1150.

[76] Ding, L., Saunders, T. L., Enikolopov, G., and Morrison, S. J. (2012). Endothelial and perivascular cells maintain haematopoietic stem cells. *Nature*, 481(7382):457.

[77] Djema, W., Bonnet, C., Mazenc, F., Clairambault, J., Fridman, E., Hirsch, P., and Delhommeau, F. (2018). Control in dormancy or eradication of cancer stem cells: Mathematical modeling and stability issues. *Journal of theoretical biology*.

[78] Djema, W., Mazenc, F., and Bonnet, C. (2015). Lyapunov stability analysis of a model describing hematopoiesis. In *Control Conference (ECC), 2015 European*, pages 2706–2711. IEEE.

[79] Djema, W., Mazenc, F., and Bonnet, C. (2016a). Analysis of a nonlinear delay differential-difference biological model. *IFAC-PapersOnLine*, 49(10):246–251.

[80] Djema, W., Mazenc, F., and Bonnet, C. (2016b). Stability of immature cell dynamics in healthy and unhealthy hematopoiesis. In *American Control Conference (ACC)*, pages 6121–6126. IEEE.

[81] Djema, W., Mazenc, F., and Bonnet, C. (2017a). Stability analysis and robustness results for a nonlinear system with distributed delays describing hematopoiesis. *Systems & Control Letters*, 102:93–101.

[82] Djema, W., Özbay, H., Bonnet, C., Fridman, E., Mazenc, F., and Clairambault, J. (2017b). Analysis of blood cell production under growth factors switching. *Proceedings of the IFAC World Congress, Toulouse*.

[83] Doherty, M. R., Smigiel, J. M., Junk, D. J., and Jackson, M. W. (2016). Cancer stem cell plasticity drives therapeutic resistance. *Cancers*, 8(1):8.

[84] Döhner, H., Estey, E. H., Amadori, S., Appelbaum, F. R., Büchner, T., Burnett, A. K., Dombret, H., Fenaux, P., Grimwade, D., Larson, R. A., et al. (2010). Diagnosis and management of acute myeloid leukemia in adults: recommendations from an international expert panel, on behalf of the european leukemianet. *Blood*, 115(3):453–474.

[85] Döhner, H., Weisdorf, D. J., and Bloomfield, C. D. (2015). Acute myeloid leukemia. *New England Journal of Medicine*, 373(12):1136–1152.

[86] Domoshnitsky, A. and Fridman, E. (2016). A positivity-based approach to delay-dependent stability of systems with large time-varying delays. *Systems & Control Letters*, 97:139–148.

[87] Durairajanayagam, D., Rengan, A. K., Sharma, R. K., and Agarwal, A. (2015). Sperm biology from production to ejaculation. In *Unexplained Infertility*, pages 29–42. Springer.

[88] Ebinger, S., Özdemir, E. Z., Ziegenhain, C., Tiedt, S., Alves, C. C., Grunert, M., Dworzak, M., Lutz, C., Turati, V. A., Enver, T., et al. (2016). Characterization of rare, dormant, and therapy-resistant cells in acute lymphoblastic leukemia. *Cancer Cell*, 30(6):849–862.

[89] Efimov, D., Perruquetti, W., Raïssi, T., and Zolghadri, A. (2013a). Interval observers for time-varying discrete-time systems. *IEEE Transactions on Automatic Control*, 58(12):3218–3224.

[90] Efimov, D., Perruquetti, W., and Richard, J.-P. (2013b). On reduced-order interval observers for time-delay systems. In *Control Conference (ECC), 2013 European*, pages 2116–2121. IEEE.

[91] Eftimie, R., Bramson, J. L., and Earn, D. J. (2011). Interactions between the immune system and cancer: a brief review of non-spatial mathematical models. *Bulletin of mathematical biology*, 73(1):2–32.

[92] Elledge, S. J. (1996). Cell cycle checkpoints: preventing an identity crisis. *Science*, 274(5293):1664.

[93] Enderling, H. (2013). Cancer stem cells and tumor dormancy. In *Systems Biology of Tumor Dormancy*, pages 55–71. Springer.

[94] Enderling, H. (2015). Cancer stem cells: small subpopulation or evolving fraction? *Integrative Biology*, 7(1):14–23.

[95] Enver, T., Pera, M., Peterson, C., and Andrews, P. W. (2009). Stem cell states, fates, and the rules of attraction. *Cell stem cell*, 4(5):387–397.

[96] Fang, Y., Zhong, L., Lin, M., Zhou, X., Jing, H., Ying, M., Luo, P., Yang, B., and He, Q. (2013). Mek/erk dependent activation of stat1 mediates dasatinib-induced differentiation of acute myeloid leukemia. *PloS one*, 8(6):e66915.

[97] Farina, L. and Rinaldi, S. (2011). *Positive linear systems: theory and applications*, volume 50. John Wiley & Sons.

[98] Ferrarini, M., Ferrero, E., Dagna, L., Poggi, A., and Zocchi, M. R. (2002). Human $\gamma\delta$ t cells: a nonredundant system in the immune-surveillance against cancer. *Trends in immunology*, 23(1):14–18.

[99] Feuring-Buske, M., Frankel, A. E., Alexander, R. L., Gerhard, B., and Hogge, D. E. (2002). A diphtheria toxin-interleukin 3 fusion protein is cytotoxic to primitive acute myeloid leukemia progenitors but spares normal progenitors. *Cancer Research*, 62(6):1730–1736.

[100] Foley, C., Bernard, S., and Mackey, M. C. (2006). Cost-effective g-csf therapy strategies for cyclical neutropenia: Mathematical modelling based hypotheses. *Journal of theoretical biology*, 238(4):754–763.

[101] Foley, C. and Mackey, M. C. (2009). Dynamic hematological disease: a review. *Journal of mathematical biology*, 58(1-2):285–322.

[102] Folkman, J. and Kalluri, R. (2004). Cancer without disease. *Nature*, 427(6977):787–787.

[103] Forys, U. and Marciniak-Czochra, A. (2003). Logistic equations in tumour growth modelling. *International Journal of Applied Mathematics and Computer Science*, 13(3):317–326.

[104] Fridman, E. (2001). New lyapunov–krasovskii functionals for stability of linear retarded and neutral type systems. *Systems & Control Letters*, 43(4):309–319.

[105] Fridman, E. (2002). Stability of linear descriptor systems with delay: a lyapunov-based approach. *Journal of Mathematical Analysis and Applications*, 273(1):24–44.

[106] Fridman, E. (2014). *Introduction to time-delay systems: Analysis and control*. Springer.

[107] Fridman, E., Bonnet, C., Mazenc, F., and Djema, W. (2016). Stability of the cell dynamics in acute myeloid leukemia. *Systems & Control Letters*, 88:91–100.

[108] Fridman, E. and Shaked, U. (2002). A descriptor system approach to h? control of linear time-delay systems. *IEEE Transactions on Automatic Control*, 47(2):253–270.

[109] Friedman, A. and Hao, W. (2015). A mathematical model of atherosclerosis with reverse cholesterol transport and associated risk factors. *Bulletin of mathematical biology*, 77(5):758–781.

[110] Friedmann-Morvinski, D. and Verma, I. M. (2014). Dedifferentiation and reprogramming: origins of cancer stem cells. *EMBO reports*, page e201338254.

[111] Gatenby, R. A. (2009). A change of strategy in the war on cancer. *Nature*, 459(7246):508–509.

[112] Geiger, T. L. and Rubnitz, J. E. (2015). New approaches for the immunotherapy of acute myeloid leukemia. *Discovery medicine*, 19(105):275.

[113] Germani, A., Manes, C., and Pepe, P. (2003). Input-output linearization with delay cancellation for nonlinear delay systems: the problem of the internal stability. *International Journal of Robust and Nonlinear Control*, 13(9):909–937.

[114] Giesl, P. (2007). *Construction of global Lyapunov functions using radial basis functions*, volume 1904. Springer.

[115] Godwin, C., Gale, R., and Walter, R. (2017). Gemtuzumab ozogamicin in acute myeloid leukemia. *Leukemia*.

[116] Goldman, A., Kohandel, M., and Clairambault, J. (2017a). Integrating biological and mathematical models to explain and overcome drug resistance in cancer. part 1: Biological facts and studies in drug resistance. *Current Stem Cell Reports*, 3(3):253–259.

[117] Goldman, A., Kohandel, M., and Clairambault, J. (2017b). Integrating biological and mathematical models to explain and overcome drug resistance in cancer, part 2: from theoretical biology to mathematical models. *Current Stem Cell Reports*, 3(3):260–268.

[118] Gouzé, J.-L., Rapaport, A., and Hadj-Sadok, M. Z. (2000). Interval observers for uncertain biological systems. *Ecological modelling*, 133(1):45–56.

[119] Gruyitch, L. T., Richard, J.-P., Borne, P., and Gentina, J.-C. (2003). *Stability domains*, volume 1. CRC Press.

[120] Gu, K., Chen, J., and Kharitonov, V. L. (2003). *Stability of time-delay systems*. Springer Science & Business Media.

[121] Gu, K. and Liu, Y. (2009). Lyapunov–krasovskii functional for uniform stability of coupled differential-functional equations. *Automatica*, 45(3):798–804.

[122] Haddad, W. M. and Chellaboina, V. (2004). Stability theory for nonnegative and compartmental dynamical systems with time delay. In *American Control Conference, 2004. Proceedings of the 2004*, volume 2, pages 1422–1427. IEEE.

[123] Haddad, W. M. and Chellaboina, V. (2005). Stability and dissipativity theory for nonnegative dynamical systems: a unified analysis framework for biological and physiological systems. *Nonlinear Analysis: Real World Applications*, 6(1):35–65.

[124] Haddad, W. M., Chellaboina, V., and Hui, Q. (2010). *Nonnegative and compartmental dynamical systems*. Princeton University Press.

[125] Haferlach, T., Schoch, C., Schnittger, S., Kern, W., Löffler, H., and Hiddemann, W. (2002). Distinct genetic patterns can be identified in acute monoblastic and acute monocytic leukaemia (fab aml m5a and m5b): a study of 124 patients. *British journal of haematology*, 118(2):426–431.

[126] Hahn, W. and Baartz, A. P. (1967). *Stability of motion*, volume 138. Springer.

[127] Hale, J. and Verduyn Lunel, S. (1993). Introduction to functional differential equations springer verlag new york. *NY Google Scholar*.

[128] Hale, J. K. (1965). Sufficient conditions for stability and instability of autonomous functional-differential equations. *Journal of Differential Equations*, 1(4):452–482.

[129] Hanoun, M., Maryanovich, M., Arnal-Estapé, A., and Frenette, P. S. (2015). Neural regulation of hematopoiesis, inflammation, and cancer. *Neuron*, 86(2):360–373.

[130] Hart, P. E., Nilsson, N. J., and Raphael, B. (1968). A formal basis for the heuristic determination of minimum cost paths. *IEEE transactions on Systems Science and Cybernetics*, 4(2):100–107.

[131] Hartwell, L. H., Kastan, M. B., et al. (1994). Cell cycle control and cancer. *Science-AAAS-Weekly Paper Edition*, 266(5192):1821–1828.

[132] Haurie, C., Dale, D. C., and Mackey, M. C. (1998). Cyclical neutropenia and other periodic hematological disorders: a review of mechanisms and mathematical models. *Blood*, 92(8):2629–2640.

[133] Haurie, C., Dale, D. C., Rudnicki, R., and Mackey, M. C. (2000). Modeling complex neutrophil dynamics in the grey collie. *Journal of theoretical biology*, 204(4):505–519.

[134] Hayden, E. C. (2009). Cutting off cancer's supply lines. *Nature*, 458(7239):686–687.

[135] Hearn, T., Haurie, C., and Mackey, M. C. (1998). Cyclical neutropenia and the peripheral control of white blood cell production. *Journal of theoretical biology*, 192(2):167–181.

[136] Hennet, J.-C. and Tarbouriech, S. (1998). Stability conditions of constrained delay systems via positive invariance. *International Journal of Robust and Nonlinear Control*, 8(3):265–278.

[137] Hirsch, P., Zhang, Y., Tang, R., Joulin, V., Boutroux, H., Pronier, E., Moatti, H., Flandrin, P., Marzac, C., Bories, D., et al. (2016). Genetic hierarchy and temporal variegation in the clonal history of acute myeloid leukaemia. *Nature communications*, 7.

[138] Hoffman, R., Silberstein, L. E., Heslop, H., and Weitz, J. (2013). *Hematology: basic principles and practice*. Elsevier Health Sciences.

[139] Hollstein, M., Sidransky, D., Vogelstein, B., Harris, C. C., et al. (1991). p53 mutations in human cancers. *Science*, 253(5015):49–53.

[140] Hon, G. C., Song, C.-X., Du, T., Jin, F., Selvaraj, S., Lee, A. Y., Yen, C.-a., Ye, Z., Mao, S.-Q., Wang, B.-A., et al. (2014). 5mc oxidation by tet2 modulates enhancer activity and timing of transcriptome reprogramming during differentiation. *Molecular cell*, 56(2):286–297.

[141] Hosing, C. (2012). Hematopoietic stem cell mobilization with g-csf. *Stem Cell Mobilization: Methods and Protocols*, pages 37–47.

[142] Iwasa, T., Okamoto, I., Suzuki, M., Nakahara, T., Yamanaka, K., Hatashita, E., Yamada, Y., Fukuoka, M., Ono, K., and Nakagawa, K. (2008). Radiosensitizing effect of ym155, a novel small-molecule survivin suppressant, in non–small cell lung cancer cell lines. *Clinical Cancer Research*, 14(20):6496–6504.

[143] Jackson, P. R., Juliano, J., Hawkins-Daarud, A., Rockne, R. C., and Swanson, K. R. (2015). Patient-specific mathematical neuro-oncology: using a simple proliferation and invasion tumor model to inform clinical practice. *Bulletin of mathematical biology*, 77(5):846–856.

[144] Jaiswal, P. K., Goel, A., Mittal, R., et al. (2015). Survivin: A molecular biomarker in cancer. *Indian Journal of Medical Research*, 141(4):389.

[145] James, D. D. *Neo-Classical Physics or Quantum Mechanics?: A New Theory of Physics*. Educreation Publishing.

[146] Jan, M. and Majeti, R. (2013). Clonal evolution of acute leukemia genomes. *Oncogene*, 32(2):135–140.

[147] Jansen, G., Gatenby, R., and Aktipis, C. A. (2015). Opinion: Control vs. eradication: Applying infectious disease treatment strategies to cancer. *Proceedings of the National Academy of Sciences of the United States of America*, 112(4):937.

[148] Jelkmann, W. (2011). Regulation of erythropoietin production. *The Journal of physiology*, 589(6):1251–1258.

[149] Jilkine, A. and Gutenkunst, R. N. (2014). Effect of dedifferentiation on time to mutation acquisition in stem cell-driven cancers. *PLoS Comput Biol*, 10(3):e1003481.

[150] Jordan, C. T., Guzman, M. L., and Noble, M. (2006). Cancer stem cells. *New England Journal of Medicine*, 355(12):1253–1261.

[151] Kanal, L. and Kumar, V. (2012). *Search in artificial intelligence*. Springer Science & Business Media.

[152] Karafyllis, I., Pepe, P., and Jiang, Z.-P. (2009). Stability results for systems described by coupled retarded functional differential equations and functional difference equations. *Nonlinear Analysis: Theory, Methods & Applications*, 71(7):3339–3362.

[153] Kareva, I. (2016a). Escape from tumor dormancy and time to angiogenic switch as mitigated by tumor-induced stimulation of stroma. *Journal of theoretical biology*, 395:11–22.

[154] Kareva, I. (2016b). Primary and metastatic tumor dormancy as a result of population heterogeneity. *Biology Direct*, 11(1):37.

[155] Kaushansky, K. (2006). Lineage-specific hematopoietic growth factors. *New England Journal of Medicine*, 354(19):2034–2045.

[156] Keener, J. and Sneyd, J. (2009a). Biochemical reactions. In *Mathematical Physiology*, pages 1–47. Springer.

[157] Keener, J. P. and Sneyd, J. (2009b). *Mathematical physiology*, volume 1. Springer.

[158] Khalil, H. K. (2002). Nonlinear systems, 3rd. *New Jewsey, Prentice Hall*, 9.

[159] Kiel, M. J., Radice, G. L., and Morrison, S. J. (2007). Lack of evidence that hematopoietic stem cells depend on n-cadherin-mediated adhesion to osteoblasts for their maintenance. *Cell stem cell*, 1(2):204–217.

[160] Kindler, T., Lipka, D. B., and Fischer, T. (2010). Flt3 as a therapeutic target in aml: still challenging after all these years. *Blood*, 116(24):5089–5102.

[161] Knapper, S., Russell, N., Gilkes, A., Hills, R. K., Gale, R. E., Cavenagh, J. D., Jones, G., Kjeldsen, L., Grunwald, M. R., Thomas, I., et al. (2016). A randomised assessment of adding the kinase inhibitor lestaurtinib to 1st-line chemotherapy for flt3-mutated aml. *Blood*, pages blood–2016.

[162] Koenig, S. and Likhachev, M. (2005). Fast replanning for navigation in unknown terrain. *IEEE Transactions on Robotics*, 21(3):354–363.

[163] Kolch, W. (2000). Meaningful relationships: the regulation of the ras/raf/mek/erk pathway by protein interactions. *Biochemical Journal*, 351(2):289–305.

[164] Kolmanovskii, V. and Myshkis, A. (1992). *Applied theory of functional differential equations*. Kluwer Acad. Pub.

[165] Kolmanovskii, V. and Myshkis, A. (1999). *Introduction to the theory and applications of functional differential equations*. Mathematics and Its Applications, Springer.

[166] Kottaridis, P. D., Gale, R. E., Frew, M. E., Harrison, G., Langabeer, S. E., Belton, A. A., Walker, H., Wheatley, K., Bowen, D. T., Burnett, A. K., et al. (2001). The presence of a flt3 internal tandem duplication in patients with acute myeloid leukemia (aml) adds important prognostic information to cytogenetic risk group and response to the first cycle of chemotherapy: analysis of 854 patients from the united kingdom medical research council aml 10 and 12 trials. *Blood*, 98(6):1752–1759.

[167] Lainey, E., Thépot, S., Bouteloup, C., Sébert, M., Adès, L., Tailler, M., Gardin, C., de Botton, S., Baruchel, A., Fenaux, P., et al. (2011). Tyrosine kinase inhibitors for the treatment of acute myeloid leukemia: delineation of anti-leukemic mechanisms of action. *Biochemical pharmacology*, 82(10):1457–1466.

[168] Lange, C. and Calegari, F. (2010). Cdks and cyclins link g1 length and differentiation of embryonic, neural and hematopoietic stem cells. *Cell Cycle*, 9(10):1893–1900.

[169] Langer, C. J. (2015). Emerging immunotherapies in the treatment of non–small cell lung cancer (nsclc): The role of immune checkpoint inhibitors. *American journal of clinical oncology*, 38(4):422–430.

[170] Langlois, G. P., Craig, M., Humphries, A. R., Mackey, M. C., Mahaffy, J. M., Bélair, J., Moulin, T., Sinclair, S. R., and Wang, L. (2017). Normal and pathological dynamics of platelets in humans. *Journal of Mathematical Biology*, pages 1–52.

[171] Leder, K., Holland, E. C., and Michor, F. (2010). The therapeutic implications of plasticity of the cancer stem cell phenotype. *PloS one*, 5(12):e14366.

[172] Lewis, T. A., Sykes, D. B., Law, J. M., Munoz, B., Rustiguel, J. K., Nonato, M. C., Scadden, D. T., and Schreiber, S. L. (2016). Development of ml390: a human dhodh inhibitor that induces differentiation in acute myeloid leukemia. *ACS Medicinal Chemistry Letters*.

[173] Ley, T. J., Ding, L., Walter, M. J., McLellan, M. D., Lamprecht, T., Larson, D. E., Kandoth, C., Payton, J. E., Baty, J., Welch, J., et al. (2010). Dnmt3a mutations in acute myeloid leukemia. *New England Journal of Medicine*, 363(25):2424–2433.

[174] Li, C., Heidt, D. G., Dalerba, P., Burant, C. F., Zhang, L., Adsay, V., Wicha, M., Clarke, M. F., and Simeone, D. M. (2007). Identification of pancreatic cancer stem cells. *Cancer research*, 67(3):1030–1037.

[175] Liu, X., Huang, J., Chen, T., Wang, Y., Xin, S., Li, J., Pei, G., and Kang, J. (2008). Yamanaka factors critically regulate the developmental signaling network in mouse embryonic stem cells. *Cell research*, 18(12):1177.

[176] Liu, X., Yu, W., and Wang, L. (2010). Stability analysis for continuous-time positive systems with time-varying delays. *IEEE Transactions on Automatic Control*, 55(4):1024–1028.

[177] Logan, J. D. (2014). *Applied partial differential equations*. Springer.

[178] Lowenberg, B., Downing, J. R., and Burnett, A. (1999). Acute myeloid leukemia. *New England Journal of Medicine*, 341(14):1051–1062.

[179] Ma, P., Song, W., and Hess, J. L. (2016). A new target for differentiation therapy in aml. *Cell Research*.

[180] Mackey, M. C. (1978). Unified hypothesis of the origin of aplastic anemia and periodic hematopoiesis. *Blood*, 51(4):941–956.

[181] Mackey, M. C., Glass, L., et al. (1977). Oscillation and chaos in physiological control systems. *Science*, 197(4300):287–289.

[182] Mackey, M. C. and Maini, P. K. (2015). What has mathematics done for biology? *Bulletin of mathematical biology*, 77(5):735–738.

[183] Mackey, M. C. and Milton, J. G. (1990). Feedback, delays and the origin of blood cell dynamics.

[184] Mackey, M. C., Ou, C., Pujo-Menjouet, L., and Wu, J. (2006). Periodic oscillations of blood cell populations in chronic myelogenous leukemia. *SIAM journal on mathematical analysis*, 38(1):166–187.

[185] Mahaffy, J. M., Bélair, J., and Mackey, M. C. (1998). Hematopoietic model with moving boundary condition and state dependent delay: applications in erythropoiesis. *Journal of theoretical biology*, 190(2):135–146.

[186] Majumder, S. and Prasad, M. S. (2016). Three dimensional d* algorithm for incremental path planning in uncooperative environment. In *Signal Processing and Integrated Networks (SPIN), 2016 3rd International Conference on*, pages 431–435. IEEE.

[187] Malisoff, M. and Mazenc, F. (2009). *Constructions of strict Lyapunov functions*. Springer Science & Business Media.

[188] Malthus, T. R. (1798). *An Essay on the Principle of Population, as it Affects the Future Imporvement of Society, with Remarks on the Speculations of Mr. Godwin, M. Condorcet, and Other Writers*. The Lawbook Exchange, Ltd.

[189] Marciniak-Czochra, A., Stiehl, T., Ho, A. D., Jäger, W., and Wagner, W. (2009). Modeling of asymmetric cell division in hematopoietic stem cells-regulation of self-renewal is essential for efficient repopulation. *Stem cells and development*, 18(3):377–386.

[190] Mazenc, F. (2015). Stability analysis of time-varying neutral time-delay systems. *IEEE Transactions on Automatic Control*, 60(2):540–546.

[191] Mazenc, F. and Bernard, O. (2011). Interval observers for linear time-invariant systems with disturbances. *Automatica*, 47(1):140–147.

[192] Mazenc, F. and Bliman, P.-A. (2006). Backstepping design for time-delay nonlinear systems. *IEEE Transactions on Automatic Control*, 51(1):149–154.

[193] Mazenc, F., Fridman, E., and Djema, W. (2015). Estimation of solutions of observable nonlinear systems with disturbances. *Systems & Control Letters*, 79:47–58.

[194] Mazenc, F. and Ito, H. (2013). Lyapunov technique and backstepping for nonlinear neutral systems. *IEEE Transactions on Automatic Control*, 58(2):512–517.

[195] Mazenc, F. and Malisoff, M. (2010). Stabilization of a chemostat model with haldane growth functions and a delay in the measurements. *Automatica*, 46(9):1428–1436.

[196] Mazenc, F. and Malisoff, M. (2016). Stability analysis for time-varying systems with delay using linear lyapunov functionals and a positive systems approach. *IEEE Transactions on Automatic Control*, 61(3):771–776.

[197] Mazenc, F., Malisoff, M., and Harmand, J. (2008). Further results on stabilization of periodic trajectories for a chemostat with two species. *IEEE Transactions on Automatic Control*, 53(Special Issue):66–74.

[198] Mazenc, F., Niculescu, S.-I., and Krstic, M. (2012). Lyapunov–krasovskii functionals and application to input delay compensation for linear time-invariant systems. *Automatica*, 48(7):1317–1323.

[199] Mead, A. J., Linch, D. C., Hills, R. K., Wheatley, K., Burnett, A. K., and Gale, R. E. (2007). Flt3 tyrosine kinase domain mutations are biologically distinct from and have a significantly more favorable prognosis than flt3 internal tandem duplications in patients with acute myeloid leukemia. *Blood*, 110(4):1262–1270.

[200] Metcalf, D. (2008). Hematopoietic cytokines. *Blood*, 111(2):485–491.

[201] Metz, J. A. and Diekmann, O. (2014). *The dynamics of physiologically structured populations*, volume 68. Springer.

[202] Michel, A. N., Hou, L., and Liu, D. (2008). *Stability of dynamical systems: continuous, discontinuous, and discrete systems*. Springer Science & Business Media.

[203] Michel, A. N., Hou, L., and Liu, D. (2015). *Stability of dynamical systems: on the role of monotonic and non-monotonic Lyapunov functions*. Springer.

[204] Michiels, W. and Niculescu, S.-I. (2014). *Stability, Control, and Computation for Time-delay Systems: An Eigenvalue-based Approach*, volume 27. Siam.

[205] M'Kendrick, A. (1925). Applications of mathematics to medical problems. *Proceedings of the Edinburgh Mathematical Society*, 44:98–130.

[206] Moisan, M. and Bernard, O. (2005). Interval observers for non monotone systems. application to bioprocess models. *IFAC Proceedings Volumes*, 38(1):43–48.

[207] Moisan, M., Bernard, O., and Gouzé, J.-L. (2009). Near optimal interval observers bundle for uncertain bioreactors. *Automatica*, 45(1):291–295.

[208] Morgan, D. O. (2007). *The cell cycle: principles of control*. New Science Press.

[209] Morrison, S. J. and Scadden, D. T. (2014). The bone marrow niche for haematopoietic stem cells. *Nature*, 505(7483):327.

[210] Murray, J. (2003). *Mathematical Biology II: Spatial Models and Biomedical Applications, vol. 18 of Biomathematics*.

[211] Murray, J. D. (2002). Mathematical biology i: an introduction, vol. 17 of interdisciplinary applied mathematics.

[212] Nakao, M., Yokota, S., Iwai, T., Kaneko, H., Horiike, S., Kashima, K., Sonoda, Y., Fujimoto, T., and Misawa, S. (1996). Internal tandem duplication of the flt3 gene found in acute myeloid leukemia. *Leukemia*, 10(12):1911–1918.

[213] Naumov, G. N., Folkman, J., and Straume, O. (2009). Tumor dormancy due to failure of angiogenesis: role of the microenvironment. *Clinical & experimental metastasis*, 26(1):51–60.

[214] Network, C. G. A. R. et al. (2013). Genomic and epigenomic landscapes of adult de novo acute myeloid leukemia. *N Engl j Med*, 2013(368):2059–2074.

[215] Ngoc, P. H. A. (2009). On positivity and stability of linear volterra systems with delay. *SIAM Journal on Control and Optimization*, 48(3):1939–1960.

[216] Ngoc, P. H. A. (2013). Stability of positive differential systems with delay. *IEEE Transactions on Automatic Control*, 58(1):203–209.

[217] Nguyen, L. V., Vanner, R., Dirks, P., and Eaves, C. J. (2012). Cancer stem cells: an evolving concept. *Nature reviews. Cancer*, 12(2):133.

[218] Niculescu, S.-I. (2001). *Delay effects on stability: a robust control approach*, volume 269. Springer Science & Business Media.

[219] Niculescu, S.-I., Verriest, E. I., Dugard, L., and Dion, J.-M. (1998). Stability and robust stability of time-delay systems: A guided tour. In *Stability and control of time-delay systems*, pages 1–71. Springer.

[220] Nielsen, M., Thomsen, J., Primdahl, S., Dyreborg, U., and Andersen, J. (1987). Breast cancer and atypia among young and middle-aged women: a study of 110 medicolegal autopsies. *British journal of cancer*, 56(6):814.

[221] Norris, D. and Stone, J. (2008). Who classification of tumours of haematopoietic and lymphoid tissues.

[222] Olgac, N. and Sipahi, R. (2002). An exact method for the stability analysis of time-delayed linear time-invariant (lti) systems. *IEEE Transactions on Automatic Control*, 47(5):793–797.

[223] Özbay, H. (1999). *Introduction to feedback control theory*. CRC Press.

[224] Özbay, H., Benjelloun, H., Bonnet, C., and Clairambault, J. (2010). Stability conditions for a system modeling cell dynamics in leukemia. *IFAC Proceedings Volumes*, 43(2):99–102.

[225] Özbay, H., Bonnet, C., Benjelloun, H., and Clairambault, J. (2012). Stability analysis of cell dynamics in leukemia. *Mathematical Modelling of Natural Phenomena*, 7(1):203–234.

[226] Özbay, H., Bonnet, C., and Clairambault, J. (2008). Stability analysis of systems with distributed delays and application to hematopoietic cell maturation dynamics. In *CDC*, pages 2050–2055.

[227] Ozbay, J. A. C. B. H., Hirsch, J. C. S. N. P., and Delhommeau, F. A discrete-maturity interconnected model of healthy and cancer cell dynamics in acute myeloid leukemia.

[228] Pardoll, D. M. (2012). The blockade of immune checkpoints in cancer immunotherapy. *Nature reviews. Cancer*, 12(4):252.

[229] Park, J.-E., Yi, H., Kim, Y., Chang, H., and Kim, V. N. (2016). Regulation of poly (a) tail and translation during the somatic cell cycle. *Molecular cell*, 62(3):462–471.

[230] Passegué, e., Jamieson, C. H., Ailles, L. E., and Weissman, I. L. (2003). Normal and leukemic hematopoiesis: are leukemias a stem cell disorder or a reacquisition of stem cell characteristics? *Proceedings of the National Academy of Sciences*, 100(suppl 1):11842–11849.

[231] Pattabiraman, D. R. and Weinberg, R. A. (2014). Tackling the cancer stem cells–what challenges do they pose? *Nature reviews. Drug discovery*, 13(7):497.

[232] Pepe, P. (2003). The liapunov's second method for continuous time difference equations. *International Journal of Robust and Nonlinear Control*, 13(15):1389–1405.

[233] Pepe, P., Karafyllis, I., and Jiang, Z.-P. (2008). On the liapunov–krasovskii methodology for the iss of systems described by coupled delay differential and difference equations. *Automatica*, 44(9):2266–2273.

[234] Perthame, B. (2006). *Transport equations in biology*. Springer Science & Business Media.

[235] Philipone, E. and Yoon, A. J. (2017). Oral soft tissue manifestations of hematologic abnormalities and diseases. In *Oral Pathology in the Pediatric Patient*, pages 129–134. Springer.

[236] Polyanin, A. D., Zaitsev, V. F., and Moussiaux, A. (2001). *Handbook of first-order partial differential equations*. CRC Press.

[237] Preziosi, L. (1996). From population dynamics to modelling the competition between tumors and immune system. *Mathematical and computer modelling*, 23(6):135–152.

[238] Pronier, E., Almire, C., Mokrani, H., Vasanthakumar, A., Simon, A., Mor, B. d. C. R. M., Massé, A., Le Couédic, J.-P., Pendino, F., Carbonne, B., et al. (2011). Inhibition of tet2-mediated conversion of 5-methylcytosine to 5-hydroxymethylcytosine disturbs erythroid and granulomonocytic differentiation of human hematopoietic progenitors. *Blood*, 118(9):2551–2555.

[239] Pronier, E. and Delhommeau, F. (2012). Role of tet2 mutations in myeloproliferative neoplasms. *Current hematologic malignancy reports*, 7(1):57–64.

[240] Pujo-Menjouet, L. (2016). Blood cell dynamics: half of a century of modelling. *Mathematical Modelling of Natural Phenomena*, 11(1):92–115.

[241] Pujo-Menjouet, L., Bernard, S., and Mackey, M. C. (2005). Long period oscillations in a g_0 model of hematopoietic stem cells. *SIAM Journal on Applied Dynamical Systems*, 4(2):312–332.

[242] Qian, H. (2012). Cooperativity in cellular biochemical processes: noise-enhanced sensitivity, fluctuating enzyme, bistability with nonlinear feedback, and other mechanisms for sigmoidal responses. *Annual review of biophysics*, 41:179–204.

[243] Quentmeier, H., Reinhardt, J., Zaborski, M., and Drexler, H. (2003). Flt3 mutations in acute myeloid leukemia cell lines. *Leukemia*, 17(1):120.

[244] Rader, J., Russell, M. R., Hart, L. S., Nakazawa, M. S., Belcastro, L. T., Martinez, D., Li, Y., Carpenter, E. L., Attiyeh, E. F., Diskin, S. J., et al. (2013). Dual cdk4/cdk6 inhibition induces cell-cycle arrest and senescence in neuroblastoma. *Clinical cancer research*, 19(22):6173–6182.

[245] Raïssi, T., Efimov, D., and Zolghadri, A. (2012). Interval state estimation for a class of nonlinear systems. *IEEE Transactions on Automatic Control*, 57(1):260–265.

[246] Reiter, R. E., Gu, Z., Watabe, T., Thomas, G., Szigeti, K., Davis, E., Wahl, M., Nisitani, S., Yamashiro, J., Le Beau, M. M., et al. (1998). Prostate stem cell antigen: a cell surface marker overexpressed in prostate cancer. *Proceedings of the National Academy of Sciences*, 95(4):1735–1740.

[247] Reya, T., Morrison, S. J., Clarke, M. F., and Weissman, I. L. (2001). Stem cells, cancer, and cancer stem cells. *nature*, 414(6859):105–111.

[248] Reynolds, A. R., Hart, I. R., Watson, A. R., Welti, J. C., Silva, R. G., Robinson, S. D., Da Violante, G., Gourlaouen, M., Salih, M., Jones, M. C., et al. (2009). Stimulation of tumor growth and angiogenesis by low concentrations of rgd-mimetic integrin inhibitors. *Nature medicine*, 15(4):392–400.

[249] Rhodes, A. and Hillen, T. (2016). Mathematical modeling of the role of survivin. *Bulletin of mathematical biology*, 78(6):1162–1188.

[250] Richard, J., Goubet-Bartholomeüs, A., Tchangani, P., and Dambrine, M. (1998). Nonlinear delay systems: Tools for a quantitative approach to stabilization. *Stability and control of time-delay systems*, pages 218–240.

[251] Richard, J.-P. (2003). Time-delay systems: an overview of some recent advances and open problems. *automatica*, 39(10):1667–1694.

[252] Röllig, C., Serve, H., Hüttmann, A., Noppeney, R., Müller-Tidow, C., Krug, U., Baldus, C. D., Brandts, C. H., Kunzmann, V., Einsele, H., et al. (2015). Addition of sorafenib versus placebo to standard therapy in patients aged 60 years or younger with newly diagnosed acute myeloid leukaemia (soraml): a multicentre, phase 2, randomised controlled trial. *The lancet oncology*, 16(16):1691–1699.

[253] Rowe, J. M. and Löwenberg, B. (2013). Gemtuzumab ozogamicin in acute myeloid leukemia: a remarkable saga about an active drug. *Blood*, 121(24):4838–4841.

[254] Russell, S., Norvig, P., and Intelligence, A. (1995). A modern approach. *Artificial Intelligence. Prentice-Hall, Egnlewood Cliffs*, 25:27.

[255] Salazar-Roa, M. and Malumbres, M. (2017). Fueling the cell division cycle. *Trends in Cell Biology*, 27(1):69–81.

[256] Salomoni, P. and Calegari, F. (2010). Cell cycle control of mammalian neural stem cells: putting a speed limit on g1. *Trends in cell biology*, 20(5):233–243.

[257] Santillan, M., Mahaffy, J. M., Belair, J., and Mackey, M. C. (2000). Regulation of platelet production: The normal response to perturbation and cyclical platelet disease. *Journal of Theoretical Biology*, 206(4):585–603.

[258] Saygin, C. and Carraway, H. E. (2017). Emerging therapies for acute myeloid leukemia. *Journal of hematology & oncology*, 10(1):93.

[259] Schaniel, C., Bruno, L., Melchers, F., and Rolink, A. G. (2002). Multiple hematopoietic cell lineages develop in vivo from transplanted pax5-deficient pre-b i–cell clones. *Blood*, 99(2):472–478.

[260] Schnerch, D., Yalcintepe, J., Schmidts, A., Becker, H., Follo, M., Engelhardt, M., and Wäsch, R. (2012). Cell cycle control in acute myeloid leukemia. *American journal of cancer research*, 2(5):508.

[261] Schreiber, R. D., Old, L. J., and Smyth, M. J. (2011). Cancer immunoediting: integrating immunity? roles in cancer suppression and promotion. *Science*, 331(6024):1565–1570.

[262] Sharpe, F. R. and Lotka, A. J. (1911). L. a problem in age-distribution. *The London, Edinburgh, and Dublin Philosophical Magazine and Journal of Science*, 21(124):435–438.

[263] Shen, C.-N., Burke, Z. D., and Tosh, D. (2004). Transdifferentiation, metaplasia and tissue regeneration. *Organogenesis*, 1(2):36–44.

[264] Shenghui, H., Nakada, D., and Morrison, S. J. (2009). Mechanisms of stem cell self-renewal. *Annual Review of Cell and Developmental*, 25:377–406.

[265] Sieff, C. A. (1987). Hematopoietic growth factors. *Journal of Clinical Investigation*, 79(6):1549.

[266] Sipahi, R., Niculescu, S.-I., Abdallah, C. T., Michiels, W., and Gu, K. (2011). Stability and stabilization of systems with time delay. *IEEE Control Systems*, 31(1):38–65.

[267] Smith, H. L. (1993). Reduction of structured population models to threshold-type delay equations and functional differential equations: a case study. *Mathematical biosciences*, 113(1):1–23.

[268] Smith, J. and Martin, L. (1973). Do cells cycle? *Proceedings of the National Academy of Sciences*, 70(4):1263–1267.

[269] Solary, E., Bernard, O., Tefferi, A., Fuks, F., and Vainchenker, W. (2014). The ten-eleven translocation-2 (tet2) gene in hematopoiesis and hematopoietic diseases. *Leukemia*, 28(3):485–496.

[270] Solomon, O. and Fridman, E. (2013). New stability conditions for systems with distributed delays. *Automatica*, 49(11):3467–3475.

[271] Solomon, O. and Fridman, E. (2015). Stability and passivity analysis of semilinear diffusion pdes with time-delays. *International Journal of Control*, 88(1):180–192.

[272] Sontag, E. D. (2008). Input to state stability: Basic concepts and results. In *Nonlinear and optimal control theory*, pages 163–220. Springer.

[273] Stentz, A. (1994). Optimal and efficient path planning for partially-known environments. In *Robotics and Automation, 1994. Proceedings., 1994 IEEE International Conference on*, pages 3310–3317. IEEE.

[274] Stentz, A. et al. (1995). The focussed dˆ* algorithm for real-time replanning. In *IJCAI*, volume 95, pages 1652–1659.

[275] Stiehl, T. and Marciniak-Czochra, A. (2011). Characterization of stem cells using mathematical models of multistage cell lineages. *Mathematical and Computer Modelling*, 53(7):1505–1517.

[276] Stiehl, T. and Marciniak-Czochra, A. (2012). Mathematical modeling of leukemogenesis and cancer stem cell dynamics. *Mathematical Modelling of Natural Phenomena*, 7(1):166–202.

[277] Stone, R. M., Mandrekar, S. J., Sanford, B. L., Laumann, K., Geyer, S., Bloomfield, C. D., Thiede, C., Prior, T. W., Döhner, K., Marcucci, G., et al. (2017). Midostaurin plus chemotherapy for acute myeloid leukemia with a flt3 mutation. *New England Journal of Medicine*, 377(5):454–464.

[278] Sykes, D. B., Kfoury, Y. S., Mercier, F. E., Wawer, M. J., Law, J. M., Haynes, M. K., Lewis, T. A., Schajnovitz, A., Jain, E., Lee, D., et al. (2016). Inhibition of dihydroorotate dehydrogenase overcomes differentiation blockade in acute myeloid leukemia. *Cell*, 167(1):171–186.

[279] Takaishi, S., Okumura, T., Tu, S., Wang, S. S., Shibata, W., Vigneshwaran, R., Gordon, S. A., Shimada, Y., and Wang, T. C. (2009). Identification of gastric cancer stem cells using the cell surface marker cd44. *Stem cells*, 27(5):1006–1020.

[280] Tata, P. R. and Rajagopal, J. (2016). Cellular plasticity: 1712 to the present day. *Current Opinion in Cell Biology*, 43:46–54.

[281] Tay, J., Levesque, J.-P., and Winkler, I. G. (2017). Cellular players of hematopoietic stem cell mobilization in the bone marrow niche. *International journal of hematology*, 105(2):129–140.

[282] Thiede, C., Steudel, C., Mohr, B., Schaich, M., Schäkel, U., Platzbecker, U., Wermke, M., Bornhäuser, M., Ritter, M., Neubauer, A., et al. (2002). Analysis of flt3-activating mutations in 979 patients with acute myelogenous leukemia: association with fab subtypes and identification of subgroups with poor prognosis. *Blood*, 99(12):4326–4335.

[283] Thorens, B. (2011). Brain glucose sensing and neural regulation of insulin and glucagon secretion. *Diabetes, Obesity and Metabolism*, 13(s1):82–88.

[284] Tsoularis, A. and Wallace, J. (2002). Analysis of logistic growth models. *Mathematical biosciences*, 179(1):21–55.

[285] Tuch, B. (2006). Stem cells-a clinical update. *Australian family physician*, 35(9):719.

[286] Tung, P.-Y. and Knoepfler, P. S. (2015). Epigenetic mechanisms of tumorigenicity manifesting in stem cells. *Oncogene*, 34(18):2288.

[287] Tyson, J. J. and Novak, B. (2015). Bistability, oscillations, and traveling waves in frog egg extracts. *Bulletin of mathematical biology*, 77(5):796–816.

[288] Uchida, N., He, D., Friera, A. M., Reitsma, M., Sasaki, D., Chen, B., and Tsukamoto, A. (1997). The unexpected g0/g1 cell cycle status of mobilized hematopoietic stem cells from peripheral blood. *Blood*, 89(2):465–472.

[289] Uhr, J. W., Scheuermann, R. H., Street, N. E., and Vitetta, E. S. (1997). Cancer dormancy: opportunities for new therapeutic approaches. *Nature medicine*, 3(5):505–509.

[290] Verriest, E. (1995). Stability of systems with distributed delays. In *Preprints of the IFAC Conference on System, Structure and Control*, pages 294–299.

[291] Vesely, M. D., Kershaw, M. H., Schreiber, R. D., and Smyth, M. J. (2011). Natural innate and adaptive immunity to cancer. *Annual review of immunology*, 29:235–271.

[292] Vidyasagar, M. (2002). *Nonlinear systems analysis*. SIAM.

[293] Visvader, J. E. and Lindeman, G. J. (2008). Cancer stem cells in solid tumours: accumulating evidence and unresolved questions. *Nature reviews. Cancer*, 8(10):755.

[294] von Wussow, U., Klaus, J., and Pagel, H. (2005). Is the renal production of erythropoietin controlled by the brain stem? *American Journal of Physiology-Endocrinology and Metabolism*, 289(1):E82–E86.

[295] Wang, E. S., Stone, R. M., Tallman, M. S., Walter, R. B., Eckardt, J. R., and Collins, R. (2016). Crenolanib, a type i flt3 tki, can be safely combined with cytarabine and anthracycline induction chemotherapy and results in high response rates in patients with newly diagnosed flt3 mutant acute myeloid leukemia (aml).

[296] Wang, G. (2013). *Analysis of Complex Diseases: A Mathematical Perspective*. CRC Press.

[297] Weinberg, R. (2013). *The biology of cancer*. Garland science.

[298] Whitman, S. P., Archer, K. J., Feng, L., Baldus, C., Becknell, B., Carlson, B. D., Carroll, A. J., Mrózek, K., Vardiman, J. W., George, S. L., et al. (2001). Absence of the wild-type allele predicts poor prognosis in adult de novo acute myeloid leukemia with normal cytogenetics and the internal tandem duplication of flt3. *Cancer research*, 61(19):7233–7239.

[299] Wilkie, K. P. and Hahnfeldt, P. (2013). Tumor–immune dynamics regulated in the microenvironment inform the transient nature of immune-induced tumor dormancy. *Cancer research*, 73(12):3534–3544.

[300] Xie, M., Lu, C., Wang, J., McLellan, M. D., Johnson, K. J., Wendl, M. C., McMichael, J. F., Schmidt, H. K., Yellapantula, V., Miller, C. A., et al. (2014). Age-related mutations associated with clonal hematopoietic expansion and malignancies. *Nature medicine*, 20(12):1472–1478.

[301] Yamada, Y., Haga, H., and Yamada, Y. (2014). Concise review: dedifferentiation meets cancer development: proof of concept for epigenetic cancer. *Stem cells translational medicine*, 3(10):1182–1187.

[302] Yan, H., Romero-López, M., Benitez, L. I., Di, K., Frieboes, H. B., Hughes, C. C., Bota, D. A., and Lowengrub, J. S. (2017). 3d mathematical modeling of glioblastoma suggests that transdifferentiated vascular endothelial cells mediate resistance to current standard-of-care therapy. *Cancer Research*, pages canres–3094.

[303] Yao, J.-C. and Link, D. C. (2017). Concise review: The malignant hematopoietic stem cell niche. *STEM CELLS*, 35(1):3–8.

[304] Yeganefar, N. (2006). *Définitions et analyse de stabilités pour les systèmes à retard non linéaires*. PhD thesis, Ecole Centrale de Lille; Université des Sciences et Technologie de Lille-Lille I.

[305] Zarrinkar, P. P., Gunawardane, R. N., Cramer, M. D., Gardner, M. F., Brigham, D., Belli, B., Karaman, M. W., Pratz, K. W., Pallares, G., Chao, Q., et al. (2009). Ac220 is a uniquely potent and selective inhibitor of flt3 for the treatment of acute myeloid leukemia (aml). *Blood*, 114(14):2984–2992.

[306] Zhang, C. C. and Lodish, H. F. (2008). Cytokines regulating hematopoietic stem cell function. *Current opinion in hematology*, 15(4):307.

[307] Zhang, X., Su, J., Jeong, M., Ko, M., Huang, Y., Park, H. J., Guzman, A., Lei, Y., Huang, Y.-H., Rao, A., et al. (2016). Dnmt3a and tet2 compete and cooperate to repress lineage-specific transcription factors in hematopoietic stem cells. *Nature Genetics*, 48(9):1014–1023.

[308] Zhou, B. O., Ding, L., and Morrison, S. J. (2015). Hematopoietic stem and progenitor cells regulate the regeneration of their niche by secreting angiopoietin-1. *Elife*, 4:e05521.

Appendix A

A step-by-step interpretation of the pseudo-code generating the optimal drug infusion strategy

Underneath the synthetic version of the pseudocode that generates the optimal drug infusion strategy, presented in Algorithm 1, there are many procedures which are sequentially ordered with the aim of determining the optimal feasible therapeutic strategy. In this section, we provide a step by step explanation and illustration of Algorithm 1, together with a given number of algorithms, which are in fact already implicitly implemented in the general Algorithm 1. More specifically, the parts of Algorithms 1 that deserve to be highlighted will be in turn rigorously formulated as separated algorithms throughout the current section. Now we are ready to start, and we naturally begin with the initialization statements in our program.

The initialization step consists in giving the fixed system parameters, structures and functions, also the initial states, the characteristic patters of the switching variables -which is certainly the key point-, as well as some program initial instructions like the therapy objectives (M^* and the `Confidence_area`) which are set by the health professionals. With a bit more detail, the initialization step involves:

- A set of positive adequate parameters. **(1) For HSCs:** γ (apoptosis rate), τ (cell-cycle actual duration), K (rate of differentiation to the lineage of interest), L (rate of self-renewing), δ (rate of death and differentiation to other lineages), f (mitosis function), $\beta(0)$, b, $\mathfrak{n}$ (parameters of the re-introduction function β). **(2) For mature cells:** μ (the degradation rate).

- The evolution profiles of the controlled biological parameters with respect to growth-factors concentrations:
  The step-like pattern: $\mathfrak{e}_2 \to \beta(\mathfrak{e}_2, 0)$, $\mathfrak{e}_3 \to \gamma(\mathfrak{e}_3)$, and, $\mathfrak{e}_4 \to K(\mathfrak{e}_4)$. An example of these evolution profiles is given in Figure 7.16.

- The size of the `Confidence_area` and the `Limit_area` are specified. It may be argued that the instructions related to the therapy objectives may depend on the diagnosis of the patient. In this case, the `Confidence_area` and the `Limit_area` are specified in the last step of the initialization phase.

Algorithm 1: The general outline of the procedure operated by the Unit of Control (UC) for the search of an optimal strategy of stabilization through multiple drug infusions

Input: Initial model parameters and explicit dependence patterns between the controlled parameters and their growth-factors concentrations. The reference M^* and the time-span between blood tests

Output: The optimized therapeutic strategy to stabilize the HSCs and mature cells total densities at a desired final steady state

Initialization: system parameters and functions, initial states, and characteristic patters

The hematopoietic system structure. The set of fixed parameters and functions of the model

The prescribed reference M^*, the prescribed `confidence_area`, and, `limit_area`

The evolution profiles of the controlled functions $\mathfrak{c}_2 \to \beta(\mathfrak{c}_2, 0)$, $\mathfrak{c}_3 \to \gamma(\mathfrak{c}_3)$, $\mathfrak{c}_4 \to K(\mathfrak{c}_4)$

Network construction:

From the first medical testings, identify the parameters of the initially activated subsystem

Identify all the hematopoietic subsystems for all the possible parameter combinations

Identify the subsystems that have strictly positive steady states inside the `limit_area`

Identify the subclass of systems that have *stable* strictly positive steady states

Set up the network connections between all the subsystems

Determine the `Goal` set using the prescribed reference M^* and `confidence_area`

if `Goal` $= \varnothing$ **then**

  return *Failure*

else

  if $M_e^{(0)}$ *is not a stable node* **then**

    Find in the neighborhood of $M_e^{(0)}$ the *cheapest* path leading to a stable node M_s

    Save the therapeutic action leading from $M_e^{(0)}$ to M_s then consider that $M_e^{(0)} \leftarrow M_s$

  else

    Continue

Real-time tracking and processing

for $i \leftarrow 1$ ***to*** `length(Goal)` **do**

  Initialize the `Open_list` with $M_e^{(0)}$. Initialize the `Closed_list` with unstable points, stable points $\notin$ `limit_area`, and points in `Goal` that are different from `Goal`(i)

  The cost of switching from $M_e^{(0)}$ to itself is set to $G\left(M_e^{(0)}, M_e^{(0)}\right) = 0$

  Compute the (Manhattan-like distance) heuristic between `Goal`(i) and each stable steady state which is inside the `limit_area` and outside the `confidence_area`

  while `Open_list` $\neq \varnothing$ **do**

    `Current_target` takes the point that has the lowest F value ($F = H + G$)

    Discover the `Successors` which are the neighbors of `Current_target`

    Ignore the neighbors in `Successors` that already belong to `Closed_list`

    Add the first-time discovered nodes in `Successors` to the `Open_list`

    Pop off `Current_target` from `Open_list` and add it to `Closed_list`

    for $j \leftarrow 1$ ***to*** `length(Successors)` **do**

      if $G(\texttt{Current\_target}) + G\left(\texttt{Current\_target}, \texttt{Successors}(j)\right) \geq G\left(\texttt{Successors(j)}\right)$ **then**

        Continue

      else

        (`Current_target` $\leftarrow$ `Successors`(j)). Cost(node)=Cost

  $\texttt{Therapeutic\_strategy}_i = \left[M_e^{(0,0,0)}, \texttt{Best\_neighbor}_1^i, \texttt{Best\_neighbor}_2^i, \ldots, \texttt{Goal}(i)\right]$

`Therapeutic_strategy` $\leftarrow$ the best strategy between the "i" strategies (`Therapeutic_strategy_`i)

return `Therapeutic_strategy`

`Time out during the treatment` ($T_{\text{treatment}}$ days)

Monitoring the patient's conditions after treatment was completed

if *Post-therapeutic analyzes reveals that* $M_e^{post\_therapy}$ *is stable and respects the* `Confidence_area` **then**

  return *Therapy has been a success!*

else

  Learn from past experience and loop to **Initialization**

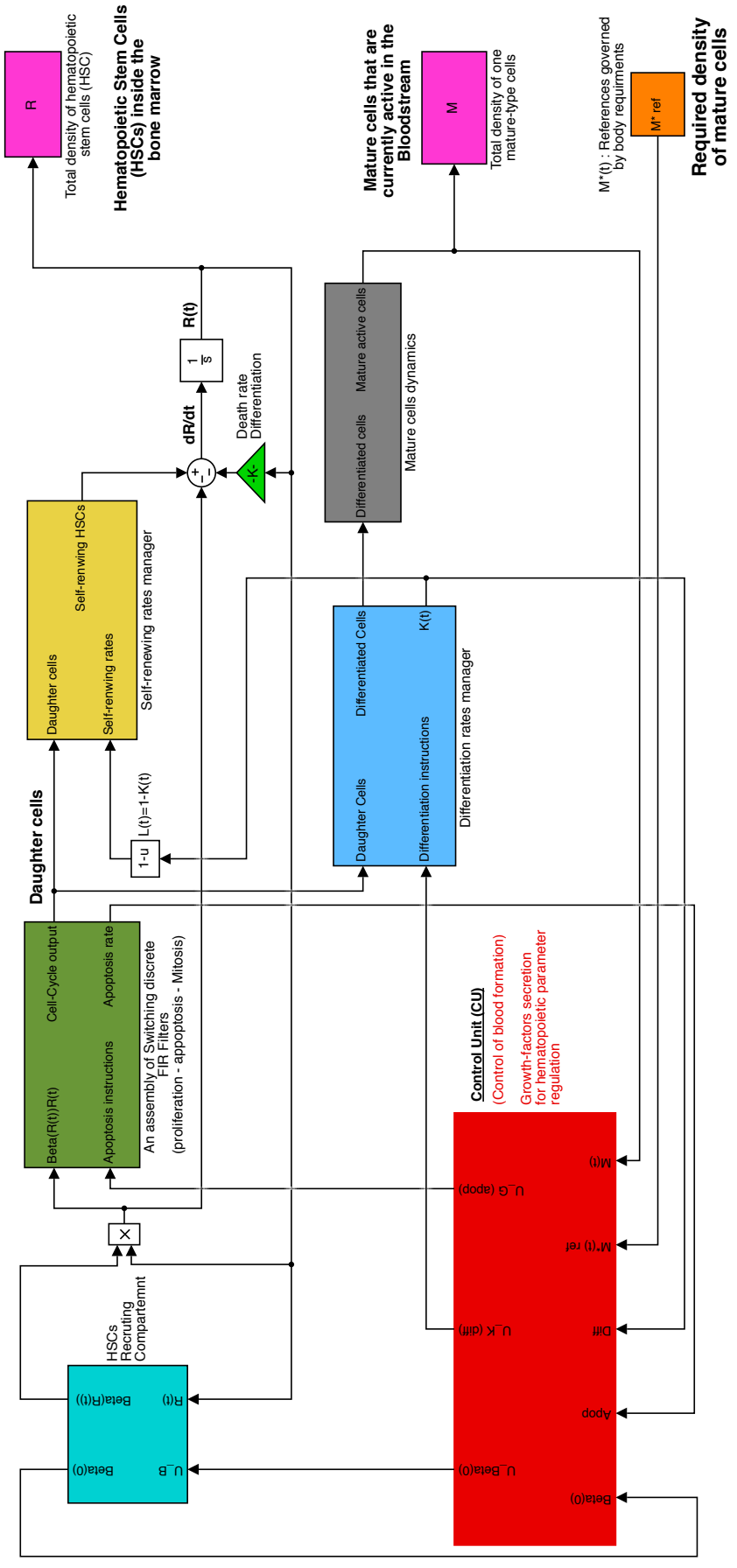

Fig. A.1 A diagram illustration of the architecture of the hematopoietic system that involves a unit of control and decision (the red box, Control Unit (CU)). It is a general architecture diagram that may apply (under slight modifications) in healthy and unhealthy hematopoiesis. It describes the HSCs dynamics R and the mature cells dynamics M. The orange block M^* is a reference generator related to the external environment. We observe that the CU is giving instructions to control the apoptosis rates (the green block represents the cell-cycle or the growth phase of the HSCs), it also affects the HSCs recruitment and differentiation mechanisms. We recall that the self-renewing rates are implicitly controlled by the CU through differentiation rates. One of the peculiarities of the unhealthy case is that the M^* is prescribed by the health professionals and the inputs of the CU, i.e. the effective parameter values and the total cell densities, are accessible only at specific time instants T_k, through blood tests.

The analysis of the results of the initial tests of the patient: In this regard, it is worth bearing in mind that a type of blood disorder is identified by the health professionals after one or more medical testings. These are of one-off and temporary measures that for our part we assume to occur every T_k days ($k \in \mathbb{N}$, not necessarily uniformly distributed). Thus, from the data collected and processed at T_0, we assume that it is possible to identify the initial total densities of HSCs and mature cells of interest (e.g. white blood cells), as well as their respective initial estimated parameters. Therefore, the monitoring of the initial parameter values gives the vector of the controlled parameters at the initial state, that we denote:

$$k \leftarrow 0, \quad \left[\beta^{(0)}, \gamma^{(0)}, K^{(0)}\right] \leftarrow \left[\beta(T_k, 0), \gamma(T_k), K(T_k)\right].$$

In the early phase of the construction of the nodes network (see Figure A.2), the `Limit_area` is clearly specified, the starting point $M^{(0)}$ is identified from initial tests, and the prescribed reference M^* together with its `Confidence_area` are defined (as therapy objectives).

Fig. A.2 Inside the `Limit_area` there is the starting point $M^{(0)}$, the prescribed reference M^* and the `Confidence_area`.

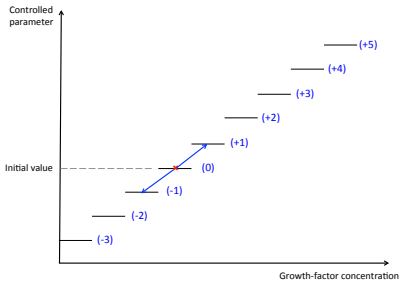

Fig. A.3 In this cartoon illustration, the exact value of p is 5. It would have been the same value if the jumps were in the opposite sense (i.e. from -5 to $+3$).

While referring to the step-like characteristic patterns giving the discrete values of the biological parameters, it is easy to determine the value of the integer p, which represents the **maximum** number of jumps that a biological parameter can perform in the increasing sense or in the decreasing one (see Figure A.3). In fact, this task can be avoided and the value of p can be initially set at an arbitrary large value that guarantees the maximum expansion of the network. On the other hand, the network expansion can be limited if p is forced to a value which is lower than its maximum possible one. In fact, p is a technical detail that is principally used to quantify the possible maximum number of nodes in the resulting networks and more importantly for notational convenience in the optimal pathway search algorithm as illustrated in the sequel.

In Figure A.3, we expect that each possible value taken by the controlled parameter represents in fact a distinct hematopoietic system, that may have a stable positive steady state which is in fact a node in our network. Our case is slightly more complicated since we are studying the case in which multiple parameters are varying under the control of different growth-factors or drugs (see Figure A.4). It is convenient to consider p as the maximum value of the individual distinct values for all the controlled parameters. We reiterate that p is simply suitable for the general statements of the Algorithms.

However, the legitimate question that raises is rather to know how to determine the adequate size of the network (i.e. the maximum expansion) measured by the number of effective nodes involved in

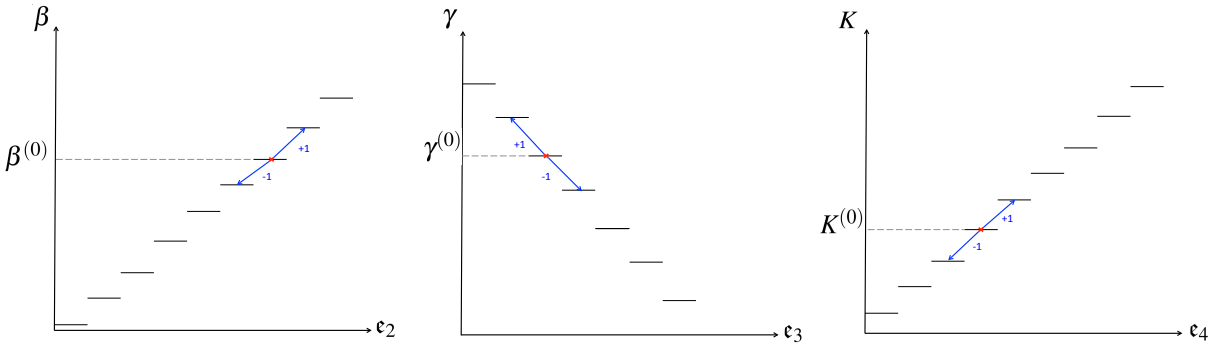

Fig. A.4 Cartoon illustration of the case of evolution profiles of three parameters: $\beta(0)$, γ and K, as it is the case in our statement. Each parameter is controlled by its own growth-factor. Since each parameter has its particular growth-factor, it follows that the variations of each controlled functionality is independent from the bahavior of the others.

it. By "adequate" we mean that a good compromise between optimal paths towards the goal nodes and the corresponding computational cost may be guaranteed. That is without doubt a problem-specific and no systematic rule can be stated, for the following reasons. Indeed, we can determine the exact number of nodes that can exist, i.e., the number of triplets $\left(\beta(0),\gamma,K\right)$ (which is overestimated by $(2p+1)^3$). However, the number of effective nodes generated by the latter triplets can be highly variable in our application. This is simply because the triplets selection are notably combined with the fixed model parameters (δ, τ,...), and all together require to satisfy strong nonlinear conditions in order to be retained as effective nodes involved in the final network. More precisely, for a triplet of controlled parameters, together with the fixed model parameters, will define a unique hematopoietic subsystem. Then, the requirements for that subsystem to be represented by one node in our network is that the following conditions hold true: i) the condition of existence of the strictly positive steady state: $\delta < \left(2(1-K(\mathfrak{e}_4))\int_0^\tau f(\ell)e^{-\gamma(\mathfrak{e}_3)\ell}d\ell\right)\beta(\mathfrak{e}_2,0)$, ii) The positive steady state does not go beyond the `Limit_area`, and, iii) the stability condition of the strictly positive steady state:

$$\delta - \frac{\partial}{\partial R}\left[\frac{\beta(\mathfrak{e}_2,0)R}{1+bR^{\mathfrak{n}}}\right]_{R=R_e} + 2(1-K(\mathfrak{e}_4))\left|\frac{\partial}{\partial R}\left[\frac{\beta(\mathfrak{e}_2,0)R}{1+bR^{\mathfrak{n}}}\right]_{R=R_e}\right|\int_0^\tau f(\ell)e^{-\gamma(\mathfrak{e}_3)\ell}d\ell > 0.$$

Therefore, according to the initial fixed model parameters and the characteristic patterns of the controlled ones, a given number of triplets is rejected during the network construction step. Furthermore, we will see that the choice of the prescribed reference M^* and the `Confidence_area` are also important elements to assess how effective is the proposed network. Indeed, even if we fix the number of nodes, it sometimes happens that many edges exist to connect the major part of the vertices, while some of them are less accessible (or completely isolated). This specific case will be illustrated in numerical simulations.

In addition, we precise that a construction without a goal is automatically rejected. In other words, a nodes network that does not contain at least one of its nodes inside the `Confidence_area` is useless. Next, a very limited nodes network (i.e. whose expansion has been limited after few iterations), and even if it involves nodes that belong to the `Confidence_area`, has certainly more chance to provide *better* and *cheapest* therapies if its expansion is increased.

We provide a generally comprehensive illustration in Figure A.5. Actually, here we want to represent the key ideas in a simple way, where we start from the point $M_e^{(0)}$. The first expanding operation creates less than $3^3 - 1 = 26$ since a part of triplets does not generate positive steady states. In this first iteration two nodes are outside the `Limit_area`, and will be rejected. All the nodes retained in the first iteration will be expanded in the next one. Here again, the way of representing the resulting nodes is caricatured since in fact many of the points created in the first iteration will be re-discovered during the second one. For instance, let us assume that among the retained nodes in the first iteration we have $M_e^{(+1,+1,0)}$ and $M_e^{(0,1,0)}$. We notice that when expanding one of them we re-discover the other one. However both of them allow emergence of novel nodes (e.g. $M_e^{(0,+2,0)}$ is one possible successor of both of them, while $M_e^{(+2,+2,-1)}$ can be a neighbor of the former point exclusively). Finally, we notice that in this example three nodes are inside the `Confidence_area`, that we group in the vector `Goal`. In fact, the way to perceive the nodes network depends entirely on which node in `Goal` is selected, as illustrated later in the part dealing with pathfinding techniques.

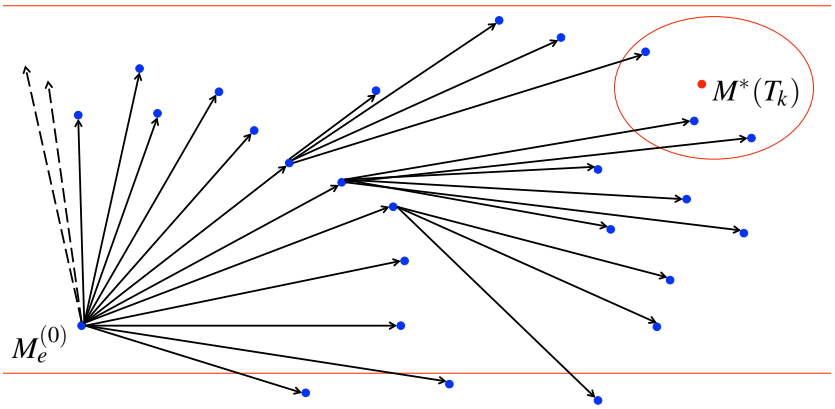

Fig. A.5 Cartoon depicting of one expected nodes network. The connections are not well-reproduced but it is to show the expansion after each iteration. The first iteration is the one that moves each parameter at the most by one step. The second iteration goes beyon this limit in the sense that new neighbors (involving +2 parameters) appear, while many common nodes will be shared. The objective is to achieve a network with reasonable size and at least one element inside the `Goal`-set, i.e. satisfying the `Confidence_area` requirements.

Using the evolution profiles and p, the vector $\mathscr{P}$ that contains all the possibly existing parameter combinations -without distinction- is created. In fact, the set $\mathscr{P}$ of possible combinations contains all the triplets of parameters, such that each possible one defines a distinct hematopoietic subsystem that could exist or not. Next, we notice that even for the existing triplets of parameters (i.e. existing hematopoietic subsystems), only a part of them will satisfy the condition of existence of the strictly positive steady states for the HSCs subpopulation. Then, we create the vector $\mathscr{M}$ that contains in an ordered sequence (according to $\mathscr{P}$) all the equilibrium points M_e that can be achieved -without distinction-. However, as previously explained, many of these points may not exist (we recall it: because the triplets do not exist, or, even if the triplet of parameters exist, it is not guaranteed that the associated hematopoietic subsystem has a positive steady state, and when it exists, it can be outside the `Limit_area`). For that reason, we need to

create the vector containing the **stable**[1] steady states. This vector containing the *effective* nodes is called $\mathscr{M}_{eff}$. The process described above is illustrated in the following memory segments (see Figure A.6 and Algorithm 2).

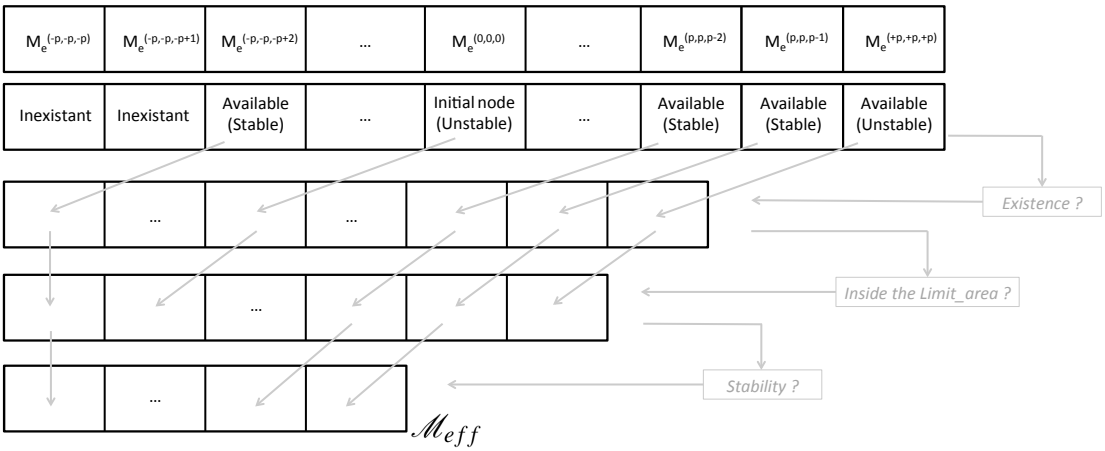

Fig. A.6 $\mathscr{M}_{eff}$ is obtained through a process of elimination of non-existing and undesirebale nodes.

Now, we remind that some data (which are the references given by the health professionals for all $t \geq 0$, and the system states and parameters at specific time instants T_k) are accessible. From them, we consider that once the vector $\mathscr{M}_{eff}$ is obtained, it comes to the vector $\mathscr{D}_{sort}$, as listed in Algorithm 2. Quite simply, it is about the search of the points in $\mathscr{M}_{eff}$ which are inside the `Confidence_area`. For that, we measure the distance between each point in the vector $\mathscr{M}_{eff}$ and the reference $M^*(T_k)$, given at $T_k \geq 0$. Then, we sort the vector $\mathscr{D}_{sort}$ in ascending order, i.e., from the smallest distance to the largest one. Technically (think about the implementation aspects), it is important to be able to connect each distance in $\mathscr{D}_{sort}$ to, first, its related point in $\mathscr{M}_{eff}$, and then to its initial location in $\mathscr{M}$. Indeed, since the position of the corresponding point in the vector $\mathscr{M}$ is entirely and uniquely determined by p, it follows that we can recursively determine the corresponding triplets of parameters. In the light of this observation, Algorithm 2 operates as follows (see also Figure A.7).

First, we keep track on the switching parameters by storing their values in a new vector $\mathscr{A}$, according to the effective M_e's values and positions in the $\mathscr{M}$ vector. Consequently, for each retained M_e in $\mathscr{M}_{eff}$, three values are added to $\mathscr{A}$, which are actually the corresponding triplet $\beta(0)$, γ and K, **in this order** (each triplet of parameters defines a distinct available hematopoietic system with a valid M_e node candidate). Then, the vector $\mathscr{D}_{sort}$ stores the distances ($d = |M_e - M^*|$) and records the corresponding

[1] In the case of healthy hematopoiesis that we will discuss in the next section, we will use from the begging the vector of positive stable steady states since the switching is allowed only between hematopoietic subsystems that possess stable strictly positive steady states.

model parameters as illustrated in Figure A.7. We observe that: $\texttt{length}(\mathscr{A}) = 3\texttt{length}\left(\mathscr{M}_{eff}\right)$ and $\texttt{length}(\mathscr{D}_{sort}) = \texttt{length}\left(\mathscr{M}_{eff}\right) + \texttt{length}(\mathscr{A})$.

Algorithm 2: Network construction

Input: Initial model parameters and explicit dependence patterns between the controlled parameters and their growth-factors concentrations. The reference M^* and the time-span between blood tests

Output: The nodes network

The parameters: μ, γ, τ, K, L, δ, $\beta(0)$, b, n, and the function f.

The evolution profiles of the controlled biological parameters

The `Confidence_area` and the `Limit_area`

Monitoring the reference of mature cell density $M^*(t)$, for all $t \geq 0$

Monitoring the controlled parameters, $\beta(t,\cdot) = \beta(\mathfrak{e}_2(t),\cdot)$, $\gamma(t) = \gamma(\mathfrak{e}_3(t))$, and, $K(t) = K(\mathfrak{e}_4(t))$, at specific time instants T_k, $k \in \mathbb{N}$

Observing the total density of HSCs, $R(t)$ and the total density of mature cells $M(t)$, at specific time instants T_k, $k \in \mathbb{N}$

First medical testings: $k \leftarrow 1$, $\left[\beta^{(0)}, \gamma^{(0)}, K^{(0)}\right] \leftarrow \left[\beta(T_k,0), \gamma(T_k), K(T_k)\right]$

Compute $R_e^{(0)}$, $M_e^{(0)}$, $d^{(0)}(T_k) = \left|M_e^{(0)} - M^*(T_k)\right|$

$\mathscr{P} \leftarrow \left[\left(\beta^{(-p)}, \gamma^{(-p)}, K^{(-p)}\right), \ldots, \left(\beta^{(-1)}, \gamma^{(-1)}, K^{(-1)}\right), \ldots, \left(\beta^{(+1)}, \gamma^{(+1)}, K^{(+1)}\right), \ldots, \left(\beta^{(+p)}, \gamma^{(+p)}, K^{(+p)}\right)\right]$

Compute the vector $\mathscr{R}$ of HSCs positive steady states, for each parameter combination from $\mathscr{P}$:

for $i \leftarrow 1$ ***to*** $\texttt{length}(\mathscr{P})$ **do**

  $\mathscr{R} \leftarrow \left[R_e^{(-p,-p,-p)}, \ldots, R_e^{(-1,-1,-1)}, \ldots, R_e^{(0,0,-1)}, R_e^{(0)}, R_e^{(0,0,+1)}, \ldots, R_e^{(+1,+1,+1)}, \ldots R_e^{(+p,+p,+p)}\right]$

Compute the vector $\mathscr{M}$ of positive steady states of mature cells for each **existing** element in $\mathscr{R}$

$\mathscr{M} \leftarrow \left[M_e^{(-p,-p,-p)}, \ldots, M_e^{(-1,-1,-1)}, \ldots, M_e^{(0,0,-1)}, M_e^{(0)}, M_e^{(0,0,+1)}, \ldots, M_e^{(+1,+1,+1)}, \ldots M_e^{(+p,+p,+p)}\right]$

Exclude the strictly positive steady states that do not exist, or do not belong to `Limit_area`, or unstable

$\mathscr{M}_{eff} \leftarrow \mathscr{M} - \{M_e \notin \texttt{limit\_area}\} - \{M_e \text{ unstable}\}$, while storing the parameters in $\mathscr{A} \leftarrow \left[a_1, a_2, a_3, \ldots, a_{3\texttt{length}(\mathscr{M}_{eff})}\right]$

Such that: $[a_1, a_2, a_3] \leftarrow \texttt{attributes\_}\mathscr{M}_{eff}(1), \ldots, [a_{3k-2}, a_{3k-1}, a_{3k}] \leftarrow \texttt{attributes\_}\mathscr{M}_{eff}(k), \quad \forall k \leq \texttt{length}(\mathscr{M}_{eff})$

Compute the vector measuring the distance between each point of $\mathscr{M}_{eff}$ and the reference $M^*(T_k)$, then sort it in ascending order, while keeping track on parameter switching by storing their values in ordered sequences

$\mathscr{D}_{sort} \leftarrow \left[(d_{\min}, \texttt{attributes\_}d_{\min}), \ldots, (d_{\max}, \texttt{attributes\_}d_{\max})\right]$

Create the vector `Goal` that contains the stable steady states from $\mathscr{M}_{eff}$ which are inside the `confidence_area`

$i \leftarrow 1$, $i' \leftarrow 1$

for $i \leftarrow 1$ ***to*** $\texttt{length}(\mathscr{D}_{sort})$ **do**

if $\mathscr{D}_{sort}(i) < \texttt{confidence\_area}$ **then**

  $\texttt{Goal}(i') \leftarrow M_e^{\texttt{attributes\_}d_i}$, $\left[\texttt{Goal}(i'+1), \texttt{Goal}(i'+2), \texttt{Goal}(i'+3)\right] \leftarrow \texttt{attributes\_}d_i$, $i' \leftarrow i'+4$, $i \leftarrow i+4$

else

  $i \leftarrow i+4$

if $\texttt{Goal} = \varnothing$ **then**

  return *Failure*

else

  return *Nodes networks constructed successfully*

Once these basic instructions are executed, we can determine one or more node networks. As previously mentioned, we simply consider that the nodes are the stable steady states belonging to $\mathscr{M}_{eff}$. However, what lurks, in reality, behind each node is a unique hematopoietic subsystem of HSCs and mature cells which is fully defined by the triplets $\left(\beta(0), \gamma, K\right)$ defining the node in question (the triplets are what we called `attributes` in Figure A.7). Next, using the vector $\mathscr{D}_{sort}$ we can determine (as shown in Algorithm 2) the vector `Goal` that contains the nodes of $\mathscr{M}_{eff}$ which are inside the `Confidence_area`. Clearly, if $d_{\min} >$ `Confidence_area`, then $\texttt{Goal} = \varnothing$, which means that the problem is ill-defined and the initial setting problems need to be revised (e.g. we have to revisit the prescribed favourable state M^*, to increase the integer p). In some singular situations (we will evoke one later in numerical examples), it is possible that it exists at least one point in `Goal`, but without any path (a succession of feasible edges that connect the nodes) to reach it. In that case it is better to focus on the other possibilities inside `Goal` or to increase the size of the network which creates in turn more suitable edges and vertices in the network.

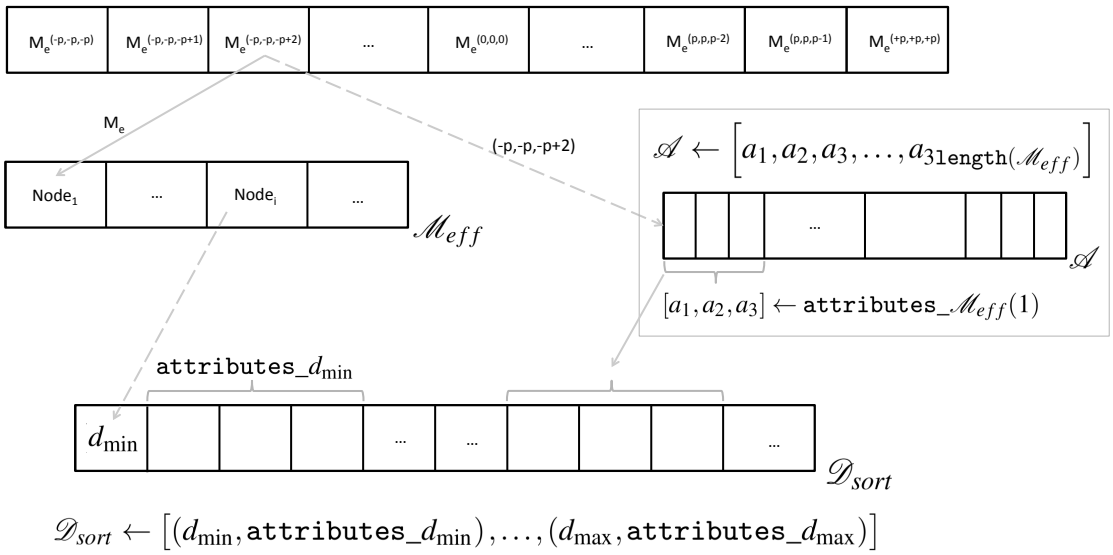

Fig. A.7 The construction of $\mathscr{D}_{sort}$ while storing the corresponding switching model parameters

For the sake of brevity, we will not spread too much on the case in which $M^{(0,0,0)}$ is an unstable steady state (which is more likely to be the case in unhealthy hematopoiesis) because several ways of interpretation may be envisaged. As previously mentioned, we just chose the path with minimum network expansion that leads to a stable node $M_s \in \mathscr{M}_{eff}$, then we pursue the reasoning as if $M_s = M^{(0,0,0)}$, in order to answer the crux of the problem: how to find the best therapeutic strategy to reach a suitable point belonging to `Goal`, from any starting point in $\mathscr{M}_{eff}$.

Remark 48. *The construction of the network we have just discussed is a bit technical, but without presenting any difficulty. This technicality results from the nature of our haematopoietic system. Indeed, these developments have a single objective, which is to determine the hematopoietic nodes network as presented in Figure 7.18 on the right, while still keeping a parallel 3D-construction as in Figure 7.18 on the left. This is striking for instance in Figure A.7, where the vector $\mathscr{M}_{eff}$ gives the nodes M_e (the stable steady states of the total density of mature cells), and the vector $\mathscr{A}$ contains the 3D coordinates of each $M_e \in \mathscr{M}_{eff}$. These steps are essential for establishing the optimal stabilization strategy (i.e. the origin of the switching signal in our overall hematopoietic system in Table-7.4. The next step is a classical application of a search algorithm on the resulting hematopoietic network (see Algorithm 3).*
In fact, we have as many hematopoietic networks as the number of nodes in the `Goal` *vector. We thus determine an optimal strategy for each point in* `Goal`*, then the overall strategy is the one with the least cost between all the strategies,*

$$\mathtt{Therapeutic\_strategy} \leftarrow \min_{i \in \{1,\ldots,\mathtt{length(Goal)}\}} \{\mathtt{Therapeutic\_strategy\_}i\}.$$

Algorithm 3: Exploration of the hematopoietic network

Input: Data (Input and Output) from Algorithm 2
Output: The optimal therapeutic strategy

if $\texttt{Goal} = \varnothing$ **then**
  Return to **Initialization**: increase p or change `Confidence_area`
else
  For each point in `Goal`, identify its corresponding nodes network and features, then search the best therapeutic strategy
  $\texttt{Total\_cost} \leftarrow 0$, `weighted_cost1`, `weighted_cost2`, `weighted_cost3`
  for $i \leftarrow 1$ ***to*** $\texttt{length(Goal)}$ **do**
    $G \leftarrow \texttt{Goal}(i)$, $\texttt{Closed\_list} \leftarrow \left\{M_e^{(0,0,0)}\right\}$, $\texttt{Cost}\left(M_e^{(0,0,0)}\right) = 0$, $\texttt{Open\_list} \leftarrow \mathscr{M}_{eff} - \texttt{Closed\_list}$
    while $\texttt{Current\_target} \neq \texttt{G}$ **do**
      Use the *Manhattan distance* to compute the heuristic
      for $j \leftarrow 1$ ***to*** $\texttt{length}(\mathscr{M}_{eff})$ **do**
        $H(j) = \left|a_{3j-2} - \texttt{Goal}(i+1)\right| + \left|a_{3j-1} - \texttt{Goal}(i+2)\right| + \left|a_{3j} - \texttt{Goal}(i+2)\right|$
      $\texttt{Current\_target} \leftarrow M_e^{(0,0,0)}$
      List the immediate stable nodes in the neighborhood of `Current_target`
      $\texttt{Immediate\_candidates} = \texttt{Open\_list} \cap \texttt{Neighbors\_of\_current}$
      for $j \leftarrow 1$ ***to*** $\texttt{length(Immediate\_candidates)}$ **do**
        Compute the `Step_cost` from `Current_target` to each point in `Immediate_candidates`
        $c(j) = \sum_{m=1}^{3} \left(\left|\texttt{attribute}_m\texttt{(Current\_target)}\right| - \left|\texttt{attribute}_m\texttt{(Immediate\_candidates(j))}\right| \right)$
        if $c(j) = 1$ **then**
          $\texttt{Step\_cost}(j) = \texttt{weighted\_cost1}$
        else
          if $c(j) = 1$ **then**
            $\texttt{Step\_cost}(j) = \texttt{weighted\_cost2}$
          else
            $\texttt{Step\_cost}(j) = \texttt{weighted\_cost3}$
        Combine all the previous elements to compute for each point in `Immediate_candidates` the `Test_score`
        $\texttt{Test\_score}(j) = H(j) + \left(\texttt{Total\_cost} + \texttt{Step\_cost}(j)\right)$
      `Best_neighbor` with **minimum** `Test_score` becomes `Current_target`
      $\texttt{Current\_target} \leftarrow \texttt{Best\_neighbor}$, $\texttt{Total\_cost} \leftarrow \texttt{Total\_cost} + \texttt{Step\_cost}(j)$
    $\texttt{Therapeutic\_strategy}_i = \left[M_e^{(0,0,0)}, \texttt{Best\_neighbor}_1^i, \texttt{Best\_neighbor}_2^i, \ldots, \texttt{Goal}(i)\right]$
  Choose the best strategy:
  $\texttt{Therapeutic\_strategy} \leftarrow \min_{i \in \{1,\ldots,\texttt{length(Goal)}\}} \left(\texttt{Therapeutic\_strategy\_}i\right)$
  return `Therapeutic_strategy`
`Time out during the treatment` ($T_{\text{treatment}}$ days)
Monitoring the patient's conditions after treatment was completed
if *Post-therapeutic analyzes reveals that* $M_e^{post\_therapy}$ *is stable and respects the* `Confidence_area` **then**
  return *Therapy has been a success!*
else
  Learn from past experience then reschedule.

The algorithm version for healthy hematopoiesis

Now, we briefly evoke the version for healthy hematopoiesis (Algorithm 4). Differently from the unhealthy case, we consider for the healthy one that the reference $M^*(t)$ is always accessible for the growth-factor secretion centers (i.e. for all $t \geq 0$), since the body sets its own objectives (e.g. according to the external environment: altitudes, presence of infections, seasonal allergies, injury, etc). In addition, the monitoring of the hematopoietic system parameters and blood cell count is available in real-time (the role of kidney for instance). It is worth mentioning that the Rule 5 has an impact on the heuristic function in this case, and the algorithm Algorithm 4 computes differently the cheapest cost for each node to reach the reference. Several features can be added in this case, since the reference is available for all $t \geq 0$, an implementation

of a D^*-like algorithm can be more suitable, however, this is beyond the scope of the current work, so as not to lengthen it excessively. In the last section of this contribution, we provide a numerical illustration that includes all the main aspects evoked throughout the work.

Algorithm 4: The general outline of the procedure operated by the Unit of Control (UC) for the search of an optimal strategy of self-stabilization in healthy hematopoiesis

Input: Actual system parameters and explicit dependence patterns between the varying parameters and their growth-factors concentrations. The reference $M^*(t)$ for all $t \geq 0$.

Output: The required optimized switching strategy to self-stabilize the HSCs and mature cells total densities at a final steady state that meets the body expectations.

Initialization: system parameters and functions, initial states, and characteristic patters

The reference $M^*(t)$ that changes according to body requirements, the `Confidence_area`, and, `Limit_area`

The evolution profiles of the controlled functions $\mathfrak{e}_2 \to \beta(\mathfrak{e}_2, 0)$, $\mathfrak{e}_3 \to \gamma(\mathfrak{e}_3)$, $\mathfrak{e}_4 \to K(\mathfrak{e}_4)$

Network construction:

Body self-test to identify the actual situation and initially activated subsystem

Identify all the hematopoietic subsystems for all the possible parameter combinations

Identify the subsystems that have strictly positive steady states inside the `limit_area`

Identify the subclass of systems that have *stable* strictly positive steady states

Set up the network connections between all the subsystems

Determine the `Goal` set using the prescribed reference M^* and `confidence_area`

if `Goal` $= \varnothing$ **then**

  return *Failure*

else

  for $i \leftarrow 1$ ***to*** `length(Goal)` **do**

    Initialize the `Open_list` with $M_e^{(0)}$. Initialize the `Closed_list` with unstable points, stable points $\notin$ `limit_area`, and points in `Goal` that are different from `Goal`(i)

    The cost of switching from $M_e^{(0)}$ to itself is set to $G\left(M_e^{(0)}, M_e^{(0)}\right) = 0$

    Compute the (Manhattan-like distance) heuristic between `Goal`(i) and each stable steady state which is inside the `limit_area` and outside the `confidence_area`

    while `Open_list` $\neq \varnothing$ **do**

      `Current_target` takes the point that has the lowest F value ($F = H + G$)

      Discover the `Successors` which are the neighbors of `Current_target`

      Ignore the neighbors in `Successors` that already belong to `Closed_list`

      Add the first-time discovered nodes in `Successors` to the `Open_list`

      Pop off `Current_target` from `Open_list` and add it to `Closed_list`

      for $j \leftarrow 1$ ***to*** `length(Successors)` **do**

        if $G(\texttt{Current\_target}) + G\left(\texttt{Current\_target}, \texttt{Successors}(j)\right) \geq G\left(\texttt{Successors(j)}\right)$ **then**

          Continue

        else

          (`Current_target` $\leftarrow$ `Successors`(j))

    $\texttt{Regulation\_strategy}_i = \left[M_e^{(0,0,0)}, \texttt{Best\_neighbor}_1^i, \texttt{Best\_neighbor}_2^i \ldots Goal(i)\right]$

  Best regulation strategy:

  `Regulation_strategy` $\leftarrow$ the best strategy between the "i" strategies (`Regulation_strategy_`i)

Monitoring the evolution of $R(t)$, $M(t)$ and $M^*(t)$, $\forall t \geq 0$

if *The regulation is not successful or* $M^*(t)$ *changes its value* **then**

  Loop to **Initialization**

else

  Stay in `standby`

  if *New requirement* $M^*(t)$ *for any* $t \geq 0$ **then**

    Break `Stanby` and loop to **Initialization**

List of publications

Peer-Reviewed Journals

[1] **W. Djema**, C. Bonnet, F. Mazenc, J. Clairambault, E. Fridman, P. Hirsch, F. Delhommeau, *Control in Dormancy or Eradication of Tumor Stem Cells: Mathematical Modeling and Stability Issues*, *Journal of Theoretical Biology (JTB)*, **(2018)**.

[2] **W. Djema**, F. Mazenc, C. Bonnet, *Stability analysis and robustness results for a nonlinear system with distributed delays describing hematopoiesis*, *Systems & Control Letters*, Vol. 102, pp. 93-101, **(2017)**.

[3] E. Fridman, C. Bonnet, F. Mazenc, **W. Djema**, *Stability of the cell dynamics in Acute Myeloid Leukemia, Systems & Control Letters*, Vol. 88, pp. 91-100, **(2016)**.

[4] F. Mazenc, E. Fridman, **W. Djema**, *Estimation of solutions of observable nonlinear systems with disturbances*, *Systems & Control Letters*, Vol. 79, pp. 47-58, **(2015)**.

Peer-Reviewed Published International Conferences

[5] **W. Djema**, C. Bonnet, H. Özbay, F. Mazenc, L. Paulevé, *A Cell Density Stabilization Technique through Drug Infusions* Submitted to *Conference on Decision & Control (CDC)*, USA, **(2018).**

[6] **W. Djema**, F. Mazenc, C. Bonnet, J. Clairambault, E. Fridman, *Stability Analysis of a Nonlinear System with Infinite Distributed Delays Describing Cell Dynamics*, To appear in the proceedings of the American Control Conference (ACC), IEEE, **(2018)**.

[6] **W. Djema**, C. Bonnet, F. Mazenc, J. Clairambault, *Introducing Cell Plasticity Mechanisms into a Class of Cell Population Dynamical Systems*, To appear in the proceedings of the American Control Conference (ACC), IEEE, **(2018)**.

[7] **W. Djema**, H. Özbay, C. Bonnet, E. Fridman, F. Mazenc, J. Clairambault, *Analysis of Blood Cell Production under Growth Factors Switching*, To appear in the proceedings of the *IFAC World Congress (IFAC WC)*, Toulouse, France, **(2017).**

[8] **W. Djema**, C. Bonnet, J. Clairambault, F. Mazenc, P. Hirsch, F. Delhommeau, *Analysis of a Model of Dormancy in Cancer as a State of Coexistence Between Tumor and Healthy Stem Cells*, In Proceedings of the IEEE *American Control Conference (ACC)*, Seattle, USA, IEEE, **(2017)**.

[9] **W. Djema**, F. Mazenc, C. Bonnet, J. Clairambault, P. Hirsch, F. Delhommeau, *Stability of a Delay System Coupled to a Delay Differential-Difference System Describing the Coexistence of Ordinary and Mutated Hematopoietic Stem Cells*, In Proceedings of the IEEE 55th *Conference on Decision and Control (CDC)*, Las Vegas, Nevada, USA, pp. 561-566, IEEE, **(2016)**.

[10] **W. Djema**, F. Mazenc, C. Bonnet, *Stability Analysis of a Differential-Difference System Through a Linear Lyapunov Functional Design,* the 5th *International Symposium on Positive Systems (POSTA)*, Roma, Italy, **(2016)**.

[11] **W. Djema**, F. Mazenc, C. Bonnet, *Analysis of a Nonlinear Delay Differential-Difference Biological Model,* Proceedings of the *IFAC Time-Delay Systems (TDS)*, IFAC-PapersOnLine 49.10, pp. 246-251. Istanbul, Turkey, **(2016)**.

[12] **W. Djema**, F. Mazenc, C. Bonnet, *Stability of Immature Cell Dynamics in Healthy and Unhealthy Hematopoiesis,* Proceedings of the *American Control Conference (ACC)*, Boston, MA, USA, pp. 6121-6126, IEEE, **(2016)**.

[13] **W. Djema**, F. Mazenc, C. Bonnet, *Lyapunov Stability Analysis of a Model Describing Hematopoiesis*, Proceedings of the *European Control Conference (ECC)*, Linz, Austria, pp. 2711-2716, IEEE, **(2015)**.

Publications choisies.

Selected Publications.

Systems and Control Letters, Elsevier, (2017), 102, pp.93 - 101

Stability Analysis and Robustness Results for a Nonlinear System with Distributed Delays Describing Hematopoiesis.[☆]

Walid Djema[a], Frédéric Mazenc[a], Catherine Bonnet[a]

[a] *Inria, Université Paris-Saclay, L2S-CentraleSupélec, 3 rue Joliot Curie, 91192, Gif-sur-Yvette, France.* walid.djema@inria.fr
frederic.mazenc@l2s.centralesupelec.fr catherine.bonnet@inria.fr

Abstract

A nonlinear system with distributed delays describing cell dynamics in hematopoiesis is analyzed -in the time-domain- via a construction of suitable Lyapunov-Krasovskii functionals (LKFs). Two interesting biological situations lead us to re-investigate the stability properties of two meaningful steady states: the 0-equilibrium for unhealthy hematopoiesis and the positive equilibrium for the healthy case. Biologically, convergence to the 0-equilibrium means the extinction of all the generations of blood cells while the positive equilibrium reflects the normal process where blood cells survive. Their analyses are slightly different in the sense that we take advantage of positivity of the system to construct linear functionals to analyze the 0-equilibrium, while we use some quadratic functionals to investigate the stability properties of the positive equilibrium. For both equilibria, we establish the exponential stability of solutions and we provide an estimate of their rates of convergence. Moreover, a robustness analysis is performed when the model is subject to some nonvanishing perturbations. Numerical examples are provided.

Keywords: Delay, Positive system, Lyapunov, Stability, Biological model.

1. Introduction

With the ultimate goal of determining a model describing cell dynamics in acute myeloid leukemia, which will be of use for the optimization of polychemotherapies, we start here with a model describing the process of fabrication of blood which was studied in [1] and revisited by input-output methods in [16]. Using an alternative approach, our aim here is to deepen the analysis as well as to solve some open issues which are of importance in practice.

Through the process of hematopoiesis, the Hematopoeitic Stem Cells (HSCs) develop into red blood cells, white blood cells, platelets and all other blood cells.

[☆] Supported by **ALMA3** project on the 'Analysis of Acute Myeloid Leukemia', through DIGITEO, Paris-Saclay.

HSCs are immature unspecialized cells able to produce cells with the same maturity level and to differentiate into specialized cells. This is a simplified development scheme, which does not take into account other cell fates -increasingly highlighted in recent years- such as cell dedifferentiation [4]. In fact, the complex cascade of signals regulating hematopoiesis is not currently clearly identified. Therefore, the importance of this biological process has motivated many theoretical and experimental works that focus on the earliest generations of immature cells since they play a critical role in blood formation, and because they are the source of several hematological disorders. The long list of works devoted to blood cells dynamics includes [1], [2], [3], [13], [16], [17], [12], [18], and [8].

Acute Myelogenous Leukemia (AML) is a serious type of cancer, which is characterized by an overproduction of abnormal myeloblasts, simultaneously with an inability to develop further into mature white blood cells (a blockade in the maturation process). Due to their overproliferation, blasts invade the bone marrow and even - sometimes - the blood circulation (Figure 1-a), which prevents adequate production of mature healthy blood cells. Since we want to emphasize on AML, we consider that the model that we focus on describes the development hierarchy leading to white cell production in the myeloid lineage.

Relying on several essential contributions by Mackey and his colleagues ([12], [18], [13], to name but a few), Adimy *et al.* introduced and analyzed in [1] a nonlinear system with distributed delays to model cell dynamics in several maturity stages. This is the model we study here, considering that it describes a cancer state when some of its biological parameters are abnormal (i.e. being different from healthy parameters, or becoming time-varying to model the effect of appropriate infused drugs) and it reflects a healthy situation when all its parameters are normal. Using a Lyapunov technique we improve some existing results in two different contexts: i) we provide theoretical conditions to eradicate cancer cells in what we assume to be a basic unhealthy situation, and, ii) we ensure the survival of healthy cells in normal hematopoiesis. A key point that we emphasize here is that the Lyapunov direct method offers strong tools to study exponential convergence of solutions, estimates on their decay rates (for both steady states), as well as estimating the basin of attraction of the positive equilibrium point and this, in our opinion, improves the way to study the phenomenon of hematopoiesis (see the concluding remarks in [16]). On the other hand, the search for a suitable Lyapunov functional is generally quite difficult, since no systematic methods apply [14, 10], and that is the challenging problem that we are dealing with in this contribution.

The paper is organized as follows. In Section 2 we briefly present the model of interest. Section 3 is devoted to the study of the 0-equilibrium of the system. We establish global exponential stability even when some parameters are time-varying, then we perform a robustness analysis. The strictly positive equilibrium X^e of the nominal system is discussed in Section 4. An estimate of its basin of attraction is proposed via a construction of a novel Lyapunov functional, that also allows us to perform a robustness analysis of the perturbed system.

2. Description of the model and known results

We revisit from [1] the model described in Figure 1-b, where for all $i \in I_n = \{1, \dots, n\}$, $n \geq 1$, x_i denotes the total density of resting cells of generation i. A resting cell is a cell that is not actively in the process of dividing. The reintroduction function from resting into proliferating subpopulation of the i-th generation is denoted $\beta_i(\cdot)$. Proliferating cells can divide between the moment they enter the proliferating phase and a maximal age $\tau_i > 0$, while the apoptosis rate, γ_i, represents the death rate of proliferating cells of the i-th generation. At each division, a proportion K_i of dividing cells goes to the next resting stage of the development hierarchy of interest, while the other part ($L_i = 1 - K_i$) stays at the same level i (self-renewing process), with the convention that $K_0 = 0$. The constant δ_i covers both the death rate of the resting cells of the i-th generation, together with their differentiation into lineages that we do not focus on.

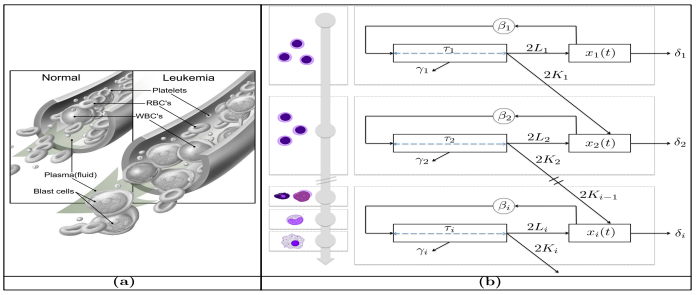

Figure 1: **(a)** Blast cells are not typically found in the circulating blood of healthy individuals. The picture is from the National Cancer Institute. **(b)** Schematic representation of the earliest stages in the myeloid lineage [1].

Finally, the dynamical system equation is in the form:

$$\begin{aligned} \dot{x}_i(t) = &- \delta_i x_i(t) - w_i(x_i(t)) + 2L_i \int_0^{\tau_i} g_i(a) w_i(x_i(t-a)) da \\ &+ 2K_{i-1} \int_0^{\tau_{i-1}} g_{i-1}(a) w_{i-1}(x_{i-1}(t-a)) da + \epsilon_i(t), \end{aligned} \tag{1}$$

for each compartment $i \in I_n$, and $t \geq 0$, with $w_i(x_i) = \beta_i(x_i)x_i$, $g_i(a) = e^{-\gamma_i a} f_i(a)$, where the f_is are $\mathcal{C}^1$ functions representing the cell division probability densities, such that $f_i(a) \geq 0$ for all $a \in [0, \tau_i]$, and $\int_0^{\tau_i} f_i(a)da = 1$, since it is assumed in [1] that the mitosis occurs before the age-limit τ_i. Moreover, biological facts induce that the parameters δ_i, L_i, K_i, τ_i and γ_i are positive for all $i \in I_n$, with $K_0 = 0$ and $K_i \in (0, 1)$ for all $i \in I_n$. The functions $\beta_i(\cdot)$ are assumed to be differentiable and decreasing functions such that $\lim_{a \to +\infty} \beta_i(a) = 0$. For a later use, we introduce the following parameters:

$$C_i = \int_0^{\tau_i} g_i(l) dl, \quad \text{and,} \quad \alpha_i = 2L_i C_i - 1, \tag{2}$$

where α_i is assumed to be strictly positive, for all $i \in I_n$ (see [16], Assumption 2). We will perform a robustness analysis of the model (1) under nonvanishing

perturbation terms $\epsilon_i(t) \in [0, \bar{\epsilon}_i]$, where $\bar{\epsilon}_i > 0$, for all $i \in I_n$ and $t \geq 0$. It is well-known that disturbances are in general due to the lack of accuracy when modeling the laws governing complex living organisms. More precisely, in the model that we study, uncertainty comes from the biological parameters and functions (e.g. the nonlinearity β_i, introduced in [12]), and from more complex phenomena which are difficult to model. In particular, the ability of differentiated cells to undergo lineage reversion (including dedifferentiation - the mechanism whereby differentiated cells regress to a less mature state [4] - and transdifferentiation from different types of cells and hierarchies) is not covered by the model illustrated in Figure 1-b. A basic representation of cells plasticity features is achieved by considering dedifferentiation and transdifferentiation as perturbation inputs. In fact, it can be proven that nonvanishing perturbations arise from cell plasticity, and uncertain re-introduction functions β_i, leading to system (1) with $\epsilon_i(t) \in (0, \bar{\epsilon}_i]$, for all $t \geq 0$.

Notation and definitions:
Throughout the paper, we analyze the stability of the model described by (1), where for all $i \in I_n = \{1, \ldots, n\}$, $x_i(t) \in \mathbb{R}^n$. The state of the system (1) at a time instant t is defined as the restriction of each component $x_i(t)$ of the solution $x(t) = (x_1(t), \ldots, x_n(t))$, on the segment $[t - \tau_i, t]$, for all $i \in I_n$. We let $x = (x_1, \ldots, x_n)$ and $\mathcal{C}_{\text{in}} = \mathcal{C}([-\tau_i, 0], \mathbb{R})$ denote the space of all continuous $\mathbb{R}$-valued functions defined on a given interval $[-\tau_i, 0]$, for all $i \in I_n$, and for all $t \geq 0$, the function x_{it} is defined by $x_{it}(m) = x_i(t + m)$ for all $m \in [-\tau_i, 0]$.

Finally, we notice that negative steady states are excluded from this study, as well as equilibria belonging to the boundaries of the positive orthant, except the origin, because of their biological irrelevance. We focus on two meaningful steady states: the 0-equilibrium denoted by $X^0 = (0, \ldots, 0)$ and the strictly positive equilibrium point denoted by $X^e = (x_1^e, \ldots, x_n^e)$, $x_i^e > 0$, for all $i \in I_n$.

We recall two simple but useful results (see [1] and [5]).

Proposition 1. *The solutions of the system (1) with positive initial conditions are positive.*

Proof. Since the nonvanishing perturbations $\epsilon_i(t)$, for all $i \in I_n$, satisfy $\epsilon_i(t) \geq 0$, for all $t \geq 0$, the proof that the positive orthant is forward invariant is similar to the one proposed in [5] for the nominal system. □

Concerning steady states for the nominal system (1), we notice that X^0 always exists. Next, without proof (available in [1] and [5]), we recall the necessary and sufficient condition of the existence of X^e of the nominal system (1):

Proposition 2. *The nominal system (1) admits a positive equilibrium point $X^e = (x_1^e, \ldots, x_n^e)$ if and only if:*

$$\beta_1(0) > \frac{\delta_1}{\alpha_1}. \tag{3}$$

Throughout Section 4, we will assume that the condition (3) is satisfied and we will analyze the stability properties of X^e using a new approach.

3. Stability analysis of the trivial steady state

3.1. Global exponential stability of the nominal system

We start by establishing global exponential stability of the origin X^0. As a corollary of this result, we prove exponential stability of X^0 when some biological parameters are uncertain or time-varying.

Theorem 1. *The nominal system (1) admits the origin, X^0, as a globally exponentially stable equilibrium point if for all $i \in I_n$, the inequalities*

$$s_i := \delta_i - (2C_iL_i - 1)\,\beta_i(0) > 0, \tag{4}$$

are satisfied. If

$$s_1 := \delta_1 - (2C_1L_1 - 1)\beta_1(0) < 0, \tag{5}$$

then no positive solution converges to X^0.

Remark 1. *i) We can readily check that if (4) is satisfied, then zero is the unique equilibrium of the nominal system (1). ii) Using a frequency domain approach, it was proved in [1] that if (5) is satisfied then the system is unstable, and that the conditions (4) guarantee local asymptotic stability of the origin. In [3], slightly more restrictive conditions than (4) (due to the fact that $L_i < 1$, for all $i \in I_n$) were given to ensure global asymptotic stability of the origin. In [5], we proved global asymptotic stability of X^0 under conditions (4). In Theorem 1 of the present paper, we extend the result of [5] to establish global exponential stability under conditions (4). iii) Even if the analytic expression of the Lyapunov functional that we will introduce in this section will be slightly different from the one used in [5], they share the common feature of being unusual since they are approximated at the origin by linear functions.*

Proof. First, let us pick a family of positive constants ρ_i, to be selected later, and define for all $i \in I_n$, the functionals

$$v_i(x_{it}) = \int_{t-\tau_i}^{t} \int_{m}^{t} e^{-\rho_i(t-m-\tau_i)} g_i(m+\tau_i-a) w_i(x_i(a)) da dm. \tag{6}$$

For all $i \in I_n$, the derivative of the functional (6) along the trajectories of the nominal system (1) satisfies

$$\begin{aligned}
\dot{v}_i(t) =& -\rho_i v_i(x_{it}) - \int_{t-\tau_i}^{t} g_i(t-a) w_i(x_i(a)) da + w_i(x_i(t)) \int_0^{\tau_i} e^{\rho_i a} g_i(a) da \\
\leq& -\rho_i v_i(x_{it}) - \int_{t-\tau_i}^{t} g_i(t-a) w_i(x_i(a)) da + w_i(x_i(t)) e^{\rho_i \tau_i} C_i,
\end{aligned}$$

where the last inequality is a consequence of (2). Let us introduce the following functional for the first compartment of hematopoietic stem cells:

$$\mathcal{V}_1(x_{1t}) = x_1(t) + 2L_1 v_1(x_{1t}). \tag{7}$$

Its derivative along the trajectories of the nominal system (1) satisfies

$$\dot{\mathcal{V}}_1(t) \leq -\delta_1 x_1(t) - 2L_1\rho_1 v_1(x_{1t}) - \left[1 - 2L_1 e^{\rho_1\tau_1} C_1\right] w_1(x_1(t)). \tag{8}$$

Since $\alpha_1 > 0$, we conclude that for all $\rho_1 > 0$, the inequality $2L_1 e^{\rho_1\tau_1} C_1 - 1 > 0$ is satisfied. Therefore, using $w_1(x_1(t)) \leq \beta_1(0)x_1(t)$, it follows from (8) that:

$$\dot{\mathcal{V}}_1(t) \leq -\left[\delta_1 - \left(2L_1 e^{\rho_1\tau_1} C_1 - 1\right)\beta_1(0)\right] x_1(t) - 2L_1\rho_1 v_1(x_{1t}). \tag{9}$$

Now, if (4) is satisfied, we choose $\rho_1 = \frac{1}{2\tau_1}\ln\left(\frac{\delta_1+\beta_1(0)+2L_1C_1\beta_1(0)}{4L_1C_1\beta_1(0)}\right)$. Then we obtain $\delta_1 - \left(2L_1 e^{\rho_1\tau_1} C_1 - 1\right)\beta_1(0) \geq \frac{s_1}{2}$. It follows that the inequality (9) gives $\dot{\mathcal{V}}_1(t) \leq -\frac{s_1}{2}x_1(t) - 2L_1\rho_1 v_1(x_{1t})$, and from the definition of $\mathcal{V}_1$, we get

$$\dot{\mathcal{V}}_1(t) \leq -\tilde{s}_1\mathcal{V}_1(x_{1t}) - \frac{s_1}{4}x_1(t), \tag{10}$$

with $\tilde{s}_1 = \min\left\{\frac{s_1}{4}, \rho_1\right\}$. Consequently, the origin of the subsystem $i = 1$ is globally exponentially stable. Next, in order to extend the result to the overall system, we introduce the following functional which takes into account the cells dynamics of the first and the second generations of immature cells:

$$\mathcal{V}_2(x_{2t}, x_{1t}) = x_2(t) + 2L_2 v_2(x_{2t}) + 2K_1 v_1(x_{1t}) + \frac{8K_1\beta_1(0)e^{\rho_1\tau_1}C_1}{s_1}\mathcal{V}_1(x_{1t}).$$

Using (10), we prove that the derivative of $\mathcal{V}_2$ along the trajectories of the nominal system (1) satisfies

$$\begin{aligned}\dot{\mathcal{V}}_2(t) \leq &-\delta_2 x_2(t) - \left(1 - 2L_2 e^{\rho_2\tau_2} C_2\right) w_2(x_2(t)) - 2L_2\rho_2 v_2(x_{2t}) \\ &- 2K_1\rho_1 v_1(x_{1t}) - \frac{8K_1\beta_1(0)e^{\rho_1\tau_1}C_1\tilde{s}_1}{s_1}\mathcal{V}_1(x_{1t}) \\ &- 2K_1 e^{\rho_1\tau_1} C_1\left[\beta_1(0) - \beta_1(x_1(t))\right] x_1(t).\end{aligned} \tag{11}$$

Using the assumption $\alpha_2 > 0$, together with the fact that the function β_2 is strictly decreasing, it follows that,

$$\begin{aligned}\dot{\mathcal{V}}_2(t) \leq &-\left[\delta_2 - \left(2L_2 e^{\rho_2\tau_2} C_2 - 1\right)\beta_2(0)\right] x_2(t) - 2L_2\rho_2 v_2(x_{2t}) \\ &- 2K_1\rho_1 v_1(x_{1t}) - \frac{8K_1\beta_1(0)e^{\rho_1\tau_1}C_1\tilde{s}_1}{s_1}\mathcal{V}_1(x_{1t}).\end{aligned} \tag{12}$$

When the conditions (4) are satisfied, we select $\rho_2 > 0$ (similarly to ρ_1), such that the inequality $\delta_2 - \left(2L_2 e^{\rho_2\tau_2} C_2 - 1\right)\beta_2(0) \geq \frac{s_2}{2}$, is satisfied. It follows from (12) that there exists a strictly positive constant $\tilde{s}_2$, such that

$$\dot{\mathcal{V}}_2(t) \leq -\tilde{s}_2\mathcal{V}_2(x_{1t}, x_{2t}) - \frac{s_2}{4}x_2(t), \tag{13}$$

is satisfied. Next, by induction, we easily check that there exist a positive constant $\tilde{s}_n$ and a family of strictly positive weighting constants λ_i and $\tilde{\lambda}_i$, such

that the derivative of the functional $\mathcal{V}(x_t) = \sum_{i=1}^{n} \left[\lambda_i x_i(t) + \tilde{\lambda}_i v_i(x_{it})\right]$, which is taking into account all the n generations of immature blood cells, along the trajectories of the nominal system (1), satisfies

$$\dot{\mathcal{V}}(t) \leq -\tilde{s}_n \mathcal{V}(x_t). \tag{14}$$

From the inequality (14) and the properties of the functional $\mathcal{V}$, we conclude that, if the conditions (4) are satisfied, the origin of the nominal model (1) is globally exponentially stable.

In order to complete the proof, we consider the case where the inequality (5) is satisfied and we show that no positive solution converges to X^0. As in [5], we prove this result by contradiction, i.e. we assume that a positive solution $x(t)$ converges to X^0. Now, we select $\rho_1 = 0$ and we observe that the derivative of the functional $\mathcal{V}_1$, introduced in (7), is given by

$$\dot{\mathcal{V}}_1(t) = \left[-\delta_1 + \alpha_1 \beta_1(x_1(t))\right] x_1(t). \tag{15}$$

When (5) is verified, using the facts that the function β_1 is decreasing and $x_1(t)$ converges to zero, we deduce that there exists $t_r > 0$ such that, for all $t \geq t_r$, $-\delta_1 + \alpha_1 \beta_1(x_1(t)) \geq \frac{-\delta_1 + \alpha_1 \beta_1(0)}{2}$. It follows from (15) that, for all $t \geq t_r$,

$$\dot{\mathcal{V}}_1(t) \geq \frac{-\delta_1 + \alpha_1 \beta_1(0)}{2} x_1(t). \tag{16}$$

From (5), and the positivity of the solutions, it follows that for all $t \geq t_r$, $\dot{\mathcal{V}}_1(t) > 0$. Consequently, we deduce that, for all $t \geq t_r$, $\mathcal{V}_1(x_{1t}) \geq \mathcal{V}_1(x_{1t_r}) > 0$. It follows that $\mathcal{V}_1(x_{1t})$ does not converge to zero. On the other hand, $\mathcal{V}_1(x_{1t})$ converges to zero because $x_1(t)$ converges to X^0. This yields a contradiction. □

Example 1. *A possible selection of the cell division probability densities, which was considered in [17] and [16], is given by* $f_i(a) = \frac{m_i}{e^{m_i \tau_i} - 1} e^{m_i a}$, *with* $m_i > 0$, *for all* $i \in I_n$. *Let us consider the following biological functions and parameters:*

	$\beta_i(x_i)$	$f_i(a)$	δ_i	L_i	τ_i	γ_i
$i = 1$	$\frac{1.22}{1+x_1^2}$	$\frac{5e^{5a}}{e^{5\tau_1}-1}$	0.9	0.85	1.2	0.22
$i = 2$	$\frac{1.33}{1+4x_2^4}$	$\frac{7e^{7a}}{e^{7\tau_2}-1}$	0.96	0.8	1.3	0.33

The form given to β_i *[12] normalizes the values taken by the total density* x_i. *Simple calculations give:* $(2L_1C_1 - 1)\,\beta_1(0) = 0.4448$, $(2L_2C_2 - 1)\,\beta_2(0) = 0.4392$. *Therefore, according to Proposition 2, the positive equilibrium of system (1) does not exist. Moreover, according to Theorem 1, the origin* $X^0 = (0, 0)$ *of system (1) is globally exponentially stable, as shown in Figure 2.*

3.2. Global exponential stability under time-varying differentiation rates

Convergence to X^0 means the eradication of all the immature blood cells. This case may be suitable when the model is assumed to describe the dynamics of unhealthy cells. Recall that one of the characteristics of leukemia is the blockade in the differentiation process, which becomes also a target for the drugs used in

treatments. From a theoretical point of view, it is interesting to consider the case where differentiation and self-renewing rates are uncertain or time varying.

In this part, we extend the result of Theorem 1 to the nominal model that describes the immature cell dynamics under time-varying differentiation rates, $K_i(t)$ for all $t \geq 0$, and $i \in I_n$, and which is given by

$$\begin{aligned} \dot{x}_i(t) = \; & 2K_{i-1}(t) \int_0^{\tau_{i-1}} g_{i-1}(a) w_{i-1}(x_{i-1}(t-a)) da \\ & + 2L_i(t) \int_0^{\tau_i} g_i(a) w_i(x_i(t-a)) da - \delta_i x_i(t) - w_i(x_i(t)), \end{aligned} \tag{17}$$

where $K_i(t) + L_i(t) = 1$ and $L_i(t) \in [L_{i\min}, L_{i\max}] \subset (0,1)$. We recall that, by convention, $K_0(t) = 0$, for all $t \geq 0$, and we assume that $K_i(\cdot)$, $L_i(\cdot)$ are of class C^0, for all $i \in I_n$. Based on Theorem 1, we prove the following result:

Corollary 1. *The conditions*

$$\overline{s}_i = \delta_i - (2L_{i\max} C_i - 1)\, \beta_i(0) > 0, \quad \forall i \in I_n, \tag{18}$$

ensure that the origin of the system (17) is globally exponentially stable.

Proof. We give some indications for the proof, which is slightly different from the one of Theorem 1. Here we consider $L_{1\max}$ instead of L_1 in the definition of the functional $\mathcal{V}_1(x_{1t})$ introduced in (7), and, similarly, we consider $L_{2\max}$, $K_{1\max} = 1 - L_{1\min}$ and $\overline{s}_1$, instead of L_2, K_1, and s_1, respectively, in the definition of the functional $\mathcal{V}_2(x_{2t}, x_{1t})$. □

Example 2. *Let us consider $n = 2$ and for all $t \geq 0$, $L_1(t) = \frac{1}{2}(1 + 0.97\cos(25t))$ and $L_2(t) = \frac{1}{2}(1 + 0.97\sin(15t))$. Sine function sounds reasonable to model the variation in differentiation rates since drugs are - usually - infused quasi-periodically. Nevertheless, many other time-varying functions may be used instead of sine ones. Let us assume that:*

	$\beta_i(x_i)$	$f_i(a)$	δ_i	τ_i	γ_i
$i=1$	$\frac{2.87}{1+x_1^2}$	$\frac{e^a}{e^{\tau_1}-1}$	0.973	0.8	0.9
$i=2$	$\frac{2.7}{1+x_2^4}$	$\frac{e^a}{e^{\tau_2}-1}$	0.965	0.7	0.97

Elementary calculations give: $\overline{s}_1 = 0.0592$, and, $\overline{s}_2 = 0.0099$. According to Corollary 1, $X^0 = (0,0)$, which is the unique equilibrium point of (17), is globally exponentially stable. Figure 3 illustrates the trajectories x_1 and x_2 for the the parameters and biological functions of Example 2.

Remark 2. *At this juncture, we emphasize that Theorem 1 and Corollary 1 complement the results of [1], [3], and [5], by establishing global exponential stability instead of asymptotic stability and by extending the result to cover the case of time-varying differentiating and self-renewing rates. Let us briefly comment these results in the AML case, in which we expect a blockade of differentiation, i.e. K_i decreases in early maturity stages. Not surprisingly, the conditions (18) suggest that therapeutic strategies to eradicate cells must be oriented towards increasing the death rates γ_i (recall that increasing the apoptosis rate γ_i decreases*

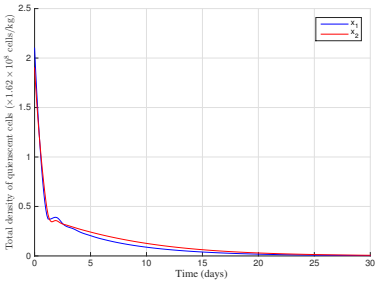

Figure 2: Trajectories of Example 1.

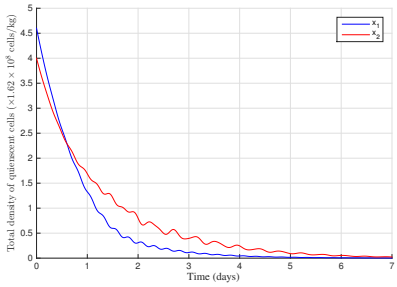

Figure 3: Trajectories of Example 2.

C_i), and δ_i, and also towards decreasing L_{imax} (i.e. increasing differentiation). Although very partial results for particular cases of AML (with myelodysplastic syndrome, MDS), and on cell cultures only, have been obtained using tyrosine kinase inhibitors (TKIs, in particular dasatinb [11]) in stimulating differentiation, the only clinically efficient case of redifferentiation therapy known until recently was by using all-trans retinoic acid (ATRA) and arsenic tri-oxide in acute promyelocytic leukemia (APL). However, this therapeutic track has lately been relaunched by establishing that inhibition of Dihydroorotate Dehydrogenase (DHODH) is efficient in releasing cells from differentiation arrest [15]. Finally, increasing apoptosis may be achieved classically by using cytosine arabinoside.

3.3. Robustness analysis of the trivial steady state

In this section, we use the strict functionals $\mathcal{V}_i$, introduced in Theorem 1, to perform a robustness analysis in the case of nonvanishing perturbations $\epsilon_i(t) \in (0, \bar{\epsilon}_i]$, for all $i \in I_n$, $t \geq 0$. Let us observe that the derivative of the functional $\mathcal{V}_1$, defined in (7), along the trajectories of the perturbed system (1), satisfies,

$$\dot{\mathcal{V}}_1(t) \leq -\tilde{s}_1 \mathcal{V}_1(x_{1t}) - \frac{s_1}{4} x_1(t) + \bar{\epsilon}_1. \tag{19}$$

We consider any constant $\theta \in (0, 1)$ and we define the family of sets:

$$\mathcal{T}_{i\bar{\epsilon}_i} = \left\{ \varphi \in \mathcal{C}\left([-\tau_i, 0], \mathbb{R}^+\right), \quad \mathcal{V}_i(\varphi) \leq \frac{\bar{\epsilon}_i}{\theta \tilde{s}_i} \right\}. \tag{20}$$

Notice for later use that the sets $\mathcal{T}_{i\bar{\epsilon}_i}$ are the smallest possible for θ close to 1. Clearly, if $x_{1t} \notin \mathcal{T}_{1\bar{\epsilon}_1}$, then (19) gives $\dot{\mathcal{V}}_1(t) \leq -(1-\theta)\tilde{s}\mathcal{V}_1(x_{1t}) - \frac{s_1}{4} x_1(t)$. Therefore, the state x_{1t} converges exponentially to the set $\mathcal{T}_{1\bar{\epsilon}_1}$. However, a refined result can be provided, in the sense that we can determine smaller positive invariant sets than the family $\mathcal{T}_{i\bar{\epsilon}_i}$. For that, let us introduce the functional,

$$\mathcal{A}_1(x_{1t}) = \mathcal{V}_1(x_{1t}) - \psi_1^\dagger x_1(t). \tag{21}$$

It is worth mentioning that the functional $\mathcal{A}_1$ is positive on the positive orthant for $\psi_1^\dagger = \frac{s_1}{8(\delta_1 + \beta_1(0))} < 1$, where s_1 is the constant defined in (4). Using the

expression of $\psi_1^\dagger$, we can check that the derivative of $\mathcal{A}_1$, along the trajectories of the perturbed system (1), satisfies:

$$\dot{\mathcal{A}}_1(t) \leq -\tilde{s}_1\mathcal{V}_1(x_{1t}) - \frac{s_1}{8}x_1(t) - 2\psi_1^\dagger L_1 \int_{t-\tau_1}^{t} g_1(t-a)w_1(x_1(a))da + (1-\psi_1^\dagger)\bar{\epsilon}_1.$$

Now, if we define the family of sets:

$$\tilde{\mathcal{T}}_{i\bar{\epsilon}_i} = \left\{ \varphi \in \mathcal{C}\left([-\tau_i, 0], \mathbb{R}^+\right), \mathcal{V}_i(\varphi) + \frac{2\psi_i^\dagger L_i}{\tilde{s}_i\theta} \int_{-\tau_i}^{0} g_i(a)w_i(\varphi)da \leq \frac{(1-\psi_i^\dagger)\bar{\epsilon}_i}{\theta\tilde{s}_i} \right\},$$

where $0 < \psi_i^\dagger < 1$, for all $i \in I_n$. Observe that $\tilde{\mathcal{T}}_{i\bar{\epsilon}_i} \subset \mathcal{T}_{i\bar{\epsilon}_i}$, for all $\psi_i > 0$. Now, notice that for all $x_{1t} \notin \tilde{\mathcal{T}}_{1\bar{\epsilon}_1}$, the derivative of the functional $\mathcal{A}_1$ satisfies,

$$\dot{\mathcal{A}}_1(t) \leq -\tilde{s}_1(1-\theta)\mathcal{V}_1(x_{1t}) - \frac{s_1}{8}x_1(t) \leq -\tilde{s}_{1\theta}\mathcal{A}_1(x_{1t}) - \frac{s_1 + \psi_1^\dagger\theta}{8}x_1(t), \quad (22)$$

where $\tilde{s}_{1\theta} = \min\{\tilde{s}_1(1-\theta), \theta/8\} > 0$, for all $\theta \in (0,1)$. Therefore, from the definition of the functional $\mathcal{A}_1$, we conclude that the state x_{1t} converges exponentially to $\tilde{\mathcal{T}}_{1\bar{\epsilon}_1}$, and the decay rate of the trajectory $x_1(t)$ is smaller than, or equal to, $\tilde{s}_{1\theta}$. On the other hand, we readily check, by contradiction, that the sets $\tilde{\mathcal{T}}_{i\bar{\epsilon}_i}$ are positively invariant (i.e. a trajectory in $\tilde{\mathcal{T}}_{i\bar{\epsilon}_i}$ remains in $\tilde{\mathcal{T}}_{i\bar{\epsilon}_i}$ for all the future time). Arguing as in the proof of Theorem 1, we generalize this result to the overall system. In other words, we have proved the following result:

Theorem 2. *If the conditions $s_i > 0$ are satisfied, for all $i \in I_n$, then the states x_{it} of the perturbed system (1), where $\epsilon_i(t) \in (0, \bar{\epsilon}_i]$, for all $t \geq 0$, converge exponentially to the sets $\tilde{\mathcal{T}}_{i\bar{\epsilon}_i}$, where $0 < \psi_i^\dagger < 1$, for all $i \in I_n$.*

4. Stability analysis of the strictly positive steady state

A strictly positive equilibrium X^e reflects the surviving of all the generations of blood cells, which is the aim of a healthy hematopoiesis. When the condition (3) is satisfied, a unique X^e exists. In this section, we answer one important open question about the problem of finding an estimate of the basin of attraction of X^e. Let us start by looking to the reintroduction functions, β_i's, from the resting to the proliferating stages. Owing to some biological considerations, Hill functions were proposed by Mackey in [12] to model β_i. Therefore, we consider,

$$\beta_i(x_i) = \frac{\beta_i(0)}{1 + b_i x_i^{\mathfrak{n}_i}}, \quad (23)$$

where $\beta_i(0) > 0$, $b_i > 0$ and $\mathfrak{n}_i \geq 2$. This typical choice was assumed in subsequent works ([1] and [16]). Actually, many other smoothly decreasing functions β_i, with a finite maximum $\beta_i(0)$ and adjustable slope and inflection point, can be chosen to match the biological assumptions [12].

Throughout this section, we consider the functions β_i in the form (23) and we indicate later for which other forms our results remain valid. Since we are

interested in the positive equilibrium X^e, we perform the change of coordinates, $\hat{x}_i = x_i - x_i^e$, for $i \in I_n$. It follows from (1) that

$$\begin{aligned}\dot{\hat{x}}_i(t) =& -\delta_i\left[\hat{x}_i(t) + x_i^e\right] - w_i\left(\hat{x}_i(t) + x_i^e\right) \\ &+ 2L_i \int_{t-\tau_i}^{t} g_i(t-a) w_i\left(\hat{x}_i(a) + x_i^e\right) da \\ &+ 2K_{i-1} \int_{t-\tau_{i-1}}^{t} g_{i-1}(t-a) w_{i-1}\left(\hat{x}_{i-1}(a) + x_{i-1}^e\right) da.\end{aligned} \tag{24}$$

However, a better representation of (24) that eases the analysis of its origin, can be obtained. Indeed, observe that, with an abuse of notation, $w_i(\hat{x}_i + x_i^e) = w_i(x_i^e) + \mu_i \hat{x}_i + R_i(\hat{x}_i)$, where,

$$\mu_i = \beta_i(x_i^e) + \beta_i'(x_i^e) x_i^e, \quad \text{and,} \quad R_i(\hat{x}_i) = \int_{x_i^e}^{x_i^e + \hat{x}_i} [\hat{x}_i + x_i^e - l] w_i^{(2)}(l) dl. \tag{25}$$

Moreover, we denote $\beta_{i*} = \delta_i + \mu_i$. It follows that (24) is equivalent to

$$\begin{aligned}\dot{\hat{x}}_i(t) =& -\beta_{i*}\hat{x}_i(t) + 2L_i\mu_i \int_{t-\tau_i}^{t} g_i(t-a)\hat{x}_i(a) da \\ &- R_i(\hat{x}_i(t)) + 2L_i \int_{t-\tau_i}^{t} g_i(t-a) R_i(\hat{x}_i(a)) da \\ &+ 2K_{i-1}\mu_{i-1} \int_{t-\tau_{i-1}}^{t} g_{i-1}(t-a)\hat{x}_{i-1}(a) da \\ &+ 2K_{i-1} \int_{t-\tau_{i-1}}^{t} g_{i-1}(t-a) R_{i-1}(\hat{x}_{i-1}(a)) da.\end{aligned} \tag{26}$$

Remark 3. *Compared with Section 3, the stability analysis of the origin of (26) is more complicated due to the shifting. Indeed, linear functionals can no longer be used since the system (26) is not positive. A common approach to investigate the stability properties of such a class of systems is by using quadratic functions or functionals, as illustrated in the sequel.*

4.1. Introductory result

To get a first intuition, let us consider the subsystem (26) for $i = 1$. A linear approximation at its origin is obtained by neglecting the terms where R_1 is present. The following linear system is obtained:

$$\dot{z}_1(t) = -\beta_{1*} z_1(t) + 2L_1\mu_1 \int_{t-\tau_1}^{t} g_1(t-a) z_1(a) da. \tag{27}$$

Let us consider the positive definite quadratic function

$$Q(a) = \frac{1}{2}a^2. \tag{28}$$

We apply the Razumikhin's theorem (see, for instance, [7]): Pick $q > 1$ and consider $t \geq 0$ such that $qQ(z_1(t)) \geq Q(z_1(a)), \quad \forall a \in (t-\tau_1, t)$. Then the derivative of Q along the trajectories of the system (27) satisfies:

$$\begin{aligned}\dot{Q}(t) &\leq -2\beta_{1*}Q(z_1(t)) + 4\sqrt{Q(z_1(t))}L_1|\mu_1| \int_{t-\tau_1}^{t} g_1(t-a)\sqrt{Q(z_1(a))}da \\ &\leq -2\left[\beta_{1*} - 2\sqrt{q}L_1|\mu_1|C_1\right]Q(z_1(t)).\end{aligned} \tag{29}$$

We conclude from Razumikhin's theorem that the condition $\beta_{1*} - 2L_1|\mu_1|C_1 > 0$ is sufficient for the asymptotic stability of the origin of the system (27). This leads us to introduce, for all $i \in I_n$, the constants

$$\varsigma_i = \beta_{i*} - 2L_i|\mu_i|C_i = \delta_i + \mu_i - 2L_i|\mu_i|C_i, \tag{30}$$

that will be of use later in the stability analysis of the nonlinear system, in the analytic expression of the quadratic Lyapunov-Krasovskii functionals and in the size of the region of attraction that we will provide.

4.2. Estimate of the basin of attraction of the positive steady state

Contrary to Section 3, the nonpositivity of the system under study motivates the use of the positive definite function (28), as well as the following functionals:

$$\Omega_i(\varphi_{it}) = \int_{t-\tau_i}^{t}\int_{l}^{t} g_i(l-a+\tau_i)Q(\varphi_i(a))dadl, \tag{31}$$

$$\Lambda_i(\varphi_{it}) = \int_{t-\tau_i}^{t} e^{l-t}\int_{l}^{t} g_i(l-a+\tau_i)Q(\varphi_i(a))dadl. \tag{32}$$

Notice that other types of functionals may be used instead of (31) and (32). However, for the sake of clarity, we use a weighted combination of them in order to compensate the distributed delayed terms and estimate the exponential decay rates. Moreover, we define for all $i \in I_n$, the following functionals:

$$S_i(\hat{x}_{it}) = \frac{1}{2}Q(\hat{x}_i(t)) + L_i|\mu_i|\Omega_i(\hat{x}_{it}), \tag{33}$$

$$N_1(\hat{x}_{1t}) = S_1(\hat{x}_{1t}) + \frac{\varsigma_1}{2C_1}\Lambda_1(\hat{x}_{1t}), \text{ and for all } i \in \{2,\dots,n\}, \tag{34}$$

$$N_i(\hat{x}_{it}, \hat{x}_{i-1t}) = S_i(\hat{x}_{it}) + \frac{\varsigma_i}{2C_i}\Lambda_i(\hat{x}_{it}) + \psi_i\Lambda_{i-1}(\hat{x}_{i-1t}), \tag{35}$$

with ς_i the constants defined in Section 4.1, and ψ_i are appropriate strictly positive constants to be selected later, for all $i \in \{2,\dots,n\}$.

Next, for a later use, we prove in Appendix A the following assertion:

Claim 1. *There exist constants $\hat{s}_i > 0$, for all $i \in I_n$, which depend on the biological parameters of the model and on the strictly positive equilibrium X^e, such that, for all $\hat{x}_i > -x_i^e$, where $x_i^e > 0$, the following inequality holds true:*

$$|R_i(\hat{x}_i)| \leq \hat{s}_i Q(\hat{x}_i), \quad \textit{where,} \quad \hat{s}_i > 0 \textit{ are given in Appendix A.} \tag{36}$$

Remark 4. *It is worth mentioning that the stability analysis which will be performed for the origin of the nonlinear system (26) is available for many other reintroduction functions β_i, as long as they satisfy the sector conditions (36).*

Furthermore, in order to ease the notation, we denote

$$I_i(\hat{x}_{it}) = \int_{t-\tau_i}^{t} g_i(t-a)Q(\hat{x}_i(a))da. \tag{37}$$

Finally, we define the constants $\tilde{k}_i = \frac{\varsigma_i}{8\hat{s}_i}$, $\hat{k}_i = \frac{\varsigma_i}{4C_iL_i\hat{s}_ie^{\tau_i}}$ and $\overline{N}_i = \min\left\{\tilde{k}_i^2, \hat{k}_i^2\right\}$. Notice that for all $i \in I_n$, $\tilde{k}_i$ and $\hat{k}_i$ are only dependent on the constant biological parameters of the model. Now, we prove the following result:

Theorem 3. *Let the system (26) be such that*

$$\varsigma_i > 0, \tag{38}$$

for all $i \in I_n$. Then all the solutions of (26) with initial conditions $\hat{\varphi}_i \in \mathcal{C}([-\tau_i, 0], (-x_i^e, +\infty))$ satisfying

$$N_i(\hat{\varphi}_i, \hat{\varphi}_{i-1}) < \overline{N}_i, \tag{39}$$

converge exponentially to the origin.

Remark 5. *Generally, Lyapunov theory provides sufficient conditions for stability. Nevertheless, due to earlier published works we can comment conditions (38). In previous works (using frequency domain approaches), it was claimed in [1] that the origin is locally asymptotically stable if $\delta_i + (2L_iC_i + 1)\,\mu_i > 0$ is satisfied. However, in [16], it was shown that the previous assertion holds true only when $-\delta_i < \mu_i < 0$. We notice that our stability conditions (38) are equivalent to those of [16] on that interval. Next, when $\mu_i > 0$, our exponential stability conditions (38) (which are provided without specifying a particular form of f_i), correspond to the conditions for local stability provided in [16] (and which have been slightly improved using Nyquist criterion for a typical selection of the functions f_i in [16]). It remains the case $\mu_i < -\delta_i$ which is not covered by the Lyapunov approach proposed here, and which was addressed in [16]. The region of attraction defined in (39) is rather difficult to interpret. In fact, based on some numerical simulations and the conjecture made in [16], we suggest that the region defined in (39) is conservative.*

Proof. First, let us observe for later use that the derivatives of the functionals Ω_i and Λ_i, for all $i \in I_n$, along the trajectories of (26) satisfy,

$$\dot{\Omega}_i(t) = C_iQ(\hat{x}_i(t)) - \int_{t-\tau_i}^{t} g_i(t-a)Q(\hat{x}_i(a))da, \quad \text{and,}$$

$$\dot{\Lambda}_i(t) \leq -\Lambda_i(\hat{x}_{it}) - e^{-\tau_i}\int_{t-\tau_i}^{t} g_i(t-a)Q(\hat{x}_i(a))da + C_iQ(\hat{x}_i(t)),$$

where the last inequality is a consequence of (2). For the sake of clarity, we will decompose now the proof of Theorem 3 in two parts: we prove the exponential stability of solutions of the first compartment ($i = 1$), and then we extend the result to any number of compartments ($i \geq 1$).

i) LKF for the first compartment: We start with the first generation of hematopoietic stem cells. Using (36), one can prove that the derivative of the function $Q(\hat{x}_1(t))$, introduced in (28), along the trajectories of (26) satisfies

$$\begin{aligned}\dot{Q}(t) \leq & 2\left[-\beta_{1*} + L_1|\mu_1|C_1\right] Q(\hat{x}_1(t)) + \hat{s}_1|\hat{x}_1(t)|Q(\hat{x}_1(t)) \\ & + 2L_1\left(|\mu_1| + \hat{s}_1|\hat{x}_1(t)|\right) I_1(\hat{x}_{1t}).\end{aligned} \tag{40}$$

It follows that the derivative of the functional N_1, introduced in (34), satisfies

$$\begin{aligned}\dot{N}_1(t) \leq & -\left[\frac{\varsigma_1}{8}Q(\hat{x}_1(t)) + \frac{\varsigma_1}{2C_1}\Lambda_1(\hat{x}_{1t})\right] + \left[\frac{\hat{s}_1}{2}|\hat{x}_1(t)| - \frac{\varsigma_1}{4}\right] Q(\hat{x}_1(t)) \\ & - \frac{\varsigma_1}{8}Q(\hat{x}_1(t)) + \left[L_1\hat{s}_1|\hat{x}_1(t)| - \frac{\varsigma_1 e^{-\tau_1}}{2C_1}\right] I_1(\hat{x}_{1t}).\end{aligned} \tag{41}$$

On the other hand, from the definition of N_1 we observe that

$$N_1(\hat{x}_{1t}) \leq \frac{1}{2}Q(\hat{x}_1(t)) + \left(\frac{\varsigma_1 + 2L_1C_1|\mu_1|e^{\tau_1}}{2C_1}\right)\Lambda_1(\hat{x}_{1t}). \tag{42}$$

From (41) and (42), we deduce that for all $\tilde{\varsigma}_1 \in \left(0, \min\left\{\frac{\varsigma_1}{4}, \frac{\varsigma_1}{\varsigma_1 + 2L_1C_1|\mu_1|e^{\tau_1}}\right\}\right)$, the derivative of the functional N_1 satisfies

$$\begin{aligned}\dot{N}_1(t) \leq & -\tilde{\varsigma}_1 N_1(\hat{x}_{1t}) + \left[\frac{\hat{s}_1}{2}|\hat{x}_1(t)| - \frac{\varsigma_1}{4}\right] Q_1(\hat{x}_1(t)) \\ & + \left[L_1\hat{s}_1|\hat{x}_1(t)| - \frac{\varsigma_1 e^{-\tau_1}}{2C_1}\right] I_1(\hat{x}_{1t}) - \frac{\varsigma_1}{8}Q(\hat{x}_1(t)).\end{aligned}$$

From the definition of N_1, which is given in (34), we notice that $|\hat{x}_1(t)| \leq 2\sqrt{N_1(\hat{x}_{1t})}$. A direct consequence is that

$$\begin{aligned}\dot{N}_1(t) \leq & -\tilde{\varsigma}_1 N_1(\hat{x}_{1t}) + \left[\hat{s}_1\sqrt{N_1(\hat{x}_{1t})} - \frac{\varsigma_1}{4}\right] Q_1(\hat{x}_1(t)) \\ & + \left[2L_1\hat{s}_1\sqrt{N_1(\hat{x}_{1t})} - \frac{\varsigma_1 e^{-\tau_1}}{2C_1}\right] I_1(\hat{x}_{1t}) - \frac{\varsigma_1}{8}Q(\hat{x}_1(t)).\end{aligned}$$

Now, we conclude that if the condition (39) is satisfied, then

$$\dot{N}_1(t) \leq -\tilde{\varsigma}_1 N_1(\hat{x}_{1t}) - \frac{\varsigma_1}{8}Q(\hat{x}_1(t)). \tag{43}$$

This allows us to conclude that the origin of the subsystem (26), for $i = 1$, is exponentially stable, with a decay rate smaller than $\tilde{\varsigma}_1$.

ii) LKF for the overall system: Here we take into account all generations of immature blood cells. We use the inequality $|\hat{x}_i(t)\hat{x}_{i-1}(a)| \leq \xi_i Q(\hat{x}_i(t)) +$

$\frac{1}{\xi_i}Q(\hat{x}_{i-1}(a))$, with $\xi_i > 0$ for all $i > 1$, and the inequality $|\hat{x}_i(t)\hat{x}_i(a)| \leq Q(\hat{x}_i(t))+Q(\hat{x}_i(a))$, for all $i \in I_n$, and we select $\psi_i = \frac{K_{i-1}|\mu_{i-1}|e^{\tau_{i-1}}}{\xi_i}+\frac{\varsigma_i e^{-\tau_i}K_{i-1}\hat{s}_{i-1}}{2L_i\hat{s}_iC_i}e^{\tau_{i-1}}$. Then the derivatives of the functions $Q(\hat{x}_i(t))$, for all $i > 1$, along the trajectories of (26) satisfy

$$\begin{aligned}\dot{Q}(t) \leq & 2\left[-\beta_{i*} + L_i|\mu_i|C_i\right]Q(\hat{x}_i(t)) + \hat{s}_i|\hat{x}_i(t)|Q(\hat{x}_i(t)) \\ & + 2L_i\left(|\mu_i| + \hat{s}_i|\hat{x}_i(t)|\right)I_i(\hat{x}_{it}) + 2K_{i-1}|\mu_{i-1}|C_{i-1}\xi_i Q(\hat{x}_i(t)) \\ & + 2K_{i-1}\left(\hat{s}_{i-1}|\hat{x}_i(t)| + \frac{|\mu_{i-1}|}{\xi_i}\right)I_{i-1}(\hat{x}_{i-1t}).\end{aligned} \tag{44}$$

Moreover, we choose $\xi_i = \frac{\varsigma_i}{4K_{i-1}|\mu_{i-1}|C_{i-1}}$. It follows that

$$\begin{aligned}\dot{N}_i(t) \leq & -\tilde{\varsigma}_i N_i(\hat{x}_i, \hat{x}_{i-1}) + \psi_i C_{i-1}Q(\hat{x}_{i-1}(t)) - \left[\frac{\varsigma_i}{8} - \frac{1}{2}\hat{s}_i|\hat{x}_i(t)|\right]Q(\hat{x}_i(t)) \\ & - \frac{\varsigma_i}{16}Q(\hat{x}_i(t)) + L_i\hat{s}_i\left[|\hat{x}_i(t)| - \frac{\varsigma_i e^{-\tau_i}}{2L_i\hat{s}_iC_i}\right]I_i(\hat{x}_{it}) \\ & + K_{i-1}\hat{s}_{i-1}\left[|\hat{x}_i(t)| - \frac{\varsigma_i e^{-\tau_i}}{2L_i\hat{s}_iC_i}\right]I_{i-1}(\hat{x}_{i-1t}),\end{aligned} \tag{45}$$

with $\tilde{\varsigma}_i > 0$. Finally, we conclude that if the conditions (39) are satisfied, then

$$\dot{N}_i(t) \leq -\tilde{\varsigma}_i N_i(\hat{x}_{it}, \hat{x}_{i-1t}) - \frac{\varsigma_i}{16}Q(\hat{x}_i(t)) + \psi_i C_{i-1}Q(\hat{x}_{i-1}(t)). \tag{46}$$

As we had done in [6], we can prove that the derivative of the functional $W(\hat{X}_t) = \sum_{i=1}^n p_i N_i(\hat{x}_{it}, \hat{x}_{i-1t})$, with an abuse of notation for N_1, and where $p_i = 2^{n-i}\prod_{k=i+1}^n \frac{8\psi_k C_{k-1}}{\varsigma_{k-1}}$, $p_n = 1$, and $\hat{X} = (\hat{x}_1, \ldots, \hat{x}_n)$, satisfies,

$$\dot{W}(t) \leq -\sum_{i=1}^n p_i\tilde{\varsigma}_i N_i(\hat{x}_{it}, \hat{x}_{i-1t}) - \frac{\varsigma_1}{8}Q(\hat{x}_1(t)) - \frac{\varsigma_n}{16}Q(\hat{x}_n(t)) - \frac{1}{2}\sum_{i=1}^{n-1}\frac{p_i\varsigma_i}{8}Q(\hat{x}_i(t)).$$

Finally, we obtain $\dot{W}(t) \leq -\varsigma W(\hat{X}_t)$, with $\varsigma = \min\{\tilde{\varsigma}_1, ..., \tilde{\varsigma}_n\} > 0$.

To summarize, by virtue of the properties of the functionals N_i, for all $i \in I_n$, and since the original system (1) is a positive system, we conclude that the set

$$\mathcal{A} = \{\varphi_i \in \mathcal{C}([-\tau_i, 0], \mathbb{R}^+) : N_i(\varphi_i - x_i^e, \varphi_{i-1} - x_{i-1}^e) < \overline{N}_i\}, \tag{47}$$

is a subset of the basin of attraction of the positive steady state of system (1). □

Example 3. *In this numerical example, we consider the system with the following biological functions and parameters for $n = 3$:*

	$\beta_i(x_i)$	$f_i(a)$	δ_i	τ_i	γ_i	K_i
$i = 1$	$\frac{0.5}{1+x_1^2}$	$\frac{10e^{10a}}{e^{10\tau_1}-1}$	0.1356	1.109402	0.3	0.05
$i = 2$	$\frac{1}{1+x_2^4}$	$\frac{10e^{10a}}{e^{10\tau_2}-1}$	0.1669	1.2	0.4	0.07
$i = 3$	$\frac{3}{1+x_3^2}$	$\frac{2e^{2a}}{e^{2\tau_2}-1}$	0.3559	1.36	0.45	0.085

From the selected parameters, it follows that

	x_i^e	α_i	ς_i	$\hat{s}_i$	$\overline{N}_i$
$i=1$	0.70036	0.40422	0.08924	0.65070	2.5935×10^{-4}
$i=2$	0.78225	0.19888	0.02329	3.00487	9.3935×10^{-7}
$i=3$	1.0050	0.20422	0.33938	2.98491	2.02×10^{-4}

We select constant initial conditions: $\varphi_1 = 0.6850$, $\varphi_2 = 0.782$ *and* $\varphi_3 = 0.979$. *Therefore, we get,* $N_1(\varphi_1 - x_1^e) = 7.16 \times 10^{-5} < \overline{N}_1$, $N_2(\varphi_2 - x_2^e, \varphi_1 - x_1^e) = 6.65 \times 10^{-7} < \overline{N}_2$, *and,* $N_3(\varphi_3 - x_3^e, \varphi_2 - x_2^e) = 1.94 \times 10^{-4} < \overline{N}_3$. *According to Theorem 3, the positive steady state* (x_1^e, x_2^e, x_3^e) *is exponentially stable (Figure 4).*

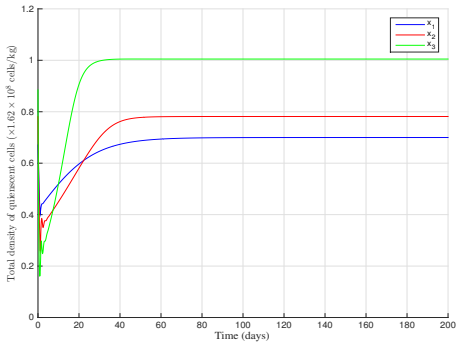

Figure 4: Trajectories x_1, x_2 and x_3 for the parameters of Example 3.

4.3. Robustness analysis of the positive equilibrium point

Here we return to the perturbed system (1), that we rewrite in a form similar to (26) by performing the change of coordinate $\hat{x}_i(t) = x_i(t) - x_i^e$. Based on the functionals constructed in Theorem 3, we prove the following result:

Corollary 2. *Let the system (26) be perturbed by nonvanishing additive disturbances* $\epsilon_i(t) \in (0, \epsilon_i]$, $\bar{\epsilon}_i > 0$, *for all* $t > 0$, *and* $i \in I_n$. *If the conditions*

$$\varsigma_i > 0 \tag{48}$$

are satisfied for all $i \in I_n$, *then all the solutions of (26) with initial conditions* $\varphi_i \in \mathcal{C}([-\tau_i, 0], \mathbb{R}^+)$ *satisfying*

$$\left(\frac{2\bar{\epsilon}_i}{\theta\tilde{\varsigma}_i}\right)^2 \leq N_i(\varphi_i - x_i^e, \varphi_{i-1} - x_{i-1}^e) < \overline{N}_i, \tag{49}$$

with $\theta \in (0,1)$, *converge exponentially to the domain,*

$$\mathcal{G}_{\bar{\epsilon}_i} = \left\{ \varphi_i \in \mathcal{C}([-\tau_i, 0], \mathbb{R}^+), \quad N_i(\varphi_i - x_i^e, \varphi_{i-1} - x_{i-1}^e) \leq \left(\frac{2\bar{\epsilon}_i}{\theta\tilde{\varsigma}_i}\right)^2 \right\}. \tag{50}$$

Proof. Let us prove the previous result for $i = 1$. Arguing as we did in the proof of Theorem 3, one can generalize to the overall system. First, observe that the derivative of $Q(\hat{x}_1(t))$ along the trajectories of the perturbed system satisfies:

$$\begin{aligned}\dot{Q}(t) \leq & 2\left[-\beta_{1*} + L_1|\mu_1|C_1\right] Q(\hat{x}_1(t)) + \hat{s}_1|\hat{x}_1(t)|Q(\hat{x}_1(t)) \\ & + 2L_1\left(|\mu_1| + \hat{s}_1|\hat{x}_1(t)|\right) I_1(\hat{x}_{1t}) + |\hat{x}_1(t)|\overline{\epsilon}_i.\end{aligned} \tag{51}$$

Consequently, the derivative of the functional N_1, introduced in (34), along the trajectories of the perturbed system, verifies

$$\begin{aligned}\dot{N}_1(t) \leq & -\left[\frac{\varsigma_1}{8}Q(\hat{x}_1(t)) + \frac{\varsigma_1}{2C_1}\Lambda_1(\hat{x}_{1t})\right] + \left[\frac{\hat{s}_1}{2}|\hat{x}_1(t)| - \frac{\varsigma_1}{4}\right] Q(\hat{x}_1(t)) \\ & - \frac{\varsigma_1}{8}Q(\hat{x}_1(t)) + \left[L_1\hat{s}_1|\hat{x}_1(t)| - \frac{\varsigma_1 e^{-\tau_1}}{2C_1}\right] I_1(\hat{x}_{1t}) + |\hat{x}_1(t)|\overline{\epsilon}_i.\end{aligned} \tag{52}$$

Using (42), and the fact that $|\hat{x}_1(t)| \leq 2\sqrt{N_1(\hat{x}_{1t})}$, we obtain

$$\begin{aligned}\dot{N}_1(t) \leq & -\tilde{\varsigma}_1 N_1(\hat{x}_{1t}) + \left[\hat{s}_1\sqrt{N_1(\hat{x}_{1t})} - \frac{\varsigma_1}{4}\right] Q_1(\hat{x}_1(t)) \\ & + \left[2L_1\hat{s}_1\sqrt{N_1(\hat{x}_{1t})} - \frac{\varsigma_1 e^{-\tau_1}}{2C_1}\right] I_1(\hat{x}_{1t}) - \frac{\varsigma_1}{8}Q(\hat{x}_1(t)) + 2\overline{\epsilon}_i\sqrt{N_1(\hat{x}_{1t})},\end{aligned}$$

where $\tilde{\varsigma}_1 \in \left(0, \min\left\{\frac{\varsigma_1}{4}, \frac{\varsigma_1}{\varsigma_1 + 2L_1C_1|\mu_1|e^{\tau_1}}\right\}\right)$. Therefore, when $N_1(\varphi_1 - x_1^e) < \overline{N}_1$ is satisfied, we deduce that

$$\dot{N}_1(t) \leq -\tilde{\varsigma}_1 N_1(\hat{x}_{1t}) - \frac{\varsigma_1}{8}Q(\hat{x}_1(t)) + 2\overline{\epsilon}_i\sqrt{N_1(\hat{x}_{1t})}. \tag{53}$$

Now, let us consider any $\theta \in (0, 1)$ and observe that for all initial conditions φ_1 satisfying $N_1(\varphi_1 - x_1^e) < \overline{N}_1$ with $\varphi_1 \notin \mathcal{G}_{\overline{\epsilon}_i}$, the inequality (53) gives

$$\dot{N}_1(t) \leq -(1-\theta)\tilde{\varsigma}_1 N_1(\hat{x}_{1t}). \tag{54}$$

We conclude that the states x_{1t} satisfying (49) converge exponentially to the invariant set $\mathcal{G}_{\overline{\epsilon}_1}$, defined in (50), such that the decay rate of the trajectory $x_1(t)$ is smaller than, or equal to, $\frac{(1-\theta)\tilde{\varsigma}_1}{2}$. □

5. Conclusion

With the aim of constantly refining and improving the modeling and the analysis of hematopoietic mechanisms, we proposed explicit constructions of suitable strict LKFs for nonlinear hematopoietic systems with distributed delays. Our approach allowed us to solve some practical and technical issues, which complement already published results on the topic. In comparison with previous works, our results provided exponential stability with an estimate on the decay rate of the solutions, and are derived without any extra assumption on the mitosis functions. Moreover, a robustness analysis was performed under

nonvanishing perturbations (that may represent dedifferentiation flux, together with model uncertainties), and we have also covered some practical situations such that time-varying differentiating rates (to model the action on the blockade in differentiation and re-differentiation). Particular emphasis was given to the positive steady state that represents healthy hematopoiesis, and for which we provided an explicit formulation of a subset of its region of attraction. Future work will enhance the role of dedifferentiation and transdifferentiation by considering hematopoietic models where cell plasticity is no more a marginal phenomenon, and cannot be considered as a perturbation, but has to be fully modeled.

References

[1] M. Adimy, F. Crauste, A. Abdllaoui, *Discrete Maturity-Structured Model of Cells Differentiation with Applications to Acute Myelogenous Leukemia*, J. Biological Systems, No. 3, pp. 395-424, (2008).

[2] M. Adimy, F. Crauste, *Mathematical Model of Hematopoiesis Dynamics with Growth Factor-dependent Apoptosis and Proliferation regulations*, Math. Comput. Modelling 49, No. 11-12, pp. 2128-2137, (2009).

[3] M. Adimy, F. Crauste, A. Abdllaoui, *Boundedness and Lyapunov function for a nonlinear system of hematopoietic stem cell dynamics*, C. R. Acad. Sci. Paris, Ser. I, 348, No. 7-8, pp. 373-377, (2010).

[4] S. Cai, X. Fu, Z. Sheng, *Dedifferentiation: a new approach in stem cell research*, Bioscience 57.8, pp. 655-662, (2007).

[5] W. Djema, F. Mazenc, C. Bonnet, *Lyapunov Stability Analysis of a Model Describing Hematopoiesis*. Proceedings of the European Control Conference (ECC), Linz, Austria, pp. 2711-2716, (2015).

[6] W. Djema, F. Mazenc, C. Bonnet, *Stability of Immature Cell Dynamics in Healthy and Unhealthy Hematopoiesis*. Proceedings of the American Control Conference (ACC), Boston, USA, pp. 6121-6126, (2016).

[7] E. Fridman, *Introduction to time-delay systems: analysis and control*, Birkhauser, Systems and Control: Foundations and Applications, Springer, (2014).

[8] E. Fridman, C. Bonnet, F. Mazenc, W. Djema, *Stability of the cell dynamics in Acute Myeloid Leukemia*. Systems & Control Letters Vol. 88, pp. 91-100, (2016).

[9] H. Khalil, *Nonlinear systems, Third Edition*. Prentice Hall, Upper Saddle River, NJ, (2002).

[10] V. Kolmanovskii, A. Myshkis, *Introduction to the Theory and Applications of Functional Differential Equations*, Kluwer Academic Publishers, Dordrecht, (1999).

[11] E. Lainey, *et al.*, *Tyrosine kinase inhibitors for the treatment of acute myeloid leukemia: Delineation of anti-leukemic mechanisms of action*, Biochemical Pharmacology 82, pp. 1457-1466, (2011).

[12] M.C. Mackey, *Unified hypothesis of the origin of aplastic anemia and periodic hematopoiesis*, Blood, 51: pp. 941-956, (1978).

[13] J. M. Mahaffy, J. Bélair, M.C. Mackey, *Hematopoietic Model with Moving Boundary Condition and State-delay: Applications in Erythropoiesis*, Journal of Theoretical Biology, 190. No. 2, pp. 135-146, (1998).

[14] M. Malisoff, F. Mazenc, *Constructions of Strict Lyapunov Functions*, Serie : Communications and Control Engineering. Spinger-Verlag London Ltd, U.K., (2009).

[15] D. B. Sykes, *et al. Inhibition of dihydroorotate dehydrogenase overcomes differentiation blockade in acute myeloid leukemia*, *Cell*, 167.1, pp. 171-186, (2016).

[16] H. Özbay, C. Bonnet, H. Benjelloun, J. Clairambault, *Stability analysis of cell dynamics in leukemia.* Math. Model Nat. Phenom., Vol. 7, No. 1, pp. 203-234, (2012).

[17] H. Özbay, C. Bonnet, J. Clairambault, *Stability analysis of systems with distributed delays and application to hematopoietic cell maturation dynamics.* Conference on Decision and Control, Mexico, pp. 2050-2055, (2008).

[18] L. Pujo-Menjouet, S. Bernard, M.C. Mackey, *Long period oscillations in a G_0 model of hematopoietic stem cells*, SIAM. J. Appl. Dynam. Syst. 4(2): pp. 312-332, (2005).

Appendix A. Proof of Claim 1

For notational convenience, we drop the subscript "i" and we use x_e instead of x_i^e to denote the positive equilibrium. Using the expression of β given in (23), we observe that for all $x_e > 0$ and $\mathfrak{z} > -x_e$, $R(\mathfrak{z}) = \beta(0)J(\mathfrak{z}) - \mu\mathfrak{z}$, where $J(\mathfrak{z}) = \frac{\mathfrak{z}+x^e}{1+b(\mathfrak{z}+x_e)^{\mathfrak{n}}} - \frac{x_e}{1+bx_e^{\mathfrak{n}}}$. First, let us study the function

$$\rho(\mathfrak{z}) = \frac{1}{1+b(\mathfrak{z}+x_e)^{\mathfrak{n}}} - \frac{1}{1+bx_e^{\mathfrak{n}}} = \frac{b\left[{x_e}^{\mathfrak{n}} - (\mathfrak{z}+x_e)^{\mathfrak{n}}\right]}{p(\mathfrak{z})},$$

where $p(\mathfrak{z}) = \left[1+b(\mathfrak{z}+x_e)^{\mathfrak{n}}\right](1+bx_e^{\mathfrak{n}})$. Observe that

$$(\mathfrak{z}+x_e)^{\mathfrak{n}} - x_e^{\mathfrak{n}} = \mathfrak{n}x_e^{\mathfrak{n}-1}\mathfrak{z} + \mathfrak{n}\int_0^{\mathfrak{z}}\int_{x_e}^{x_e+l}(\mathfrak{n}-1)m^{n-2}dmdl.$$

Consequently, $\rho(\mathfrak{z}) = -\frac{\mathfrak{n}bx_e^{\mathfrak{n}-1}}{p(\mathfrak{z})}\mathfrak{z} + \mathfrak{C}(\mathfrak{z})$, where, $\mathfrak{C}(\mathfrak{z}) = -\frac{\mathfrak{n}b(\mathfrak{n}-1)}{p(\mathfrak{z})}\int_0^{\mathfrak{z}}\int_0^l(m+x_e)^{\mathfrak{n}-2}dmdl$.

Denote $h = 1 + bx_e^{\mathfrak{n}}$ and observe that, $\frac{1}{p(\mathfrak{z})} = \frac{1}{h}\left(\rho(\mathfrak{z}) + \frac{1}{h}\right)$. It follows that $\rho(\mathfrak{z}) = -\mathfrak{n}bx_e^{\mathfrak{n}-1}\left(\frac{\rho(\mathfrak{z})}{h} + \frac{1}{h^2}\right)\mathfrak{z} + \mathfrak{C}(\mathfrak{z})$.

Consequently, we get the intermediate result:

$$\rho(\mathfrak{z}) = -\frac{\mathfrak{n}bx_e^{\mathfrak{n}-1}}{h^2}\mathfrak{z} + \mathfrak{C}(\mathfrak{z}) - \frac{\mathfrak{n}bx_e^{\mathfrak{n}-1}}{h}\rho(\mathfrak{z})\mathfrak{z}. \tag{A.1}$$

On the other hand, observe that

$$J(\mathfrak{z}) = \left(\rho(\mathfrak{z}) + \frac{1}{h}\right)\mathfrak{z} + x_e\rho(\mathfrak{z}) = \mathfrak{c}_1\mathfrak{z} + \mathfrak{c}_2\mathfrak{C}(\mathfrak{z}) + \mathfrak{c}_3\rho(\mathfrak{z})\mathfrak{z}, \tag{A.2}$$

where the last equality is a direct consequence of (A.1), with $\mathfrak{c}_1 = \frac{1}{h} - \frac{\mathfrak{n}bx_e^{\mathfrak{n}}}{h^2}$, $\mathfrak{c}_2 = x_e$ and $\mathfrak{c}_3 = \left(1 - \frac{\mathfrak{n}bx_e^{\mathfrak{n}}}{h}\right)$. Now, we readily check that

$$|\mathfrak{C}(\mathfrak{z})| \leq \frac{\mathfrak{n}b(\mathfrak{n}-1)}{p(\mathfrak{z})}\left(|\mathfrak{z}| + x_e\right)^{\mathfrak{n}-2}\frac{\mathfrak{z}^2}{2}. \tag{A.3}$$

It follows that $|\rho(\mathfrak{z})| \leq \frac{\mathfrak{n}bx_e^{\mathfrak{n}-1}}{p(\mathfrak{z})}|\mathfrak{z}| + |\mathfrak{C}(\mathfrak{z})|$. Using (A.3), we get

$$|\mathfrak{z}\rho(\mathfrak{z})| \leq \frac{\mathfrak{n}bx_e^{\mathfrak{n}-1}}{p(\mathfrak{z})}\mathfrak{z}^2 + \frac{\mathfrak{n}b(\mathfrak{n}-1)}{2p(\mathfrak{z})}\left(|\mathfrak{z}| + x_e\right)^{\mathfrak{n}-2}|\mathfrak{z}|^3. \tag{A.4}$$

From (A.2), we deduce that,

$$\begin{aligned}|J(\mathfrak{z}) - \mathfrak{c}_1\mathfrak{z}| \leq & \frac{\mathfrak{n}b(\mathfrak{n}-1)|\mathfrak{c}_3|}{2p(\mathfrak{z})}\left(|\mathfrak{z}| + x_e\right)^{\mathfrak{n}-2}|\mathfrak{z}|^3 \\ & + \left[\frac{\mathfrak{n}b(\mathfrak{n}-1)|\mathfrak{c}_2|\left(|\mathfrak{z}| + x_e\right)^{\mathfrak{n}-2}}{2p(\mathfrak{z})} + \frac{\mathfrak{n}bx_e^{\mathfrak{n}-1}|\mathfrak{c}_3|}{p(\mathfrak{z})}\right]\mathfrak{z}^2.\end{aligned}$$

Now, observe that $\frac{1}{p(\mathfrak{z})} = \frac{1}{[1+b(\mathfrak{z}+x_e)^{\mathfrak{n}}]h}$. Therefore, when $\mathfrak{z} \geq 0$, we have

$$\frac{1}{p(\mathfrak{z})} = \frac{1}{\left[1 + b(|\mathfrak{z}| + x_e)^{\mathfrak{n}}\right]h},$$

and when $\mathfrak{z} \leq 0$ (i.e. $\mathfrak{z} \in (-x_e, 0]$), we get

$$\frac{1}{p(\mathfrak{z})} \leq \frac{1}{h} \leq \frac{1 + b(2x_e)^{\mathfrak{n}}}{\left[1 + b(|\mathfrak{z}| + x_e)^{\mathfrak{n}}\right]h}.$$

Consequently, for all $\mathfrak{z} > -x_e$, we have

$$\frac{1}{p(\mathfrak{z})} \leq \frac{1 + b(2x_e)^{\mathfrak{n}}}{\left[1 + b(|\mathfrak{z}| + x_e)^{\mathfrak{n}}\right]h}.$$

We deduce that

$$|J(\mathfrak{z}) - \mathfrak{c}_1\mathfrak{z}| \leq \left[\left(\frac{\mathfrak{n}b(\mathfrak{n}-1)|\mathfrak{c}_3|(1+b(2x_e)^{\mathfrak{n}})}{2h} \right) \frac{(|\mathfrak{z}|+x_e)^{\mathfrak{n}-2}\,|\mathfrak{z}|}{1+b(|\mathfrak{z}|+x_e)^{\mathfrak{n}}} \right.$$
$$\left. + \frac{\mathfrak{n}b(\mathfrak{n}-1)|\mathfrak{c}_2|\,(|\mathfrak{z}|+x_e)^{\mathfrak{n}-2}\,(1+b(2x_e)^{\mathfrak{n}})}{2\,[1+b(|\mathfrak{z}|+x_e)^{\mathfrak{n}}]\,h} + \frac{\mathfrak{n}bx_e^{\mathfrak{n}-1}|\mathfrak{c}_3|\,(1+b(2x_e)^{\mathfrak{n}})}{[1+b(|\mathfrak{z}|+x_e)^{\mathfrak{n}}]\,h} \right] \mathfrak{z}^2.$$

By distinguishing between the two cases $|\mathfrak{z}|+x_e \geq 1$ and $|\mathfrak{z}|+x_e \leq 1$, one can prove that the following inequalities are satisfied for all $\mathfrak{z} > -x_e$,

$$\frac{(|\mathfrak{z}|+x_e)^{\mathfrak{n}-2}\,|\mathfrak{z}|}{1+b(|\mathfrak{z}|+x_e)^{\mathfrak{n}}} \leq \frac{(|\mathfrak{z}|+x_e)^{\mathfrak{n}-1}}{1+b(|\mathfrak{z}|+x_e)^{\mathfrak{n}}} \leq \max\left\{b, b^{-1}\right\}.$$

It follows that $|J(\mathfrak{z}) - \mathfrak{c}_1\mathfrak{z}| \leq \mathfrak{c}_4\mathfrak{z}^2$, with the positive constant

$$\mathfrak{c}_4 = \frac{\mathfrak{n}b(\mathfrak{n}-1)(1+b(2x_e)^{\mathfrak{n}})\,(x_e+|\mathfrak{c}_3|)\max\left\{b,b^{-1}\right\}}{2h} + \frac{\mathfrak{n}bx_e^{\mathfrak{n}-1}\,(1+b(2x_e)^{\mathfrak{n}})\,|\mathfrak{c}_3|}{h^2}.$$

On the other hand, we easily check that $\mu = \beta(0)\mathfrak{c}_1$, with μ defined in (25). It follows that $|R(\mathfrak{z})| \leq \beta(0)\mathfrak{c}_4\mathfrak{z}^2$. Since $Q(\mathfrak{z}) = \frac{1}{2}\mathfrak{z}^2$, we conclude that

$$|R(\mathfrak{z})| \leq \hat{s}Q(\mathfrak{z}), \text{ where, } \hat{s} = 2\mathfrak{c}_4\beta(0).$$

Journal of Theoretical Biology 449 (2018) 103–123

Control in Dormancy or Eradication of Cancer Stem Cells: Mathematical Modeling and Stability Issues[☆]

Walid Djema[1,*], Catherine Bonnet[2], Frédéric Mazenc[2], Jean Clairambault[3], Emilia Fridman[4], Pierre Hirsch[5], François Delhommeau[5]

Abstract

Objective: Modeling and analysis of cell population dynamics enhance our understanding of cancer. Here we introduce and explore a new model that may apply to many tissues.

Analyses: An age-structured model describing coexistence between mutated and ordinary stem cells is developed and explored. The model is transformed into a nonlinear time-delay system governing the dynamics of healthy cells, coupled to a nonlinear differential-difference system describing dynamics of unhealthy cells. Its main features are highlighted and an advanced stability analysis of several steady states is performed, through specific Lyapunov-like functionals for descriptor-type systems.

Results: We propose a biologically based model endowed with rich dynamics. It incorporates a new parameter representing immunoediting processes, including the case where proliferation of cancer cells is locally kept under check by the immune cells. It also considers the overproliferation of cancer stem cells, modeled as a subpopulation of mutated cells that is constantly active in cell division. The analysis that we perform here reveals the conditions of existence of several steady states, including the case of cancer dormancy, in the coupled model of interest. Our study suggests that cancer dormancy may result from a plastic sensitivity of mutated cells to their shared environment, different from that - fixed - of healthy cells, and this is related to an action (or lack of action) of the immune system. Next, the stability analysis that we perform is essentially oriented towards the determination of sufficient conditions, depending on all the model parameters, that ensure either a regionally (i.e., locally) stable dormancy steady state or eradication of unhealthy cells. Finally, we discuss some biological interpretations, with regards to our findings, in light of current and emerging therapeutics. These final insights are particularly formulated in the paradigmatic case of hematopoiesis and acute leukemia, which is one of the best known malignancies for which it is always hard, in presence of a clinical and histological remission, to decide between cure and dormancy of a tumoral clone.

[☆]This work is supported by ALMA3 project on the 'Analysis of Acute Myeloid Leukemia' and iCODE-Institute project funded by the idex Paris Saclay.

[*]Corresponding author: walid.djema@inria.fr

[1]W. Djema is with Inria Saclay, CentraleSupélec, Univ. Paris-Saclay & with Inria Sophia-Antipolis, Biocore and McTao teams, Université Côte d'Azur (UCA), France. walid.djema@inria.fr

[2]C. Bonnet and F. Mazenc are with Inria Saclay, Disco team, Université Paris-Saclay, CentraleSupélec, L2S (CNRS), France. catherine.bonnet@inria.fr, frederic.mazenc@inria.fr

[3]J. Clairambault is with Inria, Mamba team and with Sorbonne Université, Paris 6, UPMC, Laboratoire Jacques-Louis Lions, Paris, France. jean.clairambault@inria.fr

[4]E. Fridman is with the Department of Electrical Engineering and Systems at the School of Electrical Engineering, Tel-Aviv, Israel. emilia@eng.tau.ac.il

[5]P. Hirsch and F. Delhommeau are with Sorbonne Université, GRC n7, *Groupe de Recherche Clinique sur les Myéloproliferations Aiguës et Chroniques*, AP-HP, Hôpital Saint-Antoine, Paris, F-75012, France. pierre.hirsch@aphp.fr, francois.delhommeau@aphp.fr

Keywords: Delay, Nonlinear, Lyapunov, Cancer dormancy, Modeling.
2010 MSC: 93C23, 93C10, 93A30, 93D05, 92B05, 92C50, 80A30, 37L15, 39A30, 39A60.

Highlights *(to appear before the abstract in JTB template)*

- Modeling the cell cycle and population cell dynamics taking into account: coexistence between normal and mutated stem cells, overproliferation of cancer stem cells and sensitivity to the immune system.
- The study of existence of different steady states, including: unhealthy cells eradication and cancer cells dormancy (i.e. control in dormancy of abnormal cells).
- Construction of different types of suitable strict Lyapunov-like functionals for nonlinear delay differential-difference systems.
- Deriving stability conditions of steady states in different biological situations: a particular focus on the scenario of cancer dormancy.
- Numerical simulations, biological discussions and some therapeutic insights in the paradigmatic/exemplary case of hematopoiesis and acute myeloid leukemia.

1. Introduction and overview of the objectives

1.1. Cancer Stem Cells (SCS): a unified hypothesis to all types of cancer

Stem cells (SCs) are undifferentiated cells characterized by their ability to self-renew and their multipotency, which is the ability to differentiate into more mature and specialized cells [62], [88]. A SC that engages in the division process undergoes successive transformations until becoming, at the end of its cell cycle, two daughter cells. A heavy regulatory process controls committed cells before and during mitosis, by triggering a series of physiological events during the cycle. Even in fast-renewing tissues (e.g. gut, bone marrow and skin), cells are not always proliferating, but on the contrary, most of them are in a non-proliferating state, called resting or quiescent phase, G_0 [62]. Sometimes a pathological population of cells, that initially does not necessarily belong to the SC subpopulation, acquires self-renewing and proliferating capabilities similar to those of SCs ([28], [67]). These stem-like cells are very often out of control [76] and they are capable of initiating, developing and regenerating cancers [28], hence their designation as cancer stem cells (CSCs) [49]. Very often, CSCs are characterized by unhealthy behaviors such as excessive proliferation and loss of their differentiation faculties. This is what we observe for instance in the case

of leukemia [25]. On the other hand, it cannot be disregarded that in some cases (as in breast cancer and leukemia [6, 26]) CSCs do not overproliferate (cancer without disease [35], or, *in situ* tumor). However, even during their non-overproliferating states, CSCs remain in general distinguishable through specific markers on their surface[6] [76]. In medical research, the CSC hypothesis[7] postulates that one subpopulation of cells holds the power of initiating and regenerating cancer [28]. This stemness property in non-SCs has been first observed in leukemia, then in many other types of cancer. Not surprisingly, the study of leukemic cells became a model for many other stem-like cells [76].

1.2. Evidences and underlying assumptions about cancer dormancy

Strong evidence about the existence of a stalled growth state, commonly referred to as *tumor dormancy*, has been established many years ago when microscopic tumors were frequently encountered during autopsy examinations ([35], [64]). The most likely explanations (see [3], and also [35] and [80]) of CSCs dormancy state are: ***(H.1)*** blood and nutrient supply issues that prevent tumor growth, or at least delay its clinical manifestation [63], and ***(H.2)*** vigilance of the immune system which, in some cases, suffices to stop tumor development (see [32, 63, 80, 90, 93] and the references therein). In fact, there has been a lengthy debate on the role of the immune system in the defense against cancer: a process called *cancer immunosurveillance* [90]. The ambiguity about the immunosurveillance concept stems from the fact that often the immune system favors the development of the tumor instead of trying to eliminate it. The concept that attempts to integrate the diverse effects of the immune system on tumor progression is known as *cancer immunoediting* (see the review articles [80] and [90]). Even if it appears as an unsystematic process, an inter-

[6] For instance, stems cells in acute myeloid leukemia have some *interleukin-3receptor* α *chain* surface markers, which are not found in normal hematopoietic stems cells (see [31, 49]).

[7] The reference as *CSC paradigm* has also gained ground recently. Several subpopulations of cells, with distinct cancer-initiating powers, form actually a tumor. One subpopulation has an indefinite potential of self-renewing and shows *stem-like* status. It appears also that *stemness* might be a transient cell state that is associated to epigenetic changes [17].

est arises for cancer therapies that are immuno-oriented, bearing the name of *immunotherapy*[8]. In a similar spirit, monoclonal antibodies, e.g. gemtuzumab-ozogamicin, have been approved in the treatment protocols of some cancers (as in acute myeloid leukemia [40]), even if more trials are still needed to identify their exact benefits [40, 78]. Other cancer therapies, sometimes assimilated to immunotherapy, are using some *immune checkpoint inhibitors* (see for instance, [15], [55] and [66]). In the last part of our work, we will be shortly adopting some of these immuno-oriented concepts, associated with classical chemotherapy or targeted therapies, as it is frequently adopted in practice. More generally, the complex link between the immune system and cancer dormancy (as it is summarized in Fig. 3 of [80]) is implicitly represented in our model thanks to an extra-parameter that we introduce, as detailed in the sequel (see Section 2.2).

1.3. Is cancer dormancy a promising therapeutic option?

In a general perspective, apart from the interpretation of tumor dormancy as an observed natural phenomenon in human cancers, the idea to transform cancer into a chronic disease is in the voices of many people in the medical world nowadays [4], [39]. Indeed, the interesting issue here is about: *how can we bring CSCs from an overproliferating activity to a dormant state?* More precisely, since cancer treatments most often consist of delivering the maximum tolerable doses of drugs in order to kill clinically apparent tumors, and knowing that an incompletely eradicated cancer frequently grows again, even more aggressively than the initial one [28], the option of maintaining the tumor in dormancy is more appealing than trying to eradicate it [48]. Further discussions on the opportunities offered by cancer dormancy in therapeutics can be found for instance in [4], [39], [89] and the references therein.

The development of a relevant mathematical framework appears as a necessary tool to apprehend tumor dormancy as a biological mechanism [51], with

[8] Immunotherapy aims to help the immune system destroy cancer cells. It is given after - or at the same time as - another cancer treatment such as chemotherapy.

the ultimate goal to apply it in therapeutic settings. However, the task of mastering CSCs, i.e. bringing them into a dormant state, seems to be difficult to achieve. Indeed, one of the first dormancy-oriented therapeutic approaches in the case of solid tumors has not been very fruitful. It was based on the use of *angiogenesis inhibitors*[9] as drugs that choke off the blood supply of the tumor, in order to maintain it in dormancy. However, unexpected effects occurred in practice, and in some situations, targeting the blood vessels that feed tumors actually accelerated the spread of cancer (see [43, 77]). Therefore, it seems that tumor dormancy is more likely to be assigned to immuno-vigilance[10] (***H.2***), than to nutrient supply limitations (***H.1***). In light of the previously mentioned observations, one can say that dormancy has actually generated more issues than answers, in the process of understanding cancer. Among the open issues, we emphasize the following ones: *when a treatment protocol is elaborated for CSCs eradication with a given rate of success, how can we actually administer it (or a part of it) in order to achieve dormancy?* In addition, since eradication techniques may generate some surviving tumors which become even more aggressive than the initial ones, a key question is to determine *whether it is effective to consider the same targets and drugs, as for CSCs eradication, in order to achieve dormancy?* One can already figure out the utility of mathematical studies in such a context. Finally, we emphasize that, in the clinic of cancers today, eradication of CSCs remains the predominant treatment approach (although there is still a long way to improve the existing eradication treatment strategies [85]).

1.4. Objectives of the study - Particular insights into the hematopoietic system

We aim to provide a consistent theoretical framework for the modeling and the analysis of healthy and unhealthy cell dynamics, following different medical orientations, among which: the case where therapy aims to eradicate cancer

[9] These are substances that inhibit the growth of new blood vessels [35]

[10] In particular, cancer dormancy results from the action of adaptive immunological mechanisms, through T cells, IL-12 and IFN-gamma [80].

cells while preserving healthy ones, and the scenario that consists in maintaining healthy and unhealthy cells in a controlled stable steady-state (i.e. cancer dormancy). To that purpose, a model of coexistence between ordinary and mutated cells is introduced and analyzed. Firstly, we investigate the stability properties of the trivial steady state of the resulting model: this is equivalent to the radical case in which all the cells are eradicated. Then, we perform a stability analysis that applies to cases of cancer dormancy and unhealthy cell eradication (while healthy cells survive). For the biological motivations stated in the above sections, we will focus on the study of cancer dormancy throughout our paper.

At this juncture, we express our keen interest in the hematopoietic system. We define hematopoiesis as the process initiated by the hematopoietic SC population inside the bone marrow, that leads to the formation and continuous replenishment of all the blood cells in the body [45]. Hematopoiesis provides a model for studying and understanding all the mammalian stem cells and their niches [18], as well as all the mechanisms involved in the cell cycle, particularly cell differentiation. The hematopoietic paradigm is used in biology and medicine, as well as in the modeling and analysis of all similar processes. In [72], the author reviewed the mathematical modeling of blood cell dynamics and its related pathological disorders within the past five decades. It is within this framework that we can situate our work, as a continuity of modeling and stability analysis of blood cell dynamics. However, as for the majority of works discussed in [72], the models that we study can be used to cover other tissues and mechanisms. At this point, it is worth mentioning that pioneering works that formulated early blood cell dynamical models have been introduced for any type of cells [81], or borrowed from models describing other tissues, different from blood cell dynamics (see [16] for a dorsal epidermis cell model that inspired all the cell cycle models containing a resting phase). The interested reader is referred to [72] for more information. Therefore, we emphasize in this study the paradigmatic case of hematopoietic SCs, which are at the root of the overall hematopoietic system. Hematopoietic SCs give rise to both the myeloid

and lymphoid lineages of blood cells. The myeloid cells include many types of white blood cells (monocytes, macrophages, neutrophils, eosinophils), red blood cells (erythrocytes), and platelets (megakaryocytes). The hematopoietic process has to be well controlled [45] in order to avoid a wide range of blood disorders[11]. Acute myeloid leukemia (AML) is one of the most deadly blood malignancies. It affects the myeloid lineage and it is characterized by an overproliferation of abnormal immature white blood cells (blasts) of the myeloid lineage. Currently, AML treatment still relies on heavy chemotherapy with a high toxicity level and a low rate of success [25]. In fact, the only certain AML cure being not the result of chemotherapy, but of total bone marrow transplant that induces nearly $10-20\%$ of mortality during the manipulation and due to severe reaction, GVH, of the graft versus the host. A better understanding of the behavior of CSCs (called leukemic cells in AML) should allow us to propose some selective combined targeted therapies that lead, theoretically, to cancer dormancy. In particular, our ambition is to provide a theoretical framework, taking into account observations made by hematologists, and allowing for the suggestion of insights into cancer treatments. It is in this light that we proposed in [23] a model of cohabitation between ordinary and mutated cells in the case of the hematopoietic system. The latter model follows recent observations (made in [44] and in many other works) that associate the emergence of leukemic cells with an accumulation of several mutations, most often occurring in a standard chronological order [44], in the SC compartment. Thus, we have mathematically analyzed in [23] and [24] two categories of heterogeneous cells as illustrated in Figure 1 below, where the addition of mutations (on TET2, NPM1, FLT3) that we have considered had been established in [44]. We pursue in this work an analysis that provides a theoretical framework following different medical orientations, among which: **(i)** the case where therapy aims to eradicate cancer cells while preserving healthy cells, **(ii)** a less demanding, more realistic, sce-

[11] In particular, periodic diseases, such as cyclic neutropenia and some cases of chronic acute leukemia (see [13], [19], [58], [73], and the references therein), but also overproliferating malignant hemopathies, such as acute myeloid leukemia ([2], [23], [65]).

nario that consists in maintaining healthy and unhealthy cells in a controlled stable steady-state (cancer dormancy). Thus, our work extends the one that we proposed in [23], [24] and in a series of works: [1], [8], [9], (but see also [2], [21], [33], [38], [60], [65], [73], [83] and [84]). It is worth mentioning that the model in [9] can neither model dormancy nor the abnormal overproliferation (e.g. invasion of the bone marrow by blasts). The latter point is improved by adopting a different form of fast self-renewing process, which has been recently introduced in [1], and where a subpopulation of cells is considered to be always active in proliferation [1]. In fact, cancer dormancy has not been considered in all the previously mentioned works. This is indeed a new area in cancer therapy (see [4], [28], [48], [89]) that we want to highlight here (but see also [51] for a different approach of modeling and analysis of cancer dormancy).

1.5. Organization of the work

In light of the above mentioned remarks, the coupled model (between healthy and mutated cells as in Figure 1 below) of interest is presented in Section 2. Next, some features of the resulting coupled differential-difference model, together with the conditions of existence of our favourable steady states (reflecting dormancy and CSCs eradication), are discussed in Section 3. Then, in Section 4, the stability analysis of the case of all-cell extinction, via a construction of a linear Lyapunov-like functional, is performed (here we provide conditions for global exponential stability of the trivial steady state of the coupled model). Then, afterwards, we address in Section 5 the stability analysis, in the time-domain framework, of the cases describing cancer dormancy, and, unhealthy cells eradication (while healthy cells survive). The latter study goes through quadratic Lyapunov-like constructions (i.e. suitable degenerate functionals for the class of differential-difference systems). In fact, we are going to use two slightly different constructions: the first one is more general and relies on Linear Matrix Inequality (LMI) conditions derived via the *descriptor* method [37], applied to the linear approximation of the model around its nontrivial steady state of interest. This approach aims to provide a theoretical (sufficient) sta-

bility criterion, in the LMI form, to establish whether the steady state of a specific biological system is locally stable. The latter technique is followed by a second Lyapunov-type construction that allows us to determine *explicit* decay conditions (not in the LMI form) as well as an estimate of the decay rate of solutions and an approximation of the basin of attraction of the studied steady state. These sufficient stability conditions may be more restrictive than the LMI ones, however, they have the advantage of being easier to handle and, therefore, make it possible to interpret them biologically, from medical and therapeutic standpoints. Finally, numerical illustrations are provided and some concluding discussions, including biological interpretations of the findings, are outlined in Section 6.

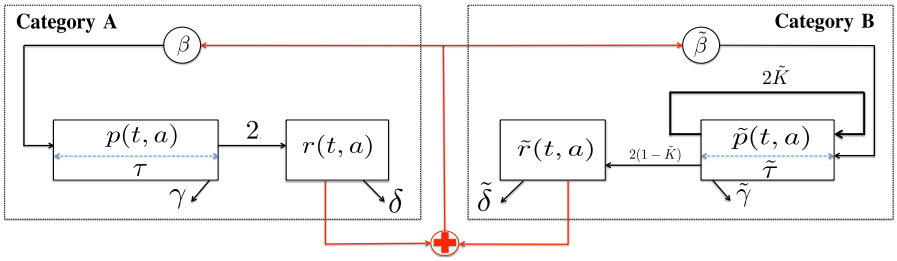

Figure 1: Schematic representation of the coupled model of interest, involving a healthy SCs compartment (on the left) and an unhealthy compartment (on the right). For the sake of simplicity, we assume that unhealthy cells are those presenting mutations that lead to cancer. Indeed, we consider that abnormal stem cells (**Category B**) have for instance a first mutation in some genes encoding enzymes in epigenetics (e.g. on TET2, DNMT3A [20, 71]), that increases the self-renewing activity of the affected cells. A more serious pathological situation arises when a second mutation, affecting this time the pathways regulating the differentiation process such as NPM1 or transcription factors, appears on some of the cells. The superposition of these two events yields a blockade in differentiation. Finally, a subsequent mutation impairing proliferation control (e.g. FLT3-ITD) appears in a subpopulation of cells that have already accumulated one or more of the previously mentioned mutations. The latter event activates an uncontrolled overproliferation of a subpopulation of cells (CSCs) and thereby causes AML [44]. Throughout this work, with a kind of abuse of notation, we use equivalently the designations: unhealthy cells, mutated cells, and CSCs. Similarly, healthy cells (**Category A**), or ordinary cells, represented on the left, are those which do not have any abnormal mutation, or those presenting some abnormalities which are not related to cancer. The definitions of the biological parameters (δ, $\tilde{\delta}$, γ, $\tilde{\gamma}$,...) are provided in Section 2.

2. A new general mathematical model involving coexistence between healthy and cancer stem cells

Our objective is to introduce a model more general than the existing ones, with regard to the recent biological features of interest, that are: cancer dormancy [26, 28], control and eradication of CSCs [48]. In particular, the compartment of unhealthy cells is hierarchized according to the severity of the mutations: cells that accumulate mutations up to that of FLT3 duplication (see Figure 1) are constantly active in proliferation (as in [1]). Our configuration allows us to reproduce and interpret the case of cancer dormancy, with the ultimate goal of providing theoretical stability conditions, along with therapeutic insights, that lead to stable dormant CSCs.

2.1. A multi-compartmental general model for healthy and unhealthy cells

We focus on the model illustrated in Figure 1, where CSCs are characterized by an ability to over-proliferate represented by the parameter $\tilde{K}$ (in $days^{-1}$), as considered in [1], and previously envisaged in [9] in a different configuration. More precisely, we notice that a subpopulation of unhealthy cells is in a permanent dividing state, namely the portion corresponding to $2\tilde{K}$, where, $0 < \tilde{K} < 1$ (as in [1] for a non-coupled model), which is different from the healthy SCs behavior (Figure 1, on the left), where daughter cells, that arise from division of healthy mother cells, leave the proliferating compartment and join necessarily the resting one. Healthy resting stem cells can stay in G_0 until their death, differentiate, or start a new proliferating cycle by being transferred through the reintroduction function β to there proliferating compartment. Indeed, we mention that as many other works (see [2, 57, 73], among others), we are considering a compartmental model in which each cell can be in a resting phase or in a proliferating one. Finally, we mention that the coupled models studied in [9, 23] do not admit a stable steady state that describes cancer dormancy, and this is an issue that we overcome here by considering a more general manner of coupling healthy and unhealthy SCs as discussed in the sequel.

Next, we denote by δ (resp. $\tilde{\delta}$) the rate, expressed in $days^{-1}$, of resting cells, which is lost either by differentiation or natural cell death for healthy SCs (resp. CSCs). A resting cell may start a cell cycle by entering in the proliferating phase during which each proliferating SC (resp. CSC) may die by apoptosis at a rate, expressed in $days^{-1}$, γ (resp. $\tilde{\gamma}$), or complete its mitosis and become two daughter cells at the end of the proliferating phase. We denote τ (resp. $\tilde{\tau}$) the average time (in *days*) taken to complete mitosis in the healthy (resp. unhealthy) proliferating compartment. For proliferation, the mechanisms regulating the entry into the cell cycle - at the cellular level - rely on some regulatory molecules that can play the role of growth factors (by stimulating the entry into proliferation of resting healthy and unhealthy cells), or, they can play the role of mitotic inhibitor ligands (meaning that mitosis proceeds normally if inhibitors are not combined with cell receptors, while it is stalled when they bind them). Consequently, we consider in our model that the transfer from the resting to the proliferating states is controlled by some reintroduction functions (as in [57, 73] and the majority of earlier works). More precisely, we let β (resp. $\tilde{\beta}$) be the reintroduction function from the healthy (resp. unhealthy) resting phase to the healthy (resp. unhealthy) proliferating phase. In addition, since healthy and unhealthy cells share the same environment (called *niches* [18] in hematopoiesis), we consider that each of the two functions β and $\tilde{\beta}$ depends simultaneously on both the total density of resting healthy cells, $x(t) = \int_0^\infty r(t,a)da$, and the total density of unhealthy resting cells, $\tilde{x}(t) = \int_0^\infty \tilde{r}(t,a)da$, where $r(t,a)$ and $\tilde{r}(t,a)$ are, respectively, the densities of resting healthy cells and resting unhealthy cells, of age $a \geq 0$, at time $t \geq 0$ [23]. This modeling approach reflects cohabitation between healthy and unhealthy cells, by considering that the entry into proliferation of healthy cells (resp. unhealthy cells) is also dependent on the total density of unhealthy cells (resp. healthy cells), the dynamics of the left and the right subpopulations in Figure 1 becoming thus strongly coupled. Thus, the choice of the arguments (i.e. coupling forms) given to the functions β and $\tilde{\beta}$ is crucial, since these arguments quantify the regulating mechanisms that affect healthy and unhealthy cells (see [57] for the case of non-coupled models).

2.2. The coupling form between ordinary and mutated cells

The functions β and $\tilde{\beta}$ represent the physiological inhibitory hormonal feedback by *Granulocyte Colony Stimulating Factors (G-CSF)* that is valid in the case of healthy as in the case of cancer cells. However, in the latter unhealthy situation, the sensitivity of the unhealthy cell population to this feedback may strongly vary. Now, the remaining issue regarding the functions β and $\tilde{\beta}$ is to select the coupling function between the total density of healthy resting cells x and the total density of mutated resting cells $\tilde{x}$ (i.e., to specify how β and $\tilde{\beta}$ actually depend on x and $\tilde{x}$). It appears that the simplest choice is to consider that both β and $\tilde{\beta}$ depend on the sum $x + \tilde{x}$, as previously considered in [9] and [23]. The latter scheme expresses a kind of absence of dominance between the populations x and $\tilde{x}$, since they show equal influence on β and $\tilde{\beta}$. However, differences actually exist between x and $\tilde{x}$ in their shared host - in particular immune - environment, mainly due to the mutations acquired by abnormal cells [46] and the reaction of the immune system. Changes that occur in mutated cell behavior may enhance the growth of cancer and result in cachexia and death [12] (see also [27, 70] for biological observations and modeling of the interaction between cancer and host environment). In our modeling approach, considering a coupling in the form $x + \tilde{x}$ means equal sensitivity of ordinary and mutated resting populations regarding the diverse proliferation regulation mechanisms, that act on the reintroduction of resting cells into proliferation. For example, due to epigenetic mutations, unhealthy cells may become less sensitive than healthy ones to the regulatory molecules secreted by the body and avoid the immune system (i.e. an immunosuppressive effect); on the other hand, healthy cells are in turn insensitive to the action of the immune system and less sensitive to drugs, since these drugs are designed to target unhealthy cells. In summary, healthy and unhealthy cells may react differently to their shared host environment (see Figure 2 below), which may result in the dominance of one subpopulation (healthy or unhealthy), or possibly in cancer dormancy [80]. Our first objective is to achieve a model that reproduces all these situations. Thus, we aim here to extend the modeling aspects by considering a more general form

of coupling functions, so that some immunological effects can be represented. For that purpose, we consider that the argument of β is $x + \tilde{x}$, while $\tilde{\beta}$ depends at the same time on a weighted combination $x + \tilde{\alpha}\tilde{x}$, where $\tilde{\alpha}$ is some positive constant. We will show later in Section 3 that actually dormancy may be found mostly when $\tilde{\alpha} \neq 1$. In an illustrative manner, Figure 2 provides a representation of the cases:

- $0 \leq \tilde{\alpha} \leq 1$: even if ordinary and mutated cells are sharing the same environment, the mutated ones are less sensitive to the regulatory system present in the host environment, that may be identified as effects of the immune system on mutated cell proliferation. Consequently, unhealthy cells may escape a part of the regulatory system, including the immune system. This appears to be in line with medical practice, since the unhealthy behavior is mainly due to genetic/epigenetic mutations that make cells partially unresponsive to the regulating system. Consequently, the case $0 \leq \tilde{\alpha} \leq 1$ suits well the untreated unhealthy behavior, in which cells avoid immune attacks and tend to get out of control, possibly leading to outgrowth of CSCs [80, 90, 95].

- $\tilde{\alpha} > 1$: this case can describe an environment where unhealthy cells are more affected by the regulatory molecules than the healthy ones. This may be partly due to the effector response of the immune system (*cancer immunosurveillance* [90]), which may explain the dormancy phenomenon as a result of an efficient immune action that contains cancer growth [93]. In other words, the case $\tilde{\alpha} > 1$ stands for a situation where proliferation of unhealthy cells may be locally kept under check by the immune system. This is the role of the innate and adaptive immunity which may lead to extrinsic tumor suppression in some rare cases, or to the adaptive immunity (T cells, IL-12, IFN-gamma) that at least may maintain cancer dormancy for long time [80].

Remark 1. *A concept of dominance between healthy and mutated cells results from $\tilde{\alpha}$, that allows for an implicit representation of the immunologic mechanisms. In fact, what really makes the difference between cells is their respective sensitivity to the immune environment. The natural feedback represented by the*

functions β and $\tilde{\beta}$ depending on their arguments x and $\tilde{x}$, is in the case of cancer cells tuned by a sensititvity parameter $\tilde{\alpha}$ that may be seen as the faculty of unhealthy cells to over-express ($\tilde{\alpha} > 1$) or hide ($\tilde{\alpha} < 1$) their surface antigens.

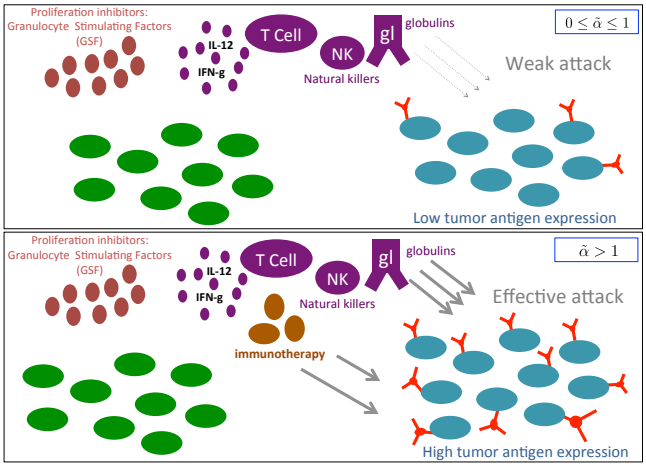

Figure 2: Cartoon illustration of healthy and unhealthy cells in their shared environment. Ordinary SCs with normal behavior are in green, while mutated ones that go through quiescence to re-start a cell cycle (i.e. not the ones having the FLT3 mutation that makes them constantly active into proliferation) are in blue. The regulation of cell proliferation may include different mechanisms: release of growth factors and mitotic regulatory molecules, T cells, natural killers, globulins, IFN-g (IFN-gamma) and IL-12 (interleukin 12). Epigenetic mutations may also play a role on the way cells react to the whole regulating system. The case $0 \leq \tilde{\alpha} \leq 1$ fits well a situation in which unhealthy cells are less sensitive to proliferation regulation than healthy ones. In this case, abnormal cells may hide their tumor antigens (an immunosuppressive state), which can be also due to the tumor variant cells that become no longer recognized and attacked by the adaptive immunity [80] and grow into insensitive cells to the entire immune effector mechanism. This condition is not enough in itself for the development of cancer, but it certainly favors it and may lead to the escape phase. On the other hand, the case $\tilde{\alpha} > 1$ represents a situation in which proliferation of unhealthy cells is more controlled than the one of healthy cells. Reasons for this include an effective action carried out by the innate and adaptive immunity (sometimes this action suffices for total tumor eradication, see e.g. [90] and Fig. 3 in [80]), but also the use of immunotherapy that acts in two ways: boosting the immune system to eliminate CSCs, and/or, enhancing the immune response by providing additional combative components such as reenabling exhausted T cells.

In addition, it can also be argued that $\tilde{\alpha} > 1$ relies on the use of drugs (immunotherapy, chemotherapy, etc) that specifically target unhealthy cells. Indeed, we recall that immunotherapy mainly enhances the immune response, and that recent chemotherapy or targeted therapies are increasingly more accurate due to the overexpression of cancer receptors (which allow them to target

unhealthy cells while the majority of healthy cells are spared). Finally, we mention that the introduction of the above considerations related to the coupling functions between x and $\tilde{x}$ will make the dynamics of the resulting model richer than earlier models, as discussed in the next sections (Section 3). To the authors' knowledge, no equivalent model exists in the literature. Next, as conventionally considered, we assume that $\tilde{\beta}$ and β are nonlinear continuous decreasing functions, and, $\lim_{\ell\to\infty}\tilde{\beta}(\ell) = \lim_{\ell\to\infty}\beta(\ell) = 0$. As in [57], [73], and all subsequent works for non-coupled models, we consider the typical Hill forms:

$$\tilde{\beta}(\ell) = \frac{\tilde{\beta}(0)}{1+\tilde{b}\ell^{\tilde{n}}}, \quad \beta(\ell) = \frac{\beta(0)}{1+b\ell^{n}} \tag{1}$$

where $\tilde{b}$, b, $\tilde{\beta}(0)$ and $\beta(0)$ are strictly positive real numbers and, $\tilde{n} \geq 2$ and $n \geq 2$. In fact, the Hill functions in (1), that belong to the family of functions with negative Schwarzian derivatives (see [5], Chap. 3) are commonly encountered in many real-life problems. Classical arguments on cooperativity of enzyme inhibition kinetics (see Chap. 1 in [52], and [75]), allow to determine the Hill-type expressions (1). The cooperative effect results in general from the fact that the binding of one regulatory molecule on one extracellular (surface) receptor of one cell will affect the binding of subsequent regulatory molecules on other receptors of the same cell. Due to the above considerations on the different sensitivities between healthy and unhealthy cells in the niches (1 and $\tilde{\alpha} \neq 1$, respectively), we can readily deduce that for given total densities x and $\tilde{x}$, the associated reintroduction functions β and $\tilde{\beta}$ actually operate according to:

$$\tilde{\beta}\left(x+\tilde{\alpha}\tilde{x}\right) = \frac{\tilde{\beta}(0)}{1+\tilde{b}\left(x+\tilde{\alpha}\tilde{x}\right)^{\tilde{n}}}, \quad \beta\left(x+\tilde{x}\right) = \frac{\beta(0)}{1+b\left(x+\tilde{x}\right)^{n}}. \tag{2}$$

2.3. Equations describing the dynamics of coupled cell populations

After the description of the particular case of the reintroduction functions β and $\tilde{\beta}$ according to the variation of the cell densities x and $\tilde{x}$ (as in Figure 3), we now focus on the dynamical equations describing the populations of cells.

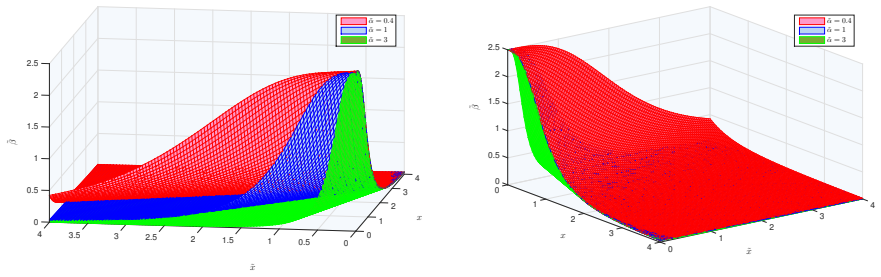

Figure 3: Illustrative example of variations of a typical $\tilde{\beta}$-surface with respect to $\tilde{x}$ and x, for different values of $\tilde{\alpha}$ (i.e. in the three possible situations: $\tilde{\alpha} > 1$, $\tilde{\alpha} = 1$, and $\tilde{\alpha} < 1$).

Similarly to x and $\tilde{x}$, we denote by y and $\tilde{y}$, respectively, the total densities of proliferating healthy and unhealthy cells: $y(t) = \int_0^{\tau} p(t,a)da$, and, $\tilde{y}(t) = \int_0^{\tilde{\tau}} \tilde{p}(t,a)da$. The age-structured PDEs describing the coupled model in Figure 1, are given for all $t > 0$ by:

$$\begin{cases} \partial_t \tilde{r}(t,a) + \partial_a \tilde{r}(t,a) = -\left[\tilde{\delta} + \tilde{\beta}\left(x, \tilde{x}, \tilde{\alpha}, t\right)\right] \tilde{r}(t,a), \quad a > 0, \\ \partial_t \tilde{p}(t,a) + \partial_a \tilde{p}(t,a) = -\tilde{\gamma}\tilde{p}(t,a), \quad 0 < a < \tilde{\tau}, \\ \partial_t r(t,a) + \partial_a r(t,a) = -\left[\delta + \beta\left(x, \tilde{x}, t\right)\right] r(t,a), \quad a > 0, \\ \partial_t p(t,a) + \partial_a p(t,a) = -\gamma p(t,a), \quad 0 < a < \tau. \end{cases} \tag{3}$$

In McKendrick-type models ([33], [56], [91]), we observe that only the death rates (δ, $\tilde{\delta}$, γ and $\tilde{\gamma}$), and the removal terms (β and $\tilde{\beta}$, since the reintroduction functions are considered as cell loss from resting cells) appear in the PDE system (3). On the other hand, the new births, which are the renewal conditions at the age $a = 0$, for resting and proliferating cells, are introduced through the following boundary conditions:

$$\begin{cases} \tilde{r}(t,0) = 2(1-\tilde{K})\tilde{p}(t,\tilde{\tau}), \\ \tilde{p}(t,0) = \tilde{\beta}\left(x, \tilde{x}, \tilde{\alpha}, t\right)\tilde{x}(t) + 2\tilde{K}\tilde{p}(t,\tilde{\tau}) \triangleq \tilde{u}(t), \\ r(t,0) = 2p(t,\tau), \\ p(t,0) = \beta\left(x, \tilde{x}, t\right)x(t), \end{cases} \tag{4}$$

for all $t > 0$, and where $\tilde{u}(t)$ represents the density of new proliferating unhealthy cells at time $t > 0$ [1]. Finally, the initial age-distributions, respectively,

$\tilde{r}(0,a) = \tilde{r}_0(a)$, for $a > 0$, $\tilde{p}(0,a) = \tilde{p}_0(a)$, for $0 < a < \tilde{\tau}$, $r(0,a) = r_0(a)$, for $a > 0$, and $p(0,a) = p_0(a)$, for $0 < a < \tilde{\tau}$, are assumed to be L^1-functions.

Now, inspired by an illustrative approach in [87], we give a biological explanation of the method of characteristics in our context. To avoid redundancy, we focus only on the unhealthy compartment. Let us define $\mathfrak{p}^*(a,s)$ as the density of unhealthy proliferating cells, of age a, that entered to the unhealthy proliferating phase at time s. This coincides with the density of unhealthy proliferating cells at time $t = a + s$ ([87]). In other words, $\mathfrak{p}^*(a,s) = \tilde{p}(a+s,a)$. Therefore,

$$\frac{\partial \mathfrak{p}^*(a,s)}{\partial a} = \frac{\partial \tilde{p}(t,a)}{\partial t}\Big|_{t=a+s} + \frac{\partial \tilde{p}(t,a)}{\partial a}\Big|_{t=a+s} = -\tilde{\gamma}\mathfrak{p}^*(a,s).$$

It follows that $\mathfrak{p}^*(a,s) = \mathfrak{p}^*(0,s)e^{-\tilde{\gamma}a}$, where $\mathfrak{p}^*(0,s) = \tilde{p}(s,0)$.

Now, let us recover $\tilde{p}$ from $\mathfrak{p}^*$ ([87]). Noticing that $\tilde{p}(t,a) = \mathfrak{p}^*(a,t-a)$, for $t > a$, we obtain, $\tilde{p}(t,a) = e^{-\tilde{\gamma}a}\tilde{p}(t-a,0)$, for all $t > a$.

Next, we define $\mathfrak{p}^{\mathfrak{v}}(t,s) = \tilde{p}(t,t+s)$, which can be interpreted as the density of unhealthy proliferating cells that are in the proliferating phase at time t, and have been in the proliferating phase at time 0, with an age $a = s$ at $t = 0$. Arguing as for $\mathfrak{p}^*$ ([87]), we find that $\frac{\partial \mathfrak{p}^{\mathfrak{v}}(t,s)}{\partial t} = -\tilde{\gamma}\mathfrak{p}^{\mathfrak{v}}(t,s)$.

Then, $\mathfrak{p}^{\mathfrak{v}}(t,s) = \mathfrak{p}^{\mathfrak{v}}(0,s)e^{-\tilde{\gamma}t}$, where $\mathfrak{p}^{\mathfrak{v}}(0,s) = \tilde{p}(0,s) = \tilde{p}_0(s)$. Recovering $\tilde{p}$ from $\mathfrak{p}^{\mathfrak{v}}$, for $a \geq t$, gives us $\tilde{p}(t,a) = e^{-\tilde{\gamma}t}\tilde{p}_0(a-t)$, for all $a \geq t$.

We deduce that we have recovered the well-known solution ([87]):

$$\tilde{p}(t,a) = \begin{cases} e^{-\tilde{\gamma}t}\tilde{p}_0(a-t), & 0 \leq t \leq a \\ e^{-\tilde{\gamma}a}\tilde{p}(t-a,0), & t > a. \end{cases} \tag{5}$$

Consequently, the first equation in (4) is then equivalent to

$$\tilde{r}(t,0) = \begin{cases} 2(1-\tilde{K})e^{-\tilde{\gamma}t}\tilde{p}_0(\tilde{\tau}-t), & 0 \leq t \leq \tilde{\tau}, \\ 2(1-\tilde{K})e^{-\tilde{\gamma}\tilde{\tau}}\tilde{p}(t-\tilde{\tau},0), & t > \tilde{\tau}. \end{cases} \tag{6}$$

From biological considerations we set, $\lim_{a\to\infty}\tilde{r}(t,a) = \lim_{a\to\infty} r(t,a) = 0$, for all fixed value of $t \geq 0$. Then, using (8), and by integrating the first equation in (3) with respect to a between 0 and $+\infty$, we determine that the long time behavior ([11]) of $\tilde{x}$ is given by $\dot{\tilde{x}}(t) = -(\tilde{\delta} + \tilde{\beta}\,(x,\tilde{x},\tilde{\alpha},t))\tilde{x}(t) + 2(1-\tilde{K})e^{-\tilde{\gamma}\tilde{\tau}}\tilde{u}(t-\tilde{\tau})$, where we recall that the density $\tilde{u}(t)$ is the one defined in (4), and represents

for all $t > 0$ the density of new unhealthy proliferating cells. Similarly, by integrating the second equation in (3) over the variable a, between 0 and $\tilde{\tau}$, and using $\tilde{p}(t, \tilde{\tau}) = \tilde{u}(t-\tilde{\tau})$, we get $\dot{\tilde{y}}(t) = -\tilde{\gamma}\tilde{y}(t) + \tilde{\beta}(x, \tilde{x}, \tilde{\alpha}, t)\tilde{x}(t) - (1 - 2\tilde{K})e^{-\tilde{\gamma}\tilde{\tau}}\tilde{u}(t-\tilde{\tau})$. Similarly, we can check that for the healthy compartment, we obtain for all $t > 0$:

$$p(t,a) = \begin{cases} e^{-\gamma t}p_0(a-t), & 0 \le t \le a \\ e^{-\gamma a}p(t-a,0), & t > a. \end{cases} \tag{7}$$

It follows that the third equation in (4) is then equivalent to:

$$r(t,0) = \begin{cases} 2e^{-\gamma t}p_0(\tau - t), & 0 \le t \le \tau, \\ 2e^{-\gamma\tau}p(t-\tau,0), & t > \tau, \end{cases} \tag{8}$$

where $p(t-\tau, 0)$ is deduced from the fourth equation in (4). Thus, using similar arguments as for the unhealthy compartment, we deduce the following overall system for all $t > 0$,

$$\begin{cases} \dot{\tilde{x}}(t) &= -\left[\tilde{\delta} + \tilde{\beta}\left(x, \tilde{x}, \tilde{\alpha}, t\right)\right]\tilde{x}(t) + 2(1-\tilde{K})e^{-\tilde{\gamma}\tilde{\tau}}\tilde{u}(t-\tilde{\tau}), \\ \dot{\tilde{y}}(t) &= -\tilde{\gamma}\tilde{y}(t) + \tilde{\beta}\left(x, \tilde{x}, \tilde{\alpha}, t\right)\tilde{x}(t) - (1-2\tilde{K})e^{-\tilde{\gamma}\tilde{\tau}}\tilde{u}(t-\tilde{\tau}), \\ \tilde{u}(t) &= \tilde{\beta}\left(x, \tilde{x}, \tilde{\alpha}, t\right)\tilde{x}(t) + 2\tilde{K}e^{-\tilde{\gamma}\tilde{\tau}}\tilde{u}(t-\tilde{\tau}), \\ \dot{x}(t) &= -\left[\delta + \beta\left(x, \tilde{x}, t\right)\right]x(t) + 2e^{-\gamma\tau}\beta\left(x, \tilde{x}, t-\tau\right)x(t-\tau), \\ \dot{y}(t) &= -\gamma y(t) + \beta\left(x, \tilde{x}, t\right)x(t) - e^{-\gamma\tau}\beta\left(x, \tilde{x}, t-\tau\right)x(t-\tau). \end{cases} \tag{9}$$

We notice that the dynamics of x, $\tilde{x}$ and $\tilde{u}$ do not depend on y and $\tilde{y}$. This (triangular) system structure leads us to study first:

$$\begin{cases} \dot{\tilde{x}}(t) = -\left[\tilde{\delta} + \tilde{\beta}\left(x(t) + \tilde{\alpha}\tilde{x}(t)\right)\right]\tilde{x}(t) + 2(1-\tilde{K})e^{-\tilde{\gamma}\tilde{\tau}}\tilde{u}(t-\tilde{\tau}), \\ \tilde{u}(t) = \tilde{\beta}\left(x(t) + \tilde{\alpha}\tilde{x}(t)\right)\tilde{x}(t) + 2\tilde{K}e^{-\tilde{\gamma}\tilde{\tau}}\tilde{u}(t-\tilde{\tau}), \\ \dot{x}(t) = -\left[\delta + \beta\left(x(t) + \tilde{x}(t)\right)\right]x(t) + 2e^{-\gamma\tau}\beta\left(x(t-\tau) + \tilde{x}(t-\tau)\right)x(t-\tau). \end{cases} \tag{10}$$

We can prove that a unique piecewise continuous solution, $(\tilde{x}(t), \tilde{u}(t), x(t))$, exists for all $t \ge 0$, when system (10) is associated with appropriate initial conditions $(\varphi_{\tilde{x}}, \varphi_{\tilde{u}}, \varphi_x)$, where, $\varphi_{\tilde{x}} \in \mathcal{C}\left([-\tau, 0], \mathbb{R}\right)$, $\varphi_x \in \mathcal{C}\left([-\tau, 0], \mathbb{R}\right)$, and, $\varphi_{\tilde{u}} \in \mathcal{C}\left([-\tilde{\tau}, 0], \mathbb{R}\right)$. Moreover, we can show that the system (10) is positive, since $\tilde{K} \in (0, 1)$. Throughout this work, only positive solutions of (10) are considered.

3. Notable features of the coupled model

In this section, we point out some properties of the model (10) that highlight its rich dynamics, according to the following possibly existing cases[12]:

Point of interest of $\tilde{x}$	0	$\tilde{x}_e$	0	$\tilde{x}_e$	$+\infty$
Point of interest of $\tilde{u}$	0	$\tilde{u}_e$	0	$\tilde{u}_e$	$+\infty$
Point of interest of x	0	0	x_e	x_e	*

❑ **Cell extinction:** clearly, $(0, 0, 0)$, is an equilibrium point of model (10). Biologically, convergence to zero is synonymous of the extinction of all the cells (both healthy and unhealthy populations). From a therapeutic standpoint, we said that we aim to address theoretical studies for the case of unhealthy cells eradication (while ensuring that healthy cells survive), and also for a dormancy steady state (where all the cells are in a stable steady state). In both situations we do not want that healthy cells vanish. However, chemotherapy always affects - to a certain extent - healthy cells. But side effects of recent chemotherapy treatments are fewer than those of the drugs used in the past, since novel molecules (targeted therapies) are designed to target overexpressed receptors corresponding to mutated cells (i.e. drugs are more accurate since they attack cells with specific extracellular receptors expressed only on mutated cells). In addition, medications are mainly acting on cells during their phase of proliferation, while it appears that most of the healthy cells are in quiescence. Therefore, we consider that only a *radical* therapy will lead to total cell eradication, and this is a situation that we want to avoid. Nevertheless, the theoretical conditions, depending on the biological functions and parameter involved in our model, that cause total cell eradication are discussed in Section 4.

❑ **Escape from dormancy in diseased cells:** one of the main concerns related to dormancy is to explain how escape from tumor dormancy can emerge (see [51] and the non-coupled model in [1] that admits unbounded solutions).

[12] Here we are considering that $\tilde{x}_e > 0$, $\tilde{u}_e > 0$ and $x_e > 0$. We can notice that $\tilde{x}_e = 0$ implies that $\tilde{u}_e = 0$, and vice versa.

Similarly to [1], we notice in the coupled model (10) that the CSC-compartment may have unbounded solutions that reproduce the unlimited cell proliferation in cancer. Indeed, from the second equation in (10) it is obvious that $2\tilde{K}e^{-\tilde{\gamma}\tilde{\tau}} > 1$, implies that, $\lim_{t\to+\infty} \tilde{u}(t) = +\infty$. It follows from the first equation in (10) that $\lim_{t\to+\infty} \tilde{x}(t) = +\infty$. This situation may reflect the escape from tumor dormancy, or the invasion of the bone marrow by the blasts as in AML.

❑ **Existence of the desired steady states $\mathfrak{D}$ and $\mathfrak{E}$:** let us start from the general case in which the point $(\tilde{x}_e, \tilde{u}_e, x_e)$ is a nonnegative steady state of (10). Therefore, it follows that this equilibrium point satisfies:

$$\begin{cases} \left[\tilde{\delta} + \tilde{\beta}(x_e + \tilde{\alpha}\tilde{x}_e)\right] \tilde{x}_e = 2(1-\tilde{K})e^{-\tilde{\gamma}\tilde{\tau}}\tilde{u}_e, \\ \tilde{\beta}(x_e + \tilde{\alpha}\tilde{x}_e)\tilde{x}_e = \left(1 - 2\tilde{K}e^{-\tilde{\gamma}\tilde{\tau}}\right)\tilde{u}_e, \\ \left[\delta - (2e^{-\gamma\tau} - 1)\,\beta(x_e + \tilde{x}_e)\right] x_e = 0, \end{cases} \tag{11}$$

where we exclude the previously discussed case of unbounded solutions by assuming that: $2\tilde{K}e^{-\tilde{\gamma}\tilde{\tau}} < 1$. Indeed, our main objective here is to determine necessary and sufficient conditions for the existence of $\mathfrak{D} = (\tilde{x}_e, \tilde{u}_e, x_e)$, where $x_e > 0$, $\tilde{x}_e > 0$ and $\tilde{u}_e > 0$, and for the existence of $\mathfrak{E} = (0, 0, x_e)$, where $x_e > 0$.

First, since β is continuous and decreasing from $\beta(0)$ to zero, we deduce from the third equation in (11) that,

$$\delta < \left[2e^{-\gamma\tau} - 1\right] \beta(0), \tag{12}$$

is a necessary and sufficient condition for the existence of x_e and $\tilde{x}_e$ such that, $x_e + \tilde{x}_e > 0$, and, $\delta - (2e^{-\gamma\tau} - 1)\,\beta(x_e + \tilde{x}_e) = 0$. In fact, the inequality (12) is a necessary and sufficient condition for the existence of $\mathfrak{E}$ (but not $\mathfrak{D}$).

Next, from the second equation in (11), we obtain that $\tilde{u}_e = \frac{\tilde{\beta}(x_e + \tilde{\alpha}\tilde{x}_e)\tilde{x}_e}{1 - 2\tilde{K}e^{-\tilde{\gamma}\tilde{\tau}}}$.

By substituting $\tilde{u}_e$ in the first equation of (11), we get:

$$\left[\tilde{\delta} - \frac{2e^{-\tilde{\gamma}\tilde{\tau}} - 1}{1 - 2\tilde{K}e^{-\tilde{\gamma}\tilde{\tau}}}\tilde{\beta}(x_e + \tilde{\alpha}\tilde{x}_e)\right] \tilde{x}_e = 0. \tag{13}$$

The fact that $\tilde{\beta}$ is continuous and decreasing implies that the condition,

$$\tilde{\delta} < \left[\frac{2e^{-\tilde{\gamma}\tilde{\tau}} - 1}{1 - 2\tilde{K}e^{-\tilde{\gamma}\tilde{\tau}}}\right]\tilde{\beta}(0), \tag{14}$$

is necessary and sufficient for the existence of x_e and $\tilde{x}_e$, such that, $x_e + \tilde{\alpha}\tilde{x}_e > 0$, and, $\tilde{\delta} - \frac{2e^{-\tilde{\gamma}\tilde{\tau}}-1}{1-2\tilde{K}e^{-\tilde{\gamma}\tilde{\tau}}}\tilde{\beta}(x_e + \tilde{\alpha}\tilde{x}_e) = 0$. Obviously, we notice that, $2\tilde{K}e^{-\tilde{\gamma}\tilde{\tau}} < 1 < 2e^{-\tilde{\gamma}\tilde{\tau}}$. In fact, the condition (14) is a necessary and sufficient condition for the existence of $(\tilde{x}_e, \tilde{u}_e, 0)$, where $\tilde{x}_e > 0$ and $\tilde{u}_e > 0$.

It is worth mentioning that, if the condition (12) is satisfied (i.e. the necessary and sufficient condition for the existence of $\mathfrak{E}$), together with the condition

$$\tilde{\delta} > \left[\frac{2e^{-\tilde{\gamma}\tilde{\tau}} - 1}{1 - 2\tilde{K}e^{-\tilde{\gamma}\tilde{\tau}}}\right]\tilde{\beta}(0), \tag{15}$$

then $(0, 0, 0)$ and $\mathfrak{E}$ are the unique existing steady states of the studied model. Let us now focus on the case where both x_e and $\tilde{x}_e$ are simultaneously strictly positive (and then $\tilde{u}_e$ is strictly positive). In the latter situation, we get,

$$\begin{cases} x_e + \tilde{\alpha}\tilde{x}_e = \tilde{\beta}^{-1}(\tilde{\mu}), \\ x_e + \tilde{x}_e = \beta^{-1}(\mu), \end{cases} \tag{16}$$

where, $\mu = \frac{\delta}{2e^{-\gamma\tau}-1}$, and, $\tilde{\mu} = \frac{\tilde{\delta}\left(1-2\tilde{K}e^{-\tilde{\gamma}\tilde{\tau}}\right)}{2e^{-\tilde{\gamma}\tilde{\tau}}-1}$. Consequently, we get,

$$\begin{cases} x_e = \frac{1}{\tilde{\alpha}-1}\left[\tilde{\alpha}\beta^{-1}(\mu) - \tilde{\beta}^{-1}(\tilde{\mu})\right], \\ \tilde{x}_e = \frac{1}{\tilde{\alpha}-1}\left[\tilde{\beta}^{-1}(\tilde{\mu}) - \beta^{-1}(\mu)\right], \\ \tilde{u}_e = \frac{\tilde{\delta}}{2e^{-\tilde{\gamma}\tilde{\tau}}-1}\tilde{x}_e. \end{cases} \tag{17}$$

Now, we distinguish between the following two situations:

The case $\tilde{\alpha} = 1$: Here we notice that,

$$\begin{cases} x_e + \tilde{x}_e = \tilde{\beta}^{-1}(\tilde{\mu}) = \beta^{-1}(\mu), \\ \tilde{u}_e = \frac{\tilde{\delta}}{2e^{-\tilde{\gamma}\tilde{\tau}}-1}\tilde{x}_e, \end{cases} \tag{18}$$

which is either an impossible case if the biological parameters are such that $\tilde{\beta}^{-1}(\tilde{\mu}) \neq \beta^{-1}(\mu)$, or, when $\tilde{\beta}^{-1}(\tilde{\mu}) = \beta^{-1}(\mu)$, it corresponds to a *continuum* equilibrium point (the infinite possible values of x_e and $\tilde{x}_e$ that satisfy the first equation in (18)). We want to avoid the latter continuum equilibrium points since that case has no concrete biological signification.

The case $\tilde{\alpha} > 1$ or $0 < \tilde{\alpha} < 1$: First, we focus on the case $0 < \tilde{\alpha} < 1$. We recall from earlier discussion that, biologically, $0 < \tilde{\alpha} < 1$ means that CSCs are less sensitive than ordinary cells to their shared environment composed by regulatory mitotic molecules (due to epigenetic mutations for instance, unhealthy cells no longer respond to inhibitory signals and continue to proliferate). More generally, $\tilde{\alpha} < 1$ plays the role of a mitigating factor of the effect of regulatory molecules that attenuate the entrance frequency into proliferation. Now, from (17), we deduce that a sufficient condition for the existence of $\mathfrak{D}$ when $\tilde{\alpha} < 1$, is given by: $\tilde{\alpha}\beta^{-1}(\mu) < \tilde{\beta}^{-1}(\tilde{\mu}) < \beta^{-1}(\mu)$.

On the other hand, we observe that when $\tilde{\alpha} > 1$, then, from (17), we deduce that a sufficient condition for the existence of $\mathfrak{D}$ is given by: $\beta^{-1}(\mu) < \tilde{\beta}^{-1}(\tilde{\mu}) < \tilde{\alpha}\beta^{-1}(\mu)$. We summarize the overall discussion in the following result:

Proposition 1. ***(i)*** *For all $\tilde{\alpha} > 0$, if the conditions*

$$\tilde{\delta} > \left[\frac{2e^{-\tilde{\gamma}\tilde{\tau}} - 1}{1 - 2\tilde{K}e^{-\tilde{\gamma}\tilde{\tau}}}\right]\tilde{\beta}(0), \quad \textit{and,} \quad \delta > \left[2e^{-\gamma\tau} - 1\right]\beta(0), \tag{19}$$

are satisfied, then $(0,0,0)$ is the unique equilibrium point of the system (10). Note that in fact $(0,0,0)$ is always a steady state of the system (10).

(ii) *For all $\tilde{\alpha} > 0$, the condition*

$$\delta < \left[2e^{-\gamma\tau} - 1\right]\beta(0), \tag{20}$$

is a necessary and sufficient conditions for the existence of the steady state, $\mathfrak{E} = (0,0,x_e)$, where $x_e > 0$, for the system (10).

(iii) *For all* $\tilde{\alpha} > 0$*, if the conditions*

$$\tilde{\delta} > \left[\frac{2e^{-\tilde{\gamma}\tilde{\tau}} - 1}{1 - 2\tilde{K}e^{-\tilde{\gamma}\tilde{\tau}}}\right]\tilde{\beta}(0), \quad \textit{and,} \quad \delta < \left[2e^{-\gamma\tau} - 1\right]\beta(0), \tag{21}$$

are satisfied, then $(0, 0, 0)$ *and* $\mathfrak{E} = (0, 0, x_e)$ *are the unique steady states of system* (10)*.*

(iv) *For all* $\tilde{\alpha} > 0$*, the condition*

$$\tilde{\delta} < \left[\frac{2e^{-\tilde{\gamma}\tilde{\tau}} - 1}{1 - 2\tilde{K}e^{-\tilde{\gamma}\tilde{\tau}}}\right]\tilde{\beta}(0), \tag{22}$$

is a necessary and sufficient condition for the existence of the steady state $(\tilde{x}_e, \tilde{u}_e, 0)$ *where,* $\tilde{x}_e > 0$ *and* $\tilde{u} > 0$*, for the system* (10)*.*

(v) *For all* $\tilde{\alpha} > 0$*, if the conditions*

$$\tilde{\delta} < \left[\frac{2e^{-\tilde{\gamma}\tilde{\tau}} - 1}{1 - 2\tilde{K}e^{-\tilde{\gamma}\tilde{\tau}}}\right]\tilde{\beta}(0), \quad \textit{and,} \quad \delta > \left[2e^{-\gamma\tau} - 1\right]\beta(0), \tag{23}$$

are satisfied, then $(0, 0, 0)$ *and* $(\tilde{x}_e, \tilde{u}_e, 0)$ *are the unique steady states of system* (10)*.*

(vi) *For all* $\tilde{\alpha} > 0$*, the conditions*

$$\tilde{\alpha} \neq 1, \quad \tilde{\delta} < \left[\frac{2e^{-\tilde{\gamma}\tilde{\tau}} - 1}{1 - 2\tilde{K}e^{-\tilde{\gamma}\tilde{\tau}}}\right]\tilde{\beta}(0), \quad \textit{and,} \quad \delta < \left[2e^{-\gamma\tau} - 1\right]\beta(0), \tag{24}$$

are necessary, but not sufficient, for the existence of $\mathfrak{D} = (\tilde{x}_e, \tilde{u}_e, x_e)$*.*

(vii) *We denote* $\mu = \frac{\delta}{2e^{-\gamma\tau}-1}$*, and,* $\tilde{\mu} = \frac{\tilde{\delta}\left(1-2\tilde{K}e^{-\tilde{\gamma}\tilde{\tau}}\right)}{2e^{-\tilde{\gamma}\tilde{\tau}}-1}$*. If the conditions,*

$$\begin{cases} 0 < \tilde{\alpha} < 1, \quad \mu < \beta(0), \quad \tilde{\mu} < \tilde{\beta}(0), \\ \tilde{\alpha}\beta^{-1}(\mu) < \tilde{\beta}^{-1}(\tilde{\mu}) < \beta^{-1}(\mu), \\ 2\tilde{K}e^{-\tilde{\gamma}\tilde{\tau}} < 1 < 2e^{-\tilde{\gamma}\tilde{\tau}}, \end{cases} \tag{25}$$

or,

$$\begin{cases} \tilde{\alpha} > 1, \quad \mu < \beta(0), \quad \tilde{\mu} < \tilde{\beta}(0), \\ \beta^{-1}(\mu) < \tilde{\beta}^{-1}(\tilde{\mu}) < \tilde{\alpha}\beta^{-1}(\mu), \\ 2\tilde{K}e^{-\tilde{\gamma}\tilde{\tau}} < 1 < 2e^{-\tilde{\gamma}\tilde{\tau}}, \end{cases} \tag{26}$$

are satisfied, then a unique strictly positive dormancy steady state $\mathfrak{D} = (\tilde{x}_e, \tilde{u}_e, x_e)$, *exists and is given by* (17).

Remark 2. ***(1)*** *Obviously, uniqueness in Proposition 1-****(vii)*** *means the existence of a unique isolated strictly positive equilibrium point* $\mathfrak{D}$, *but the trivial steady state and the points* $\mathfrak{E} = (0, 0, x_e)$, $(\tilde{x}_e, \tilde{u}_e, 0)$ *are also steady states of system* (10). ***(2)*** *We can check that when the positive steady states exists, then*

$$y_e = \frac{1}{\gamma}(1 - e^{-\gamma\tau})\beta(x_e + \tilde{x}_e)x_e, \quad \text{and,} \quad \tilde{y}_e = \frac{1}{\tilde{\gamma}}(1 - e^{-\tilde{\gamma}\tilde{\tau}})\tilde{u}_e, \tag{27}$$

where y_e *(resp.* $\tilde{y}_e$*) is the positive steady state of the total density of proliferating healthy (resp. unhealthy) cells.* ***(3)*** *The third condition in* (25)-(26) *expresses an interesting relationship between the fast-self renewing ability* $\tilde{K}$, *the apoptosis rate of malignant cancer cells* $\tilde{\gamma}$, *and their average cell-cycle duration* $\tilde{\tau}$. *We notice that even if* $\tilde{K}$ *is relatively important (and knowing that it is not easy to act on* $\tilde{K}$ *by drug infusions since its high value is due to FLT3 mutations) it is still possible to guarantee the existence of a dormancy state by increasing* $\tilde{\tau}\tilde{\gamma}$. *However, the increase must be moderate to not exceed the upper-bound* $\tilde{\gamma}\tilde{\tau} <$ $\ln(2)$. ***(4)*** *Finally, we notice that other cases can be discussed if biologically needed. For instance, adding the restriction,* $2\tilde{\beta}^{-1}(\tilde{\mu}) < (1 + \tilde{\alpha})\,\beta^{-1}(\mu)$, *to the conditions* (25)-(26), *ensures that* $x_e > \tilde{x}_e$, *which can reasonably be the expected situation of dormant tumors without forming clinically apparent cancers.*

Now, we motivate our stability analysis through some preliminary numerical observations that highlight the rich dynamics of the model that we introduced in this work. In particular, we point out the different possible behaviors of the nonlinear differential-difference system (10) according to its associated initial conditions. The latter fact emphasizes the importance of determining mathe-

matically an estimate of the region of attraction of each steady state of interest.

Example 1. *Let us consider the following biological functions and parameters for cells in Category A (Cat. A) and Category B (Cat. B):*

Cat. A:	$\tau = 1.11$	$\delta = 0.1$	$\gamma = 0.1$	$\beta(m) = \frac{3}{1+m^4}$		
Cat. B:	$\tilde{\tau} = 0.9$	$\tilde{\delta} = 0.36$	$\tilde{\gamma} = 0.32$	$\tilde{\beta}(m) = \frac{2}{1+m^4}$	$\tilde{\alpha} = 0.6$	$\tilde{K} = 0.54$

For the considered set of parameters and functions, a unique dormancy steady state $\mathfrak{D}$ *exists and is given by* $\mathfrak{D} = (\tilde{x}_e, \tilde{u}_e, x_e)$*, where* $\tilde{x}_e = 0.6573$*,* $\tilde{u}_e = 0.4737$ *and* $x_e = 1.5255$*. This steady state is shown in Figure 4-(a). However, the latter point is not the unique equilibrium point of the system. Indeed, the 0-equilibrium* $(0, 0, 0)$*, and the points:* $\mathfrak{E} = (0, 0, 2.1826)$ *and* $(3.1998, 2.3060, 0)$*, also exist*[13]*. When we select the constant initial conditions* $\varphi_x(t) = \varphi_{\tilde{x}}(t) = 2$*, for all* $t \in [-\tau, 0]$*, and* $\varphi_{\tilde{u}}(t) = 1$*, for all* $t \in [-\tilde{\tau}, 0]$*, we observe that the trajectories converge to* $(3.1998, 2.3060, 0)$*, as illustrated in Figure 4-(b), where unhealthy cells survive (the attractive point seems to be stable), while the healthy cells vanish (converge to zero). By changing the initial condition of* $\tilde{u}$*, from the previous value to* $\varphi_{\tilde{u}}(t) = 0.1$*, for all* $t \in [-\tilde{\tau}, 0]$*, we observe that the trajectories converge to* $\mathfrak{E}$*, as illustrated in Figure 4-(c). Moreover, the steady states in Figures 4-(b)-(c) seem to be stable (each one has its region of attraction). Lyapunov theory offers strong tools to establish the regional stability properties of the steady states, provided that a suitable Lyapunov functional is found for the studied model. Now, let us modify the value of* $\tilde{K}$ *by increasing it to* $\tilde{K} = 0.6680$*. It follows that* $2\tilde{K}e^{-\tilde{\gamma}\tilde{\tau}} - 1 = 0.017$*, which implies that the trajectories of the unhealthy compartment are unbounded (similarly to [1]). Numerical simulations in that case, for arbitrary initial conditions, are given in Figure 4-(d).*

[13] One may notice the relationship that exists between the three different non-trivial steady states. In fact, the x_e-value in $\mathfrak{E}$ corresponds to the sum $x_e + \tilde{x}_e$ of the dormancy steady state $\mathfrak{D}$, while the $\tilde{x}_e$-value in the steady state $(\tilde{x}_e, \tilde{u}_e, 0)$ corresponds to the value $\frac{x_e + \tilde{\alpha}\tilde{x}_e}{\tilde{\alpha}}$, where x_e and $\tilde{x}_e$ in the latter fraction are the corresponding values in the dormancy steady state $\mathfrak{D}$.

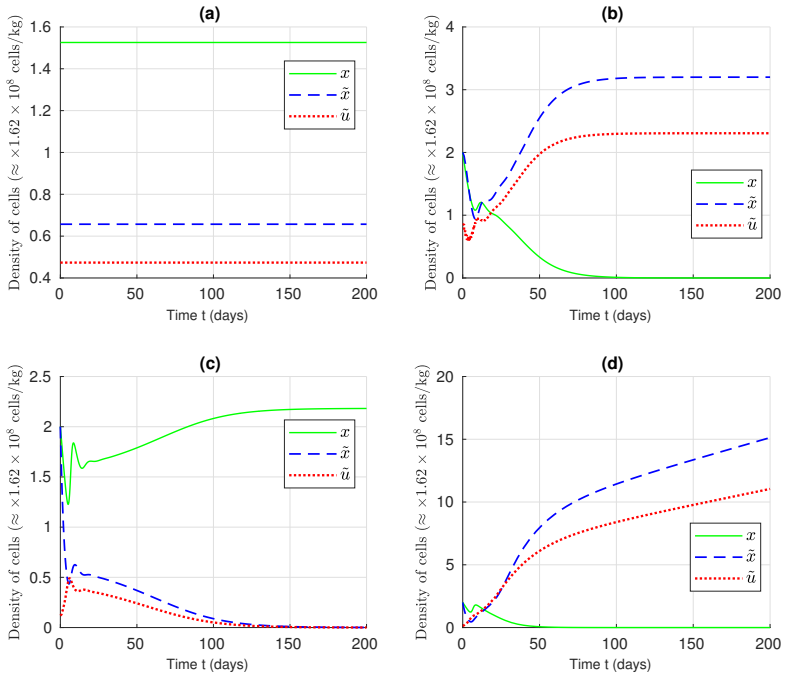

Figure 4: **(a)** Trajectories of the model whose parameters are given in Example 1, when they started on the Dormancy steady state $\mathfrak{D}$, where $\tilde{x}_e = 0.6573$, $\tilde{u}_e = 0.4737$ and $x_e = 1.5255$. We mention that in this case, numerical simulations show that $\mathfrak{D}$ is unstable, i.e. for arbitrary small perturbation on the initial conditions, trajectories do not converge towards $\mathfrak{D}$. **(b)** Trajectories of the model whose parameters are given in Example 1, when they started from the initial conditions given by: $\varphi_x(t) = \varphi_{\tilde{x}}(t) = 2$, for all $t \in [-\tau, 0]$, and $\varphi_{\tilde{u}}(t) = 1$, for all $t \in [-\tilde{\tau}, 0]$. The steady states $\mathfrak{D}$ and $\mathfrak{E}$ both exist in this case, however, we notice that the trajectories rather converge to another equilibrium point, that seems stable, and which is given by $(3.1998, 2.3060, 0)$. **(c)** All the model parameters and the initial conditions are similar to **(b)**, except the initial condition for $\tilde{u}$ which is no given by: $\varphi_{\tilde{u}}(t) = 0.1$, for all $t \in [-\tilde{\tau}, 0]$. In this case, the trajectories converge to $\mathfrak{E} = (0, 0, 2.1826)$. **(d)** Now, we modify the value of $\tilde{K}$, that we incrase to 0.6680, and we observe that for any initial conditions the trajectories $\tilde{x} \to +\infty$ and $\tilde{u} \to +\infty$, when t goes to $+\infty$.

Example 2. *Now, let us consider the following functions and parameters:*

Cat. A:	$\tau = 1.25$	$\delta = 0.2$	$\gamma = 0.2$	$\beta(m) = \frac{1}{1+m^2}$		
Cat. B:	$\tilde{\tau} = 1.66$	$\tilde{\delta} = 0.1$	$\tilde{\gamma} = 0.2$	$\tilde{\beta}(m) = \frac{1.2}{1+5m^4}$	$\tilde{\alpha} = 0.4$	$\tilde{K} = 0.3$

The steady states $(0, 0, 0)$, $\mathfrak{E} = (0, 0, x_e)$, $(\tilde{x}_e, \tilde{u}_e, 0)$, *and* $\mathfrak{D} = (\tilde{x}_e, \tilde{u}_e, x_e)$, *of the corresponding system, exist. If we select the constant initial conditions* $\varphi_x(t) = 1.55$, *and* $\varphi_{\tilde{x}}(t) = 1$, *for all* $t \in [-\tau, 0]$, *and* $\varphi_{\tilde{u}}(t) = 0.3$, *for all* $t \in$

$[-\tilde{\tau}, 0]$, *we observe that the trajectories are unstable as illustrated in Figure 5-(a), knowing that the dormancy steady state here is* $\mathfrak{D} = (0.3445, 0.0792, 0.9926)$. *For instance, we recall that in hematopoietic systems, oscillations are associated to many periodic diseases (e.g. cyclic neutropenia and some types of chronic leukemia). Now, let us consider random constant initial conditions and let us keep constant all the biological parameters, except the value of* $\tilde{\alpha}$, *that we consider as* 0.2, *and then* 0.6 *in a second case. As shown in Figure 5-(b), we note that by increasing the value of* $\tilde{\alpha}$ *from* 0.2 *to* 0.6, *the trajectories become stable. Thus, it appears that* $\tilde{\alpha}$ *may have, at least in this example, a stabilizing (or destabilizing) effect on the trajectories of the studied model.*

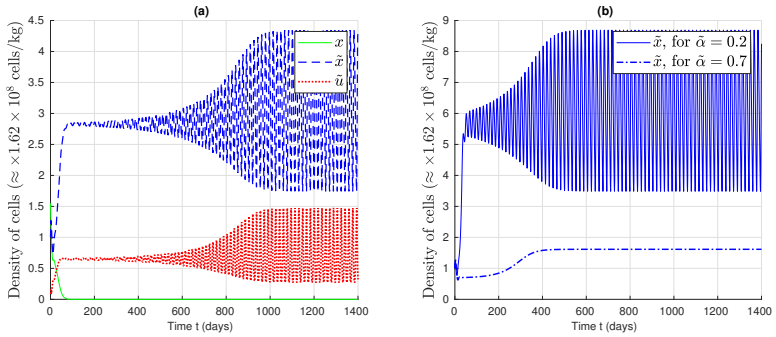

Figure 5: Trajectories of the model in Example 2. **(a)** Unstable (oscillatory) solutions corresponding to the constant initial conditions $\varphi_x(t) = 1.55$, $\varphi_{\tilde{x}}(t) = 1$, for all $t \in [-\tau, 0]$, $\varphi_{\tilde{u}}(t) = 0.3$, for all $t \in [-\tilde{\tau}, 0]$. **(b)** Stabilizing effect of $\tilde{\alpha}$. In this illustration, all the parameters, as well as initial conditions, are identical, except the value of $\tilde{\alpha}$. In the first case, $\tilde{\alpha} = 0.2$: the trajectories are unstable. By increasing $\tilde{\alpha}$ to 0.7 the trajectories become stable.

Example 3. *Finally, let us consider the following functions and parameters:*

Cat. A:	$\tau = 1.25$	$\delta = 0.1$	$\gamma = 0.2$	$\beta(m) = \frac{1}{1+m^2}$		
Cat. B:	$\tilde{\tau} = 0.7$	$\tilde{\delta} = 0.2$	$\tilde{\gamma} = 0.1$	$\tilde{\beta}(m) = \frac{2}{1+2m^4}$	$\tilde{\alpha} = 2$	$\tilde{K} = 0.5$

The conditions of existence of $\mathfrak{D} = (\tilde{x}_e, \tilde{u}_e, x_e)$ *are satisfied, and in this case we have:* $\tilde{x}_e = 0.6833$, $\tilde{u}_e = 0.1580$ *and* $x_e = 1.45599$. *For the constant initial conditions* $\varphi_x(t) = 0.1$ *and* $\varphi_{\tilde{x}}(t) = 1.5$, *for all* $t \in [-\tau, 0]$, *and* $\varphi_{\tilde{u}}(t) = 1.5$ *for all* $t \in [-\tilde{\tau}, 0]$, *it appears that* $\mathfrak{D}$ *is stable as illustrated in Figure 6.*

At this juncture, we deduce that the coupled system (10) under study has some interesting dynamical features. Firstly, we saw that the solutions of the

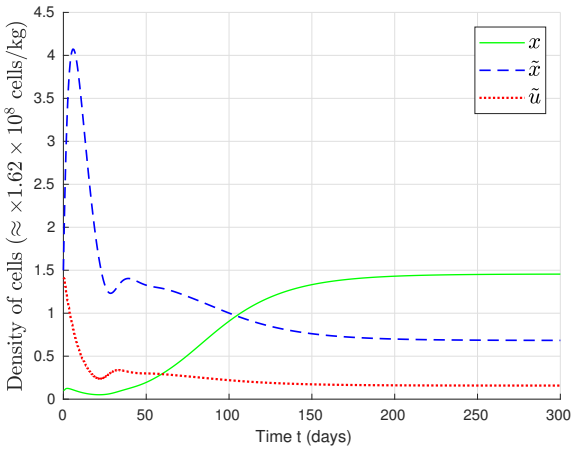

Figure 6: Trajectories of the model given in Example 3. Here the dormancy steady state $\mathfrak{D}$ exists and is given by: $\tilde{x}_e = 0.6833$, $\tilde{u}_e = 0.1580$ and $x_e = 1.45599$. Convergence to the dormancy steady state $\mathfrak{D}$ (which seems stable) is obtained starting from the constant initial conditions: $\varphi_x(t) = 0.1$ and $\varphi_{\tilde{x}}(t) = 1.5$, for all $t \in [-\tau, 0]$, and $\varphi_{\tilde{u}}(t) = 1.5$ for all $t \in [-\tilde{\tau}, 0]$.

coupled system can be bounded or unbounded (as in the non-coupled model [1]). In the former case, several steady states may exist and their values depend on the different biological parameters of the model. The existence of the steady states of interest ($\mathfrak{D}$ and $\mathfrak{E}$) are governed by some non-intuitive conditions on the biological parameters involved in the system (see Proposition 1). In addition, we saw that according to the initial conditions associated with the model trajectories, the bounded solutions may converge to one among several possible steady states, i.e. the stability of each steady state is regional (local). In the general case, the steady states of the system (10) are not always stable, but on the contrary, we noticed that oscillations may emerge, as in Example 2. Our objective now is to determine exponential stability conditions for the steady states of interest (which are: all-cell extinction, $\mathfrak{E}$ and $\mathfrak{D}$).

4. Stability analysis of the extinction of all the cells

In this section, we perform a stability analysis of the 0-equilibrium of the system (10). From a biological standpoint, this is a case that we want to avoid, as

discussed in the previous section (see the first point, *Cell extinction*), since it is synonymous of an excessive therapy that not only alters unhealthy populations, but also leads to the extinction of healthy cells in the coupled model.

Here we introduce the following functional:

$$\begin{aligned}\mathcal{W}\left(\tilde{x}_t, \tilde{u}_t, x_t\right) =& \tilde{x}(t) + x(t) + \psi_1 \int_{t-\tilde{\tau}}^{t} e^{\rho_1^*(\ell-t)} \tilde{u}(\ell) d\ell \\ &+ \psi_2 \int_{t-\tau}^{t} e^{\rho_2^*(\ell-t)} \beta\left(x(\ell) + \tilde{x}(\ell)\right) x(\ell) d\ell,\end{aligned} \tag{28}$$

where, $\psi_1 = \psi_{11} + \psi_{12}$, $\psi_{11} = 1 + \frac{\tilde{\delta}}{\tilde{\beta}(0)}$, $\psi_{12} = -\frac{\psi^*}{3(\overline{K}-\tilde{K})\tilde{\beta}(0)}$, $\overline{K} = \frac{1}{2}e^{\tilde{\gamma}\tilde{\tau}}$, $\psi^* = (\tilde{\beta}(0) + \tilde{\delta})\overline{K} - \tilde{\beta}(0) - \tilde{K}\tilde{\delta}$, and, $\psi_2 = 2\psi_3 e^{-\gamma\tau}$, where, ψ_3, together with ρ_1^* and ρ_2^*, are strictly positive constants that we will choose later.

We can readily check that if $2\tilde{K}e^{-\tilde{\gamma}\tilde{\tau}} < 1$ (that we can rewrite as $\tilde{K} < \overline{K}$), and $\psi^* > 0$, (i.e. $\psi_{12} < 0$), we obtain $\psi_1 > 0$. It follows that the functional $\mathcal{W}$ is nonnegative. We notice also that $\mathcal{W}$ is an unusual Lyapunov-Krasovskii functional (LKF) candidate, since it can be used only because the system (10) is positive. In addition, it is a *degenerate* LKF candidate (since $\mathcal{W} = 0$ does not imply $\tilde{u} = 0$) which is usually the case for differential-difference systems. This will also be the case when we investigate the stability properties of the dormancy steady state, where we will construct a quadratic degenerate LKF.

Thanks to the functional $\mathcal{W}$, we prove in Appendix A the following result:

Theorem 1. *If the conditions*

$$\left(2e^{-\gamma\tau} - 1\right)\beta(0) < \delta, \qquad 0 < \psi^*, \qquad \text{and,} \qquad 2\tilde{K}e^{-\tilde{\gamma}\tilde{\tau}} < 1, \tag{29}$$

are satisfied, then the trivial steady state of system (10) is globally exponentially stable with a decay rate larger than, or equal to, ψ_4 (defined in Appendix A).

Remark 3. ***(1)*** *The conditions (29) exclude the existence of any steady state different from the trivial one.* ***(2)*** *We can interpret the cell extinction as a result of an excessive therapy that affects also healthy cells so that their apoptosis rate, γ, increases until becoming greater than the ratio $\frac{\ln(2)}{\tau}$, or, until the*

*death rate and differentiation rate, i.e. δ, becomes greater than $(2e^{-\gamma\tau}-1)\,\beta(0)$ (which is a less demanding condition in comparison to $\gamma > \frac{\ln(2)}{\tau}$). **(3)** Arguing as in [1, 22], we can prove that the conditions (29) are also necessary for the exponential stability of the 0-equilibrium. **(4)** Finally, we deduce from Theorem 1 that all-cell extension results from uncorrelated conditions between the healthy and unhealthy compartments. Indeed, we note that the last two conditions in (29) relate to the unhealthy compartment, since only unhealthy parameters are involved. Moreover, these conditions are similar to those giving global asymptotic stability in [1] for a non-coupled model. The biological interpretation is that cell extension occurs if and only if both the healthy and unhealthy compartments are enable to regenerate themselves autonomously. In other words, it appears that the coupling has no effect on the stability of the 0-equilibrium since the conditions for total-cell eradication imply extinction of both the unhealthy and healthy compartments, as if they were separated (not coupled). This observation will not hold when we study dormancy (and non-zero steady states).*

5. Stability analysis of favourable steady states: $\mathfrak{D}$ (dormancy) and $\mathfrak{E}$ (CSCs eradication)

Here we will emphasize on the dormancy steady state $\mathfrak{D} = (\tilde{x}_e, \tilde{u}_e, x_e)$, where all the components of the steady state are different from zero (i.e. $\tilde{x}_e > 0$, $\tilde{u}_e > 0$, $x_e > 0$). In fact, we will highlight the case of dormancy $\mathfrak{D}$, since it is clearly the most general one. Indeed, from the analysis of $\mathfrak{D}$, it becomes possible to evaluate the regional stability properties of $\mathfrak{E} = (0, 0, x_e)$ (which are partially investigated in [23], when $\tilde{\alpha} = 1$), and also of the steady state $(\tilde{x}_e, \tilde{u}_e, 0)$.

5.1. A new representation of the system

Now, we want to investigate the stability properties of $\mathfrak{D}$ when it exists. Thus, we assume that the conditions given in *Proposition 1*-**(vii)** are satisfied and we perform the classical changes of coordinates: $\tilde{X} = \tilde{x} - \tilde{x}_e$, $\tilde{U} = \tilde{u} - \tilde{u}_e$,

and $X = x - x_e$. Therefore, from (10), it follows that for all $t \geq 0$,

$$\begin{cases} \dot{\tilde{X}}(t) = -\left[\tilde{\delta} + \tilde{\beta}(X(t) + \tilde{\alpha}\tilde{X}(t) + x_e + \tilde{\alpha}\tilde{x}_e)\right](\tilde{X}(t) + \tilde{x}_e) \\ \qquad\qquad +2(1-\tilde{K})e^{-\tilde{\gamma}\tilde{\tau}}(\tilde{U}(t-\tilde{\tau}) + \tilde{u}_e), \\ \tilde{U}(t) + \tilde{u}_e = \tilde{\beta}(X(t) + \tilde{\alpha}\tilde{X}(t) + x_e + \tilde{\alpha}\tilde{x}_e)(\tilde{X}(t) + \tilde{x}_e) \\ \qquad\qquad +2\tilde{K}e^{-\tilde{\gamma}\tilde{\tau}}(\tilde{U}(t-\tilde{\tau}) + \tilde{u}_e), \\ \dot{X}(t) = -\left[\delta + \beta(X(t) + \tilde{X}(t) + x_e + \tilde{x}_e)\right](X(t) + x_e) \\ \qquad\qquad +2e^{-\gamma\tau}\beta(X(t-\tau) + \tilde{X}(t-\tau) + x_e + \tilde{x}_e)(X(t-\tau) + x_e). \end{cases} \tag{30}$$

To ease the analysis of the above system, we rewrite it in a more convenient form. Observe that for all $\mathfrak{z} > -\mathfrak{e}$, $\mathfrak{e} > 0$, where, $\mathfrak{z} = X + \tilde{X}$ and $\mathfrak{e} = x_e + \tilde{x}_e$, we have, with an abuse of notation,

$$\beta(\mathfrak{z} + \mathfrak{e}) = \beta(\mathfrak{e}) + \theta\mathfrak{z} + R(\mathfrak{z}), \tag{31}$$

where β is the Hill-function defined in (1), $\theta = \beta'(\mathfrak{e})$, and, $R(\mathfrak{z}) = \int_{\mathfrak{e}}^{\mathfrak{e}+\mathfrak{z}} (\mathfrak{z} + \mathfrak{e} - \ell)\beta^{(2)}(\ell)d\ell$. Next, for all $\tilde{\mathfrak{z}} > -\tilde{\mathfrak{e}}$, $\tilde{\mathfrak{e}} > 0$, where, $\tilde{\mathfrak{z}} = X + \tilde{\alpha}\tilde{X}$, and, $\tilde{\mathfrak{e}} = x_e + \tilde{\alpha}\tilde{x}_e$, we get similarly to (31),

$$\tilde{\beta}\left(\tilde{\mathfrak{z}} + \tilde{\mathfrak{e}}\right) = \tilde{\beta}(\tilde{\mathfrak{e}}) + \tilde{\theta}\tilde{\mathfrak{z}} + \tilde{R}(\tilde{\mathfrak{z}}), \tag{32}$$

where, $\tilde{\theta} = \tilde{\beta}'(\tilde{\mathfrak{e}})$, and, $\tilde{R}(\tilde{\mathfrak{z}}) = \int_{\tilde{\mathfrak{e}}}^{\tilde{\mathfrak{e}}+\tilde{\mathfrak{z}}} (\tilde{\mathfrak{z}} + \tilde{\mathfrak{e}} - \ell)\tilde{\beta}^{(2)}(\ell)d\ell$. Therefore, using (31)-(32), and by simplifying some terms using (11), we get the system,

$$\begin{cases} \dot{\tilde{X}}(t) = -\mathfrak{a}_1\tilde{X}(t) - \mathfrak{a}_2 X(t) + \mathfrak{a}_3\tilde{U}(t-\tilde{\tau}) + F(X(t), \tilde{X}(t)), \\ \tilde{U}(t) = \mathfrak{a}_4\tilde{X}(t) + \mathfrak{a}_2 X(t) + \mathfrak{a}_5\tilde{U}(t-\tilde{\tau}) - F(X(t), \tilde{X}(t)), \\ \dot{X}(t) = -\mathfrak{a}_6 X(t) - \mathfrak{a}_7\tilde{X}(t) + \mathfrak{a}_8 X(t-\tau) + \mathfrak{a}_9\tilde{X}(t-\tau) + G(X_t, \tilde{X}_t), \end{cases} \tag{33}$$

$$\begin{aligned} \text{where,} \qquad F(X(t), \tilde{X}(t)) = &-\tilde{\theta}\left[\tilde{\alpha}\tilde{X}^2(t)) + X(t)\tilde{X}(t)\right] \\ &- \tilde{R}(X(t) + \tilde{\alpha}\tilde{X}(t))(\tilde{X}(t) + \tilde{x}_e), \end{aligned} \tag{34}$$

$$
\begin{aligned}
G(X_t, \tilde{X}_t) = &- \theta \left[X^2(t) + X(t)\tilde{X}(t)\right] - R(X(t) + \tilde{X}(t))(X(t) + x_e) \\
&+ 2e^{-\gamma\tau}\theta \left[X^2(t-\tau) + X(t-\tau)\tilde{X}(t-\tau)\right] \\
&+ 2e^{-\gamma\tau} R(X(t-\tau) + \tilde{X}(t-\tau))(X(t-\tau) + x_e),
\end{aligned} \tag{35}
$$

and where the constant parameters $\mathfrak{a}_i$ are given by:

$$
\begin{cases}
\mathfrak{a}_1 = \tilde{\delta} + \tilde{\beta}(x_e + \tilde{\alpha}\tilde{x}_e) + \tilde{\alpha}\tilde{\theta}\tilde{x}_e, \quad \mathfrak{a}_2 = \tilde{\theta}\tilde{x}_e, \quad \mathfrak{a}_3 = 2(1 - \tilde{K})e^{-\tilde{\gamma}\tilde{\tau}}, \\
\mathfrak{a}_4 = \tilde{\beta}(x_e + \tilde{\alpha}\tilde{x}_e) + \tilde{\alpha}\tilde{\theta}\tilde{x}_e, \mathfrak{a}_5 = 2\tilde{K}e^{-\tilde{\gamma}\tilde{\tau}}, \ \mathfrak{a}_6 = \delta + \beta\left(x_e + \tilde{x}_e\right) + \theta x_e, \\
\mathfrak{a}_7 = \theta x_e, \quad \mathfrak{a}_8 = 2e^{-\gamma\tau}\left[\beta\left(x_e + \tilde{x}_e\right) + \theta x_e\right], \quad \mathfrak{a}_9 = 2e^{-\gamma\tau}\theta x_e.
\end{cases} \tag{36}
$$

We notice that if the trajectories of (33) converge exponentially to the 0-equilibrium, then the positive trajectories of the system (10) converge exponentially to $\mathfrak{D}$. Now, we are going to state and prove some sector conditions on the nonlinear terms R and $\tilde{R}$. Then, we deduce some upper-bounds on the nonlinear terms F and G. For that purpose, we prove in Appendix B through lengthy calculations that there exist strictly positive constants $\mathfrak{s}$, $\tilde{\mathfrak{s}}$, $\mathfrak{m}$ and $\tilde{\mathfrak{m}}$, satisfying:

$$
|R(\mathfrak{z})| \leq \mathfrak{s}|\mathfrak{z}|, \quad \text{and} \quad |\tilde{R}(\tilde{\mathfrak{z}})| \leq \tilde{\mathfrak{s}}|\tilde{\mathfrak{z}}|, \tag{37}
$$

$$
|R(\mathfrak{z})| \leq \mathfrak{m}\mathfrak{z}^2, \quad \text{and} \quad |\tilde{R}(\tilde{\mathfrak{z}})| \leq \tilde{\mathfrak{m}}\tilde{\mathfrak{z}}^2, \tag{38}
$$

for all $\mathfrak{z} > -\mathfrak{e}$ ($\mathfrak{z}$ and $\mathfrak{e}$ are defined before (31)), and for all $\tilde{\mathfrak{z}} > -\tilde{\mathfrak{e}}$ ($\tilde{\mathfrak{z}}$ and $\tilde{\mathfrak{e}}$ are defined before (32)). Moreover, using (37) and (38), we can determine strictly positive constants $\mathfrak{c}_i$, $i = \{1, \ldots, 6\}$, such that the following quadratic upper bounds hold true:

$$
\left|F(X, \tilde{X})\right| \leq \mathfrak{c}_1 Q(X) + \mathfrak{c}_2 Q(\tilde{X}), \tag{39}
$$

$$
\left|G(X_t, \tilde{X}_t)\right| \leq \mathfrak{c}_3 Q(X(t)) + \mathfrak{c}_4 Q(\tilde{X}(t)) + \mathfrak{c}_5 Q(X(t-\tau)) + \mathfrak{c}_6 Q(\tilde{X}(t-\tau)). \tag{40}
$$

Remark 4. ***(1)*** *The upper-bounds given in (37), (38), (39), and, (40), will not intervene when we determine the decay conditions and the decay rate of the*

solutions. However, their effect appears in the size of the basin of attraction that we will provide. Actually, if the constants $\mathfrak{s}$, $\tilde{\mathfrak{s}}$, $\mathfrak{m}$, $\tilde{\mathfrak{m}}$, *in* (37)-(38), *as well as the constants* $\mathfrak{c}_i$ *in* (39)-(40), *are large, then the size of the basin of attraction shrinks accordingly.* ***(2)*** *By comparing the present study with [23], we notice that [23] was devoted to the study of a model which was simpler than the system* (33) *under study in this paper. Indeed, the model in [23] can be obtained by putting* $\tilde{\alpha} = 1$ *and by eliminating all the terms where* $\tilde{x}_e$ *is present in equations* (33), (36), (34) *and* (35). ***(3)*** *It is worth mentioning that the stability results that we will determine later apply for a wide range of functions* β *and* $\tilde{\beta}$, *as long as the sector conditions* (37) *and* (38) *are satisfied.*

Now, we want to perform a stability analysis of the trivial steady state of the (shifted) model using its representation in (33): we recall that the 0-equilibrium of (33) can be $\mathfrak{D}$ or $\mathfrak{E}$ of (10). For meeting such a purpose, strong tools are provided by Lyapunov theory, in the analysis of nonlinear differential-difference systems with possibly piecewise continuous solutions (see e.g. [41], [50], [61], [68], and the references therein). However, finding a suitable LKF is not an easy task. In addition, the provided stability conditions can be conservative. So, we adopt the following strategy that highlights our biological aims:

① Firstly, we use the *descriptor method* [37] that allows us to provide a local (Lyapunov-based) stability result for our biological model. The advantage of this approach is that it provides an effective tool (formulated as an LMI condition) to check if a steady state of a specific biological model (defined by its set of parameters) is locally stable.

② In order to address the following issue: *How can we provide realistic stability conditions that can be interpreted and satisfied under the effect of drugs?*, the first approach will be slightly modified in a second time. Thus, we establish a different result (that can be seen as a particular formulation of the first approach) which relies on the analytic construction of a suitable Lyapunov-like functional, specific for the studied biological system. The latter approach allows us to provide more explicit decay conditions than the common LMI-type

approaches. We point out that even if the second construction provides more conservative conditions than the LMI ones, they have the advantage of being more easily (biologically) understandable. It is to this end that, in the last section, we show how the decay conditions can be interpreted, in practice, according to the biological context of hematopoiesis and leukemia.

In summary, we determine throughout this section some exponential decay conditions (along with an estimate of the decay rate of the solutions and a region of attraction of the favourable steady states), via two complementary approaches: the descriptor method that provides local stability results for the general structure of the studied system, and, a suitable explicit Lyapunov-like construction that allows us to address the regional stability properties of the dormancy steady state. The latter decay conditions lend themselves more easily than the LMI ones to medical interpretations.

5.2. Stability analysis using the descriptor method

In this section, we consider as a first step only continuous solutions of the system in (33) and we study the linear approximation of the state $col\left\{X, \tilde{X}\right\}$, that we denote $Z = col\left\{Z_1, Z_2\right\}$. Then, by neglecting the nonlinear terms F and G in (33), we rewrite the studied system in the following compact form:

$$\begin{cases} \dot{Z}(t) = B_0 Z(t) + B_1 Z(t-\tau) + B_2 \tilde{U}\left(t-\tilde{\tau}\right), \\ \tilde{U}(t) = B_3 Z(t) + B_4 \tilde{U}\left(t-\tilde{\tau}\right), \end{cases} \tag{41}$$

for all $t \geq 0$, where B_i are given by (we recall that $\mathfrak{a}_i$ are defined in (36)),

$$\begin{aligned} B_0 &= -\begin{pmatrix} \mathfrak{a}_6 & \mathfrak{a}_7 \\ \mathfrak{a}_2 & \mathfrak{a}_1 \end{pmatrix}, \quad B_1 = \begin{pmatrix} \mathfrak{a}_8 & \mathfrak{a}_9 \\ 0 & 0 \end{pmatrix}, B_2 = \begin{pmatrix} 0 \\ \mathfrak{a}_3 \end{pmatrix}, \\ B_3 &= \begin{pmatrix} \mathfrak{a}_2 & \mathfrak{a}_4 \end{pmatrix}, \quad \text{and,} \quad B_4 = \mathfrak{a}_5 = 2\tilde{K}e^{-\tilde{\gamma}\tilde{\tau}}. \end{aligned} \tag{42}$$

Next, we consider some symmetric positive definite matrices $P > 0$, $S > 0$, $J > 0$, of appropriate dimension, together with a strictly positive constant $\tilde{\mathfrak{a}}$,

and we verify that the derivative of the functional,

$$\begin{aligned} V\left(Z_t,\tilde{U}_t\right) =& Z(t)^T P Z(t) + \int_{t-\tau}^{t} Z^T(\ell) S Z(\ell) d\ell + \\ &+ \tilde{\mathfrak{a}} \int_{t-\tilde{\tau}}^{t} \tilde{U}^2(\ell) d\ell + \tau \int_{t-\tau}^{t} (\ell+\tau-t)\, \dot{Z}^T(\ell) J \dot{Z}(\ell) d\ell, \end{aligned} \tag{43}$$

along the trajectories of (41), is given by,

$$\begin{aligned} \dot{V}(t) = & Z^T(t)\left[P+P^T\right]\dot{Z}(t) + Z^T(t) S Z(t) - Z^T(t-\tau) S Z(t-\tau) \\ & -\tau \textstyle\int_{t-\tau}^{t} \dot{Z}^T(\ell) J \dot{Z}(\ell) d\ell + \tau^2 \dot{Z}^T(t) J \dot{Z}(t) + \tilde{\mathfrak{a}}\left(\tilde{U}^2(t) - \tilde{U}^2(t-\tilde{\tau})\right). \end{aligned}$$

First, we notice that an upper-bound of $\dot{V}$ is given by,

$$\begin{aligned} \dot{V}(t) \leq & Z^T(t)\left[P+P^T\right]\dot{Z}(t) + Z^T(t) S Z(t) - Z^T(t-\tau) S Z(t-\tau) \\ & +\tau^2 \dot{Z}^T(t) J \dot{Z}(t) - Z^T(t) J Z(t) + Z^T(t) J Z(t-\tau) \\ & + Z^T(t-\tau) J Z(t) - Z^T(t-\tau) J Z(t-\tau) + \tilde{\mathfrak{a}} \tilde{U}^2(t) - \tilde{\mathfrak{a}} \tilde{U}^2(t-\tilde{\tau}) \\ & + 2\left[Z^T(t)\overline{P}^T + \dot{Z}^T(t)\overline{\overline{P}}^T\right] \underbrace{\left[B_0 Z(t) + B_1 Z(t-\tau) + B_2 \tilde{U}\left(t-\tilde{\tau}\right) - \dot{Z}(t)\right]}_{=0}, \end{aligned} \tag{44}$$

which, in fact, directly follows from the Jensen's Inequality given by,

$$\begin{aligned} -\tau \int_{t-\tau}^{t} \dot{Z}^T(\ell) J \dot{Z}(\ell) d\ell \leq & -\int_{t-\tau}^{t} \dot{Z}^T(\ell) d\ell J \int_{t-\tau}^{t} \dot{Z}(\ell) d\ell \\ = & -\left[Z(t) - Z(t-\tau)\right]^T J \left[Z(t) - Z(t-\tau)\right], \end{aligned}$$

and where $\overline{P}$ and $\overline{\overline{P}}$ that appear in (44) are some free-weighting matrices of appropriate dimension. Then, it follows that,

$$\dot{V}(t) \leq \eta^T(t) \Phi \eta(t) + \tilde{\mathfrak{a}} \tilde{U}^2(t),$$

where η is an augmented state defined by,

$$\eta^T(t) = \left[\begin{array}{cccc} Z(t) & \dot{Z}(t) & Z(t-\tau) & \tilde{U}(t-\tilde{\tau}) \end{array}\right], \tag{45}$$

and the matrix Φ is given by,

$$\Phi = \begin{pmatrix} S - J + \overline{p}^T B_0 + B_0^T \overline{P} & P - \overline{P}^T + B_0^T \overline{\overline{P}} & J + \overline{P}^T B_1 & \overline{P}^T B_2 \\ * & \tau^2 J - \overline{\overline{P}}^T - \overline{\overline{P}} & \overline{\overline{P}}^T B_1 & \overline{\overline{P}}^T B_2 \\ * & * & -S - J & 0 \\ * & * & * & -\tilde{\mathfrak{a}} \end{pmatrix}. \tag{46}$$

Noticing that, $\tilde{U}(t) = \begin{bmatrix} B_3 & 0 & 0 & B_4 \end{bmatrix} \eta(t)$, it follows that,

$$\tilde{\mathfrak{a}} \tilde{U}^2(t) = \eta^T(t) E \eta(t), \quad \text{where,} \quad E = \begin{bmatrix} B_3 & 0 & 0 & B_4 \end{bmatrix}^T \tilde{\mathfrak{a}} \begin{bmatrix} B_3 & 0 & 0 & B_4 \end{bmatrix}.$$

Therefore, by applying Schur complement, we conclude that $\dot{V}(t) < 0$ is satisfied provided that the following LMI:

$$\Psi = \begin{pmatrix} S - J + \overline{P}^T B_0 + B_0^T \overline{P} & P - \overline{P}^T + B_0^T \overline{\overline{P}} & J + \overline{P}^T B_1 & \overline{P}^T B_2 & B_3^T \tilde{\mathfrak{a}} \\ * & \tau^2 J - \overline{\overline{P}}^T - \overline{\overline{P}} & \overline{\overline{P}}^T B_1 & \overline{\overline{P}}^T B_2 & 0 \\ * & * & -S - J & 0 & 0 \\ * & * & * & -\tilde{\mathfrak{a}} & B_4^T \tilde{\mathfrak{a}} \\ * & * & * & * & -\tilde{\mathfrak{a}} \end{pmatrix} < 0, \tag{47}$$

holds. Next, by following arguments of [36] we deduce from $\Psi < 0$ that the last block in (47) satisfies $\begin{pmatrix} -\tilde{\mathfrak{a}} & B_4^T \tilde{\mathfrak{a}} \\ * & -\tilde{\mathfrak{a}} \end{pmatrix} < 0$. The latter implies by Schur complement that $-I + B_4^T B_4 < 0$. Hence, the eigenvalues of B_4 are inside the unit circle, i.e. the difference equation $\tilde{U}(t) = B_4 \tilde{U}(t - \tilde{\tau})$ is stable for all $\tilde{\tau} > 0$. The latter, together with $\dot{V} < 0$, guarantees the asymptotic stability of the system (41). We mention that it is possible to extend the stability result to the nonlinear system (33), using the functional V (i.e. providing some conditions on the nonlinear terms F and G as in [37], Section 3.11). However, since it seems actually difficult to interpret the LMI (47) as a combined targeted therapy for the studied biological system, we slightly modify our Lyapunov approach by

designing, in the next section, a suitable specific LKF for the studied system that provides explicit (sufficient) stability conditions for the dormancy steady state of the nonlinear system (33). The functional that we are going to propose has some similarities with the functional V. Actually, in the next section, we are going to select some matrices P, S and J, together with the constant $\tilde{\mathfrak{a}}$, involved in the above construction. Thus, we will determine analytically some upper-bounds on $\dot{V}$, through classical inequalities. Not surprisingly, the latter approach increases the *conservatism* of the sufficient stability condition in the LMI form (the LMI condition is given by (47)). That is the price of determining more biologically exploitable results (i.e. explicit exponential decay conditions with an estimate on the decay rate of the solution and a subset of the basin of attraction of the trivial steady state of the nonlinear system (33)).

5.3. Obtaining Explicit Exponential Decay Conditions

We focus on the coupled system using its representation in (33), with possibly piecewise continuous solutions. Firstly, let us introduce the quadratic function:

$$\mathfrak{Q}(X,\tilde{X}) = Q(X) + \lambda_1 Q(\tilde{X}), \text{ where, } Q(\ell) = \tfrac{1}{2}\ell^2, \tag{48}$$

and $\lambda_1 = 2$. This is equivalent to put $P = diag\{1/2, 1\}$ in V of the previous section. Next, we consider the following operators,

$$\mathcal{Y}(\tilde{\varphi}) = \int_{-\tilde{\tau}}^{0} e^{\rho_1 \ell} Q(\tilde{\varphi}(\ell)) d\ell, \quad \text{and,} \tag{49}$$

$$\mathcal{S}(\varphi) = \int_{-\tau}^{0} e^{\rho_2 \ell} Q(\varphi(\ell)) d\ell, \tag{50}$$

where, $\varphi \in \mathcal{C}([-\tau, 0], \mathbb{R})$, $\tilde{\varphi} \in \mathcal{C}([-\tilde{\tau}, 0], \mathbb{R})$, and ρ_1, ρ_2, are strictly positive constants that we determine later. In fact, observe that, compared to the integral terms in V of the previous section, $\mathcal{S}$ and $\mathcal{Y}$ have exponential functions -in the integral terms- that make it possible to get a lower-bound on the exponential decay of the solutions. Next, in the quest for explicit decay conditions, we are going to substitute $\dot{X}$ and $\dot{\tilde{X}}$ when computing the derivative of $\mathfrak{Q}$ (which is

not the approach adopted in the descriptor method, where $\dot{X}$ and $\dot{\tilde{X}}$ were not replaced). Thus, the derivative of $\mathfrak{Q}$ along the trajectories of (33), satisfies

$$\begin{aligned}\dot{\mathfrak{Q}}(t) =& -2\mathfrak{a}_1\lambda_1 Q(\tilde{X}(t)) - 2\mathfrak{a}_6 Q(X(t)) - (\mathfrak{a}_2\lambda_1 + \mathfrak{a}_7)\, X(t)\tilde{X}(t) \\ &+ \mathfrak{a}_3\lambda_1\tilde{X}(t)\tilde{U}(t-\tilde{\tau}) + \mathfrak{a}_8 X(t)X(t-\tau) + \mathfrak{a}_9 X(t)\tilde{X}(t-\tau) \\ &+ \lambda_1\tilde{X}(t)F(X(t),\tilde{X}(t)) + X(t)G(X_t,\tilde{X}_t).\end{aligned} \tag{51}$$

Notice that the derivative of $\mathcal{Y}(\tilde{U}_t)$, for almost all $t \geq 0$, is

$$\dot{\mathcal{Y}}(t) = Q(\tilde{U}(t)) - e^{-\rho_1\tilde{\tau}}Q(\tilde{U}(t-\tilde{\tau})) - \rho_1\mathcal{Y}(\tilde{U}_t). \tag{52}$$

Now, using the second equation in (33), we obtain

$$\begin{aligned}\dot{\mathcal{Y}}(t) =& -\rho_1\mathcal{Y}(\tilde{U}_t) + \mathfrak{a}_4^2 Q(\tilde{X}(t)) + \mathfrak{a}_2^2 Q(X(t)) - (e^{-\rho_1\tilde{\tau}} - \mathfrak{a}_5^2)Q(\tilde{U}(t-\tilde{\tau})) \\ &+ \mathfrak{a}_2\mathfrak{a}_4 X(t)\tilde{X}(t) + \mathfrak{a}_2\mathfrak{a}_5 X(t)\tilde{U}(t-\tilde{\tau}) + \mathfrak{a}_4\mathfrak{a}_5\tilde{X}(t)\tilde{U}(t-\tilde{\tau}) \\ &+ Q(F(\tilde{X}(t),X(t))) - F(X(t),\tilde{X}(t))\left[\mathfrak{a}_4\tilde{X}(t) + \mathfrak{a}_2 X(t) + \mathfrak{a}_5\tilde{U}(t-\tilde{\tau})\right],\end{aligned}$$

where the $\mathfrak{a}_i$'s and F are defined after (33). Similarly, we compute the derivatives of the functionals $\mathcal{S}(X_t)$ and $\mathcal{S}(\tilde{X}_t)$. By combining the previous intermediate results (i.e. $\dot{\mathfrak{Q}}$, $\dot{\mathcal{Y}}$ and $\dot{\mathcal{S}}$), we deduce that the time derivative of the functional,

$$V^\dagger(X_t,\tilde{X}_t,\tilde{U}_t) = \mathfrak{Q}(X(t),\tilde{X}(t)) + \lambda_2\mathcal{S}(X_t) + \lambda_3\mathcal{S}(\tilde{X}_t) + \lambda_4\mathcal{Y}(\tilde{U}_t), \tag{53}$$

where λ_2, λ_3 and λ_4 are positive constants to be chosen later, along the trajectories of (33) is given, for almost all $t \geq 0$, by:

$$\begin{aligned}\dot{V}^\dagger(t) =& -\left[2\lambda_1\mathfrak{a}_1 - \lambda_3 - \lambda_4\mathfrak{a}_4^2\right]Q(\tilde{X}(t)) - \left[2\mathfrak{a}_6 - \lambda_2 - \lambda_4\mathfrak{a}_2^2\right]Q(X(t)) \\ &- \rho_2\lambda_3\mathcal{S}(\tilde{X}_t) - \rho_2\lambda_2\mathcal{S}(X_t) - \rho_1\lambda_4\mathcal{Y}(\tilde{U}_t) - \lambda_4\left[e^{-\rho_1\tilde{\tau}} - \mathfrak{a}_5^2\right]Q(\tilde{U}(t-\tilde{\tau})) \\ &- \lambda_2 e^{-\rho_2\tau}Q(X(t-\tau)) - \lambda_3 e^{-\rho_2\tau}Q(\tilde{X}(t-\tau)) + \mathfrak{a}_2\mathfrak{a}_5\lambda_4 X(t)\tilde{U}(t-\tilde{\tau}) \\ &- \left[\mathfrak{a}_2\lambda_1 + \mathfrak{a}_7 - \lambda_4\mathfrak{a}_2\mathfrak{a}_4\right]X(t)\tilde{X}(t) + \mathfrak{a}_8 X(t)X(t-\tau) + \mathfrak{a}_9 X(t)\tilde{X}(t-\tau) \\ &+ \left[\mathfrak{a}_3\lambda_1 + \mathfrak{a}_4\mathfrak{a}_5\lambda_4\right]\tilde{X}(t)\tilde{U}(t-\tilde{\tau}) - \mathfrak{a}_5\lambda_4 F(X(t),\tilde{X}(t))\tilde{U}(t-\tilde{\tau}) \\ &+ X(t)G(X_t,\tilde{X}_t) + \lambda_4 Q(F(\tilde{X}(t),X(t))) - \lambda_4 F(X(t),\tilde{X}(t))\left[\mathfrak{a}_4\tilde{X}(t) + \mathfrak{a}_2 X(t)\right].\end{aligned}$$

Next, we recall that for strictly positive constants, $\nu_i > 0$, $i = 1$ to 5, (that we will choose later), we have the following inequalities: $\left|X\tilde{X}\right| \leq \frac{1}{\nu_1}Q(X)+\nu_1 Q(\tilde{X})$, $|X(t)X(t-\tau)| \leq \frac{1}{\nu_2}Q(X(t)) + \nu_2 Q(X(t-\tau))$, $\left|X(t)\tilde{X}(t-\tau)\right| \leq \frac{1}{\nu_3}Q(X(t)) + \nu_3 Q(\tilde{X}(t-\tau))$, $\left|\tilde{X}(t)\tilde{U}(t-\tilde{\tau})\right| \leq \frac{1}{\nu_4}Q(\tilde{X}(t)) + \nu_4 Q(\tilde{U}(t-\tilde{\tau}))$, $\left|X(t)\tilde{U}(t-\tilde{\tau})\right| \leq \frac{1}{\nu_5}Q(X(t)) + \nu_5 Q(\tilde{U}(t-\tilde{\tau}))$. Therefore, it follows that the derivative $\dot{V}^\dagger(t)$ satisfies, for almost all $t \geq 0$, the following inequality:

$$\begin{aligned}
\dot{V}^\dagger(t) \leq & -\left[2\lambda_1\mathfrak{a}_1 - \mathfrak{b}_1\right] Q(\tilde{X}(t)) - \left[2\mathfrak{a}_6 - \mathfrak{b}_2\right] Q(X(t)) - \rho_2\lambda_3\mathcal{S}(\tilde{X}_t) \\
& - \rho_2\lambda_2\mathcal{S}\left(X_t\right) - \rho_1\lambda_4\mathcal{Y}(\tilde{U}_t) - \left[\lambda_4 e^{-\rho_1\tilde{\tau}} - \mathfrak{b}_3\right] Q(\tilde{U}(t-\tilde{\tau})) \\
& - \left[\lambda_2 e^{-\rho_2\tau} - \mathfrak{b}_4\right] Q\left(X(t-\tau)\right) - \left[\lambda_3 e^{-\rho_2\tau} - \mathfrak{b}_5\right] Q(\tilde{X}(t-\tau)) \\
& + \lambda_4 Q(F(\tilde{X}(t), X(t))) - \mathfrak{a}_5\lambda_4 F(X(t), \tilde{X}(t))\tilde{U}(t-\tilde{\tau}) \\
& + X(t)G(X_t, \tilde{X}_t) - \lambda_4 F(X(t), \tilde{X}(t))\left[\mathfrak{a}_4\tilde{X}(t) + \mathfrak{a}_2 X(t)\right],
\end{aligned} \tag{54}$$

where,

$$\begin{cases}
\mathfrak{b}_1 = & \lambda_3 + \lambda_4\mathfrak{a}_4^2 + \nu_1\left|\mathfrak{a}_2\lambda_1 + \mathfrak{a}_7 - \lambda_4\mathfrak{a}_2\mathfrak{a}_4\right|, \\
\mathfrak{b}_2 = & \lambda_2 + \lambda_4\mathfrak{a}_2^2 + \frac{|\mathfrak{a}_2\lambda_1 + \mathfrak{a}_7 - \lambda_4\mathfrak{a}_2\mathfrak{a}_4|}{\nu_1} + \frac{|\mathfrak{a}_8|}{\nu_2} + \frac{|\mathfrak{a}_9|}{\nu_3} + \frac{|\mathfrak{a}_2\mathfrak{a}_5|\lambda_4}{\nu_5}, \\
\mathfrak{b}_3 = & \lambda_4\mathfrak{a}_5^2 + \nu_4\left|\mathfrak{a}_3\lambda_1 + \mathfrak{a}_4\mathfrak{a}_5\lambda_4\right| + \nu_5\lambda_4\left|\mathfrak{a}_2\mathfrak{a}_5\right|, \\
\mathfrak{b}_4 = & \nu_2|\mathfrak{a}_8|, \quad \text{and}, \quad \mathfrak{b}_5 = \nu_3|\mathfrak{a}_9|.
\end{cases} \tag{55}$$

Now we are ready to determine decay conditions that ensure the regional exponential stability of the trivial steady state of the system (33). The terms where F and G are involved in (54) will be used only to determine a subset of the basin of attraction of the trivial steady state of the system (33).

Let us focus on the constant which is multiplied by $Q(\tilde{U}(t-\tilde{\tau}))$ in (54). Using the inequality $|\mathfrak{a}_3\lambda_1 + \mathfrak{a}_4\mathfrak{a}_5\lambda_4| \leq \lambda_1|\mathfrak{a}_3| + \lambda_4|\mathfrak{a}_4\mathfrak{a}_5|$, we notice that the inequality $\lambda_4 e^{-\rho_1\tilde{\tau}} - \mathfrak{b}_3 > 0$ is verified if

$$\lambda_4\left(e^{-\rho_1\tilde{\tau}} - \mathfrak{a}_5^2 - \nu_4|\mathfrak{a}_4\mathfrak{a}_5| - \nu_5|\mathfrak{a}_2\mathfrak{a}_5|\right) - \nu_4\lambda_1|\mathfrak{a}_3| > 0. \tag{56}$$

For later use, we set $\mathfrak{d}_1 \triangleq \lambda_4\left(e^{-\rho_1\tilde{\tau}} - \mathfrak{a}_5^2 - \nu_4|\mathfrak{a}_4\mathfrak{a}_5| - \nu_5|\mathfrak{a}_2\mathfrak{a}_5|\right) - \nu_4\lambda_1|\mathfrak{a}_3|$.

We deduce that the first decay condition is given by:

$$\mathfrak{a}_5^2 + \nu_4|\mathfrak{a}_4\mathfrak{a}_5| + \nu_5|\mathfrak{a}_2\mathfrak{a}_5| < 1. \tag{57}$$

Indeed, the previous condition is necessary to guarantee that (56) is satisfied. Now, let us select $\nu_4 = \frac{1}{2}|\mathfrak{a}_4|^{-1}$, and $\nu_5 = \frac{1}{2}|\mathfrak{a}_2|^{-1}$, for $\mathfrak{a}_4 \neq 0$ and $\mathfrak{a}_2 \neq 0$. Using the definitions of $\mathfrak{a}_i$'s, ν_4 and ν_5, it follows that the first decay condition (57) is equivalent to

$$(2\tilde{K}e^{-\tilde{\gamma}\tilde{\tau}})^2 + 2\tilde{K}e^{-\tilde{\gamma}\tilde{\tau}} < 1. \tag{58}$$

Remark 5. *One notices that we have deliberately chosen* $\nu_4 = \frac{1}{2}|\mathfrak{a}_4|^{-1}$, *and,* $\nu_5 = \frac{1}{2}|\mathfrak{a}_2|^{-1}$, *and that these choices are not unique. Indeed, our objective here is to determine a sufficient decay condition that involves only the unhealthy parameters of the permanently dividing subpopulation (for instance, the subpopulation with FLT3-type mutations in AML) which are,* $\tilde{K}$, $\tilde{\tau}$ *and* $\tilde{\gamma}$. *For that purpose, we derive a decay condition involving only the parameter* $\mathfrak{a}_5$. *Therefore,* ν_4 *and* ν_5 *are used in order to compensate* $\mathfrak{a}_4$ *and* $\mathfrak{a}_2$. *A more general form is given by* $\nu_4 = \tilde{\nu}_4|\mathfrak{a}_4|^{-1}$, $\nu_5 = \tilde{\nu}_5|\mathfrak{a}_2|^{-1}$, *where* $\tilde{\nu}_4 > 0$, *and,* $\tilde{\nu}_5 > 0$. *In this case, the decay condition* (58) *rewrites as,* $(2\tilde{K}e^{-\tilde{\gamma}\tilde{\tau}})^2 + 2\left(\tilde{\nu}_4 + \tilde{\nu}_5\right)\tilde{K}e^{-\tilde{\gamma}\tilde{\tau}} < 1$.

Now, notice that a direct consequence of the inequality (58) is that for all $\rho_1 \in \left(0, \frac{1}{\tilde{\tau}}\ln\left(\frac{5}{1+4\left[\mathfrak{a}_5^2+\mathfrak{a}_5\right]}\right)\right)$, we get $e^{-\rho_1\tilde{\tau}} - \left[\mathfrak{a}_5^2 + \mathfrak{a}_5\right] > \frac{1-\left[\mathfrak{a}_5^2+\mathfrak{a}_5\right]}{5} > 0$. Consequently, we deduce that $\mathfrak{d}_1$, which is defined right after (56), and which is now equal to: $\mathfrak{d}_1 = \lambda_4\left(e^{-\rho_1\tilde{\tau}} - \left[\mathfrak{a}_5^2 + \mathfrak{a}_5\right]\right) - \nu_4\lambda_1|\mathfrak{a}_3|$, satisfies the inequality, $\mathfrak{d}_1 > 0$, for all $\lambda_4 = \frac{\tilde{\lambda}_4\lambda_1\nu_4|\mathfrak{a}_3|}{e^{-\rho_1\tilde{\tau}}-\left[\mathfrak{a}_5^2+\mathfrak{a}_5\right]} > 0$, where $\tilde{\lambda}_4 > 1$. Next, using the inequality,

$$\left|F(X(t), \tilde{X}(t))\tilde{U}(t-\tilde{\tau})\right| \leq \frac{2|\mathfrak{a}_5|\lambda_4}{\mathfrak{d}_1}Q(F(X(t), \tilde{X}(t))) + \frac{\mathfrak{d}_1}{2|\mathfrak{a}_5|\lambda_4}Q(\tilde{U}(t-\tilde{\tau}),$$

it follows from (54) that,

$$\begin{aligned}\dot{V}^{\dagger}(t) \leq & -\left[2\lambda_1\mathfrak{a}_1-\mathfrak{b}_1\right]Q(\tilde{X}(t))-\left[2\mathfrak{a}_6-\mathfrak{b}_2\right]Q(X(t))-\frac{\mathfrak{d}_1}{2}Q(\tilde{U}(t-\tilde{\tau}))\\ & -\rho_2\lambda_2\mathcal{S}(X_t)-\rho_2\lambda_3\mathcal{S}(\tilde{X}_t)-\left[\lambda_2e^{-\rho_2\tau}-\mathfrak{b}_4\right]Q(X\left(t-\tau\right))\\ & -\left[\lambda_3e^{-\rho_2\tau}-\mathfrak{b}_5\right]Q(\tilde{X}(t-\tau))-\rho_1\lambda_4\mathcal{Y}(\tilde{U}_t)+H(X_t,\tilde{X}_t),\end{aligned} \tag{59}$$

where,

$$\begin{aligned}H\left(X_t,\tilde{X}_t\right)=&\left(\lambda_4+\frac{2\left(\mathfrak{a}_5\lambda_4\right)^2}{\mathfrak{d}_1}\right)Q(F(X(t),\tilde{X}(t)))+X(t)G(X_t,\tilde{X}_t)\\ &-\lambda_4F(X(t),\tilde{X}(t))\left[\mathfrak{a}_4\tilde{X}(t)+\mathfrak{a}_2X(t)\right].\end{aligned} \tag{60}$$

Arguing similarly, we select ν_2 and ν_3 that compensate the terms $\mathfrak{a}_8$ and $\mathfrak{a}_9$ (for $|\mathfrak{a}_8|\neq 0$, and $|\mathfrak{a}_9|\neq 0$). For instance, we can consider $\nu_2=\frac{1}{6|\mathfrak{a}_8|}$ and $\nu_3=\frac{1}{6|\mathfrak{a}_9|}$. Then, we put, for instance, $\lambda_2=\lambda_3=\frac{1}{3}$. We notice that our choices of ν_2 and ν_3 in this case are equivalent to $\mathfrak{b}_4=\mathfrak{b}_5=\frac{1}{6}$, and it follows that for all $\rho_2\in\left(0,\frac{1}{\tau}\ln\left(\frac{\lambda_2}{\mathfrak{b}_4}\right)\right)$, we obtain in this case $e^{-\rho_2\tau}>\frac{2}{3}$. Thus, we end up with[14]

$$\begin{aligned}\mathfrak{d}_2&\triangleq\lambda_2e^{-\rho_2\tau}-\mathfrak{b}_4=\tfrac{1}{3}\left(e^{-\rho_2\tau}-\tfrac{1}{2}\right)>\tfrac{1}{18},\\ \mathfrak{d}_3&\triangleq\lambda_3e^{-\rho_2\tau}-\mathfrak{b}_5=\tfrac{1}{3}\left(e^{-\rho_2\tau}-\tfrac{1}{2}\right)>\tfrac{1}{18}.\end{aligned} \tag{61}$$

Finally, by selecting $\nu_1=\lambda_1=2$, all the setting parameters involved in the functional $V^{\dagger}$ are now chosen. We conclude that if the decay conditions $\mathfrak{d}_4\triangleq 2\lambda_1\mathfrak{a}_1-\mathfrak{b}_1>0$, and $\mathfrak{d}_5\triangleq 2\mathfrak{a}_6-\mathfrak{b}_2>0$, are satisfied, then (59) satisfies for almost all $t\geq 0$,

$$\begin{aligned}\dot{V}^{\dagger}(t)\leq & -3\overline{\mathfrak{d}}V^{\dagger}(X_t,\tilde{X}_t,\tilde{U}_t)-\frac{\mathfrak{d}_4}{2}Q(\tilde{X}(t))-\frac{\mathfrak{d}_5}{2}Q(X(t))-\frac{\mathfrak{d}_1}{2}Q(\tilde{U}(t-\tilde{\tau}))\\ & -\mathfrak{d}_2Q(X(t-\tau))-\mathfrak{d}_3Q(\tilde{X}(t-\tau))+H(X_t,\tilde{X}_t),\end{aligned}$$

[14] Similarly to ν_4 and ν_5 in Remark 5, the choices of ν_2 and ν_3 are not unique (and, similarly, those of λ_2 and λ_3 either). In Example 4, we are going to use different numerical values that also satisfy $\mathfrak{d}_2>0$ and $\mathfrak{d}_3>0$.

where $\overline{\mathfrak{d}} = \frac{1}{3}\min\left\{\frac{\mathfrak{d}_4}{2\lambda_1}, \frac{\mathfrak{d}_5}{2}, \rho_1, \rho_2\right\}$. Next, in Appendix C, we focus on the nonlinear function H, defined right after (59), in order to define a subset of the basin of attraction of the trivial steady state of system (33). By following the arguments given in Appendix C, we prove that in a well-defined region (defined in terms of the initial conditions) we get:

$$\dot{V}^{\dagger}(t) \leq -2\overline{\mathfrak{d}}V^{\dagger}(X_t, \tilde{X}_t, \tilde{U}_t), \quad \text{for almost all} \quad t \geq 0. \tag{62}$$

We integrate this inequality and we obtain for all $t \geq 0$,

$$V^{\dagger}(X_t, \tilde{X}_t, \tilde{U}_t) \leq e^{-2\overline{\mathfrak{d}}t}V^{\dagger}\left(\varphi_{X_t}, \varphi_{\tilde{X}_t}, \varphi_{\tilde{U}_t}\right). \tag{63}$$

Consequently, we get for all $t \geq 0$, $X^2(t) + \lambda_1\tilde{X}^2(t) \leq 2e^{-2\overline{\mathfrak{d}}t}V^{\dagger}\left(\varphi_X, \varphi_{\tilde{X}}, \varphi_{\tilde{U}}\right)$. We conclude that the trajectories $X(t)$ and $\tilde{X}(t)$ converge exponentially to the trivial steady state of the shifted system, with a decay rate larger than, or equal to, $\overline{\mathfrak{d}}$. By classical arguments, we observe from the second equation in (33) that, since $2\tilde{K}e^{-\tilde{\gamma}\tilde{\tau}} < 1$, $\tilde{U}(t)$ converges exponentially to zero when $X(t)$ and $\tilde{X}(t)$ converge exponentially to the zero.

To summarize, we considered that $\mathfrak{D}$ (or $\mathfrak{E}$) exists and we rewrote the studied system (10) in the form (33). Next, we proved that if the decay conditions ((58), $\mathfrak{d}_4 > 0$, $\mathfrak{d}_5 > 0$) are satisfied, then the trajectories of (33) associated with initial conditions belonging to the set $\mathcal{B}$, converge exponentially to 0-equilibrium of the shifted system (33), with a decay rate larger than, or equal to, $\overline{\mathfrak{d}}$. By explicitly rewriting the decay conditions, we summarize our findings in Section 5 as follows:

Theorem 2. ***(A)*** *Assume that $\mathfrak{D}$ (resp. $\mathfrak{E}$) exists, then consider the shifted system (33), such that its trivial steady state corresponds to $\mathfrak{D}$ (resp. $\mathfrak{E}$) of (10). If there exist matrices P, S, J, $\overline{P}$ and $\overline{\overline{P}}$, of appropriate dimension, and a positive constant $\tilde{\mathfrak{a}}$, that satisfy the LMI (47), then the trivial steady state of the shifted system (33), which is $\mathfrak{D}$ (resp. $\mathfrak{E}$) of (10), is locally asymptotically stable.*

(B) *Assume that system (10) admits a positive steady state* $\mathfrak{D}$ *(i.e. (25) or (26) in Proposition 1-**(vii)** hold). If*

$$\begin{aligned} &i) \quad \left(2\tilde{K}e^{-\tilde{\gamma}\tilde{\tau}}\right)^2 + 2\tilde{K}e^{-\tilde{\gamma}\tilde{\tau}} < 1, \\ &ii) \quad \tfrac{\mathfrak{b}_1}{4} - \tilde{\alpha}\tilde{\theta}\tilde{x}_e < \tilde{\beta}\left(x_e + \tilde{\alpha}\tilde{x}_e\right) + \tilde{\delta}, \\ &iii) \quad \tfrac{\mathfrak{b}_2}{2} - \theta x_e < \beta(x_e + \tilde{x}_e) + \delta, \end{aligned} \tag{64}$$

are satisfied, ensuring also that $\mathfrak{d}_2 > 0$ *and* $\mathfrak{d}_3 > 0$*, then* $\mathfrak{D}$ *is regionally exponentially stable with a decay rate larger than, or equal to,* $\overline{\mathfrak{d}}$*, and with basin of attraction defined by:*

$$\begin{aligned} \mathcal{B}^{\dagger} = \Big\{ \varphi_x \in \mathcal{C}\left([-\tau, 0], \mathbb{R}^+\right), \varphi_{\tilde{x}} \in \mathcal{C}\left([-\tau, 0], \mathbb{R}^+\right), \varphi_{\tilde{u}} \in \mathcal{C}\left([-\tilde{\tau}, 0], \mathbb{R}^+\right) \Big| \\ V^{\dagger}\left(\varphi_x - x_e, \varphi_{\tilde{x}} - \tilde{x}_e, \varphi_{\tilde{u}} - \tilde{u}_e\right) < \overline{V}^{\dagger} \Big\}. \end{aligned} \tag{65}$$

(C) *Assume that* $\mathfrak{E}$ *exists (Proposition 1-**(ii)**), and consider that* $\tilde{x}_e = 0$ *in (64). If the conditions (64) are satisfied (for* $\tilde{x}_e = 0$*), then* $\mathfrak{E}$ *of (10) is regionally exponentially stable with a decay rate* $\mathfrak{d}$ *and basin of attraction defined by (65), where we consider now that* $\tilde{x}_e = \tilde{u}_e = 0$ *in (65).*

Example 4. *In this example, we assume that* $\tilde{\alpha} = 5$*. For the unhealthy compartment, we consider the parameters given in Table 1, while for the healthy case we consider the parameters of Table 2.*

We want to investigate the stability properties of the dormancy steady state: $\mathfrak{D} = (\tilde{x}_e, \tilde{u}_e, x_e)$*, where,* $\tilde{x}_e = 0.0217$*,* $\tilde{u}_e = 0.0593$*, and* $x_e = 0.2535$*. Obviously, if the decay conditions (64) are satisfied, then the LMI (47) admits a solution.*

$\tilde{\delta}$	$\tilde{\gamma}$	$\tilde{\tau}$	$\tilde{\beta}(m)$	$\tilde{K}$	$\tilde{u}_e$	$\tilde{x}_e$
0.928	0.4	1	$\frac{2.78}{1+3m^2}$	0.2	0.05938567	0.02179864

Table 1: Parameters of the unhealthy compartment, and the values of $\tilde{x}_e$ and $\tilde{u}_e$.

δ	γ	τ	$\beta(m)$	x_e
0.168	0.001	0.12	$\frac{0.219}{1+4m^2}$	0.25354595

Table 2: Parameters of the healthy hematopoetic stem cell compartment, and the value of x_e.

We check that the decay conditions (64) are verified:

$$\begin{aligned}
&\textbf{\textit{(i)}} \quad 1-2\tilde{K}e^{-\tilde{\gamma}\tilde{\tau}}-\left(2\tilde{K}e^{-\tilde{\gamma}\tilde{\tau}}\right)^2=0.659979347>0,\\
&\textbf{\textit{(ii)}} \quad \tilde{\beta}\left(x_e+\tilde{\alpha}\tilde{x}_e\right)+\tilde{\delta}-\left(\tfrac{\mathfrak{b}_1}{4}-\tilde{\alpha}\tilde{\theta}\tilde{x}_e\right)=0.987350196>0,\\
&\textbf{\textit{(iii)}} \quad \beta\left(x_e+\tilde{x}_e\right)+\delta-\left(\tfrac{\mathfrak{b}_2}{2}-\theta x_e\right)=0.000149333>0,
\end{aligned} \tag{66}$$

where we consider: $\lambda_1=2$, $\lambda_2=\lambda_3=0.261780$, $\lambda_4=2.205796$, $\tilde{\lambda}_4=2$, $\nu_1=2$, $\nu_2=\frac{1}{4|\mathfrak{a}_8|}=1.301858$, $\nu_3=\frac{1}{4|\mathfrak{a}_9|}=1.736024$, $\nu_4=\frac{1}{2|\mathfrak{a}_4|}=0.302151$, $\nu_5=\frac{1}{2|\mathfrak{a}_2|}=7.374022$, $\rho_1=\frac{1}{10\tilde{\tau}}\ln\left(\frac{5}{1+4(\mathfrak{a}_5^2+\mathfrak{a}_5)}\right)=0.075074$ *and* $\rho_2=\frac{1}{10\tau}\ln\left(\frac{\lambda_2}{\mathfrak{b}_4}\right)=0.038369$. *For these numerical values, we check that* $\mathfrak{d}_2=\mathfrak{d}_3=0.010577>0$. *Therefore, according to Theorem 2, the dormancy steady state,* $\mathfrak{D}=(0.0217,0.0593,0.2535)$, *is regionally exponentially stable, as illustrated in Figure 4. This example will be revisited in the next section, in the practical situation of therapeutic strategies.*

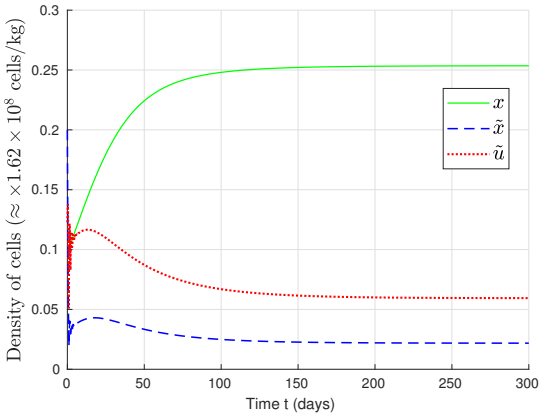

Figure 7: Trajectories of the system of the numerical example 4 (Tables 1-2). In this case, the dormancy steady state $\mathfrak{D}$ exists, such that $\tilde{x}_e=0.0217$, $\tilde{u}_e=0.0593$. The sufficient local stability conditions given in *Theorem 2-(B)* are satisfied, as shown in (66), and the trajectories of the system converge exponentially to $\mathfrak{D}$.

6. Concluding comments on the findings and possible therapeutic strategies oriented towards cancer dormancy

A first remark is that CSC dormancy probably results from complex relationships between the different biological parameters involved in this process, that are difficult to elicit, let alone to be understood. This observation concerns the stability properties (decay conditions in Theorem 2), but also the conditions of existence of dormancy (Proposition 1-**(vii)**), along with the role of the sensitivity parameter $\tilde{\alpha}$. This should lead us to develop further the mathematical framework sketched here, in order to help us understand the mechanisms behind dormancy. In the current section, we emphasize the main case of hematopoiesis and AML. In fact, experiments on fresh blood samples of patients with hyperleukocytosis may allow to identify the apoptosis and differentiation rates in the specific case of AML. However, there is no immediate prospect for estimating the proliferation functions $\tilde{\beta}$ and β, as well as the fast self-renewing parameter $\tilde{K}$. In addition, cancer dormancy is not easily traceable at the current time, since clinical manifestation of cancer is detectable only when tumor size exceeds a given threshold. Thus, model identification is a highly topical open issue, and our attention is only focused on the qualitative asymptotic behavior of our model, which is otherwise in line with the biological observations in this field. Nevertheless, as a first step, the analysis that we performed throughout this paper reveals that our theoretical results may suggest some therapeutic guidelines to eradicate aggressive CSCs ($\mathfrak{E}$), or to bring them to dormancy ($\mathfrak{D}$), as discussed in the sequel.

1) Towards the adoption of a common therapeutic strategy to yield states $\mathfrak{D}$ and $\mathfrak{E}$? It cannot be claimed that convergence to the steady state $\mathfrak{D}$ and the steady state $\mathfrak{E}$ should share the same therapeutic roadmap, since a crucial difference lies in their conditions of existence. For instance, $\mathfrak{E}$ exists even if $\tilde{\delta} > \frac{2e^{-\tilde{\gamma}\tilde{\tau}}-1}{1-2\tilde{K}e^{-\tilde{\gamma}\tilde{\tau}}}\tilde{\beta}(0)$ (see Proposition 1), while the reverse situation is required in order to allow for the existence of dormancy $\mathfrak{D}$, in addition to other conditions. We recall that in our system, the conditions of existence of the

steady states of interest are a type of *red lines*, that must not be crossed when elaborating a treatment strategy.

On the other hand, when we focus on the stability conditions, wondering how therapeutic actions can make the biological system go into the direction of the decay conditions (64), we realize that the respective decay conditions of $\mathfrak{D}$ and $\mathfrak{E}$ are substantially similar. More precisely, our sufficient stability conditions suggest that the biological parameters that can be targeted in order to satisfy (64), in either of the two states $\mathfrak{D}$ or $\mathfrak{E}$, are similar (but not identical). In this sense, we can state that a common therapeutic strategy for $\mathfrak{D}$ and $\mathfrak{E}$ can be proposed. So, in light of the existing therapies and recent clinical trials that highlight novel effective molecules as potential drugs in AML, we briefly discuss how a combined therapy - mostly composed of targeted therapies and standard chemotherapy - may satisfy the theoretical conditions (64).

First, we observe that the condition **(B-i)** in Theorem 2 provides a restriction on the dynamics of over-proliferating cells, since $\tilde{K}$, $\tilde{\gamma}$ and $\tilde{\tau}$ are involved. Satisfying the previous condition relies in increasing the product $\tilde{\gamma}\tilde{\tau}$, and decreasing $\tilde{K}$. Increasing $\tilde{\gamma}\tilde{\tau}$ means that we extend the average duration of the cell cycle $\tilde{\tau}$ and/or increase the apoptosis rate $\tilde{\gamma}$ in the population of unhealthy cells. Leukemic cells may be targeted by drugs such as quizartinib (AC220 [94]) or erlotinib [54] to increase $\tilde{\tau}$, while cytosine arabinoside can be used to increase the apoptosis rate $\tilde{\gamma}$. Moreover, quizartinib can be used to decrease the fast self-renewal rate $\tilde{K}$. In fact, $\tilde{K}$ is expected to be the hardest parameters to modify in practice, due to preexisting mutations in epigenetic control genes (DNMT3A, TET2). However, new *FLT3 inhibitors*, such as midostaurin[15], have achieved good performance (see the recent quantitative results provided in [85]) and are now approved for use along with chemotherapy to target leukemic cells in AML.

Next, in the conditions **(B-ii)** and **(B-iii)** of Theorem 2, the targets can be the parameters δ and $\tilde{\delta}$ (mainly $\tilde{\delta}$, since it is the unhealthy parameter) that

[15] Midostaurin is a multi-targeted protein kinase inhibitor, which can be active against oncogenic CD135 (FMS-like tyrosine kinase 3 receptor, FLT3). [25, 85]

appear in the right hand sides of the corresponding inequalities. We recall that $\tilde{\delta}$ includes the death rate and the differentiation rate of unhealthy resting cells. In practice, increasing $\tilde{\delta}$ means that we should increase the differentiation rates, which can be achieved in the case of leukemia by infusing dasatinib [54], that targets most of the tyrosine kinases including the c-KIT gene. In fact, it was thought that drugs promoting re-differentiation of CSCs in many cancers are not effective in the specific case of AML. However, this therapeutic option has been relaunched recently after successful clinical trials, where *dihydroorotate dehydrogenase (DHODH) inhibitors* restored differentiation of leukemic cells in AML [86]. Finally, increasing $\beta(0)$ and $\tilde{\beta}(0)$ can be performed by using G-CSF molecules [34]. These are the main common targets shared by $\mathfrak{D}$ and $\mathfrak{E}$.

2) Constraints and spillover risks of CSCs eradication: Increasing the parameters $\tilde{\delta}$, $\tilde{\gamma}$ and $\tilde{\tau}$ (using some of the previously mentioned molecules or their equivalent), promotes the existence of the state $\mathfrak{E}$, together with its stability. However, it may exclude the steady state $\mathfrak{D}$, by violating its conditions of existence. Furthermore, an excessive therapy that affects also healthy cells leads, theoretically, to the extinction of all the cells (*Theorem 1*). At the other extreme, insufficient drug dose might not successfully stop CSCs from overproliferation (when $2\tilde{K}e^{-\tilde{\gamma}\tilde{\tau}} > 1$). The overproliferating behavior may be worsened by CSC resistance to drugs. Thus, dormancy $\mathfrak{D}$ appears as a delicate intermediate equilibrium between the cancer progression and CSC eradication.

3) Specific constraints related to dormancy: In the *common strategy* that aims to satisfy the condition (64), we noticed that drugs have to increase the product $\tilde{\gamma}\tilde{\tau}$. On the other hand, we recall from Proposition 1-**(vii)** that the condition $1 < 2e^{-\tilde{\gamma}\tilde{\tau}}$ is necessary for the existence of $\mathfrak{D}$. Thus, the therapy action in this case has to take into account this supplementary condition. We infer from this remark that the probability to achieve the dormancy steady state $\mathfrak{D}$ by using the classical strategies that consist in giving the maximum tolerated dose of drugs during the treatment period [28], is therefore very low. Indeed, since a high dose is expected to yield $1 > 2e^{-\tilde{\gamma}\tilde{\tau}}$, the condition of existence of $\mathfrak{D}$ is then violated. The multiple restrictions on the biological parameters listed

in *Proposition 1* show that the existence of $\mathfrak{D}$ is more difficult to achieve than the existence of $\mathfrak{E}$. However, we suggest that infusing G-CSF molecules appears to favour the existence of a dormancy steady state, since increasing (relatively) $\beta(0)$ seems to go in the right direction in order to satisfy both the existence and the stability conditions of $\mathfrak{D}$.

4) The suggestion of therapeutic strategies that achieve dormancy: In light of the above discussion, we propose to implement what can be considered as a simple theoretical therapeutic strategy that aims to achieve a stable dormancy steady state. More precisely, we consider an hematopoietic system with the clinical symptoms that we expect when facing some overproliferating malignant hemopathies. This ranges from a blockade in differentiation mechanisms to the survival of abnormal cells, along with a high rate of self-renewal activity. We will in fact check that in the absence of adequate treatment, the unhealthy population will proliferate abundantly. Then, in a second time, our objective is to stabilize the total cell density, through multiple drug infusions of a combined therapy that is in line with our theoretical results (i.e. the decay conditions in *Theorem 2*). In other words, we aim to bring the hematopoietic system from an initial abnormal overproliferating state into a dormant stable steady state. For that purpose, let us assume that the initial parameters of the unhealthy compartment are those given in Table 3. In fact, we have deliberately chosen an intuitive set of parameters that matches specific dysfunctions in overproliferating malignant hemopathies (particularly the condition $2\tilde{K}e^{-\tilde{\gamma}\tilde{\tau}} > 1$).

$\tilde{\delta}$	$\tilde{\gamma}$	$\tilde{\tau}$	$\tilde{\beta}(m)$	$\tilde{K}$	$\tilde{\alpha}$
0.25	0.1	0.2	$\frac{2.78}{1+m^3}$	0.55	0.8

Table 3: The set of initial (i.e. before treatment) parameters of the unhealthy compartment.

On the other hand, we assume that the parameters of the healthy compartment are those given in Example 4, and we consider that the therapy to be administrated has a negligible effect on ordinary cells.

In medical practice, usually the hematopoietic system is targeted through

chemotherapy or targeted therapy (a combination of two or three drugs), sometimes infused along with a complementary treatment. All these drugs have in fact molecular targets (e.g. dasatinib targets BCR/Abl, Src, ephrin receptors, c-Kit and many other tyrosine kinases), that result in a modification of some biological mechanisms (e.g. generally, dasatinib increases proliferation, and differentiation in AML [30]). It should be borne in mind that the functional effect resulting from the molecular action of the infused drugs, varies in practice according to several facts (for instance, the buildup of many types of mutations by some individuals). However, when we put aside all the intermediate complications that may exist in practice, we can take a shortcut that associates to each infused drug its most likely action on one or several biological functions (that are: differentiation, apoptotis, and so on), with a certain amount of confidence. Thus, we can roughly state from medical practice some major families of molecules that can be used in the case of AML or other cancers, according to their expected effect on the biological functionalities.

Fast self-renewing ($\tilde{K}$)	Quizartinib, midostaurin Dihydroorotate dehydrogenase (DHODH) inhibitors
Apoptosis ($\tilde{\gamma}$)	Daunorubicin, cytosine arabinoside, volasertib
Differentiation ($\tilde{\delta}$)	Dihydroorotate dehydrogenase (DHODH) inhibitors
Cell cylce dur. ($\tilde{\tau}$)	Quizartinib, erlotinib, volasertib

Table 4: Here we associate the most likely (clinically established) effect of some advanced drugs/molecules on the biological features of the hematopoietic system, in the specific case of AML (without focussing neither on the molecular mechanisms behind each drug action, or on the possible mutual interactions that may exist between drugs within some combinations). The case of the sensitivity paprameter $\tilde{\alpha}$ is discussed later, in Remark 7.

Remark 6. ***(i)*** *One notices that some molecules in Table 4 are expected to modify more than one model parameter. For instance, the DHODH inhibitor, which is a differentiation re-activator, may decrease $\tilde{K}$ and increase $\tilde{\delta}$, since both actions seem to promote a return into normal differentiation.* ***(ii)*** *The volasertib (recognized as orphan drug for AML since 2014), belongs to the family of Polo-like kinase (Plk) inhibitors. It can be used in the treatment of AML to promote apoptosis and cell cycle arrest (see for instance [10]). In fact, the list of drugs given in Table 4 is not exhaustive and can be enlarged, for instance, to: histone deacetylase (HDAC) inhibitors (vorinostat and panobinostat), and the*

family of aurora kinase inhibitors (AZD115).

Now, we observe that the biological parameters considered in Table 3 imply that $2\tilde{K}e^{-\tilde{\gamma}\tilde{\tau}} = 1.078$. It follows that, theoretically, if AML is not treated, unhealthy cells will invade the bone marrow and possibly the bloodstream. In Figure 8, we illustrate the evolution of cell densities for the selected model parameters, where we observe the unbounded proliferation of unhealthy cells.

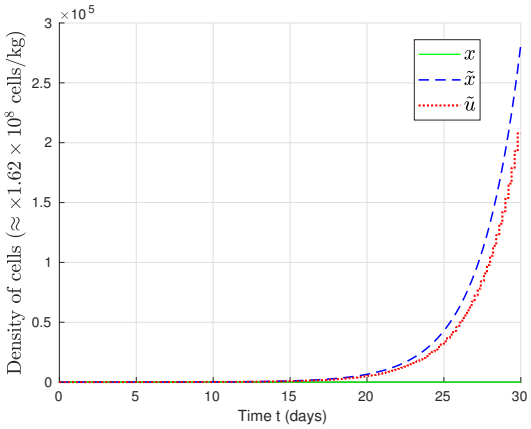

Figure 8: Trajectories of the system for the (non-treated) model parameters of Table 3.

Remark 7. *We expect that $\tilde{\alpha}$ is less than* 1 *before therapy, then it starts to increase when therapy is applied (an immunostimulating effect of cytotoxic drugs, elicited e.g. in [96, 95]), and then greater than* 1 *when the immune system has learnt to counter the dodges of cancer cells (such as hiding their tumor antigens or achieving inactivation of antibodies, e.g. by glycosylation), or when the reduction of the tumor burden has made immune cells proportionally more efficient in their encounters with cancer cells, or also when successful immunotherapy is used to directly target cancer cells.*

Actually, the elaboration of an *optimal* therapeutic strategy[16] is beyond the

[16]The optimal therapy requires the determination of the best infusion planning, that takes into account drug toxicity and other practical considerations (e.g. how the doses of each drug type are spread over the duration of the therapy). These points deserve a separated study.

scope of this work. Here, we are suggesting a theoretical therapeutic strategy, that can be based on some suitable combination of drugs (listed in Table 4, or others similar ones). We assume that the resulting evolution patterns of the biological model parameters are those illustrated in Figure 9. In fact, we can distinguish between two evolution trends, nested within one another as follows:

1) The first series of infusions aims to decrease $\tilde{K}$ (fast self-renewing rate), to increase $\tilde{\tau}$ (cell-cycle duration), and to increase $\tilde{\gamma}$ (apoptosis rate). It is worth mentioning that the direction of the change in the model parameters (i.e. by increasing/decreasing the model parameters values) is in line with the observed effect of the drugs listed in Table 3. This treatment phase is expected to limit the expansion of CSCs. We also assume that the first treatment phase is accompanied by a slight increase of the value of $\tilde{\alpha}$ (see Remark 7).

2) The second phase of the treatment aims, on the one hand, to maintain the trend given for the parameters ($\tilde{K}$, $\tilde{\tau}$, $\tilde{\gamma}$), and on the other hand, to reactivate the differentiation of unhealthy cells (using DHODH inhibitors, for instance) and to increase the sensitivity parameter $\tilde{\alpha}$ with more virulence than in the first series of infusions (e.g. using a suitable immunotherapeutic action, Remark 7).

Remark 8. *It seems legitimate to wonder whether the reactivation of differentiation of CSCs is a good strategy to fight cancer. The answer is argued for instance in [28], where it is explained how CSCs can initiate and regenerate cancers, while differentiated cancer cells (called CCs [28]) will inevitably die out (see the section "Cancer stem cells and non-stem cancer cells", [28]). Thus, promoting the differentiation of CSCs into CCs appears as a sustainable way to both limit cancer progression, and avoid the escape from cancer dormancy.*

Now, let us assume that an adequate combination of drugs has been fixed. We can highlight one suggestion among other possibilities, in which we propose:

① a shock treatment through chemotherapy that promotes apoptosis $\tilde{\gamma}$ and cell arrest $\tilde{\tau}$ (using volasertib for both objectives), and targeting $\tilde{K}$ using AC220 (which has also a suitable effect on cell arrest $\tilde{\tau}$),

② followed by a more differentiation-oriented treatment (using drugs based

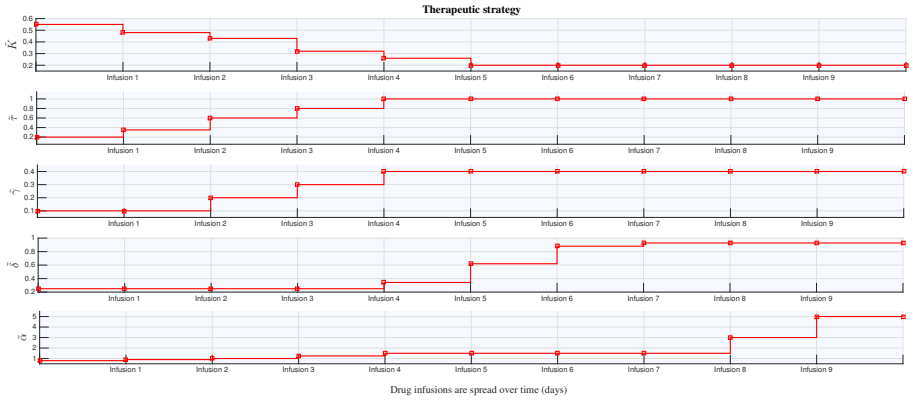

Figure 9: An illustrative therapeutic strategy that gradually modifies five model parameters, using adequates drugs: this can be achieved using a mixture of standard chemotherapy or targeted therapies, along with complementary molecules and/or immunotherapeutic actions.

on DHODH inhibitors) and mitotic/proliferation inhibition of unhealthy cells (possibly using some immunotherapy-based drugs, or vincristine, see also [79]).

We aim through the selected therapy to achieve an evolution pattern of the model parameters as close as possible to the idealistic ones given in Figure 9.

Remark 9. *The treatment protocol that we suggest have many similarities with classical methods in AML therapeutics [79]. We can mention in particular the* ***3+7*** *most famous strategy, which is also based on two main separated phases (7 days of intensive induction through cytarabine, plus 3 days of an anthracycline [79]), and then possibly followed by consolidation chemotherapy and hematopoietic cell transplant [25, 79].*

Next, we apply the therapeutic strategy given in Figure 9 to our model, starting the first infusion at $t = 1$ day, and considering a fixed treatment step of 1 day between successive infusions (another choice may be envisaged if needed). One notices that the model parameters after *Infusion* 9 are those given in Example 4, for which the decay conditions (64) of Theorem 2 are satisfied.

The evolution of the ordinary and mutated cell densities is shown in Figure 10. It is worth mentioning that in practice, the treatment of AML is spread over several separated phases. For instance, in the recent experimental work

[85], an AML (FLT3-type) therapy based on midostaurin and chemotherapy, has been separated into two *induction phases*, a *consolidating phase* and *maintenance phase* (59% of patients that have undergone the previously mentioned therapeutic protocol, then underwent bone marrow transplant, have reached the complete remission state [85]). Similarly, in our example, we assume that after *Infusion* 9, a consolidating and a maintenance phases continue so as to correct, adjust, strengthen, and fortify the desired dormancy state of the hematopoietic system (which is the state described by the set of parameters of *Infusion* 9).

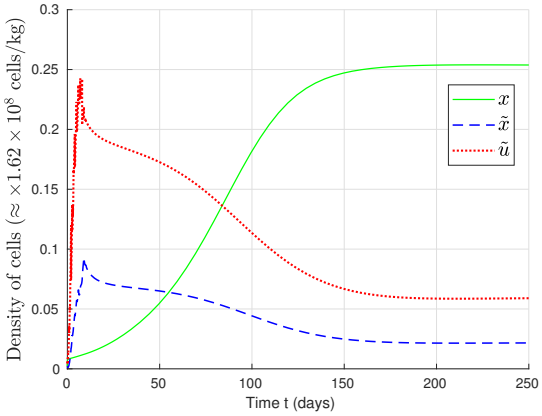

Figure 10: The evolution of the total densities of healthy and unhealthy cells (resp. $x(t)$ and $\tilde{x}(t)$) and $\tilde{u}(t)$, when we apply the theoretical therapeutic strategy illustrated in Figure 9. If we do not change the parameter values, the model behaves as in Figure 8 (i.e. CSCs over-proliferate). However, in the case of treated cancer, the trajectories converge to a dormancy stable steady state, under the effect of the suggested therapy.

We conclude this work by referring to Table 1 in [79], which summarizes a number of emerging promising AML therapies, that open up other possibilities to act on cancerous hematopoietic systems. Many of these strategies can in fact be implemented and discussed within the modeling and analysis framework that we introduced in our current work. It is worth mentioning that the addition of midostaurin to chemotherapy resulted in a 22% lower risk of death among patients, in comparison to another more classical treatment (see [85]). Notice that, most of the molecules listed in [79] (and the references therein) are in early phases of development and trials, but they participate greatly, as

well as many multidisciplinary works, to nourish this hope of moving towards systematic treatments for cancer, in general, and leukemia, in particular.

References

[1] M. Adimy, A. Chekroun, T.M. Touaoula, *Age-Structured and Delay Differential-Difference Model Of Hematopoietic Stem Cell Dynamics*, Discret And Continuous Dynamical Systems Series B, Volume 20, Number 9, pp. 2765-2791, (2015).

[2] M. Adimy, F. Crauste, A. Abdllaoui, *Discrete Maturity-Structured Model of Cells Differentiation with Applications to Acute Myelogenous Leukemia*, J. Biological Systems, No. 3, pp. 395-424, (2008).

[3] J.A. Aguirre-Ghiso, *Models, mechanisms and clinical evidence for cancer dormancy*, Nature Reviews Cancer, 7(11), pp. 834-846, (2007).

[4] J.A. Aguirre-Ghiso, *The problem of cancer dormancy: understanding the basic mechanisms and identifying therapeutic opportunities*, Cell Cycle, Taylor & Francis Online, Vol. 5(6), pp. 1740-1743, (2006).

[5] M. Ahsen, H. Özbay, S. I. Niculescu, *Analysis of deterministic cyclic gene regulatory network models with delays*, Birkhäuser, (2015).

[6] M.G. Al-Asadi, G. Brindle, M. Castellanos, S.T. May, K.I. Mills, N.H. Russell, C.H. Seedhouse, M. Pallis, *A molecular signature of dormancy in CD34+ CD38-acute myeloid leukaemia cells*, Blood, Oncotarget, 8(67), p.111405, (2017).

[7] B. Alberts , D. Bray, K. Hopkin, A. Johnson, J. Lewis, M. Raff, K. Roberts, P. Walter, *Essential Cell Biology, Fourth Edition*, Garland Science, pp. 865, (2013).

[8] J. L. Avila, *et al.*, *A coupled model for healthy and cancerous cells dynamics in Acute Myeloid Leukemia,* IFAC Proceedings Volumes 47.3: pp. 7529-7534, (2014).

[9] J.L. Avila, C. Bonnet, J. Clairambault, H. Özbay, S.I. Niculescu, F. Merhi, R. Tang, J.P. Marie, *A new model of cell dynamics in acute myeloid leukemia involving distributed delays*. IFAC TDS, pp. 55-60, (2012).

[10] J.M. Brandwein, *Targeting polo-like kinase 1 in acute myeloid leukemia. Therapeutic advances in hematology*, 6(2), pp. 80-87, (2015).

[11] J. Bélair, M.C. Mackey, J.M. Mahaffy, *Age-structured and Two-delay Models for Erythropoiesis*, Math. Biosci. 128. No. 1-2, pp. 317-346, (1995).

[12] N. Bellomo, G. Forni, *Dynamics of tumor interaction with the host immune system,* Mathematical and computer modelling, 20(1), pp.107–122, (1994).

[13] S. Bernard, J. Bélair, M.C. Mackey, *Oscillations in cyclical neutropenia: new evidence based on mathematical modeling*, Journal of theoretical biology, 223(3), pp.283-298, (2003).

[14] H. M. Blau, T. R. Brazelton, and J. M. Weimann, *The Evolving Concept Review of a Stem Cell: Entity or Function?*, Cell, Vol. 105, pp. 829-841, (2001).

[15] J.R. Brahmer, D.M. Pardoll, *Immune checkpoint inhibitors: making immunotherapy a reality for the treatment of lung cancer,* Cancer immunology research, 1(2), pp. 85–91, (2013).

[16] F.J. Burns, J.F. Tannock, *On the existence of a G_0-phase in the cell cycle*, Cell Tissue Kinetics, 3:321–334, (1970).

[17] C.L. Chaffer, Brueckmann, I., Scheel, C., Kaestli, A.J., Wiggins, P.A., Rodrigues, L.O., Brooks, M., Reinhardt, F., Su, Y., Polyak, K. and Arendt, L.M., 2011. *Normal and neoplastic nonstem cells can spontaneously convert to a stem-like state*, Proceedings of the National Academy of Sciences, 108(19), pp.7950-7955, (2011).

[18] G. M. Crane, E. Jeffery, S.J. Morrison, *Adult haematopoietic stem cell niches*, Nature Reviews Immunology, (2017).

[19] C. Colijn, M. C. Mackey, *A mathematical model of hematopoiesisI. Periodic chronic myelogenous leukemia*, Journal of Theoretical Biology, 237(2), pp.117-132, (2005).

[20] F. Delhommeau, S. Dupont, V. Della Valle, C. James, S. Trannoy, A. Massé, O. Kosmider, J.P. Le-Couedic, F. Robert, A. Alberdi, Y. Lécluse, I. Plo, F.J. Dreyfus, C. Marzac, N. Casadevall, C. Lacombe, S.P. Romana, P. Dessen, J. Soulier, F. Viguié , M. Fontenay, W. Vainchenker, O.A. Bernard, *Mutation in TET2 in Myeloid Cancers*, New England Journal of Medicine, 360(22):2289-30, (2009).

[21] W. Djema, F. Mazenc, C. Bonnet, *Stability analysis and robustness results for a nonlinear system with distributed delays describing hematopoiesis*, Systems & Control Letters, Elsevier, Vol. 102, pp. 93-101, (2017).

[22] W. Djema, F. Mazenc, C. Bonnet, *Analysis of a Nonlinear Delay Differential-Difference Biological Model*, IFAC-PapersOnLine, IFAC Conference on Time-Delay Systems, Vol. 49, No. 10, pp. 246-251, (2016).

[23] W. Djema, F. Mazenc, C. Bonnet, J. Clairambault, P. Hirsch, F. Delhommeau, *Stability of a Delay System Coupled to a Delay Differential-Difference System Describing the Coexistence of Ordinary and Mutated Hematopoietic Stem cells*, the 55^{th} Conference on Decision and Control, Las Vegas, USA, (2016).

[24] W. Djema, F. Mazenc, C. Bonnet, J. Clairambault, P. Hirsch, F. Delhommeau, *Analysis of a Model of Dormancy in Cancer as a State of Coexistence Between Tumor and Healthy Stem Cells*, *Proceedings* of the American Control Conference, Seattle, USA, (2017).

[25] H. Döhner, D.J. Weisdorf, C.D. Bloomfield, *Acute Myeloid Leukemia*, N. Engl. J. Med. 373, pp. 1136-1152, (2015).

[26] S. Ebinger, E. Z. Özdemir, C. Ziegenhain, S. Tiedt, C. C. Alves, M. Grunert, M. Dworzak, C. Lutz, V. A. Turati, T. Enver, H. P. Horny, *Characterization of Rare, Dormant, and Therapy-Resistant Cells in Acute Lymphoblastic Leukemia*, **Cancer Cell**, 30(6), pp. 849-862, (2016).

[27] R. Eftimie, J.L. Bramson, D.J. Earn, *Interactions between the immune system and cancer: a brief review of non-spatial mathematical models,* Bulletin of mathematical biology, 73(1), pp. 2–32, (2011).

[28] H. Enderling, *Cancer Stem Cells and Tumor Dormancy*, Sys. Biol. of Tumor Dormancy, Springer NY, pp. 55-71, (2013).

[29] T. Enver, M. Pera, C. Peterson, P.W. Andrews, *Stem cell states, fates, and the rules of attraction*, Cell Stem Cell 4, pp. 387-397, (2009).

[30] Y. Fang, L. Zhong, M. Lin, X. Zhou, H. Jing, M. Ying, M., Luo, P., Yang, B. and He, Q., *MEK/ERK dependent activation of STAT1 mediates dasatinib-induced differentiation of acute myeloid leukemia*, PloS one, 8(6), p.e66915, (2013).

[31] M. Feuring-Buske, A.E. Frankel, R.L. Alexander, B. Gerhard, D.E. Hogge, *A diphtheria toxin-interleukin 3 fusion protein is cytotoxic to primitive acute myeloid leukemia progenitors but spares normal progenitors*, Cancer Research, 62(6), pp. 1730-1736, (2002).

[32] M. Ferrarini, E. Ferrero, L. Dagna, A. Poggi, M. R. Zocchi, *Human T cells: a nonredundant system in the immune-surveillance against cancer*, Trends in immunology, 23(1), pp. 14-18, (2002).

[33] C. Foley, M.C. Mackey, *Dynamic hematological disease: a review*, J. Math. biology, 58.1-2: pp. 285-322, (2009).

[34] C. Foley, , S. Bernard, M.C. Mackey, *Cost-effective G-CSF therapy strategies for cyclical neutropenia: Mathematical modelling based hypotheses*, Journal of theoretical biology 238.4: pp. 754-763, (2006).

[35] J. Folkman, R. Kalluri, *Cancer without disease*, Nature, 427(6977), pp. 786-787, (2004).

[36] E. Fridman *Stability of linear descriptor systems with delay: a Lyapunov-based approach,* Journal of Mathematical Analysis and Applications, 273(1), pp. 24-44, (2002).

[37] E. Fridman, *Introduction to time-delay systems: analysis and control*, Birkhauser, Systems and Control: Foundations and Applications, 2014.

[38] E. Fridman, C. Bonnet, F. Mazenc, W. Djema, *Stability of the cell dynamics in Acute Myeloid Leukemia*, Systems & Control Letters 88, pp. 91-100, (2016).

[39] R. A. Gatenby, *A change of strategy in the war on cancer*, Nature, 459(7246), pp. 508-509, (2009).

[40] C.D. Godwin, R.P. Gale, R.B. Walter, *Gemtuzumab ozogamicin in acute myeloid leukemia*, Leukemia, (2017).

[41] K. Gu, Y. Liu. *Lyapunov-Krasovskii Functional for Uniform Stability of Coupled Differential-Functional Equations.* Automatica, Vol 45, No. 3, pp. 798-804, (2009).

[42] J.K. Hale, *Sufficient conditions for stability and instability of autonomous functional-differential equations*, Journal of Differential Equations, vol. 1, pp. 452-482, (1965).

[43] E.C. Hayden, *Cutting off cancer's supply lines*, Nature, 458(7239), p.686-687, (2009).

[44] P. Hirsch, Y. Zhang, R. Tang, V. Joulin, H. Boutroux, E. Pronier, H. Moatti, P. Flandrin, C. Marzac, D. Bories, F. Fava, *Genetic hierarchy and temporal variegation in the clonal history of acute myeloid leukaemia,* Nature communications, 7, p.12475, (2016).

[45] R. Hoffman, E.J. Benz, L.E. Silberstein, H. Heslop, J. Weitz, J. Anastasi, *Hematology: Basic Principles and Practice*, 6^{th} Edition, Elsevier, Churchill Livingstone, (2012).

[46] M. Hollstein, D. Sidransky, B. Vogelstein, C.C. Harris, *p53 mutations in human cancers,* Science, 253(5015), pp. 49–53, (1991).

[47] C. Hosing, *Hematopoietic Stem Cell Mobilization with G-CSF*, Methods Mol Biol. 904:37-47, (2012).

[48] G. Jansen, R. Gatenby, C.A. Aktipis, *Control vs. eradication: Applying infectious disease treatment strategies to cancer*, Proceedings of the National Academy of Sciences of United States of America, vol. 112, no. 4, pp. 937-938, (2015).

[49] C.T. Jordan, M.L. Guzman, M. Noble, *Cancer stem cells*, New England Journal of Medicine, 355(12), pp.1253-1261, (2006).

[50] I. Karafyllis, P. Pepe, Z.P. Jiang, *Stability results for systems described by coupled retarded functional differential equations and functional difference equations*, Nonlinear Anal. Theory Methods Appl. 71, 3339–3362, (2009).

[51] I. Kareva, *Primary and Metastatic Tumor Dormancy as a Result of Population Heterogeneity*, Biology direct, 11(1), p.37., (2016).

[52] J.P. Keener, J. Sneyd, *Mathematical physiology*, Vol. 1, New York: Springer, (2009).

[53] V. Kolmanovskii, A. Myshkis, *Introduction to the Theory and Applications of Functional Differential Equations*, Kluwer Academic Publishers, Dordrecht, (1999).

[54] E. Lainey, S. Thépot, C. Bouteloup, M. Sébert, L. Adès, M. Tailler, C. Gardin, S. Botton, A. Baruchel, P. Fenaux, G. Kroemer, S. Boehrer, *Tyrosine kinase inhibitors for the treatment of acute myeloid leukemia: Delineation of anti-leukemic mechanisms of action*, Biochemical Pharmacology 82, pp. 1457-1466, (2011).

[55] C.J. Langer, *Emerging Immunotherapies in the Treatment of Nonsmall Cell Lung Cancer (NSCLC): The Role of Immune Checkpoint Inhibitors,* American journal of clinical oncology, 38(4), pp. 422–430, (2015).

[56] A.G. McKendrick, *Applications of mathematics to medical problems*, Proceedings of the Edinburgh Mathematical Society 44, pp. 98-130, (1925).

[57] M.C. Mackey, *Unified hypothesis of the origin of aplastic anemia and periodic hematopoiesis*, Blood 51, pp. 941-956, (1978).

[58] M.C. Mackey, L. Pujo-Menjouet, J. Wu, *Periodic oscillations of blood cell populations in chronic myelogenous leukemia*, SIAM journal on mathematical analysis, 38(1), pp.166-187, (2006).

[59] M. Malisoff, F. Mazenc, *Constructions of Strict Lyapunov Functions*, Serie : Communications and Control Engineering. Spinger-Verlag London Ltd, U.K., 2009.

[60] A. Marciniak-Czochra, T. Stiehl, A.D. Ho, W.Jäger, W. Wagner, *Modeling of asymmetric cell division in hematopoietic stem cellsregulation of self-renewal is essential for efficient repopulation*, Stem cells and development, 18(3), pp.377-386, (2009).

[61] A.N. Michel, L. Hou, D. Liu, *Stability of Dynamical Systems: Continuous, Discontinuous, and Discrete Systems*, Systems & Control: Foundations & Applications, Birkhäuser, 2nd Ed. (2015).

[62] D. Morgan, *The Cell Cycle: Principles of Control*, Primers in Biology Series, Oxford University Press, pp. 297, (2006).

[63] G.N. Naumov, J. Folkman, O. Straume, *Tumor dormancy due to failure of angiogenesis: role of the microenvironment.* Clin Exp Metastasis, 26(1):5160, (2009).

[64] M. Nielsen, J. Thomsen, S. Primdahl , U. Dyreborg, J. Andersen, *Breast cancer and atypia among young and middle-aged women: a study of 110 medicolegal autopsies*, Br. J. Cancer. 56(6):8149, (1987).

[65] H. Özbay, C. Bonnet, H. Benjelloun, J. Clairambault, *Stability analysis of cell dynamics in leukemia.* Math. Model Nat. Phenom., Vol. 7, No. 1, pp. 203-234, (2012).

[66] D.M. Pardoll, *The blockade of immune checkpoints in cancer immunotherapy,* Nature reviews. Cancer, 12(4), pp. 252, (2012).

[67] E. Passegué, C. H. Jamieson, L. E. Ailles, I. L. Weissman, *Normal and leukemic hematopoiesis: Are leukemias a stem cell disorder or a reacquisition of stem cell characteristics?*, Proc. Natl. Acad. Sci., Regenerative Medicine, USA 100 (Suppl 1), pp. 11842-11849, (2003).

[68] P. Pepe, *The Liapunov's second method for continuous time difference equations*, International Journal of Robust and Nonlinear Control, 13(15), pp.1389-1405, (2003).

[69] P. Pepe, I. Karafyllis, Z.P. Jiang, *On the Liapunov-Krasovskii methodology for the ISS of systems described by coupled delay differential and difference equation*, Automatica, 44. pp. 2266-2273, (2008).

[70] L. Preziosi, *From population dynamics to modelling the competition between tumors and immune system. Mathematical and computer modelling*, 23(6), pp. 135–152, (1996).

[71] E. Pronier, F. Delhommeau, *Inhibition of TET2-mediated conversion of 5-methylcytosine to 5-hydroxymethylcytosine disturbs erythroid and granulomonocytic differentiation of human hematopoietic progenitors*, Blood, 118(9), pp. 2551–2555, (2011).

[72] L. Pujo-Menjouet, *Blood cell dynamics: half of a century of modelling*, Mathematical Modelling of Natural Phenomena, 11(1), pp. 92–115, (2016).

[73] L. Pujo-Menjouet, S. Bernard, M.C. Mackey, *Long period oscillations in a G_0 model of hematopoietic stem cells*, SIAM. J. Appl. Dynam. Syst. 4(2), pp. 312-332, (2005).

[74] E. Pronier, F. Delhommeau, *Role of* TET2 *Mutations in Myeloproliferative Neoplasms*, Curr. Hematol. Malig. Rep., 7, pp. 57–64, (2012).

[75] H. Qian, *Cooperativity in cellular biochemical processes: Noise-enhanced sensitivity, fluctuating enzyme, bistability with nonlinear feedback, and other mechanisms for sigmoidal responses*, Annual review of biophysics, 41, pp.179-204, (2012).

[76] T. Reya, S.J. Morrison, M.F. Clarke, I.L. Weissman, *Stem cells, cancer, and cancer stem cells*, nature, 414(6859), pp. 105–111, (2001).

[77] A.R. Reynolds, *et al.*, *Stimulation of tumor growth and angiogenesis by low concentrations of RGD-mimetic integrin inhibitors,* Nature medicine, 15(4), pp. 392-400, (2009).

[78] J.M. Rowe, B.Löwenberg, *Gemtuzumab ozogamicin in acute myeloid leukemia: a remarkable saga about an active drug*, Blood, 121(24), pp. 4838-4841, (2013).

[79] C. Saygin, H.E. Carraway, *Emerging therapies for acute myeloid leukemia*, Journal of hematology & oncology, 10(1), p.93, (2017).

[80] R.D. Schreiber, L.J. Old, M.J. Smyth, *Cancer immunoediting: integrating immunity's roles in cancer suppression and promotion*, Science, 331(6024), pp. 1565-1570, (2011).

[81] J. A. Smith, L. Martin, *Do cells cycle?. Proceedings of the National Academy of Sciences*, 70(4), pp. 1263–1267, (1973).

[82] E. Solary, O.A. Bernard, A. Tefferi, F. Fuks, W. Vainchenker, *The Ten-Eleven Translocation-2 (TET2) gene in hematopoiesis and hematopoietic diseases*, Leukemia, 28, pp. 485–496, (2014).

[83] T. Stiehl, A. Marciniak-Czochra, *Characterization of stem cells using mathematical models of multistage cell lineages,* Mathematical and Computer Modelling, 53(7), pp.1505-1517, (2011).

[84] T. Stiehl, A. Marciniak-Czochra, *Mathematical modeling of leukemogenesis and cancer stem cell dynamics*, Mathematical Modelling of Natural Phenomena, 7(1), pp.166-202, (2012).

[85] R.M. Stone, S.J. Mandrekar, B.L. Sanford, K. Laumann, S. Geyer, C.D. Bloomfield, C. Thiede, T.W. Prior, K. Döhner, G. Marcucci, F. Lo-Coco, *Midostaurin plus Chemotherapy for Acute Myeloid Leukemia with a FLT3 Mutation*, New England Journal of Medicine, (2017).

[86] D. B. Sykes, Y. S. Kfoury, F. E. Mercier, M. J. Wawer, J. M. Law, M. K. Haynes, T. A. Lewis, A. Schajnovitz, E. Jain, D. Lee, H. Meyer, *Inhibition of dihydroorotate dehydrogenase overcomes differentiation blockade in acute myeloid leukemia*, Cell, 167(1), pp. 171-186, (2016).

[87] H.R. Thieme, *Mathematics in Population Biology*, Princeton Series in Theoretical and Computational Biology. Princeton University Press, (2003).

[88] B. Tuch, *Stem cells - a clinical update,* Australian family physician, 35(9), pp. 719, (2006).

[89] J.W. Uhr, R.H. Scheuermann, N.E. Street, E.S. Vitetta, *Cancer dormancy: opportunities for new therapeutic approaches,* Nature medicine, 3(5), pp. 505-509, (1997).

[90] M.D. Vesely, *et al.*, *Natural innate and adaptive immunity to cancer*, Annual review of immunology, 29, pp.235-271, (2011).

[91] G.C. Wake, *The Solution and the Stability of a Nonlinear Age-Structured Population model*, The ANZIAM Journal, 45(02): pp. 153-165, (2003).

[92] G. Wang, *Analysis of Complex Diseases: A Mathematical Perspective*, CRC Press, (2013).

[93] K.P. Wilkie, P. Hahnfeldt, *Tumorimmune dynamics regulated in the microenvironment inform the transient nature of immune-induced tumor dormancy*, J. Cancer Research, 73(12), pp. 353444, (2013).

[94] P.P. Zarrinkar, *AC220 is a uniquely potent and selective inhibitor of FLT3 for the treatment of acute myeloid leukemia (AML)*, Blood, 114(14): pp. 2984–2992, (2009).

[95] L. Zitvogel, A. Tesniere, G. Kroemer, *Cancer despite immunosurveillance: immunoselection and immunosubversion*, Nature Reviews Immunology, 6(10), pp. 715-727, (2006).

[96] L. Zitvogel, L. Apetoh, F. Ghiringhelli, G. Kroemer, *Immunological aspects of cancer chemotherapy*, Nature Reviews Immunology, 8(1), pp. 58-73, (2008).

Acknowledgement: We would like to thank the A.E. and the reviewers of JTB for their valuable comments. We also thank professors P. Pepe and M. Adimy, referees of the PhD thesis of W. Djema, for the stimulating discussions we had on the topic.

Appendix A. Proof of Theorem 1 (cell extinction)

Simple calculations show that the derivative of $\mathcal{W}$, defined in (28), along the trajectories of (10), satisfies, for almost all $t \geq 0$,

$$\begin{aligned}
\dot{\mathcal{W}}(t) = & \left[-\tilde{\delta} + (\psi_1 - 1)\,\tilde{\beta}\,(x(t) + \tilde{\alpha}\tilde{x}(t))\right]\tilde{x}(t) \\
& - \left[\psi_1(e^{-\rho_1^*\tilde{\tau}} - 2\tilde{K}e^{-\tilde{\gamma}\tilde{\tau}}) - 2(1-\tilde{K})e^{-\tilde{\gamma}\tilde{\tau}}\right]\tilde{u}(t-\tilde{\tau}) \\
& - \left[\delta + (1-\psi_2)\,\beta(x(t)+\tilde{x}(t))\right]x(t) - \psi_1\rho_1^*\int_{t-\tilde{\tau}}^{t} e^{\rho_1^*(\ell-t)}\tilde{u}(\ell)d\ell \\
& - (\psi_3 e^{-\rho_2^*\tau} - 1)2e^{-\gamma\tau}\beta\,(x(t-\tau) + \tilde{x}(t-\tau))\,x(t-\tau) \\
& - \psi_2\rho_2^*\int_{t-\tau}^{t} e^{\rho_2^*(\ell-t)}\beta\,(x(\ell) + \tilde{x}(\ell))\,x(\ell)d\ell.
\end{aligned}$$

Now, according to (29), the conditions $2\tilde{K}e^{-\tilde{\gamma}\tilde{\tau}} < 1$ and $\psi^* > 0$ are satisfied. It follows that for all $\rho_1^* \in \left(0, \frac{1}{\tilde{\tau}}\ln\left(\frac{k}{1+2(k-1)\tilde{K}e^{-\tilde{\gamma}\tilde{\tau}}}\right)\right)$, where $k > 1$ is a constant

that we will select later, we get $0 < \frac{1-2\tilde{K}e^{-\tilde{\gamma}\tilde{\tau}}}{k} < e^{-\rho_1\tilde{\tau}} - 2\tilde{K}e^{-\tilde{\gamma}\tilde{\tau}} < 1 - 2\tilde{K}e^{-\tilde{\gamma}\tilde{\tau}}$. On the other hand, using the definition of ψ_1, we can readily check that:

$$\psi_1\left(1-2\tilde{K}e^{-\tilde{\gamma}\tilde{\tau}}\right) - 2\left(1-\tilde{K}\right)e^{-\tilde{\gamma}\tilde{\tau}} > 0.$$

Therefore, we can notice that for all $k \in \left(1, \frac{\left(1-2\tilde{K}e^{-\tilde{\gamma}\tilde{\tau}}\right)\psi_1}{2(1-\tilde{K})e^{-\tilde{\gamma}\tilde{\tau}}}\right)$, the constant:

$$\overline{k} = \psi_1\left(\frac{1-2\tilde{K}e^{-\tilde{\gamma}\tilde{\tau}}}{k}\right) - 2\left(1-\tilde{K}\right)e^{-\tilde{\gamma}\tilde{\tau}},$$

is strictly positive. Next, since $\tilde{\beta}$ is decreasing, and using the fact that $\psi_{11} > 1$, it follows that $(\psi_{11}-1)\,\tilde{\beta}\,(x(t)+\tilde{\alpha}\tilde{x}(t)) \leq (\psi_{11}-1)\,\tilde{\beta}(0)$. From the previous intermediate results, we conclude that for all $t \geq 0$, $-\tilde{\delta}+(\psi_1-1)\,\tilde{\beta}\,(x(t)+\tilde{\alpha}\tilde{x}(t)) \leq \psi_{12}\tilde{\beta}\,(x(t)+\tilde{\alpha}\tilde{x}(t))$, where, $\psi_{12} < 0$. Now, we assume that the third decay condition, $\delta > (2e^{-\gamma\tau}-1)\,\beta(0)$, is satisfied, and we put $\psi_3 = \frac{2\beta(0)+(\delta+\beta(0))e^{\gamma\tau}}{4\beta(0)}$. Therefore, it is easy to check that, in this case, we have $\psi_3 \in \left(1, \frac{\delta+\beta(0)}{2\beta(0)}e^{\gamma\tau}\right)$. It follows that $\delta + (1-\psi_2)\,\beta(0)$ is positive. For later use we denote $\delta^* = \delta + (1-\psi_2)\,\beta(0)$. Next, by selecting $\rho_2^* = \frac{1}{2\tau}\ln\left(\frac{2\psi_3}{\psi_3+1}\right) > 0$, we deduce that $\psi_3 e^{-\rho_2\tau} - 1$ is positive. For later use we denote $\rho^* = \psi_3 e^{-\rho_2^*\tau} - 1$. We conclude that $\dot{\mathcal{W}}(t)$ satisfies, for almost all $t \geq 0$,

$$\begin{aligned}\dot{\mathcal{W}}(t) \leq & \psi_{12}\tilde{\beta}\,(x(t)+\tilde{\alpha}\tilde{x}(t))\,\tilde{x}(t) - \psi_1\rho_1\int_{t-\tilde{\tau}}^{t} e^{\rho_1(\ell-t)}\tilde{u}(\ell)d\ell \\ & - \overline{k}\tilde{u}(t-\tilde{\tau}) - 2\rho^* e^{-\gamma\tau}\beta\,(x(t-\tau)+\tilde{x}(t-\tau))\,x(t-\tau) \\ & - \delta^* x(t) - \psi_2\rho_2\int_{t-\tau}^{t} e^{\rho_2(\ell-t)}\beta\,(x(\ell)+\tilde{x}(\ell))\,x(\ell)d\ell,\end{aligned} \tag{A.1}$$

where, $\psi_{12} < 0$, $\overline{k} > 0$, $\delta^* > 0$, and, $\rho^* > 0$. By integrating the previous inequality (A.1), we deduce that the functional $\mathcal{W}$ is bounded over $[0, +\infty)$. From the definition of $\mathcal{W}$, it follows that for all $t \geq 0$, the trajectories $\tilde{x}(t)$ and $x(t)$ are bounded by, respectively, the positive constants $\tilde{x}_s$ and x_s. A direct

consequence is that for almost all $t \geq 0$,

$$\begin{aligned}\dot{\mathcal{W}}(t) \leq & \psi_{12}\tilde{\beta}\left(x_s + \tilde{\alpha}\tilde{x}_s\right)\tilde{x}(t) - \psi_1\rho_1 \int_{t-\tilde{\tau}}^{t} e^{\rho_1(\ell-t)}\tilde{u}(\ell)d\ell \\ & - \delta^* x(t) - \psi_2\rho_2 \int_{t-\tau}^{t} e^{\rho_2(\ell-t)}\beta\left(x(\ell) + \tilde{x}(\ell)\right)x(\ell)d\ell.\end{aligned}$$

We conclude that for almost all $t \geq 0$, we have,

$$\dot{\mathcal{W}}(t) \leq -\psi_4 \mathcal{W}\left(\tilde{x}_t, \tilde{u}_t, x_t\right), \tag{A.2}$$

where $\psi_4 = \min\left\{-\psi_{12}\tilde{\beta}(x_s + \tilde{\alpha}\tilde{x}_s), \delta^*, \rho_1^*, \rho_2^*\right\} > 0$. Now, by integrating the inequality (A.2), we deduce that for all $t \geq 0$,

$$\mathcal{W}\left(\tilde{x}_t, \tilde{u}_t, x_t\right) \leq e^{-\psi_4 t}\mathcal{W}\left(\varphi_{\tilde{x}}, \varphi_{\tilde{u}}, \varphi_x\right). \tag{A.3}$$

It follows from the definition of $\mathcal{W}$ that $\tilde{x}$ and x converge exponentially to zero with a decay rate larger than, or equal to, ψ_4. From the second equation in (10), we note that the linearity in $\tilde{u}$ and the fact that $2\tilde{K}e^{-\tilde{\gamma}\tilde{\tau}} < 1$, imply that $\tilde{u}$ converges exponentially to the 0-equilibrium of the shifted system when $\tilde{x}$ and x also converge exponentially to zero. This concludes the proof of Theorem 1.

Appendix B. Determining $\mathfrak{s}$, $\tilde{\mathfrak{s}}$, $\mathfrak{m}$, and $\tilde{\mathfrak{m}}$, in (37) and (38)

Since R and $\tilde{R}$ have similar forms, we prove the desired results only for R. Using the expression of β given in (1), we rewrite for all $\mathfrak{e} > 0$ and $\mathfrak{z} > -\mathfrak{e}$,

$$R(\mathfrak{z}) = \beta(0)\left(\frac{1}{1 + b(\mathfrak{z} + \mathfrak{e})^n} - \frac{1}{1 + b\mathfrak{e}^n}\right) - \theta\mathfrak{z}. \tag{B.1}$$

Obviously, when $|\mathfrak{z}| > 1$, we have

$$\frac{|R(\mathfrak{z}|}{|\mathfrak{z}|} \leq \frac{2\beta(0) + |\theta|}{|\mathfrak{z}|} \leq 2\beta(0) + |\theta|. \tag{B.2}$$

To address the case where $|\mathfrak{z}| \leq 1$ for all $\mathfrak{z} > -\mathfrak{e}$ and $\mathfrak{e} > 0$, we consider first the function:

$$\rho^{\dagger}(\mathfrak{z}) = \frac{1}{1+b(\mathfrak{z}+\mathfrak{e})^n} - \frac{1}{1+b\mathfrak{e}^n} = \frac{b\left[\mathfrak{e}^n - (\mathfrak{z}+\mathfrak{e})^n\right]}{q(\mathfrak{z})},$$

where $q(\mathfrak{z}) = \left[1+b(\mathfrak{z}+\mathfrak{e})^n\right](1+b\mathfrak{e}^n)$. Using,

$$(\mathfrak{z}+a)^n - a^n = na^{n-1}\mathfrak{z} + n(n-1)\int_0^{\mathfrak{z}}\int_a^{a+l} m^{n-2}dmdl,$$

we deduce that,

$$\rho^{\dagger}(\mathfrak{z}) = -nb\mathfrak{e}^{n-1}\frac{\mathfrak{z}}{q(\mathfrak{z})} + \mathfrak{C}(\mathfrak{z}), \tag{B.3}$$

where $\mathfrak{C}(\mathfrak{z}) = -nb(n-1)\frac{1}{q(\mathfrak{z})}\int_0^{\mathfrak{z}}\int_0^{\ell}(m+\mathfrak{e})^{n-2}dmd\ell$. We ease the notation by considering $h = 1+b\mathfrak{e}^n$. Then, by noticing that $\frac{1}{q(\mathfrak{z})} = \frac{1}{h}\left(\rho^{\dagger}(\mathfrak{z}) + \frac{1}{h}\right)$, it follows that $\rho^{\dagger}(\mathfrak{z}) = -nb\mathfrak{e}^{n-1}\left(\frac{\rho^{\dagger}(\mathfrak{z})}{h} + \frac{1}{h^2}\right)\mathfrak{z} + \mathfrak{C}(\mathfrak{z})$. Consequently,

$$\rho^{\dagger}(\mathfrak{z}) = -\frac{nb\mathfrak{e}^{n-1}}{h^2}\mathfrak{z} + \mathfrak{C}(\mathfrak{z}) - \frac{nb\mathfrak{e}^{n-1}}{h}\rho^{\dagger}(\mathfrak{z})\mathfrak{z}. \tag{B.4}$$

We recall that, by definition, $\theta = \beta'(\mathfrak{e}) = \beta(0)\frac{nb\mathfrak{e}^{n-1}}{h^2}$. Therefore,

$$\rho^{\dagger}(\mathfrak{z}) + \frac{\theta}{\beta(0)}\mathfrak{z} = \mathfrak{C}(\mathfrak{z}) - \frac{nb\mathfrak{e}^{n-1}}{h}\rho^{\dagger}(\mathfrak{z})\mathfrak{z}. \tag{B.5}$$

On the other hand, observe that (B.1) is equivalent to $R(\mathfrak{z}) = \beta(0)\left[\rho^{\dagger}(\mathfrak{z}) - \frac{\theta}{\beta(0)}\mathfrak{z}\right]$. By combining the last equality with (B.5), we get the intermediate consequence,

$$\frac{R(\mathfrak{z})}{\beta(0)} = \mathfrak{C}(\mathfrak{z}) - \frac{nb\mathfrak{e}^{n-1}}{h}\rho^{\dagger}(\mathfrak{z})\mathfrak{z}. \tag{B.6}$$

Now, we readily check that

$$|\mathfrak{C}(\mathfrak{z})| \leq \frac{nb(n-1)}{q(\mathfrak{z})}\left(|\mathfrak{z}|+\mathfrak{e}\right)^{n-2}\frac{\mathfrak{z}^2}{2}. \tag{B.7}$$

From (B.3) we deduce that $\left|\rho^{\dagger}(\mathfrak{z})\right| \leq \frac{nb\mathfrak{e}^{n-1}}{q(\mathfrak{z})}|\mathfrak{z}| + |\mathfrak{C}(\mathfrak{z})|$. Using (B.7), it follows that

$$\left|\mathfrak{z}\rho^{\dagger}(\mathfrak{z})\right| \leq \frac{nb\mathfrak{e}^{n-1}}{q(\mathfrak{z})}\mathfrak{z}^2 + \frac{nb(n-1)}{2q(\mathfrak{z})}\left(|\mathfrak{z}|+\mathfrak{e}\right)^{n-2}|\mathfrak{z}|^3. \tag{B.8}$$

Consequently, from (B.6), and using (B.7) and (B.8), we obtain the upper bound,

$$\begin{aligned}\frac{|R(\mathfrak{z})|}{\beta(0)} \leq & \frac{(nb)^2(n-1)\mathfrak{e}^{n-1}}{2hq(\mathfrak{z})}\left(|\mathfrak{z}|+\mathfrak{e}\right)^{n-2}|\mathfrak{z}|^3 \\ & + \left[\frac{nb(n-1)}{2q(\mathfrak{z})}\left(|\mathfrak{z}|+\mathfrak{e}\right)^{n-2} + \frac{\left(nb\mathfrak{e}^{n-1}\right)^2}{hq(\mathfrak{z})}\right]\mathfrak{z}^2.\end{aligned} \tag{B.9}$$

On the other hand, we observe that, $\frac{1}{q(\mathfrak{z})} = \frac{1}{[1+b(\mathfrak{z}+\mathfrak{e})^n]h}$. Therefore, when $\mathfrak{z} \geq 0$, we have, $\frac{1}{q(\mathfrak{z})} = \frac{1}{[1+b(|\mathfrak{z}|+\mathfrak{e})^n]h}$, and when $\mathfrak{z} \leq 0$, then $\mathfrak{z} \in (-\mathfrak{e}, 0]$. Thus, $\frac{1}{q(\mathfrak{z})} \leq \frac{1}{h} \leq \frac{1+b(2\mathfrak{e})^n}{[1+b(|\mathfrak{z}|+\mathfrak{e})^n]h}$. Consequently, for all $\mathfrak{z} > -\mathfrak{e}$, we have,

$$\frac{1}{q(\mathfrak{z})} \leq \frac{1+b(2\mathfrak{e})^n}{\left[1+b(|\mathfrak{z}|+\mathfrak{e})^n\right]h}. \tag{B.10}$$

From (B.10) and (B.9), we deduce that

$$\begin{aligned}\frac{|R(\mathfrak{z})|}{\beta(0)} &\leq \left[\mathfrak{p}_1\frac{1+\left(|\mathfrak{z}|+\mathfrak{e}\right)^{n-2}}{1+b\left(|\mathfrak{z}|+\mathfrak{e}\right)^n} + \mathfrak{p}_2\frac{\left(|\mathfrak{z}|+\mathfrak{e}\right)^{n-2}|\mathfrak{z}|}{1+b\left(|\mathfrak{z}+\mathfrak{e}\right)^n}\right]\mathfrak{z}^2 \\ &\leq \left[\mathfrak{p}_1\frac{1+\left(|\mathfrak{z}|+\mathfrak{e}\right)^{n-2}}{1+b\left(|\mathfrak{z}|+\mathfrak{e}\right)^n} + \mathfrak{p}_2\frac{\left(|\mathfrak{z}|+\mathfrak{e}\right)^{n-1}}{1+b\left(|\mathfrak{z}+\mathfrak{e}\right)^n}\right]\mathfrak{z}^2,\end{aligned}$$

where the positive constants $\mathfrak{p}_1$ and $\mathfrak{p}_2$ are given by:

$$\mathfrak{p}_1 = \left[1+b(2\mathfrak{e})^2\right]^n \max\left\{\frac{nb(n-1)}{2h}, \frac{\left(nb\mathfrak{e}^{n-1}\right)^2}{h^2}\right\},$$

and, $\mathfrak{p}_2 = \frac{\left((nb)^2(n-1)\mathfrak{e}^{n-1}\right)\left(1+b(2\mathfrak{e})^n\right)}{2h^2}$. Next, observe that:
case 1: if $|\mathfrak{z}|+\mathfrak{e} \leq 1$, then $\frac{1+(|\mathfrak{z}|+\mathfrak{e})^{n-2}}{1+b(|\mathfrak{z}|+\mathfrak{e})^n} \leq 2$, and, $\frac{(|\mathfrak{z}|+\mathfrak{e})^{n-1}}{1+b(|\mathfrak{z}+\mathfrak{e})^n} \leq 1$.
case 2: if $|\mathfrak{z}|+\mathfrak{e} > 1$, then $\frac{1+(|\mathfrak{z}|+\mathfrak{e})^{n-2}}{1+b(|\mathfrak{z}|+\mathfrak{e})^n} \leq \bar{b}$, and, $\frac{(|\mathfrak{z}|+\mathfrak{e})^{n-1}}{1+b(|\mathfrak{z}+\mathfrak{e})^n} \leq \bar{b}$, where,

$\overline{b} = \max\left\{1, \frac{1}{b}\right\}$. Therefore, in both cases, we proved that:

$$|R(\mathfrak{z})| \leq \mathfrak{m}\mathfrak{z}^2, \tag{B.11}$$

where, $\mathfrak{m} = \beta(0)\max\left\{\mathfrak{p}_1 \max\left\{2, b^{-1}\right\}, \mathfrak{p}_2\overline{b}\right\}$.

Now, recall that $R(\mathfrak{z}) = \beta(0)\left[\rho^\dagger(\mathfrak{z}) - \frac{\theta}{\beta(0)}\mathfrak{z}\right]$. From (B.11), we get,

$$\frac{|\beta(0)\rho^\dagger(\mathfrak{z}) - \theta\mathfrak{z}|}{|\mathfrak{z}|} \leq \mathfrak{m}|\mathfrak{z}|. \tag{B.12}$$

Therefore, we observe that if $|\mathfrak{z}| \leq 1$, the inequality (B.12) implies that

$$|\beta(0)\rho^\dagger(\mathfrak{z}) - \theta\mathfrak{z}| \leq \mathfrak{m}|\mathfrak{z}|. \tag{B.13}$$

From (B.2) and (B.13), we conclude that, for all $\mathfrak{z} > -\mathfrak{e}$ and $\mathfrak{e} > 0$, we have,

$$|R(\mathfrak{z})| \leq \mathfrak{s}|\mathfrak{z}|, \tag{B.14}$$

where $\mathfrak{s} = \max\{\mathfrak{m}, 2\beta(0) + |\theta|\}$.

Finally, based on (B.11), (B.14) and similar results for $\tilde{R}$, one can easily determine constants $\mathfrak{c}_i$ so that (39) and (40) are satisfied.

Appendix C. Subsequent steps in the proof of Theorem 2

Now, we focus on the function H, defined after (59). We recall that there exist $\mathfrak{c}_i > 0$, $i = 1, \ldots, 6$ such that (39) and (40) are satisfied. In addition, from the expression of $V^\dagger$, defined in (53), we notice that since $\lambda_1 = 2$, we get,

$$V^\dagger(X_t, \tilde{X}_t, \tilde{U}_t) \geq \frac{\mathfrak{c}_1}{\max\{\mathfrak{c}_1, \mathfrak{c}_2\}}Q(X(t)) + \frac{\mathfrak{c}_2}{\max\{\mathfrak{c}_1, \mathfrak{c}_2\}}Q(\tilde{X}(t),$$

$$\left|\tilde{X}(t)\right| \leq \sqrt{V^\dagger(X_t, \tilde{X}_t, \tilde{U}_t)}, \quad \text{and,} \quad |X(t)| \leq \sqrt{2V^\dagger(X_t, \tilde{X}_t, \tilde{U}_t)}.$$

By combining the previous inequalities, we get the following upper bound:

$$\begin{aligned}\left|H(X_t,\tilde{X}_t)\right| \leq\, & v{V^\dagger}^2(X_t,\tilde{X}_t,\tilde{U}_t)+\mathfrak{c}_5\sqrt{2V^\dagger(X_t,\tilde{X}_t,\tilde{U}_t)}Q(X(t-\tau))\\ &+\left[\lambda_4\mathfrak{c}_1(\mathfrak{a}_4+\mathfrak{a}_2)+\mathfrak{c}_3\right]\sqrt{2V^\dagger(X_t,\tilde{X}_t,\tilde{U}_t)}Q(X(t))\\ &+\left[\lambda_4\mathfrak{c}_2(\mathfrak{a}_4+\mathfrak{a}_2)+\mathfrak{c}_4\right]\sqrt{2V^\dagger(X_t,\tilde{X}_t,\tilde{U}_t)}Q(\tilde{X}(t))\\ &+\mathfrak{c}_6\sqrt{2V^\dagger(X_t,\tilde{X}_t,\tilde{U}_t)}Q(\tilde{X}(t-\tau)),\end{aligned} \tag{C.1}$$

where, $v=\frac{\left(\mathfrak{d}_1\lambda_4+2(\mathfrak{a}_5\lambda_4)^2\right)\max\{\mathfrak{c}_1,\mathfrak{c}_2\}^2}{2\mathfrak{d}_1}$. A direct consequence is that the time derivative of $V^\dagger$ satisfies for almost all $t\geq 0$,

$$\begin{aligned}\dot{V}^\dagger(t)\leq &-2\overline{\mathfrak{d}}V^\dagger(X_t,\tilde{X}_t,\tilde{U}_t)-\frac{\mathfrak{d}_1}{2}Q(\tilde{U}(t-\tilde{\tau}))\\ &-\left[\overline{\mathfrak{d}}-vV^\dagger(X_t,\tilde{X}_t,\tilde{U}_t)\right]V^\dagger(X_t,\tilde{X}_t,\tilde{U}_t)\\ &-\left[\frac{\mathfrak{d}_4}{2}-\left(\lambda_4\mathfrak{c}_2(\mathfrak{a}_4+\mathfrak{a}_2)+\mathfrak{c}_4\right)\sqrt{2V^\dagger(X_t,\tilde{X}_t,\tilde{U}_t)}\right]Q(\tilde{X}(t))\\ &-\left[\mathfrak{d}_2-\mathfrak{c}_5\sqrt{2V^\dagger(X_t,\tilde{X}_t,\tilde{U}_t)}\right]Q(X(t-\tau))\\ &-\left[\frac{\mathfrak{d}_5}{2}-\left(\lambda_4\mathfrak{c}_1(\mathfrak{a}_4+\mathfrak{a}_2)+\mathfrak{c}_3\right)\sqrt{2V^\dagger(X_t,\tilde{X}_t,\tilde{U}_t)}\right]Q(X(t))\\ &-\left[\mathfrak{d}_3-\mathfrak{c}_6\sqrt{2V^\dagger(X_t,\tilde{X}_t,\tilde{U}_t)}\right]Q(\tilde{X}(t-\tau)).\end{aligned} \tag{C.2}$$

Consequently, for all initial conditions belonging to the set

$$\mathcal{B}=\left\{(\varphi_X,\varphi_{\tilde{X}},\varphi_{\tilde{U}})\in\mathcal{C}_\tau\times\tilde{\mathcal{C}}_\tau\times\tilde{\mathcal{C}}_{\tilde{\tau}}\;\middle|\;V^\dagger\left(\varphi_X,\varphi_{\tilde{X}},\varphi_{\tilde{U}}\right)<\overline{V}^\dagger\right\}, \tag{C.3}$$

where, with an abuse of notation, we consider the spaces of continuous functions: $\mathcal{C}_\tau=\mathcal{C}\left([-\tau,0],(-x_e,+\infty)\right)$, $\tilde{\mathcal{C}}_\tau=\mathcal{C}\left([-\tau,0],(-\tilde{x}_e,+\infty)\right)$, and, $\tilde{\mathcal{C}}_{\tilde{\tau}}=\mathcal{C}\left([-\tilde{\tau},0],(-\tilde{u}_e,+\infty)\right)$, as well as the upper bound: $\overline{V}^\dagger=\min\{\frac{\overline{\mathfrak{d}}}{v},u_1^2,u_2^2,u_3^2,u_4^2\}$, where, $u_1=\frac{\mathfrak{d}_4}{8(\lambda_4\mathfrak{c}_2(\mathfrak{a}_4+\mathfrak{a}_2)+\mathfrak{c}_4)}$, $u_2=\frac{\mathfrak{d}_5}{8(\lambda_4\mathfrak{c}_1(\mathfrak{a}_4+\mathfrak{a}_2)+\mathfrak{c}_3)}$, $u_3=\frac{\mathfrak{d}_4}{4\mathfrak{c}_5}$, and, $u_4=\frac{\mathfrak{d}_3}{4\mathfrak{c}_6}$,
1140 we finally find that the derivative of the functional $V^\dagger$ satisfies:

$$\dot{V}^\dagger(t)\leq-2\overline{\mathfrak{d}}V^\dagger(X_t,\tilde{X}_t,\tilde{U}_t),\text{ where }\overline{\mathfrak{d}}>0,\text{ for almost all }t\geq 0.$$